A Serendipitous Survey of Galaxy Clusters with XMM-Newton

Michael Davidson

Institute for Astronomy
School of Physics

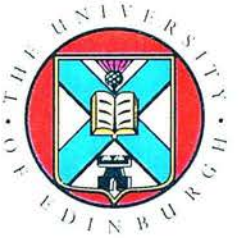

University of Edinburgh
Doctor of Philosophy

December 2005

Abstract

We present the first release of the XMM Cluster Survey (XCS), a serendipitous survey of clusters of galaxies using archival XMM-Newton data.

In this thesis we describe in detail the automated pipeline used to search the XMM images for extended sources. We also discuss techniques for the identification of clusters which are already known. We perform a rigorous set of tests designed to validate and quantify the effectiveness of the algorithms. Furthermore, we have developed a methodology for describing quantitatively the survey selection function and include the implications for the XCS constraints on the cosmological parameters σ_8 and Ω_m.

We compile three main catalogues from the set of 63327 detected sources. The first is a statistically well-defined sample of 142 known clusters and 1622 new candidates. The second is a smaller list of 90 XCS cluster candidates identified in the non-statistical sample. Finally, we include for completeness the point sources detected in the survey. We also describe the database used to store and access the survey data and source lists.

Strategies for the long-term follow-up of the catalogues in the low, medium and high redshift regimes are investigated. We have measured photometric redshifts for 219 new candidate clusters out to $z \sim 0.3$.

We conclude with the discoveries in the XCS of the most distant X-ray cluster currently known, at $z = 1.5$, and a likely supercluster at $z = 0.9$.

Declaration

I declare that this thesis is not substantially the same as any that I have submitted for a degree or diploma or other qualification at any other University. I further state that no part of my thesis has already been or is being concurrently submitted for any such degree, diploma or other qualification.

This thesis is the outcome of my own work except where specifically indicated in the text.

Michael Davidson
Edinburgh,
December 2005.

Acknowledgements

If you only read one page of this thesis, read this. It is often said that the life of a PhD student is an isolated one yet it is hard to reconcile this with the length of the list of people I really must thank. Without the help and support offered so freely from family, friends and colleagues I would never have been capable of completing this project. On second thoughts, without some of these friends the thesis would have been finished much earlier but I wouldn't have had nearly as much fun.

First and foremost I must thank my family, in particular Mum, Dad, Martin, Christine, Damien and Alex. Throughout my life they have moved mountains to help me in whatever I have chosen to do. This assistance has been delivered in many forms - innumerable phone calls and letters, a well-timed gift of a Spitfire tea towel and even the arrival of a new member of the family. Also, I must not fail to acknowledge the considerable financial support given over the years. Even when I announced my plan to quit a respectable job with excellent prespects in order to re-enter the murky world of academia I received nothing but encouragement. I expect I am about to test my family's nerves once more with my unconventional career detours - I remind them that they have given me the freedom and inclination to do so!

I settled into Edinburgh very easily, due to the good fortune of beginning the PhD at the same time as Miller, Jess, Emma and Rachel. Although our projects were very different it always felt as though we were working together. In fact, the Reading Groups over the first few months meant that we *had* to (although I'm informed by others that things were much tougher in their day..!). I must mention Ben, the original IDL guru. Thanks for answering so many questions - without your example I would never have been able to run wtransform on quite so many machines (run, Ben, run!). It would be neglectful not to thank Mairi who often endured frankly unreasonable streams of foul language in the office (see Chapter 3 especially) yet could still offer productive advice. Tom, you rarely offered advice but that beer was greatly appreciated!

At no point during the PhD have I appreciated my friends more than over the

past number of months spent writing the thesis. There were few things which reached me over that period of time. Examples include Portuguese food, port and lengthy discussions about music (read evangelical rants), thanks to Rita. I hope to enjoy complimentary chouriço and quince-based preserves for quite a while, courtesy of Mr Dylan. A regular 'commitment' without which I may have lost touch with reality is the Monday night pub quiz. The craic and, let's be candid, the beer supplied by the whole team is unmissible. Martin, Ross, Jo, Matt and Michael, in particular are thanked for their deep pockets and rapier wit. The often necessary Tuesday morning lie-ins also helped set my body clock (essential when weeks pass by without seeing the sun shine!). Olivia has an unheard of talent at defusing even the worst PhD panic. Whether it was caused by broken code, thesis structure, pre-viva stress, or otherwise you were always there to listen and help. You convinced me that the thesis was in no way like a broken pencil.

Many other friends have certainly earned a nod but, as I'd like you to read all the way to the end of these acknowledgements I will do so briefly. I'd like to thank Anita, Barney, Caz, Dan, Elizabeth, Emma R, Eric, Iain Turbitt, Ian, Michael Osborne, Michele, Niall, Paul, Simon and Tom K. Note the alphabetical order!

Of course, I must thank my supervisor, Bob Mann, for the assistance and guidance offered throughout the past 3 years and for the opportunity to join the XCS project. Furthermore, I'm immensely greatful to the whole XCS collaboration, in particular to Kivanc for devoting so much effort on making the best of the XMM data, and to Kathy Romer for her leadership of the project, constant encouragement and limitless patience with regards delivery of the final catalogue! I am also indebted to John Peacock for providing a different perspective on the project and for making available his galaxy sample which has proved tremendously useful for this thesis.

At this point, I would like to acknowledge and thank the Institute of Astronomy and James F. Hosie who, via the Royal Astronomical Society Hosie Bequest, funded the PhD project. In addition, I am grateful to have received funding for visits to the University of Sussex from the Visitors Grant.

Finally, I thank my examiners, Prof. Jim Dunlop and Prof. Trevor Ponman, for a viva which (against all odds!) was an enjoyable and memorable experience.

Michael Davidson
Edinburgh
March 2006

For my grandfather.

Contents

Chapter 1

Introduction

Galaxy clusters are dense regions of the Universe containing gas, galaxies and dark matter. These component elements interact to form an environment rich in interesting phenomena. Furthermore, the evolution of clusters is tied closely to the development of the Universe as a whole. By compiling a large sample of galaxy clusters we hope to gain insight into these processes. The copious emission of X-rays from hot gas in clusters makes this possible.

In this thesis we present the first release of the XMM Cluster Survey (XCS, Romer et al. 2001). The XCS is, primarily, a catalogue of clusters of galaxies with well-defined selection criteria. The project takes advantage of the huge archive of images taken by the XMM satellite to reap the largest ever sample of clusters selected by their X-ray emission.

This work reports the creation and analysis of the source catalogues. In Chapter 2 we describe in detail the XMM-Newton satellite, the observation archives and the derivation of the fundamental XCS resources, namely, the X-ray images and exposure maps. The development and implementation of the source detection algorithms is discussed in depth in Chapter 3 before the compilation of the key catalogues and databases is covered in Chapter 4. A major strength of the XCS is that it is well-characterised and will become more so in the future. The simulations to validate the algorithms and measure the survey selection function are presented in Chapter 5, and the initial power of XCS to constrain cosmology is highlighted. Efforts to confirm and find redshifts for the new cluster candidates in the low, medium and high redshift

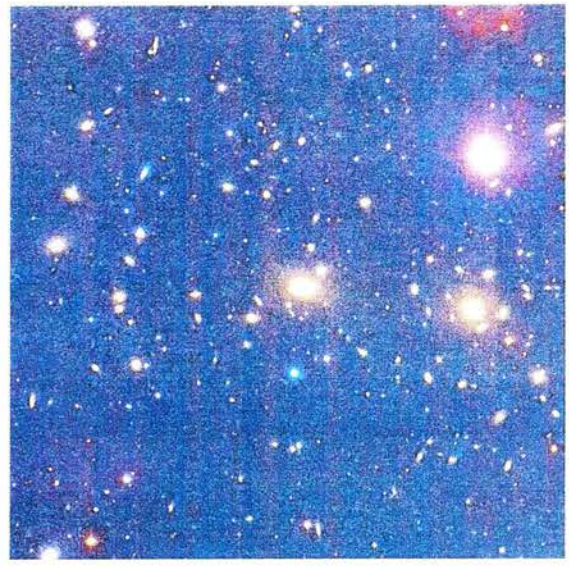

Figure 1.1: The Coma Cluster, which contains over 1000 member galaxies. This image is $\sim$ 30' by 30'. To provide scale, this is approximately the same size as the full moon. Image credit: O. Lopez-Cruz (INAOEP) et al., AURA, NOAO, NSF.

regimes are explored in Chapter 6. This culminates in the discovery of the most distant cluster of galaxies currently known, at $z = 1.5$.

First, however, we shall provide some background into the relevant physics at work in galaxy clusters. We then outline the XCS project and its scientific objectives.

1.1 Clusters of Galaxies

The study of galaxy clusters has a long history. To the naked eye, in a dark sky, the hazy regions of light which are our closest neighbouring galaxies can just be discerned. If our eyes were only slightly more sensitive the spectacle of the night sky would be even greater. Looking south, particularly to the constellations of Virgo and Coma Berenices (Figure 1.1), these indistinct objects form conglomerations which can be picked out easily from the thousands of stars nearby. The advent of the telescope revealed these clusters to be immensely rich environments, in stark contrast to other parts of the sky.

1.1.1 Current Paradigm

The field of cluster physics is wide and progressing rapidly. Over time, however, a standard picture of galaxy clusters and their place in the Universe has formed (e.g. Rosati et al. 2002; Mushotzky 2004). There are many exceptions, as will be discussed

later, but it is still useful to set the scene for what is to follow.

Clusters of galaxies form from the gravitational collapse of over-dense peaks in the primordial density field. They continue to evolve through mergers; a scheme known as hierarchical structure formation. Given time and isolation they become relaxed, often with one massive central galaxy. This object is termed the Brightest Cluster Galaxy (BCG) and is usually found at the bottom of the gravitational potential well of the cluster. Extreme examples of isolated elliptical galaxies with extensive X-ray haloes, known as fossil groups, support this scenario (for instance, Ponman et al. 1994; Jones et al. 2003).

The composition of clusters has been under question ever since Zwicky (1933) calculated the velocity dispersion of the member galaxies of the Coma cluster. The mass derived was far in excess of that which could be accounted for from the visible galaxies alone. This result was subsequently confirmed for other clusters and through measurements of gravitational lensing of light (for recent reviews see, for example, Fort and Mellier 1994; Bartelmann and Schneider 2001; Refregier 2003). Typical cluster masses are $\sim 10^{15} M_{\odot}$, confirming their unique position as the most massive bound objects in the Universe. The majority ($\sim 80\%$) of this mass is in the form of 'dark matter'; hot intra-cluster gas contributes $\sim 15\%$ and stars and galaxies provide only the small amount remaining. The baryonic and non-baryonic components are consistent with those found from Wilkinson Microwave Anisotropy Probe (WMAP, Spergel et al. 2003) observations of the Cosmic Microwave Background (CMB).

All rich clusters are thought to contain a population of early type galaxies which conform to a colour-magnitude relation, known as the red sequence (e.g. Postman et al. 1996; Gladders and Yee 2000, 2005). This is expected to arise given that old, elliptical galaxies in clusters ought to form at a similar epoch (and from gas of the same composition). They would then co-evolve with the cluster and, hence, provide a reliable redshift estimator.

Several relationships between cluster parameters have been found, both empirically and through theory. In general, cluster bolometric luminosity and temperature have been shown to be related as $L_X \propto T_X^3$ over a wide range of brightnesses (for example, Markevitch 1998; Arnaud and Evrard 1999). Similarly, the cluster mass can be related to its temperature as $M_{vir} \propto T^{3/2}$ (for instance, Eke et al. 1998; Finoguenov et al. 2001; Arnaud et al. 2005). There is evidence for deviation from these relationships, particularly at low masses and extremes of redshift (e.g. Helsdon and Ponman 2000; Del Popolo et al. 2005).

1.1.2 Key Physics

Having reviewed the broad properties of clusters we shall now discuss some of the physics most relevant to the XCS project and this thesis. Much of the content to follow has been derived from sources including Carroll and Ostlie (1996), Rybicki and Lightman (1986) and Peacock (1999).

The basic properties of an ideal cluster can be found easily. A first assumption will be that the cluster is dynamically relaxed, which may prove not to be true for recently disturbed systems. A condition for the cluster to be relaxed is that the typical crossing time should be less than the age of the cluster. From Carroll and Ostlie (1996), for a cluster of size R, and assuming that the age is that of the Hubble time, t_H, then the crossing time condition is

$$t_{cross} \approx \frac{R}{\sigma_v} \lesssim t_H$$

for the inner regions of a cluster, where the radial velocity dispersion σ_v is of order 10^3 km s^{-1}. Furthermore, if the cluster is virialized then, following Zwicky's example, the virial theorem can be combined with the equation for the gravitational potential energy of a spherical cluster to give an estimated mass as

$$M_{virial} \simeq \frac{5R\sigma_v^2}{G}.$$

While it was clear from this analysis that the majority of the mass of a cluster was not in the form of galaxies, it was only when X-ray observations became possible that it was revealed that a large portion of the missing mass was intracluster gas (Giacconi et al. 1971). Gas trapped in the potential well of the cluster can be expected to be in thermal equilibrium with the galaxies, leading to a relation for the gas temperature

$$k_B T \simeq \mu m_p \sigma_v^2$$

where m_p is the proton mass and μ is the mean molecular weight ($\mu = 0.6$ for a primordial composition with a 76% fraction contributed by hydrogen). Thus, one expects the temperature to be of the order of 10^7 K, or 1 - 10 keV, and hence the gas to be completely ionized. The reason for the abundance of X-rays detected from clusters is now evident; the emissivity of such a plasma is dominated by thermal bremsstrahlung radiation.

Bremsstrahlung Emission

Given the typical mass of a cluster, and the assumption that its gas will be virialized, we expect there to exist plentiful quantities of hot plasma. The dominant mechanism for emission from such a plasma under these circumstances is bremsstrahlung radiation. Bremsstrahlung emission, the radiation process whereby a free electron emits a photon as it passes close to (and is 'braked') by an ion, has a characteristic spectrum. Knowing this spectrum it is possible to map the density and temperature of a cluster and thus also its mass distribution.

Without providing a full derivation of bremsstrahlung emissivity, the expected form can be obtained. The rate of energy loss as two charged particles pass near each other is proportional to i) the ionic charges, ii) the number density of ions, n_e^2, and iii) the inverse of their relative velocity, v. For thermal emission from a fully ionized plasma, where the velocity $v \propto T^{\frac{1}{2}}$ (a Maxwell-Boltzmann distribution), the emission per unit volume of gas is therefore $\propto T^{-\frac{1}{2}} n_e^2$. The final bremsstrahlung emissivity equation (e.g. Peacock 1999; Rybicki and Lightman 1986) can be quoted as

$$\epsilon_\nu / \mathrm{Wm}^{-3}\mathrm{Hz}^{-1} = 6.8 \times 10^{-32}\, T^{-\frac{1}{2}}\, n_e^2\, e^{-\frac{h\nu}{kT}}\, G(\nu, T)$$

where G is the quantum mechanical Gaunt factor, $G \simeq 1 + \log_{10}(kT/h\nu)$.

The emissivity equation is a vital observational tool for clusters. Measurable quantities such as X-ray spectra can be used to access the temperature and density profile of clusters. In the simple case of a spherical cluster in hydrostatic equilibrium knowledge of the density and the temperature can be combined with the assumption of an ideal gas to arrive at the cluster mass profile

$$\frac{\mathrm{d}P}{\mathrm{d}r} = -\frac{GM(<r)\rho}{r^2}$$

and

$$P = \frac{\rho k T}{\mu m_p}$$

lead to

$$M(<r) = -\frac{kTr}{\mu m_p G}\left(\frac{\mathrm{d}\ln\rho}{\mathrm{d}\ln r} + \frac{\mathrm{d}\ln T}{\mathrm{d}\ln r}\right)$$

where m_p is the proton mass and μ is the mean molecular weight as defined earlier.

Canonical Cluster Profile

The shape of the X-ray emission expected from a galaxy cluster can be predicted by assuming a canonical model of a cluster. If the cluster gas and galaxies are isothermal, in hydrostatic equilibrium and have isotropic velocity dispersions then a parameter β can be defined

$$\beta \equiv \frac{\mu m_p \sigma_r^2}{kT}$$

where σ_r is the radial velocity dispersion. The quantity β represents the ratio of the energy per unit mass in the galaxies and dark matter to that in the gas. By solving the mass profile equation above (e.g. Bahcall and Lubin 1994) we find that $\rho_{gas} \propto \rho_{gals}^{\beta}$.

Now, the distribution of galaxies in clusters has been observed to be well-fitted to a King model (King 1972; Cavaliere and Fusco-Femiano 1976).

$$\rho_{gals} \propto \left[1 + \left(\frac{r}{r_c}\right)^2\right]^{-\frac{3}{2}}$$

where r_c is a scale radius. Hence, under the aforementioned assumptions, the gas density should have the form

$$\rho_{gas} \propto \left[1 + \left(\frac{r}{r_c}\right)^2\right]^{-\frac{3\beta}{2}}$$

Furthermore, for an isothermal cluster bremsstrahlung emissivity is $\propto \rho_{gas}^2$ and thus $\epsilon \propto [1 + (r/r_c)^2]^{-3\beta}$. After projecting this three dimensional emission on to the plane of the sky the final surface brightness profile is determined

$$S(R) \propto \left[1 + \left(\frac{R}{r_c}\right)^2\right]^{-3\beta+\frac{1}{2}}$$

where R is the radius in cylindrical coordinates. This 'beta' model for the cluster emission has been shown to provide a good fit for many clusters (Neumann 2005a; Vikhlinin et al. 1999; Mulchaey et al. 2003), with $0.5 \lesssim \beta \lesssim 1.3$. However, the value of β has large variance which may suggest that one or more of the explicit assumptions is invalid. For instance, hydrostatic equilibrium is unlikely in a cluster undergoing a major merger. Often, the model is found to fit well for the outer regions of a cluster but poorly in the centre. Possible causes for this deviation include AGN activity in the BCG (or otherwise) and cooling of the core (e.g. Böhringer et al. 2005).

Observational Cosmology

We require a framework to describe how observable quantities are related to the underlying properties of the Universe. Examples which assume that the Universe is isotropic, homogeneous on large scales and in which energy is conserved are known as Friedmann-Robertson-Walker (FRW) models. Following the example set by Peacock (1999) the Robertson-Walker metric can be expressed in the form

$$c^2 \mathrm{d}\tau^2 = c^2 \mathrm{d}t^2 - R^2(t)[\mathrm{d}r^2 + S_k^2(r)\,\mathrm{d}\psi^2]$$

with the space-time curvature

$$S_k = \begin{cases} \sin r & k = 1 \quad \text{Positive curvature} \\ \sinh r & k = -1 \quad \text{Negative curvature} \\ r & k = 0 \quad \text{Flat} \end{cases}$$

where the coordinates are comoving and $\mathrm{d}\psi$ is the angular separation of two points on the sky. $R(t)$ is the scale factor at time, t, such that the proper distance between an observer and radial coordinate is $R(t)r$.

The expansion of the Universe, first confirmed by Hubble (1929), causes radiation emitted from a distant object to undergo an effective Doppler shift, known as the redshift. Light of frequency, ν_e, emitted at time, t_e will have a frequency, ν_o, when observed at time, t_o. The redshift can also be written in terms of the scale factor

$$\frac{\nu_e}{\nu_o} \equiv 1 + z = \frac{R(t_o)}{R(t_e)}.$$

The dynamics of the FRW model highlight the significance of the value of k, in terms of the geometry of the Universe. The development of the scale factor can be described by the equation

$$\dot{R}^2 - \frac{8\pi G}{3}\rho R^2 = -kc^2$$

There is thus a critical density which will result in a flat, Euclidean Universe ($k = 0$). Defining Hubble's constant as $H \equiv \dot{R}/R$ leads to

$$\rho_c = \frac{3H^2}{8\pi G}$$

and a density parameter Ω can be found to relate a general ρ to the critical value

$$\Omega \equiv \frac{\rho}{\rho_c} = \frac{8\pi G\rho}{3H^2}$$

Evidence for flatness ($\Omega = 1$) is very compelling, for instance from the cosmic microwave background (Spergel et al. 2003). However, as will discussed later, the rate of evolution of structure in the Universe and the observed brightness of supernovae (Riess et al. 1998) suggest that the matter contribution to the critical density is rather small ($\Omega_m \sim 0.3$) and that the remainder is in the form of vacuum energy ($\Omega_\Lambda \sim 0.7$).

In order to calculate observationally-useful quantities such as flux density and surface brightness we must have a solution to the Friedmann equation. Neglecting the contribution to Ω from radiation the solution can be quoted as

$$R_0\,\mathrm{d}r = \frac{c}{H_0}[(1-\Omega)(1+z)^2 + \Omega_\Lambda + \Omega_m(1+z)^3]^{-1/2}\,\mathrm{d}z$$

and so the distance-redshift relation is

$$R_0 S_k(r) = \frac{c}{H_0}\int_0^z [(1-\Omega)(1+z')^2 + \Omega_\Lambda + \Omega_m(1+z')^3]^{-1/2}\,\mathrm{d}z'.$$

For a generalized cosmology this must be integrated numerically. We can now revisit the FRW metric to determine the proper transverse size of an object

$$\mathrm{d}l = \mathrm{d}\psi\, R_0 S_k(r)/(1+z).$$

This equation is crucial if we wish to predict the apparent angular size of a source as a function of redshift and cosmology.

After considering cosmological factors, such as time dilation, the flux density of a source is

$$S_\nu(\nu_0) = \frac{L_\nu(\,[1+z]\nu_0\,)}{4\pi R_0^2 S_k^2(r)(1+z)}.$$

The specific intensity I_ν from a source with surface brightness B_ν is thus

$$I_\nu(\nu_0) = \frac{B_v(\,[1+z]\nu_0\,)}{(1+z)^3}.$$

In practice, the bolometric equivalents of these relations (obtained by integration over a frequency band) are more useful

$$S_{\mathrm{tot}} = \frac{L_{\mathrm{tot}}}{4\pi R_0^2 S_k^2(r)(1+z)^2}$$

and

$$I_{\mathrm{tot}} = \frac{B_{\mathrm{tot}}}{(1+z)^4}.$$

A luminosity distance can then be defined

$$d_L = (1+z)R_0 S_k(r).$$

The relations set out above are vital for the study of clusters at high redshifts in general cosmologies.

Cosmological Mass Function

Galaxy clusters can be used to trace the evolution of structure in the Universe and hence to reveal the underlying cosmology. The current theory of hierarchical structure formation is that initial over-densities in the primordial density field collapse to form small Cold Dark Matter (CDM) haloes first. These haloes then merge to create larger and larger bound systems. A natural outcome of such a scheme is a population of objects in the Universe with an evolving range of masses. This distribution is known as the Mass Function (MF), $n(M,z)$. The rate at which the haloes merge is sensitive to the overall mass density in the Universe, Ω_m. The density perturbations can only develop when the Universe is matter-dominated. A low value of Ω_m delays the switch from radiation-dominance to matter-dominance (e.g. Viana and Liddle 1996; Mo and White 2002). The abundance of haloes above a given mass at a particular epoch (usually the present) constrains the amplitude of the initial density fluctuations. These two factors thus uncover the shape and normalization of the Mass Function. Clusters of galaxies, being very massive objects, lie at the extreme tail of the mass distribution and are therefore ideal for studying cosmological structure formation. A small change in the observed abundance of clusters has a large consequence for the inferred population as a whole. By looking at how the number of clusters observed varies with mass and redshift we can derive constraints on the features discussed above.

Large numerical simulations have been used to investigate to validity of cosmological structure formation models. It is often found that the density of the structures which develop can be well-fitted to a particular family of profiles (known as NFW, e.g. Navarro et al. 1997a; Moore et al. 1999). The generalized shape is

$$\rho\left(\frac{r}{r_s}\right) = \frac{\rho_s}{\left(\frac{r}{r_s}\right)^{\alpha}\left(1+\frac{r}{r_s}\right)^{3-\alpha}}$$

where the characteristic radius r_s and ρ_s are related to the mass of the halo. This profile has also been shown to apply for real cluster observations over a large range of radii and mass (e.g. Pointecouteau et al. 2005).

The key parameter in structure formation is the normalization of the power spectrum of the initial density field. This is usually quantified in a term known as σ_8. We can assume that the initial density fluctuations evolve linearly with time until the present day. The current amplitude of the density fluctuations, found by averaging within spheres of radius $8h^{-1}$ Mpc, is σ_8. It is important that σ_8 is known accurately if Ω_m is to be determined as they are jointly-constrained. This is apparent if one considers the epoch at which most density fluctuations have started to collapse. A given cluster abundance at this epoch could arise through a combination of high Ω_m with low σ_8, or vice versa.

It is very difficult to measure cluster masses directly. Gravitational lensing techniques have been shown to do so (e.g. Miralda-Escude 1995; Allen 1998; Smith et al. 2005) but only for a small number of objects. X-ray observations offer the most efficient method for mass determination, although they must use an observable proxy. The depth of a cluster potential well is set by the mass of its dark matter halo. Assuming that the intra-cluster gas is virialized then there is a relation between its temperature (measurable from the X-ray spectrum) and its mass. This $M-T$ relation is one of the most useful to connect observation to predictions from theory. The precise form of the $M-T$ relation is still not known but is typically assumed to have the form $M \propto T^{3/2}$. There is evidence for this scaling, at least at low redshift (e.g. Arnaud et al. 2005), although the normalization is uncertain.

As a final extension, a relatively large number of X-ray photons is required to measure the cluster temperature, unlike its luminosity. Hence, a large sample of cluster masses can be obtained through use of a luminosity-temperature ($L-T$) relation, in combination with a $M-T$ conversion. This is not a preferred method as uncertainties in both relations (for instance, in the normalization and evolution of $L-T$) can bias the results.

1.2 X-ray Astronomy

It has only been possible to study the X-ray sky for 40 years and yet the most distant regions of the Universe are now within reach. X-rays are absorbed by the Earth's atmosphere and so the development of X-ray astronomy is governed by advances in space technology. Ever since the first, unexpected, discovery of the cosmic X-ray source Scorpius X-1 during an early rocket flight (Giacconi et al. 1962) each new mission has taken great steps forward in sensitivity. With the current generation of telescopes,

NASA's Chandra and the European Space Agency's XMM-Newton, it is possible to detect objects with fluxes as low as $\sim 10^{-17}$ erg cm^{-2} s^{-1} (Alexander et al. 2003a). This represents a rate of maturity matched by few scientific disciplines. The award of the Nobel Prize in 2002 to the leader of the team which discovered Sco X-1, Prof. Riccardo Giacconi, is an indication of the crucial role X-ray astronomy plays in science today.

The first major X-ray mission was Uhuru (Giacconi et al. 1972) which produced a catalogue of X-ray sources, including several objects at high galactic latitudes shown to be clusters of galaxies. The High Energy Astronomy Observatory (HEAO-1) provided the evidence that cluster radiation was dominated by thermal bremsstrahlung emission and made measurements of the X-ray background from 3 - 50 keV (Marshall et al. 1980). However, both HEAO and Ariel V, which followed, suffered from a large beam size. Therefore, the development of the technology required to focus X-rays for imaging brought forth a surge of enhanced-quality data via Einstein (Giacconi et al. 1979). The Einstein Medium Sensitivity Survey (EMSS, Gioia et al. 1990) covered almost 800 square degrees and detected 835 serendipitous sources, so setting the trend for cluster detection through large area surveys. ESA's EXOSAT operated in the mid-1980s and made great advances in the study of variability in black holes and neutron stars (e.g. Berger and van der Klis 1994).

The 1990s brought several missions specializing in either imaging or spectroscopy and precision timing. The Roentgensatellite (ROSAT) was a joint program of Germany, the United Kingdom and the United States. ROSAT discovered a huge number of X-ray sources through an all-sky survey performed during its nine year mission. Its excellent imaging resolution ($\sim 3''$) enabled it to resolve the majority ($\sim 70\%$) of the X-ray background (McHardy et al. 1998). The Advanced Satellite for Cosmology and Astrophysics (ASCA) obtained detailed spectra for many X-ray sources and made the first observation of gravitational redshift by a black hole (Nandra et al. 1999). The Rossi X-ray Timing Explorer (RXTE) and BeppoSAX have proved to be invaluable for studying rapid variation in a wide variety of sources (e.g. Mattson and Weaver 2004).

We are currently experiencing a golden age in X-ray astronomy with two major complementary missions ongoing. As previously mentioned, Chandra and XMM-Newton have been collecting data for several years and are generating an ever-increasing amount of science. XMM-Newton can see deeper than any previous mission. It has recently made observations of a supernova which occurred over 25 years ago (Immler et al. 2005) and of high velocity matter in a black hole accretion disc (Turner et al. 2004). Chandra,

with its superb spatial resolution (0.5") is invaluable, for example it has mapped structure in the Centaurus cluster (Figure 1.2, Sanders and Fabian 2002) and cold fronts in the cores of the galaxy clusters (e.g. Hallman and Markevitch 2004).

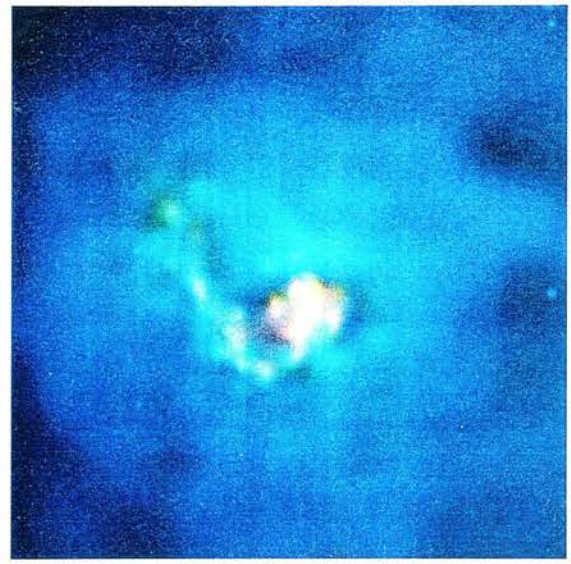

Figure 1.2: The Centaurus Cluster. Image credit: NASA/IoA/J. Sanders & A. Fabian.

However, XMM-Newton has features, such as huge collecting power and good resolution, which make its suitability for our project unique. Thus, we will be concentrating primarily on XMM-Newton in this thesis.

1.3 The History of Cluster Surveys

With the advent of the telescope came a period of systematic mapping of the sky. The most significant of the early surveys were those performed by Messier and Herschel, who discovered many hundreds of 'nebulae', many of which are in fact galaxies. Messier, Herschel and Méchain noted that these nebulae were more often to be found in certain regions of the sky, for instance in Virgo, and thus should be accredited with the discovery of galaxy clusters. However, the first systematic survey of galaxy clusters was performed, through huge effort, by identifying regions where there was an over-density of galaxies on photographic plates (Abell 1958).

Since Abell in 1958 there have been many projects surveying clusters, some over the whole sky and others using small area, deep searches. The optical surveys can be divided into two broad classes: the ones created by looking for concentrations of galaxies by eye, for instance, Zwicky (1966), and those which are automated using digital images

and machine-based algorithms (e.g. Lumsden et al. 1992; Dalton et al. 1997). Optical surveys suffer from a variety of problems including spurious detections of poor clusters because of variations in the density of field galaxies, difficulty in distinguishing between real clusters and projection artifacts, and uncertainty in the selection function (e.g. van Haarlem et al. 1997). Although this last issue is improved when automated searches are used, optical galaxy cluster surveys are usually limited to low redshifts. Progress has also been made in compensating for the colour variations towards higher redshifts and indeed colour-colour relations are now successfully being used to estimate the redshifts of candidates (for example, the Red Sequence Cluster Survey, Gladders 2000). In fact, a $z = 1.27$ cluster has been found by Stanford et al. (1997a). No doubt further advances will be forthcoming when Sloan Digital Sky Survey and UKIRT Infrared Deep Sky Survey[1] (e.g. Lawrence et al. 2002, Lawrence et al. 2006, in prep.) data are exploited, pushing into the near-infrared to extend selection to higher redshifts. However, as discussed earlier, the great mass of these clusters leads to the presence of vast quantities of hot gas throughout and so X-rays provide a more efficient means for detecting clusters. In X-rays there is high contrast between the peaked cluster emission and the background thus reducing problems with projection effects.

Numerous X-ray surveys were performed with ROSAT, notably the All-Sky Survey (RASS, Truemper 1993), the Bright Cluster Sample (BCS, Ebeling et al. 1998), the Northern ROSAT All Sky Survey (NORAS, Bohringer et al. 2000) and the ROSAT-ESO Flux Limited X-ray survey (REFLEX, Böhringer et al. 2001). The ROSAT data archive is still being exploited, for instance, the Massive Cluster Survey (MACS, Ebeling et al. 2001). The potential to carry out serendipitous cluster surveys came into its own with ROSAT. There were many pointed observations performed after the all sky survey was completed. Serendipitous surveys based on these data include the ROSAT International X-ray/Optical Survey (RIXOS, Castander et al. 1995), the ROSAT Deep Cluster Survey (RDCS, Rosati et al. 1998), the Serendipitous High-Redshift Archival ROSAT Cluster Survey (SHARC, Collins et al. 1997) and the Wide Angle ROSAT Pointed X-ray Survey (WARPS, Scharf et al. 1997). These surveys have been great successes and have highlighted the scientific results which can be reaped from archival sources.

[1] http://www.ukidss.org

Member	Institution
Chris Collins	ARI, Liverpool John Moores University
Michael Davidson	IfA, Edinburgh
Matt Hilton	ARI, Liverpool John Moores University
Scott Kay	Oxford University
Kate Land	Imperial College
Andrew Liddle	University of Sussex
Bob Mann	IfA, Edinburgh
Chris Miller	NOAO/CTIO
Bob Nichol	University of Portsmouth
Kathy Romer	University of Sussex
Kivanc Sabirli	Carnegie Mellon University
Adam Stanford	Lawrence Livermore National Laboratory
Pedro Viana	Universidade do Porto
Mike West	University of Hawaii, Hilo

Table 1.1: The XCS Collaboration (December 2005).

1.4 The XMM Cluster Survey

The XCS (Romer et al. 2001) is a major project to create and exploit a catalogue of clusters from the XMM archives. It was first mooted in the late 1990s and the collaboration was formalized subsequent to the successful launch of XMM. Since then XCS has grown in size and its current membership is presented in Table 1.1. By the end of the XMM mission XCS shall have discovered several thousand clusters out to $z > 1$ over an area ~ 500 square degrees. Its place, in comparison to previous cluster surveys is shown in Figure 1.3. It will also have measured directly the cluster temperatures for all candidates with at least 500 photons, which (as discussed above) are essential for cosmological studies. As there are no new X-ray satellites planned for the near future the exploitation of the XCS catalogues is guaranteed to continue well into the next decade. The significance of cluster astrophysics to cosmology, taken alongside the cosmic microwave background and Type Ia supernovae, is undoubted. We shall now outline some specific scientific aims in more detail.

Evolution of Cluster Properties XCS will compile a homogeneous sample of clusters with temperature measurements. It will thus be possible to obtain a self-consistent

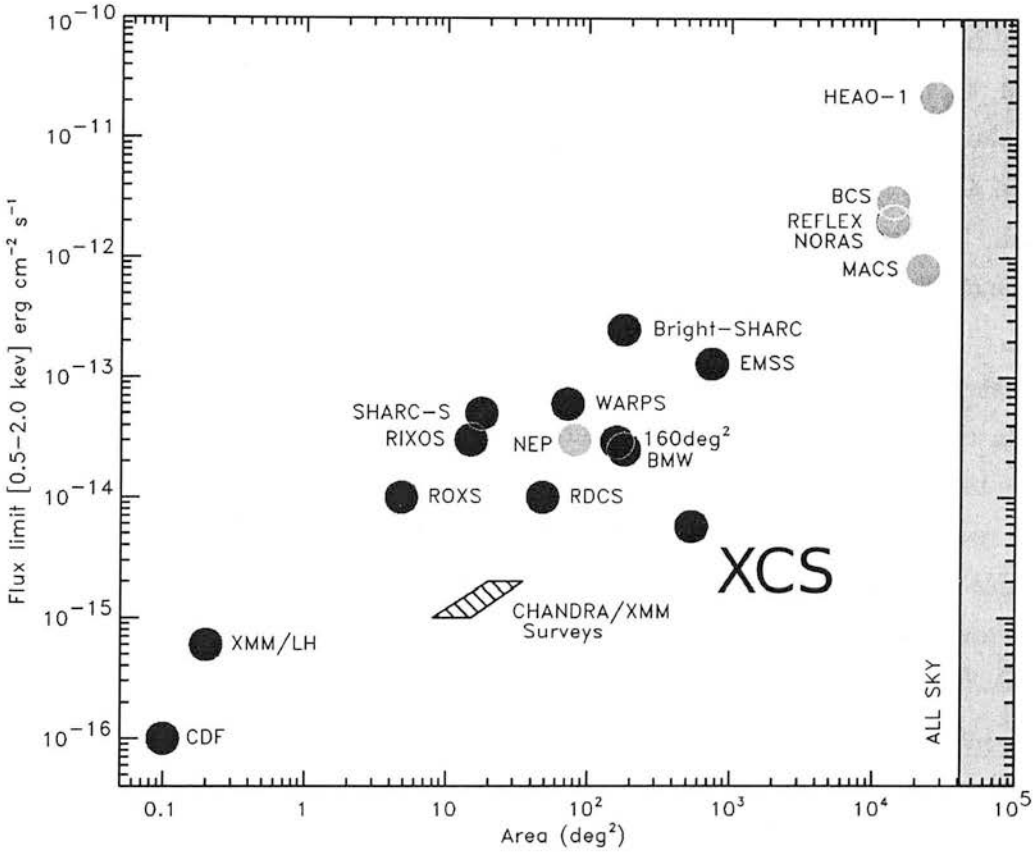

Figure 1.3: A summary of previous serendipitous and pointed X-ray cluster surveys (dark and light shaded circles respectively). The likely position for XCS, when it is complete, is also shown. It should be noted that a serendiptious survey of extended sources, such as XCS, has no uniform flux limit. The figure is adapted from Rosati et al. (2002).

$L_X - T_X$ relation for a wide range of temperatures and redshifts. This will confirm the presence of any deviation from either the self-similar model ($L \propto T^2$) or the observed general fit ($L \propto T^3$). Hence, non-gravitational processes such as heating, which are more evident in low-mass clusters, can be studied. Knowledge of the $L_X - T_X$ relation is also vital if accurate cosmological constraints are to be obtained.

With a large and uniform sample of clusters we shall be able to answer many of the questions regarding the observed surface brightness profiles. For instance, improved X-ray background estimates will enable cluster emission to be traced well beyond the virial radius. Our catalogue should also contain cooling core clusters, permitting the complex feedback between heating and cooling to be investigated.

In addition, the metallicity of the intra-cluster medium (ICM) can be analysed in detail. This is expected to reveal much information about the star formation history of the cluster galaxies.

Constraints on Cosmological Parameters The power of cluster surveys to constrain cosmological parameters has already been covered in Section 1.1.2. The XCS seeks to measure values (at the 95% confidence level) for σ_8 and Ω_m to within 5% and 10% respectively. Ultimately, after extensive follow-up of the XCS clusters we should be able to constrain Ω_Λ to within 15% (e.g. Viana et al. 2002). These constraints compare favourably to the values obtained by Spergel et al. (2003) of 11% for σ_8 and 14% for Ω_m(CMB data only).

Additional Science There is a huge range of complementary science to be performed beside the primary goals set out above. These include studies of the interaction between cluster galaxies and the ICM and their evolution. Additionally, clusters are known to magnify distant galaxies through gravitational lensing (for instance, Walsh et al. 1979; Inada et al. 2005). Sensitive sub-millimetre observations may reveal background galaxies out to $z = 5$ and beyond (for example with SCUBA-2, Audley et al. 2004). Finally, XCS is likely to be a cornerstone of many future projects, particularly those utilizing the CMB and Sunyaev-Zeldovich effect (SZ, e.g. Sunyaev and Zeldovich 1972; Pierpaoli and Anthoine 2005; Bond et al. 2005; Geisbüsch et al. 2005). Foreground objects such as galaxy clusters are a major contaminant in cosmological CMB studies and must therefore be masked. Joint constraints on the cosmological parameters from X-ray, SZ and optical techniques are likely to be the tightest for many years to come.

Galaxy clusters have become both a pillar of observational cosmology and a lab-

oratory for various interesting phenomena. A large survey with a telescope such as XMM-Newton will be invaluable.

Chapter 2

XMM-Newton

The project which became the X-ray Multi-Mirror (XMM) mission was first conceived in the late 1970s. The development and success of previous X-ray satellites, such as EXOSAT (Taylor et al. 1981), provided justification for the European Space Agency (ESA) to commit to a major mission. The project progressed through various assessment and design phases in the 1980s and 1990s before the commencement of the industrial phase in 1994[1]. The whole-life cost of XMM was budgeted at $\sim$ £500m which is approximately half the price of NASA's Chandra mission. The actual cost of the mission up to the end of the first two years of operation was close to this target, and was paid for by the constituent nations of ESA. Provisional funding until 31 March 2010 has been secured for the project[2].

XMM aims to provide unprecedented spectroscopic and imaging coverage of the X-ray sky. Its name was changed at launch to XMM-Newton to honour Sir Isaac Newton who played a founding role in the subject of spectroscopy by separating white light into its constituent colours. XMM-Newton has the largest collecting area of any X-ray satellite so can look deeper into the Universe than ever before.

A selection of the most relevant XMM specifications are provided in Table 2.1.

[1]ESA Bulletin Number 100, John Credland, http://www.esa.int/esapub/pi/bulletinPI.htm.
[2]http://www.esa.int/esaCP/SEM31GVLWFE_index_0.html

Property	Value
Imaging Spectral Range	0.1 - 12.0 keV
RGS Spectral Range	0.35 -2.5 keV
Collecting Area at 1.5 keV	4300 cm^2
Collecting Area at 8.0 keV	1800 cm^2
Mass	3800 kg
Focal Length	7.5 m
On-Axis FWHM PSF	5"
Mission Lifetime	At least until 31 March 2010
MOS Pixel Size	1.1"
pn Pixel Size	4.1"
EPIC FOV	$\sim 30'$
RGS FOV	$\sim 5'$

Table 2.1: Pertinent XMM specifications, from the XMM Users Handbook and the XMM-Newton Science Operations Centre.

2.1 The Satellite

In this section we discuss the key features of the satellite, from the orbit through to its imaging technology and instrument payload.

2.1.1 Launch and Orbit

XMM-Newton was launched on 10 December 1999 on an Ariane 5 rocket from Kourou in French Guiana. With a launch weight of 3800 kg and dimensions of 10 by 16 metres XMM is the most massive satellite so far launched by ESA. This stage of the mission was an undoubted success and the telescope was placed within 1.5 km of its planned orbit. Hence, much of the satellite's positioning fuel was conserved, leaving enough potentially for a 10 year mission.

The chosen orbit is highly elliptical and extends to almost one third of the way to the moon (an apogee of 114,000 km). This orbit enables very long uninterrupted observations to be made and ensures efficient contact with the ground stations in French Guiana, Australia and Chile.

2.1.2 Spacecraft

It is useful to have an awareness of the design and operation of the satellite in order to understand the provenance of the scientific data. An overview of the spacecraft layout

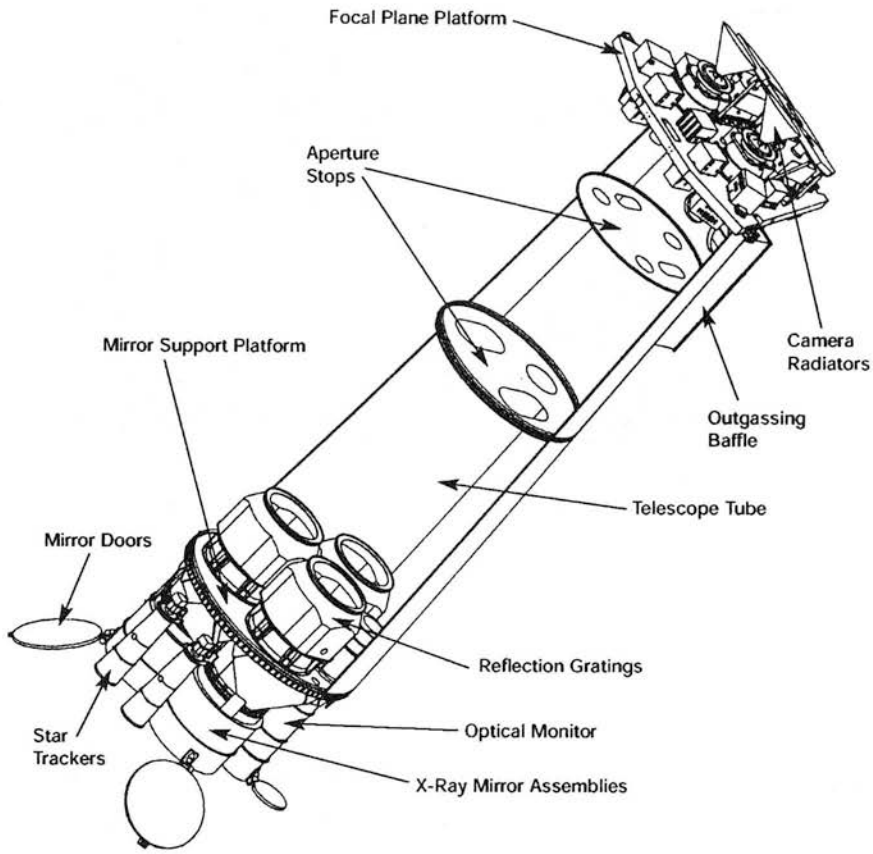

Figure 2.1: Schematic diagram of the XMM structure, from "An Overview of the XMM Observatory System", Barre et al., ESA Bulletin 100.

is shown in Figure 2.1. The telescope is designed around the three mirror modules (discussed in detail below). At one end is the Service Module which contains many of the essential operational systems of the satellite, such as

- Orbit and Attitude Control, through use of eight small hydrazine gas jets
- Electrical Power, provided by the solar panels (omitted from Figure 2.1 for the sake of clarity)
- Telemetry
- Thermal Control

The Telescope Tube itself encloses the aperture stops and baffles. At the other end is the Focal Plane Platform upon which the mission instruments are mounted, including the cameras and spectrometers.

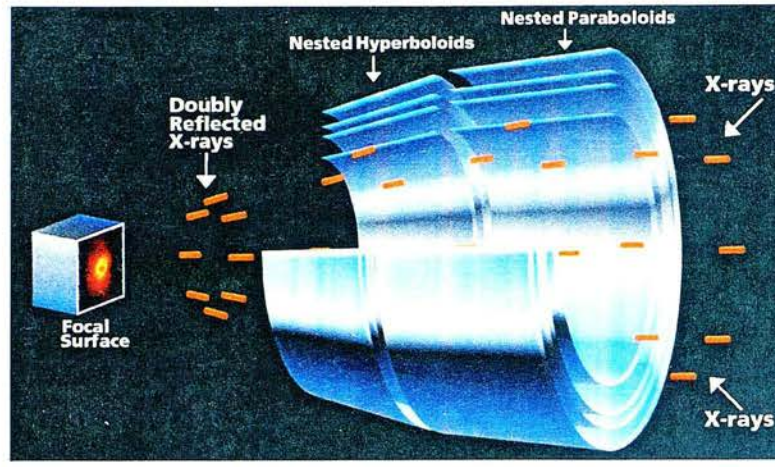

Figure 2.2: Grazing incidence reflection from hyperbolic and parabolic mirrors is used to focus X-rays on to a focal plane on which lies an imager. Image credit: NASA (http://chandra.harvard.edu/resources/illustrations/teleSchemGraz3D.html).

2.1.3 X-ray Mirrors

The XMM mirrors are a considerable engineering achievement. Imaging in X-rays is a difficult technical challenge because their energy is so high that they must be focussed by grazing incidence reflection (Figure 2.2). The solution found to maximize the collecting area of the telescope was to use a set of 58 co-aligned concentric nested mirrors (Figure 2.3).

There are three such sets of mirrors, each of which has a focal length of 7.5m. Each mirror has a nickel substrate and a reflective gold coating to ensure efficient focussing of X-rays with energies up to 10 keV. The mirror nests were constructed and aligned with very high precision[3] . However, the trauma of launch caused a degree of misalignment, which was expected.

2.1.4 European Photon Imaging Camera

At the prime focus of the three mirror modules lies the European Photon Imaging Camera (EPIC). There are two different imager technologies used: Metal Oxide Semiconductor (MOS) and pn. Two of the three cameras are of the MOS variety, which have been proven in previous missions. These were developed by Leicester University and are nominally identical, save for a relative rotation of 90 degrees (to fill in chip gaps). Each camera has seven Charged Couple Devices (CCDs) of 600 by 600 pixels.

[3]The four mirrors of Chandra are more precisely cast but at the price of lower collecting area.

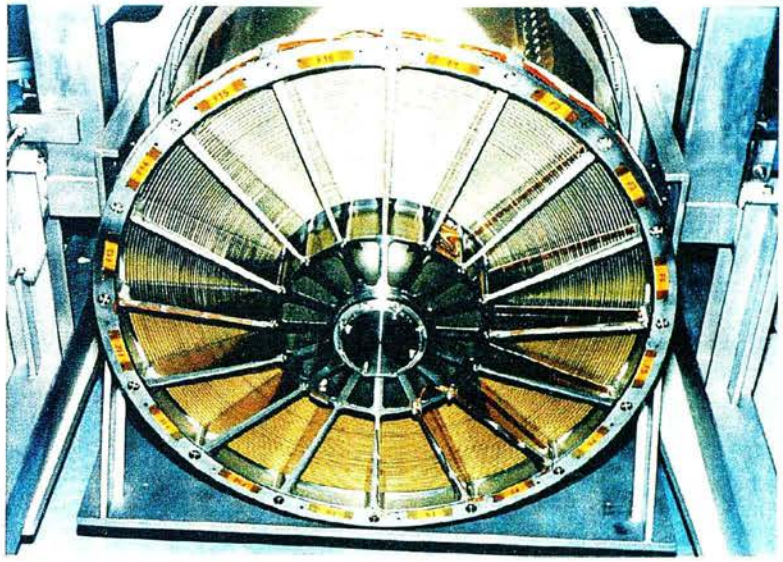

Figure 2.3: Photograph of an XMM mirror module. Image credit: Max-Planck-Institut für extraterrestrische Physik (http://wave.xray.mpe.mpg.de/xmm/mission/overview).

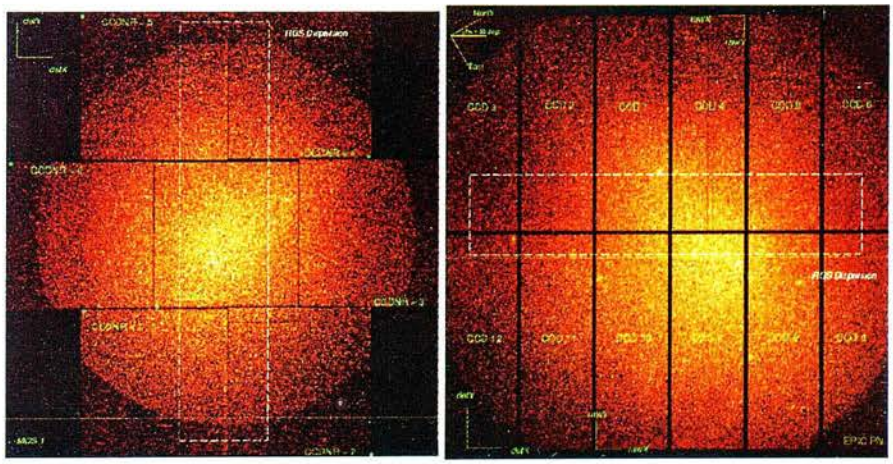

Figure 2.4: Layout of the chips in the MOS cameras (left) and pn camera (right). Image credit: XMM Users' Handbook.

The third telescope uses a pn camera. The pn imager is a new technology developed jointly by the Max-Planck-Institut für extraterrestrische Physik (Garching) and the Astronomisches Institut Tübingen. It is a back-illuminated device of 12 CCDs of 64 by 189 pixels. As a consequence of the X-ray photons not having to pass through as much material before being detected the pn camera is more sensitive than the MOS. The layout of both the MOS and pn chip configurations are shown in Figure 2.4.

Both types of camera are designed to record not only the position and time of arrival of each photon but also its energy. This enables moderate resolution imaging spectroscopy ($\frac{E}{\Delta E} \sim 20 - 50$) to be performed at no extra cost. The cameras also have high time resolution which helps in the analysis of variable sources. To increase the flexibility and performance of XMM the cameras can operate in a number of different modes. These vary in read-out frequency, from the standard full-frame which takes advantage of the entire field of view (FOV) of 30' (at a low temporal resolution), to the pn's Burst mode, offering exceptionally short read-out times. Not all of these modes are suitable for the XCS (in particular, the Timing and Small Window mode observations).

In addition, there is a filter wheel with a choice of 6 different settings ranging from 'Closed' through 'Thin' and 'Thick' to 'Open'. The filter chosen will depend on the optical brightness of the target and background objects. Pointings requiring use of the thick filter are unlikely to be suitable for XCS. The closed filter is primarily used for calibration of the instrumental background and to provide the detectors from damage (Section 2.1.6).

XMM's flexibility in these regards, in fact, makes the task of XCS more difficult. This is due to the increased inhomogeneity of the archive the modes and filters bring. Also, characterisation must be carried out for all of the modes and filters in turn, introducing an additional uncertainty through dilution of the available calibration time.

2.1.5 Reflection Grating Spectrometer

XMM is primarily a spectroscopic mission and thus has two high resolution spectrometers onboard. Each of the two MOS telescopes has a reflection grating in the light-path to divert approximately half of the light away from the imagers and towards a secondary focus (Figure 2.5). In contrast, the pn mirror module feeds light directly to the imager (Figure 2.6).

We shall not say any more about the spectrometers as the contribution of this thesis to XCS utilizes almost exclusively the X-ray images rather than spectra. However, XCS has made excellent progress finding cluster redshifts using X-ray spectra from XMM (Sabirli et al. in prep).

2.1.6 Other Instruments

The EPIC and RGS are the prime instruments onboard XMM but there are also others important to the overall success of the mission. There is a 30cm UV/Optical Moni-

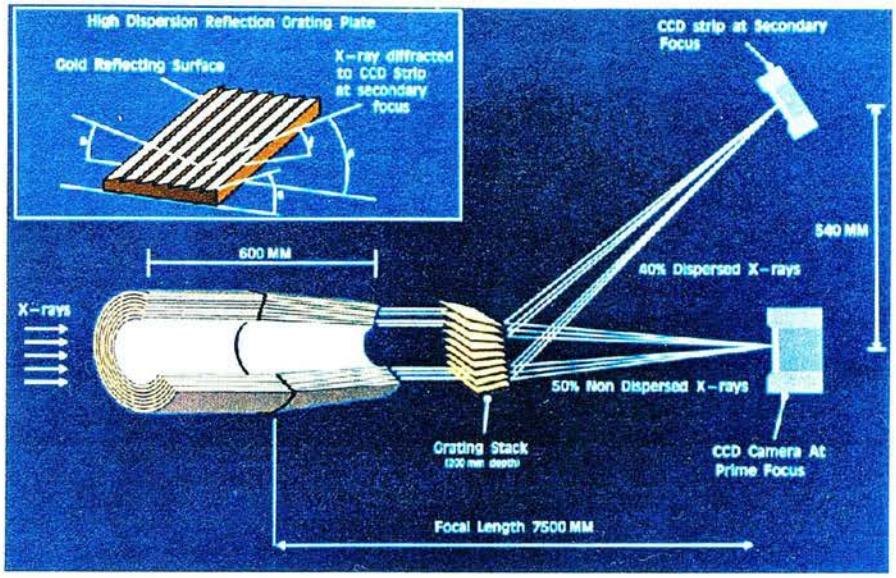

Figure 2.5: Light path for the X-rays in the two MOS mirror modules, which are equiped with both an imager and a spectrometer. Image credit: XMM Users' Handbook.

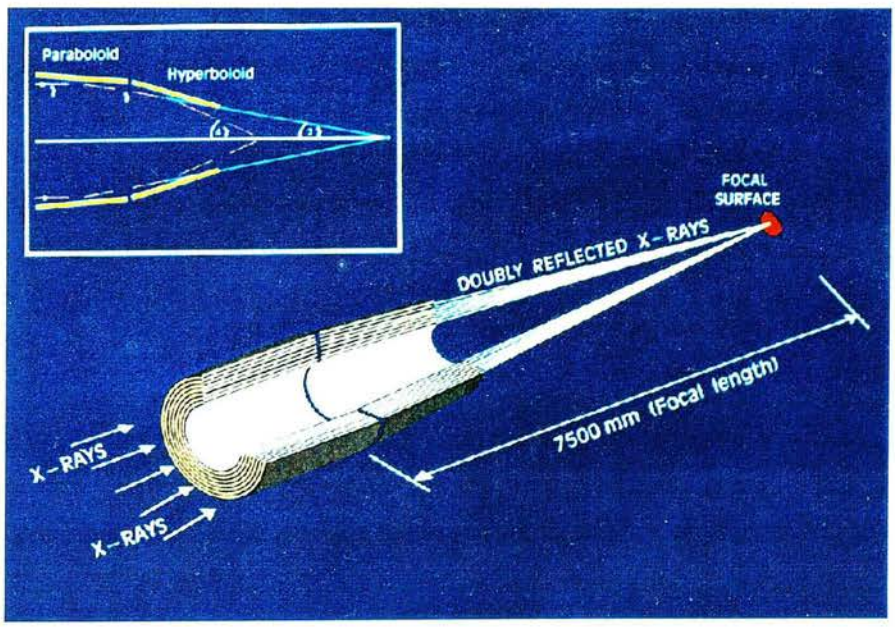

Figure 2.6: Light path for the X-rays in the pn mirror module. Image credit: XMM Users' Handbook.

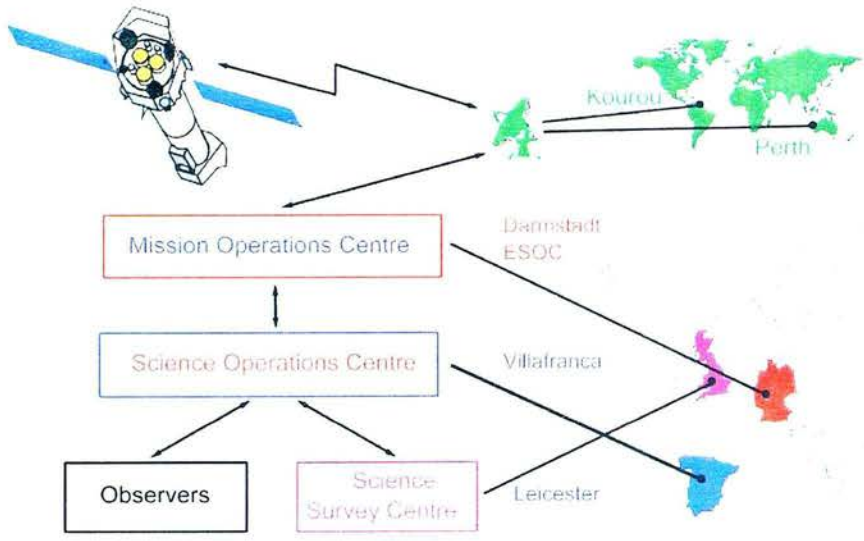

Figure 2.7: Mission architecture of the XMM mission. Image credit: ESA Bulletin Number 100, John Credland.

tor telescope used for shallow optical follow-up of each pointing (and also useful for guidance and astrometry). Furthermore, there is the EPIC Radiation Monitor (ERM) experiment. The first of its two main goals is to study the radiation belts and solar particle background (important in itself and for the operation of the EPIC). Secondly, it protects XMM from solar flares and while it is within the radiation belts by closing the EPIC cameras when high backgrounds are detected.

Typically, all of XMM's instruments operate in synchrony thereby providing simultaneous imaging, spectral and optical coverage for every pointing. Each observation can contain several exposures, subject to technical interuptions or otherwise.

2.2 Management and Access

Many thousands of people have been involved in the XMM mission, from construction to operations and end-users. Here we present an overview of the organisational infrastructure through which an observation proposal progresses before culminating in the final pipeline products from XMM.

2.2.1 Mission Architecture

A schematic of the mission architecture is shown in Figure 2.7. The various aspects of operation are clearly delegated and the geographical distribution of work is set out.

- **Mission Operations Centre** Controls the day-to-day technical operations of the satellite including communications through the various ground stations. It is located at the European Space Operations Centre in Darmstadt, Germany.

- **Science Operations Centre** Responsible for the scientific exploitation of XMM, from observation proposals through to calibration and archiving of data (based at Villafranca, Spain).

- **Survey Science Centre** Performs pipeline reduction of the archive and compiles catalogues of point sources. It is a consortium of eight European institutes lead from Leicester University.

2.2.2 Archive

The raw data files for each observation are archived by the Science Operations Centre (SOC) and are made available online through the XMM Science Archive[4] (XSA). To maximise the scientific output of the mission the Principal Investigator of each proposal has exclusive access to the data for one year only, after which they are publicly available. Everything required to produce images and spectra from the data is accessible in this manner.

2.2.3 Calibration

XMM carries a complex set of instruments using cutting edge technology. As such there are many issues which need to be addressed before reliable scientific data can be obtained. In fact, calibration is an ongoing process as the characteristics of the satellite change throughout its lifetime. The SOC performs calibration for XMM and makes the files available through its webpages[5].

- **Mirrors** For each of the telescopes there are calibration files which describe, for instance, the collecting area as a function of X-ray energy and how the Point Spread Function (PSF) varies with energy and off-axis angle. The choice of filter will affect these results also.

- **Spacecraft** At any given time an observer needs to know the precise attitude of the spacecraft and details of the systems such as time frames.

[4] http://xmm.vilspa.esa.es/external/xmm_data_acc/xsa/index.shtml
[5] ftp://xmm.vilspa.esa.es/pub/ccf/constituents/

- **Instruments** As with any scientific instruments the EPIC and RGS responses need to be carefully calibrated. Fundamental CCD properties such as the Charge Transfer Inefficiencies, bad pixels and quantum efficiencies have non-linear responses and therefore must be analysed in detail.

Some of these properties are known from pre-launch tests performed on the ground but many need to be measured in orbit. Continual degradation of the cameras due to exposure to radiation in space is expected and there are occasionally more serious events such as the micro-meteorite strike in early 2005 (see Section 6.5.1).

It should be noted that most effort is expended on the on-axis response of the instruments. There are many acknowledged ongoing deficiencies in the off-axis calibration[6] which is troublesome for a serendipitous survey like XCS. However, we shall demonstrate in Chapters 3 and 5 our efforts to overcome the various difficulties.

2.3 Data Reduction and Products

The requirements of XCS from the XMM archive are unique so use of the standard pipeline products is not appropriate. The data reduction for XCS has been performed by Sabirli (in prep.) and the description below outlines the procedures therein. Much of the XCS reduction is carried out using tasks from the Science Analysis System[7] (SAS) package of tools from the SOC.

2.3.1 XCS Local Archive

As previously discussed, XMM operates all of its instruments simultaneously and hence produces a vast quantity of data (of the order of 500Gb per year between $\sim$ 700 pointings). Mirroring and processing these data presents a considerable challenge for the project. XCS runs several large Terabyte RAID machines in Sussex and Edinburgh to store the raw data and reduced products.

2.3.2 Image and Exposure Map Creation

For each exposure there exists an event list which contains the position, time of arrival and energy of every detected photon. Not all of these photons should be used when

[6] See, for example, the discussion on relative flux offsets between the cameras in the documents XMM-SOC-CAL-TN-0023 and XMM-SOC-CAL-TN-0018 from the XMM Calibration pages at http://xmm.vilspa.esa.es/external/xmm_sw_cal/calib/documentation/index.shtml

[7] http://xmm.vilspa.esa.es/external/xmm_sw_cal/sas_frame.shtml

creating an image. Some will be detections of particles such as cosmic rays or other instrumental artefacts. Cosmic rays produce counts in the surrounding pixels in certain common patterns, so they can be easily identified and removed.

The X-ray background varies dramatically with time. There is a fuller discussion of this in the Algorithms chapter (Section 3.2.2) but suffice it to say here that time periods in which the background is flaring are excised through creation of Good Time Interval files.

Thus, a soft band image for each camera can be created by using `evselect`[8] to select the photon events in the 0.5 - 2.0 keV energy range, after filtering out dubious patterns, time periods and bad pixels. Hard band images and exposure maps (2 to 10 keV) are produced in precisely the same manner.

An exposure map is an image containing the effective exposure time a given pixel is available to receive photons. It is made by folding together the various mirror and detector responses, along with the filtering applied when creating the corresponding image. The SAS task `EEXPMAP`[9] is used to generate the exposure maps for XCS. Errors (and approximations) in the intrumental response models here can have significant consequences on source properties, for instance fluxes. As an example, `EEXPMAP` generates exposure maps using a single energy in each band. The seriousness of this approximation depends on the spectrum of the source in question and the width of the band. The primary band for XCS (0.5 to 2.0 keV) is quite narrow so the error should be minimal. Flux calibration against other X-ray missions is performed in Section 5.2.1.

Finally, XCS is looking for faint diffuse emission, which is intrinsically low signal-to-noise relative to the X-ray background. To increase the depth of the survey and quality of the statistics measured we decided that it was essential to merge the images from all three cameras MOS1, MOS2 and pn. This is a simple procedure for the images (they are directly co-added) but slightly more complicated for exposure maps. On account of the significantly different responses of the cameras each one must be weighted by their respective Energy Conversion Factor (ECF) before being merged. The ECF is the conversion between count-rate of a source and its flux. Here, it is taken to have a standard power law point source spectrum with photon index of 1.7, corrected for the appropriate nH column density from the Dickey and Lockman (1990) map. This is not entirely appropriate for cluster emission but the effect of this assumption will be measured through simulations (Section 5.2.2).

[8] http://xmm.vilspa.esa.es/sas/current/doc/evselect/

[9] http://xmm.vilspa.esa.es/sas/current/doc/eexpmap/

Chapter 3

Source Detection Algorithms

3.1 Introduction

The problem of source detection in images exists in virtually all branches and wavebands of astronomy. There has been much work carried out in recent years to automate the task as it can, in principle, be stated clearly in a few steps which are valid for most types of data (for instance optical, X-ray or radio). Firstly, a statistical significance that a pixel has more signal than background must be chosen. Next, an hypothesis test must be carried out on each pixel of the image to determine whether it belongs to the background or to an object. Lastly, these significant pixels should be combined in some manner to form objects. A brief search of the literature reveals many techniques to do this, though most are variants of a few core methods. Each of these has merits and deficiencies and it is soon realised that before an algorithm can be chosen (or written) it is essential to understand properly the issues affecting the data in question, and specify what is required from the final product. Hence, the structure of this chapter will be as follows: we will initially review the requirements of an algorithm as applied to the XCS project, then we will assess the suitability of a selection of commonly used methods before setting out a full description of the algorithms in their final form.

3.2 Challenges for XCS Algorithms

The nature of the job at hand is different for a large serendipitous survey such as XCS than for a project which only has to create source lists for a small number of images.

We must face all of the obstacles encountered in any X-ray observation but we must be able to overcome them automatically and speedily if we are going to search for clusters in the entire XMM archive.

3.2.1 Aims

The primary aim of the algorithm is straightforward; to detect and correctly classify clusters of galaxies in the X-ray images. This can be expanded by saying that the code should also be able to de-blend close point sources as well as coping with point sources (AGN) embedded in the extended clusters. The ability to cope with such artefacts is as important as being able to detect clusters if contamination of the catalogue is to be minimised. Another aim is that the code should be fast enough in order to perform detection on many hundreds of thousands of simulated clusters in real images for the purpose of determining the selection function of the survey. By selection function we mean here the detection efficiency of the code as a function of the cluster type, redshift, luminosity, observation, position and so on. This topic will be covered in depth in Chapter 5 but it should be kept in mind that a balance between efficiency and computation time will steer the final form of the algorithms. Furthermore, we must have confidence in the measured source properties; for instance flux, classification and cluster profile, and be able to provide the errors on these values based on careful statistics and numerical simulations.

3.2.2 Issues

XMM suffers from all the usual problems associated with X-ray telescopes, plus a few of its own. These can be broadly divided into instrumental, calibration and statistical difficulties.

PSF

Large point spread functions (PSFs) are a generic feature of X-ray telescopes due to the difficulty in focussing high energy photons. The XMM mirror configuration (Section 2.1.3) means that not only is the PSF large but it grows larger, and deviates from circular symmetry, off-axis. Worse still, the effect is not even azimuthally symmetric about the optical axis, as can be seen in the pre-launch test (Figure 3.1).

There are several PSF models currently available, as included in the Current Cal-

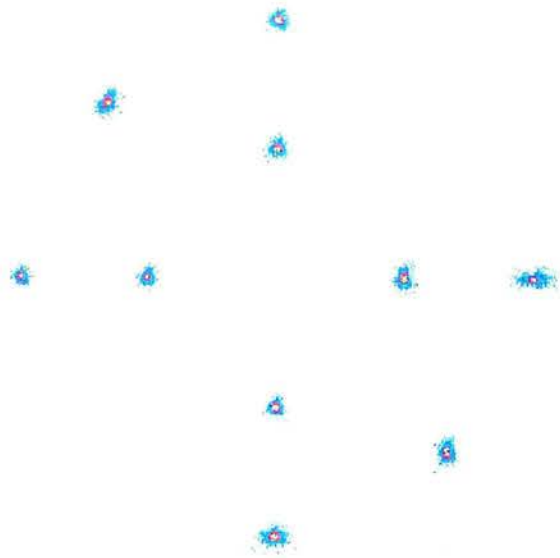

Figure 3.1: Pre-launch test carried out at the Panter facility showing the shape of the PSF across the field of view (7' and 14') of a MOS camera (logarithmic scale), from the XMM Users' Handbook.

ibration Files[1]. Some are based on simulations of the mirror modules and others on real observations.

1. Low Accuracy This method constructs a single bi-dimensional Gaussian with parameters dependent on energy and off-axis angle. Although this is very straightforward it does not properly represent the shape of the PSF at medium to high off-axis angles. It also fails to take into account the azimuthal variation.

2. Medium Accuracy This is based on a library of PSF images created through numerical simulations of the mirror modules. For a given energy and off-axis angle an image can be produced by interpolation of the library images. In the Science Analysis System (SAS) task `CALVIEW` the model PSF for any azimuthal angle can be obtained. It should be noted that this is just a rotated version of the library image at the same off-axis angle and hence does not contain any more structure. It may not reproduce the true PSF at high off-axis angle as there is evidence that it develops twin peaks with extensive wings (Figure 3.2). This is the only two dimensional PSF model available.

[1] http://xmm.vilspa.esa.es/external/xmm_sw_cal/calib/index.shtml

3. High Accuracy This is an analytical model constructed from the superposition of three Gaussian profiles (to attempt to model both the core and wings of the PSF). It has been superceded by the Extended accuracy model.

4. Extended Accuracy Through extensive studies of a sample of real detected point sources by Ghizzardi (2001)[2] the PSF was parameterised for both MOS cameras and the pn camera. Here, the PSF consists of an analytic King Model (plus a constant background):

$$PSF = A\left[1 + \left(\frac{r}{r_c}\right)^2\right]^{-\alpha} + B$$

where the fitted parameters are the core radius, r_c, the slope, α, the normalization, A and a constant background, B. The King model provides a better fit to both the core and the wings of the PSF than a Gaussian, and shares the property of being analytical. There are a number of disadvantages to this model; the range of validity is limited to energies less than 5 keV (not too critical for XCS) and off-axis angle less than 7' (more so). Crucially however, the fits are of the *azimuthallt averaged* PSF at each off-axis position (note that there is no explicit FOV azimuthal dependence, only rotation of the image). This model may prove useful for classification purposes, when the azimuthal average of each candidate object can be calculated, but not for simulations due to the lack of spatial structure. The Extended Accuracy model has the advantage of being measured using observations of real sources and thus should include the effects of the wings of the PSF.

An illustrative example is shown in Figure 3.2.

The uncertainty in the PSF will have implications for classification, as will be discussed in Section 3.5.5.

Vignetting

The optics of the telescope cause the effective exposure to vary significantly over the field of view, an effect known as vignetting. Vignetting can be rather severe in X-ray telescopes; for instance, the XMM exposure falls by approximately 60% at the edge (Figure 3.3).

It can also be seen that the vignetting is a function of energy thus the effective area of the telescope must be carefully measured for the band used. Exposure maps

[2] http://xmm.vilspa.esa.es/docs/documents/CAL-TN-0022-1-0.ps.gz

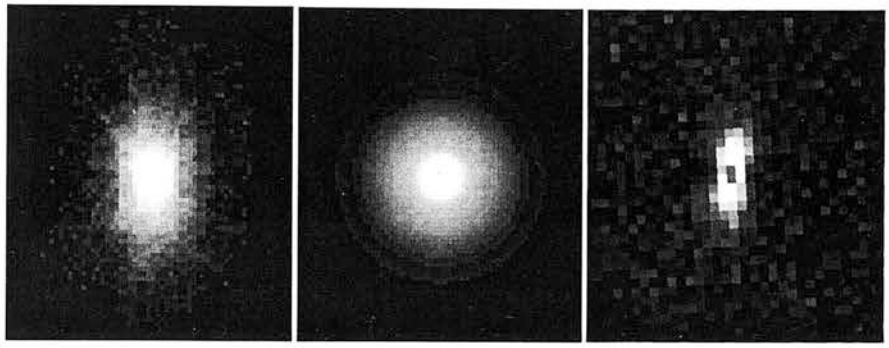

Figure 3.2: Left) The model PSFs from CALVIEW for an off-axis angle of 10', azimuthal angle=90 ° using the Medium accuracy model; middle) likewise for the Extended accuracy model (2D image generated from 1D profile); right) real twin-peaked source at an off-axis angle of 14'.

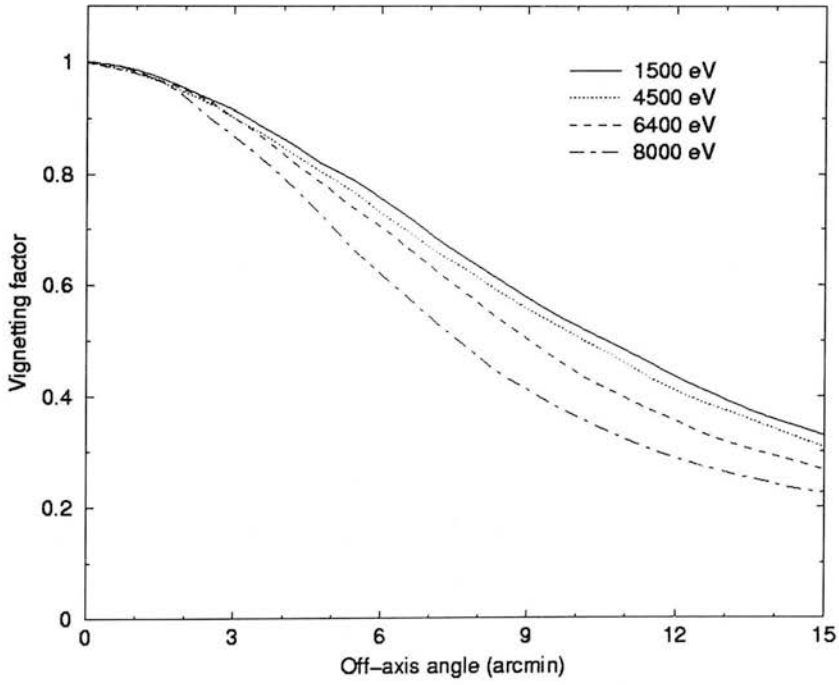

Figure 3.3: Vignetting function as a function of off-axis angle (0' - 15', based on simulations), at a few selected energies, for the pn camera (XMM Users' Handbook).

are calculated using the SAS task `EEXPMAP`, which also takes into account the chip gaps present in each camera. Recent calibration work[3] has shown that it is likely that the in-orbit vignetting profile is consistent with the optical axis being off-centre by around 1 arcminute. This needs to be taken into consideration as the standard calibration files did not include this effect at the time the observations were reduced and thus flux errors of $\sim 10\%$ could be introduced. A efficacious detection algorithm will be able to use this exposure information. Vignetting can be especially important when deriving properties of extended sources because the exposure varies across the object itself.

X-ray Background

The X-ray background in XMM is comprised of several components which vary continually in magnitude and relative intensity. In each image there will be a vignetted background (soft X-rays from the Galaxy and the local bubble, hard X-rays from AGN and soft protons from the Sun being channelled into the telescope) along with an unvignetted internal background from interactions of high energy cosmic rays with the telescope itself. Along with this, there is the instrumental background (e.g. read-out noise). Hence, it becomes very difficult to disentangle and model the background in a given image in order to remove it. It is important that significance thresholds can be calculated in light of this. Additionally, the level of protons originating from the Sun is wildly variable, sometimes ruining entire observations. The space 'weather' is worst at the most distant end of the orbit lying outside of the Earth's radiation belts. The periods of flaring background must be excised from the data (Figure 3.4 shows an example) and so often much exposure time is lost.

Statistical

A fundamental problem in X-ray astronomy is that most sources have a low count rate and thus typically we must deal with small integer numbers of photons (most pixels in an image will record no photons whatsoever). One must then take care with every operation performed on the images as they lie squarely in the low-counts statistical regime. Issues as seemingly straightforward as finding the goodness-of-fit of data to a model suddenly become non-trivial and the potential biases can enter the survey.

One way to boost the signal from a source is to merge the images and exposure maps from the three individual cameras MOS1, MOS2 and pn. Later we will discuss

[3] http://xmm.vilspa.esa.es/docs/documents/CAL-SRN-0156-1-3.ps.gz

why it is risky but essential to do this without knowing fully the characteristics of each camera.

Keeping the above in mind we will now review some possible detection algorithms.

3.3 Review of Detection Algorithms

X-ray astronomy has made great use of techniques originally developed for optical images, after modification to deal with the variable PSF and Poisson counts. They each have advantages and disadvantages.

Sliding Cells The sliding cell algorithm has been used in X-ray missions including Einstein, ROSAT, Chandra and XMM, for example, Gioia et al. (1990) and Voges et al. (2001). A square box (typically a few pixels on a side) is moved pixel by pixel over the image and the Signal-to-Noise ratio (SNR) measured. This is done by modelling the counts inside the box as the signal and the noise as the counts in an annulus outside the box. If the SNR exceeds a pre-defined threshold then the box at that position is flagged as an object. These objects plus a surrounding region are then excised leaving a 'cheese' which is interpolated by use of a spline to make a background image. The image can then be re-scanned using a new, improved, threshold obtained from the background image to produce a final object list.

The XMM SAS task for sliding cell detection is `EBOXDETECT`. It is often used in

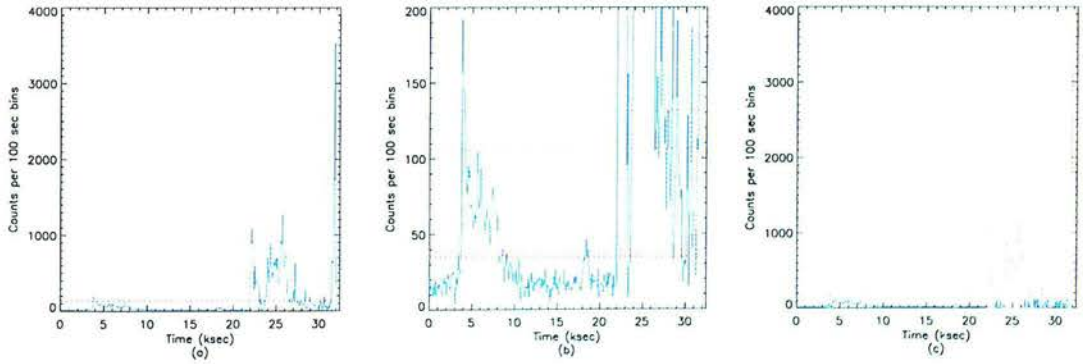

Figure 3.4: Left) The initial light curve is blue/solid, and the mean of the uncut light curve is red/dashed. Centre) The same with reduced vertical scale. The decrease in the mean of the light curve using successive 3σ cut cleaning can be seen from the mean of the remaining exposure which is red/dashed. Right) The original high-energy light curve, now with the filtered flaring regions shown as red/dashed and the remainder as blue/solid (Courtesy of K. Sabirli).

combination with a Maximum Likelihood calculation, for example in the SAS task EMLDETECT, to help flag extended sources. EMLDETECT simultaneously fits up to six neighbouring sources using the Medium accuracy PSF model and can provide an estimate of the source extent by convolving the PSF with either a Gaussian or Beta model surface brightness profile. The documentation[4] warns that the extent can only be calculated for bright sources and the code will default to finding point source properties if not bright enough. The XMM-Newton Serendipitous Source Catalogue[5] (XMMSSC) team is aware of the difficulties encountered in extended source detection and they do not attempt to classify the objects in their catalogue (XMM-Newton Survey Science Centre 2003).

This is a fast and robust algorithm which requires few assumptions about the input image and background to be made. However, it is clearly optimised for the detection of point sources. Extended objects (i.e. clusters of galaxies) are often low signal-to-noise sources and are hard to separate from the noisy and variable background. The procedure also performs poorly at separating close objects and obtaining accurate fluxes of extended features, (for example, Valtchanov et al. 2001). These problems are evident in the XMMSSC source lists for the Lynx field (Figure 3.5). Looking ahead, the final XCS source list (Figure 3.22) demonstrates the improvement.

Voronoi Tessellation and Percolation Voronoi Tessellation and Percolation (VTP, Ebeling and Wiedenmann 1993; Ebeling 1993) has been used on the ROSAT WARPS survey (Scharf et al. 1997) and is the algorithm chosen for another serendipitous survey using Chandra (Boschin 2003). The method looks for areas of enhanced surface brightness in an input image and is designed to highlight non-Poissonian structure. It works on sparse images by creating a polygon around each individual photon (the Voronoi Tessellation) by joining the non-crossing perpendicular bisectors of the nearest neighbour photons, and so the surface brightness here is simply the reciprocal area of the polygon. Pixels with more than one photon must be treated differently (optimized towards small pixel CCDs, such as those onboard Chandra). Significant pixels (i.e. due to objects) are chosen by comparing the distribution function of the inverse areas of the photons to that expected from a Poisson distribution. This defines a threshold above which pixels are flagged. The set of significant pixels is then percolated to form objects.

[4] http://xmm.vilspa.esa.es/sas/current/doc/emldetect/node3.html
[5] http://xmmssc-www.star.le.ac.uk/

This sounds ideal for detecting extended objects without making assumptions about the background or the source. In practice VTP is a troublesome technique. It has various issues which each must be dealt with in a contrived manner. Through its very nature VTP will blend objects and the large PSF of XMM only serves to exacerbate the effect. The solution Boschin (2003) use is to define three different surface brightness thresholds, then work out at what surface brightness threshold level the sources become blended, which is rather inelegant. Another serious handicap was emphasized by Valtchanov et al. (2001) regarding the inability of VTP to restore fluxes and positions of clusters. Again, Boschin (2003) introduce a factor to correct for missing flux. On considering these concerns, and the lengthy computational time required, we felt that VTP cannot be the well understood, robust procedure we need.

Neural Networks It is worth mentioning here the use of neural network based systems, in particular *SExtractor* (Bertin and Arnouts 1996), as it is used for source detection by the XMM-LSS project (Refregier et al. 2002). *SExtractor* was originally developed to detect and classify stars and galaxies and so it was trained on simulated optical images. By careful selection of the parameters used it can be, and often is,

Figure 3.5: A portion of the XMMSSC source list for the Lynx Field. Various artefacts can be seen and the extended objects are split into many sources.

applied to X-ray images. While this may produce adequate results, the artificial modifications of the parameters (i.e. treating a single PSF size as the 'seeing' parameter and classification based on 'stellarity') means that the technique is not naturally tuned for use in X-ray astronomy.

Wavelets and Multiscale Analysis The rationale behind this technique is a desire to be able to emphasize objects of a chosen scale in an image and thus understand sources in terms of their interscale relations. It is fast, stable and copes very well with point objects through to very extended features: there is much background to this topic, for example, Starck et al. (1998). Wavelet analysis has been shown to be effective at detecting low surface brightness objects in astronomical images (Valtchanov et al. 2001; Starck and Pierre 1998). Previous X-ray cluster surveys have used wavelet detection, for example, the Brera Multi-scale Wavelet survey (Lazzati et al. 1999) and the 160 Square Degree survey (Vikhlinin et al. 1998). There is a SAS task, `EWAVELET`[6] specifically to perform wavelet detection on XMM images. Early trials proved this to be unsatisfactory as it produces a source list which often fails to recover much of the flux from extended sources due to the methods used to calculate thresholds and form objects. `EWAVELET` does not fully account for the exposure variation across the field and estimates detection thresholds through use of the numerical approximations of Damiani et al. (1997). This method is inappropriate for sparse images and irregular exposure maps where the the statistics are non-Gaussian. An arbitrary additional threshold based on the gradient of the exposure map is applied to assist with detections near chip gaps. Also, `EWAVELET` produces background maps by simply smearing the image. As seen in Figure 3.6, while it detects the clusters in the Lynx field, it severely underestimates their extent. Furthermore, the detection is limited to the creation of circular, rather than elliptical, sources which is not ideal considering the PSF variation. This result was confirmed by Valtchanov et al. (2001). These problems can be overcome through careful design of new algorithms. Wavelet analysis is the basis of our chosen detection algorithm and so it is helpful to go into some mathematical detail.

3.4 Wavelet-based Detection

In this section we discuss the theory behind the wavelet transform and methods to estimate thresholds.

[6] http://xmm.vilspa.esa.es/sas/current/doc/ewavelet/index.html

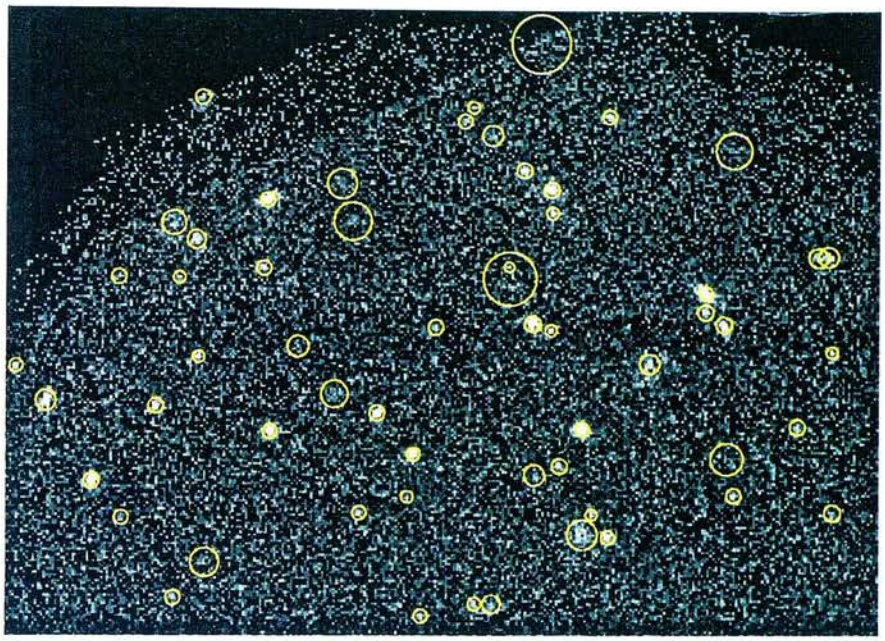

Figure 3.6: A extract from the source list generated by the SAS task `EWAVELET` for the Lynx field, highlighting the difficulty it has in reconstructing extended objects.

3.4.1 The Wavelet Transform

In many ways the wavelet transform is similar to the well-known Fourier transform. The difference lies in the fact that, with wavelets, features can be localised in *physical* space as well as frequency space. Essentially, a function of a certain scale, such as the Mexican Hat (Figure 3.7), is translated pixel by pixel across the image, taking the convolution with the image at each point. This convolution provides a measure of the correlation between the wavelet and the image, i.e. how well the wavelet matches the image here. The wavelet is then scaled in order to select objects of larger sizes and the process described above is repeated.

In order to be suitable as a wavelet the function must obey some scaling relations and, if all image information is to be retained to allow exact restoration from the wavelet transform, the mean of the function must be zero. There are many possible wavelet functions and so it is left to the user to choose the most appropriate for the task at hand. Generally, the wavelet is chosen to be as close as possible in profile to the kind of object which is to be emphasized in the image. The Morlet-Grossman definition of the continuous wavelet transform of a 1D signal is

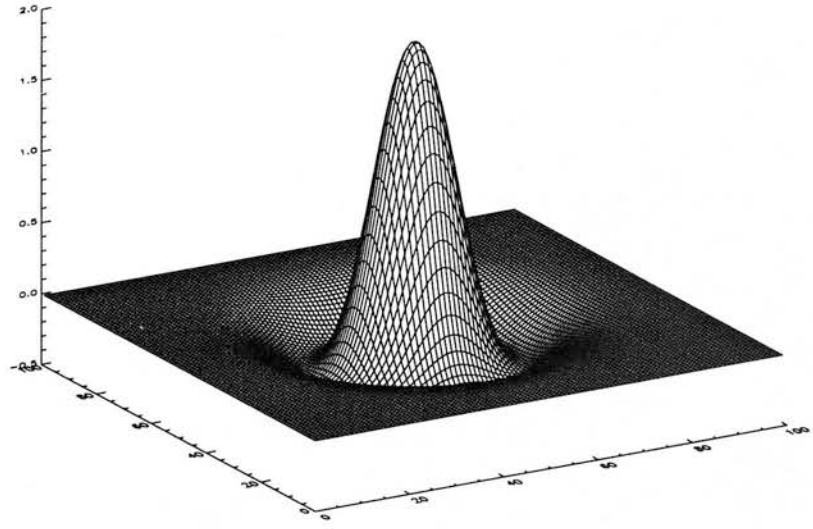

Figure 3.7: A typical Mexican Hat mother wavelet, with the negative annulus clearly visible.

$$C(\sigma, a) = \frac{1}{\sqrt{\sigma}} \int_{-\infty}^{+\infty} D(x)\, W^*\left(\frac{x-a}{\sigma}\right) \mathrm{d}x$$

where $C(\sigma, a)$ is the wavelet correlation coefficient of the data $D(x)$ using the wavelet $W(x)$ of scale σ at position a. It should be noted that a 2D scaling function can be written as the product of two valid 1D functions, $\phi(x, y) = \phi(x)\,\phi(y)$. The 1D transform above can then be generalized for use on 2D images. The wavelet is derived from a mother function, W'_m, which itself is generated using the derivative of the scaling function, $\phi(x, y)$:

$$W'_m\left(\frac{x}{\sigma_x}, \frac{y}{\sigma_y}\right) = -\left(\sigma_x \frac{\partial}{\partial \sigma_x} + \sigma_y \frac{\partial}{\partial \sigma_y}\right) \phi\left(\frac{x}{\sigma_x}, \frac{y}{\sigma_y}\right).$$

This can seem quite abstract; a summary and illustrative example can be useful.

Procedure for finding wavelet coefficients

i) Specify the scaling function $\phi(x)$ associated with the desired mother wavelet

ii) Generate the family of wavelets from this mother wavelet

iii) Calculate the correlation images by scalar product of each wavelet with the data

i) The scaling function used is the Gaussian function. This has been chosen because the mother wavelet function it creates is the Mexican Hat, which is appropriate for finding astronomical sources, which are often symmetrical and centrally-peaked (Figure 3.7).

$$\phi\left(\frac{x}{\sigma_x}, \frac{y}{\sigma_y}\right) = \frac{1}{2\pi\sigma_x\sigma_y} \exp\left(-\frac{x^2}{2\sigma_x^2} - \frac{y^2}{2\sigma_y^2}\right) ,$$

which leads to:

$$\begin{aligned} W'_m\left(\frac{x}{\sigma_x}, \frac{y}{\sigma_y}\right) &= \frac{1}{2\pi\sigma_x\sigma_y}\left[2 - \frac{x^2}{\sigma_x^2} - \frac{y^2}{\sigma_y^2}\right] e^{-\frac{x^2}{2\sigma_x^2} - \frac{y^2}{2\sigma_y^2}} \\ &= \frac{1}{2\pi\sigma_x\sigma_y} W_m\left(\frac{x}{\sigma_x}, \frac{y}{\sigma_y}\right) \end{aligned}$$

where W_m is often the function used as the wavelet (the normalisation can be included elsewhere). This notation is chosen to be consistent with `WAVDETECT` (Freeman et al. 2002).

ii) The mother wavelet can be translated and dilated to generate the family of wavelet functions:

$$W'(a, b; \sigma_x, \sigma_y; x, y) \equiv \frac{1}{\sigma_x\sigma_y} W'_m\left(\frac{x-a}{\sigma_x}, \frac{y-b}{\sigma_y}\right)$$

where σ_x and σ_y are the dilation parameters in the x and y directions (typically these are the same) and a and b are the translation parameters.

iii) If the image data is D and the value $D_{i,j} \equiv D(i,j)$ then the correlation value of the image with the discretized wavelet W is

$$\begin{aligned} C_{i,j} &= \sum_{i'}\sum_{j'} W_{i-i',j-j'}\, D_{i',j'} \\ &\equiv < W \star D >_{i,j} . \end{aligned}$$

In this manner the complete set of wavelet correlation coefficient images for the chosen scales can be computed. These will only be meaningful once we can assess their significance, as compared to the values expected from statistical variations in the background.

3.4.2 Calculation of Thresholds: Initial Efforts with MR/1

Review of the literature on the subject of detection algorithms and practical experimentation had led us to the decision that a wavelet-based technique was best. However, it was still unclear which wavelet code would be used or if we would have to write our own. The field of wavelet analysis has grown enormously since the mid-1990s and there is indeed an overwhelming quantity of material, both theory and application, available to study. Books tend to be aimed at either a non-technical level (for example, orientated towards medicine or engineering) where only the application is important, or at a highly mathematical level where every statement is accompanied by a proof. As non-experts we needed to build some intuition about how best to use and understand wavelets without the fundamentals being obscured by details. We found the ideal text for this purpose in Starck et al. (1998) which provides a suitable depth of material along with some excellent illustrations and examples. In addition, the authors of this text have also released a package of code implementing the algorithms described therein, MR/1[7]. This package had already been used by other X-ray projects working on extended sources e.g. Valtchanov et al. (2001). Thus, we felt that MR/1 could be the core of the source detection algorithms.

One of the most appealing features of MR/1 is the ability to compute wavelet thresholds which are valid for even very sparse images with Poisson noise. After thresholding, objects can be created. The decision to be made can be phrased as: given a wavelet coefficient $C_{i,j}$, calculated by the convolution of n photons with the wavelet function, could it have been produced by the noise? Assuming that the photons due to the noise are independent then the wavelet coefficient arising from the photons lying within the support K of the wavelet (that is, where the wavelet is non-zero) results from the sum $\sum_{k \in K} n_k$ of variables with the same distribution as the wavelet function. If the wavelet coefficient of the data is significantly greater than that which could be expected from n independent variables then it is likely not to be noise.

The distribution of one photon will be the histogram H_1 of the wavelet function. Thus if there are n photons then the distribution of the sum (S_n) will be that of n autoconvolutions of H_1, $H_n = H_1 \otimes H_1 \otimes \ldots \otimes H_1$. The histograms evolve with increasing numbers of counts, converging to a Gaussian as expected from the central limit theorem.

The variable S_n can be reduced to assist in comparison:

[7] http://www.multiresolution.com

$$c = \frac{S_n - E(S_n)}{\sigma(S_n)}$$

where $E(S_n)$ and $\sigma(S_n)$ are respectively the expectation value and standard deviation of the distribution. Hence, the cumulative distribution function is

$$F_n(c) = \int_{-\infty}^{c} H_n(u)\,\mathrm{d}u$$

This enables us to set thresholds c_{min} and c_{max} such that $F(c_{min}) = \epsilon$ and $F(c_{max}) = 1 - \epsilon$ where ϵ is a chosen confidence level. The wavelet coefficient must also be reduced via

$$C_j^r(x,y) = \frac{C_j(x,y)}{\sqrt{n}\sigma_{W_j}}$$

where σ_W is the standard deviation of the undilated mother wavelet function. A wavelet coefficient is thus significant if

$$F(C^r) > c_{max} \qquad \text{or} \qquad F(C^r) < c_{min}$$

As in Starck et al. (1998), the significant pixels in each wavelet plane need to be connected to form the 'segmentation image' at that scale. A set of connected wavelet coefficients is known as a *structure* and structures within different wavelet planes are connected to form *objects* by way of the *interscale relation.* A structure S_j^1 at scale j is said to be connected to a structure S_{j+1}^2 at scale $j+1$ if S_{j+1}^2 contains the pixel in S_j^1 with the maximum wavelet coefficient. In this way, objects can be identified in wavelet transform space and can be divided into sub-objects. The objects are then reconstructed iteratively using 2D Gaussian profiles. An example of a reconstruction image is given in Figure 3.8.

We used the MR/1 task `mr_detect` to do this. The output of `mr_detect` is a source list containing source position, source counts, fitted ellipse parameters, signal-to-noise ratio and other properties.

During the time we were using MR/1 we were also working on classification schemes. These will be discussed in detail in the classification section (3.5.5). It will suffice to say here that a simple wavelet ratio profile technique was used throughout this period for the selection of candidates. This involved comparing the relative wavelet coefficient magnitudes of a source to those expected from the PSF. Although this method was later superceded it proved to be quite successful, for example the re-detection of the

three high redshift clusters in the Lynx field and the creation of the early candidate lists. The results were also used in a preliminary study looking at correlations between XMM sources and SDSS quasars and galaxy overdensities (Land et al. 2004). However, as our experience and understanding of wavelets grew it became apparent that MR/1 was not perfect and an alternative was required.

Limitations of MR/1

One of the fundamental difficulties we are faced with in this project is object detection based on very small numbers of photons. It is sensible, therefore, to get the most out of our data by merging the images from the three cameras. Unfortunately, this introduces new problems.

One of the strengths of wavelet analysis is that a signal that varies smoothly on large scales is automatically removed from the cleansed image. In our case this means that for a single XMM image the effect of the vignetted background can be more or less neglected when detecting objects. There are small areas in each image (near the edge of the field of view and either side of chip gaps) where the calculated thresholds are unreliable and spurious sources are detected. This issue is not too serious when the individual images are being used (i.e. before merging) because a simple off-axis angle limit could be imposed and objects near chip gaps could be flagged as possibly spurious.

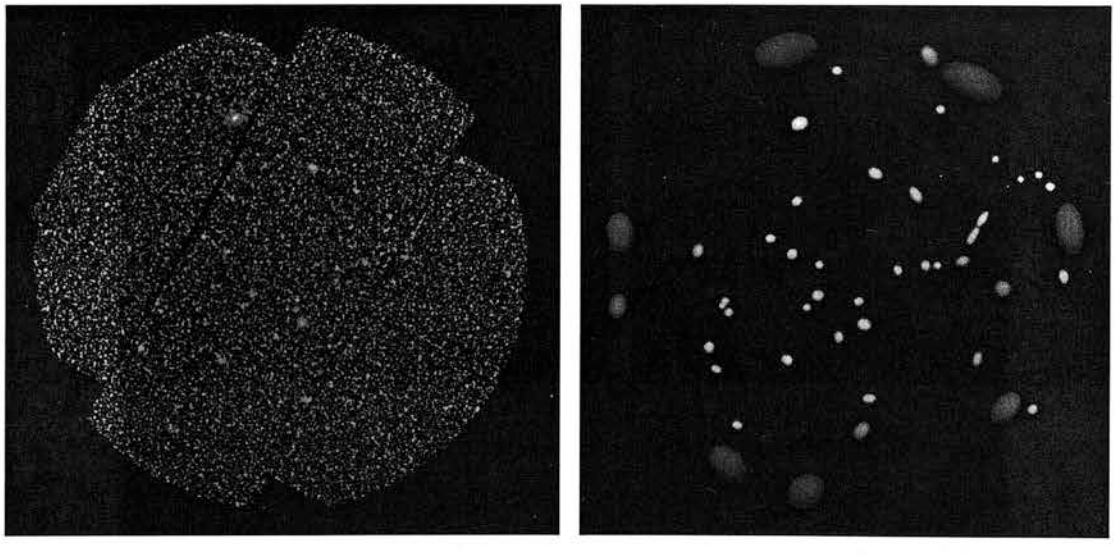

Figure 3.8: Wavelet analysis on a sample image (left) using MR/1 code detected the objects shown in the figure on the right.

When we began using MR/1 on merged images it became apparent that many more spurious sources were being created. This was due to a much larger fraction of the field of view being close to a chip gap, the fact that the chip geometry was different for MOS and pn, and that the cameras could operate in various modes (such as full frame or single chip for faster readout). Essentially, there was far greater variation in the effective exposure over the field of view and there was no facility in MR/1 to use the information present in the merged exposure maps.

At first we hoped to be able to calculate analytically the exposure corrections for the wavelet thresholds. This could be achieved by simulating several thousand 'fake' background images using the exposure map and then calculating the transform of each image. Thus, for each pixel and scale, we could recover the distribution of wavelet coefficients for a range of background levels. This was not possible because there is too much variation in the ratio of the exposure times of the cameras for each observation. Instead of calculating the corrections on a few template merged exposure maps we would have had to calculate them for each and every observation and this would have been too computationally intensive. The principle is sound but it is not suitable for a project of this size.

MR/1 also fails on the key criterion of being able to carry out extensive simulations. As a commercial product requiring licenses for each machine, it is not as simple to run it on a large number of CPUs when simulating the hundreds of thousands of clusters, as compared to other software.

While potentially foreseeable, this, coupled with a need to have more control over the source reconstruction algorithm, meant that the limit of the work we could do with MR/1 had been reached. What was necessary was an algorithm which could correct for the exposure variations when calculating wavelet thresholds. This led us back to the commonly used piece of code, `WAVDETECT`.

3.4.3 Calculation of Thresholds: `WAVDETECT`

The package `WAVDETECT` (Freeman et al. 2002) was written to be a mission-independent wavelet source detection code and consists of two components. The first, `wtransform`, calculates wavelet thresholds and computes the wavelet transform of the image, while the second, `wrecon`, takes the output from `wtransform` and uses it to form objects. It is commonly used for the analysis of Chandra data as it is part of the Chandra Interactive Analysis of Observations[8] (`CIAO`) package and is often used with XMM data as it is

[8] http://cxc.harvard.edu/ciao/

superior to the SAS code `EWAVELET`. We initially passed over `WAVDETECT` in favour of MR/1 because of apparent difficulties it had in reconstructing extended objects (it requires the PSF size as a function of off-axis angle in order to define an object cell). Subsequently, however, the author of `WAVDETECT`, Peter Freeman, has become involved in XCS and has made available the source code for `WAVDETECT`, which has proved tremendously useful. We have been able to modify substantially the code to tune it for use with XMM and in particular we have written our own object reconstruction code to be used instead of `wrecon`.

The ability to compute exposure-weighted wavelet significance values is one of the most appealing features of `wtransform`. If one considers only the negative area of the support of the wavelet function (NW), which should, in the ideal circumstances, contain only background counts, then the background can be estimated:

$$\begin{aligned} B_{i,j} &= E_{i,j}\, B_{\mathrm{norm},i,j} \\ &= E_{i,j}\, \frac{< NW \star D >_{i,j}}{< NW \star E >_{i,j}} \end{aligned}$$

where $B_{\mathrm{norm},i,j}$ is the normalized expected number of counts at pixel (i,j) and $< NW \star D >_{i,j}$ and $< NW \star E >_{i,j}$ are respectively the scalar products of the negative annulus with the data and the exposure map. If one has the probability distribution of the correlation coefficients given the background signal, i.e. $p(C|B_{i,j})$, then the significance of a given measured coefficient can be computed. If the user specifies a significance threshold, S_o, then by combining the background level with the known distribution of probabilities, the coefficient threshold $C_{i,j,o}$ can be determined:

$$S_o = \int_{C_{i,j,o}}^{\infty} \mathrm{d}C\, p(C|B_{i,j})$$

The only way to find the distribution $C_{i,j,o}(S_o, B_{i,j})$ is by carrying out extensive simulations. Freeman simulated over 50,000 1024×1024 pixel images and it is the results of these simulations which are used in `wtransform`.

As discussed in the MR/1 section, in the ideal world the simulations would be performed for each XMM image in turn to ensure the exposure variations are accounted for exactly but this is not computationally practical so the correlation images must be modified. The measured correlation coefficient is

$$C_{i,j} = < W \star D >_{i,j} = < W \star B >_{i,j} + \Delta C_{i,j}$$

where $B_{i,j}$ is the estimated background intensity and $\Delta C_{i,j}$ is the noise (and source count) contribution to $C_{i,j}$.

If, as in Freeman et al. (2002), we ignore the latter term and rewrite the former so that its dependence on exposure variations is explicit:

$$\begin{aligned} < W\star B >_{i,j} &= < W\star EB_{\rm norm} >_{i,j} \\ &= \sum_{i'}\sum_{j'} W_{i-i',j-j'} E_{i',j'} B_{{\rm norm},i',j'} \\ &= \sum_{i'}\sum_{j'} W_{i-i',j-j'} \left(E_{i,j} B_{{\rm norm},i',j'} - (E_{i,j} - E_{i',j'}) B_{{\rm norm},i',j'} \right) \\ &= E_{i,j} < W\star B_{\rm norm} >_{i,j} - < W\star(\delta EB_{\rm norm}) >_{i,j} \end{aligned}$$

The quantity $\delta E_{i,j;i',j'}$ encapsulates exposure variability within the wavelet support, and thus the $< W\star(\delta EB_{\rm norm}) >_{i,j}$ term carries this effect through to $C_{i,j}$; subtracting this term from $C_{i,j}$ yields an "exposure-corrected" quantity

$$\begin{aligned} C_{{\rm cor},i,j} &= C_{i,j} - < W\star(\delta EB_{\rm norm}) >_{i,j} \\ &= C_{i,j} - < W\star EB_{\rm norm} >_{i,j} + E_{i,j} < W\star B_{\rm norm} >_{i,j} \end{aligned}$$

It is this quantity that is compared with the distribution $p(C|B_{i,j})$ to determine whether (i,j) is a source pixel. If $B_{\rm norm}$ is constant (or linear) within the wavelet support then

$$C^{\rm approx}_{{\rm cor},i,j} = C_{i,j} - B_{{\rm norm},i,j} < W\star E >_{i,j}$$

Because $< W\star E >$ is computed only once, Freeman dubs this the 'fast' exposure correction, as opposed to the 'full' exposure correction $C_{{\rm cor},i,j}$. The acute variation in the exposure maps for XMM makes it necessary for us to use the 'full' correction in our detection.

In summary, `wtransform` enables the correlation images to be corrected for exposure variation, thus greatly improving the quality of the source lists.

3.5 XCS Automated Pipeline Algorithms, XAPA

Here we set out in detail the modified detection and reconstruction algorithms and explain their features. We then present the results from a few typical observations

to illustrate the effectiveness and limits of the algorithms. The entire code is quite complex because of the various problems laid out above. However, broadly speaking, there are four code modules which are called from the pipeline (sometimes more than once). It is best to set out schematics of the full pipeline before explaining each module in detail.

3.5.1 Algorithm Flowcharts

Figure 3.9 depicts the `md_detect` code which performs the wavelet transform and calls `md_recon` to construct objects.

Figure 3.10 describes how `md_recon` takes the wavelet coefficient images, thresholds them and then calculates structures and objects.

Figure 3.11 explains how source properties and classifications are calculated for the input source list.

Figure 3.12 summarizes the various algorithms used to cleanse the source list of a variety of artefacts.

Figure 3.13 shows the procedure for calculating the final properties for the sources in the cleaned lists.

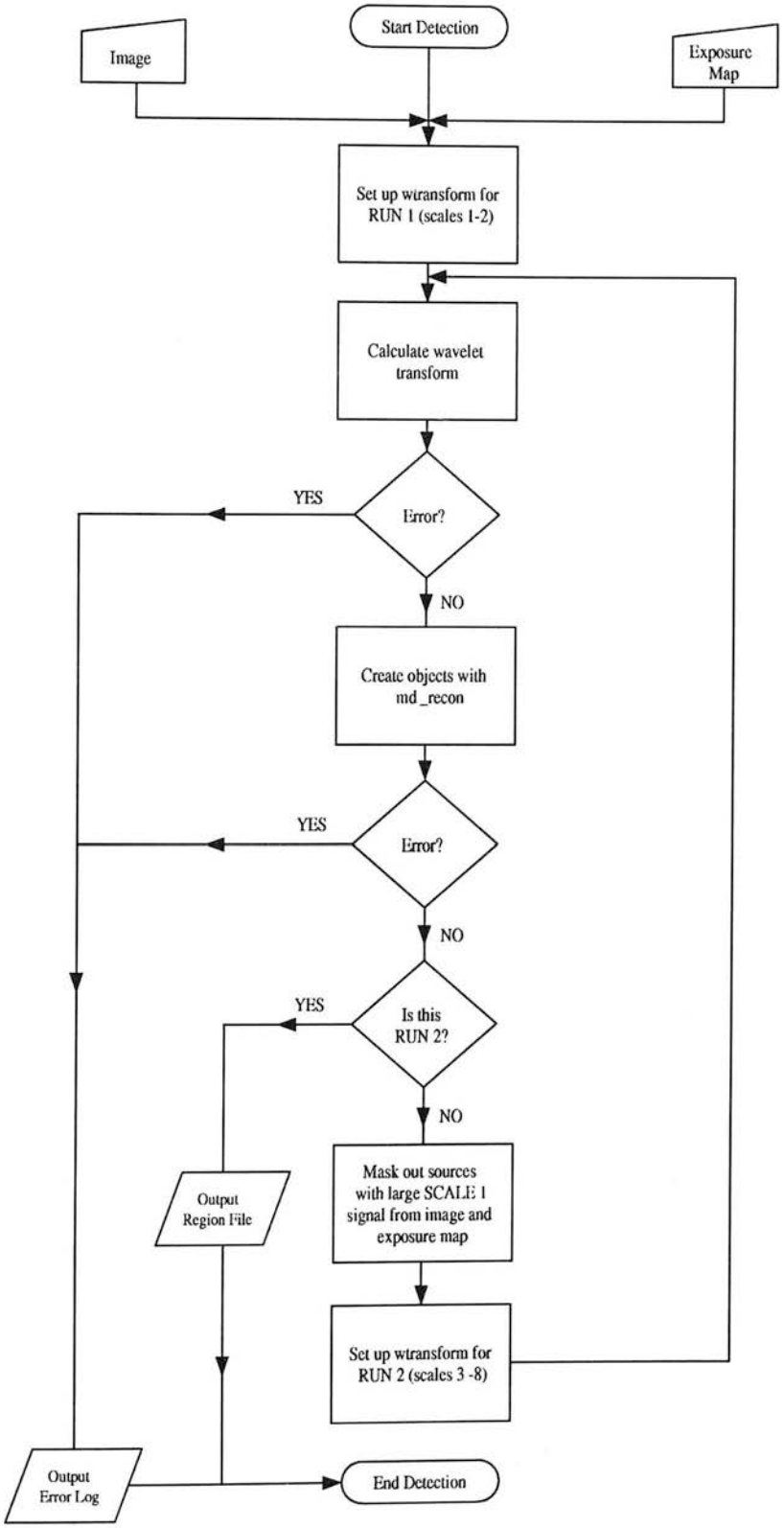

Figure 3.9: `md_detect` flowchart.

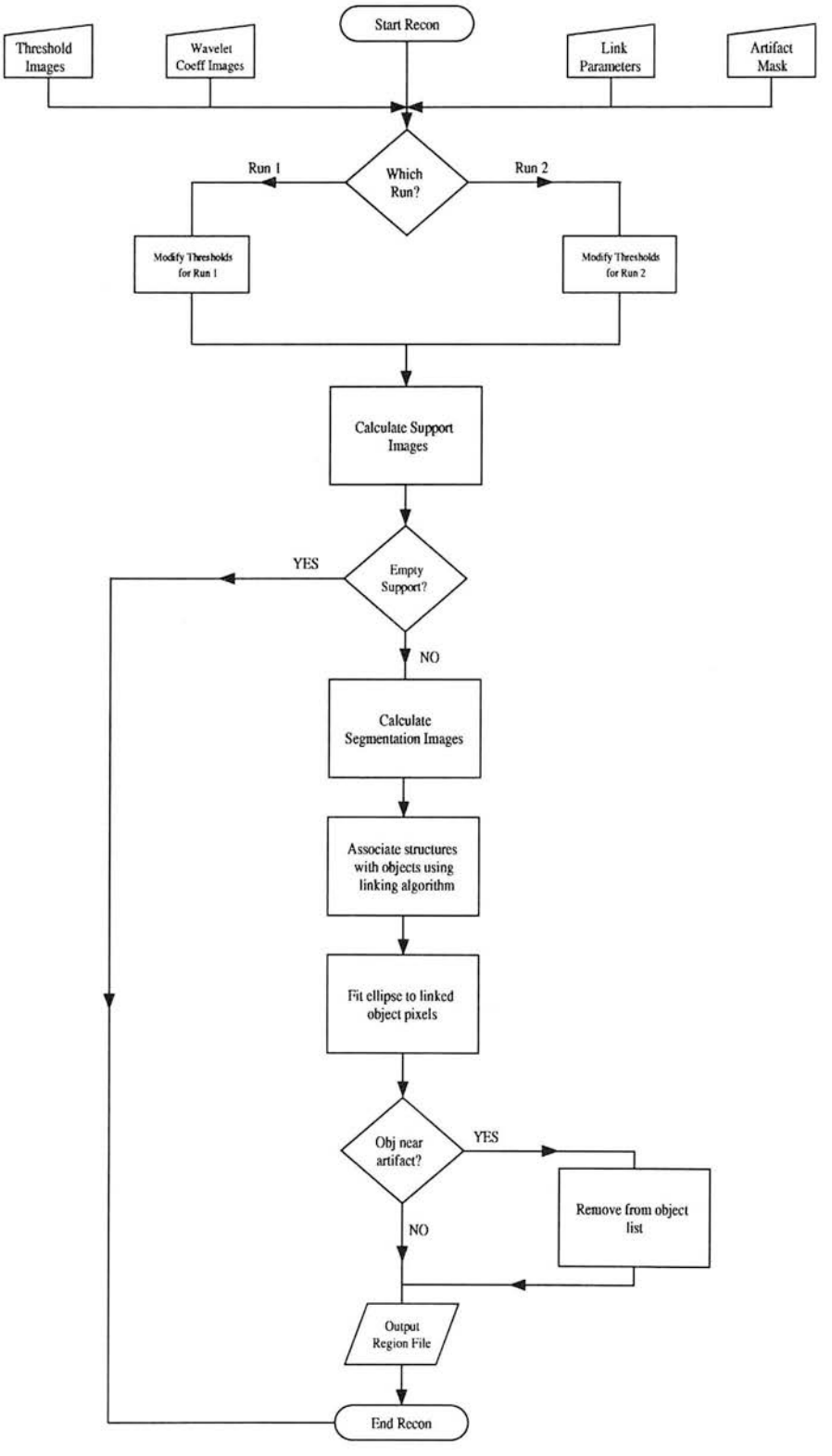

Figure 3.10: `md_recon` flowchart.

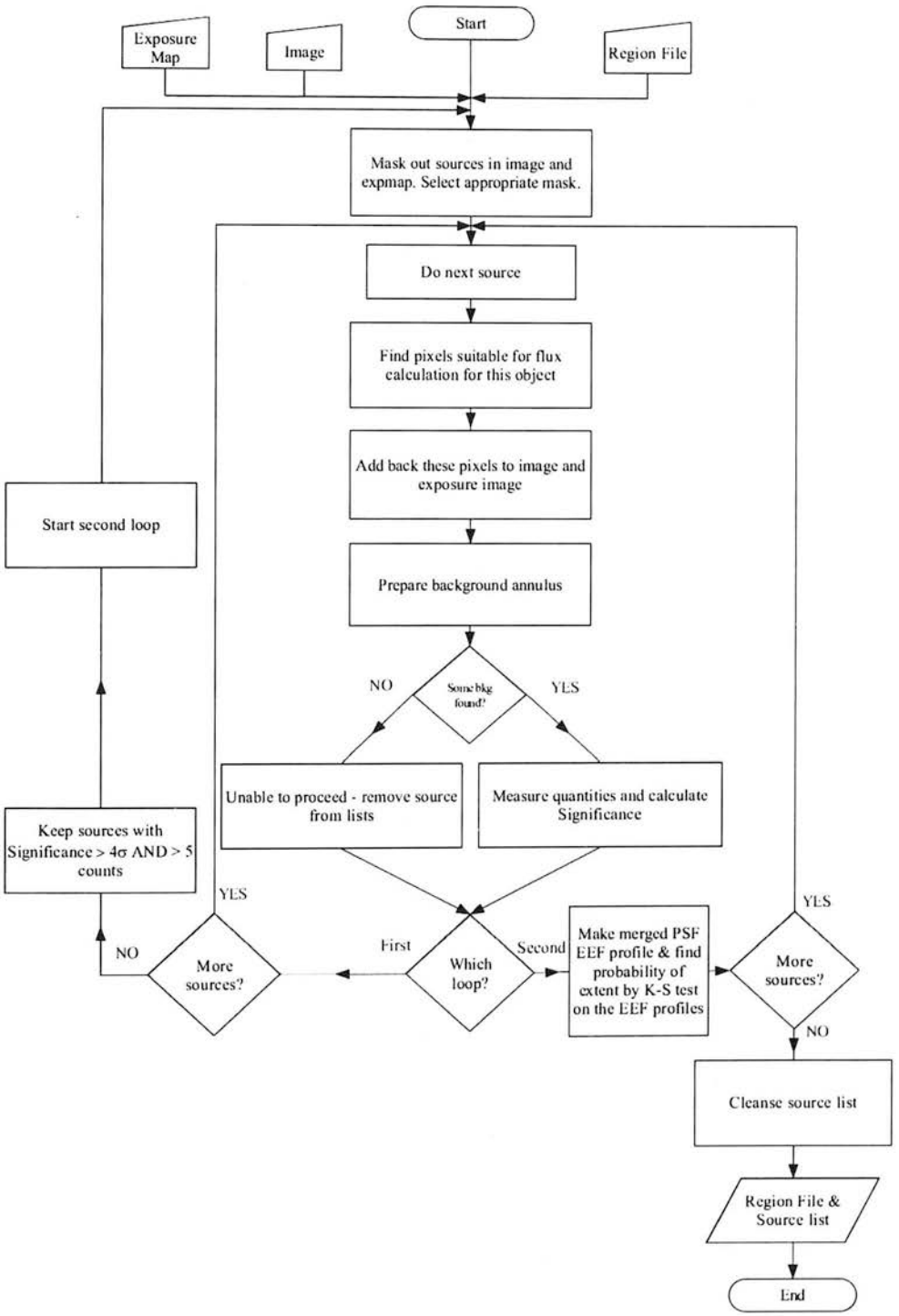

Figure 3.11: `find_srcprop` flowchart.

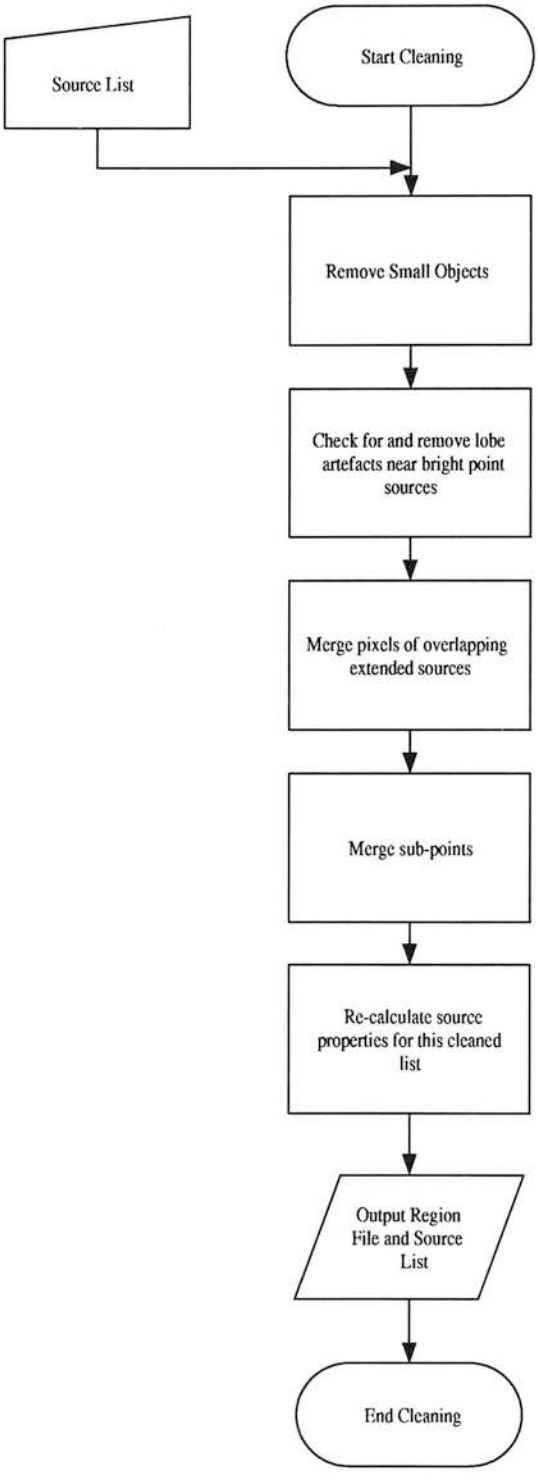

Figure 3.12: Cleaning flowchart.

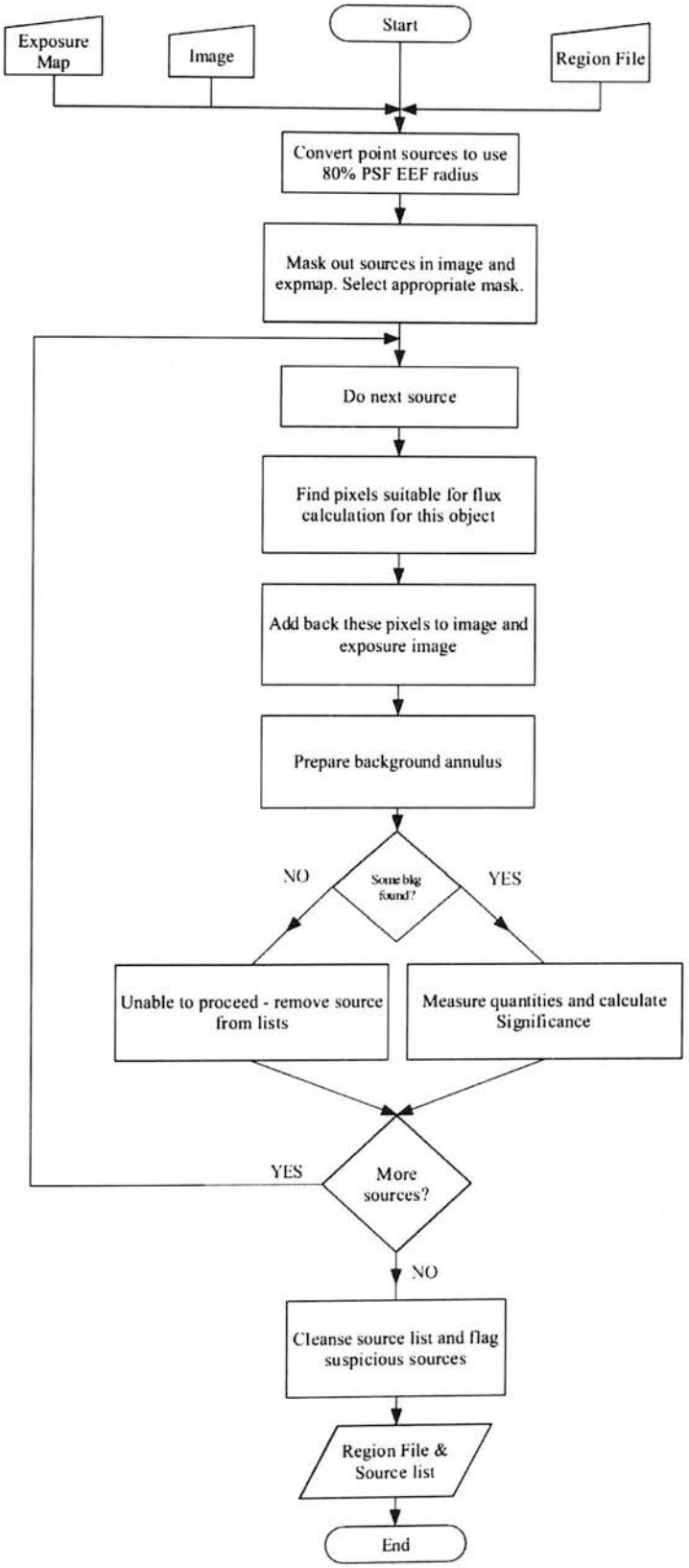

Figure 3.13: `find_srcprop_final` flowchart.

3.5.2 Inputs

For any particular XMM observation the three cameras run simultaneously and produce a set of event lists from which images can be extracted in the 0.5 - 2.0 keV band. This energy band was chosen to maximise the signal-to-noise ratio for cluster emission by excluding much of the Galactic and hard particle background. Although sensitivity to low temperature groups ($T < 2$ keV) is lost through use of this band, it has been shown by Scharf (2002) to be close to optimal for a wide range of higher temperature clusters to $z = 1$. There are usually three such images but, depending on the camera configuration and problems during the exposure, there can be fewer or more with a mixture of 'scheduled' and 'unscheduled' exposures caused by the observation being interrupted. To boost the detectability of faint clusters these images are directly co-added. It should be noted here that they are not 'flattened' to remove vignetting (for example, with the SAS task `EVIGWEIGHT`), as is often done, because of the unrealistic treatment of sparse images. If this is done then the counts in each pixel are boosted to reflect the effect of reduced exposure relative to the maximum. Obviously, this means that a pixel with zero counts remains with zero counts and so the scale properties of the background are seriously biased. If the exposure was really increased then counts would be detected in the gaps and photons would not necessarily land in the same pixel again. Furthermore, the non-vignetted particle background is also scaled upwards in an unrealistic manner. We believe that it is acceptable to use `EVIGWEIGHT` only to determine properties of sources found using non-wavelet methods. By co-adding the vignetted images you arrive at a true merged image. The challenge is to have an appropriate merged exposure map to accompany the image. We generate the exposure map by the following procedure (Sabirli, in prep.)

- Check which images were used in the creation of the merged image
- Generate exposure maps for these images individually
- Check the instrument, submode, filter information
- Check the number density of absorbing hydrogen (nH) in the direction of the pointing
- Use this value to correct the Energy Conversion Factor (ECF) from the ECF tables, which are a function of submode and filter
- Multiply each exposure map with its estimated ECF

- Merge all relevant modified exposure maps

This ensures that the exposure map reflects the relative sensitivity of the cameras used to produced the merged image.

The XMM archive consists of observations of a range of targets and not all are suitable for the XCS project. Only if there exists significant area where a new extended source could be discovered is the observation kept. Thus, observations of supernova remnants, crowded star clusters, large nearby galaxies or galaxy clusters or very bright point sources are not suitable and are removed. Also, if the exposure time of the observation is extremely low or the camera mode is unusable the observation can be removed from the XCS list. As of February 2005 this leaves 1847 XCS-suitable observations which have been made public and have been reduced. This sample defines the input to the first XCS catalogue (Chapter 4).

Additionally, masks have been made for each merged image to remove a range of objects and artefacts. These include bright point sources displaying prominent diffraction spikes, target clusters, hot pixels, streaks due to Out-of-Time events (when photons are registered as the CCD is being read out, creating a line of counts between the source and the read-out node) and areas containing ghost images (caused by sources outside of the field of view). The image and exposure image are multiplied by the mask before being passed on to the pipeline.

3.5.3 Detection and Object Creation

Discussed previously was the wavelet transform package `WAVDETECT` which consists of two pieces of code; the first, `wtransform`, to calculate wavelet coefficients and significance thresholds, and the second, `wrecon`, to use this information to reconstruct the sources in the image. Although the code is excellent at reconstructing point sources it can at times have problems with extended sources due to how `wrecon` characterises the scale of the source. It looks for local maxima in flux space (the smoothed image minus the normalised background) and selects the pixels for which this is the local maximum in flux space in order to define a source cell (the scale used is the one closest to the PSF size). Hence, if a source has more than one maximum in flux then it can be divided (as happens often with extended sources). Furthermore, it can suffer from scale pollution; an effect which will be discussed in Section 3.5.3 (see Figure 3.14 for an example). Seeing how powerful the wtransform portion of the package is we decided to use it but write our own reconstruction code, `md_recon`, to form objects. This is the

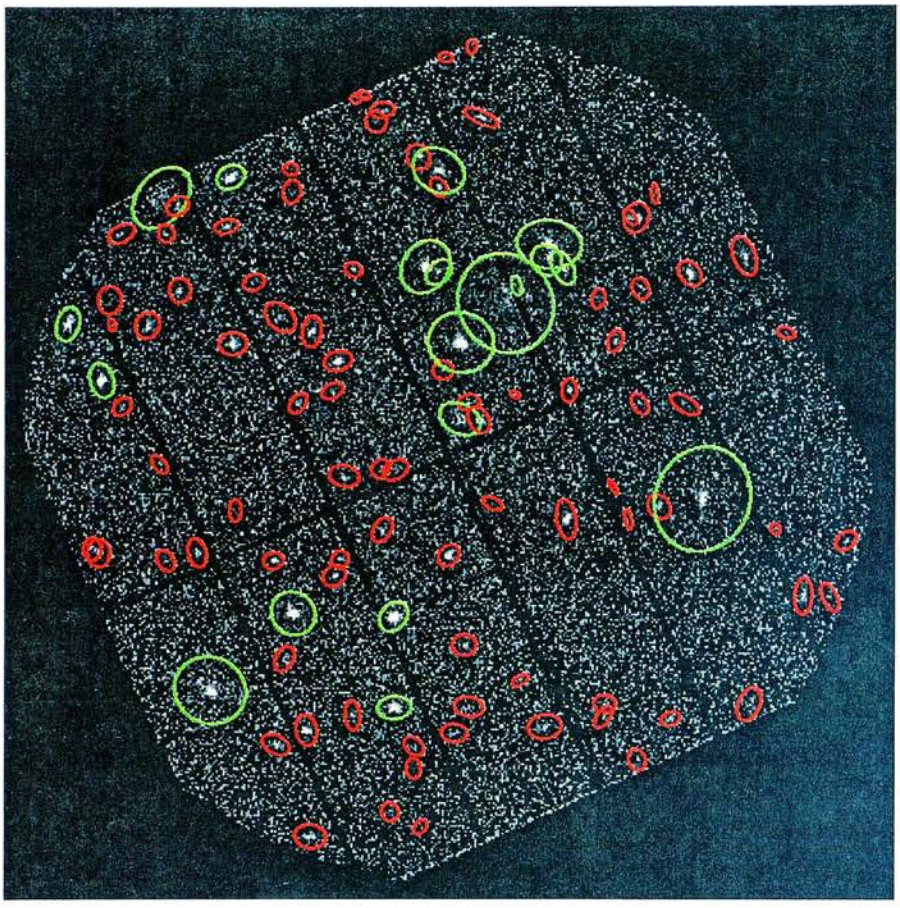

Figure 3.14: The effect of scale pollution in `wrecon`. The point sources with large green ellipses have been mistakenly classified as extended.

stage where it is vital to have control over the pipeline and no other available package would be flexible enough.

md_recon Once `wtransform` has calculated the set of wavelet coefficient images and significance threshold images it is trivial to combine these to make the set of support images. These are simply the images containing the significant pixels at each scale. Initial tests revealed problems with blending and size estimation but these could be alleviated by simply raising the wavelet thresholds of the three largest scales (the 8, 16 and 32 pixel scales) by factors of 3, 5 and 7 respectively. Ordinarily, this would invalidate the source reconstruction but since we do not rely on the properties of wavelets explicitly for source properties this is acceptable. Using these support images and a series of rules defining a *vision model*, the multi-scale objects can be formed. We shall use the same terminology as MR/1: a structure is a connected set of pixels in a support

image at a particular scale; an object is a set of connected structures at different scales. The vision model we have created works as follows:

1. Find objects with their root at scale i, i.e. $S_i(x, y, \text{scale} < i) = 0$ for all scales $< i$ where S_i is the support image at scale i.

2. Check to see if there is a structure in the scale above at this position.

3. If there is, and the maximum of the structure above lies within the lower structure then these two structures are linked, so the image pixels belonging to the object are the pixels of structure_1 plus the pixels of structure_2.

4. The process of upward linking continues until the condition in step 2 is not satisfied at which time the object is terminated. When each scale has been scanned for root structures and they have been propagated in the 'tree-like' fashion then for each object created there exists a set of image pixels belonging to it. An ellipse can then be fitted to these regions and a source list created.

This vision model is capable of finding point-like sources, extended sources and, crucially, it can cope with both point sources in extended sources and close pairs of points which should be separated rather then blended. An example to illustrate how the vision model works can be seen in Figure 3.15.

The code itself allows the beginning root scale and ending root scale for the search to be specified along with the maximum depth of an object tree. This feature will be used for a two-stage object reconstruction process, as will be covered now.

md_detect `md_detect` is the wrapper for the calls of `wtransform` and `md_recon`. One problem with wavelet analysis is that very bright compact objects can 'pollute' the wavelet signal at all scales. Consider the signal created by a delta function; any wavelet function convolved with a delta function returns a copy of the wavelet function itself. Although this is an extreme example, a bright point source will present a significant signal not only on small spatial scales but also on longer ones. This can seriously hinder detection of true extent which may be on the limit of detectibility. As a solution to this we have used a two step detection using 9 wavelet scales (numbered according to increasing size, corresponding to $\sqrt{2}$, 2, $2\sqrt{2}$, 4, $4\sqrt{2}$, 8, $8\sqrt{2}$, 16 and 32 image pixels). In this, rather than detect directly from scales 1 to 9, we detect on scales 1 to 3 first (Run1) before masking some of these sources from the data and continuing detection from scales 3 to 9 (Run2).

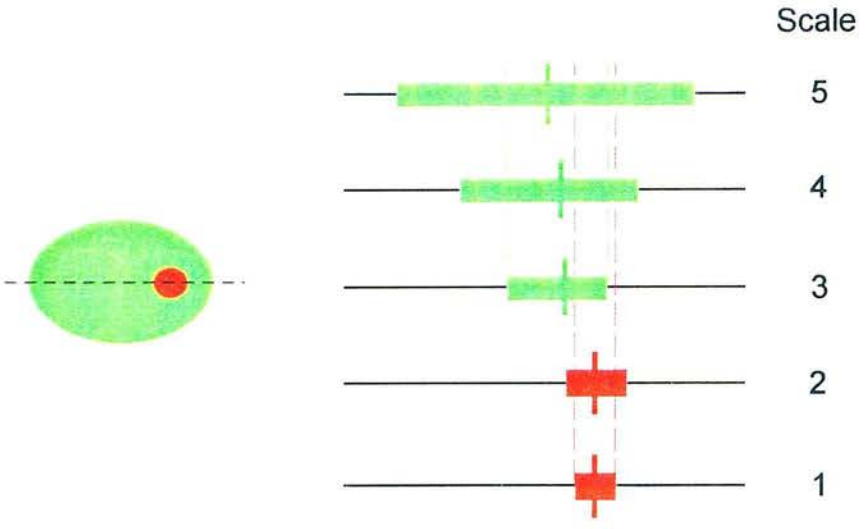

Figure 3.15: Illustration of the 'tree' vision model. Left) The source configuration showing a point source embedded in a larger source. The dashed line indicates a 1D cut through the sources. Right) A schematic of the significant pixels at each scale showing how the structures are connected to form objects. The vertical bars denote the position of the maximum coefficient at each scale. The maximum of scale 3 lies outside of the structure of scale 1 hence a new object is started.

Not all sources are masked, only those which have a significant signal on the first scale (this is a preliminary classification as mostly bright points should be selected this way; if any extended sources are masked then they should be re-detected in the second step, unlike point sources). Occasionally, extended sources do present a large central first scale signal, for instance if they contain a point source or the density profile is cuspy. If this happens then the central source can cause the Run2 detection of the extent proper to be removed as a likely lobe around a bright Run1 source (see Section 3.5.6). Thus, the true extent of the source is underestimated, as illustrated in Figure 3.16.

To mitigate against this another simple test is performed. A grid of 5 by 5 pixels, Q, centred on the source is extracted from the image. The quantity representing the 'cuspiness', C, of the central region is calculated:

$$C = \frac{\text{Max } [Q(i,j)] - \text{Min } [Q(i,j)]}{\text{Max } [Q(i,j)]}$$

If $C > 0.85$, that is, a flatter profile compared to a real point source then the source is removed from the Run1 list. There remains the possibility that genuinely extended

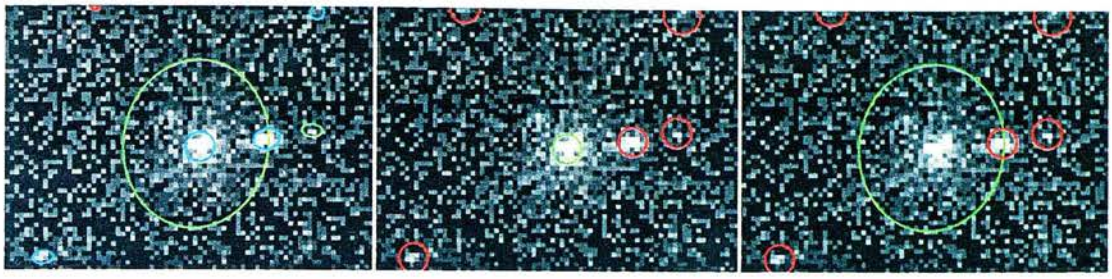

Figure 3.16: Illustration of the effect of extended source cuspiness. Left) The original Run1 (blue) and Run2 (green) detections. Middle) The final source list if the cuspiness test is not performed (Extent: green, Points: red). Right) The final source list after the cuspiness test (Extent is green and points are red).

sources could be mistakenly removed by this filter. The significance of this issue will be quantified as part of the selection function simulations (Chapter 5), however, visual checking confirms that it is not severe.

After both runs are complete the two lists are combined and passed on to the next stage of the pipeline.

At this point the process is still far from being finished. Although objects have been created from significant pixels the overall significance of the object needs to be calculated and other source properties measured, including the probability of extent.

3.5.4 Initial Source Properties

It is important to create the best possible source lists from the XMM images. To do this, the sources must be correctly identified, classified and have their fluxes estimated reasonably. Thus, the process consists of several stages, each of which takes the information known about each source and uses it to make a better list.

find_srcprop The first task is to remove any sources which are statistically of low significance. This is done not only so as to prevent spurious detections but also to ensure that the properties of genuine sources can be calculated accurately. An example of the kind of object to be removed are the edge-effect sources which have been detected through wavelet thresholds being underestimated (this would be a much graver problem if not for `wtransform`'s use of the exposure information).

To achieve this the source and background apertures used must be chosen carefully. Throughout the pipeline these apertures will change, depending on the information

available. The various apertures used are summarised in Table 3.1. In the following the term "*ellaxes*" refers to the ellipse as fitted to the object region[9] (hence $3 * ellaxes$ refers to an ellipse with three times the measured major and minor axes). As an example, in the initial run of `find_srcprop` the flux for a source not masked in Run1 of `md_detect` can be calculated. This can be achieved by masking out all of the sources from the image and then adding back one source only (consisting of its $1 * ellaxes$ pixels plus the unique $3 * ellaxes$ pixels, i.e. not also belonging to another source) as in seen in Figure 3.17.

[9]This region is defined as the union of the set of object pixels at each scale. The ellipse is fitted to this irregular shape with unbiased pixel-weighting.

Algorithm	Source Type	Aperture Configuration	
`find_srcprop`	Masked in Run1	Mask:	Run1 sources masked at $2 * ellaxes$
		Flux Aperture:	$1 * ellaxes+$ unique $3 * ellaxes$
		Bkg Aperture:	Inner radius of $2 * ellaxes$, 400 pix
	Other	Mask:	All sources masked at $3 * ellaxes$
		Flux Aperture:	$1 * ellaxes+$ unique $3 * ellaxes$
		Bkg Aperture:	Inner radius of $3 * ellaxes$, 2000 pix
`find_srcprop_extmerge`	All	Mask:	All sources masked at $3 * ellaxes$
		Flux Aperture:	$1 * ellaxes+$ unique $3 * ellaxes$
		Bkg Aperture:	Inner radius of $3 * ellaxes$, 2000 pix
`find_srcprop_final`	Point	Mask:	Point sources masked at $2 * ellaxes$
		Flux Aperture:	$1 * ellaxes$
		Bkg Aperture:	Inner radius of $2 * ellaxes$, 400 pix
	Extended	Mask:	All sources masked at $3 * ellaxes$
		Flux Aperture:	$(1 * ellaxes$ with points masked out at $1 * ellaxes) +$ unique $3 * ellaxes$
		Bkg Aperture:	Inner radius of $3 * ellaxes$, 2000 pix

Table 3.1: A summary of the apertures and masks used throughout the pipeline for the calculation of source properties.

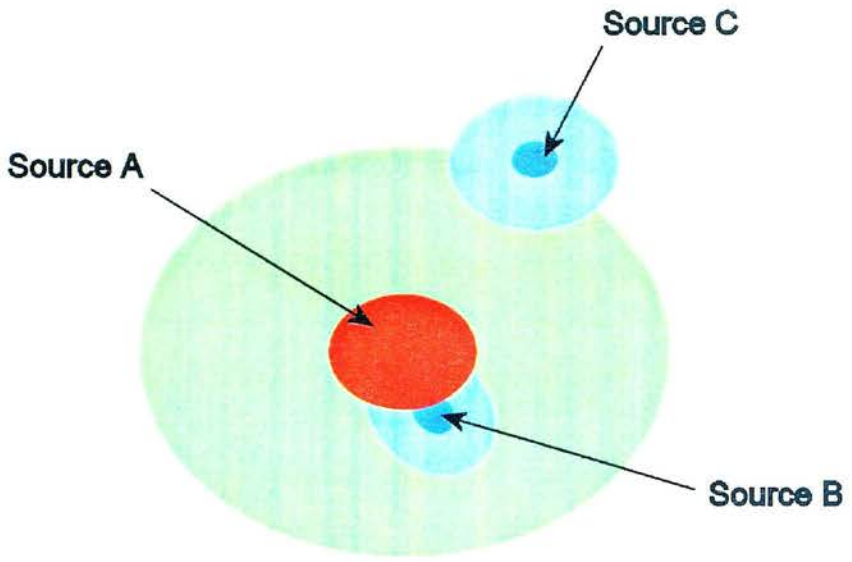

Figure 3.17: A diagram showing how the aperture used to measure source flux is created. The source to be measured is *Source A* and there are also two other objects nearby (*Source B* and *Source C*). Both the $1 * ellaxes$ and $3 * ellaxes$ ellipses are shown for each source (red and green respectively for *Source A* and dark blue and light blue for *B* and *C*). Hence, the area used to calculate the flux for *Source A* is the red plus the green region.

It is necessary for this complex set of flux apertures to be used if point sources embedded in extent are to be identified.

Of course, the level of the background must be assessed also. An elliptical annulus is placed around the source position (the inner edge varies but usually at $3 * ellaxes$ and outer edge increased until there are at least 2000 background pixels or no more area is available). A smaller background annulus is used for point sources so that they can be fitted in the presence of extent, i.e. AGN in clusters. The background countrate can be calculated:

$$b_{pix} = \frac{b}{\bar{E}' \times a'}$$

where b is the total number of counts in the annulus, $\bar{E}'$ the mean exposure in the annulus and a' the number of pixels in the annulus. This can be regarded as an acceptable estimate of the background (both instrumental and astrophysical) at that point in the field of view. The assumption that vignetting in minimal across the size of the annulus is a reasonable one for most sources, although of course for the largest there will be error introduced at this step. There is little alternative in this case although it

is hoped that empirical background maps will be one of the by-products of XCS.

With the estimate of b_{pix} one can calculate the expected number of background counts in the source aperture:

$$b_a = b_{pix} \times \bar{E} \times a$$

where $\bar{E}$ is the mean exposure in the aperture and a the number of pixels in the aperture. This value is one of the most important in the pipeline. Once b_a is known then it is possible to assess the significance of the detected source. In the parlance of astronomy, source significance is often quoted in terms of signal-to-noise ratio (SNR) or multiples of sigma but this can be frequently misleading. The significance of a source in the Poisson regime cannot be felt intuitively. There are ways to calculate SNRs but the trivial expressions must be discarded and various approximations made in order to arrive at an effective standard deviation of the background. For instance, Gehrels (1986) found an analytical approximation for the Poisson error corresponding to the confidence limit equivalent to a Gaussian 1σ, which is more accurate for the low counts regime

$$\sigma_g \simeq 1 + \sqrt{0.75 + \mu}$$

where μ is the Poisson expectation value. It is still not at all valid to then proceed to assign significances to sources by, for example, dividing the source counts by the standard deviation. This will create a list of '$N\sigma$' sources but a misleading one as the underlying distribution is not Gaussian.

The most statistically meaningful measure of significance in this Poisson regime is the probability that the background could, by chance, produce the detected number of counts in the source aperture. If one has calculated b_a then this is the expectation value of the background in the source aperture, the Poisson distribution mean. Then using the cumulative Poisson distribution the probability of the background presenting more than the measured number of counts, t, is calculated. This is the probability of the detection not being caused by the background and its interpretation is simple.

Sometimes it is desired to know the Gaussian 'equivalent' of this probability. It is possible to find the Gaussian cut-off value for any given confidence limit. As an example, a significance probability of 0.0000317 corresponds to a Gaussian 4σ source.

After doing this the source counts are obtained by simply subtracting the expected background counts in the expanded source aperture (Figure 3.17) from the total number

of counts in the aperture.

When all of the source significances are known a preliminary cleansing of the list is made by removing sources detected at less than '4σ'. The process above is then repeated to improve the accuracy of the remaining sources.

3.5.5 Classification

The ideal situation when trying to classify objects is to have a good two dimensional model of the PSF but unfortunately this is not the case. Therefore, it was decided to use the best available model (the Extended model) which is a radially averaged one, with a limited validity over the field of view. For each camera the SAS tool `CALVIEW` was used, by hand, to produce a set of Encircled Energy profiles at a range of off-axis angles at intervals of 1' out to 15'. A typical set of profiles is seen in Figure 3.18. Strikingly, even though the shape of the PSF changes considerably towards large off-axis angles, the encircled energy profile is only a weak function of angle.

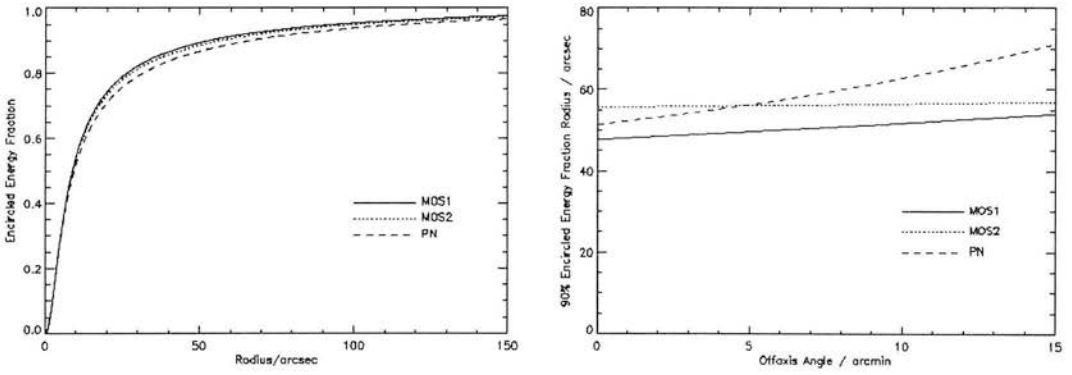

Figure 3.18: Left) The Encircled Energy Profiles at an off-axis angle of 12'. Right) The variation of the 90% EEF radius across the field of view.

Classification is based on making a null hypothesis, calculating a test statistic and then comparing this statistic to a threshold to determine whether the null hypothesis can be rejected at a particular confidence limit. Here the null hypothesis is that the source being tested is a point source. The cumulative nature of the encircled energy profile along with the existence of a library of PSF EEFs leads naturally to the choice of the Kolmogorov-Smirnov (K-S) test. The K-S test uses the maximum difference, d, between the cumulative distributions of two sets of data as the statistic. Note that standard χ^2 cannot be used to compare the profiles as the bins are correlated and there

is no choice but to bin the data.

Before carrying out the test, one must first make a merged EEF profile at the source position which reflects the weightings of the individual cameras used to make the image. These weightings are found by multiplying the mean exposure for a camera by the Energy Conversion Factor (ECF) appropriate for that camera and correcting for the nH value for the observation (using the map of Dickey and Lockman 1990). They are then normalised such that the total of the camera weightings equal 1. The individual EEF profiles are then multiplied by their weighting factor and added to create the merged EEF profile.

When measuring the EEF profile of the data themselves one must take care to subtract properly the contribution expected from the background. If this is not done correctly, large statistical errors can enter (consider the number of pixels in the inner radial bins; there are only a handful and so the number of background counts expected in them has a large variance). The solution to this is to subtract the expectation value for the number of background counts in a given bin (equal to the number of pixels in the bin $\times$ mean exposure in the bin $\times$ b_{pix}) from the total number measured. Doing this produces the best possible EEF profile of the source.

The probability of the source being point-like, $p(point)$, can then be obtained by applying a K-S test on the merged PSF EEF and the data EEF. In our studies with SDSS point sources (Land et al. 2004) we confirmed that the positional accuracy for point sources is roughly one pixel. Thus, the probability is calculated for a 9 pixel grid (± 0.5 pixels in x and y) around the source position and the highest probability of the source being a point (best fitting) is the one chosen.

Monte-Carlo Simulations Calculating these goodness-of-fits is only the first stage in classification; the next is the choice of a meaningful threshold statistic to compare them to. Clearly, the reliability of the $p(point)$ values is a function of the position on the field of view, the background level, the number of source counts, the proximity of neighbouring sources and many other factors. Choosing a fixed threshold would not be appropriate as it would not take these factors into account.

Because we use the actual data in our estimation of the PSF EEF model (by measuring the background component) we cannot strictly use the analytical expression for the K-S confidence threshold. The only option in this case is to perform a set of Monte-Carlo (MC) simulations for *every* source. Although this is computationally expensive it is vital to prevent misclassification. The bootstrap resampling process involves generat-

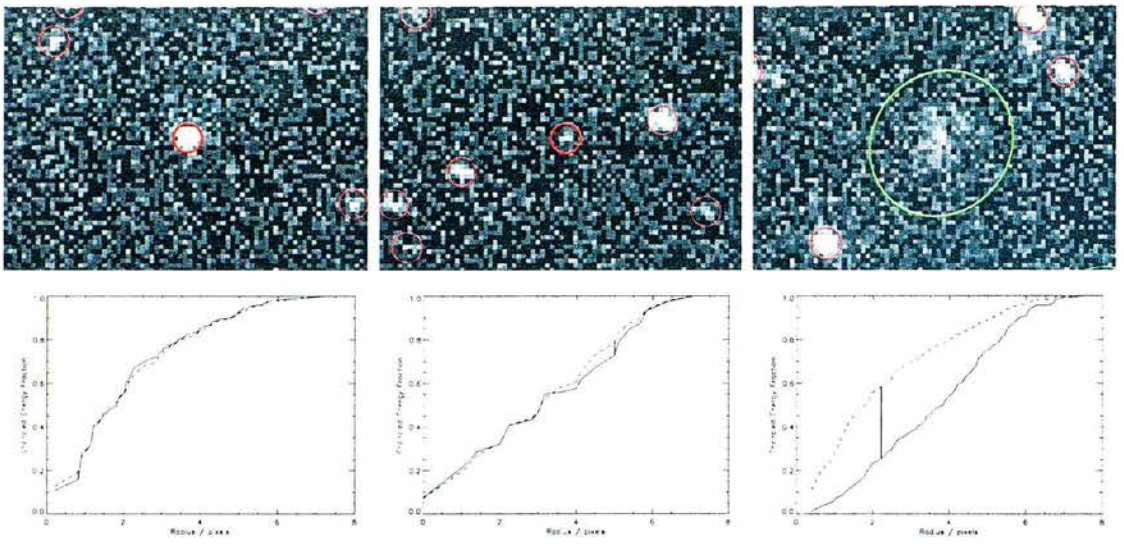

Figure 3.19: A selection of three sources which highlight the typical classification performance in various brightness and profile regimes. The solid line is the EEF profile as measured from the data, the dashed line is the model profile and the thick vertical line is the maximum difference, d, between them. From left to right; a bright point source with $p(point) = 0.805$, a fainter point source with $p(point) = 0.550$ and a moderately bright extended source with $p(point) = 0.000$.

ing 200 realisations of the PSF EEF model and populating them with the same number of counts as measured in the data. Each of these realisations can be compared to the model and a empirical distribution of the K-S d values found. If none of the simulated distributions returns a d value as great as the measured value then an approximate upper limit on the probability of the source being truly a point is 0.005. Simulations replicate the statistical scatter in the EEF profile due to the small number of photons used. There is clearly room for inaccuracy in classification here but there is no viable alternative available currently. The classification methodology will later be shown to be reasonable and effective in Section 5.2. A selection of example EEF profile fits is shown in Figure 3.19. The test is clearly capable of discrimination between point and extended source profiles.

Classification can be summarised as:

- Calculate merged PSF EEF profile
- Measure background-subtracted source EEF profile
- Perform K-S test to obtain d
- Compare d to the MC d distribution for a source with this number of counts

- If d is less than the 200 MC ds then the source is classified as extended.

3.5.6 Cleaning

Although we have a source list with classifications at this stage in the pipeline there are still many unwanted features in it. There are several algorithms to remove these and improve the source list.

Remove Small Sources While technically there is no reason why a faint source should not have only one significant pixel such sources should be removed as they are either too faint to be useful or are hot pixels.

Lobe Artefact Removal This is a particularly important and hazardous procedure. As has been discussed earlier there exists no reliable two dimensional model of the PSF. Empirically, it is known that it becomes distorted (banana-like) towards high off-axis angles and much structure is introduced into the wings. As seen in Figure 3.20, frequently the wings of a moderate-to-bright point source get detected. If this happens (as it should because they do in fact contain source counts) then they will not be classified as very point-like. If these sources are not excised from the lists then not only will the count rate for the point source be underestimated but crucially they will pollute the cluster catalogue with false negatives. We have arrived at a pragmatic solution after many trials. For each '$\geq 4\sigma$' source classified as point-like and bright Run1 objects (to be called Source A), we perform the following check:

- Measure the source counts for Source A, S_A.
- Measure the source counts, S_{Ext}, for any extended sources within $3 * ellaxes$ of Source A.
- If $S_{Ext} < 5 \times S_A$ then the extended source is removed.

This should remove the majority of such artefacts.

There is, however, the possibility of erroneously removing genuine extended emission if it happens to contain a bright point source. For the meantime, this eventuality must be acknowledged and its effect will be accounted for in the selection function simulations.

Merge Overlapping Extent One inbuilt feature of the reconstruction algorithm is the ability to detect sources within sources (e.g. AGN emission within clusters). This is accomplished by growing the object tree upwards through the scales and branching off into new objects. While this works exactly as intended, if the maximum of the source at each scale shifts significantly from the position of the root (as it might if the cluster is non-spherical or if there is bright point source emission) then the extended source can be divided into overlapping sources, for instance, a source detected at scales 3 to 6 and the same one at 7 to 9. It is not until after the classification step that it is known which sources can be 'recombined'. Once we know that two extended sources are overlapping it makes sense to take the pixels belonging to the sources in question, merge them and recalculate its properties (using the `find_srcprop_extmerge` code). This ensures that in most cases the cluster flux and morphology is recovered well. An example is shown in Figure 3.21.

Merge Sub-Points An analogous situation can arise with point sources, too, especially when the PSF is elongated in which case the root position (determined typically at scale 1) is not coincident with the position of the maximum even at scales 2 and 3. After classification it is known that these sources are both point-like and so, if one source is completely contained within another then the first can be excised from the list, and properties recalculated.

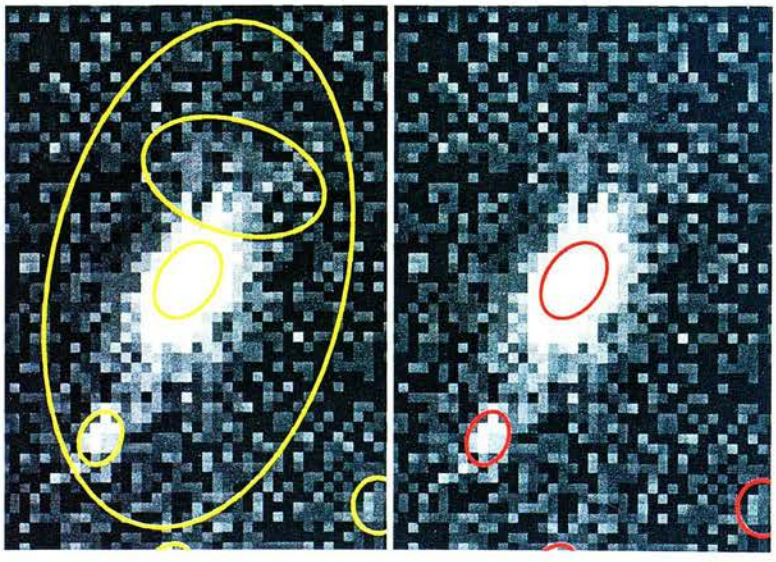

Figure 3.20: The lobe detections around a bright point source, before and after the lobe removal.

The pipeline has now finished and the source list and properties can be written to file. Using this final source list we also derive the source properties found using the individual images rather than the merged image. We thus have a source list for each exposure and a merged source list in which, for example, the sum of the source counts from the individual cameras equals the value calculated in from the merged image.

3.5.7 Final Source Properties

With the knowledge of the source classifications and brightnesses it is possible to repeat and improve the measurement of source properties.

`find_srcprop_final` This stage is substantially similar to the initial source property code. However, the key difference is that the objects classified as being points can have their ellipses altered to that expected from the PSF, and from then on they are treated as points. Not only does this improve the flux recovery of the point sources themselves but it also helps extended sources, after the internal points have been excised.

3.5.8 Flagging

Even after a considerable amount of effort has been applied developing a vision model and cleansing there can still be a variety of artefacts in the final lists. These occur because of the fundamental uncertainties in relevant parameters such as the PSF and the background level. Rather than make the cleansing algorithms so conservative that many genuine extended sources are removed, we have introduced a set of tests to flag

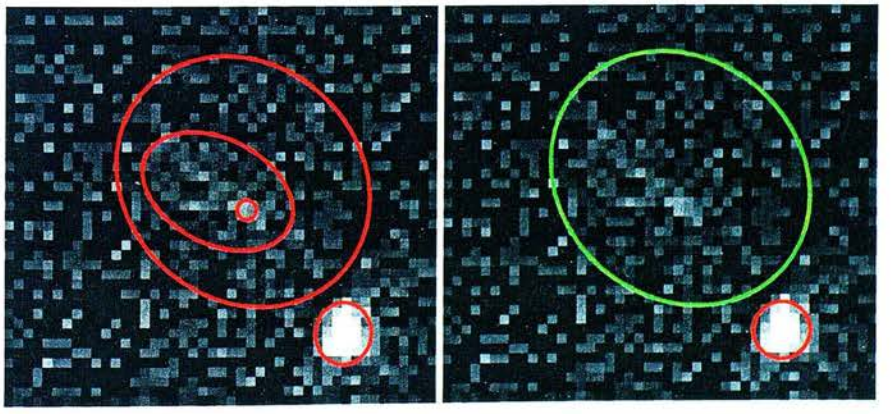

Figure 3.21: An example of how when there are several detections of an extended source they can be merged to improve the source properties.

potentially misleading sources.

Flag PSF-sized Extended Sources Possibly the most severe source of contamination of the lists is misclassified point sources. Particularly at large off-axis angles and high count-rates it is not infrequent for the flaws in the PSF model to cause an obvious point source to be classified as extended. Experience has shown that the majority of these sources can be identified by simply comparing the detected source size to that expected of the PSF. These sources can then be flagged, without too great a loss of real extended sources. The true effect of this on the extended source lists cannot be quantified until the full selection function simulations are performed. However, it is likely that it will be minimal as the discerning power of the algorithms will be dominated by the errors in the PSF model.

Flag Extended Sources with Internal Points Although the vision model is designed to cope with a range of scenarios occasionally it does happen that flux in the envelope of bright point sources is detected as a separate object, i.e. it appears as an extended detection with a point source detected within. It is important to detect this flux (otherwise it would pollute the background estimation of other sources) but so as not to contaminate the genuine candidate lists they must be flagged. If an extended source has a large proportion of its overall flux made up of the contribution of internal point sources then it is flagged as suspicious. The criterion for flagging is passed if the point source flux is $\geq 1.3\times$ the extended source contribution. This also covers the eventuality of extended detections of close-knit groups of point sources.

Flag Extended Sources with Internal Run1 Sources There is one final extension to the test described above. Usually sources which are detected in Run1 of `md_detect` are point sources. However, for the reasons mentioned previously, these are not always correctly classified leading to sources which seem to be extended but are in fact due to the configurations discussed in the second test. So, as a generalisation, this test checks for extended sources with a large proportion of their overall flux made up of the contribution of internal Run1 sources. The criterion here is tightened so that a source is flagged if the internal Run1 source counts contribution is greater than or equal to the extended source counts.

Ellipse Colour	Description
Red	Point source
Green	Extended source
Magenta	PSF-sized extended source
Blue	Extended source with significant point source contribution
Cyan	Extended source with significant Run1 contribution
Yellow	Extended source with less than 10 counts

Table 3.2: Summary of source types corresponding to ellipse colours.

3.6 Examples

Although the only rigorous way to assess the pipeline is to carry out extensive simulations it is still instructive to show the output of a selection of observations. In this way it should be possible to judge whether the pipeline is performing satisfactorily. The ellipse colours correspond to the source types in Table 3.2.

Observation 0085150101 This field is not an average one as it contains (at least) three high redshift clusters, which are all properly recovered. It can be seen that when the source counts are high the classification is very good (Figure 3.22). A few point sources have been removed from the list as they have been misclassified due to blending effects of nearby points.

Observation 0083280101 This is a typical field with little to cause problems. There are a couple of low significance cluster candidates visible in Figure 3.23.

Observation 0091140201 This is an observation of the A1983 cluster of galaxies. The target cluster itself is well-recovered and several point sources are detected within the extended emission.

Figure 3.22: Source list for 0085150101.

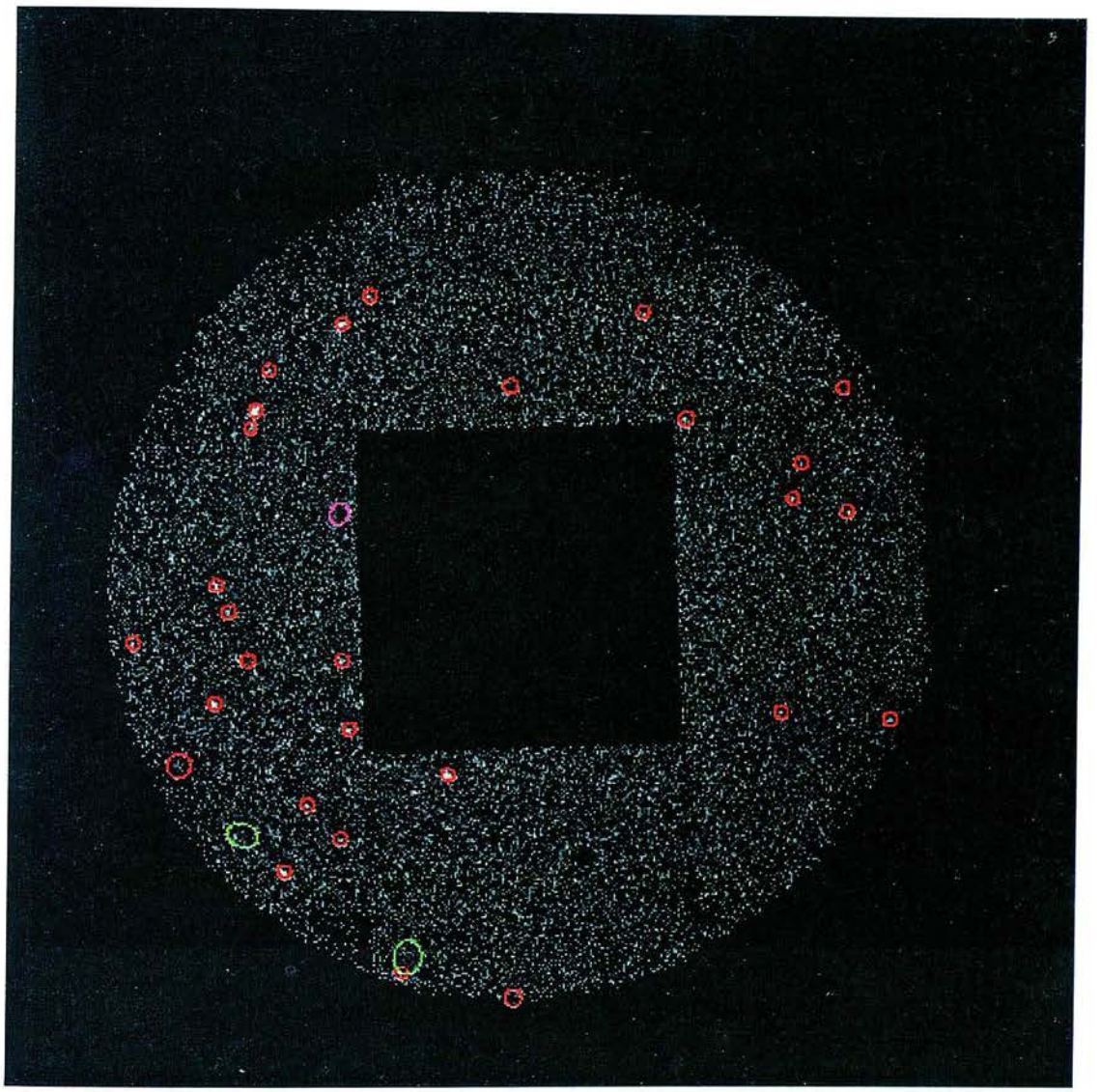

Figure 3.23: Source list for 0083280101.

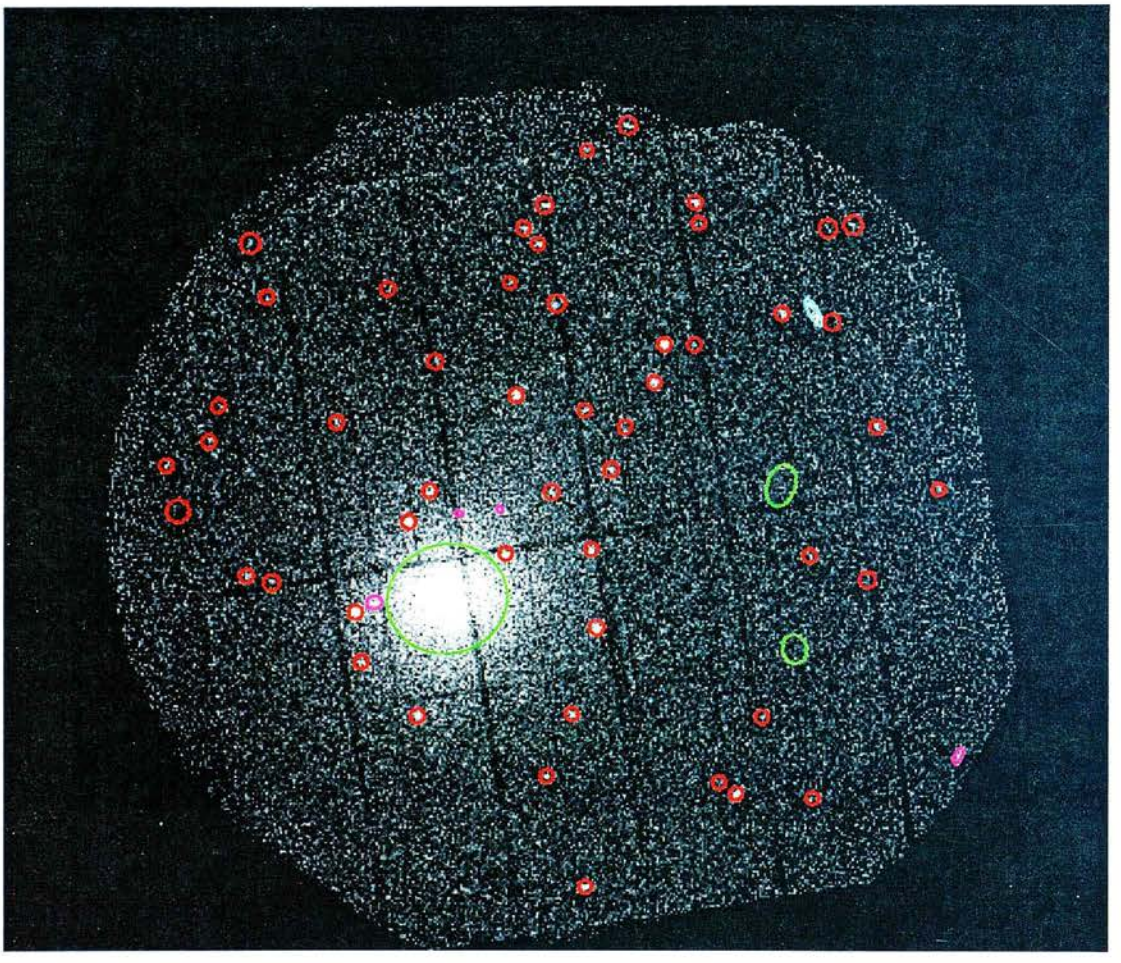

Figure 3.24: Source list for 0091140201.

Chapter 4

Catalogues & Survey Area

Here we describe the steps taken to move from the XAPA pipeline source lists to the final XCS catalogues. Then we discuss the database used to store and manipulate these catalogues, before presenting the initial calculation of the survey area.

4.1 Preparation

4.1.1 Observation Log

The first and most fundamental table in the XCS is the XMM observation log. This consists of the 1847 of the 2413 publicly available observations selected as suitable for XCS, as of February 2005. Given in Table A.1 of the Appendices are the key properties of each observation. The columns are mostly self-explanatory. The 'Type' column refers to the category of the pointing target (Table 4.1). The 'StatSam' column refers to whether the pointing is suitable for the XCS Statistical Sample (see Section 4.2.1).

4.1.2 Removal of Duplicate Sources

The pipeline produces a separate source list for each of the $\sim$ 2000 XMM images in the archive. These source lists are concatenated to form a raw master source list, containing all of the objects detected in the archive (74296 sources). Since it is not uncommon for multiple observations of the same area of sky to be performed the list will contain duplicate entries for some objects.

Pointing Type	Description
1	AGN, QSOs, BL-Lacs and XRB
2	Galaxies and Galactic Surveys
3	Groups of Galaxies, Clusters of Galaxies, and Superclusters
4	Stars, White Dwarf and Solar System
5	Supernovae, Supernova Remnants, Diffuse Emission
6	White Dwarf Binaries, Neutron Star Binaries, Cataclysmics
7	X-ray Background and Surveys

Table 4.1: Summary of XMM pointing types.

To remove duplicate sources an appropriate matching radius needs to be chosen. The positional accuracy of the survey is much higher for point sources than for extended sources so it makes sense to use a different radius for each type. The accuracy for point sources varies as a function of off-axis and azimuthal angles (amongst other parameters). However, for simplicity we use a single value for the radius. As will be shown in the Veroncat point source analysis (Section 5.2.1) a suitable radius is 5".

The case for extended sources is less straightforward because of the sheer variety of species. The positional accuracy for large diffuse objects, such as low redshift clusters, can be very poor (of the order of many arcminutes). It is very hard to pick a radius which takes all of this into account without being overly conservative. Fortunately, pointings containing the largest diffuse sources will have been flagged as unsuitable for XCS so it becomes justifiable to use a fixed matching radius of 2' for extended sources.

For both point-like and extended sources the source with the greatest number of soft-band counts in a matching set is chosen to remain in the concatenated list. Of course, the others in the set are given a flag to point to their catalogue source. As an aside, these sets of detections of the same source are useful for assessing the scatter in measured properties, such as flux (see Figure 5.8).

After this operation the remaining sources (58154 points, 5173 extended) comprise the Master Source List.

4.1.3 Literature Searches

A large number of extant surveys, in multiple wavebands, are available online in databases such as the NASA Extragalactic Database[1] (NED) and SIMBAD[2]. The value

[1] http://nedwww.ipac.caltech.edu/

[2] http://simbad.u-strasbg.fr/

of the XCS catalogues could be greatly increased if a significant fraction of the detections are matched to sources in other catalogues. Not only does this reduce the mammoth task of follow-up for the XCS but, by utilizing the literature data for known clusters (e.g. redshifts), XCS science can begin immediately. However, this is a notoriously difficult problem (see for instance, Sutherland and Saunders 1992; Mann et al. 1997, and Section 6.1.4). Astronomical catalogues (including our own) tend to be inhomogeneous, contaminated and incomplete. Without knowing the detailed astrophysics of each species of source and characteristics of the catalogues it is not apparent whether an association is likely to be real or coincidental.

A thorough association of the XCS is beyond the scope of this thesis, although it is important that we cross-match our cluster candidates with literature sources. The aim is to separate the list of extended candidates into re-detections of known clusters (or other X-ray emitting diffuse objects) and new candidates. This is accomplished by searching the NED and SIMBAD databases for the most common diffuse X-ray sources, namely clusters and groups of galaxies, supernovae and remnants, HII regions (such as those around ionizing OB stars), and low redshift galaxies. For the same reasons as discussed above, a single matching radius of 2' is used for the association tests. This is adequate for all but the closest, largest clusters of galaxies. Frequently, their catalogue positions were measured using optical data and since the cluster galaxies do not always follow the cluster gas (particularly in merging systems) the X-ray centroid can be more than 2' from the optical centroid. There are not enough of these sources to alter the statistical conclusions of the XCS as, typically, they are the target object of the XMM pointing.

Neither NED or SIMBAD have complete lists of the known clusters of galaxies. A recent project, the X-Rays Clusters Database[3] (BAX) has attempted to gather known clusters from many locations and make them accessible in one archive. Therefore, we also query this database in addition to NED and SIMBAD.

As a last check we have also gathered a small number of clusters which we have found by hand in the literature and are not present in the previously mentioned databases, for instance, the $z = 1.4$ cluster presented in Mullis et al. (2005). By doing these literature tests we should have the best possible chance of correctly identifying known clusters, and of separating the non-cluster X-ray emission from the possible cluster candidates.

[3]http://bax.ast.obs-mip.fr/

4.1.4 Caveats

Over two years of work has been spent developing and optimizing XAPA. Given the number of difficulties and uncertainties associated with XMM it produces exceptionally good source lists, but through thorough manual checking there are some known deficiencies. None of these should affect the value of the XCS.

Occasionally, close pairs of point sources are mistakenly removed from the source lists. This is caused by the classification failing on both point sources (due to stray source counts from the other), thus each is flagged as being a possible lobe of the other. Of course, XCS is not a point source survey so this has no effect on the primary science. It is mentioned here to explain the apparent lack of detection of some obvious sources. This bug will be corrected in the next release of the XCS catalogues.

A more serious, but not threatening, problem is with the code to flag extended sources which have been detected as roughly the same size as the PSF (i.e. potentially misclassified point sources, see Section 3.5.8). Even though the cuspiness test works most of the time there are a few cases in which clearly extended sources have been mistakenly flagged as being PSF-sized. These are small in number so it is not worth further effort at this stage. The magnitude of the issue will be eventually be quantified in the selection function simulations. Furthermore, an additional catalogue of these sources has been compiled by hand (see the discussion below). Naturally, these will be excluded from statistical analysis of the archive but they are useful for other cluster physics.

4.2 Catalogues

There are many possible catalogues which could be created from the Master Source List. In fact, this is one of the strongest features of XCS; no other comparable catalogue of both point-like and diffuse X-ray sources exists, or will exist in the foreseeable future. Once the Master Source List is made publicly available other groups will be able to extract objects for a huge number of projects, for instance AGN or supernovae studies. In this way the legacy of XCS will be long lasting.

However, here we compile the set of catalogues most directly relevant to the XCS, namely a statistical cluster sample, a sample of other new cluster candidates, and a catalogue of the detected point sources.

4.2.1 Statistical Cluster Sample

To fulfil some of the goals of XCS, in particular the cosmology objectives, we must compile a large, unbiased sample of clusters and cluster candidates. It is straightforward to select the extended sources from the Master Source List but, to improve the sample, some must be filtered out. Firstly, only *serendipitously* detected clusters are useful for an unbiased sample. That is, clusters which are the pointing target are not selected from random positions in the sky and therefore should be discounted. Secondly, to minimize contamination and boost the constraining power of the selection function, some clusters which have been flagged as being in certain pointing types are not used. Specifically, there is a greater chance of candidates in cluster or SNR pointings being associated with the target source, so these pointings are excluded.

An additional, simple test to ensure that no target objects are included filters out any sources flagged as being within 2' of the target position.

To ensure the cleanest possible list for the statistical sample sources flagged by the algorithms as suspect (Section 3.5.8) are not considered. The literature tests discussed above are also used to flag potential non-cluster sources.

After applying these filters 1764 candidates remain. These will be a mixture of both new candidates (1622) and serendipitously re-detected known clusters (142). Where available, the details of the known clusters are included in the table. The Statistical Cluster Sample is presented in Appendices B.1 (known clusters) and C.1 (new candidates).

The description of the table columns is as follows:

- **Id** IAU XCS name of the source.
- **Literature Name** Literature name of the source.
- **Obsid** XMM observation in which the source was found.
- **RA** Right Ascension of the source (J2000.0).
- **Dec** Declination of the source (J2000.0).
- $\boldsymbol{\theta}$ Off-axis angle of the source in arcminutes.
- **Scts** Source counts in 0.5-2.0 keV band.
- $\boldsymbol{t_{max}}$ The average exposure time over the source (seconds). The maximum value for the set of exposures used to create the merged data is used.

- **Flux** Flux in 0.5-2.0 keV, using Point Source ECF ($\times 10^{-14}$ erg/cm^2/s).

- σ_F 1σ error in flux ($\times 10^{-14}$ erg/cm^2/s).

- **Sig** Significance of source, $-log(P)$, where P is the probability of the source being a background fluctuation. A 'NaN' indicates that P is so close to zero that $-log(P)$ is undefined using the current machine accuracy, i.e. the source is extremely significant.

- **FN_P** Approximate probability of the source being a false negative, i.e. the probability that a point source at this position and with this number of counts would be misclassified. The spatial profile of the candidate is not considered in the calculation of this probability and therefore the attribute can be misleading. It is most reliable when the source size is similar to that expected of the PSF.

- **Flags** This is a set of binary flags. The first digit is 1 if the source is found in the BAX archive otherwise it is 0. Similarily, the second digit represents whether the source is a cluster or group in KnownNEDObject, the third digit whether it is a cluster or group in KnownSIMBADObject and the fourth is 1 if the source has a match with the KnownOtherCluster table.

- **z** The literature redshift, where available from the archives.

- z_{est} The XCS estimated cluster redshifts (see Section 6.2).

- σ_z The 1σ error on the XCS estimated cluster redshift (see Section 6.2).

- z_{flag} The reliability flag for the XCS estimated cluster redshift (see Section 6.2).

4.2.2 Manual Cluster Candidates Sample

As mentioned in the caveats discussion, the algorithms are not perfect and occasionally a good cluster candidate is removed from the list. These have been identified by eye and are listed in Table D.1 of the Appendices. This sample of 90 is useful for cluster physics and evolution. The candidates have not yet been investigated in detail.

The table column descriptions are the same as those given for the Statistical Cluster Sample. There is an additional column with a comment on why the candidate was excluded.

4.2.3 Point Sources

The largest catalogue of all is of X-ray point sources (58154). It is too large to be included in this thesis but is, of course, available online (see Section 4.3). This is a considerable resource which will be used by XCS for studies of neutron stars (amongst other applications). However, we anticipate that this catalogue will be exploited mostly by other groups.

4.3 Database

The tables included in this thesis cover only a small fraction of the overall survey, simply due to the sheer quantity of data available. It has always been a stated aim of the project to make as much of these data as possible accessible to the astronomy community. Naturally, the only way to do this is via an online database and, hence, into the Virtual Observatory (Mann et al. 2002).

A database is, in essense, a set of tables connected in a logically consistent manner. After all of the tables were designed, in terms of content, they were populated and implemented in the form of a database.

A summary of the content and structure of the database is best shown in the form of an Entity Relation Diagram (Figure 4.1). This uses standard database terminology and notation to denote how the tables which constitute the database relate to each other. Most of the information is in the linestyle and connectors used to link the tables:

- **Solid Line** Complete one-to-one relation between entries in the tables.
- **Solid-Dashed Line** Partial one-to-one relation (i.e. every entry in Table A has a counterpart in Table B, but not vice versa.)
- **Dashed Line** Some entries in Table A have counterparts in Table B and vice versa.
- **Crow's Foot** One-to-many relation between the table entries.

The samples discussed above (the XCS Statistical Sample, Manual Cluster Candidates and Point Sources) are created by constructing a query incorporating the necessary criteria. This is known as a 'view'. The set of views so far created are also presented in Figure 4.1.

The complete database contains considerably more information than the tables in the appendices, in particular they include much intermediate data relating to the

reduction of the XMM pointing and the detection pipeline. There is too much to be described in detail here. For further elaboration see Appendix E.1 and the database schema and description pages online[4].

The XCS database is implemented using Microsoft SQL Server 2000 and can be queried using the well-known Structured Query Language (SQL). SQL is an intuitive language and the queries constructed are typically transparent. The database has a web-based interface[5] which is currently restricted to the XCS collaboration but will ultimately be public. An illustrative example of a simple XCS query and its results is shown in Figure 4.2.

[4]http://www.roe.ac.uk/~mdv/xcs_browser.html
[5]http://www-wfau.roe.ac.uk:8080/xmm/sql.html

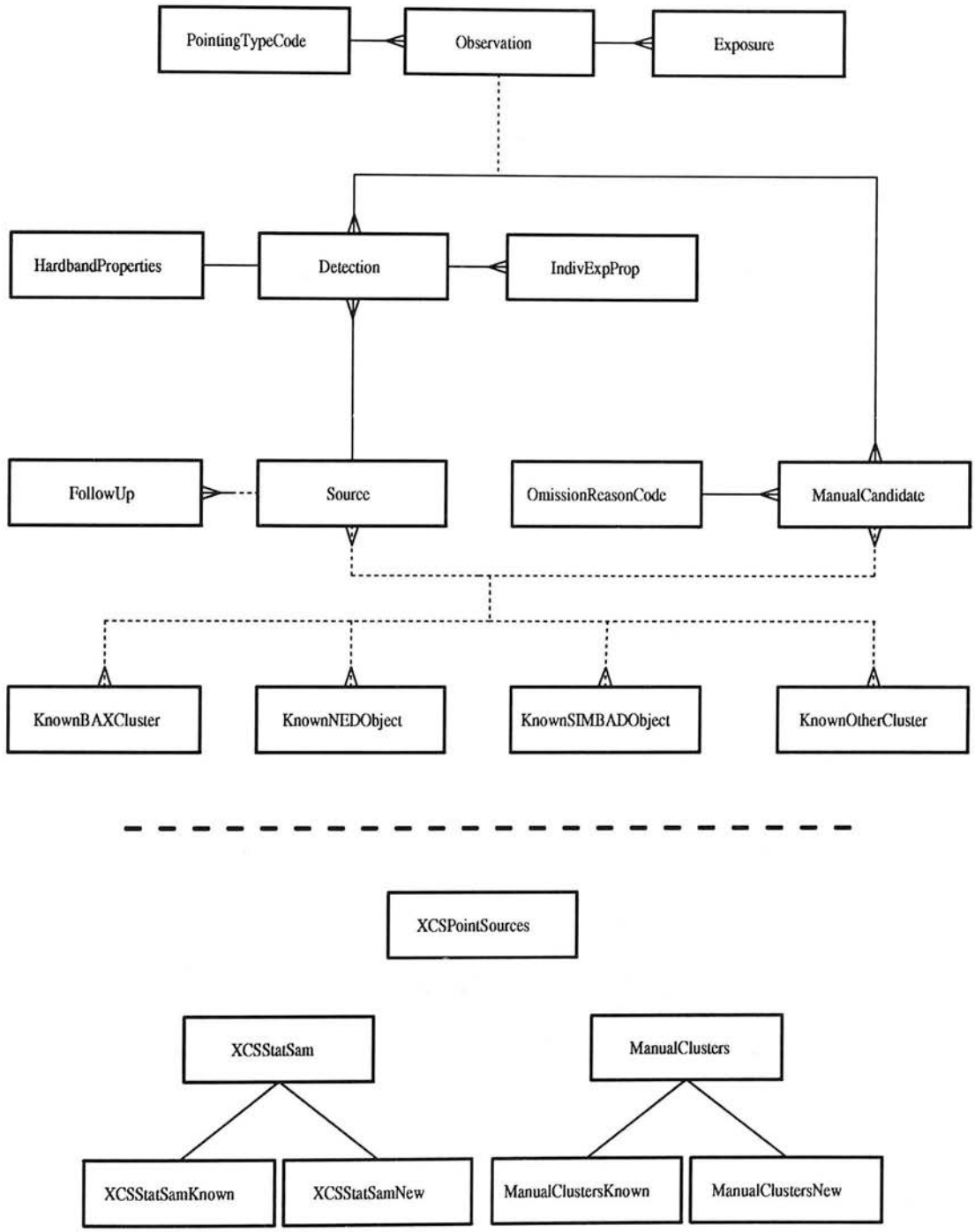

Figure 4.1: The Entity Relation Diagram for the XCS database. Also shown, below the ERD, is a selection of views of the source table.

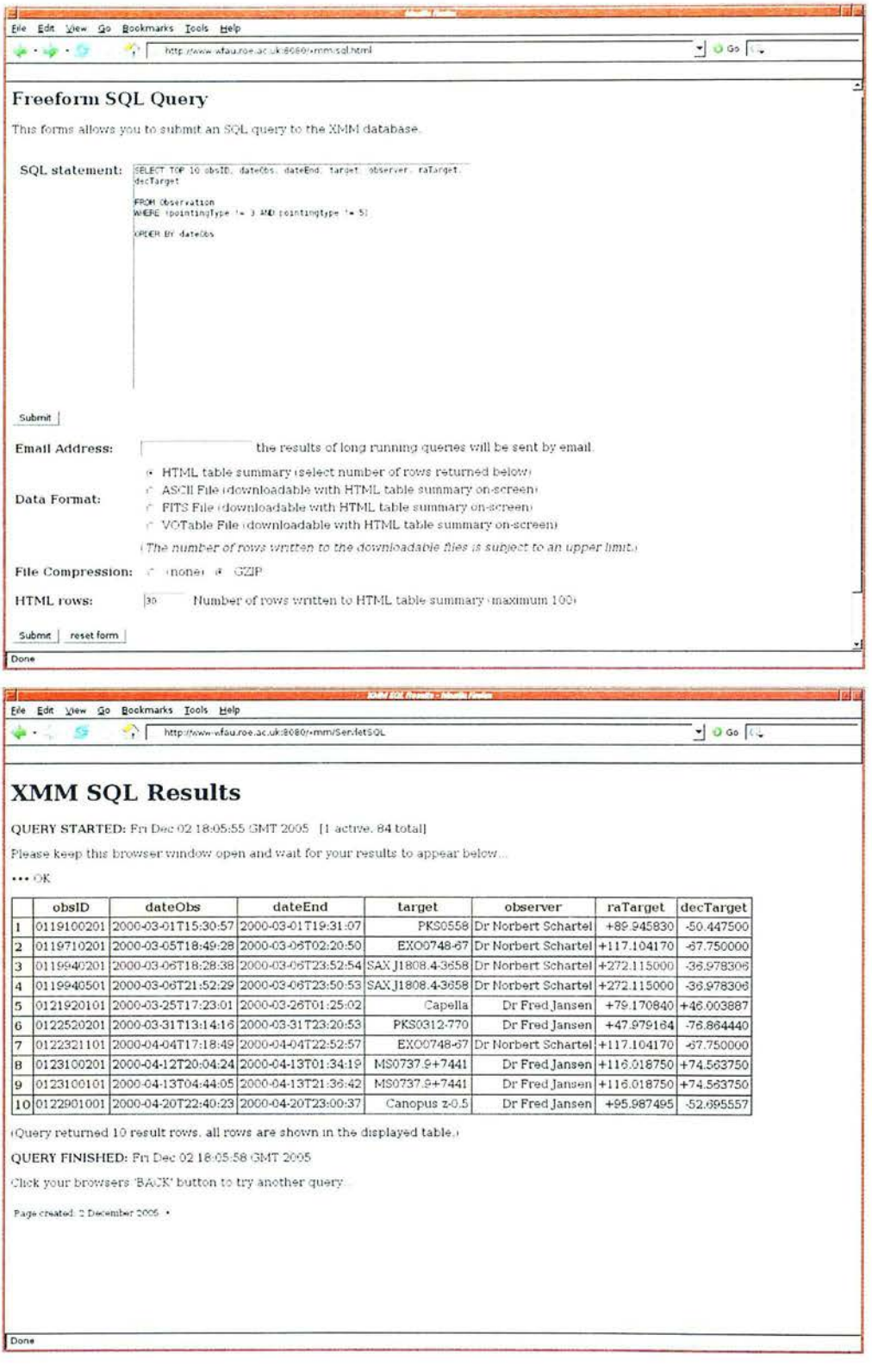

	obsID	dateObs	dateEnd	target	observer	raTarget	decTarget
1	0119100201	2000-03-01T15:30:57	2000-03-01T19:31:07	PKS0558	Dr Norbert Schartel	+89.945830	-50.447500
2	0119710201	2000-03-05T18:49:28	2000-03-06T02:20:50	EXO0748-67	Dr Norbert Schartel	+117.104170	-67.750000
3	0119940201	2000-03-06T18:28:38	2000-03-06T23:52:54	SAX J1808.4-3658	Dr Norbert Schartel	+272.115000	-36.978306
4	0119940501	2000-03-06T21:52:29	2000-03-06T23:50:53	SAX J1808.4-3658	Dr Norbert Schartel	+272.115000	-36.978306
5	0121920101	2000-03-25T17:23:01	2000-03-26T01:25:02	Capella	Dr Fred Jansen	+79.170840	+46.003887
6	0122520201	2000-03-31T13:14:16	2000-03-31T23:20:53	PKS0312-770	Dr Fred Jansen	+47.979164	-76.864440
7	0122321101	2000-04-04T17:18:49	2000-04-04T22:52:57	EXO0748-67	Dr Norbert Schartel	+117.104170	-67.750000
8	0123100201	2000-04-12T20:04:24	2000-04-13T01:34:19	MS0737.9+7441	Dr Fred Jansen	+116.018750	+74.563750
9	0123100101	2000-04-13T04:44:05	2000-04-13T21:36:42	MS0737.9+7441	Dr Fred Jansen	+116.018750	+74.563750
10	0122901001	2000-04-20T22:40:23	2000-04-20T23:00:37	Canopus z-0.5	Dr Fred Jansen	+95.987495	-52.695557

Figure 4.2: An example of a simple XCS SQL query and the results returned.

4.4 Initial Survey Area

Seemingly one of the easiest-to-state properties of a survey is its area. This is not true even for point source surveys but especially so for inhomogeneous extent surveys like XCS. The fundamental quality to be calculated is the volume surveyed over which a certain species of object would have been detected (above a given significance). For the same survey this volume would be significantly different for two different species of cluster. When one has knowledge of the real population of clusters in the Universe then it might eventually be valid to state a single figure for the survey volume, but of course this is not currently available! Instead of picking arbitrarily one variety of cluster and using it to derive the survey volume, we have chosen to tackle this in two stages.

Firstly, we can calculate the 'geometrical' solid angle of the Statistical Sample survey by summing the unique area of each observation after application of the masks. To review, the masks in question are:

- **Initial Mask** This mask was created by hand for each pointing before detection began. Its purpose is to remove extremely bright sources from the images, especially point sources with very evident diffraction spikes. Also removed at this stage are streaks caused by out-of-time events, and bad pixels.

- **Target Mask** This is a simple 2' mask around the target of the pointing. This is not literally masked from the image but, since any cluster found to lie near the target by chance would be flagged as suspicious, the region must not be included in these area calculations.

- **Literature Extended Source Mask** As in the target mask, genuine new candidates lying within 2' of a known extended source in the literature would not reach the statistical cluster sample therefore the area must be discounted.

The masks reduce the geometrical area of the survey from 236.5 to 168.2 square degrees[6]. This can be thought of as the maximum possible survey area for any source type. Although the area has been cut significantly we believe it is justified by the improved purity of the sample and less contaminated follow-up.

[6] An additional observational constraint is the influence of the Galaxy and the Magellanic Clouds. Optical follow-up in these regions of the sky can difficult because of extinction and the presence of dense star fields. The final survey area may be reduced further by such problems. The degree of this problem is yet to be ascertained.

Secondly, we can calculate the effective area for a range of realistic cluster types. Using the selection function simulations (Chapter 5) we can estimate the survey area for a grid of cluster species. This is done by measuring the detection efficiency for a cluster with a given profile, luminosity and redshift and then scaling the geometrical area by this factor, i.e.

$$\text{Cluster Area} = \text{Cluster Detection Efficiency} \times \text{Geometrical Area}$$

As will be discussed in the next chapter, these simulations will take several years. However, in this manner a true picture of the survey volume will be established.

Chapter 5

Simulations

While the source catalogues as presented are interesting resources, their value can be increased greatly by carefully quantifying the algorithms used to create them. Aside from the benefits gained from being able to have confidence in the source parameters, it would be impossible to make any use of the clusters for cosmology without doing so.

Firstly, the techniques used to generate simulated clusters are discussed before these are used (along with external data sets) to validate the performance of the pipeline algorithms. After this, the survey selection function methodology is described and the initial cosmological constraining power of the survey is measured.

5.1 Simulation Methodology

The guiding principle of these simulations is to create sources as similar as possible to those expected to be observed in the real images. This requires inclusion of as much of the relevant physics as is practical, folding the model through the instrumental responses and processing it in precisely the same manner as a genuine observation. Furthermore, due to the large number of simulations to be performed, the code must be simple, fast and easy to run on many computers.

5.1.1 Surface Brightness Models

The emission of X-rays from clusters of galaxies is a complicated process and depends on the 3-dimensional distribution of mass. As discussed earlier in Section 1.1.2 the

dominant process is that of bremsstrahlung, the strength of which is proportional to the local gas density and temperature. Given a physical model of the matter distribution the emission can be simulated and then projected on to the plane of the sky to obtain the surface brightness profile of the cluster. Several different models have been found to be useful for describing the surface brightness profiles of real clusters. A selection of these are available for use in the simulations. The following models should allow most realistic scenarios to be simulated:

Beta Model The physical motivation behind the β profile has been outlined in the Introduction (Section 1.1.2). It is known to be a successful model but its limits are becoming apparent, as will be discussed further in Chapter 6. The surface brightness profile for a β model can be described as

$$S \propto \frac{1}{\left[1 + \left(\frac{r}{r_c}\right)^2\right]^{3\beta - 0.5}}$$

where r is the radial distance, β is the shape parameter and r_c is a characteristic core radius.

Navarro, Frenk & White Again, the NFW profile (Navarro et al. 1997b; Nevalainen et al. 1999; Thomas et al. 2001) has often been used to describe cluster emission over a wide range of masses and radial distances. It is less straightforward to project the emission expected from the density distribution in order to obtain a surface brightness map. In practice, the emission from the density profile

$$\rho(r) = \frac{\rho_0}{\left(\frac{r}{r_s}\right)\left(1 + \frac{r}{r_s}\right)^2}$$

where ρ_0 is the central density and r_s a scale length, is numerically integrated.

Point Source The point source model simply uses the Medium Accuracy PSF. Its corresponding surface brightness profile is a delta function which, when convolved with the PSF, results in the desired source probability density function.

Double Beta This is much like the β model described above but, to alleviate the core/outskirts problem, the inner and outer regions are fitted separately (with the correct boundary conditions). This should provide a more appropriate model for clusters with peaked centres, such as those with cooling cores.

Hydrodynamical Simulations Large numerical simulations of clusters are including more and more realistic physics. They thus offer a 'laboratory' for studying clusters in more detail than can currently be resolved observationally. The surface brightness profiles obtained from large simulations will ultimately comprise a library of cluster states, encompassing clusters in various states of merging and AGN activity and at different redshifts. Members of the XCS collaboration have made considerable progress along these lines already (for instance, Kay et al. 2004; Onuora et al. 2003). With them, the impact of the various assumptions used when making the models above (for instance, isothermality) can be assessed.

In addition, by combining the Point Source model with, for instance, the β model, the effect of AGN contamination can be characterised.

5.1.2 Creation of Cluster Image

In the following discussion the β model is used for illustration. The methodology is easily extended to the other surface brightness profiles mentioned above.

Cluster Profile A 201 by 201 pixel image, S of the β profile is created:

$$S_i \propto \frac{1}{\left[1+\left(\frac{\theta_i}{\theta_s}\right)^2\right]^{3\beta-0.5}}$$

where θ_i is the distance in radians of pixel i to the cluster centre, and θ_s is the apparent angular size of the core radius r_c in radians. θ_s is calculated using the IDL Astrolib function `zang`[1]. S is then normalised to give a total probability of 1, creating a PDF. This 201 by 201 pixel image corresponds approximately to 15' by 15'.

Addition of Cluster Photons When simulating the fake source both the profile and the cluster bolometric luminosity are specified. The cluster image is created by calculating a rate image for each exposure used in making the XMM image, adding the appropriate number of photons to it, and then merging the individual images with the actual XMM image. This is done as follows:

1. The cluster PDF is positioned within the image and then convolved with the appropriate Medium Accuracy PSF.

[1] http://idlastro.gsfc.nasa.gov/ftp/pro/astro/zang.pro

2. The absorbed count rate is calculated using grids calculated using XSPEC[2] (Arnaud 1996, Sabirli et al. in prep.), for the appropriate camera, filter, T, z, neutral hydrogen density and unabsorbed bolometric luminosity.

3. The unvignetted PDF is normalised to the absorbed count rate, thus creating a rate image for the exposure.

4. By multiplying the rate image by the exposure map a 'count' image is made. This accounts for factors such as vignetting, masking and chip gaps. The correct number of photons, n, to add is found by summing this count image and rounding.

5. A modified, exposure map-corrected PDF is obtained by normalising the rate image to 1. The individual cluster image is thus made by adding n counts at random to this PDF.

6. Finally, each of the individual cluster images are co-added to the real XMM image.

Ideally, a more realistic PSF would be used for convolution with the cluster profile. This would improve the accuracy of the simulations of sources with limited spatial extent (i.e. the structure in the wings of the PSF would be accounted for). However, the Medium Accuracy PSF is the only 2D model currently available.

5.1.3 XAPA Processing and Matching

The XMM images with the fake clusters are processed with XAPA in precisely the same way as a normal image. One slight difference is that source properties are only calculated for objects found within 4' of the input cluster position in order to save CPU time. Once processing is complete the source list is compared to the real source list (without the fake cluster). If there are sources in the former which are not in the latter then then source closest to the input position is chosen as the match (with extended sources given priority over point sources).

After the source has been matched the usual flags are recorded and association tests performed. Of course, these fake clusters should not be associated with known real sources but sometimes will be through chance alone. This false association issue will be discussed in a Section 5.2.2.

[2]http://heasarc.gsfc.nasa.gov/docs/xanadu/xspec/

5.2 Validation of XAPA

Now that we have the means to simulate fake sources it is timely to confirm that XAPA is indeed capable of the required performance. The key tests which must be passed relate to the code's ability to measure positions and fluxes accurately and classify sources reliably. We shall approach this task by treating separately sources known to be point-like or extended.

5.2.1 Point Sources

The required resource here is a large, independent sample of X-ray detected point sources which cover (or at least approach) the depth accessible with XMM. We cannot use a set of simulated point sources for this purpose because of the uncertainties with the PSF model (it would not make sense to classify a source using the same model used to generate it). The existing catalogues in the literature each have advantages and disadvantages and there is no single appropriate sample.

Positional Accuracy

To check the recovery of positions for point sources it is not required for the literature sample to have X-ray properties. All that is required is a list of objects which would be expected to appear point-like in X-rays. A suitable catalogue is Véron-Cetty and Véron (2003), hereafter known as Veroncat, which contains $\sim$ 50000 AGN, quasars and BL Lac objects across a wide region of sky. This catalogue has 2613 matches with the XCS Source table (using a 10" pairing radius). Both point-like and extended XCS sources were matched and this fact will be used later in the Classification Section.

The plots in Figure 5.1 confirm that the point source positions are being accurately recovered. There appears to be no systematic offset in either the x or y directions. The 95% matching radius is 7.8" (less than two pixels). While this level of accuracy is acceptable it is a little larger than expected. This is due to the uncertainties in the shape of the PSF towards large off-axis angles. There is an decrease in positional accuracy in the innermost regions of the FOV due to the presence of the target object and occasionally contribution from the host galaxy, in the case of AGN. Ideally, we would investigate the θ, ϕ and source counts dependence of the positional accuracy using Veroncat but unfortunately the sample size is not large enough to do so. However, the θ dependence has been measured using a small number of annuli (Figure 5.2). The resolution of other X-ray point source catalogues is not high enough to be useful.

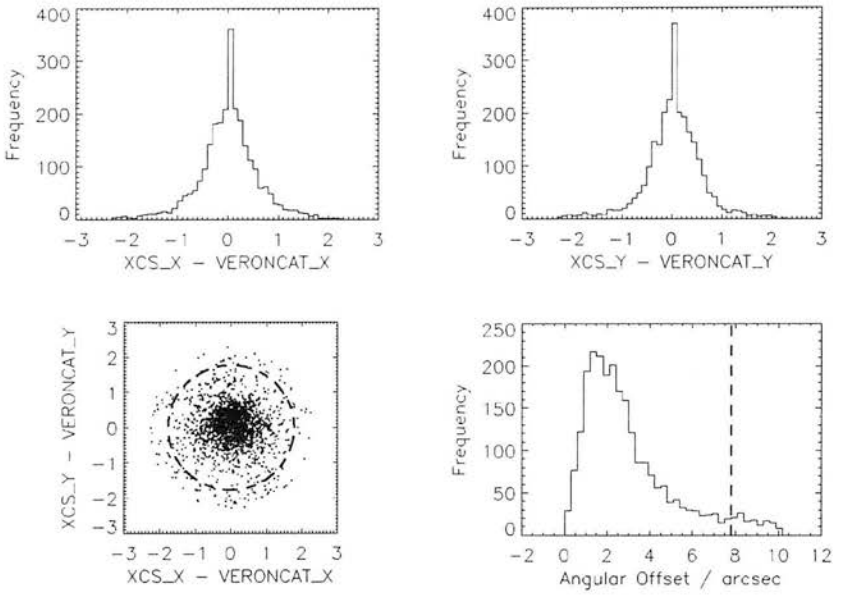

Figure 5.1: Top) Offsets in the x and y pixel positions between XCS and the Veron-Cetty catalogue. Bottom left) 2-dimensional offsets (in pixels) show no systematic bias; and bottom right) absolute offset between the two catalogues (the dashed line in both of these plots represents the 95% matching region).

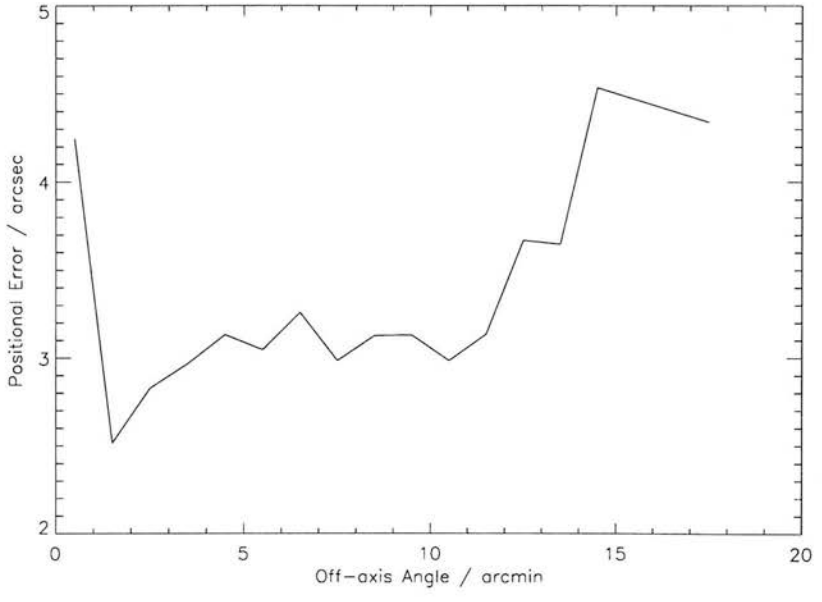

Figure 5.2: The point source positional error as a function of off-axis angle, found using Veroncat matches.

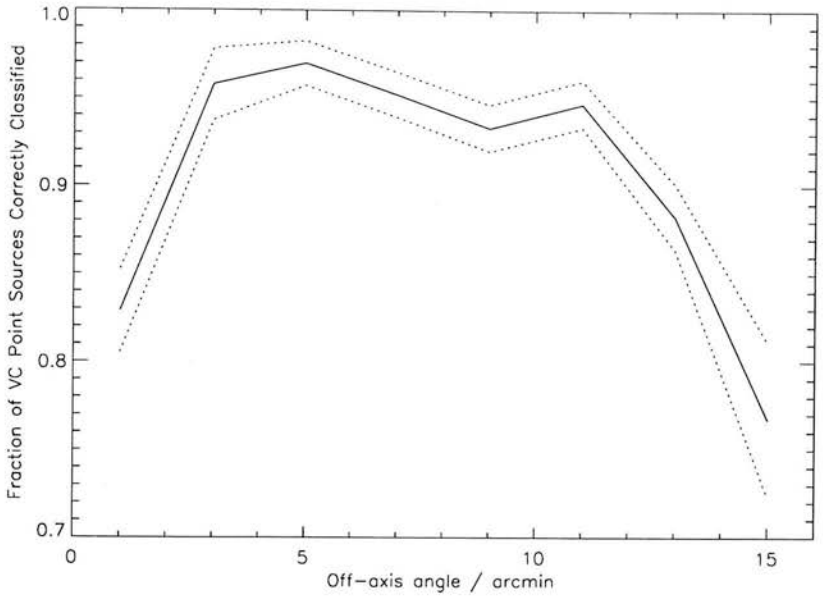

Figure 5.3: The effect of off-axis angle on the ability of XAPA to correctly classify Veroncat point sources. The dotted lines are the 1σ errors.

Classification

Classification is, in essence, a hypothesis test where the null hypothesis is that a source is point-like. Real point sources can either be classified correctly (true positive) or incorrectly (false negative). The Veroncat enables us to measure these probabilities as a function of source counts and off-axis angle, which are the two most influential parameters. The first plot (Figure 5.3) shows the simple dependence of the classification accuracy on the off-axis angle of the source. The slight dip in accuracy at low θ is due to detections of nearby galaxies (being truly extended in X-rays) having internal points present in the XCS catalogue. These are usually the XMM pointing target hence are at low off-axis angles.

Next, we turn to the sources in each θ bin and calculate the source counts dependence of classification. For this we look at the relative number of point-like and extended sources found as a function of θ and source counts. Implicit in this work is the assumption that the true ratio between the two kinds of sources is constant. As seen in Figure 5.4 the brightness of the source has a strong effect on whether it will be classified correctly. Each θ bin displays a similar shape with the classification accuracy being poor at low source counts, peaking and then falling gradually as the object becomes brighter. This is to be expected as the differences between the model and real PSFs

will be most apparent in the high counts regime. Again, there is a possibility that some of the brightest sources in the Veroncat sample, which are taken to be point-like, are actually not unresolved.

These two dependencies can be combined to form a 2D array containing the true positive probabilities as a function of θ and source counts (Figure 5.5). Thus, given (θ, counts) for an extended source we can estimate the probability that it is in fact a false negative.

Flux Recovery

Flux recovery for unresolved sources should be relatively straightforward. The two-dimensional profile of the PSF is less important and so we can rely on the EEF values previously measured. We cannot use the Veroncat because it does not contain X-ray fluxes so we must look to other catalogues. Preferably, the catalogues used will have been compiled using observations from X-ray telescopes other than XMM. This is so the absolute rather than relative calibration can be assessed. Two major missions are promising; ROSAT and Chandra. The ROSAT point source catalogues are very large (for instance, White et al. 2000) but unfortunately only count-rates are quoted, not fluxes. The uncertainty associated with the ROSAT and XMM ECFs makes direct comparison rather difficult. Presumably, there are still ongoing issues with the ROSAT calibration otherwise source fluxes would have been released. A similar problem affects the large CHAMP survey with Chandra (Wilkes and et al. 2001) which does not make fluxes readily available. The only major surveys which provide fluxes in their catalogues (other than XMMSSC) are Chandra Deep Field North (CDFN, Alexander et al. 2003b) and Chandra Serendipitous Extragalactic X-Ray Source ID (SEXSI, Eckart et al. 2003). For this reason we use these two surveys as comparators.

Using a 10" matching radius we found 366 CDFN and 195 SEXSI sources with counterparts in the XCS. A comparison of the fluxes is presented in Figure 5.6. The sample sizes are quite limited but there is no egregious bias between the XCS and Chandra fluxes. This is encouraging as the Chandra fluxes are expected to be well-calibrated due to the excellent resolution of the telescope.

It is instructive to look at the relation between the XCS fluxes and the quoted individual camera fluxes from XMMSSC. As is apparent from Figure 5.7 the samples agree broadly but there is a definite offset between the surveys (and between the individual cameras). We find a systematic bias of $\sim$ 20% for MOS1 and MOS2 and $\sim$ 10% for

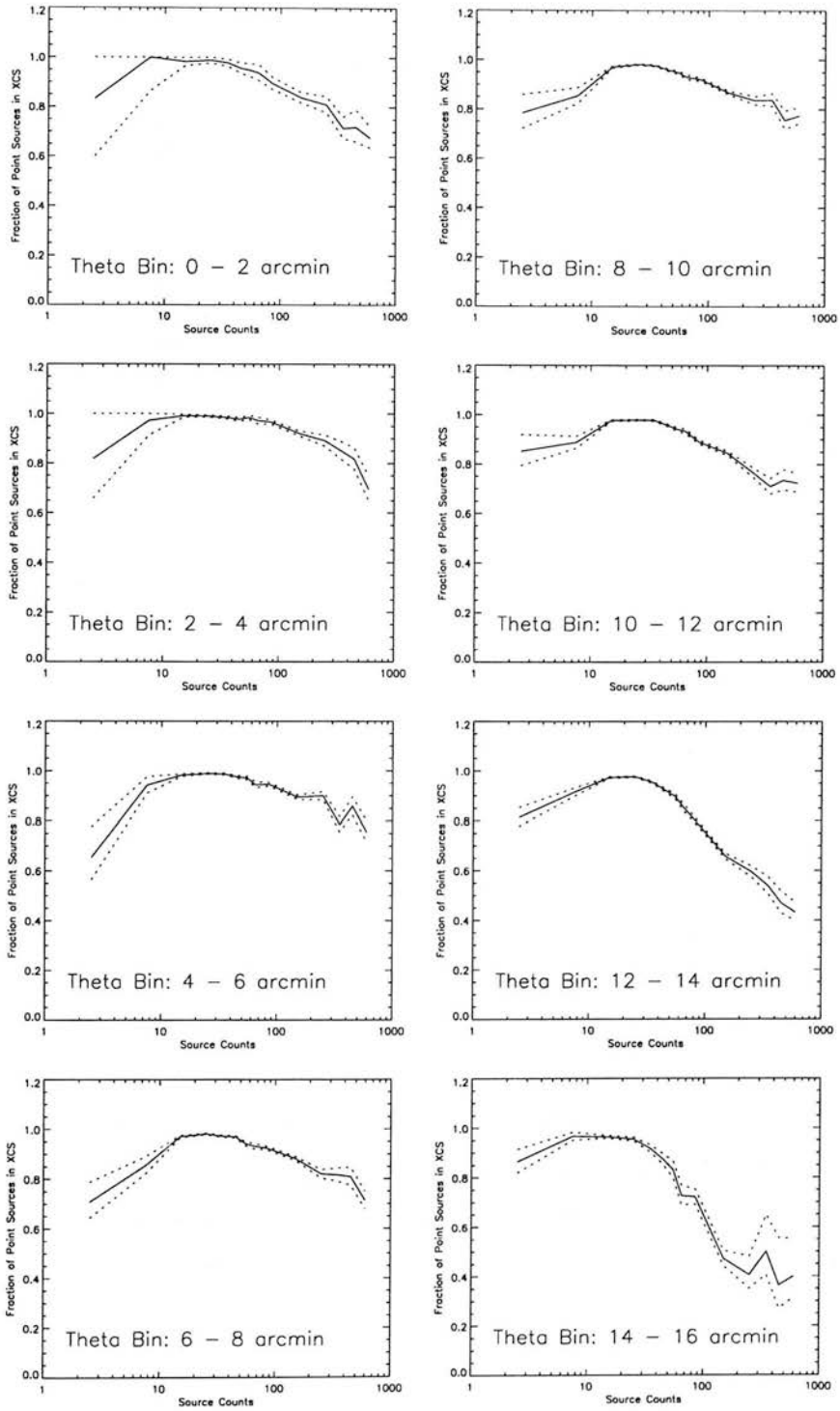

Figure 5.4: The effect of the X-ray source counts on the relative number of extended and point-like sources. Dotted lines are the 1σ errors.

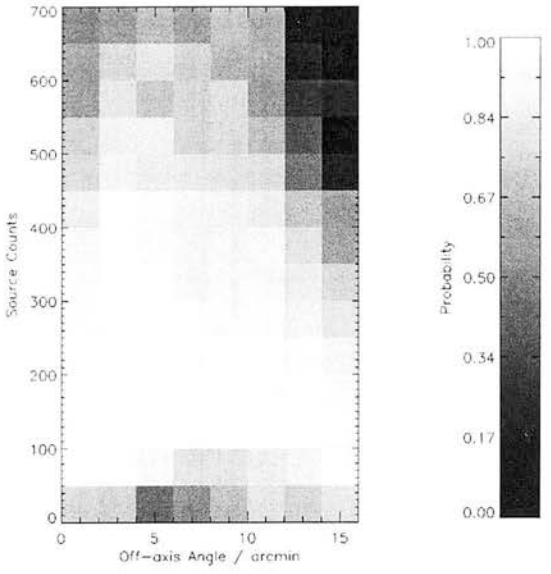

Figure 5.5: The two dimensional array containing the probability that a point source will be correctly classified, as a function of off-axis angle and source counts. The slight dip in accuracy at off-axis angle $\sim 5'$ and low source counts is due to the geometry of the MOS CCDs. The focal surface of XMM is curved and so the CCDs do not lie on a plane; the central chip is positioned behind the others (Figure 2.4). Hence, some sources lying close to the edges of the central chip are misclassified.

pn. This relative offset is well-known in the XMM Calibration documents[3] and is still not completely resolved[4]. It is beyond the scope of this thesis to provide an in-depth calibration of XMM but we believe that the above work confirms the reliabilty of our point source flux estimates.

Finally, we have measured the empirical scatter in the fluxes measured by XCS. To do this we selected a set of sources which had been observed in more than one pointing (there are ~ 2700 such sources). The scatter for the source fluxes is apparent in Figure 5.8. Also shown are the XCS scatter predictions. The XCS error estimate agrees in general with the true scatter found in the flux measurements.

5.2.2 Extended Sources

No such uniform sample of accurate positions and fluxes exists for X-ray extended sources. By their very nature, it is harder to define the centre and size of extended

[3]http://xmm.vilspa.esa.es/docs/documents/CAL-TN-0023-2-1.ps.gz
[4]http://xmm.vilspa.esa.es/docs/documents/CAL-TN-0018.pdf

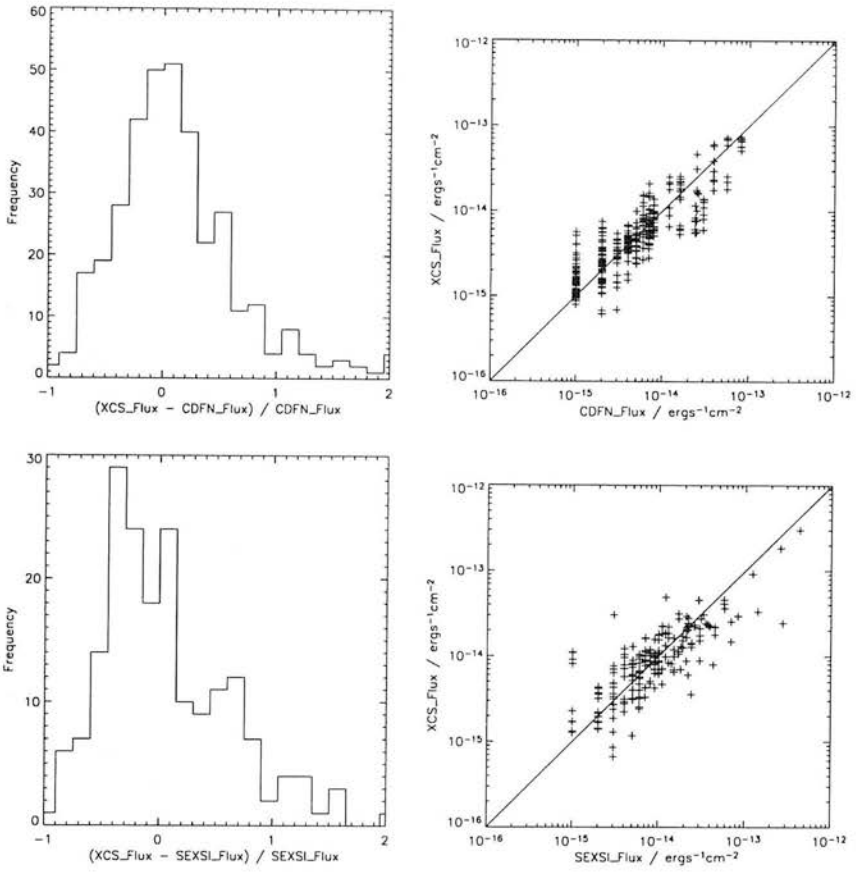

Figure 5.6: Comparison between XCS and Chandra point source fluxes using the CDFN and SEXSI surveys.

objects. We can still measure the algorithm's success using a simulated set of ideal clusters. From these, we can estimate the impact of each of the assumptions that are made in the pipeline and identify any biases. A set of 10000 canonical clusters was used for these tests. These are isothermal β profile clusters with a core radius of 160 kpc and $\beta = 0.66$, with no ellipticity and a temperature of 3 keV. The cosmology is concordance ($\Omega_m = 0.3$. $\Omega_\Lambda = 0.7$, $q = -0.55$). There are 10 logarithmically-spaced bins in luminosity from 0.056 to 10.0×10^{44} erg/s and ten linear bins in redshift from 0.2 to 2.0. They are placed into random XMM pointings from the Statistical Sample (i.e. those selected as suitable for XCS, excluding cluster and SNR pointings).

Positional Accuracy

The recovered position offsets are shown in Figure 5.9. Clearly, the positional error is slightly larger than that measured for point sources but it is still quite acceptable.

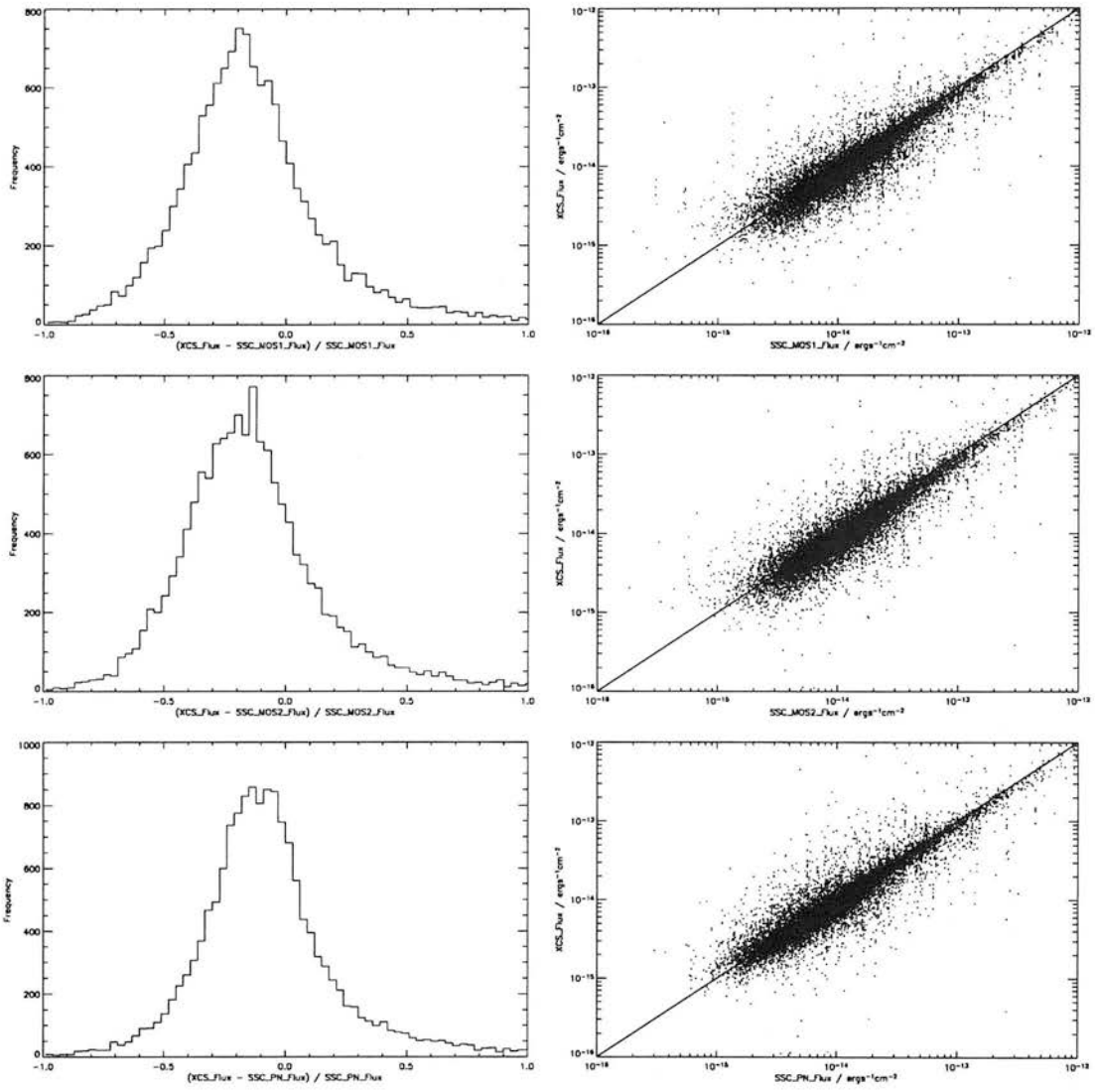

Figure 5.7: Comparison between the individual camera point source fluxes as found by the XMMSSC and XCS.

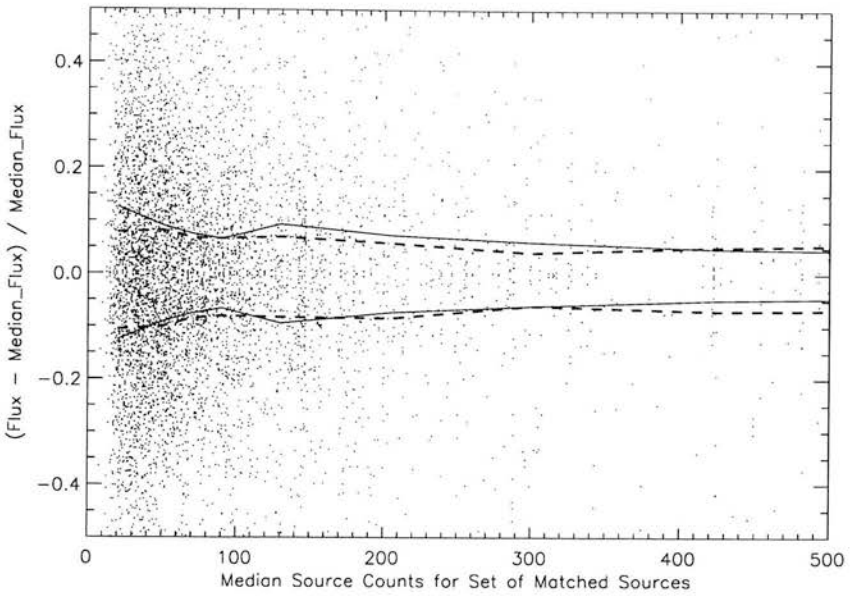

Figure 5.8: Scatter in XCS fluxes for sets of sources with multiple observations. The solid line denotes the predicted upper and lower 68% Gehrels error limits on the scatter while the dashed line shows the measured values.

Little more can be said at this stage about the position recovery for extended sources as this simulation used only one species of cluster.

Classification

By design we know that the input sources are extended. Thus, we can use the set of simulations to measure the false positive (classified as point-like) and true negative (classified as extended) probabilities. In the same manner as Section 5.2.1, we have broken these results down to measure their dependence on off-axis angle and source counts (Figures 5.10 and 5.11). The large error envelopes for the innermost annuli are due to the small number of sources being simulated in these areas.

Again, these results apply only to one (simple) variety of cluster. A fuller analysis must wait until the selection function has been fully quantified (see later). However, it is reasonable to conclude that the classification algorithms are behaving as desired.

Flux Recovery

We can use the simulations to assess the impact of the assumptions made in the algorithms.

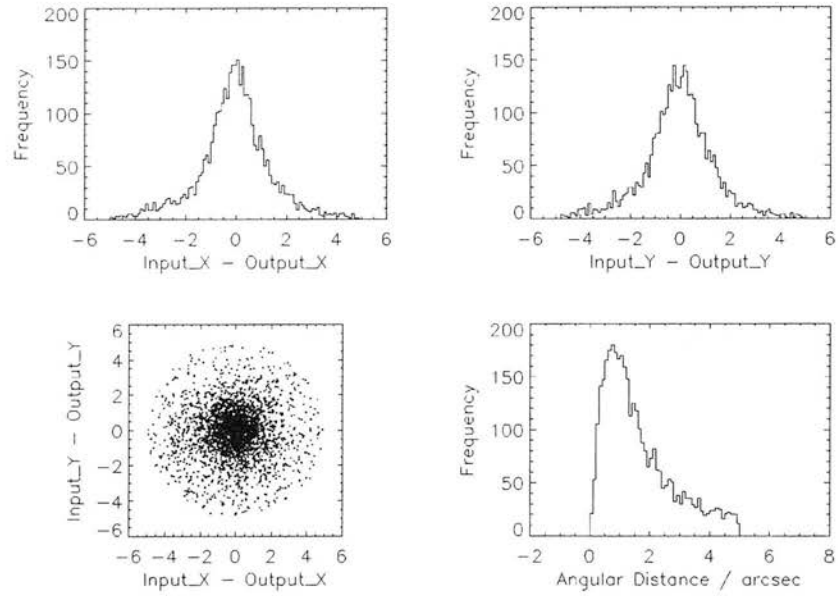

Figure 5.9: As Figure 5.1 but for the simulated extended sources.

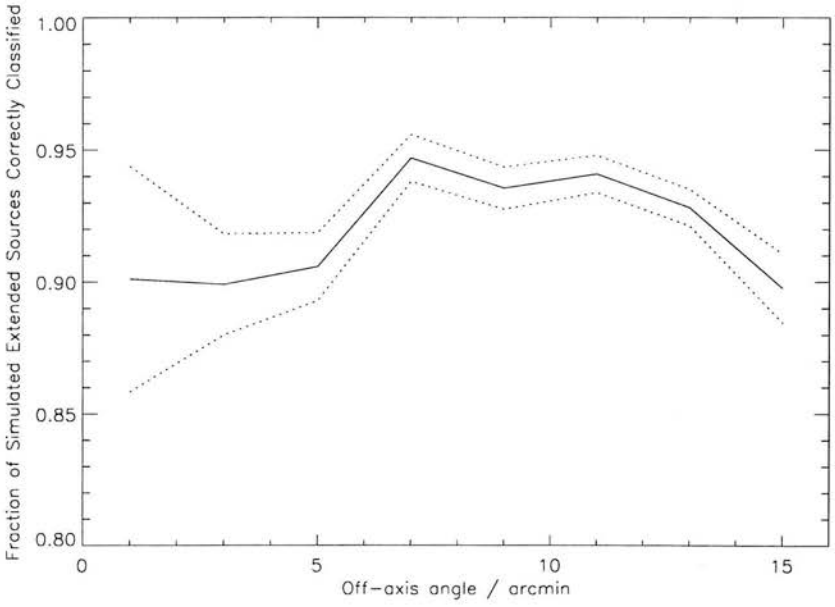

Figure 5.10: The effect of off-axis angle on the ability of XAPA to correctly classify simulated extended sources (canonical β model). The dotted lines are the 1σ errors.

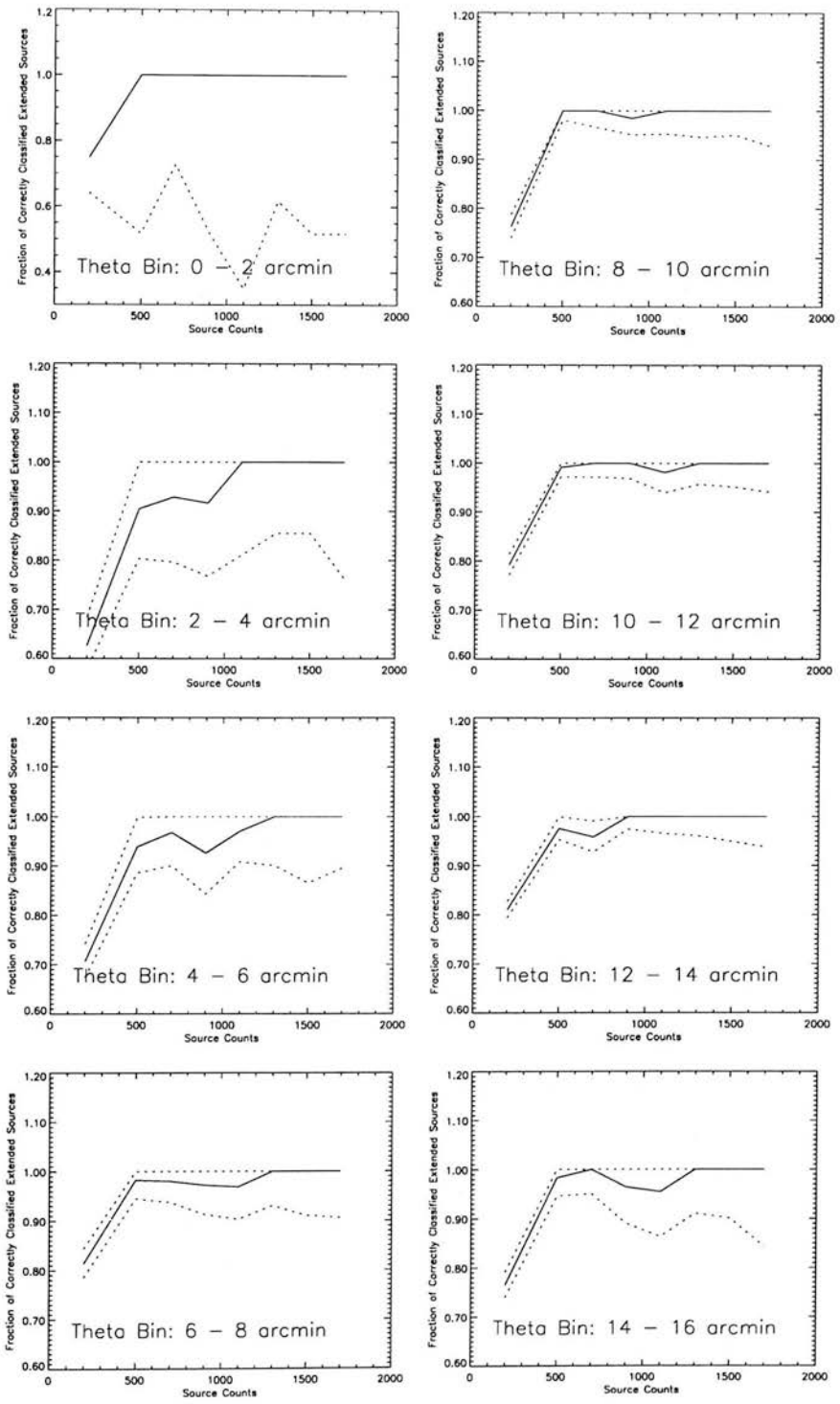

Figure 5.11: As Figure 5.4 but for the simulated extended sources.

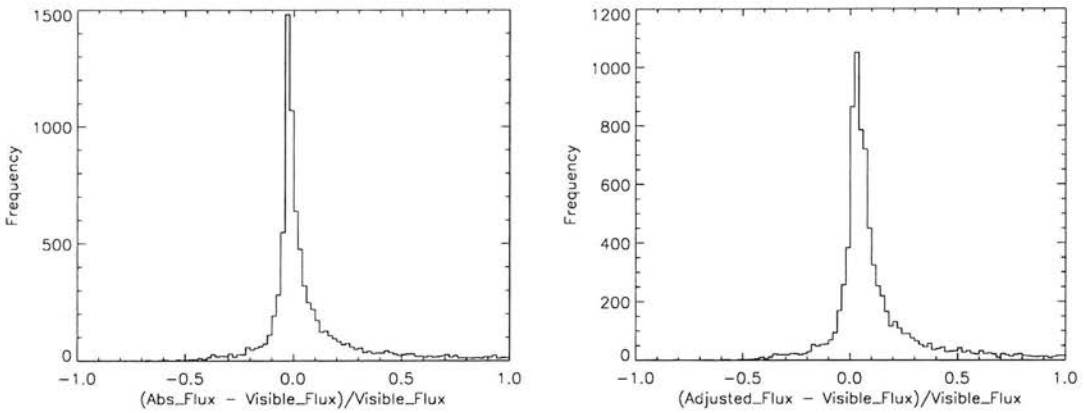

Figure 5.12: Left) Comparison of flux visible in the merged cluster image with the actual absorbed flux; right) comparison of flux visible in the merged cluster image with the absorbed flux after adjustment due to use of a 201 by 201 pixel grid.

Limited β Profile In theory, the cluster emission for a β profile extends out to infinity. By placing all of the emission within a 15' box we will over-estimate the true flux. We wish to estimate the size of this effect. To assess this, we made the profiles using a 1001 by 1001 pixel array ($\sim 1.2°$) and then extracted the central 201 by 201 pixels. Assuming all of the flux falls within the larger box, using a 201 by 201 pixel box causes an over-estimation between 4.5 and 10.0%, depending on the redshift of the cluster.

Input Fluxes Are the merged cluster images correct? Do they have the desired flux and what is the effect of chip gaps? The simulations produce the results shown in Figure 5.12. These plots are as expected. The visible flux is higher than the actual flux by approximately 3%, due to the truncation issue mentioned above. The value is less than the 4.5 to 10.0% predicted because of flux lost to chip gaps, for example. The second plot in Figure 5.12 provides a value of $\sim 3\%$ for this loss, so when the two factors are combined the adjusted flux is indeed $\sim 6\%$, in agreement with the prediction.

Use of Point ECFs The standard pipeline calculates fluxes using the merged image and exposure map. The merged exposure map is created by weighting the individual exposure maps by the appropriate *point source* ECF. We need to evaluate the size of the effect of using this exposure map rather than one weighted by the correct *cluster* ECFs. Obviously, in the real catalogue we cannot know in advance which ECFs to

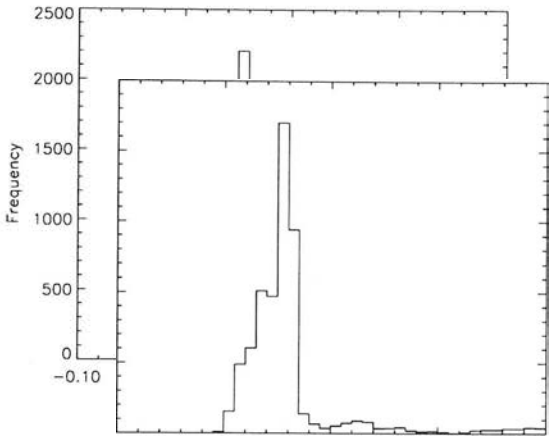

Figure 5.13: A comparison of the flux visible in the merged images when the point source ECFs are used instead of the correct cluster ECFS.

use but in the simulations we do know the ECFs so can measure the severity of this problem. To do this we created a second merged exposure map, correctly weighted by the cluster ECFs. We can then compare the visible flux (point ECFs) with the visible flux (cluster ECFs)[5]. As seen in Figure 5.13, using point source ECFs as standard leads to a $\sim 3\%$ bias in the calculation of visible flux.

The last thing to look at is the overall performance, in terms of flux restoration, of the pipeline from the actual unabsorbed flux through to the merged flux which would be recorded in the catalogue. It is useful to do this in three stages.

1. **Merged Flux versus Visible Flux, calculated with Point ECFs** Since the merged fluxes assume implicitly the point ECFs it is instructive to first compare these to the visible fluxes found using the same assumption. This is a test of how well the pipeline algorithms recover the flux in the image. Figure 5.14 shows that the code performs well, with the flux recovery centred around 92.5% of the visible flux. The slight peak at -1 is due to erroneous matching of the cluster with a low count fluctuation in the source list. XAPA is susceptible to this because of the necessity to calculate classifications using bootstrap resampling. When the fluxes are plotted against each other they are seen to behave as expected, with increasing scatter towards low input fluxes.

2. **Merged Flux versus Visible Flux, calculated with Cluster ECFs** This is

[5]When answering the second issue we use the correct *cluster* ECF weighted exposure map to measure the visible flux.

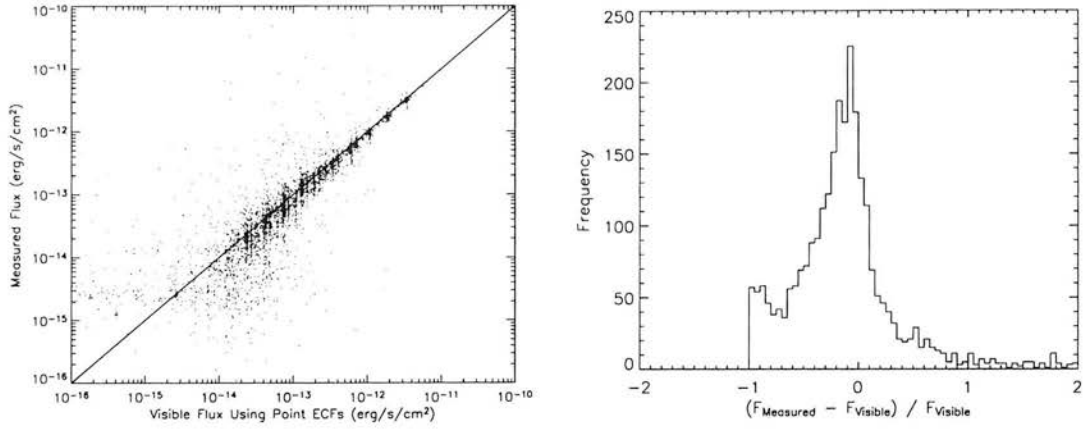

Figure 5.14: Comparison of measured fluxes with visible fluxes, calculated using point source ECFs.

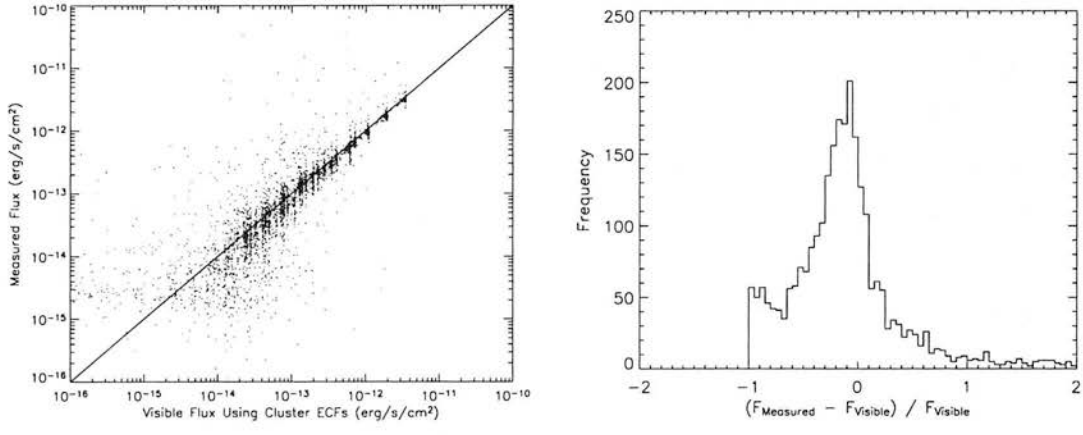

Figure 5.15: Comparison of measured fluxes with visible fluxes, calculated using cluster ECFs.

now repeated but using the more realistic fluxes. This has only a modest influence on the flux recovery (Figure 5.15). Again, there are no untoward features in the flux-flux plot.

3. **Merged Flux versus actual Unabsorbed Flux** This is the key result. The overall performance of the algorithms is such that $\sim 90\%$ of the real cluster flux is automatically recovered, without making any assumption about the cluster profile or spectrum. Figure 5.16 indicates a tendency for fluxes to be systematically high in the faint regime (below $\sim 5 \times 10^15$) and also that they become systematically

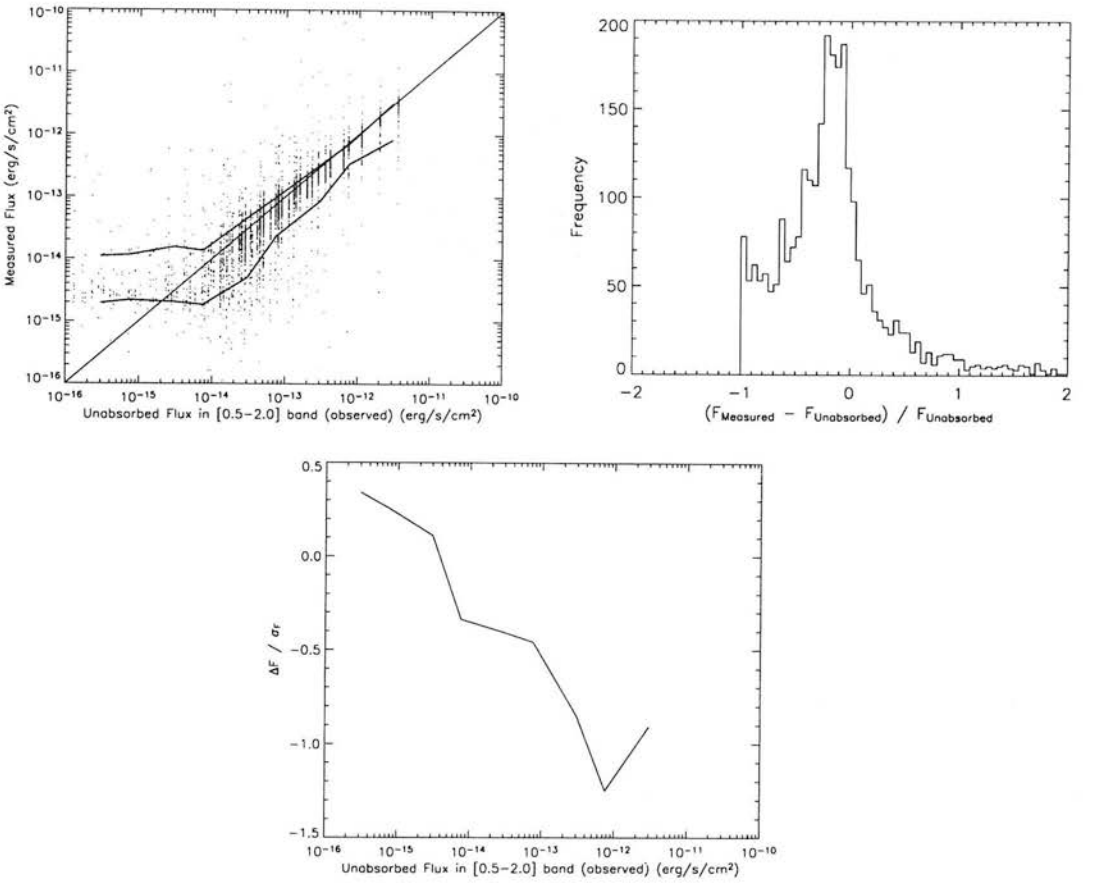

Figure 5.16: Comparison of measured fluxes with actual unabsorbed fluxes. The thick solid lines in the upper left plot denote the 68% confidence intervals for the measured fluxes, binned in unabsorbed flux. The lower plot shows the level of offset in flux recovery, quantified by the difference between the median recovered flux and the true flux.

lower as the true flux increases. However, this is to be expected for extended sources and the effect shall be quantified thoroughly as part of the selection function simulations (Section 5.3).

Association

The simulated clusters clearly should not be associated with any real sources in the literature tests. Inevitably, some will through chance alone. The number of these falsely-associated sources in the 10000 simulations provides an estimate of the probability that a real cluster candidate would be flagged as suspicious (Figure 5.17). These plots show that the rate of false flagging is very low ($\sim 5\%$). Most of the matches are

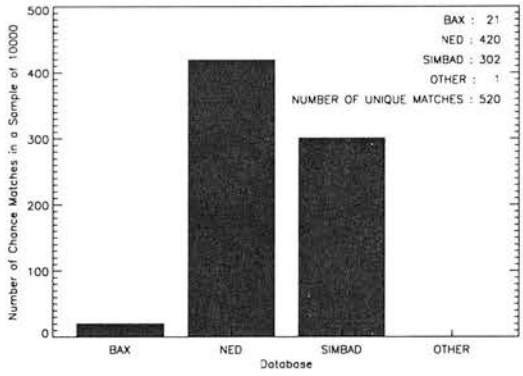

Figure 5.17: Rate of false source assocation found by generating 10000 random positions and matching them with the literature databases.

with low redshift galaxies and HII sources. While the association algorithms will certainly remove some genuine candidates the disadvantages are balanced by the improved purity of the XCS source lists.

5.3 Survey Selection Function

The validation of the algorithms has been successful and so we are able to begin the process of full characterisation.

5.3.1 Motivation

Many authors have shown how the abundance of clusters and its evolution with redshift can provide important cosmological information (for example, Gunn and Gott 1972; Oukbir and Blanchard 1997; Eke et al. 1996; Kitayama and Suto 1997). Improved technology has revealed the complexity of clusters and highlighted the necessity of careful analysis of the number counts. The influence of the cosmological parameters needs to be disentangled from biases in the detection algorithms and from natural variation in the cluster population. The flux observed from a distant cluster, and thus its probability of being detected, is affected by the cosmology. The survey selection function provides the connection between the true and observed cluster populations. In general, the survey selection function, Φ, can be defined as

$$\Phi\left[\mathrm{P}\left(>n\right) \mid L,\, z,\, T,\, \Omega_m,\, \Omega_\Lambda,\, \text{profile...}\right]$$

where P ($> n$) is the probability that a cluster of luminosity L, redshift z, temperature T in a cosmology (Ω_m, Ω_Λ) and with a given profile will be detected with at least n source photons.

The standards for survey selection functions have been set by projects such as Rosati et al. (1995); Vikhlinin et al. (1998); Adami et al. (2000). All of the above surveys (and our own) share a similar principle. We wish to find the probability that a cluster with a given set of parameters and under a certain cosmology would be found by the algorithms used to compile our statistical sample. This can be achieved, largely through brute force, by simulating sources with properties spanning the parameter range of interest, placing them in the XMM images, running XAPA and checking whether they would appear in the catalogue.

5.3.2 Batch Processing

For even a conservative choice of free parameters the number of simulations necessary is formidable. The three dominant parameters in terms of detection efficiency are expected to be cluster redshift, luminosity and temperature.

Run Configuration

For each combination of morphological (surface brightness profile, ellipticity, point source contamination) and cosmological (Ω_m, Ω_Λ) parameters we perform 70000 simulations. This is called a run and consists of 10 redshifts (linearly spaced from 0.1 to 1.0), 10 luminosities (logarithmically spaced from 0.178 to 31.623 $\times 10^{44}$ erg/s) and 7 temperatures (linear spacing from 2 to 8 keV). Each combination is repeated in 100 XMM pointings to reproduce the variance between fields.

Once the morphological and cosmological parameters have been chosen a file containing the configuration for the 70000 proposed simulations is created. This is done as follows

- 100 observation IDs are selected at random from the list of XCS StatSam pointings.
- Random off-axis and azimuthal angles are generated, ensuring a uniform probability across the field of view.
- Random orientations are chosen for the sources (this applies only to non-symmetrical profiles).
- The source configurations are output to file.

Processing

The simulation code has been designed to allow it to be run easily on as many machines as possible (all that is required is IDL and $\sim$ 100 Mb of disk space). The run of 70000 simulations is first divided into batches. The batch size is chosen to balance the load between the various computers working at the same time. A large batch size might mean a considerable wait for a particularly slow (or otherwise engaged) machine to finish before the run is complete. This would be an inefficient use of resources as many other machines could be left idle during such a period. For the current XCS set-up of 66 computers based at the ROE a batch size of 50 sources has been found to work well.

When a machine has been allocated a batch of sources it begins working through them one at a time. The machine reads the source parameters from the run configuration file and proceeds to generate the fake cluster, place it in the XMM image and run XAPA in precisely the same manner as described above in the Validation Section.

Depending on other users' processes, the typical run duration is one week. While this is not prohibitive we aim ultimately to have additional machines working on the task, either at other XCS member institutions or by gaining access to supercomputers (for instance, COSMOS[6]).

Example Results

The results for a typical run with a 3 keV beta model ($\beta = 0.66$, $r_c = 160$ kpc) in a concordance cosmology are shown in Figure 5.18.

The behaviour of the selection function is much as expected for this species of cluster. The detection efficiencies increase towards lower redshifts and higher luminosities, where the apparent brightness is greatest.

The numerical results obtained from this run, in the form which is useful for cosmology, are also presented in Table 5.1.

[6]http://www.damtp.cam.ac.uk/cosmos/Public/index.html

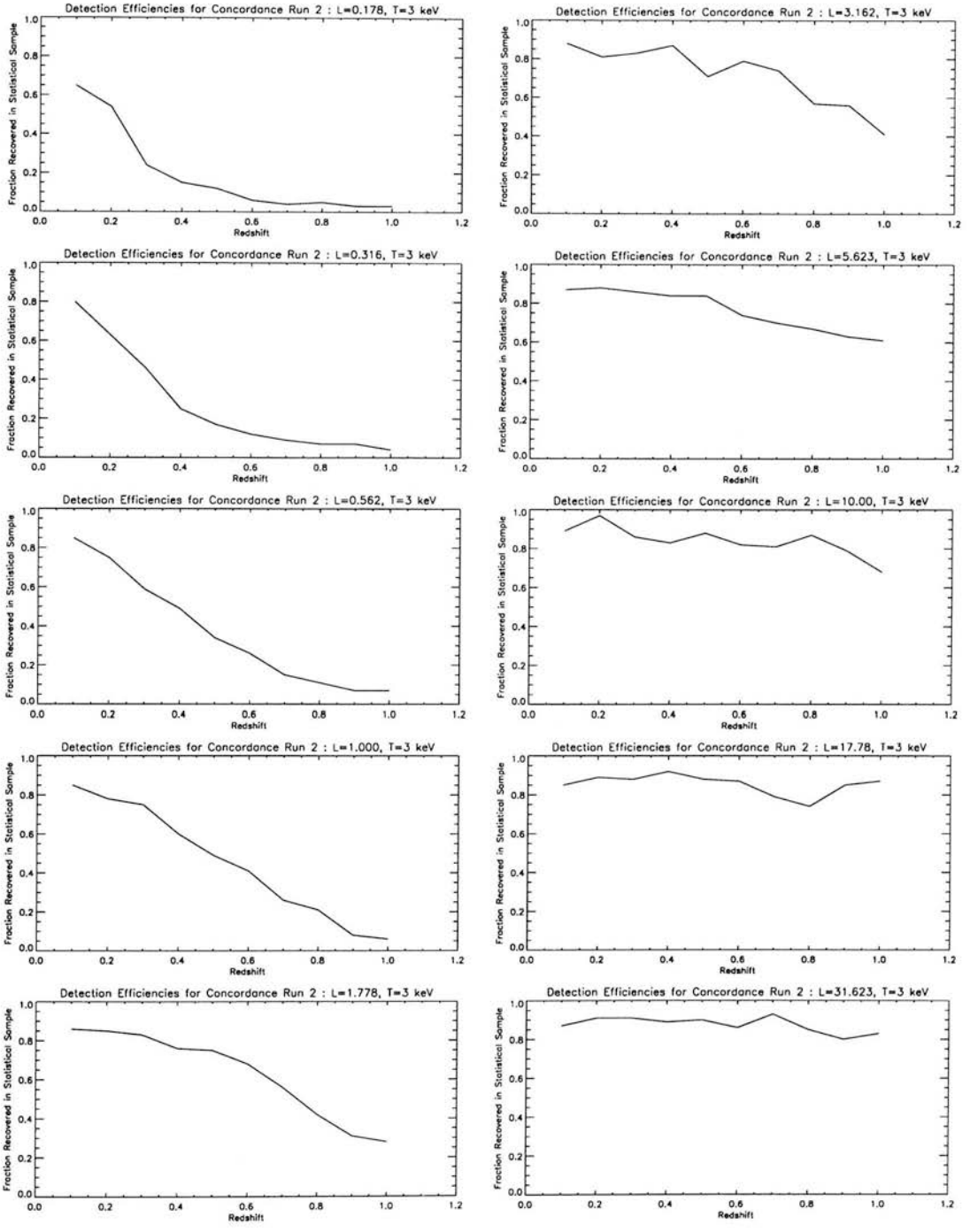

Figure 5.18: An example set of results from a selection function run.

z	L_{44} erg/s	DetEff_0	DetEff_{100}	DetEff_{250}	DetEff_{500}	DetEff_{1000}	DetEff_{2000}
0.1	0.178	0.65	0.60	0.54	0.44	0.27	0.11
0.1	0.316	0.80	0.74	0.69	0.62	0.47	0.26
0.1	0.562	0.85	0.82	0.82	0.75	0.61	0.43
0.1	1.000	0.85	0.85	0.85	0.82	0.71	0.62
0.1	1.778	0.86	0.85	0.85	0.85	0.83	0.76
0.1	3.162	0.88	0.88	0.88	0.87	0.84	0.78
0.1	5.623	0.87	0.87	0.87	0.87	0.87	0.84
0.1	10.000	0.89	0.88	0.88	0.88	0.88	0.86
0.1	17.783	0.85	0.85	0.85	0.85	0.85	0.85
0.1	31.623	0.87	0.86	0.86	0.86	0.86	0.86
0.2	0.178	0.54	0.39	0.25	0.14	0.01	0.00
0.2	0.316	0.63	0.51	0.33	0.18	0.09	0.02
0.2	0.562	0.75	0.68	0.62	0.43	0.17	0.10
0.2	1.000	0.78	0.72	0.70	0.60	0.40	0.20
0.2	1.778	0.85	0.84	0.80	0.72	0.62	0.40
0.2	3.162	0.81	0.81	0.78	0.72	0.67	0.55
0.2	5.623	0.88	0.88	0.87	0.84	0.80	0.68
0.2	10.000	0.97	0.97	0.97	0.97	0.93	0.89
0.2	17.783	0.89	0.89	0.88	0.87	0.86	0.82
0.2	31.623	0.91	0.91	0.91	0.91	0.91	0.89
0.3	0.178	0.24	0.15	0.06	0.00	0.00	0.00
0.3	0.316	0.46	0.25	0.17	0.06	0.02	0.00
0.3	0.562	0.59	0.49	0.31	0.16	0.06	0.00
0.3	1.000	0.75	0.66	0.56	0.36	0.18	0.03
0.3	1.778	0.83	0.75	0.66	0.52	0.33	0.10
0.3	3.162	0.83	0.80	0.75	0.64	0.56	0.36
0.3	5.623	0.86	0.85	0.80	0.73	0.61	0.48
0.3	10.000	0.86	0.85	0.82	0.78	0.70	0.59
0.3	17.783	0.88	0.88	0.87	0.85	0.82	0.75
0.3	31.623	0.91	0.89	0.89	0.89	0.86	0.81
0.4	0.178	0.15	0.03	0.01	0.01	0.00	0.00
0.4	0.316	0.25	0.15	0.03	0.01	0.00	0.00
0.4	0.562	0.49	0.39	0.21	0.07	0.01	0.01
0.4	1.000	0.60	0.49	0.35	0.17	0.05	0.00
0.4	1.778	0.76	0.70	0.51	0.29	0.16	0.04
0.4	3.162	0.87	0.79	0.66	0.53	0.31	0.10
0.4	5.623	0.84	0.79	0.75	0.65	0.42	0.25
0.4	10.000	0.83	0.83	0.78	0.70	0.59	0.44
0.4	17.783	0.92	0.92	0.91	0.84	0.77	0.68
0.4	31.623	0.89	0.89	0.88	0.86	0.80	0.73
0.5	0.178	0.12	0.03	0.01	0.01	0.00	0.00
0.5	0.316	0.17	0.08	0.03	0.00	0.00	0.00
0.5	0.562	0.34	0.24	0.12	0.01	0.00	0.00
0.5	1.000	0.49	0.36	0.20	0.05	0.00	0.00
0.5	1.778	0.75	0.64	0.40	0.20	0.04	0.01
0.5	3.162	0.71	0.63	0.49	0.35	0.20	0.03
0.5	5.623	0.84	0.78	0.70	0.62	0.42	0.13
0.5	10.000	0.88	0.83	0.78	0.68	0.55	0.30
0.5	17.783	0.88	0.86	0.79	0.73	0.63	0.54
0.5	31.623	0.90	0.87	0.84	0.81	0.73	0.62
0.6	0.178	0.06	0.01	0.00	0.00	0.00	0.00
0.6	0.316	0.12	0.04	0.01	0.00	0.00	0.00
0.6	0.562	0.26	0.15	0.01	0.00	0.00	0.00
0.6	1.000	0.41	0.26	0.14	0.05	0.00	0.00
0.6	1.778	0.68	0.47	0.24	0.05	0.02	0.00
0.6	3.162	0.79	0.66	0.50	0.27	0.06	0.02
0.6	5.623	0.74	0.67	0.59	0.42	0.20	0.09
0.6	10.000	0.82	0.74	0.68	0.57	0.35	0.16
0.6	17.783	0.87	0.83	0.74	0.67	0.57	0.38
0.6	31.623	0.86	0.86	0.83	0.76	0.67	0.52
0.7	0.178	0.04	0.00	0.00	0.00	0.00	0.00
0.7	0.316	0.09	0.00	0.00	0.00	0.00	0.00
0.7	0.562	0.15	0.05	0.03	0.02	0.01	0.01
0.7	1.000	0.26	0.16	0.06	0.01	0.00	0.00
0.7	1.778	0.56	0.38	0.13	0.06	0.01	0.00

0.7	3.162	0.74	0.55	0.31	0.11	0.06	0.00
0.7	5.623	0.70	0.54	0.41	0.24	0.12	0.01
0.7	10.000	0.81	0.71	0.58	0.48	0.30	0.12
0.7	17.783	0.79	0.74	0.66	0.56	0.44	0.23
0.7	31.623	0.93	0.91	0.84	0.77	0.66	0.43
0.8	0.178	0.05	0.01	0.01	0.01	0.00	0.00
0.8	0.316	0.07	0.01	0.00	0.00	0.00	0.00
0.8	0.562	0.11	0.00	0.00	0.00	0.00	0.00
0.8	1.000	0.21	0.11	0.03	0.01	0.00	0.00
0.8	1.778	0.42	0.23	0.12	0.01	0.00	0.00
0.8	3.162	0.57	0.40	0.25	0.09	0.01	0.00
0.8	5.623	0.67	0.55	0.36	0.17	0.09	0.01
0.8	10.000	0.87	0.73	0.62	0.42	0.22	0.08
0.8	17.783	0.74	0.70	0.62	0.52	0.34	0.15
0.8	31.623	0.85	0.84	0.77	0.70	0.60	0.39
0.9	0.178	0.03	0.00	0.00	0.00	0.00	0.00
0.9	0.316	0.07	0.00	0.00	0.00	0.00	0.00
0.9	0.562	0.07	0.02	0.00	0.00	0.00	0.00
0.9	1.000	0.08	0.04	0.00	0.00	0.00	0.00
0.9	1.778	0.31	0.18	0.03	0.01	0.00	0.00
0.9	3.162	0.56	0.33	0.15	0.04	0.02	0.00
0.9	5.623	0.63	0.50	0.28	0.15	0.06	0.00
0.9	10.000	0.79	0.63	0.49	0.30	0.12	0.01
0.9	17.783	0.85	0.81	0.70	0.52	0.28	0.10
0.9	31.623	0.80	0.76	0.68	0.57	0.44	0.25
1.0	0.178	0.03	0.00	0.00	0.00	0.00	0.00
1.0	0.316	0.04	0.01	0.01	0.00	0.00	0.00
1.0	0.562	0.07	0.01	0.01	0.00	0.00	0.00
1.0	1.000	0.06	0.01	0.00	0.00	0.00	0.00
1.0	1.778	0.28	0.14	0.05	0.00	0.00	0.00
1.0	3.162	0.41	0.31	0.10	0.01	0.00	0.00
1.0	5.623	0.61	0.41	0.20	0.08	0.00	0.00
1.0	10.000	0.68	0.57	0.43	0.19	0.10	0.00
1.0	17.783	0.87	0.78	0.61	0.46	0.20	0.07
1.0	31.623	0.83	0.74	0.69	0.62	0.32	0.13

Table 5.1: Example Detection Efficiency table.

The table also includes the detection efficiencies as a function of detected source counts. This is crucial; if a cluster is detected with a sufficient number of photons (~ 500) then it is possible to obtain an X-ray redshift without further dedicated follow-up. This subset of clusters is very valuable for constraining cosmology, as is discussed in the next section.

5.4 Constraints on Cosmology

One of the fundamental science aims of XCS is to constrain the values of the cosmological parameters Ω_m, Ω_Λ and σ_8. To do this the abundance of clusters as a function of redshift and temperature must be measured so that they can be compared to predictions.

5.4.1 Parameter Estimation Methodology

The XCS parameter estimation methodology has been set out in detail in Viana et al. (2006, in prep.). The method consists of two stages; 1000 mock XCS catalogues are generated and then the most likely underlying cosmology is determined.

The mock catalogues contain $T > 2$ keV, $z < 2$ clusters which are X-ray luminous enough for X-ray temperatures to be obtained without further follow-up. They are created by drawing randomly from a Poisson distribution with the mean number of clusters, as a function of T and z, as expected from the fiducial model with $\Omega_m = 0.3$, $\Omega_\Lambda = 0.7$ and $\sigma_8 = 0.8$. The mass function used is that of Jenkins et al. (2001) and Evrard et al. (2002), which has been shown to be appropriate for a wide range of cluster masses. There are several important assumptions made:

- $M_{500} - T_X$ relation is normalized to the present day cluster number density and evolves self-similarly
- $L_X - T_X$ relation is assumed not to evolve with redshift
- Scatter in the above relations and errors in L_X, T_X and z are not considered.

Some of these assumptions are more reasonable than others. The $M-T$ relation has been shown to be consistent with self-similar evolution in both simulations (e.g. Muanwong et al. 2002) and observations (e.g. Ota and Mitsuda 2004a; Ettori et al. 2004b), with only a small scatter. This may not be true at the scale of groups (for instance, Ponman et al. 1999; Davé et al. 2002). It is unlikely, however, that the non-evolving $L - T$ is realistic (e.g. Ettori et al. 2004a). The 'no-evolution' assumption predicts the lowest number of XCS clusters and therefore results in conservative estimates for the cosmological parameters. XCS should eventually derive a more appropriate $L - T$ relation. Work is currently being performed to assess the significance of the scatter on the observational parameters L_X, T_X and z (Viana et al. in prep). The dominant factor is the estimate of z. Random scatter of up to 20% in the photometric redshifts appears to be acceptable, although systematic errors would be more serious. Overall, the assumptions are valid but with the caveat that stronger constraints will eventually be obtained.

The likelihood method is based on that described in Holder et al. (2001) which uses the Cash (1979) extension to χ^2 minimization. However, the XCS technique (Viana et al. 2006, in prep) considers not only the observed number of clusters when finding the best-fitting parameters, but also the distribution of cluster properties (z, T_X and

Run ID	Ω_m	Ω_Λ
1	0.22	0.78
2	0.26	0.74
3	0.30	0.70
4	0.34	0.66
5	0.38	0.62

Table 5.2: First set of concordance cosmology runs to be performed.

L_X). The probability distributions for the cosmological parameters of interest are then found by marginalizing over the other parameters.

5.4.2 Initial Selection Function Runs

As explained above, it is important that the selection function of the survey is known to sufficient accuracy. However, this is a computationally open-ended task and a first order, gross profile of the function can be found by performing a relatively small number of runs.

The first set of runs to be performed and analysed are summarized in Table 5.2. For these, canonical clusters ($\beta = 0.66$, $r_c = 160$ kpc, $e = 0.0$) in flat universes ($\Omega_m + \Omega_\Lambda = 1$) are used.

The predicted constraints arising from this small set of simulations are discussed in the next section.

5.4.3 Predicted Constraints Based on 240 Clusters

Likelihood distributions that result from using the XCS selection function obtained for the cosmologies in Table 5.2 have been calculated. The distributions for Ω_m and σ_8 are shown in Figure 5.19. These constraints assume that we will eventually measure temperatures for $\sim$ 240 clusters from the archive. The XCS-NOAO survey (Section 6.5.2) will provide the redshifts necessary for X-ray temperature measurements within a timescale of three years.

For contrast, we also include the predicted constraints found under the assumption that the XCS selection function does not depend on Ω_m (Figure 5.20). The difference between these two sets of figures is striking (and works in our favour). Including the dependence of the XCS selection function on Ω_m leads to tighter constraints on the cosmological parameters. The cosmological constraints improve as the predicted nor-

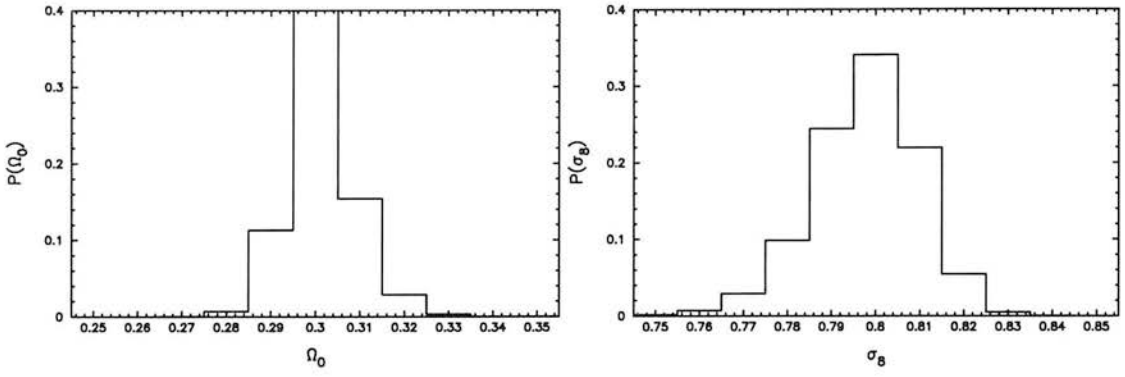

Figure 5.19: The predicted marginalized probability distributions for Ω_m and σ_8, based on the initial five concordance cosmology simulation runs (95% confidence level). Figure courtesy of P. Viana.

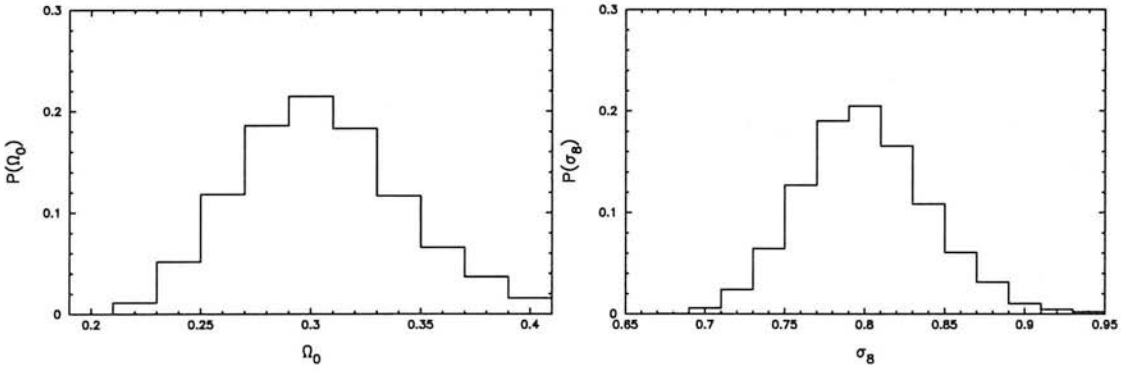

Figure 5.20: As Figure 5.19 but under the assumption that the XCS selection function is independent of the cosmology. Figure courtesy of P. Viana.

malization and distribution of temperatures for each combination of $(\Omega_m, \Omega_\Lambda)$ become increasingly different. With the current XCS selection function we predict that Ω_m and σ_8 shall be constrained within $\sim 15\%$ and $\sim 4\%$ respectively. On the other hand, this highlights a potential sensitivity of the algorithms which must be mapped fully before the results can be relied upon.

5.4.4 Projected Selection Function Runs

The process of measuring redshifts and temperatures for the XCS clusters will take several years and so there is plenty of time for the selection function simulations to be performed. The choice of runs will be dynamic; the results of previous simulations will inform the direction of later ones. This will ensure that the parameter space will

Run ID	Ω_m	Ω_Λ
6	0.28	0.72
7	0.32	0.68

Table 5.3: Second set of concordance cosmology runs to be performed.

Run ID	Ω_m	Ω_Λ
8	0.26	0.60
9	0.26	0.80
10	0.30	0.60
11	0.30	0.80
12	0.34	0.60
13	0.34	0.80

Table 5.4: Proposed set of non-flat cosmology runs to be performed, with Ω_Λ as a free parameter.

be covered efficiently, focussing on variables which are most sensitive to the underlying cosmology.

Analysis of the initial set of cosmologies has confirmed that the constraining power of the survey will be maximised by concentrating future simulations on a smaller range around the concordance cosmology. As such, the next runs to be performed are presented in Table 5.3.

Once these are complete the assumption of flatness will be lifted, allowing Ω_Λ to vary freely and be fitted. The Ω_Λ runs are presented in Table 5.4 and shall take approximately two months of processing time.

Other planned runs cover a selection of morphologies; a range of β models, NFW models and ellipticities. By the time these runs are completed a significant fraction of clusters will have the data necessary to produce the first XCS constraints on cosmology.

Chapter 6

XCS Statistical Sample

The purpose of this chapter is to begin the process of adding value to the statistically-defined sample of cluster candidates in the XCS, hereafter known as the XCS StatSam. This shall be done by, wherever possible, confirming the existence of the clusters of galaxies and obtaining redshifts for them. The full follow-up and exploitation of the StatSam will take the XCS collaboration several years and is therefore beyond the scope of this thesis. However, we shall explore a few interesting examples before outlining the proposed optical follow-up programme for the catalogue.

6.1 Cluster Confirmation

Even though great care has been taken in the preparation of the XCS candidate lists we expect them to contain a number of false sources. This is due to the necessary balance between survey completeness and reliability. Here we present a variety of methods designed to confirm the reality of our candidates and to help in the selection of the highest redshift clusters.

6.1.1 Archival Imaging Surveys

Mnay of the potential sources of contamination of the survey can be spotted trivially through examination of the available archival data on the candidate's position. The most useful optical surveys are the Digitized Sky Survey (DSS, Lasker et al. 1990), SuperCOSMOS Sky Survey (SSS, Hambly et al. 2001) and the Sloan Digital Sky Survey

(SDSS, Stoughton et al. 2002). The DSS and SSS are invaluable because they have coverage of the whole sky, with the SSS probing slightly fainter ($R \sim 19$ compared to ~ 18), thus ensuring excellent overlap with the XCS. The SDSS explores deeper than either of these surveys but it is not full-sky. Its current survey area is 6670 square degrees, confined mostly to the northern hemisphere. SDSS also provides 3-colour JPEG images which assists the assessment of a candidates veracity as clusters often appear as close associations of red galaxies.

Although, the primary reason for using these catalogues is to look for obvious over-densities of galaxies at the cluster position they also reveal non-cluster emission. These can be close blends of point sources, parts of very low redshift galaxies, star clusters or detections of individual galaxies. They can also be used to spot putative XMM PSF lobe sources if the candidate lies very close to a bright star, for example.

Use of other wavebands, for instance the VLA-NVSS radio survey (Condon et al. 1998) and 2MASS (Kleinmann et al. 1994) in the infrared, can help identify sources such as AGN, although this may not be conclusive due to the presence of AGN in clusters of galaxies.

However, it is not always straightforward to decide which (if any) visible galaxies truly have a physical association with the X-ray emission. The eye can be misleading, especially if there is no obvious Brightest Cluster Galaxy (BCG) or if the source is a poor, loose group. Ideally, we could cross-correlate our candidate lists with a carefully selected group/cluster catalogue.

6.1.2 Existing Group/Cluster Catalogues

The ultimate resource for the task at hand would be an all-sky catalogue of galaxies with spectroscopic redshifts, complete to the redshift limit of XCS (~ 1.5). Of course, this is fanciful and in reality we desire a large area catalogue with well-defined selection criteria. It should be emphasized here that it is beyond the ambition of the current work to generate a group catalogue.

Since Huchra and Geller (1982) galaxy redshift surveys have been used to compile group catalogues. Traditionally, the algorithm used to do so has been of the Friends-of-Friends (FoF) variety in which linking lengths are specified and galaxies above a certain over-density are associated. There have been several such catalogues, making use mostly of the 2dfGRS and more recently the SDSS (for example, Eke et al. 2004; Weinmann et al. 2005; Merchán and Zandivarez 2005; Miller et al. 2005). The properties of these catalogues are summarized in Table 6.1. While great care has been taken in the

Group/Galaxy Catalogue	Area	N	z	N_{gals}
2PIGG : 2dfGRS	~ 1500 deg^2	~ 29000	< 0.2	2+
SDSSDR3GG : SDSS SpectroDR3	4188 deg^2	10864	< 0.3	4+
Weinmann : SDSS SpectroDR2	~ 1950 deg^2	~ 53000	< 0.2	2+
C4 : SDSS SpectroDR2	~ 2600 deg^2	~ 748	< 0.17	10+

Table 6.1: Summary of a sample of existing group catalogues. The number of groups in each catalogue is N and the minimum number of galaxies required is N_{gals}.

creation of these catalogues, in practice they are of limited use to the XCS. The main reason for this is the small number of cross-matches found between them and the XCS StatSam. This can be attributed to a set of circumstances. The most relevant is the choice of galaxies used for each catalogue. All of the existing large group catalogues are based on galaxy redshift catalogues which are typically limited by apparent magnitude. Thus, galaxies fainter than the limit are 'invisible' to the group-finder. The implicit assumption appears to be that the luminosity function of the group galaxies is identical to that of the population as a whole. This leads to an unavoidable bias towards low redshift groups because higher redshift ones have only a few (if any) galaxies in the magnitude range.

This is confirmed by the small number of matches actually found when matching with, for instance 2PIGG, is carried out. Neglecting the small effect of overlapping XCS area, the expected maximum number of 2PIGG matches in the XCS StatSam should be of the order of 250 (scaling to the XCS area in the 2PIGG survey and assuming that all the groups are X-ray emitting). The observed number of matches is only 11. One of these is a known group, 4 are good new candidates and the remainder are unconfirmed or possible artifacts. Given that there may be little X-ray emission from many of the poor 2PIGG groups it is not altogether surprising that there are so few matches. The matched known group, XMMXCS J220206.1-315909.0 (Figure 6.1), is at z=0.009 and, being so close, is not typical of the XCS candidates.

A further issue with spectroscopic galaxy redshift surveys is fibre collision. There is a minimum separation distance a pair of galaxies can have before it becomes impossible to obtain spectra simultaneously for them due to the optical fibres colliding. It is possible for observations to be repeated but usually one of the galaxies is left without a measured redshift. The relevant collision distances are 55" for SDSS and 30" for 2dfGRS. This affects compact or distant groups most severely as only the BCG is measured and the

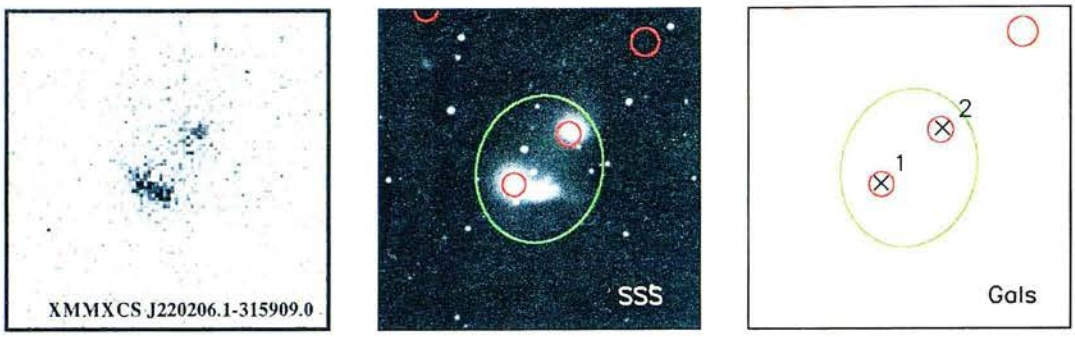

Figure 6.1: From left to right; X-ray image for XMMXCS J220206.1-315909.0, optical image with detected X-ray sources (green ellipses for extended sources and red for points), and the matched galaxy positions.

others are missed. It is expected that the XCS StatSam will contain many such sources which will therefore go unmatched.

Similar effects are seen with the other existing group catalogues (SDSSDR3GG and SDSS-Weinmann). Seeing as these catalogues are created from limited (albeit large) areas of sky it seems that they offer only minimal help to the process of XCS cluster confirmation. They may provide piecemeal matches to a handful of clusters but shall not be adequate for the task as a whole.

6.1.3 SSS/2MASS Galaxy Catalogue

As previously mentioned, in order to make significant headway in the confirmation of XCS clusters the ideal resource would be a moderately deep, large area, uniform catalogue of galaxies. Such a catalogue can be compiled by utilising existing all-sky surveys, thus providing a multi-wavelength sample of galaxies.

SuperCOSMOS Sky Survey

Over the past twenty years there has been a considerable effort spent on digitizing the vast quantity of archival imaging data stored as photographic plates. Having the data in digital form greatly enhances the scientific potential of the surveys, enabling relatively straightforward synergy with external databases. Of these projects, for instance, APM (Kibblewhite et al. 1984), COSMOS (MacGillivray and Stobie 1984) and DSS (Lasker et al. 1990), the SuperCOSMOS Sky Survey (Hambly et al. 2001) is the most ambitious.

The SSS has used plates from the UK Schmidt Telescope (UKST), ESO Schimdt

and Palomar Schmidt telescopes to cover the entire sky in two wavebands (B and R) and two epochs (in R). A third band, I, has full coverage in the southern hemisphere and is scheduled to be complete in the north in spring 2006. In addition to the imaging data, source detection has been performed with care being taken over classification, deblending and photometry. The SSS catalogues are available through the SuperCOSMOS Science Archive[1] (SSA). The SSA is a phenomenal data source containing over 1 billion unique sources and 2.5Tb of imaging data. An additional benefit is the pixel size of 0.7", smaller than previous sky surveys including DSS-I and DSS-II.

In terms of photometry and astrometry, the SSS is a well-defined and accurate survey (positional errors are $< 0.3''$ and $\sigma_{B,R} < 0.3$ mag). By heeding the appropriate flags and caveats a sample of galaxies in the SSS has been made available in the form of the "ReliableGalaxies" view of the SSA database[2].

Two Micron All Sky Survey

The Two Micron All Sky Survey (2MASS) is another ambitious project which has mapped the entire sky in the infra-red waveband. Between 1997 and 2001 two automated 1.3m telescopes, one in the North (Mt. Hopkins, Arizona) and one in the South (CTIO, Chile), scanned almost the full sky. They were equipped with cameras to enable simultaneous imaging in three bands, J (1.25 micron), H (1.65 micron) and Ks (2.17 micron) with a resolution of 1". Included with the final All-Sky Data Release[3] were the Point Source Catalog (PSC) and Extended Source Catalog (XSC), Jarrett et al. (2000), containing, respectively, 471 and 1.6 million unique sources. The PSC comprises unresolved sources which are almost exclusively stars in the Milky Way and Magellanic Clouds. Resolved sources are identified by a combination of features including whether they can be fitted to a single PSF, their size, central surface brightness and colours. The composition of the XSC is 97% galaxies with the remainder a variety of galactic objects such as planetary nebulae, young stellar objects and HII regions. When the area around masked bright stars (and other small instrumental effects) is accounted for, the XSC covers 98% of the sky.

The stated magnitude limits for each of the bands are 15.0, 14.2 and 13.5 for J, H and K. While there are many different methods for measuring the flux and magnitudes of extended sources there is no general scheme for doing so and this must be borne in mind

[1]The SSA can be accessed at http://surveys.roe.ac.uk/ssa.

[2]See http://surveys.roe.ac.uk/ssa/www/ssa_browser.html.

[3]Available from http://www.ipac.caltech.edu/2mass/releases/allsky/index.html.

in the following work. Definition and measurement of the errors on the magnitudes near the limits is also difficult. Due to the extensive calibration work done by the 2MASS team it is reasonable to use the catalogued values.

SuperCOSMOS All-Sky Galaxy Catalogue

Both the SSS and 2MASS cover practically the whole sky to approximately the same depth ($z \sim 0.3$) and with similar resolution. Thus, there should be many cross-matches between galaxies detected in SSS (B and R bands) and the 2MASS XSC (J, H and K bands). This cross-matching has been performed by John Peacock (in prep.) who has produced a catalogue, the SuperCOSMOS All-Sky Galaxy Catalogue (SASGC), containing the extinction-corrected 5-band data with positions for each galaxy. There is considerable background in the literature to the subject of association of sources in different catalogues (for example, Sutherland and Saunders 1992; Mann et al. 1997) but as a first approximation using a fixed matching radius of 10", as has been done for SASGC, is acceptable. This is especially true when the angular resolution of the data is good, as is the case for these optical and infrared surveys. This matching radius is also comparable to the minimum angular size of galaxies reliably detectable in the 2MASS XSC.

The SASGC contains 1645874 unique sources. Not all galaxies have been detected in all five bands (or occasionally the magnitude estimation fails). However, this issue is small; 1250018 galaxies have full 5-band information and 97.3% have at least three magnitudes.

6.1.4 Association of Galaxies with XCS Candidates

It is expected that many of the XCS candidates will have galaxies visible in the archival optical/IR data, if only the BCG. By employing a quantitative statistic to describe the probability of an association between the X-ray emission and the SASGC galaxies we can make strides into the task of cluster confirmation. Indeed, we shall also be able to identify non-cluster candidates such as extended emission from individual galaxies. As will be discussed later in this chapter, we shall even be able to obtain redshifts for a significant fraction of our candidates in this automated fashion.

For a given XCS candidate we search for matching SASGC galaxies within a fixed matching radius of 3' (candidates larger than this are unlikely to be detected by the algorithms). The question is then "what is the probability that this is a chance match?". Rather than answering this question by *a priori* methods such as the Likelihood Ratio,

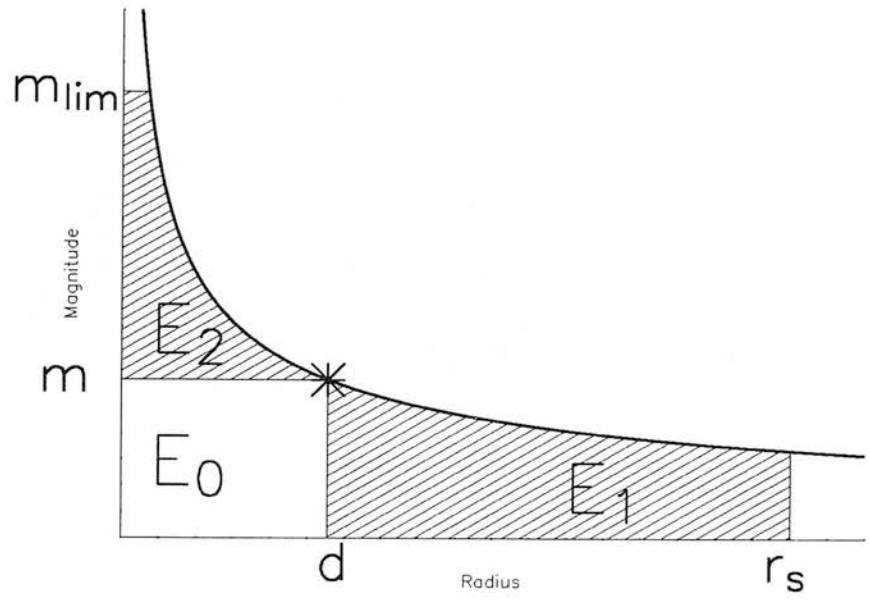

Figure 6.2: A sketch of the relevant probabilities E_0, E_1 and E_2. The thick line is the locus of constant chance probability P^*. The star symbol denotes the position on the locus of the putative cluster member.

which requires (unknown) information on the underlying population, we choose to follow the example set by Browne & Cohen (1978), Downes et al. (1986) and Serjeant et al. (2003).

In their Poisson Clustering Hypothesis the above question is addressed by calculating the probability that a galaxy of magnitude m at a distance d from the X-ray position is there by chance. If the surface density of galaxies with magnitudes $\leq m$ is $N[\leq m]$ then the expected number to be found $\leq d$ is

$$E_0 = \pi d^2 N[\leq m]$$

If this expected value is small then the Poisson probability of matching with at least one object is $P \approx E_0$. However, to properly assess the chance of a random match we must also consider both brighter and fainter galaxies which, by their nature, will have lower and higher surface densities respectively. For a given probability P^* there will be galaxies with magnitudes $\leq m$ at $r \geq d$ and similarly ones $\geq m$ at $r \leq d$ (see Figure 6.2 for an illustration).

The expected number of matches with $P \leq P^*$ is then $E = E_0 + E_1 + E_2$, where E_1 and E_2 are the contributions from brighter and fainter objects. These values can be

calculated for a survey with a maximum search radius r_s and limiting magnitude $m_{\rm lim}$

$$\begin{aligned} E_1 &= \int_d^{r_s} N[\leq m_{\rm max}(r)]\ 2\pi r\ {\rm d}r \\ E_2 &= \int_m^{m_{\rm lim}} n(m)\,{\rm d}m \int_0^{r_{\rm max}(m)} 2\pi r\ {\rm d}r \end{aligned}$$

where $r_{\rm max}$ and $m_{\rm max}$ are the maximum radius and magnitude which could satisfy the constant probability condition. They are related to the probability E_0 as

$$\begin{aligned} E_0 &= \pi r^2 N[\leq m_{\rm max}(r)] \\ E_0 &= \pi r_{\rm max}^2 N[\leq m]. \end{aligned}$$

The integrals for E_1 and E_2 can thus be performed

$$\begin{aligned} E_1 &= \int_d^{r_s} \frac{2E_0}{r}\,{\rm d}r \\ &= 2E_0 \ln\left(\frac{r_s}{d}\right) \\ &= E_0 \ln\left(\frac{r_s^2}{d^2}\right) \end{aligned}$$

and

$$\begin{aligned} E_2 &= \int_m^{m_{\rm lim}} n(m)\,{\rm d}m\ \pi r_{\rm max}^2(m) \\ &= \int_{N[\leq m]}^{N[\leq m_{\rm lim}]} {\rm d}N[\leq m]\ \pi r_{\rm max}^2(m) \\ &= \int_{N[\leq m]}^{N[\leq m_{\rm lim}]} \frac{E_0}{N[\leq m]}\,{\rm d}N[\leq m] \\ &= E_0 \ln\left(\frac{N[\leq m_{\rm lim}]}{N[\leq m]}\right) \end{aligned}$$

leading to

$$E = E_0\left[1 + \ln\left(\frac{r_s^2 N[\leq m_{\rm lim}]}{d^2 N[\leq m]}\right)\right].$$

Defining a new probability $E_c \equiv \pi r_s^2 N[\leq m_{\rm lim}]$ and recalling that $E_0 = \pi d^2 N[\leq m]$ results in the modified expectation value

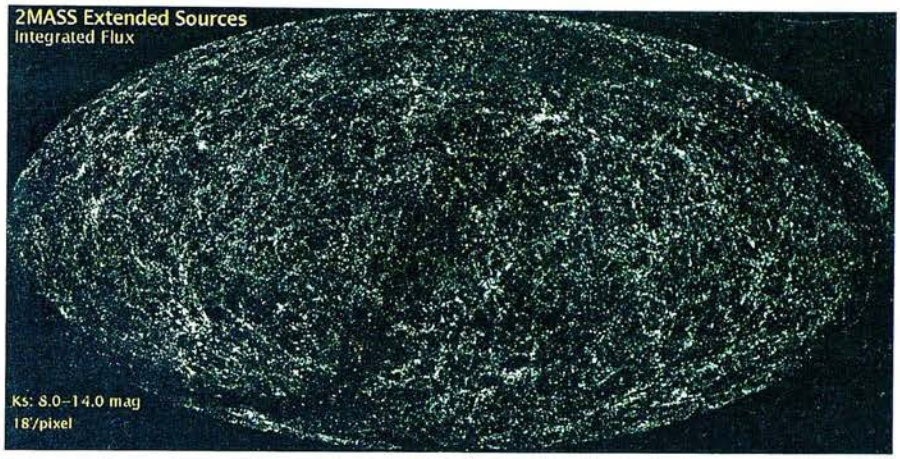

Figure 6.3: Aitoff projection of the distribution of the XSC sources (Credit: 2MASS).

$$E = P^*[1 + \ln(E_c/E_0)].$$

The probability that a galaxy (with P^*) has been matched by chance is thus $[1 - \exp(-E)]$.

For SASGC we found that almost the entire sample had K magnitudes (99.97%) so we used this band and a maximum search radius of 3' for the matching. This is a more reliable estimate of the probability that the match is due to chance, but there are several causes of uncertainty.

It has been known for many years that the distribution of galaxies on the sky is not uniform and so the assumption of a single SASGC galaxy density is invalid. This can be illustrated beautifully by simply plotting the positions of the 2MASS XSC galaxies (Figure 6.3).

Clearly, there is significant non-Gaussianity in the distribution of mass (or galaxies, at least). This can be quantified by counting the galaxies in cells on the sky. The distribution of the counts is shown in Figure 6.4.

If the cells were Poisson sampling from an underlying Gaussian distribution then we would expect the histogram to be a Gaussian with an analytically-predictable width. In fact, the width is greater than expected from Poisson statistics and the distribution is better fitted by a lognormal model, as first noted by Hubble (1934). This shape often arises when small deviations are compounded multiplicatively, as occurs during gravitational collapse. This is a well-known feature. The lognormal distribution is inconvenient to work with, unlike the Poisson distribution, as it has a more complicated

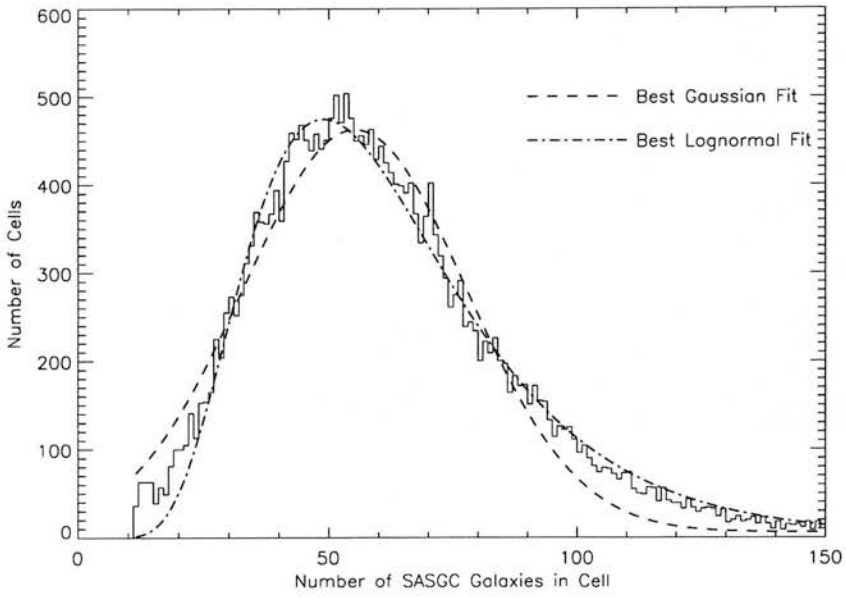

Figure 6.4: The distribution of galaxy cell-counts for SASGC. The lognormal model provides a better fit for the range of clustering strength.

expectation and variance. Thus, as an approximation, we have divided the sky into 400 equal area cells. We then assume that the distribution within each cell is Poissonian rather than lognormal. Smaller cells would lead to better local surface density estimates but, unfortunately, due to the requirement of binning in K magnitude as well as position, shot noise would introduce large errors in these estimates. The chosen scale should deal with the most egregious local clustering.

With the above points in mind, we then decided which SASGC galaxies were associated with XCS candidates by imposing a (rather arbitrary) threshold chance-probability of 0.10. The value may not be entirely accurate but it should allow us to state with reasonable confidence whether or not a match is likely to be due to chance. Simulations have been performed to check the actual probability of a chance match. A large number (54400) positions where generated at random from the XCS distribution of RAs and Decs and matched with SASGC. The measured rate of false matches was 0.03, lower than the desired 0.10 but indicative that the measured probabilities are conservative.

The number of sources in the XCS StatSam with at least one matched SASGC galaxy is encouraging. Of the known clusters in the StatSam there were 53 matches out of 142, and of the new candidates there were 219 from 1622. The rate of matching is clearly higher for the known sample (35% compared to 15%) but this is to be expected as

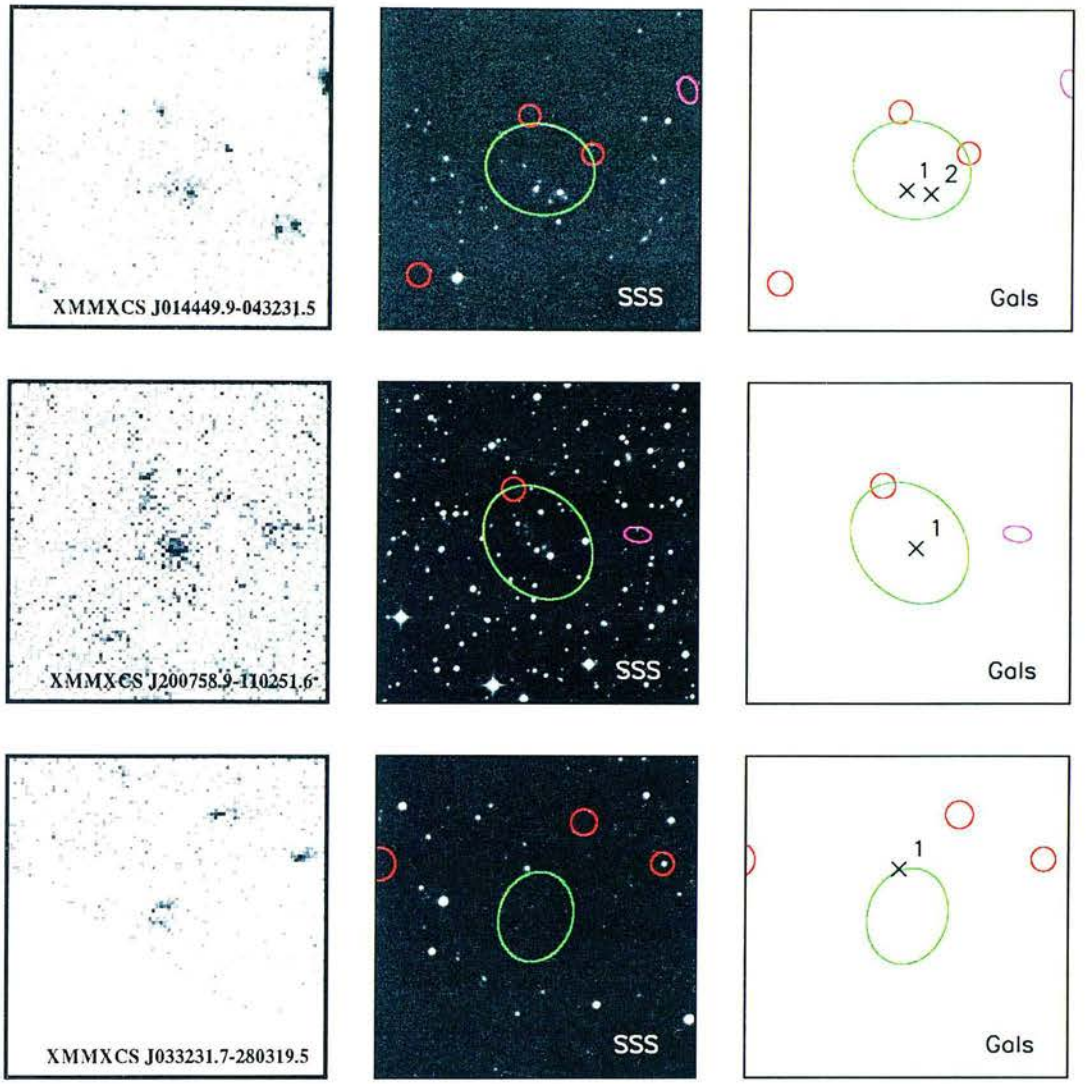

Figure 6.5: Three examples of the new candidate matches. Top) A secure match with two galaxies; middle) a good match with only the BCG; and bottom) a chance match of a galaxy with a pair of blended point sources at the edge of the FOV.

the known cluster sample will be, in general, at lower redshift. The majority of matched sources are with only one galaxy (often the BCG, such as XMMXCS J200758.9-110251.6 in Figure 6.5). There are a handful of obviously erroneous matches, comparable in number to that predicted by chance alone (around 4 in the known sample). The new candidates also appear to be mostly successful matches. Some of these were observed in August 2005 using the University of Hawaii's 2.2m telescope (see Section 6.2.4). A selection of illustrative examples is presented in Figure 6.5.

Catalogue	Area	N	z	Reference
2dfGRS	~ 1500 deg^2	221414	< 0.2	Colless et al. (2003)
6dfGRS	~ 20000 deg^2	~ 90000	< 0.3	Jones et al. (2004)
CfA ZCAT	~ 30000 deg^2	~ 433246	< 0.3	Huchra et al. (1996)
SDSS DR4	4783 deg^2	565715	< 0.3	Adelman-McCarthy (2005)
UZC	~ 20000 deg^2	19372	< 0.07	Falco et al. (1999)

Table 6.2: Summary of a sample of existing galaxy redshift catalogues.

While this information is useful, the most valuable information on a cluster candidate is its redshift.

6.2 Redshifts

In general, the redshift of a cluster of galaxies is measured by obtaining spectra for several galaxies appearing to be part of the cluster, fitting redshifts to the spectra then confirming an overdensity. In practice this process requires time and resources. Imaging observations need to be performed in order to pick galaxies for further spectroscopic study. If we hope to complete the follow-up of a survey of the size of the XCS, in a reasonable timescale, we need to find a way to use existing data as much as possible. Pointed follow-up observations can then be prioritized for the remaining candidates.

6.2.1 Spectroscopic Galaxy Redshifts

Given that we expect most of our candidates to be at low redshifts (less than $z \sim 0.3$, depending on the results of the selection function) the obvious approach is to look for individual galaxies with spectroscopic redshifts in the literature. Since the advent of multi-object spectrometers there have been been several galaxy redshift surveys probing to moderate depths. A selection of major surveys along with their areas, depths and number of galaxies is presented in Table 6.2. By combining the 2dfGRS, 6dfGRS, CfA ZCAT, SDSS DR4 and UZC catalogues we instantly have a large (686246 sources) sample of spectroscopic redshifts, albeit with some duplicates. Unsurprisingly, a large fraction of these were matched to counterparts in the SASGC using a simple 10" pairing radius (Peacock et al. in prep.). Of the 1645874 SASGC galaxies 361050 have spectroscopic redshifts in the literature. The distribution of these matches reaches out to $z \sim 0.4$ (Figure 6.6).

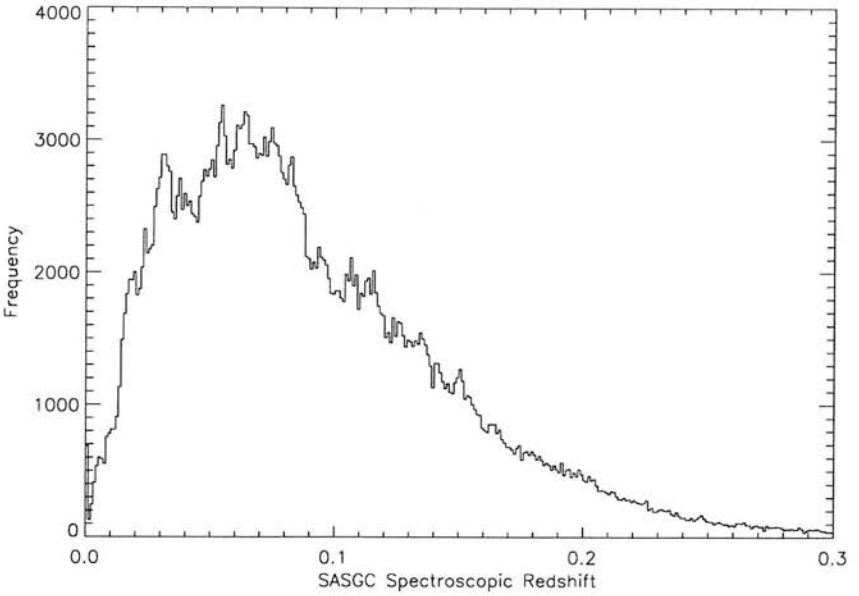

Figure 6.6: The distribution of the galaxies in the SASGC with matched spectroscopic objects in the merged catalogues.

6.2.2 Photometric Galaxy Redshifts

The combination of the 5-band SASGC catalogue with the sample of spectroscopic redshifts opens up the possibility of estimating photometric redshifts. The photometric redshifts for SASGC were incomplete at the beginning of this work therefore we derive XCS values. There exist several methods of doing so such as spectral template fitting (e.g. Bolzonella et al. 2000) or a linear combination of magnitudes (e.g. Connolly et al. 1995) but we choose to use a neural network method. Artificial Neural Networks (ANNs) have, in recent years, been used many times in the literature for this purpose and for morphology classification (e.g. Odewahn et al. 2001; Ball et al. 2004; Vanzella et al. 2004). They provide a proven, fast and easily-implemented solution.

Artificial Neural Networks

Artificial Neural Networks (ANNs) were first proposed in the 1940s. Inspired by biological brains, Warren McCulloch, Walter Pitts, Donald Hebb and others began work on neuron functionality and how they could be simulated electronically. Neural networks solve problems by using feedback with training sets to 'learn' without explicit intervention or knowledge of the system behind the problem.

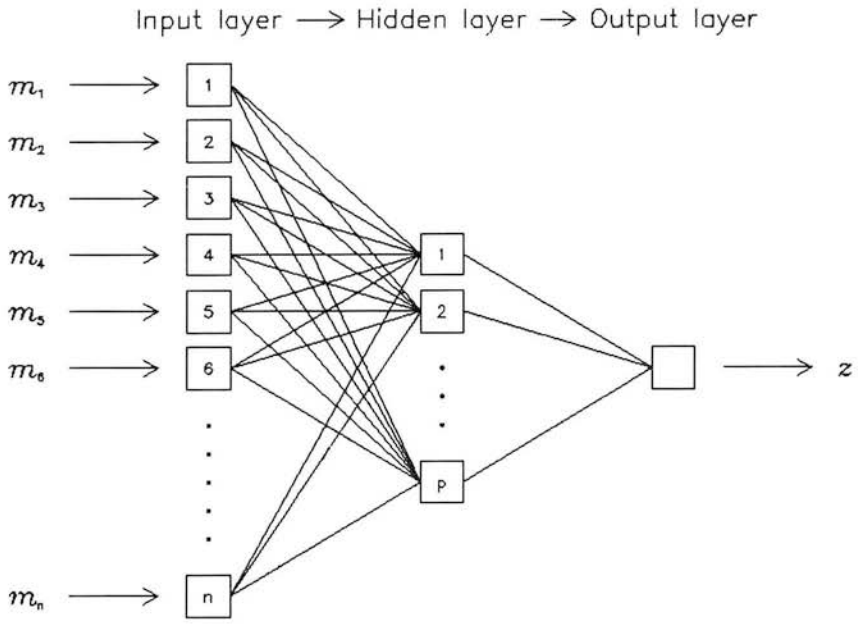

Figure 6.7: A schematic diagram of the architecture of an ANN, with input magnitudes, hidden layers and the output node returning the redshift. Figure adapted from Firth et al. (2003).

The principles behind ANNs are quite simple. A set of inputs (one for each source of information) are connected to the first layer of the network; these are known as the input nodes. Each node in each layer is connected to every other node (see Figure 6.7). The final layer is called the output and has a node for each desired parameter. A set of training data (i.e. correct outputs for a given set of inputs) can then be used to 'teach' the network how to predict the outputs for any new set of inputs. This is achieved by calculating a Cost Function, representing the goodness of the prediction, then iteratively changing the weights on each node to minimize this function.

The software we have chosen to use is `ANNz` (Collister and Lahav 2004). `ANNz` has been shown to produce some very promising results when used on SDSS data (Collister and Lahav 2004) and is elegant in implementation. One program, `annz_net`, is used to create a network architecture (i.e. the number and size of layers). Then `annz_train` takes the training data (5-band magnitudes and the true spectroscopic redshifts) and uses it to teach the network (create node weights). This code also uses a separate set of data to validate the training. Finally, photometric redshifts for the sample are estimated by feeding them into `annz_test`.

One weakness (or strength) of artificial neural networks is that they are very poor at extrapolation and perform best when shown inputs similar to those seen before. This sets a definite upper limit on the redshifts we can expect reliable estimates for. The limit will be set by the depth at which the training data becomes sparse, i.e. $z \sim 0.3$.

We used the spectroscopic SASGC, as described above, to train and test the network. The 361050 galaxies are divided at random as follows; 200000 for the training set, 50000 for validation and the remaining 111050 for our own testing.

The choice of network architecture is very much a trial-and-error process. There must be enough nodes and layers in order to cope with the number of available inputs and to represent the complexity of the underlying system but too many leads to unfeasibly large computation times and diminishing returns. The best compromise we found was 5.10.10.10.1, i.e. five input nodes (the magnitudes), three hidden layers of 10 nodes each, and one output (the photometric redshift). This may not be the optimal architecture but, as we shall show, it performs adequately for our purposes.

Results

The 111050 spectroscopic SASGC galaxies were used to measure the efficacy of the `ANNz` photometric redshifts. The performance of the code in reproducing unbiased redshift estimates is shown in Figure 6.8.

These results are better than we could have anticipated. For redshifts out to 0.3 there is almost no systematic offset (the maximum fractional error is less than 10% for $z > 0.01$). The empirical spread in the recovered redshifts can also be used to estimate the error as a function of photometric redshift.

Another important question is whether the estimated photometric redshifts come from the same population as the spectroscopic sample used for training. As seen in Figure 6.9, they do indeed come from a slightly deeper redshift ($z \sim 0.085$ compared to $z \sim 0.074$) but this lies within the range of the training data. Of course, we must check the results for the all of the SASGC galaxies without spectroscopic redshifts (1284824 sources).

The histograms of the 5-band magnitudes (Figure 6.9) show that, as expected, the photometric objects are indeed fainter than the training data but that they lie within the range of the spectroscopic sample. This is encouraging as it appears that the samples overlap significantly and thus there will not be a problem with extrapolation. We believe this provides reasonable support for the reliability of the photometric redshift estimates for the SASGC.

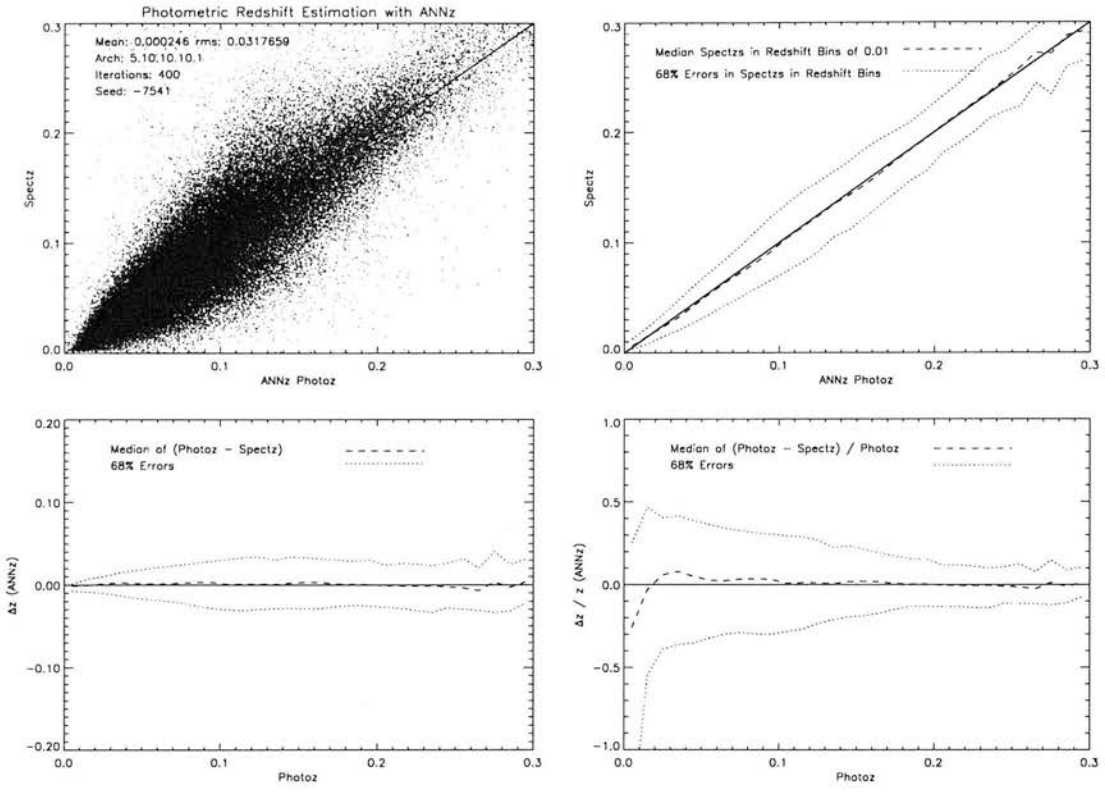

Figure 6.8: Four figures showing the neural network-based redshifts and 1σ errors.

6.2.3 Estimation of Cluster Redshifts

With the galaxy redshifts (both spectroscopic and photometric) now available we can attempt to estimate cluster redshifts for the XCS candidates. The majority of candidates have only one matched galaxy but some have multiple matches. The accuracy of the cluster redshifts is expected to improve with the number of matched galaxies. In order to estimate the cluster redshift and variance we used the weighted mean method to combine the galaxy redshifts and errors. Assuming that the galaxies provide n independent estimates z_j, with associated error σ_j, for the cluster redshift then the weighted mean is

$$\bar{z}_w = \frac{\sum_{j=1}^{n} w_j z_j}{\sum_{j=1}^{n} w_j}$$

where the weights $w_j = 1/\sigma_j^2$. The best estimate for the variance of $\bar{z}_w$ is

$$\sigma_w^2 = \frac{1}{\sum_{j=1}^{n} \frac{1}{\sigma_j^2}}$$

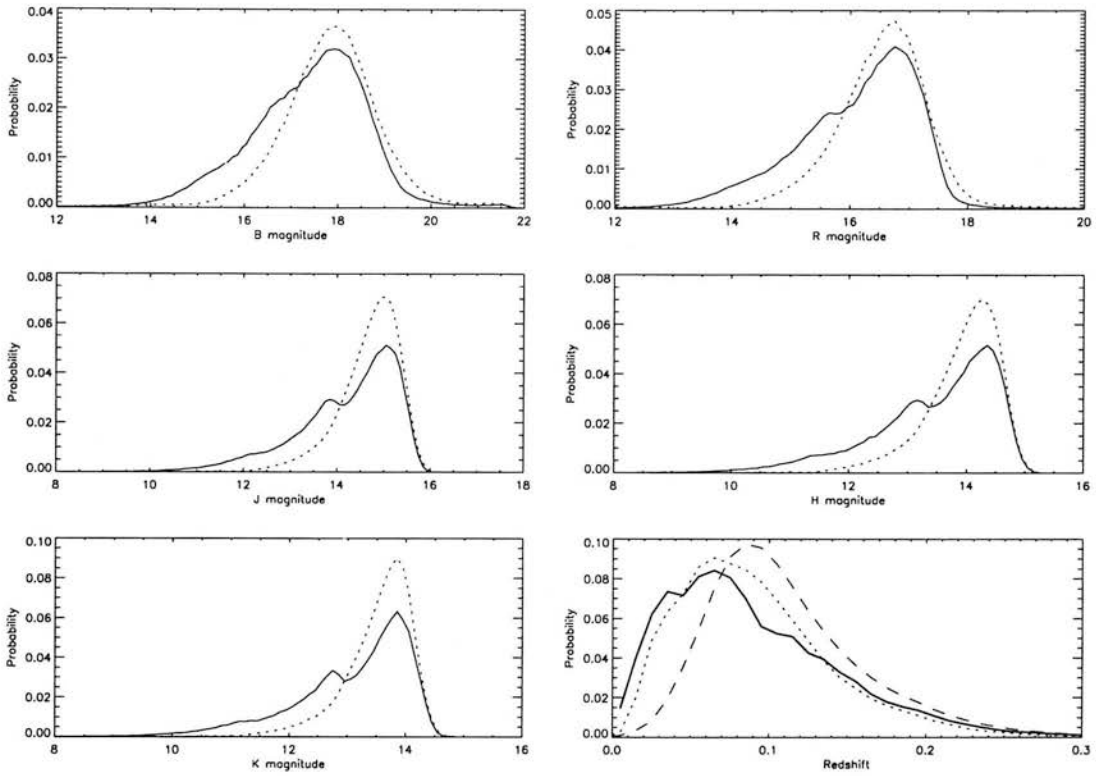

Figure 6.9: The first five plots show the distribution of the magnitudes for the spectroscopic and photometric samples (solid and dotted lines respectively). The figure at the bottom right confirms that the training set represent the whole sample. In this plot, the solid line is the redshift distribution of the galaxies with spectroscopic redshifts, the dotted distribution of the photometric estimates for this spectroscopic sample, and the dashed line is for the galaxies with only photometric values.

Reliability of Cluster Redshifts

While we have shown that the photometric redshift estimates are reasonable there are several factors that may introduce errors into the cluster redshifts. There is the possibility that the matched galaxy is falsely associated with the X-ray emission. Also, although we usually match with the BCG, clusters are not always regular in shape due to merging or otherwise, and so can be elongated in redshift. More seriously, the potential remains for cluster galaxies to form a different population in 5-band magnitude space than the SASGC galaxies in general.

The sample of known clusters serendipitously rediscovered in the XCS StatSam can be used to check our cluster redshifts. Of the 142 known clusters, 53 had matches with at least one SASGC galaxy. Not all of these clusters had reliable redshifts in the

literature; some had only photometric estimates, some redshifts came from untraceable sources and some were missing altogether. Keeping only those with solid spectroscopic redshifts reduced the sample to 29 for which it was possible to estimate XCS redshifts.

Plotting these spectroscopic redshifts against the XCS estimated redshifts (Figure 6.10) is quite revealing. Overall, there is good agreement. Having at least one galaxy with a spectroscopic redshift greatly improves the accuracy and reduces the error on the estimated cluster redshift. There are some notable outliers, however. Furthermore, these outliers are all underestimates which suggests a systematic cause. Examination of the optical images for these sources reveals that typically there are several other galaxies close to the matched galaxy (see Figure 6.11 for an example). These appear to be physically closer than the resolution of 2MASS ($\sim 10''$) so all of the galaxies are merged into one detection. Incompleteness of the XSC has been studied recently and appears to confirm that many of the missed galaxies are missed and are present only in the Point Source Catalog (McIntosh et al. 2005). If this hypothesis is true then it would explain the one-sided nature of the apparent offset. The flux from several galaxies at the same redshift is being attributed to a single galaxy. Hence this galaxy appears to `ANNz` to be brighter (and therefore closer) than it truly is. The size of this effect can be quantified approximately by calculating the factor which, when applied to the 5-band fluxes, would cause `ANNz` to return the correct redshift. For the nine photometric clusters this factor ranges from 0.12 to 0.37. This rough estimate is not unreasonable considering the potential number of unresolved galaxies.

A possible solution to the blending issue is to only use the B and R magnitudes for the prediction. The optical SSS survey has a higher resolution and is deeper then 2MASS thus the galaxies close to the BCG can be resolved. Initial tests of the neural network (and other techniques) using 2-band data have been promising, however this work is ongoing. The use of colour-magnitude diagrams is also being considered as a way to identify troublesome candidate redshifts.

Undeniably, these issues cast some uncertainty on the photometric cluster redshifts. A great deal can still be gained by using a simple scoring system to rate the reliability of the matches. If a candidate has at least one spectoscopic redshift it is awarded a Reliability Score of 1 as it is very likely to be an accurate estimate. If there are two or more photometric redshifts then a score of 2 is given. The additional matches tend to be to galaxies in less crowded regions of the cluster where the blending issue is not as serious. Finally, if there is only one photometric match then a score of 3 is assigned. These redshifts may be quite inaccurate and will require further attention. In general,

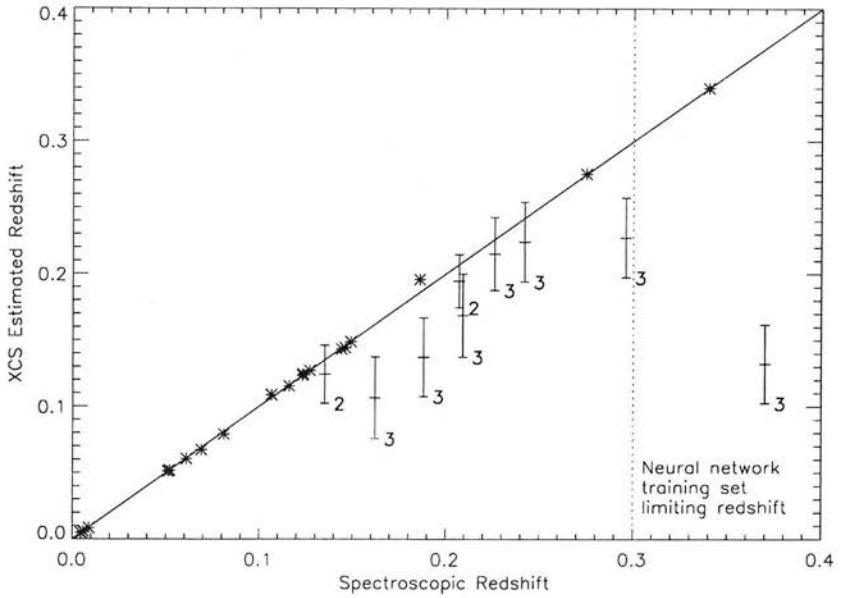

Figure 6.10: The redshift estimation ability of XCS, for reliable spectroscopic clusters. The reliability score for the XCS estimates are also shown. Scores and error bars for the clusters with at least one spectroscopic match (star symbols) are not shown for clarity.

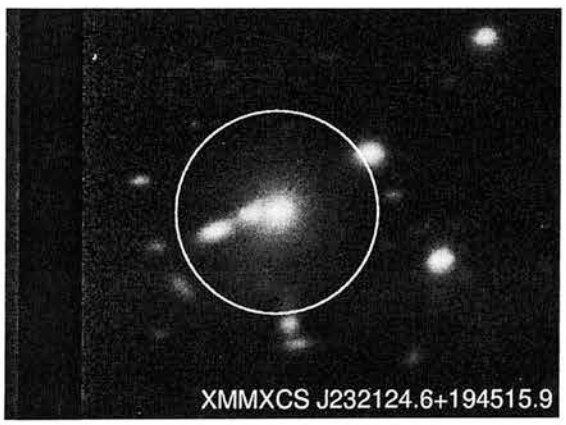

Figure 6.11: An example of blending of galaxies in 2MASS as seen in the optical UH 2.2m image. The galaxies within the $\sim 10''$ resolution of the 2MASS XSC (the white circle) are blended into a single detection.

XCS Name	Other Name	XCS Redshift	Reliability Score
XMMXCS J131302.4+351944.4	ZwCl 1310.6+3536	0.26 ± 0.03	3
XMMXCS J111926.5+210650.8	NSC J111192+210546	0.175 ± 0.001	1
XMMXCS J230247.4+084812.9	[B2002a] 36	0.05 ± 0.02	3
XMMXCS J012358.7-350733.2	SCG 0121-3521	0.0197 ± 0.0007	1

Table 6.3: XCS redshifts for those without any value in the literature.

they may be lower limits for the true redshift.

6.2.4 First Predictions

Preliminary redshifts estimated using these techniques have been obtained. There are 219 new candidates in the StatSam with estimated redshifts ($\sim$ 15%). Here we discuss the first examples.

Known Clusters

As mentioned earlier, four of the known clusters in the literature have no estimated redshift at all (neglecting for now the other exclusions). These clusters are presented in Table 6.3 along with the XCS redshifts for them.

The redshifts range from 0.05 up to 0.26. Two of them are Score 1 matches and thus should be reliable while the others should be regarded as likely lower limits.

In this work we have only considered literature clusters lying in the StatSam pointings of the XCS archive. These initial results are promising enough to recommend the technique for use on the whole sky. There should be a moderate number of other literature clusters (without X-ray information) for which redshifts can be obtained using SASGC.

UH 2.2m Clusters

Time was awarded to observe a set of XCS candidates in August 2005 on the UH 2.2m in Hawaii. Eleven clusters were successfully imaged during the run and of these eight have SASGC matches. They are presented in Table 6.4.

The scores are either 2 or 3 so the redshifts are still only preliminary but the clusters have been confirmed. Spectral template fitting is currently ongoing for this sample (Hilton et al., in prep) and shall be used for validation of the XCS estimates.

XCS Name	XCS Redshift	Reliability Score
XMMXCS J014449.9-043231.5	0.13 ± 0.02	2
XMMXCS J200758.9-110251.6	0.08 ± 0.02	3
XMMXCS J205405.6-154728.5	0.18 ± 0.02	2
XMMXCS J223228.7+391518.3	0.27 ± 0.04	3
XMMXCS J223633.7+342959.3	0.06 ± 0.02	3
XMMXCS J232124.6+194515.9	0.25 ± 0.03	3
XMMXCS J232221.3+193855.8	0.16 ± 0.03	3
XMMXCS J235109.5+201538.2	0.20 ± 0.03	3

Table 6.4: XCS redshifts for the SASGC matches observed with the UH 2.2m.

6.3 Confirmed High Redshift Clusters

We now change focus from the low to the high redshift regime. Arguably, one of the strongest features of XCS is its predicted ability to increase the number of very high redshift clusters known. The population at $z > 1$ is interesting both because of the leverage they provide to the cosmological predictions and for cluster evolution.

6.3.1 Rediscovered $z > 1$ Clusters

Existing surveys (for instance, Böhringer et al. 2001; Ebeling et al. 2001; Rosati et al. 1998; Collins et al. 1997) have had great success in finding clusters out to redshifts of 0.8 or 0.9 but struggle to break the $z = 1$ barrier. This is to be expected due to the severe $(1+z)^4$ surface brightness dimming affecting X-ray imaging. Sunyaev-Zeldovich surveys (e.g. Holder et al. 2000; Schulz and White 2003) offer a potential solution to this problem but the technology at present is not sensitive enough to reach these depths. X-ray selection shall remain the most reliable way to discover them for a number of years to come.

As of November 2005 there are eight spectroscopically confirmed systems of galaxies at $z > 1$ (see Table 6.5). Where XMM coverage is available, all of these clusters are rediscovered by XCS. One (RDCS J1252.9-2927) is not included in the StatSam as it is the target of the XMM image and thus is not a serendipitous rediscovery.

These were relatively easy detections and our pipeline properties are usually consistent with the literature values. Results such as these provide justification for belief that many more high redshift clusters are present in the XCS StatSam and that a stream of others will continue to be discovered throughout the lifetime of XMM.

XCS Name	Literature Name	z	Reference
XMMXCS J223520.3-255742.2	XMMU J2235.3-2557	1.393	Mullis et al. (2005)
XMMXCS J084834.5+445340.9	RDCS J0848.6+4453	1.273	Stanford et al. (1997b)
XMMXCS J084859.0+445149.6	RDCS J0848.9+4452	1.265	Rosati et al. (1999)
No XMM Coverage	RDCS J0910+5422	1.11	Stanford et al. (2002)
XMMXCS J125254.7-292718.4	RCDS J1252.9-2927	1.237	Rosati et al. (2004)
XMMXCS J105343.6+573518.6	RX J1053.7+5735	1.14	Hashimoto et al. (2004)
XMMXCS J022709.4-041806.4	XLSS J022708.7-041759	1.0	Andreon et al. (2005)
XMMXCS J022404.2-041327.9	XLSS J022403.9-041328	1.05	Andreon et al. (2005)

Table 6.5: Summary of all known clusters at $z > 1$ (November 2005).

A handful of our high redshift candidates have been followed-up already. To pick the *crème de la crème* of the new candidates from the StatSam we first select those with existing moderately deep optical imaging from the Isaac Newton Telescope Wide Field Survey (INT-WFS, McMahon et al. 2001) or ESO Imaging Survey (EIS, Nonino et al. 1999). If the candidates are at low to moderate redshift then they should be visible in these surveys. The X-ray detections are also checked for any possible artifacts or poor statistics. In this manner, the first high redshift candidates were selected for large-telescope follow-up.

6.3.2 A Supercluster at z=0.9?

In February 2005 one of the candidates, XMMXCS J130601.6+180142.3, was observed with Keck (Figure 6.12). Of the redshifts obtained there were three concurrent at $z = 0.93$. Once spectra are taken for more of the apparent members this redshift can be confirmed more conclusively.

While this is a worthy example of a high redshift cluster on its own, the XMM observation in which XMMXCS J130601.6+180142.3 was discovered is special. It is one of the 'richest' XCS pointings (0017940101) as it has at least six excellent cluster candidates within (including XMMXCS J130601.6+180142.3). The bright point source target is easily excised even though there was extensive out-of-time event streaking. The XMM image with sources is shown in Figure 6.13.

If a candidate contains enough photons it should be possible to measure its redshift by looking for lines in its X-ray spectrum. It takes quite a large number of counts to do this with reasonable accuracy, of the order at least 500 to 1000 (Sabirli et al., in prep.). XMMXCS J130601.6+180142.3 is not bright enough to use this technique (having only

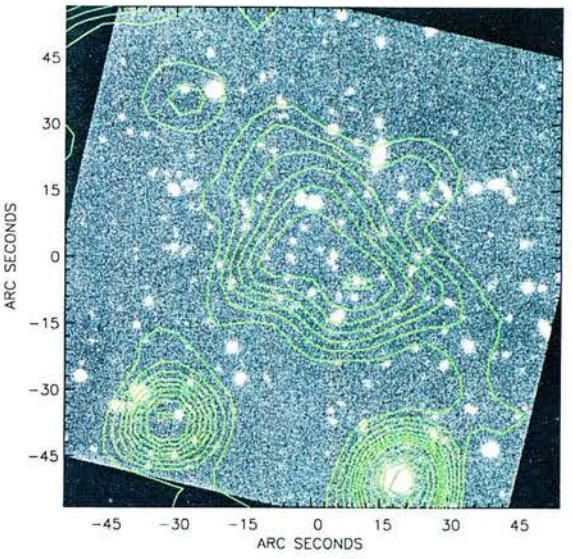

Figure 6.12: Keck R band image of XMMXCS J130601.6+180142.3 with X-ray contours (arbitrary contour levels).

59 photons), which is partly why it was chosen for deep optical follow-up. However, the brightest cluster candidate in the pointing, XMMXCS J130526.8+181156.4, has over 2200 counts and thus should have an acceptable spectrum. It is unusual to have a high-redshift cluster with this many counts so it was initially suspected that the source was at moderate redshift. This candidate yielded an X-ray redshift of $0.912^{+0.059}_{-0.078}$ (90% confidence region) through its Fe line (K. Sabirli, private communication).

Two confirmed clusters at $z \sim 0.92$ are not quite sufficient to declare this system a supercluster. It should not be a surprise that such a system could be seen as structure formation theories predict that cluster assembly is very much active at $z \sim 1$ and so superclustering should be quite common. The typical separation of the candidates ($\sim 10'$) corresponds to a physical scale of ~ 10 Mpc at this redshift. This is small, in supercluster terms, where you would typically expect a size $\sim 10 - 20$ Mpc (see, for instance, Small et al. 1998), but there may yet be further structure beyond the field-of-view of XMM.

This pointing will be the subject of further deep optical and IR observations. Work is underway to determine an X-ray redshift for the second brightest candidate, XMMXCS J130534.8+175659.5. Hopefully, observations with the large format Suprime-Cam on Suburu, following the example of Nakata et al. (2005), should permit

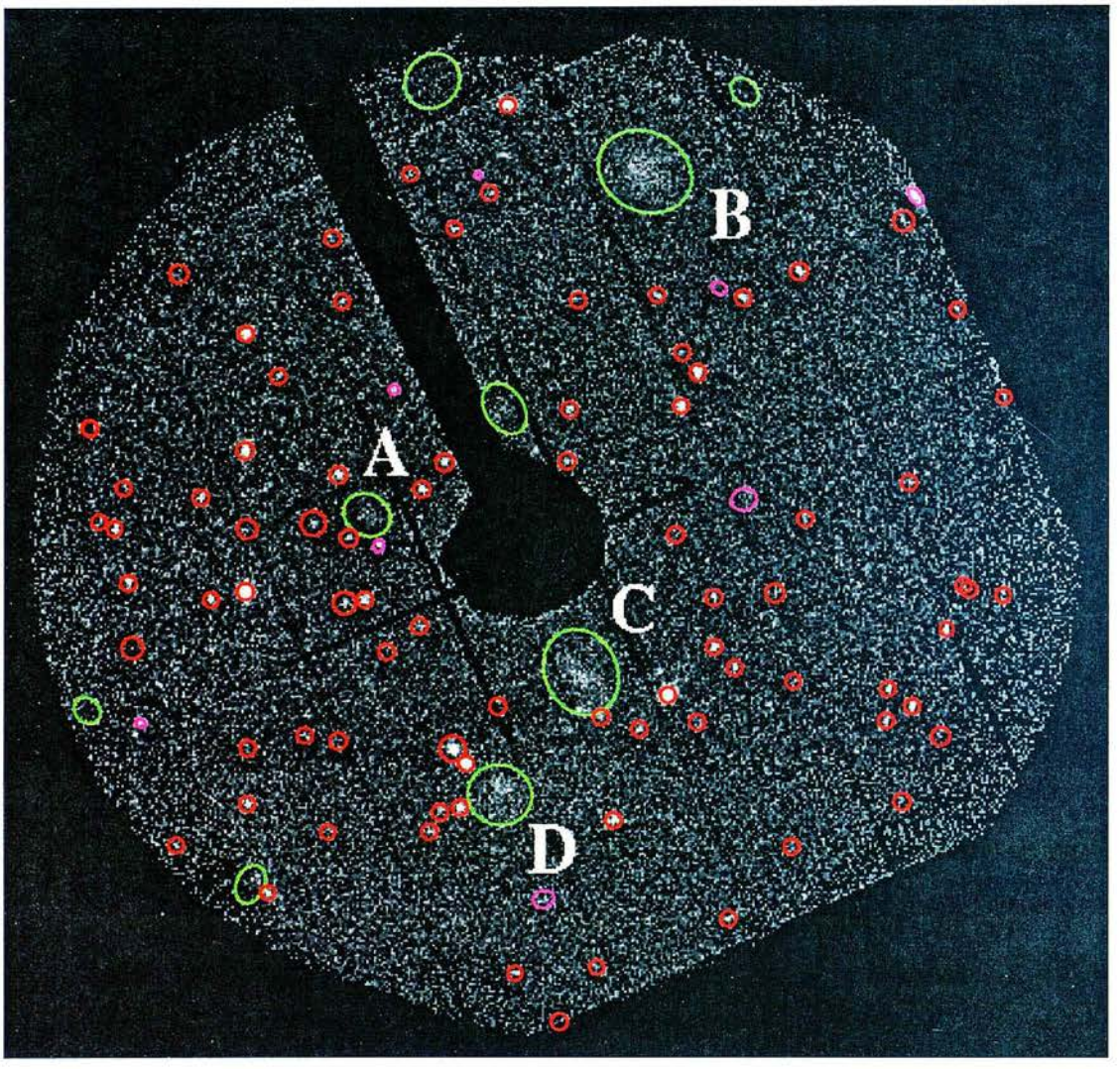

Figure 6.13: XMM Observation 0017940101. There are clearly several extended sources in this field. Source 'A' has been spectroscopically confirmed at $z = 0.93$ and 'B' has an X-ray redshift of 0.92. Sources 'C' and 'D' are under investigation.

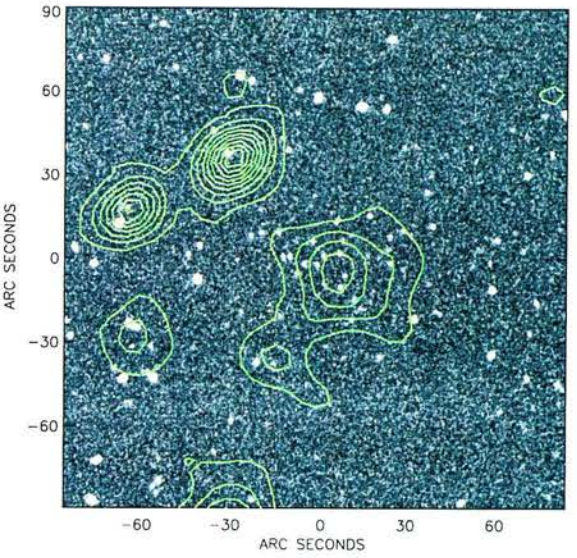

Figure 6.14: Palomar K band image of XMMXCS J221559.4-173815.5 with X-ray contours (arbitrary contour levels).

any evidence of superclustering to be traced beyond the field-of-view of XMM.

6.3.3 A Cluster at z=1.5

XMM is delivering on its promise to discover the most distant ever clusters. As discussed earlier, the $z = 1$ barrier is regularly breached. Recently, Mullis et al. (2005) announced the discovery of XMMU J2235.3-2557, having the highest redshift of any in this sample at $z = 1.393$. XCS has since confirmed the detection of the most distant cluster yet known, at $z = 1.45$.

XMMXCS J221559.4-173815.5 was first flagged as a possible high-z candidate through its appearance in the INT-WFS and EIS images. The EIS I-band image was just deep enough (~ 24) to enable a mask to be prepared for a handful of putative members. Spectroscopy was obtained using this mask with DEIMOS on Keck in September 2005 resulting in three galaxy redshifts concurrent at $z = 1.45$. Further spectroscopy with DEIMOS increased provisionally the number of confirmed cluster members to five. Additionally, a 3000s Ks band image was taken at Palomar (Figure 6.14). As shown in Figure 6.15 the colour-magnitude diagram, I-K vs K, shows evidence for a possible red sequence at I-K ~ 4.5 which is the appropriate value for passively evolving early type galaxies at $z = 1.45$.

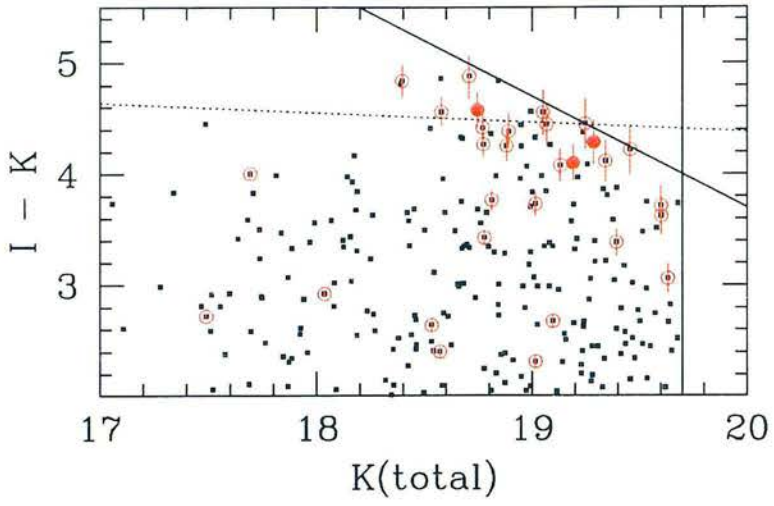

Figure 6.15: Colour - Magnitude plot for XMMXCS J221559.4-173815.5. The black points are are all galaxies within 7' of the X-ray centre, red circles are within 1' and the solid red circles are the spectroscopic members. The expected colour-magnitude relation for non-evolving early type galaxies at $z = 1.5$ is the dotted line. Figure courtesy of Adam Stanford.

r_c / kpc	$L_x[0.5-2.0$ keV$]$ / 10^{44} erg/s	L_{bol} / 10^{44} erg/s	$F_x[0.5-2.0$ keV$]$ / erg/s/cm^2
150.0	1.725	5.217	1.56×10^{14}
194.4	2.092	6.329	1.89×10^{14}

Table 6.6: The luminosities contained within r_{200} for two values of the core radius. The first (150 kpc) is a canonical cluster. The second core radius has been obtained using the empirical $r_c - r_{200}$ relation of Neumann and Arnaud (1999).

X-ray analysis of XMMXCS J221559.4-173815.5 has been performed by K. Sabirli (in prep.) who derives a temperature of $kT = 4.06 \pm 1.06$ keV. The large error reflects the limited number of X-ray photons (431) available for the fitting of the emission. A $\beta = 0.66$ beta model was assumed after this and the best-fit temperature used to estimate r_{200}. This is the radius at which the enclosed mean mass density falls below 200 times the critical density of the Universe. It provides a characteristic mass for a cluster. For a beta model the luminosity contained within r_{200} depends on the choice of core radius, r_c. The X-ray properties for two values of r_c are presented in Table 6.6.

Also shown in Table 6.6 are the fluxes expected by extrapolation of the two models. These compare favourably to the pipeline detection flux of $1.75 \pm 0.19 \times 10^{14}$ erg/cm^2/s in the 0.5-2.0 keV band. This illustrates one of the strengths of using a model-free

detection algorithm.

Further pointed observations of this cluster by XMM, Chandra and Keck should hopefully be forthcoming. While it is clearly possible to discover clusters with X-rays in this high redshift regime it may prove difficult to push much beyond $z \sim 1.5$. This is not so much an effect of surface brightness dimming but of selection of candidates for long observations with large telescopes. Distant candidates may still seen but will be hard to separate from large number of artifacts in the archive with a similar low number of photons. It is very much a 'needle in a haystack' situation; $z \sim 0.9$ clusters are visible in ROSAT images, if it is known where to look. Undoubtedly, XCS will be a premier X-ray resource for these objects.

6.4 Morphology

Cluster morphology, the spatial distribution of gas and galaxies, is important for several reasons. Not only is it interesting in its own right for studies of cluster physics, in particular evolution and merging, but it is relevant in the context of cosmology.

The canonical cluster has evolved over the years since the hydrostatic, isothermal model was developed. The beta model (see Section 5.1.1) had great success describing the surface brightness of the clusters of galaxies observed by the first generation of X-ray telescopes. Later, other models were found to provide good fits, such as the NFW (Section 5.1.1) profile which is attractive due to the ease with which it can be integrated with cosmological predictions. With improved X-ray technology has come the realisation that clusters could no longer be treated simply as relaxed spherical systems. However, there is still comparative value in the results obtained under this assumption.

6.4.1 Beta Model Profiles

There has been much previous work on the relative merits of the Beta and NFW models (e.g. Neumann and Arnaud 1999; Wu and Xue 2000; Neumann 2005b). In the spirit of what is to follow, we shall only consider the former as it is still the first-order model used during X-ray analysis. It also has the benefit of being easily coded and simple to fit.

Automated Model Fitting

Numerous issues must be addressed before it could be possible to obtain best-fitting beta models for the StatSam candidates. As noted by several authors (for instance, Ota and Mitsuda 2004b; Neumann and Arnaud 1999) the best-fitting beta model can depend on the choice of a set of factors.

Point Source Masking Point sources embedded in the cluster emission can severely contaminate the beta model fit. Ideally, the point source itself could be fitted in 2D and subtracted from the data. This can prove to be difficult without an accurate 2D model of the PSF. Without such a model the best option is to mask out the point source rather than subtract it. The masking radius must be quite conservative if the wings of the PSF are to be excised but unfortunately this can leave little cluster emission to fit a beta model.

Choice of Inner Radius The surface brightness near the centre of clusters is known to deviate from the hydrostatic equilibrium prediction necessary for the beta model to be valid. Central AGN activity or the presence of a cooling flow can cause a steepening of the profile. Thus, there are circumstances when the central region should be masked out. The minimum radius to be used for beta fitting can depend on redshift and the degree of core cooling. Many of our candidates cannot be adequately fitted if any standard core is assumed. This also rules out the possibility of using a double beta model (essentially, fitting the core and outer regions separately).

Choice of Outer Radius One weak point of the beta model is that, mathematically, it predicts emission out to infinity. Obviously, in reality the cluster profile is limited and there is a radius at which it becomes impossible to distinguish genuine emission from the background. In many cases it is hard to determine this radius and so it can be left as a free parameter in the fit. It cannot be too large otherwise the errors in the background and from contamination will dominate the fit.

Goodness-of-Fit Without revisiting the discussion on the difficulty of calculating a mathematically rigorous goodness-of-fit statistic (see the work on classification in Section 3.5.5), many of the same problems arise here. The standard measures (χ^2) are used only as a guide.

Limited Knowledge of Redshifts Having cluster redshifts for the full sample would make a uniform analysis easier. A fixed core radius could be used, removing a degree of freedom from the fits. This is not yet the case so the beta modelling must be done with angular rather than absolute sizes.

The above concerns need to be heeded but there are a large number of examples where acceptable fits can be found.

Method

Much of the methodology for the beta model fitting is similar to that used in for the selection function simulations. There we specified a physical beta model, transformed it to the correct cosmology and then folded it through the instrumental responses including convolution with the PSF. Here we generate a set of functions, varying a number of parameters:

- β : the slope parameter
- r_c : the angular size of the core radius
- x_c : the x position of the cluster
- y_c : the y position of the cluster
- Peak: the normalisation of the beta model
- Bkglevel: background photons per pixel per second (assume non-vignetted)
- e : the ellipticity
- ϕ : the orientation of the profile

The IDL code `MPFIT2DFUN` by Craig Markwardt[4] can be supplied with this function and a set of weights (assumed to be uniform) and it finds the best parameters by performing a Levenberg-Marquardt least-squares fit. `MPFIT2DFUN` allows individual parameters to be assigned, amongst other attributes, minimum and maximum values, thus protecting against unphysical fits.

The data supplied to `MPFIT2DFUN` is the 1.5' by 1.5' extracted subimage of the merged XMM images. Point sources are masked out using the expected 80% EEF radius; this removes the worst of the contamination while leaving as much cluster emission as possible. No inner radius is specified to maintain generality.

[4] http://cow.physics.wisc.edu/~craigm/idl/idl.html

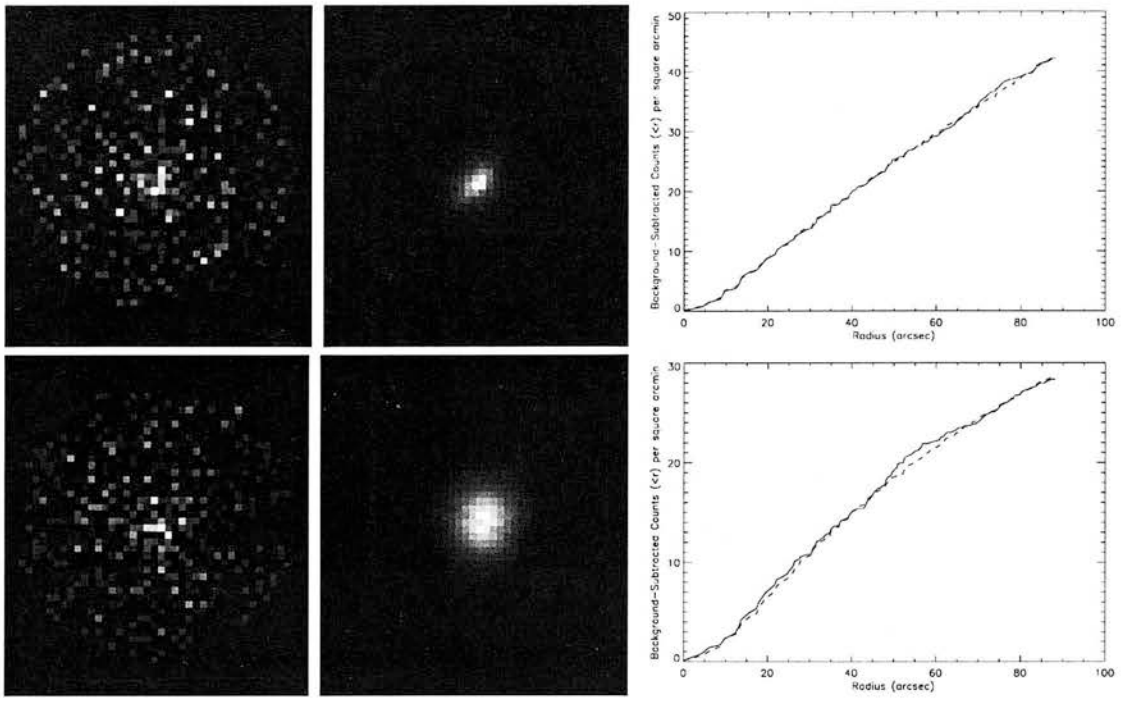

Figure 6.16: Three examples of well-fitting beta models, XMMXCS J000429.1+633127.1 and XMMXCS J001042.5-112743.3. From left to right, XMM merged image, best-fit model and 1D radial cumulative profiles (solid line is the data and dotted line the model).

Results

As expected, the results from this simplistic automated procedure are mixed. There are examples with excellent fits (for example those in Figure 6.16) but the majority cannot be relied upon. The most common problem is caused by the relative number of source counts to background counts. For faint sources the code tends to fit to the background rather than the candidate's emission. A similar problem occurs for low redshift candidates which have large spatial extent and thus have rather flat profiles in the extracted central regions.

Unfortunately, it appears that such an automated approach is not suitable. However, there are a few individual examples worthy of discussion.

XMMXCS J130601.6+180142.3 This is the spectroscopically confirmed $z = 0.9$ cluster which is suspected of being part of a supercluster. The fits below are not perfect but do illustrate the ability to fit a model with only a small number of counts available. The best-fit parameters ($\beta = 2.0$, $r_c = 317$ kpc) are not physically reasonable. A beta

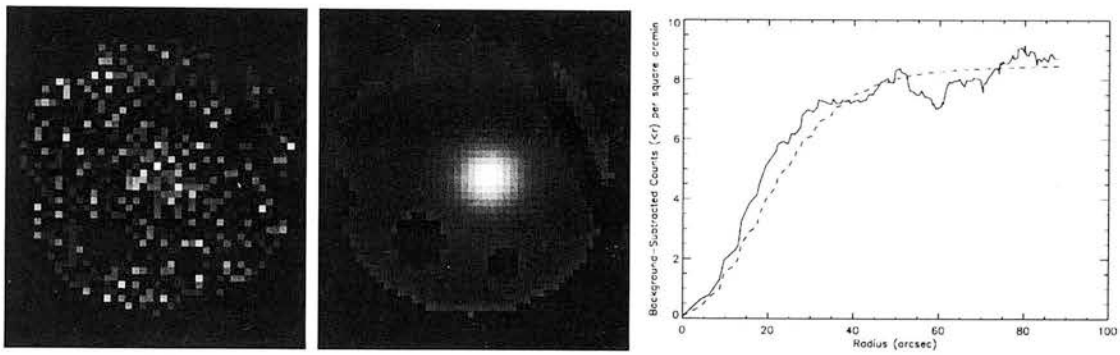

Figure 6.17: As Figure 6.16 but for XMMXCS J130601.6+180142.3.

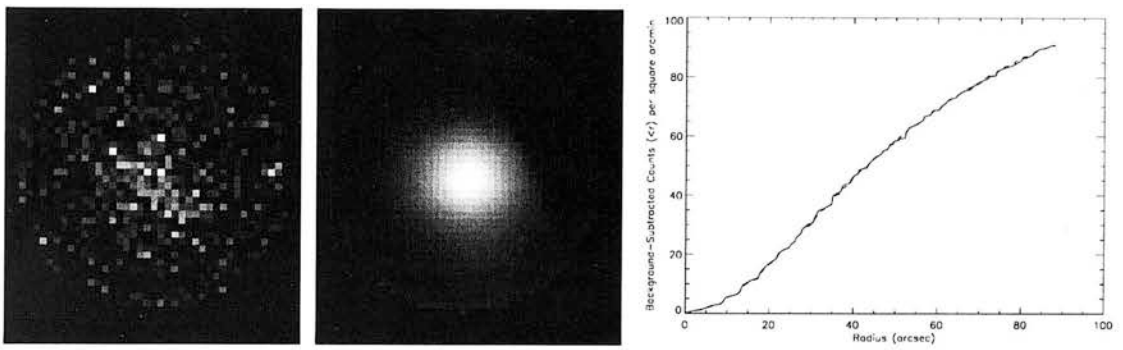

Figure 6.18: As Figure 6.16 but for XMMXCS J121334.9+025350.7.

value greater than the canonical 2/3 could be due to exclusion of the outer regions but the degeneracy between β and r_c is the more likely cause of the values.

XMMXCS J121334.9+025350.7 One of the best-fitting candidates is XMMXCS J121334.9+025350.7 (RX J1213.5+0253, $z = 0.409$, Mullis et al. 2003). As seen in Figure 6.18, the fit is exceptional. There are several reasons for this. Firstly (and most importantly), the cluster candidate has a large number of counts (> 2000) within the 1.5' aperture. More than this, it is also apparently relaxed and regular and has no obvious point source contamination. The exposure map beneath the cluster is mostly flat (not always the case). These fortuitous conditions are reflected in the best-fitting parameters of the model: $\beta = 0.73$ and $r_c = 241$ kpc. These suggest that the fit is physically realistic.

In summary, beta model fitting (or otherwise) cannot be entirely automated. It is recommended that the code is used semi-interactively as each individual cluster is followed-up. Doing so will ensure that the masks are adequate and that suitable

radii are chosen. Ultimately, once an improved XMM PSF model is available, point source masking will be straightforward and automated cluster profile fitting may yet be possible.

6.5 Optical Follow-up

Previously in this chapter we have discussed our efforts to confirm candidate clusters in the low and high redshift regimes (through SASGC and large telescopes, such as Keck, respectively). Now we turn to the middle ground at which we expect the bulk of new XCS clusters to be discovered.

6.5.1 Projected Candidate Numbers

XCS has already compiled a formidable cluster candidate catalogue and the project is far from finished. This first release of XCS candidates is based on XMM observations from March 2000 to November 2004. Since then XCS has obtained a further 291 pointings, which have been reduced but not yet added to the databases. That number will only increase because of existing proprietary data becoming public and the ongoing support for the XMM mission. Technical failures aside, such as a micro-meteorite strike more serious than the one which disabled a chip on the MOS1 camera in March 2005, XMM will continue to function until 2010. After extrapolating the current catalogue size and area the predicted final XCS release will have approximately 3500 candidates clusters.

A fraction of these (around 15%) should have secure confirmations and redshifts from the SASGC and literature but this leaves a large number requiring dedicated optical observations.

6.5.2 The XCS-NOAO Programme

The XCS-NOAO is a major survey to follow up cluster candidates in $\sim$ 330 XMM pointings. It was proposed in March 2005 and the first observations were taken in November 2005.

The facilities of the National Optical Astronomy Observatory (NOAO) are ideally suited to our purposes. Homogeneous multi-band optical imaging of the XMM pointings will be gathered using the 4m KPNO telescope in the North and 4m CTIO in the South. The two-band (SDSS r' and z') data from the MOSAIC cameras should be deep enough to provide photometric redshifts out to redshifts of ~ 1 (Andreon et al. 2005). By the

end of the three year programme of observations XCS shall have an X-ray selected catalogue of unprecendented uniformity and depth.

Through careful use of a targeting algorithm an observing strategy can be chosen to maximize the science obtained from the XCS-NOAO pointings. The most valuable science, such as the $L - T$ relation, requires temperatures for the clusters. Only the brightest clusters can yield X-ray temperatures so these should be given high priority. However, these are relatively sparse and much other information can be gained from the fainter candidates. As an example, the putative $z > 1$ candidates are unlikely to have enough counts for a temperature measurement yet the NOAO data can be used to select them for deeper observations. With this in mind the XMM pointings can be ranked and the most fruitful selected for the XCS-NOAO survey.

An XMM pointing could be ranked highly if it contains a few bright candidates or many faint ones (or somewhere in between). A scoring system has been devised:

- Each new candidate in the XCS StatSam is given a score equal to its position in the source counts ordered list, i.e. the brightest will have a large score.
- Each XMM pointing has a rating equal to the sum of the scores of the candidates within.

In practice, several different lists must be used in parallel. Weather conditions or paucity of candidates in certain RA/Dec ranges can reduce the amount of useful time available during a run. To counter these effects we generate three ranked lists. The first is the complete list without any counts cut (i.e. containing candidates down to a handful of photons). The second only uses candidates with more than 250 counts and the third only uses candidates with more than 500 counts. Essentially, the difference between these lists is the balance between clusters bright enough for temperature measurements and possible high-z candidates. The bright lists are subsets of the complete lists and so contain some of the same pointings but, crucially, they are in a different order. A summary of the number of pointings in each list for the November 2005 KPNO run is given in Table 6.7.

This should give us enough flexibility to maximise the number of good candidates in the event of not being able to observe 10 fields a night. In summary, we shall use primarily the 250 counts list unless time is short in which case we can change to targets in the 500 counts list. If there are sparse pointings for a particular time of night then additional candidates can be found in the complete list of pointings. The lists will

Counts Threshold	Number of Pointings	Number of Candidates
5	255	570
250	81	103
500	35	41

Table 6.7: Summary of the three pointing lists to be used for the XCS-NOAO programme.

change slightly during the course of the three year programme as more candidates are discovered. By the end of the survey in 2008 we predict that at least 500 candidates in the $\sim$ 330 pointings will have been observed by the XCS-NOAO project.

Chapter 7

Conclusions

The XCS has performed a large area serendipitous survey of galaxy clusters using archival XMM images. This thesis details the construction and validation of the source detection algorithms and describes the database created to access the results. A number of catalogues have been derived from the database, primarily lists of previously known clusters and new candidates. The methodology for the characterisation of the survey selection function is outlined and the preliminary results are presented. The ability of XCS to constrain the cosmological parameters σ_8 and Ω_m is discussed, based on the current selection function. Progress has been made on the follow-up of cluster candidates in the low, medium and high redshift regimes. Photometric techniques are used with optical and infrared data in order to assist in the identification of clusters at $z < 0.3$. We also discuss a strategy to ensure efficient optical follow-up through the XCS-NOAO programme. Finally, we highlight some initial successes, in particular, the discovery of the most distant X-ray selected cluster at $z = 1.5$.

7.1 Source Detection Algorithms

The XCS requires use of a complex set of algorithms to obtain clean source lists with reliable properties. We have developed a pipeline, known as XAPA, to detect, classify, characterise and cleanse sources in the merged XMM exposures. The essential elements of XAPA are summarized below.

- The core of the detection algorithms is based on a two-stage wavelet transform

with exposure-corrected coefficent thresholds being used to identify source pixels.

- Significant pixels on several scales are connected to form objects using a linking algorithm designed to ensure efficacious source separation. A variety of source types can be detected; from point-like through to those which are extended over many arcminutes. The object creation process is independent of any model.

- Classification is performed using a Kolmogorov-Smirnov test on each source's encircled energy profile, with Monte-Carlo simulations providing an empirical statistic distribution.

- A series of tests is carried out to cleanse the source lists of artefacts, for example mis-classified points, and any remaining suspicious objects are flagged.

Validation tests on the algorithms concluded that they perform well. The positional accuracy (95% confidence limit) for point sources is 7.8" and there is no observed significant systematic offset in the measured fluxes. More than 90% of point-like objects are classified correctly over a wide range of off-axis angle and brightness ($\theta \lesssim 10'$ and $\lesssim 500$ source counts). Initial simulations confirm that there is no offset in the recovered positions of extended sources. A classification accuracy of $> 90\%$ can be expected for the full field-of-view. A careful analysis of the measured properties reveals that $\sim 90\%$ of the unabsorbed flux from a canonical beta model is recovered.

No other algorithms exist which can use merged X-ray data so effectively and detect objects with a range of scales across the whole field-of-view.

7.2 Catalogues & Database

The XCS pipeline creates a large quantity of data on the detected sources. A database is the most practical means of manipulating such a dataset. The XCS database contains all pertinent information on the XMM observations used and the sources detected within, plus many intermediate attributes. The key features of the XCS catalogues are below.

- XCS contains 74296 detections at $> 4\sigma$ significance (Gaussian equivalent), of which 63327 are unique X-ray sources. More than 90% (58154) of the sources are classified as point-like and the remainder, 5173, as extended.

- Literature searches using several external databases of extragalactic objects have been performed for the purpose of identifying re-discovered clusters and removing emission from non-cluster sources.

- A number of catalogues most relevant to the XCS have been derived from the database. A set of criteria have been chosen in order to define an XCS Statistical Sample of sources. The Statistical Sample consists of 142 known clusters and 1622 new candidates. A further, non-statistical, sample of 90 cluster candidates has been compiled by eye.

- The XCS Statistical Sample area is currently 170 square degrees and is on track to reach the final target of 500 square degrees by the end of the project.

The database can be queried through the Web, enabling straightforward access for the XCS collaboration (and eventually the astronomy community). It shall be a unique resource as no similar survey of point and extended sources is planned for many years.

7.3 Cosmological Parameters

We have developed a methodology for determining the survey selection function, i.e. the probability of a cluster with a given redshift, luminosity and temperature being found in the Statistical Sample. This value is measured for a range of cluster parameters through simulation, on a large number of machines, of a set of fake clusters.

The selection function can be used in conjunction with dark matter halo mass functions from large numerical simulations. By comparing the observed number of clusters, as a function of mass, with that expected from N-body simulations the most likely underlying cosmology can be obtained.

Predictions have been made for the preliminary constraining power of XCS when temperatures, and thus masses, have been measured for ~ 240 clusters.

- The current amplitude of cosmological density fluctuations, σ_8, should be constrained to within 4% of its true value.

- The current matter density, Ω_m, shall be determined with an accuracy of 15%.

- Subject to further selection function simulations and follow-up observations, constraints shall be obtained on the vacuum energy of the Universe, Ω_Λ.

The simulations are ongoing and are intended to continue until the end of the project (not before 2010). The constraints from XCS are independent of those from the CMB and supernovae and thus joint constraints are likely to be very strong.

7.4 Cluster Follow-up

We have explored techiques for the follow-up of the XCS cluster candidates and have presented several notable successes achieved so far. Highlights include

- **Low Redshift Confirmations** We have associated the XCS Statistical Sample with an optical/infra-red galaxy survey (SASGC, Peacock, in prep.). Through use of a Poisson clustering technique we have obtained matches for $\sim 35\%$ of the known clusters and $\sim 15\%$ of the new candidates in the Statistical Sample.

- **Photometric Redshifts** We have extended SASGC by using a neural network to estimate photometric redshifts for 1284824 galaxies. The photometric redshift sample has a median depth of $z = 0.085$ and is potentially reliable to $z \sim 0.3$.

- **Cluster Redshifts** These values (plus a sample of spectroscopic galaxy redshifts) has enabled XCS to estimate cluster redshifts for the SASGC matches. The set of 219 new candidate redshifts represents a significant fraction of the required follow-up.

- **Morphology** We have begun a process of automatic measurement of the X-ray morphology for the XCS clusters. Although we have had success with bright clusters, there is still work to be done.

- **Clusters at High Redshift** A likely super-cluster at $z = 0.9$ has been discovered. This reaffirms both the value of serendipitous surveys and the ability of the project to measure X-ray temperatures at high redshift. Furthermore, the most distant X-ray selected cluster currently known (at $z = 1.5$) has been found by XCS.

- **XCS-NOAO** An efficient observing strategy to maximize XCS science has been designed for the XCS-NOAO programme. This will ensure a large sample of cluster redshifts and temperatures are available by the end of 2008.

All of the infra-structure required for XCS to achieve its primary scientific goals of measuring the evolution in cluster parameters (such as the $L - T$ relation) and constraining cosmology is now in place.

7.5 Future Work

It is time for the exploitation of the XCS catalogues to begin in earnest. Execution of the follow-up schemes outlined previously is already underway. However, there are several developments which could assist greatly in the task.

- Currently, photometric redshifts are found only for galaxies which are visible in both the SuperCOSMOS (Hambly et al. 2001) and 2MASS Jarrett et al. (2000) archives. Many galaxies are visible only in the optical surveys and thus a method to derive reliable redshifts from the B and R band data alone would be very beneficial. Looking further ahead, the analysis technique could be extended to use data from the next generation of infrared surveys such as UKIDSS (Lawrence et al. 2002).

- Our sample of sources which are extended in X-rays and have optical/IR coverage is ideal for a homogeneous study of fossil groups. It should be possible to use this information to justify dedicated follow-up observations with XMM and Chandra for a large sample of such systems.

- We expect there to be several additional releases of the catalogues as further XMM observations are made and become public. Very little effort is required to include this new information and to correct the small number of bugs found in the code (Section 4.1.4). It is hoped that, eventually, the survey can be improved through use of a more accurate PSF and background model.

Clusters at $z > 1$ are being discovered routinely for the first time, opening a window on to a critical period of structure formation. Many new avenues of research are likely to arise as the optical and X-ray follow-up programmes continue. The possibilities for XCS are captivating.

Bibliography

Abell, G. O.: 1958, ApJS **3**, 211

Adami, C., Ulmer, M. P., Romer, A. K., Nichol, R. C., Holden, B. P., and Pildis, R. A.: 2000, ApJS **131**, 391

Adelman-McCarthy, J. K.: 2005, *ArXiv Astrophysics e-prints*

Alexander, D. M., Bauer, F. E., Brandt, W. N., Schneider, D. P., Hornschemeier, A. E., Vignali, C., Barger, A. J., Broos, P. S., Cowie, L. L., Garmire, G. P., Townsley, L. K., Bautz, M. W., Chartas, G., and Sargent, W. L. W.: 2003a, *ArXiv Astrophysics e-prints* pp 4392–+

Alexander, D. M., Bauer, F. E., Brandt, W. N., Schneider, D. P., Hornschemeier, A. E., Vignali, C., Barger, A. J., Broos, P. S., Cowie, L. L., Garmire, G. P., Townsley, L. K., Bautz, M. W., Chartas, G., and Sargent, W. L. W.: 2003b, AJ **126**, 539

Allen, S. W.: 1998, MNRAS **296**, 392

Andreon, S., Valtchanov, I., Jones, L. R., Altieri, B., Bremer, M., Willis, J., Pierre, M., and Quintana, H.: 2005, MNRAS **359**, 1250

Arnaud, K. A.: 1996, in *ASP Conf. Ser. 101: Astronomical Data Analysis Software and Systems V*, pp 17–+

Arnaud, M. and Evrard, A. E.: 1999, MNRAS **305**, 631

Arnaud, M., Pointecouteau, E., and Pratt, G. W.: 2005, A&A **441**, 893

Audley, M. D., Holland, W. S., MacIntosh, M. J., Fairley, A. E., Robson, E. I., Irwin, K. D., Duncan, W. D., Walton, A., Ade, P. A. R., Fich, M., Kycia, J., Halpern, M., Naylor, D., Mitchell, G., and Bastien, P.: 2004, *American Astronomical Society Meeting Abstracts* **205**,

Böhringer, H., Schuecker, P., Guzzo, L., Collins, C. A., Voges, W., Schindler, S., Neumann, D. M., Cruddace, R. G., De Grandi, S., Chincarini, G., Edge, A. C., MacGillivray, H. T., and Shaver, P.: 2001, A&A **369**, 826

Bahcall, N. A. and Lubin, L. M.: 1994, ApJ **426**, 513

Ball, N. M., Loveday, J., Fukugita, M., Nakamura, O., Okamura, S., Brinkmann, J., and Brunner, R. J.: 2004, MNRAS **348**, 1038

Bartelmann, M. and Schneider, P.: 2001, Phys. Rep. **340**, 291

Berger, M. and van der Klis, M.: 1994, A&A **292**, 175

Bertin, E. and Arnouts, S.: 1996, A&AS **117**, 393

Böhringer, H., Burwitz, V., Zhang, Y.-Y., Schuecker, P., and Nowak, N.: 2005, ApJ **633**, 148

Bohringer, H., Voges, W., Huchra, J. P., McLean, B., Giacconi, R., Rosati, P., Burg, R., Mader, J., Schuecker, P., Simic, D., Komossa, S., Reiprich, T. H., Retzlaff, J., and Trumper, J.: 2000, *VizieR Online Data Catalog* **212**, 90435

Bolzonella, M., Miralles, J.-M., and Pelló, R.: 2000, A&A **363**, 476

Bond, J. R., Contaldi, C. R., Pen, U.-L., Pogosyan, D., Prunet, S., Ruetalo, M. I., Wadsley, J. W., Zhang, P., Mason, B. S., Myers, S. T., Pearson, T. J., Readhead, A. C. S., Sievers, J. L., and Udomprasert, P. S.: 2005, ApJ **626**, 12

Boschin, W.: 2003, *Memorie della Societa Astronomica Italiana* **74**, 440

Browne, I. W. A. and Cohen, A. M.: 1978, MNRAS **182**, 181

Carroll, B. W. and Ostlie, D. A.: 1996, *An introduction to modern astrophysics*, Reading, Mass. : Addison-Wesley Pub., c1996.

Cash, W.: 1979, ApJ **228**, 939

Castander, F. J., Bower, R. G., Ellis, R. S., Aragon-Salamanca, A., Mason, K. O., Hasinger, G., McMahon, R. G., Carrera, F. J., Mittaz, J. P. D., Perez-Fournon, I., and Lehto, H. J.: 1995, Nature **377**, 39

Cavaliere, A. and Fusco-Femiano, R.: 1976, A&A **49**, 137

Colless, M., Peterson, B. A., Jackson, C., Peacock, J. A., Cole, S., Norberg, P., Baldry, I. K., Baugh, C. M., Bland-Hawthorn, J., Bridges, T., Cannon, R., Collins, C., Couch, W., Cross, N., Dalton, G., De Propris, R., Driver, S. P., Efstathiou, G., Ellis, R. S., Frenk, C. S., Glazebrook, K., Lahav, O., Lewis, I., Lumsden, S., Maddox, S., Madgwick, D., Sutherland, W., and Taylor, K.: 2003, *ArXiv Astrophysics e-prints*

Collins, C. A., Burke, D. J., Romer, A. K., Sharples, R. M., and Nichol, R. C.: 1997, ApJ **479**, L117+

Collister, A. A. and Lahav, O.: 2004, PASP **116**, 345

Condon, J. J., Cotton, W. D., Greisen, E. W., Yin, Q. F., Perley, R. A., Taylor, G. B., and Broderick, J. J.: 1998, AJ **115**, 1693

Connolly, A. J., Csabai, I., Szalay, A. S., Koo, D. C., Kron, R. G., and Munn, J. A.: 1995, AJ **110**, 2655

Dalton, G. B., Maddox, S. J., Sutherland, W. J., and Efstathiou, G.: 1997, MNRAS **289**, 263

Damiani, F., Maggio, A., Micela, G., and Sciortino, S.: 1997, ApJ **483**, 350

Davé, R., Katz, N., and Weinberg, D. H.: 2002, ApJ **579**, 23

Del Popolo, A., Hiotelis, N., and Peñarrubia, J.: 2005, ApJ **628**, 76

Dickey, J. M. and Lockman, F. J.: 1990, *ARAA* **28**, 215

Downes, A. J. B., Peacock, J. A., Savage, A., and Carrie, D. R.: 1986, MNRAS **218**, 31

Ebeling, H.: 1993, *Ph.D. Thesis*

Ebeling, H., Edge, A. C., Bohringer, H., Allen, S. W., Crawford, C. S., Fabian, A. C., Voges, W., and Huchra, J. P.: 1998, MNRAS **301**, 881

Ebeling, H., Edge, A. C., and Henry, J. P.: 2001, ApJ **553**, 668

Ebeling, H. and Wiedenmann, G.: 1993, Phys. Rev. E **47**, 704

Eckart, M. E., Harrison, F. A., Helfand, D. J., Laird, E., Mao, P. H., and Stern, D.: 2003, *Astronomische Nachrichten* **324**, 180

Eke, V. R., Baugh, C. M., Cole, S., Frenk, C. S., Norberg, P., Peacock, J. A., Baldry, I. K., Bland-Hawthorn, J., Bridges, T., Cannon, R., Colless, M., Collins, C., Couch, W., Dalton, G., de Propris, R., Driver, S. P., Efstathiou, G., Ellis, R. S., Glazebrook, K., Jackson, C., Lahav, O., Lewis, I., Lumsden, S., Maddox, S., Madgwick, D., Peterson, B. A., Sutherland, W., and Taylor, K.: 2004, MNRAS **348**, 866

Eke, V. R., Cole, S., and Frenk, C. S.: 1996, MNRAS **282**, 263

Eke, V. R., Navarro, J. F., and Frenk, C. S.: 1998, ApJ **503**, 569

Ettori, S., Borgani, S., Moscardini, L., Murante, G., Tozzi, P., Diaferio, A., Dolag, K., Springel, V., Tormen, G., and Tornatore, L.: 2004a, MNRAS **354**, 111

Ettori, S., Tozzi, P., Borgani, S., and Rosati, P.: 2004b, A&A **417**, 13

Evrard, A. E., MacFarland, T. J., Couchman, H. M. P., Colberg, J. M., Yoshida, N., White, S. D. M., Jenkins, A., Frenk, C. S., Pearce, F. R., Peacock, J. A., and Thomas, P. A.: 2002, ApJ **573**, 7

Falco, E. E., Kurtz, M. J., Geller, M. J., Huchra, J. P., Peters, J., Berlind, P., Mink, D. J., Tokarz, S. P., and Elwell, B.: 1999, PASP **111**, 438

Finoguenov, A., Reiprich, T. H., and Böhringer, H.: 2001, A&A **368**, 749

Firth, A. E., Lahav, O., and Somerville, R. S.: 2003, MNRAS **339**, 1195

Fort, B. and Mellier, Y.: 1994, A&A Rev. **5**, 239

Freeman, P. E., Kashyap, V., Rosner, R., and Lamb, D. Q.: 2002, ApJS **138**, 185

Gehrels, N.: 1986, ApJ **303**, 336

Geisbüsch, J., Kneissl, R., and Hobson, M.: 2005, MNRAS **360**, 41

Ghizzardi, S.: 2001, *In Flight Calibration of the PSF for the MOS1 and MOS2 Cameras*, Technical report, Milano Calibration Team, Istituto di Fisica Cosmica

Giacconi, R., Branduardi, G., Briel, U., Epstein, A., Fabricant, D., Feigelson, E., Forman, W., Gorenstein, P., Grindlay, J., Gursky, H., Harnden, F. R., Henry, J. P., Jones, C., Kellogg, E., Koch, D., Murray, S., Schreier, E., Seward, F., Tananbaum, H., Topka, K., Van Speybroeck, L., Holt, S. S., sBecker, R. H., Boldt, E. A., Serlemitsos, P. J., Clark, G., Canizares, C., Markert, T., Novick. R., Helfand, D., and Long, K.: 1979, ApJ **230**, 540

Giacconi, R., Gursky, H., Paolini, F. R., and Rossi, B. B.: 1962, *Physical Review Letters* **9**, 439

Giacconi, R., Kellogg, E., Gorenstein, P., Gursky, H., and Tananbaum, H.: 1971, ApJ **165**, L27+

Giacconi, R., Murray, S., Gursky, H., Kellogg, E., Schreier, E., and Tananbaum, H.: 1972, ApJ **178**, 281

Gioia, I. M., Maccacaro, T., Schild, R. E., Wolter, A., Stocke, J. T., Morris, S. L., and Henry, J. P.: 1990, ApJS **72**, 567

Gladders, M. D.: 2000, *American Astronomical Society Meeting* **197**, 0

Gladders, M. D. and Yee, H. K. C.: 2000, AJ **120**, 2148

Gladders, M. D. and Yee, H. K. C.: 2005, ApJS **157**, 1

Gunn, J. E. and Gott, J. R. I.: 1972, ApJ **176**, 1

Hallman, E. J. and Markevitch, M.: 2004, ApJ **610**, L81

Hambly, N. C., MacGillivray, H. T., Read, M. A., Tritton, S. B., Thomson, E. B., Kelly, B. D., Morgan, D. H., Smith, R. E., Driver, S. P., Williamson, J., Parker, Q. A., Hawkins, M. R. S., Williams, P. M., and Lawrence, A.: 2001, MNRAS **326**, 1279

Hashimoto, Y., Barcons, X., Böhringer, H., Fabian, A. C., Hasinger, G., Mainieri, V., and Brunner, H.: 2004, A&A **417**, 819

Helsdon, S. F. and Ponman, T. J.: 2000, MNRAS **315**, 356

Holder, G., Haiman, Z., and Mohr, J. J.: 2001, ApJ **560**, L111

Holder, G. P., Mohr, J. J., Carlstrom, J. E., Evrard, A. E., and Leitch, E. M.: 2000, ApJ **544**, 629

Hubble, E.: 1929, *Proceedings of the National Academy of Science* **15**, 168

Hubble, E.: 1934, ApJ **79**, 8

Huchra, J. P. and Geller, M. J.: 1982, ApJ **257**, 423

Huchra, J. P., Geller, M. J., Clemens, C. M., Tokarz, S. P., and Michel, A.: 1996, *VizieR Online Data Catalog* **7193**, 0

Immler, S., Fesen, R. A., Van Dyk, S. D., Weiler, K. W., Petre, R., Lewin, W. H. G., Pooley, D., Pietsch, W., Aschenbach, B., Hammell, M. C., and Rudie, G. C.: 2005, ApJ **632**, 283

Inada, N., Burles, S., Gregg, M. D., Becker, R. H., Schechter, P. L., Eisenstein, D. J., Oguri, M., Castander, F. J., Hall, P. B., Johnston, D. E., Pindor, B., Richards, G. T., Schneider, D. P., White, R. L., Brinkmann, J., Szalay, A. S., and York, D. G.: 2005, AJ **130**, 1967

Jarrett, T. H., Chester, T., Cutri, R., Schneider, S., Skrutskie, M., and Huchra, J. P.: 2000, AJ **119**, 2498

Jenkins, A., Frenk, C. S., White, S. D. M., Colberg, J. M., Cole, S., Evrard, A. E., Couchman, H. M. P., and Yoshida, N.: 2001, MNRAS **321**, 372

Jones, D. H., Saunders, W., Colless, M., Read, M. A., Parker, Q. A., Watson, F. G., Campbell, L. A., Burkey, D., Mauch, T., Moore, L., Hartley, M., Cass, P., James, D., Russell, K., Fiegert, K., Dawe, J., Huchra, J., Jarrett, T., Lahav, O., Lucey, J., Mamon, G. A., Proust, D., Sadler, E. M., and Wakamatsu, K.-i.: 2004, MNRAS **355**, 747

Jones, L. R., Ponman, T. J., Horton, A., Babul, A., Ebeling, H., and Burke, D. J.: 2003, MNRAS **343**, 627

Kay, S. T., Thomas, P. A., Jenkins, A., and Pearce, F. R.: 2004, MNRAS **355**, 1091

Kibblewhite, E. J., Bridgeland, M. T., Bunclark, P. S., and Irwin, M. J.: 1984, in *Astronomical Microdensitometry Conference*, pp 277–+

King, I. R.: 1972, ApJ **174**, L123+

Kitayama, T. and Suto, Y.: 1997, ApJ **490**, 557

Kleinmann, S. G., Lysaght, M. G., Pughe, W. L., Schneider, S. E., Skrutskie, M. F., Weinberg, M. D., Price, S. D., Matthews, K., Soifer, B. T., and Huchra, J. P.: 1994, Ap&SS **217**, 11

Land, K. R., Nichol, R. C., Davidson, M., Sabirli, K., Romer, A. K., Liddle, A. R., Collins, C. A., Kay, S. T., Mann, R. G., Viana, P. T. P., and West, M. J.: 2004, *XMM Cluster Survey: X-ray source identification using the Sloan Digital Sky Survey*, astro-ph/0405225

Lasker, B. M., Sturch, C. R., McLean, B. J., Russell, J. L., Jenkner, H., and Shara, M. M.: 1990, AJ **99**, 2019

Lawrence, A., Hambly, N., Mann, B., Irwin, M., McMahon, R. G., Lewis, J. R., and Adamson, A. J.: 2002, in *Survey and Other Telescope Technologies and Discoveries. Edited by Tyson, J. Anthony; Wolff, Sidney. Proceedings of the SPIE, Volume 4836, pp. 418-425 (2002).*, pp 418–425

Lazzati, D., Campana, S., Rosati, P., Panzera, M. R., and Tagliaferri, G.: 1999, ApJ **524**, 414

Lumsden, S. L., Nichol, R. C., Collins, C. A., and Guzzo, L.: 1992, MNRAS **258**, 1

MacGillivray, H. T. and Stobie, R. S.: 1984, *Vistas in Astronomy* **27**, 433

Mann, R. G., Oliver, S. J., Serjeant, S. B. G., Rowan-Robinson, M., Baker, A., Eaton, N., Efstathiou, A., Goldschmidt, P., Mobasher, B., Sumner, T. J., Danese, L., Elbaz, D., Franceschini, A., Egami, E., Kontizas, M., Lawrence, A., McMahon, R., Norgaard-Nielsen, H. U., Perez-Fournon, I., and Gonzalez-Serrano, J. I.: 1997, MNRAS **289**, 482

Mann, R. G., The Astrogrid Consortium, Lawrence, A., Davenhall, C., Mann, B., McMahon, R., Irwin, M., Walton, N., Rixon, G., Watson, M., Osborne, J., Page, C., Allan, P., Giaretta, D., Perry, C., Pike, D., Sherman, J., Murtagh, F., Harra, L., Bentley, B., Mason, K., and Garrington, S.: 2002, in *ASP Conf. Ser. 281: Astronomical Data Analysis Software and Systems XI*, pp 3–+

Markevitch, M.: 1998, ApJ **504**, 27

Marshall, F. E., Boldt, E. A., Holt, S. S., Miller, R. B., Mushotzky, R. F., Rose, L. A., Rothschild, R. E., and Serlemitsos, P. J.: 1980, ApJ **235**, 4

Mattson, B. J. and Weaver, K. A.: 2004, ApJ **601**, 771

McHardy, I. M., Jones, L. R., Merrifield, M. R., Mason, K. O., Newsam, A. M., Abraham, R. G., Dalton, G. B., Carrera, F., Smith, P. J., Rowan-Robinson, M.,

Wegner, G. A., Ponman, T. J., Lehto, H. J., Branduardi-Raymont, G., Luppino, G. A., Efstathiou, G., Allan, D. J., and Quenby, J. J.: 1998, MNRAS **295**, 641

McIntosh, D. H., Bell, E. F., Weinberg, M. D., and Katz, N.: 2005, *ArXiv Astrophysics e-prints*

McMahon, R. G., Walton, N. A., Irwin, M. J., Lewis, J. R., Bunclark, P. S., and Jones, D. H.: 2001, *New Astronomy Review* **45**, 97

Merchán, M. E. and Zandivarez, A.: 2005, ApJ **630**, 759

Miller, C. J., Nichol, R. C., Reichart, D., Wechsler, R. H., Evrard, A. E., Annis, J., McKay, T. A., Bahcall, N. A., Bernardi, M., Boehringer, H., Connolly, A. J., Goto, T., Kniazev, A., Lamb, D., Postman, M., Schneider, D. P., Sheth, R. K., and Voges, W.: 2005, AJ **130**, 968

Miralda-Escude, J.: 1995, ApJ **438**, 514

Mo, H. J. and White, S. D. M.: 2002, MNRAS **336**, 112

Moore, B., Quinn, T., Governato, F., Stadel, J., and Lake, G.: 1999, MNRAS **310**, 1147

Muanwong, O., Thomas, P. A., Kay, S. T., and Pearce, F. R.: 2002, MNRAS **336**, 527

Mulchaey, J. S., Davis, D. S., Mushotzky, R. F., and Burstein, D.: 2003, ApJS **145**, 39

Mullis, C. R., McNamara, B. R., Quintana, H., Vikhlinin, A., Henry, J. P., Gioia, I. M., Hornstrup, A., Forman, W., and Jones, C.: 2003, ApJ **594**, 154

Mullis, C. R., Rosati, P., Lamer, G., Böhringer, H., Schwope, A., Schuecker, P., and Fassbender, R.: 2005, ApJ **623**, L85

Mushotzky, R. F.: 2004, in *Clusters of Galaxies: Probes of Cosmological Structure and Galaxy Evolution*, pp 124–+

Nakata, F., Kodama, T., Shimasaku, K., Doi, M., Furusawa, H., Hamabe, M., Kimura, M., Komiyama, Y., Miyazaki, S., Okamura, S., Ouchi, M., Sekiguchi, M., Ueda, Y., Yagi, M., and Yasuda, N.: 2005, MNRAS **357**, 1357

Nandra, K., George, I. M., Mushotzky, R. F., Turner, T. J., and Yaqoob, T.: 1999, ApJ **523**, L17

Navarro, J. F., Frenk, C. S., and White, S. D. M.: 1997a, ApJ **490**, 493

Navarro, J. F., Frenk, C. S., and White, S. D. M.: 1997b, ApJ **490**, 493

Neumann, D. M.: 2005a, A&A **439**, 465

Neumann, D. M.: 2005b, A&A **439**, 465

Neumann, D. M. and Arnaud, M.: 1999, A&A **348**, 711

Nevalainen, J., Markevitch, M., and Forman, W.: 1999, ApJ **526**, 1

Nonino, M., Bertin, E., da Costa, L., Deul, E., Erben, T., Olsen, L., Prandoni, I., Scodeggio, M., Wicenec, A., Wichmann, R., Benoist, C., Freudling, W., Guarnieri, M. D., Hook, I., Hook, R., Mendez, R., Savaglio, S., Silva, D., and Slijkhuis, R.: 1999, A&AS **137**, 51

Odewahn, S. C., Gal, R. R., de Carvalho, R. R., Djorgovski, S. G., Mahabal, A. A., Brunner, R., Lopes, P., and DPOSS Team: 2001, *Bulletin of the American Astronomical Society* **33**, 1462

Onuora, L. I., Kay, S. T., and Thomas, P. A.: 2003, MNRAS **341**, 1246

Ota, N. and Mitsuda, K.: 2004a, A&A **428**, 757

Ota, N. and Mitsuda, K.: 2004b, A&A **428**, 757

Oukbir, J. and Blanchard, A.: 1997, A&A **317**, 1

Peacock, J. A.: 1999, *Cosmological Physics*, Cosmological Physics, by John A. Peacock, pp. 704. ISBN 052141072X. Cambridge, UK: Cambridge University Press, January 1999.

Pierpaoli, E. and Anthoine, S.: 2005, *Advances in Space Research* **36**, 757

Pointecouteau, E., Arnaud, M., and Pratt, G. W.: 2005, A&A **435**, 1

Ponman, T. J., Allan, D. J., Jones, L. R., Merrifield, M., McHardy, I. M., Lehto, H. J., and Luppino, G. A.: 1994, Nature **369**, 462

Ponman, T. J., Cannon, D. B., and Navarro, J. F.: 1999, Nature **397**, 135

Postman, M., Lubin, L. M., Gunn, J. E., Oke, J. B., Hoessel, J. G., Schneider, D. P., and Christensen, J. A.: 1996, AJ **111**, 615

Refregier, A.: 2003, ARA&A **41**, 645

Refregier, A., Valtchanov, I., and Pierre, M.: 2002, A&A **390**, 1

Riess, A. G., Filippenko, A. V., Challis, P., Clocchiatti, A., Diercks, A., Garnavich, P. M., Gilliland, R. L., Hogan, C. J., Jha, S., Kirshner, R. P., Leibundgut, B., Phillips, M. M., Reiss, D., Schmidt, B. P., Schommer, R. A., Smith, R. C., Spyromilio, J., Stubbs, C., Suntzeff, N. B., and Tonry, J.: 1998, AJ **116**, 1009

Romer, A. K., Viana, P. T. P., Liddle, A. R., and Mann, R. G.: 2001, ApJ **547**, 594

Rosati, P., Borgani, S., and Norman, C.: 2002, ARA&A **40**, 539

Rosati, P., della Ceca, R., Burg, R., Norman, C., and Giacconi, R.: 1995, ApJ **445**, L11

Rosati, P., della Ceca, R., Norman, C., and Giacconi, R.: 1998, ApJ **492**, L21+

Rosati, P., Stanford, S. A., Eisenhardt, P. R., Elston, R., Spinrad, H., Stern, D., and Dey, A.: 1999, AJ **118**, 76

Rosati, P., Tozzi, P., Ettori, S., Mainieri, V., Demarco, R., Stanford, S. A., Lidman, C., Nonino, M., Borgani, S., Della Ceca, R., Eisenhardt, P., Holden, B. P., and Norman, C.: 2004, AJ **127**, 230

Rybicki, G. B. and Lightman, A. P.: 1986, *Radiative Processes in Astrophysics*, Radiative Processes in Astrophysics, by George B. Rybicki, Alan P. Lightman, pp. 400. ISBN 0-471-82759-2. Wiley-VCH , June 1986.

Sanders, J. S. and Fabian, A. C.: 2002, MNRAS **331**, 273

Scharf, C.: 2002, ApJ **572**, 157

Scharf, C. A., Jones, L. R., Ebeling, H., Perlman, E., Malkan, M., and Wegner, G.: 1997, ApJ **477**, 79

Schulz, A. E. and White, M.: 2003, ApJ **586**, 723

Serjeant, S., Dunlop, J. S., Mann, R. G., Rowan-Robinson, M., Hughes, D., Efstathiou, A., Blain, A., Fox, M., Ivison, R. J., Jenness, T., Lawrence, A., Longair, M., Oliver, S., and Peacock, J. A.: 2003, MNRAS **344**, 887

Small, T. A., Ma, C.-P., Sargent, W. L. W., and Hamilton, D.: 1998, ApJ **492**, 45

Smith, G. P., Kneib, J.-P., Smail, I., Mazzotta, P., Ebeling, H., and Czoske, O.: 2005, MNRAS **359**, 417

Spergel, D. N., Verde, L., Peiris, H. V., Komatsu, E., Nolta, M. R., Bennett, C. L., Halpern, M., Hinshaw, G., Jarosik, N., Kogut, A., Limon, M., Meyer, S. S., Page, L., Tucker, G. S., Weiland, J. L., Wollack, E., and Wright, E. L.: 2003, ApJS **148**, 175

Stanford, S. A., Elston, R., Eisenhardt, P. R., Spinrad, H., Stern, D., and Dey, A.: 1997a, AJ **114**, 2232

Stanford, S. A., Elston, R., Eisenhardt, P. R., Spinrad, H., Stern, D., and Dey, A.: 1997b, AJ **114**, 2232

Stanford, S. A., Holden, B., Rosati, P., Eisenhardt, P. R., Stern, D., Squires, G., and Spinrad, H.: 2002, AJ **123**, 619

Starck, J.-L., Murtagh, F., and Bijaoui, A.: 1998, *Image processing and data analysis. The multiscale approach*, Image processing and data analysis. The multiscale approach, Publisher: Cambridge, UK: Cambridge University Press, 1998, ISBN: 0521590841

Starck, J.-L. and Pierre, M.: 1998, A&AS **128**, 397

Stoughton, C., Lupton, R. H., Bernardi, M., Blanton, M. R., Burles, S., Castander, F. J., Connolly, A. J., Eisenstein, D. J., Frieman, J. A., Hennessy, G. S., Hindsley, R. B., Ivezić, Ž., Kent, S., Kunszt, P. Z., Lee, B. C., Meiksin, A., Munn, J. A., Newberg, H. J., Nichol, R. C., Nicinski, T., Pier, J. R., Richards, G. T., Richmond, M. W., Schlegel, D. J., Smith, J. A., Strauss, M. A., SubbaRao, M., Szalay, A. S., Thakar, A. R., Tucker, D. L., Vanden Berk, D. E., Yanny, B., Adelman, J. K., Anderson, J. E., Anderson, S. F., Annis, J., Bahcall, N. A., Bakken, J. A., Bartelmann, M., Bastian, S., Bauer, A., Berman, E., Böhringer, H., Boroski, W. N., Bracker, S., Briegel, C., Briggs, J. W., Brinkmann, J., Brunner, R., Carey, L., Carr, M. A., Chen, B., Christian, D., Colestock, P. L., Crocker, J. H., Csabai, I., Czarapata, P. C., Dalcanton, J., Davidsen, A. F., Davis, J. E., Dehnen, W., Dodelson, S., Doi, M., Dombeck, T., Donahue, M., Ellman, N., Elms, B. R., Evans, M. L., Eyer, L., Fan, X., Federwitz, G. R., Friedman, S., Fukugita, M., Gal, R., Gillespie, B., Glazebrook, K., Gray, J., Grebel, E. K., Greenawalt, B., Greene, G., Gunn, J. E., de Haas, E., Haiman, Z., Haldeman, M., Hall, P. B., Hamabe, M., Hansen, B., Harris,

F. H., Harris, H., Harvanek, M., Hawley, S. L., Hayes, J. J. E., Heckman, T. M., Helmi, A., Henden, A., Hogan, C. J., Hogg, D. W., Holmgren, D. J., Holtzman, J., Huang, C.-H., Hull, C., Ichikawa, S.-I., Ichikawa, T., Johnston, D. E., Kauffmann, G., Kim, R. S. J., Kimball, T., Kinney, E., Klaene, M., Kleinman, S. J., Klypin, A., Knapp, G. R., Korienek, J., Krolik, J., Kron, R. G., Krzesiński, J., Lamb, D. Q., Leger, R. F., Limmongkol, S., Lindenmeyer, C., Long, D. C., Loomis, C., Loveday, J., MacKinnon, B., Mannery, E. J., Mantsch, P. M., Margon, B., McGehee, P., McKay, T. A., McLean, B., Menou, K., Merelli, A., Mo, H. J., Monet, D. G., Nakamura, O., Narayanan, V. K., Nash, T., Neilsen, E. H., Newman, P. R., Nitta, A., Odenkirchen, M., Okada, N., Okamura, S., Ostriker, J. P., Owen, R., Pauls, A. G., Peoples, J., Peterson, R. S., Petravick, D., Pope, A., Pordes, R., Postman, M., Prosapio, A., Quinn, T. R., Rechenmacher, R., Rivetta, C. H., Rix, H.-W., Rockosi, C. M., Rosner, R., Ruthmansdorfer, K., Sandford, D., Schneider, D. P., Scranton, R., Sekiguchi, M., Sergey, G., Sheth, R., Shimasaku, K., Smee, S., Snedden, S. A., Stebbins, A., Stubbs, C., Szapudi, I., Szkody, P., Szokoly, G. P., Tabachnik, S., Tsvetanov, Z., Uomoto, A., Vogeley, M. S., Voges, W., Waddell, P., Walterbos, R., Wang, S.-i., Watanabe, M., Weinberg, D. H., White, R. L., White, S. D. M., Wilhite, B., Wolfe, D., Yasuda, N., York, D. G., Zehavi, I., and Zheng, W.: 2002, AJ **123**, 485

Sunyaev, R. A. and Zeldovich, Y. B.: 1972, *Comments on Astrophysics and Space Physics* **4**, 173

Sutherland, W. and Saunders, W.: 1992, MNRAS **259**, 413

Taylor, B. G., Andresen, R. D., Peacock, A., and Zobl, R.: 1981, *Space Science Reviews* **30**, 479

Thomas, P. A., Muanwong, O., Pearce, F. R., Couchman, H. M. P., Edge, A. C., Jenkins, A., and Onuora, L.: 2001, MNRAS **324**, 450

Truemper, J.: 1993, *Science* **260**, 1769

Turner, T. J., Miller, L., George, I. M., and Reeves, J. N.: 2004, *American Astronomical Society Meeting Abstracts* **205**,

Valtchanov, I., Pierre, M., and Gastaud, R.: 2001, A&A **370**, 689

van Haarlem, M. P., Frenk, C. S., and White, S. D. M.: 1997, MNRAS **287**, 817

Vanzella, E., Cristiani, S., Fontana, A., Nonino, M., Arnouts, S., Giallongo, E., Grazian, A., Fasano, G., Popesso, P., Saracco, P., and Zaggia, S.: 2004, A&A **423**, 761

Véron-Cetty, M.-P. and Véron, P.: 2003, A&A **412**, 399

Viana, P. T. P. and Liddle, A. R.: 1996, MNRAS **281**, 323

Viana, P. T. P., Romer, A. K., Liddle, A. R., Mann, R. G., Collins, C. A., Nichol, R. C., and West, M. J.: 2002, in *On the nature of dark energy*, AIP

Vikhlinin, A., Forman, W., and Jones, C.: 1999, ApJ **525**, 47

Vikhlinin, A., McNamara, B. R., Forman, W., Jones, C., Quintana, H., and Hornstrup, A.: 1998, ApJ **502**, 558

Voges, W., Henry, J. P., Briel, U. G., Böhringer, H., Mullis, C. R., Gioia, I. M., and Huchra, J. P.: 2001, ApJ **553**, L119

Walsh, D., Carswell, R. F., and Weymann, R. J.: 1979, Nature **279**, 381

Weinmann, S. M., van den Bosch, F. C., Yang, X., and Mo, H. J.: 2005, *ArXiv Astrophysics e-prints*

White, N. E., Giommi, P., and Angelini, L.: 2000, *VizieR Online Data Catalog* **9031**, 0

Wilkes, B. J. and et al.: 2001, in *ASP Conf. Ser. 232: The New Era of Wide Field Astronomy*, pp 47–+

Wu, X.-P. and Xue, Y.-J.: 2000, ApJ **542**, 578

XMM-Newton Survey Science Centre, C.: 2003, *VizieR Online Data Catalog* **9037**, 0

Zwicky, F.: 1933, *Helvetica Physica Acta* **6**, 110

Zwicky, F.: 1966, in *California Inst. Techn., 3 (1966)*, pp 0–+

Appendix A

Observation Log

Obsid	Field Name	RA(J2000)	Dec(J2000)	t_{exp}/ s	Type	StatSam
0000110101	XTE J0421+560	04 19 42.1	+55 59 58	24378	6	Y
0001730601	HD47129	06 37 24.0	+06 08 07	18530	4	Y
0001930101	IRAS F00235+1024	00 26 07.0	+10 41 21	16286	1	Y
0001930301	IRAS F12514+1027	12 54 00.0	+10 11 11	21721	1	Y
0002740101	CFHT-Pl-12	03 53 55.1	+23 23 38	22179	4	Y
0002740301	Denis-J1228	12 28 13.8	-15 47 11	8677	4	Y
0002740501	Cha-Ha-3	11 07 52.9	-77 36 56	22804	4	Y
0002940101	NGC4968	13 07 05.9	-23 40 36	7091	1	Y
0002940401	NGC1410	03 41 10.8	-01 17 57	1497	1	Y
0002942301	NGC424	01 11 27.5	-38 05 01	7608	1	Y
0002942401	UGC2608	03 15 01.4	+42 02 09	2737	1	Y
0002960101	3C465	23 38 29.0	+27 01 53	10968	1	Y
0002970101	3C449	22 31 20.6	+39 21 30	21068	1	Y
0002970201	3C66B	02 23 11.4	+42 59 31	19143	1	Y
0004010101	3C58	02 05 37.7	+64 49 42	7574	5	N
0004010201	3C58	02 05 37.7	+64 49 42	22033	5	N
0004210201	G16.7+0.1	18 20 56.8	-14 19 40	8400	5	N
0004610201	NEP5281	18 21 38.1	+68 27 52	5105	3	N
0004610301	NEP5281	18 21 38.1	+68 27 52	13700	3	N
0004610401	NEP5281	18 21 38.1	+68 27 52	4610	3	N
0005010101	Mkn478	14 42 07.4	+35 26 23	24082	1	Y
0005010201	Mkn478	14 42 07.4	+35 26 23	9800	1	Y
0005010301	Mkn478	14 42 07.4	+35 26 23	25966	1	Y
0006010301	Beta Geminorum	07 45 18.9	+28 01 34	34459	4	Y
0006010401	Beta Hydri	00 25 45.1	-77 15 18	35135	4	Y
0006220201	NGC 4507	12 35 34.8	-39 54 55	42775	1	Y
0006810101	Akn 564	22 42 39.3	+29 43 31	6846	1	Y
0006810301	Akn 564	22 42 39.3	+29 43 31	8589	1	Y
0007420701	Galactic Plane 07	14 01 48.3	-62 10 31	11992	7	Y
0007420801	Galactic Plane 08	13 59 09.0	-61 49 43	12784	7	Y
0007420901	Galactic Plane 09	13 59 56.0	-61 22 19	9568	7	Y
0007421001	Galactic Plane 10	13 57 22.0	-61 01 23	11100	7	Y
0007421101	Galactic Plane 11	13 58 09.3	-60 34 01	11114	7	Y
0007421201	Galactic Plane 12	13 55 40.3	-60 12 58	13259	7	Y
0007421301	Galactic Plane 13	13 56 27.9	-59 45 38	15836	7	Y
0007421401	Galactic Plane 14	13 54 03.5	-59 24 28	12058	7	Y
0007421501	Galactic Plane 15	13 54 51.2	-58 57 11	14190	7	Y
0007421601	Galactic Plane 16	14 05 13.5	-62 03 39	12206	7	Y
0007421701	Galactic Plane 17	14 02 33.0	-61 43 05	12319	7	Y
0007421801	Galactic Plane 18	14 03 16.4	-61 15 37	7690	7	Y
0007421901	Galactic Plane 19	14 00 41.2	-60 54 55	9784	7	Y
0007422001	Galactic Plane 20	14 01 25.1	-60 27 29	10041	7	Y
0007422101	Galactic Plane 21	13 58 54.9	-60 06 39	11784	7	Y
0007422201	Galactic Plane 22	13 59 39.1	-59 39 16	11837	7	Y
0007422301	Galactic Plane 23	13 57 13.7	-59 18 18	14940	7	Y
0007422401	Galactic Plane 24	13 57 58.2	-58 50 58	12319	7	Y
0007425001	Galactic Plane 18	14 03 16.4	-61 15 37	6784	7	Y
0008020101	RXJ0439.8-6809	04 39 49.7	-68 09 02	12500	6	Y
0008220201	HD 111812	12 51 41.9	+27 32 27	39732	4	Y
0008820301	HD168112	18 18 30.0	-12 10 00	11318	4	Y
0008820601	HD168112	18 18 30.0	-12 10 00	13520	4	Y
0008830101	ms2137-23	21 40 15.2	-23 39 41	12400	3	N
0009220301	Mrk 3	06 15 36.3	+71 02 15	2100	1	Y
0009220401	Mrk 3	06 15 36.3	+71 02 15	8170	1	Y
0009220501	Mrk 3	06 15 36.3	+71 02 15	7271	1	Y
0009220601	Mrk 3	06 15 36.3	+71 02 15	11989	1	Y
0009220701	Mrk 3	06 15 36.3	+71 02 15	6800	1	Y
0009220901	Mrk 3	06 15 36.3	+71 02 15	7586	1	Y
0009221001	Mrk 3	06 15 36.3	+71 02 15	6598	1	Y
0009221601	Mrk 3	06 15 36.3	+71 02 15	7488	1	Y
0009650101	AO Psc	22 55 18.0	-03 10 41	31442	6	Y
0009650201	FO Aqr	22 17 55.5	-08 21 05	19577	6	Y
0010620101	V1309 Ori	05 15 41.4	+01 04 41	24309	6	Y
0011420101	NGC 2264 north	06 40 43.3	+09 51 00	37811	4	Y
0011430201	CTA1	00 07 02.0	+73 02 59	37224	5	N

0011450101	SMC X-1	01 17 05.1	-73 26 35	43138	6	Y
0011830201	CSO 755	15 25 53.9	+51 36 49	29953	1	Y
0011830401	CSO 755	15 25 53.9	+51 36 49	6710	1	Y
0012440301	PB5062	22 05 09.8	-01 55 18	29059	1	Y
0012660101	2EG 2227+6122	22 29 05.0	+61 14 16	24355	5	N
0012830101	NGC 1399	03 38 29.3	-35 27 01	10642	2	Y
0012850101	C0720.8+7109	07 20 46.8	+71 09 40	2311	3	N
0012850201	C1256.0+2556	12 56 02.9	+25 56 45	25051	3	N
0012850601	C0720.8+7109	07 20 46.8	+71 09 40	4900	3	N
0012850701	C0720.8+7109	07 20 46.8	+71 09 40	8700	3	N
0012940101	MR2251-178	22 54 06.0	-17 34 55	62616	1	Y
0013140101	NGC 5506	14 13 14.9	-03 12 27	17438	1	Y
0013140201	NGC 5506	14 13 14.9	-03 12 27	12321	1	Y
0014740601	a0447-0627	04 47 48.6	-06 27 51	2340	1	Y
0016140101	RX J0002+6246	00 02 55.5	+62 46 17	24161	5	N
0017540101	A868	09 45 25.2	-08 39 06	7607	3	N
0017740201	Galactic Ridge 2	18 44 26.5	+00 58 21	17070	5	N
0017740401	Galactic Ridge 1	18 51 44.7	+00 08 58	27468	5	N
0017740501	Galactic Ridge 1	18 51 44.7	+00 08 58	21464	5	N
0017740601	Galactic Ridge 2	18 44 26.5	+00 58 21	22234	5	N
0017740701	Galactic Ridge 2	18 44 26.5	+00 58 21	22147	5	N
0017940101	GP Com	13 05 43.5	+18 01 02	47695	6	Y
0018540101	HD 5980	00 59 26.8	-72 09 55	26875	4	Y
0018741001	A2055	15 18 46.0	+06 13 60	7436	3	N
0018741101	A2104	15 40 06.0	-03 18 30	2116	3	N
0018741701	A3888	22 34 32.8	-37 43 59	7107	3	N
0020540401	RXJ1309.9+3222	13 09 55.6	+32 22 31	48261	3	N
0021140201	Stephans Quintet	22 36 03.3	+33 59 08	43739	2	Y
0021140801	IC1262	17 32 59.7	+43 44 38	405	2	Y
0021140901	IC1262	17 32 59.7	+43 44 38	4795	2	Y
0021540101	NGC 5846	15 06 29.3	+01 36 21	28659	2	Y
0021540201	NGC 4649	12 43 39.7	+11 33 09	49307	2	Y
0021540501	NGC 5846	15 06 29.3	+01 36 21	15369	2	Y
0021740101	3C 223	09 39 52.8	+35 53 58	29237	1	Y
0021740201	3C 284	13 11 04.6	+27 28 07	43498	1	Y
0021750101	AlphaTrA	16 48 39.9	-69 01 40	12959	4	Y
0021750201	BetaDra	17 30 25.8	+52 18 05	7358	4	Y
0021750401	AlphaTrA	16 48 39.9	-69 01 40	10020	4	Y
0021750501	AlphaTrA	16 48 39.9	-69 01 40	27335	4	Y
0021750601	AlphaTrA	16 48 39.9	-69 01 40	6310	4	Y
0021750701	AlphaTrA	16 48 39.9	-69 01 40	28086	4	Y
0021751001	BetaDra	17 30 25.8	+52 18 05	3115	4	Y
0022140101	HD148937	16 33 52.4	-48 06 40	15129	5	N
0022140601	HD148937	16 33 52.4	-48 06 40	12743	5	N
0022740101	Lockman Hole	10 52 43.0	+57 28 48	12482	7	Y
0022740201	Lockman Hole	10 52 43.0	+57 28 48	42160	7	Y
0022740301	Lockman Hole	10 52 43.0	+57 28 48	34484	7	Y
0022940101	IRAS18325-5926	18 36 58.1	-59 24 09	61211	1	Y
0024140101	GammaTau	04 19 47.6	+15 37 40	52347	4	Y
0024940201	WR110	18 07 57.0	-19 23 57	25190	4	Y
0025540101	IC1623	01 07 46.6	-17 30 22	7684	1	Y
0025540301	NGC2623	08 38 23.0	+25 45 17	11196	1	Y
0025540401	NGC2633	08 48 04.7	+74 05 52	13005	1	Y
0025541001	NGC7479	23 04 56.6	+12 19 23	9600	1	Y
0025541601	NGC520	01 24 35.0	+03 47 29	12520	1	Y
0025541701	NGC2633	08 48 04.7	+74 05 52	8795	1	Y
0025740101	CL1604+4304	16 04 19.5	+43 04 34	4400	3	N
0025740201	CL1324+3011	13 24 50.4	+30 11 26	37661	3	N
0025740401	CL1604+4304	16 04 19.5	+43 04 34	15700	3	N
0026340101	Holmberg I	09 40 29.1	+71 11 19	25860	2	Y
0026340201	Sextans A	10 11 05.6	-04 41 28	11100	2	Y
0026340301	IC 2574	10 28 21.2	+68 24 43	21922	2	Y
0027340101	NGC 3923	11 51 02.1	-28 48 23	37417	2	Y
0028540201	3C 184	07 39 24.3	+70 23 11	37449	3	N
0028540301	3C 322	15 35 01.2	+55 36 51	10948	3	N
0028540601	3C 184	07 39 24.3	+70 23 11	38583	3	N
0028540801	3C 184	07 39 24.3	+70 23 11	14761	3	N

0028740101	NGC 55 (West)	00 14 32.8	-39 10 46	30271	7	Y
0028740201	NGC 55 (East)	00 15 46.0	-39 15 28	33012	7	Y
0028740301	NGC 3184	10 18 40.0	+41 25 11	23506	7	Y
0029340101	SV Cam	06 41 19.1	+82 16 02	24926	4	Y
0029740101	MCG–6-30-15	13 35 53.7	-34 17 45	59855	1	Y
0029740701	MCG–6-30-15	13 35 53.7	-34 17 45	102443	1	Y
0029740801	MCG–6-30-15	13 35 53.7	-34 17 45	115247	1	Y
0030140201	A3530	12 55 30.7	-30 19 53	4794	3	N
0030140301	A3532	12 57 22.0	-30 22 03	14615	3	N
0030540101	XTE J1748-288	17 48 05.1	-28 28 26	27517	6	Y
0030540201	XTE J1748-288	17 48 05.1	-28 28 26	3838	6	Y
0031740101	PSR J0034-0534	00 34 21.8	-05 34 37	27354	5	N
0032140101	1saxJ1218.0+4738	12 18 03.0	+47 38 36	3349	7	Y
0032140201	1saxJ2302.5+0836	23 02 29.6	+08 36 33	8310	7	Y
0032140401	1saxj0140.2-6748	01 40 13.2	-67 48 51	7204	7	Y
0032140501	1saxj0646.7-4432	06 46 42.5	-44 32 29	12571	7	Y
0032140701	1saxj2331.9+1938	23 31 53.7	+19 38 03	10673	7	Y
0032140801	1saxj1649.9+0454	16 49 59.7	+04 53 18	2600	7	Y
0032141201	1saxj1305.2-1020	13 05 13.2	-10 20 59	13559	7	Y
0032340301	HD 81809	09 27 46.8	-06 04 16	5720	4	Y
0032341301	HD 81809	09 27 46.8	-06 04 16	4560	4	Y
0032342201	HD 81809	09 27 46.8	-06 04 16	5800	4	Y
0032342301	HD 81809	09 27 46.8	-06 04 16	7558	4	Y
0032940101	4U1755-33	17 58 39.9	-33 48 27	18119	6	Y
0033540601	pg 1206+459	12 08 58.0	+45 40 36	7198	1	Y
0033540901	PG 1630+377	16 32 01.1	+37 37 50	15200	1	Y
0033541001	pg 2302+029	23 04 45.0	+03 11 46	12510	1	Y
0035940201	NGC 4214	12 15 38.7	+36 19 42	13600	2	Y
0035940301	NGC 5253	13 39 56.4	-31 38 25	36838	2	Y
0036140201	XB 1323-619	13 26 36.0	-62 08 10	48853	6	Y
0036540101	SDSS033829.31+00215	03 38 29.3	+00 21 56	20668	1	Y
0037980101	XMM_LSS_1	02 22 40.0	-03 49 60	14559	7	Y
0037980201	XMM_LSS_2	02 24 00.0	-03 49 60	13372	7	Y
0037980301	XMM_LSS_3	02 25 20.0	-03 49 60	13468	7	Y
0037980401	XMM_LSS_4	02 26 40.0	-03 49 60	11799	7	Y
0037980501	XMM_LSS_5	02 28 00.0	-03 49 60	16066	7	Y
0037980601	XMM_LSS_6	02 22 00.0	-03 30 00	13375	7	Y
0037980701	XMM_LSS_7	02 23 20.0	-03 30 00	12376	7	Y
0037980801	XMM_LSS_8	02 24 40.0	-03 30 00	11569	7	Y
0037980901	XMM_LSS_9	02 25 60.0	-03 30 00	14020	7	Y
0037981001	XMM_LSS_10	02 27 20.0	-03 30 00	13363	7	Y
0037981101	XMM_LSS_11	02 22 40.0	-03 10 00	12579	7	Y
0037981201	XMM_LSS_12	02 24 00.0	-03 10 00	11520	7	Y
0037981301	XMM_LSS_13	02 25 20.0	-03 10 00	7466	7	Y
0037981401	XMM_LSS_14	02 26 40.0	-03 10 00	13169	7	Y
0037981501	XMM_LSS_15	02 28 00.0	-03 10 00	11570	7	Y
0037981601	XMM_LSS_16	02 23 20.0	-02 49 60	12772	7	Y
0037981701	XMM_LSS_17	02 24 40.0	-02 49 60	5256	7	Y
0037981801	XMM_LSS_18	02 25 60.0	-02 49 60	16294	7	Y
0037981901	XMM_LSS_19	02 27 20.0	-02 49 60	13062	7	Y
0037982001	XMM_LSS_20	02 20 40.0	-04 49 60	16856	7	Y
0037982101	XMM_LSS_21	02 21 20.0	-04 30 00	15563	7	Y
0037982201	XMM_LSS_22	02 22 00.0	-04 10 00	13873	7	Y
0037982301	XMM_LSS_23	02 19 60.0	-04 30 00	10672	7	Y
0037982401	XMM_LSS_24	02 20 40.0	-04 10 00	18281	7	Y
0037982501	XMM_LSS_25	02 21 20.0	-03 49 60	11978	7	Y
0037982601	XMM_LSS_26	02 20 40.0	-03 30 00	14850	7	Y
0037982701	XMM_LSS_27	02 21 20.0	-03 10 00	17301	7	Y
0037990101	PSRJ2043+2740	20 43 43.5	+27 40 56	16564	5	N
0038540201	IC 2980	11 57 30.0	-73 41 06	6900	2	Y
0038540301	NGC7010	21 04 40.0	-12 20 18	14745	2	Y
0038540401	NGC3332	10 40 29.0	+09 10 59	5900	2	Y
0038541101	NGC766	01 58 42.0	+08 20 54	5799	2	Y
0039140101	IRAS F15307+3252	15 32 44.0	+32 42 47	12607	1	Y
0039340101	RXJ1532.9+3021	15 32 53.8	+30 21 00	13000	3	N
0040140201	WR114	18 23 16.3	-13 43 26	16674	4	Y
0040140301	WR1	00 43 28.4	+64 45 35	9212	4	Y

0041150101	NGC 7009	21 04 10.9	-11 21 50	38317	5	N
0041160101	PDS 456	17 28 19.8	-14 15 56	44437	1	Y
0041170101	CFRS3h	03 02 38.6	+00 07 40	47032	7	Y
0041170201	cfrs10h	10 00 40.4	+25 14 20	45039	7	Y
0041180301	NGC 3091 group	10 00 12.0	-19 38 24	21002	3	N
0041750101	BLANCO1	00 02 48.0	-30 00 00	51187	4	Y
0042340201	RXCJ0043.4-2037	00 43 24.2	-20 37 21	12342	3	N
0042340301	RXCJ0232.2-4420	02 32 17.1	-44 20 43	13254	3	N
0042340501	RXCJ0307.0-2840	03 07 04.0	-28 40 15	13340	3	N
0042340701	RXCJ0516.7-5430	05 16 43.8	-54 30 37	13759	3	N
0042340801	RXCJ0528.9-3927	05 28 56.2	-39 27 49	9000	3	N
0042341001	RXCJ1131.9-1955	11 31 56.6	-19 55 33	12399	3	N
0042341101	RXCJ2011.3-5725	20 11 22.8	-57 25 43	198	3	N
0042341201	RXCJ2308.3-0211	23 08 23.1	-02 11 32	3478	3	N
0042341301	RXCJ2337.6+0016	23 37 40.9	+00 16 34	13362	3	N
0042341601	RXCJ0437.1+0043	04 37 10.2	+00 43 35	7661	3	N
0042341801	RXCJ0532.9-370i	05 32 56.4	-37 01 34	11500	3	N
0044350101	IRAS00317-2142	00 34 13.8	-21 26 21	15269	2	Y
0044350201	IRAS20051-1117	20 07 51.5	-11 08 33	5560	2	Y
0044350501	IRAS20051-1117	20 07 51.5	-11 08 33	14133	2	Y
0044740201	Beta Vir	11 50 41.6	+01 45 53	48196	4	Y
0044740601	HD39060	05 47 17.1	-51 03 60	69216	4	Y
0044741301	70 Oph	18 05 27.2	+02 29 58	9155	4	Y
0044741401	70 Oph	18 05 27.2	+02 29 58	9206	4	Y
0045940301	AXJ0341.4-4453	03 41 24.4	-44 53 02	27207	1	Y
0046540201	AX J1845.0-0300	18 45 00.0	-03 00 00	10561	5	N
0046940201	WARPJ0943.7+1644	09 43 43.7	+16 44 19	4941	3	N
0046940401	WARPJ0943.7+1644	09 43 43.7	+16 44 19	14963	3	N
0047540601	SN1998S	11 46 06.1	+47 28 56	23153	5	N
0047940101	QR And	00 19 50.0	+21 56 54	48062	6	Y
0048740101	NAB 0205+024	02 07 49.9	+02 42 56	24392	1	Y
0049150101	Magellanic Bridge	02 15 15.0	-73 58 60	6819	7	Y
0049150201	Magellanic Bridge	02 15 30.0	-74 01 00	7220	7	Y
0049150301	Magellanic Bridge	02 15 30.0	-74 01 00	19458	7	Y
0049340201	NGC 7252	22 20 45.0	-24 40 43	26384	2	Y
0049340301	NGC 3921	11 51 07.0	+55 04 45	25346	2	Y
0049350101	Proxima Centauri	14 29 42.1	-62 40 45	59124	4	Y
0049540101	CM Draconis: Oct200	16 34 20.0	+57 09 48	3996	4	Y
0049540301	CM Draconis	16 34 19.9	+57 09 47	21464	4	Y
0049540401	CM Draconis	16 34 19.9	+57 09 47	21100	4	Y
0050140201	Cl0024+17	00 26 36.0	+17 09 45	47975	3	N
0050150101	PMN 0525-3343	05 25 06.2	-33 43 06	13808	1	Y
0050150301	PMN 0525-3343	05 25 06.2	-33 43 06	22949	1	Y
0050940101	Baades Window	18 03 24.0	-29 59 24	18121	5	N
0050940201	Baades Foreground	17 57 24.8	-29 55 18	19057	5	N
0050940301	Bulge-8	18 19 20.2	-32 22 08	11457	5	N
0050940401	Bulge-12	18 35 25.8	-34 36 56	11922	5	N
0051590101	2S0921-630	09 22 34.7	-63 17 42	59027	6	Y
0051590201	2S0921-630	09 22 34.7	-63 17 42	6333	6	Y
0051610101	grb980425	19 35 13.9	-52 51 56	21271	5	N
0051760101	PG 1244+026	12 46 35.3	+02 22 08	8599	1	Y
0051760201	PG 1404+226	14 06 21.9	+22 23 47	14299	1	Y
0051940101	XGPS_001	18 25 08.1	-11 51 28	7652	7	Y
0051940201	XGPS_002	18 27 38.5	-12 10 51	8585	7	Y
0051940301	XGPS_003	18 25 53.9	-11 30 15	9139	7	Y
0051940401	XGPS_004	18 28 24.1	-11 49 36	9135	7	Y
0051940501	XGPS_005	18 26 39.5	-11 09 01	9358	7	Y
0051940601	XGPS_006	18 29 09.6	-11 28 21	3700	7	Y
0052140201	NGC3665 Group	11 24 43.4	+38 45 44	32495	3	N
0052140301	HCG 15	02 07 39.0	+02 08 18	30774	3	N
0054540101	PSR B1046-58	10 48 12.6	-58 32 04	19248	5	N
0054540501	PSR B1823-13	18 26 13.2	-13 34 47	16232	5	N
0054540701	PSR B1823-13	18 26 13.2	-13 34 47	21356	5	N
0055140101	LP 944-20	03 39 34.6	-35 25 51	45488	4	Y
0055990201	Arp270	10 49 52.8	+32 58 56	18153	2	Y
0055990301	Arp222	23 39 54.2	-12 17 31	13863	2	Y
0055990501	Mrk266	13 38 17.6	+48 16 34	18148	2	Y

0056020301	RX J0256.5+0006	02 56 33.0	+00 06 12	18874	7	Y
0056020401	RX J0426.1+1655	04 26 07.3	+16 55 12	18669	7	Y
0056020701	RX J1200.8-0328	12 00 48.0	-03 27 51	29182	7	Y
0056020901	RX J1241.5+3250	12 41 33.1	+32 50 23	20465	7	Y
0056021001	RX J1308.5+5342	13 08 32.6	+53 42 19	28045	7	Y
0056021601	RX J2237.0-1516	22 37 00.0	-15 16 08	24178	7	Y
0056022201	RX J0318.2-0301	03 18 25.3	-03 01 34	20264	7	Y
0056030101	xi Boo A	14 51 22.8	+19 06 05	58530	4	Y
0056340101	NGC 4261	12 19 23.2	+05 49 31	28861	1	Y
0056340201	NGC 6251	16 32 32.0	+82 32 16	34958	1	Y
0057560301	ERO field	14 49 28.6	+09 00 01	38425	1	Y
0057570101	NGC 2527	08 04 47.2	-28 07 52	25837	4	Y
0057740301	c1252.9-2927	12 52 54.2	-29 27 07	67153	3	N
0057740401	c1252.9-2927	12 52 54.2	-29 27 07	67764	3	N
0058940101	0917+75	09 22 11.4	+74 59 31	27518	1	Y
0058940301	1401-33	14 04 16.6	-34 02 22	19317	1	Y
0058940701	1253+275	12 55 25.0	+27 13 46	17968	1	Y
0059140101	NGC 4258	12 18 57.5	+47 18 14	12106	1	Y
0059140201	NGC 4258	12 18 57.5	+47 18 14	11662	1	Y
0059140401	NGC 4258	12 18 57.5	+47 18 14	5912	1	Y
0059140901	NGC 4258	12 18 57.5	+47 18 14	13211	1	Y
0059750201	N1_2	16 11 06.0	+54 56 24	2097	7	Y
0059752301	N1_U_1	16 10 60.0	+54 13 25	7500	7	Y
0059752401	N1_U_2	16 10 60.0	+54 13 25	5302	7	Y
0059752601	N1_U_4	16 10 60.0	+54 13 25	9000	7	Y
0059753001	N1_U_3	16 10 60.0	+54 13 25	474	7	Y
0059760101	HD104237	12 00 05.1	-78 11 35	6542	4	Y
0059800101	LSBC F568-6	10 39 53.0	+20 50 49	14065	2	Y
0059830101	NGC 4593	12 39 39.0	-05 20 39	67549	1	Y
0060370101	SBS 1542+541	15 43 59.4	+53 59 04	8416	1	Y
0060370201	Q1246-057	12 49 13.9	-05 59 19	40149	1	Y
0060370901	SBS 1542+541	15 43 59.4	+53 59 04	23893	1	Y
0061540101	Markarian 6	06 52 12.3	+74 25 37	3175	1	Y
0061940101	278-010	13 31 52.5	+11 16 44	7041	1	Y
0061940201	031-001	21 38 07.6	-42 36 14	4708	1	Y
0061940301	122-013	16 30 54.2	+78 11 05	4990	1	Y
0061940901	122-013	16 30 54.2	+78 11 05	5837	1	Y
0062340101	2E 0453.8-6834	04 53 37.0	-68 29 29	9375	5	N
0062940401	HE2149-2745	21 52 00.7	-27 31 50	23089	1	Y
0064600101	3C 98	03 58 54.4	+10 26 02	13219	1	Y
0064600301	3C 98	03 58 54.4	+10 26 02	11063	1	Y
0064940101	SAX J1808.4-3658	18 08 27.5	-36 58 42	36039	6	Y
0065140201	Abell 85	00 42 30.8	-09 41 29	12500	3	N
0065760201	PKS0521-365	05 22 58.0	-36 27 31	31637	1	Y
0065770101	G1	00 32 46.9	+39 34 42	7392	6	Y
0065790101	RXJ 095208.7-014818	09 52 08.7	-01 48 18	9257	3	N
0065820101	NGC 1333	03 28 60.0	+31 15 00	43787	4	Y
0065820201	Serpens exposure 2	18 30 00.0	+01 13 00	19983	4	Y
0065820301	Serpens exposure 1	18 30 00.0	+01 13 00	5677	4	Y
0065820501	Serpens exposure 1	18 30 00.0	+01 13 00	12038	4	Y
0065820601	Serpens exposure 2	18 30 00.0	+01 13 00	19547	4	Y
0066940101	NGC 2547	08 10 12.0	-49 13 00	35827	4	Y
0066950201	UGC 6614	11 39 11.7	+17 07 22	11797	2	Y
0066950301	NGC 7589	23 18 15.6	+00 16 00	7447	2	Y
0066950401	NGC 7589	23 18 15.6	+00 16 00	12383	2	Y
0067140101	Sz 6	10 59 07.1	-77 01 49	29586	4	Y
0067140201	Sz 6	10 59 07.1	-77 01 49	37805	4	Y
0067140301	Sz 6	10 59 07.1	-77 01 49	6269	4	Y
0067170101	Phoenix field	01 12 52.0	-45 33 10	43319	7	Y
0067190101	ESO 198-G24	02 38 19.6	-52 11 33	26533	1	Y
0067340201	Field II	18 04 01.7	-42 32 42	11673	5	N
0067340301	Field III	18 08 30.4	-31 20 32	16069	5	N
0067340401	Field IV	17 26 05.8	+02 19 26	14097	5	N
0067340501	Field V	16 42 16.9	+03 10 54	14088	5	N
0067340601	Field VI	16 07 13.5	+08 04 42	14257	5	N
0067540201	Mrk 348	00 48 47.2	+31 57 25	15431	1	Y
0067750101	Cen X-4	14 58 22.0	-31 40 08	35314	6	Y

0068940101	CL1	05 33 44.0	-24 11 01	60734	3	N
0068940601	CL1	05 33 44.0	-24 11 01	33810	3	N
0069750101	epsilon CMa	06 58 37.5	-28 58 20	45244	4	Y
0070340101	WJ0035.9+8513	00 35 59.3	+85 13 17	7553	3	N
0070340201	WJ1008.7+5342	10 08 47.8	+53 42 03	20106	3	N
0070340301	WJ1103.6+3555	11 03 37.1	+35 55 18	8198	3	N
0070340401	WJ1350.8+6007	13 50 50.3	+60 07 32	5717	3	N
0070340501	WJ1226.9+3332	12 27 16.0	+33 32 22	20054	3	N
0070340701	WJ1342.8+4028	13 42 48.8	+40 28 19	35080	3	N
0070341201	WJ1559.1+6353	15 59 10.0	+63 53 06	21820	3	N
0070740101	mkn 841	15 04 01.2	+10 26 16	11219	1	Y
0070740301	mkn 841	15 04 01.2	+10 26 16	12115	1	Y
0070940101	NGC 3044	09 53 40.8	+01 34 46	6230	2	Y
0070940401	NGC 3044	09 53 40.8	+01 34 46	13653	2	Y
0071340201	NGC 3585	11 13 16.8	-26 45 21	18002	1	Y
0071340301	NGC 4494	12 31 23.5	+25 46 32	29729	1	Y
0071340501	NGC 5322	13 49 15.2	+60 11 26	17945	1	Y
0071740501	A 0538-66	05 35 40.8	-66 51 54	20600	6	Y
0072340601	H0917-74	09 19 51.4	-07 35 35	7405	7	Y
0072340701	MRK 464	13 55 53.5	+38 34 29	7661	7	Y
0073140201	1RXSJ160518.8+32490	16 05 18.8	+32 49 07	27777	5	N
0073140301	1RXSJ160518.8+32490	16 05 18.8	+32 49 07	25675	5	N
0073140501	1RXSJ160518.8+32490	16 05 18.8	+32 49 07	22017	5	N
0073340201	GRS 1009-45	10 13 36.3	-45 04 32	18000	6	Y
0073740101	3C 391	18 49 30.0	-00 57 00	1669	5	N
0073740201	3C 391	18 49 30.0	-00 57 00	5214	5	N
0073740301	3C 391	18 49 30.0	-00 57 00	6893	5	N
0074140101	4U 1608-52	16 12 43.0	-52 25 23	6006	6	Y
0074140201	4U 1608-52	16 12 43.0	-52 25 23	12800	6	Y
0075940101	30 Ari	02 36 57.7	+24 38 53	26282	4	Y
0075940301	30 Ari	02 36 57.7	+24 38 53	47146	4	Y
0079570201	S 308	06 53 30.0	-23 43 00	22661	5	N
0080940101	PKS 2155-304	21 58 51.8	-30 13 29	56791	1	Y
0080940301	PKS 2155-304	21 58 51.8	-30 13 29	46000	1	Y
0081340201	MKN 231	12 56 14.2	+56 52 25	21600	1	Y
0081340301	IRAS23128-59	23 15 47.1	-59 03 16	16200	1	Y
0081340401	IRAS20551-42	20 58 27.0	-42 39 06	14812	1	Y
0081340501	IRAS20100-41	20 13 29.9	-41 47 35	20725	1	Y
0081340601	IRAS17208-00	17 23 22.0	-00 17 00	15500	1	Y
0081340801	IRAS12112+03	12 13 46.1	+02 48 41	22522	1	Y
0081340901	IRAS22491-18	22 51 49.4	-17 52 23	22475	1	Y
0081341001	IRAS19254-72	19 31 21.6	-72 39 22	18190	1	Y
0081341101	IRAS15250+36	15 26 59.5	+35 58 38	18845	1	Y
0081341401	IRAS14348-14	14 37 38.3	-15 00 23	17997	1	Y
0082140301	NGC3623	11 18 55.2	+13 05 34	32803	2	Y
0082340101	PG1115+080	11 18 16.9	+07 45 59	57848	1	Y
0082990101	3C 277.2	12 53 33.0	+15 42 29	38569	1	Y
0083000101	B3 0731+438	07 35 21.9	+43 44 20	28678	1	Y
0083000301	3C 257	11 23 09.2	+05 30 19	30678	1	Y
0083150401	A1302	11 33 14.0	+66 22 56	4779	3	N
0083150601	A2241	16 59 44.0	+32 36 54	203	3	N
0083150801	A2241	16 59 44.0	+32 36 54	4097	3	N
0083151001	A2241	16 59 44.0	+32 36 54	2500	3	N
0083210101	1SAXJ2054.3-1556	20 54 18.6	-15 55 42	9599	1	Y
0083210201	1SAXJ2337.8-5625	23 37 49.1	-56 24 34	9666	1	Y
0083210701	1SAXJ2011.9-8758	20 11 58.3	-87 57 57	10104	1	Y
0083240201	RX J0911.4+0551	09 11 27.5	+05 50 52	19363	3	N
0083280101	1700-37	17 03 56.8	-37 50 39	24241	6	Y
0083280301	1700-37	17 03 56.8	-37 50 39	19419	6	Y
0083280401	1700-37	17 03 56.8	-37 50 39	29255	6	Y
0083950101	4C34.16	04 00 54.8	+34 43 10	22425	3	N
0083960101	Mkn 279	13 53 03.4	+69 18 30	24438	2	Y
0084030101	M104	12 39 59.4	-11 37 23	42373	2	Y
0084140101	MS0205.7+3509	02 08 38.1	+35 23 12	38310	1	Y
0084140501	MS0205.7+3509	02 08 38.1	+35 23 12	14672	1	Y
0084190201	UX UMa	13 36 41.1	+51 54 49	44015	6	Y
0084200101	SMC Pointing 1	00 56 41.7	-72 20 24	12571	6	Y

0084200801	SMC Pointing 8	00 54 31.7	-73 40 56	20570	6	Y
0084230201	Abell 68	00 37 06.4	+09 09 20	27837	3	N
0084230401	Abell 267	01 52 41.8	+01 00 43	17300	3	N
0084230601	Abell 773	09 17 52.8	+51 43 38	16821	3	N
0084230701	Abell 963	10 17 03.6	+39 02 56	26768	3	N
0084230901	Abell 1763	13 35 19.0	+40 59 56	19895	3	N
0084960101	Galactic Halo	03 20 09.8	-62 26 29	9769	5	N
0084960201	Galactic Halo	03 32 54.9	-63 27 50	12156	5	N
0085030101	ngc2685	08 55 35.1	+58 44 01	5520	7	Y
0085100101	NGC 625	01 35 07.2	-41 26 09	788	2	Y
0085150101	Lynx.3A	08 49 12.0	+44 50 24	42862	7	Y
0085150201	Lynx.3A_NW	08 49 06.4	+44 51 24	37514	7	Y
0085150301	lLynx.3A_SE	08 49 17.6	+44 49 24	34675	7	Y
0085170101	RX J1011.2+5545	10 11 12.4	+55 44 50	30317	1	Y
0085220101	The Antennae	12 01 52.8	-18 51 54	18720	2	Y
0085220201	The Antennae	12 01 52.8	-18 51 54	51529	2	Y
0085280201	NGC6366	17 27 44.3	-05 04 36	8720	6	Y
0085280301	M 13	16 41 41.4	+36 27 37	15006	6	Y
0085280501	NGC6366	17 27 44.3	-05 04 36	27576	6	Y
0085280601	NGC6366	17 27 44.3	-05 04 36	16680	6	Y
0085280801	M 13	16 41 41.4	+36 27 37	13800	6	Y
0085281001	NGC6366	17 27 44.3	-05 04 36	18100	6	Y
0085580101	NOVA Mus 1998	11 56 09.0	-65 34 21	7041	6	Y
0085580201	NOVA Sco 1998	17 55 25.0	-31 01 42	7937	6	Y
0085580301	NOVA Sgr 1998	18 21 40.5	-27 31 38	9146	6	Y
0085580401	NOVA Oph 1998	17 31 59.8	-19 13 56	7369	6	Y
0085580501	NOVA Sco 1997	17 54 11.2	-30 02 53	6938	6	Y
0085580801	NOVA Mus 1998	11 56 09.0	-65 34 21	7114	6	Y
0085580901	NOVA Mus 1998	11 56 09.0	-65 34 21	5991	6	Y
0085581001	NOVA Sco 1998	17 55 25.0	-31 01 42	7929	6	Y
0085581101	NOVA Sco 1998	17 55 25.0	-31 01 42	5992	6	Y
0085581201	NOVA Sgr 1998	18 21 40.5	-27 31 38	6642	6	Y
0085581301	NOVA Sgr 1998	18 21 40.5	-27 31 38	9183	6	Y
0085581401	NOVA Oph 1998	17 31 59.8	-19 13 56	7593	6	Y
0085581501	NOVA Sco 1997	17 54 11.2	-30 02 53	2200	6	Y
0085581601	NOVA Sco 1997	17 54 11.2	-30 02 53	4400	6	Y
0085581701	NOVA Oph 1998	17 31 59.8	-19 13 56	6521	6	Y
0085582001	NOVA Oph 1998	17 31 59.8	-19 13 56	7895	6	Y
0085640101	IRAS05189-2524	05 21 01.4	-25 21 45	9992	1	Y
0085640201	UGC 05101	09 35 51.6	+61 21 11	34078	1	Y
0085680501	GX 339-4	17 02 49.4	-48 47 23	7566	6	Y
0085680601	GX 339-4	17 02 49.4	-48 47 23	11533	6	Y
0085960101	GS1124-68	11 26 26.6	-68 40 32	33196	6	Y
0086360301	V410 Tau	04 18 31.2	+28 27 16	59929	4	Y
0086360401	V410 Tau	04 18 31.2	+28 27 16	30662	4	Y
0086750101	FIRST 1016+5209	10 16 14.3	+52 09 16	7722	1	Y
0087940101	G337.2-0.7	16 39 30.0	-47 49 60	38575	5	N
0088020201	IRAS F21243-4501	21 27 38.2	-44 48 54	17739	1	Y
0089210601	SNR 0450-709	04 50 30.0	-70 50 24	53479	5	N
0089210701	N 120	05 18 42.0	-69 39 30	23445	5	N
0089370501	Saturn	05 55 30.3	+22 07 46	22342	4	Y
0089370601	Saturn	05 55 31.5	+22 07 45	20865	4	Y
0089370701	Saturn	05 55 32.5	+22 07 42	16085	4	Y
0089940101	B335	19 37 01.0	+07 34 11	12166	4	Y
0089940201	L1448-C	03 25 40.0	+30 43 60	25386	4	Y
0089940801	B335	19 37 01.0	+07 34 11	8669	4	Y
0089940901	B335	19 37 01.0	+07 34 11	14359	4	Y
0089960301	NGC5548	14 17 59.5	+25 08 12	65191	1	Y
0089960401	NGC5548	14 17 59.5	+25 08 12	27538	1	Y
0090010101	RBS1223	13 08 48.6	+21 27 09	16050	5	N
0090020101	ngc 3998	11 57 56.1	+55 27 13	10997	1	Y
0090050601	3c445	22 23 49.6	-02 06 12	22719	1	Y
0090050701	PICTOR A	05 19 49.7	-45 46 44	16032	1	Y
0090070101	Q 0144-3938	01 46 12.5	-39 23 05	32667	1	Y
0090070201	UM 269	00 43 19.7	+00 51 15	20523	1	Y
0091140201	A1983	14 52 44.0	+16 44 48	31881	3	N
0091140401	MKW9	15 32 29.2	+04 40 54	31951	3	N

0091770101	NGC 1316	03 23 50.0	-37 16 60	43680	2	Y
0092140101	Centaurus B	13 46 49.0	-60 24 30	30260	1	Y
0092360101	3EG 0616-3310/1	06 17 47.0	-32 55 12	11765	5	N
0092360201	3EG 0616-3310/2	06 17 47.0	-33 25 12	13777	5	N
0092360301	3EG 0616-3310/3	06 15 24.0	-33 25 12	10966	5	N
0092360401	3EG 0616-3310/4	06 15 24.0	-32 55 12	14229	5	N
0092360501	3EG 1249-8330/1	12 57 52.0	-83 15 00	11354	5	N
0092360601	3EG 1249-8330/2	12 57 52.0	-83 45 00	12046	5	N
0092360701	3EG 1249-8330/3	12 40 12.0	-83 45 00	5187	5	N
0092360801	3EG 1249-8330/4	12 40 12.0	-83 15 00	15739	5	N
0092790101	EZ CMa	06 54 13.0	-23 55 42	12105	4	Y
0092800101	APM 08279+5255	08 31 41.6	+52 45 18	16869	1	Y
0092800201	APM 08279+5255	08 31 41.6	+52 45 18	74186	1	Y
0092820101	PSR 1259-63/SS2883	13 02 47.7	-63 50 09	11309	6	Y
0092820201	PSR 1259-63/SS2883	13 02 47.7	-63 50 09	3485	6	Y
0092820301	PSR 1259-63/SS2883	13 02 47.7	-63 50 09	38235	6	Y
0092820801	PSR 1259-63/SS2883	13 02 47.7	-63 50 09	7260	6	Y
0092821201	PSR 1259-63/SS2883	13 02 47.7	-63 50 09	10890	6	Y
0092850101	PG 1407+265	14 09 23.8	+26 18 21	9800	2	Y
0092850201	PKS 2135-147	21 37 45.2	-14 32 55	32980	2	Y
0092850501	PG 1407+265	14 09 23.8	+26 18 21	41111	2	Y
0092970201	ESO 197-G010	01 53 38.4	-49 37 01	13600	2	Y
0092970301	ESO263-G048	10 30 47.6	-46 19 40	9212	2	Y
0092970501	NGC5266	13 43 01.9	-48 10 09	8841	2	Y
0092970801	IC 4320	13 44 03.7	-27 13 54	7120	2	Y
0093030101	Abell 1689	13 11 29.4	-01 20 29	37569	3	N
0093030201	RX J2129.6+0005	21 29 37.8	+00 05 38	47006	3	N
0093160201	BR 0351-1034	03 53 47.0	-10 25 19	18100	1	Y
0093160701	Q1028-0844	10 28 37.7	-08 44 24	6988	1	Y
0093190301	NGC 7770	23 51 22.5	+20 05 47	31618	2	Y
0093190501	NGC 2341	07 09 12.0	+20 36 06	28518	2	Y
0093550401	Z And	23 33 40.0	-15 17 02	22241	6	Y
0093552701	Z And	23 33 39.9	+48 49 06	19931	6	Y
0093552801	Z And	23 33 39.9	+48 49 06	5418	6	Y
0093630101	NGC 1052	02 41 04.8	-08 15 21	15603	1	Y
0093640301	IRAS 10173+0828	10 19 59.9	+08 13 34	14785	2	Y
0093640401	IC 0883	13 20 35.3	+34 08 23	19704	2	Y
0093640701	NGC 7552	23 16 11.0	-42 34 59	17247	2	Y
0093640901	IC 0342	03 46 49.7	+68 05 45	9600	2	Y
0093641001	NGC 660	01 43 01.8	+13 38 30	11139	2	Y
0093641101	NGC 3627	11 20 15.0	+12 59 30	10510	2	Y
0094170101	Mkn 180	11 36 26.4	+70 09 27	6531	1	Y
0094310101	SSA22	22 17 34.2	+00 15 01	57595	7	Y
0094310201	SSA22	22 17 34.2	+00 15 01	70703	7	Y
0094360201	NGC 5033	03 13 27.5	+36 35 38	12266	1	Y
0094360501	NGC 5033	13 13 27.5	+36 35 38	11516	1	Y
0094360601	NGC 4736	12 50 53.0	+41 07 14	9553	1	Y
0094360701	NGC 4736	12 50 53.0	+41 07 14	12000	1	Y
0094381101	1ES0347-121	03 49 23.2	-11 59 27	5100	1	Y
0094382101	1ES0120+340	01 23 08.7	+34 20 49	5800	1	Y
0094382501	1es0323+022	03 26 13.9	+02 25 15	5101	1	Y
0094382701	1ES1028+511	10 31 18.5	+50 53 36	5796	1	Y
0094383101	1ES0414+009	04 16 52.4	+01 05 24	9100	1	Y
0094383201	1ES1255+244	12 57 31.9	+24 12 40	5958	1	Y
0094383401	1ES0145+138	01 48 29.7	+14 02 18	4958	1	Y
0094383501	1ES1959+650	19 59 59.9	+65 08 55	6507	1	Y
0094400101	VII Zw 031	05 16 38.9	+79 40 11	31738	1	Y
0094400301	IRAS 07598+6508	08 04 33.1	+64 59 49	18866	1	Y
0094401201	Mrk 463	13 56 02.7	+18 22 19	25910	1	Y
0094530401	3C192	08 05 35.0	+24 49 50	20889	1	Y
0094530501	PKS1637-77	16 44 16.1	-77 15 48	719	1	Y
0094740101	H1320+551	13 22 49.2	+54 55 29	17753	1	Y
0094740201	H1419+480	14 21 29.6	+47 47 27	9318	1	Y
0094780101	Pleiades-1	03 47 18.0	+24 22 31	36439	4	Y
0094790201	Hawaii 167	03 57 22.0	+01 10 56	21498	1	Y
0094800101	MS1054.4-0321	10 57 00.0	-03 37 27	27680	3	N
0094800201	MS1137.5+6625	11 40 23.0	+66 08 41	25800	3	N

0095810401	Zeta Puppis (comple	08 03 35.0	-40 00 12	37588	4	Y
0096010101	IRAS13349+2438	13 37 19.0	+24 23 03	41806	1	Y
0096020101	Mkn 766	12 18 26.0	+29 48 46	28575	1	Y
0098610101	4U1624-49	16 28 04.0	-49 12 03	22436	6	Y
0098610201	4U1624-49	16 28 04.0	-49 12 03	56362	6	Y
0098810101	WW Hor	02 36 11.5	-52 19 14	23512	6	Y
0099010101	UZ For	03 35 28.7	-25 44 23	19294	6	Y
0099020301	OY Car	10 06 22.3	-70 14 05	50887	6	Y
0099030101	DP Leo	11 17 16.0	+17 57 41	17900	6	Y
0099320101	lam Andromeda	23 37 33.8	+46 27 29	28238	4	Y
0099840101	Magellanic Bridge	02 15 22.0	-74 00 00	12091	7	Y
0100240101	HD 117555	13 30 47.0	+24 13 59	28727	4	Y
0100240201	HD 117555	13 30 47.0	+24 13 59	35300	4	Y
0100240401	HD 33798	05 15 15.5	+47 10 15	21452	4	Y
0100240701	UZ LIB	15 32 23.0	-08 32 05	17792	4	Y
0100240801	UZ LIB	15 32 23.0	-08 32 05	26211	4	Y
0100240901	HD 223460	23 49 41.0	+36 25 33	5989	4	Y
0100241001	HD 223460	23 49 41.0	+36 25 33	9090	4	Y
0100241101	HD 199178	20 53 53.0	+44 23 11	7156	4	Y
0100241201	HD 199178	20 53 53.0	+44 23 11	5754	4	Y
0100440101	PHL 5200	22 28 30.4	-05 18 55	44957	1	Y
0100640101	NGC 188	00 44 22.0	+85 20 25	34824	4	Y
0100640201	NGC 188	00 44 22.0	+85 20 25	57198	4	Y
0100650101	44 Boo	15 03 47.3	+47 39 15	17440	4	Y
0100650201	VW Cep	20 37 21.5	+75 36 01	11100	4	Y
0100650301	VW Cep	20 37 21.5	+75 36 01	11458	4	Y
0101040101	Mrk 335	00 06 19.6	+20 12 17	33940	1	Y
0101040201	Fairall 9	01 23 46.1	-58 48 21	28994	1	Y
0101040301	NGC 3227	10 23 30.6	+19 51 54	35803	1	Y
0101040401	IC 4329a	13 49 19.2	-30 18 34	12744	1	Y
0101040501	ESO 141-G55	19 21 14.2	-58 40 13	36748	1	Y
0101440101	alpha Persei	03 26 16.0	+48 50 29	51887	4	Y
0101440201	IC2602	10 42 41.0	-64 21 01	33756	4	Y
0101440301	NGC2024	05 38 44.8	-02 36 00	42375	4	Y
0101440401	Praesepe	08 39 58.0	+19 32 29	45074	4	Y
0101440501	VB71	04 28 35.0	+15 57 45	40293	4	Y
0101440601	VB50	04 24 13.0	+14 45 30	41020	4	Y
0101440701	HD283572	04 21 59.0	+28 18 08	31499	4	Y
0101440801	SU Aurigae	04 55 59.0	+30 34 02	124933	4	Y
0101441501	VB50	04 24 13.0	+14 45 30	39074	4	Y
0101640101	NGC 6240	16 52 58.6	+02 24 04	16986	1	Y
0101640201	Mrk 1014	01 59 50.2	+00 23 41	7934	1	Y
0101640401	Mrk 273	13 44 42.1	+55 53 13	22272	1	Y
0101640601	NGC 6240	16 52 58.6	+02 24 04	9800	1	Y
0101640801	Arp 220	15 34 57.1	+23 30 16	13410	1	Y
0101640901	Arp 220	15 34 57.1	+23 30 16	14570	1	Y
0102040101	B2 1721+34	17 23 20.8	+34 17 59	6833	1	Y
0102040201	B2 1128+31	11 31 09.4	+31 14 07	23300	1	Y
0102040301	B2 1028+31	10 30 59.1	+31 02 56	25829	1	Y
0102040401	PG 0804+761	08 10 58.5	+76 02 43	2233	1	Y
0102040501	MARK 1383	14 29 06.6	+01 17 06	3264	1	Y
0102040601	MARK 876	16 13 57.2	+65 43 09	3200	1	Y
0102040701	Q 0056-363	00 58 37.3	-36 06 05	14997	1	Y
0102041201	B2 1721+34	17 23 20.8	+34 17 59	5400	1	Y
0102041301	MARK 876	16 13 57.2	+65 43 09	6987	1	Y
0102640101	M33_1	01 33 51.0	+30 39 37	10408	2	Y
0102640201	M33_2	01 34 40.0	+30 57 48	16038	2	Y
0102640301	M33_3	01 33 32.0	+30 52 13	11073	2	Y
0102640401	M33_4	01 32 51.0	+30 36 49	12265	2	Y
0102640501	M33_5	01 33 02.0	+30 21 24	11760	2	Y
0102640601	M33_6	01 34 08.0	+30 46 06	5652	2	Y
0102640701	M33_7	01 34 10.0	+30 27 00	10965	2	Y
0102640801	M33_8	01 34 51.0	+30 42 22	2047	2	Y
0102640901	M33_9	01 34 04.0	+30 57 25	7200	2	Y
0102641001	M33_10	01 33 07.0	+30 45 02	9153	2	Y
0102641101	M33_11	01 32 46.0	+30 28 19	10500	2	Y
0102641201	M33_12	01 33 38.0	+30 21 49	11699	2	Y

0102642001	M33_8	01 34 51.0	+30 42 22	11343	2	Y
0102642101	M33_13	01 34 34.0	+30 34 11	12269	2	Y
0102642201	M33_14	01 34 56.0	+30 50 52	13865	2	Y
0102642301	M33_15	01 33 33.0	+30 33 07	12250	2	Y
0103060101	PKS 2126-158	21 29 12.2	-15 38 41	20112	1	Y
0103060201	Q1442+2931	14 44 53.7	+29 19 05	29353	1	Y
0103060301	Q0000-263	00 03 22.9	-26 03 17	39486	1	Y
0103060401	PKS 2149-306	21 51 55.6	-30 27 54	23865	1	Y
0103260401	PSR J0631+1036	06 31 27.6	+10 36 58	7702	5	N
0103260501	PSR B0740-28	07 42 49.1	-28 22 44	1000	5	N
0103260601	PSR B0823+26	08 26 51.3	+26 37 26	49405	5	N
0103260701	PSR B0906-49	09 08 35.5	-49 13 07	7250	5	N
0103260901	PSR B1221-63	12 24 22.2	-64 07 54	6461	5	N
0103261001	PSR B1449-64	14 53 32.7	-64 13 16	5686	5	N
0103261101	PSR B1634-45	16 37 58.7	-45 53 27	1257	5	N
0103261201	PSR B1719-37	17 22 59.2	-37 12 04	6668	5	N
0103261301	PSR B1742-30	17 45 56.3	-30 40 24	7600	5	N
0103262401	PSR B0740-28	07 42 49.1	-28 22 44	6066	5	N
0103262501	PSR B0136+57	01 39 19.8	+58 14 32	5981	5	N
0103262801	PSR B0540+23	05 43 09.7	+23 29 06	7668	5	N
0103460801	McNaught-Hartley	16 16 28.7	+12 12 22	13172	4	Y
0103460901	McNaught-Hartley	16 17 02.1	+12 24 18	14390	4	Y
0103461001	McNaught-Hartley	16 17 37.0	+12 36 58	11789	4	Y
0103660101	PG 1411+442	14 13 48.3	+44 00 14	32283	1	Y
0103660201	PG 0844+349	08 47 42.4	+34 45 05	18394	1	Y
0103660301	Mark 304	22 17 12.1	+14 14 21	17222	1	Y
0103860101	PMN J0623-6436	06 23 08.0	-64 36 21	8245	2	Y
0103860201	ESO 602- G 031	22 36 56.0	-22 13 12	8200	2	Y
0103860301	UGC 12138	22 40 18.0	+08 03 16	6691	2	Y
0103860501	NGC 7158	21 56 56.0	-11 39 32	7551	2	Y
0103860601	CGCG 21-63	15 16 40.0	+00 14 54	13293	2	Y
0103860701	MCG -02-14-009	05 16 21.0	-10 33 40	4948	2	Y
0103860801	UGC 3973	07 42 33.0	+49 48 30	1989	2	Y
0103860901	ESO 244- G 017	01 20 20.0	-44 07 43	21394	2	Y
0103861001	Mrk 609	03 25 25.0	-06 08 30	9126	2	Y
0103861201	IIZw 177	22 19 19.0	+12 07 57	12011	2	Y
0103861301	NGC 7331	22 37 06.0	+34 25 19	4070	2	Y
0103861501	AM2354-304S	23 57 28.0	-30 27 39	1428	2	Y
0103861601	ESO 113- G 010	01 05 17.0	-58 26 13	7100	2	Y
0103861701	ESO 15- IG 011	04 35 16.0	-78 01 57	7995	2	Y
0103861801	MK 728	11 01 01.0	+11 02 46	9109	2	Y
0103862001	ESO 15- IG 011	04 35 16.0	-78 01 57	6600	2	Y
0103862101	UGC 3973	07 42 33.0	+49 48 30	5900	2	Y
0103862701	MCG -01-13-025	04 51 41.0	-03 48 34	7666	2	Y
0103863001	MCG -01-13-025	04 51 41.0	-03 48 34	6500	2	Y
0103863101	NGC 7331	22 37 06.0	+34 25 19	9470	2	Y
0103863201	Z 1121.5+0630	11 24 08.0	+06 12 56	8661	2	Y
0104060101	LMC deep field	05 31 20.0	-65 57 38	37884	6	Y
0104060201	LMC deep field	05 31 20.0	-65 57 38	23964	6	Y
0104460301	RIDGE_3	18 27 32.0	-11 29 19	11035	7	Y
0104460401	RIDGE_4	18 28 19.0	-11 07 11	11919	7	Y
0104460701	RIDGE_1	18 25 56.0	-12 13 33	7890	7	Y
0104460801	RIDGE_2	18 26 44.0	-11 51 26	9319	7	Y
0104460901	RIDGE_5	18 29 06.0	-10 45 03	13155	7	Y
0104860101	[HB89] 0420-388	04 22 14.8	-38 44 53	14112	1	Y
0104860201	[HB89] 0438-436	04 40 17.1	-43 33 09	12175	1	Y
0104860501	RX J122135.6+280613	12 21 35.6	+28 06 14	36485	1	Y
0104860601	[HB89] 2000-330	20 03 24.1	-32 51 45	19557	1	Y
0104861001	[SP89] 1107+487	11 10 38.5	+48 31 16	32895	1	Y
0105070101	1WGA J1220.3+0641	12 20 18.1	+06 41 16	9711	7	Y
0105070201	1WGA J1216.9+3743	12 16 57.1	+37 43 35	5298	7	Y
0105460101	RXJ1712.6-2414	17 12 36.0	-24 14 41	8900	6	Y
0105460301	RXJ1548.2-4528	15 48 14.0	-45 28 45	18394	6	Y
0105460501	RXJ1548.2-4528	15 48 14.0	-45 28 45	17701	6	Y
0105460601	RXJ1712.6-2414	17 12 36.0	-24 14 41	16742	6	Y
0105870101	PKS 0745-19	07 47 31.5	-19 17 40	22136	3	N
0105870201	PKS 0745-19-offset	07 48 24.5	-19 06 00	39680	3	N

0106060201	Virgo 2	12 30 50.0	+13 03 30	7770	3	N
0106060301	Virgo 3	12 30 50.0	+13 23 30	7891	3	N
0106060401	Virgo 4	12 30 50.0	+13 43 30	11341	3	N
0106060501	Virgo 5	12 30 50.0	+14 03 30	15448	3	N
0106060601	Virgo 6	12 30 50.0	+14 23 30	10962	3	N
0106060701	Virgo 7	12 30 50.0	+14 43 30	12952	3	N
0106060901	Virgo 9	12 30 50.0	+15 23 30	12300	3	N
0106061001	Virgo 10	12 30 50.0	+15 43 30	8900	3	N
0106061101	Virgo 11	12 30 50.0	+16 03 30	12939	3	N
0106061201	Virgo 12	12 30 50.0	+16 23 30	15248	3	N
0106061301	Virgo 13	12 30 50.0	+17 53 30	15624	3	N
0106061401	Virgo 8	12 30 50.0	+15 03 30	8220	3	N
0106260101	RXJ1856.6-3754	18 56 35.3	-37 54 34	56895	5	N
0106260201	RXJ0806.4-4123	08 06 23.0	-41 22 33	13723	5	N
0106460101	Cl0939+472	09 43 00.0	+46 59 30	46580	3	N
0106660101	LBQS 2212-1759	22 15 31.7	-17 44 06	57067	1	Y
0106660201	LBQS 2212-1759	22 15 31.7	-17 44 06	49120	1	Y
0106660401	LBQS 2212-1759	22 15 31.7	-17 44 06	33086	1	Y
0106660501	LBQS 2212-1759	22 15 31.7	-17 44 06	8064	1	Y
0106660601	LBQS 2212-1759	22 15 31.7	-17 44 06	94352	1	Y
0106860101	NGC 1313	03 18 14.0	-66 30 00	26677	5	N
0106860201	NGC 4321	12 22 55.0	+15 49 12	24801	5	N
0107460601	NGC 3516	11 06 47.5	+72 34 07	95136	1	Y
0107460701	NGC 3516	11 06 47.5	+72 34 07	114306	1	Y
0107660201	PG 1440+356	14 42 07.5	+35 26 23	21457	1	Y
0107860201	RXJ1120.1	11 20 07.0	+43 18 05	21254	3	N
0107860301	RXJ1701.3	17 01 23.0	+64 14 08	10800	3	N
0107860401	SHARC4	03 37 45.0	-25 22 26	26960	3	N
0107860501	Vik 59	08 47 11.0	+34 49 16	57800	3	N
0108060401	AXAF Ultra Deep F	03 32 26.7	-27 48 20	23210	7	Y
0108060501	AXAF Ultra Deep F	03 32 29.3	-27 48 40	43853	7	Y
0108060601	AXAF Ultra Deep F	03 32 28.0	-27 48 50	48882	7	Y
0108060701	AXAF Ultra Deep F	03 32 26.7	-27 48 40	77410	7	Y
0108061801	AXAF Ultra Deep F	03 32 28.0	-27 48 30	55241	7	Y
0108061901	AXAF Ultra Deep F	03 32 28.0	-27 48 10	43053	7	Y
0108062101	AXAF Ultra Deep F	03 32 29.3	-27 48 20	44478	7	Y
0108062301	AXAF Ultra Deep F	03 32 28.0	-27 48 10	81953	7	Y
0108460201	Abell 2597	23 25 21.0	-12 07 12	15913	3	N
0108460301	Abell 2670	23 54 09.0	-10 24 00	18808	3	N
0108670101	ZW 3146	10 23 40.0	+04 11 24	53451	3	N
0108670201	E1455+2232	14 57 14.0	+22 20 24	36261	3	N
0108860101	NGC 4325	12 23 06.7	+10 37 10	20941	3	N
0108860501	NGC 2563	08 20 35.6	+21 04 08	20961	3	N
0108860701	NGC 5129	13 24 09.7	+13 58 33	18482	3	N
0109060101	rho Oph cloud	16 25 17.0	-24 16 48	47743	4	Y
0109060201	Sco Cen field	16 13 60.0	-23 00 00	50106	4	Y
0109060301	L1551 cloud	04 31 39.0	+18 10 00	55643	4	Y
0109070101	RE1034+396	10 34 38.6	+39 38 28	14805	1	Y
0109070201	E1346+266	13 48 35.0	+26 22 07	54667	1	Y
0109070401	REJ2248-511	22 48 41.2	-51 09 54	13844	1	Y
0109070601	REJ2248-511	22 48 41.2	-51 09 54	14423	1	Y
0109080101	PG1202+281	12 04 42.1	+27 54 11	16879	1	Y
0109080201	PG1309+355	13 12 17.8	+35 15 21	26666	1	Y
0109080301	PG1322+659	13 23 49.5	+65 41 48	10975	1	Y
0109080401	PG1352+183	13 54 35.8	+18 05 18	9690	1	Y
0109080501	PG1415+451	14 17 00.6	+44 56 06	23331	1	Y
0109080601	PG1444+407	14 46 45.9	+40 35 06	19100	1	Y
0109080701	PG1048+342	10 51 43.4	+33 59 27	28892	1	Y
0109080801	PG1114+445	11 17 06.4	+44 13 33	40481	1	Y
0109080901	PG1427+480	14 29 43.0	+47 47 27	37963	1	Y
0109081001	PG1402+261	14 05 16.1	+25 55 34	12085	1	Y
0109081101	PG1626+554	16 27 55.9	+55 22 31	2279	1	Y
0109100201	LSS3074	13 26 59.7	-62 01 48	9926	4	Y
0109110101	WR46	12 05 19.0	-62 03 08	71741	4	Y
0109120101	HD108	00 06 03.0	+63 40 48	36158	4	Y
0109130201	NGC 526A	01 23 54.2	-35 03 56	10811	2	Y
0109130301	MRK590	02 14 33.5	-00 46 00	10807	2	Y

0109130601	ESO103-G35	18 38 20.3	-65 25 42	11222	2	Y
0109130701	MCG-2-58-22	23 04 43.4	-08 41 08	10490	2	Y
0109131001	H0557-385	05 58 02.0	-38 20 05	4551	2	Y
0109131101	3C120	04 33 11.1	+05 21 16	11865	2	Y
0109141301	Mkn766	12 18 26.5	+29 48 46	96118	1	Y
0109141401	NGC4051	12 03 09.7	+44 31 53	89141	1	Y
0109270301	M31North2	00 45 20.0	+41 56 09	36221	6	Y
0109270401	M31North3	00 46 38.0	+42 16 20	53777	6	Y
0109270701	M31North1	00 44 01.0	+41 35 57	57290	6	Y
0109280101	WR40	11 06 17.0	-65 30 35	22623	4	Y
0109460101	RX J0132-65	01 32 42.0	-65 54 32	7100	4	Y
0109460201	RX J0153-59	01 54 01.1	-59 47 49	7299	4	Y
0109460701	RE J0531-46	05 31 35.3	-46 24 08	6013	4	Y
0109460801	RE J1141-6410	11 41 23.0	-64 10 15	7620	4	Y
0109460901	BY Cam	05 42 49.1	+60 51 31	5148	4	Y
0109461001	EU Cnc	08 51 27.0	+11 46 58	9384	4	Y
0109461201	RX J1002-19	10 02 11.7	-19 25 38	5800	4	Y
0109461301	RX J1007-20	10 07 34.6	-20 17 33	6829	4	Y
0109461401	RX J1015+09	10 15 34.7	+09 04 42	5800	4	Y
0109461701	AN UMa	11 04 25.7	+45 03 15	6919	4	Y
0109461801	ST LMi	11 05 39.8	+25 06 29	11363	4	Y
0109461901	AR UMa	11 15 44.7	+42 58 23	3952	4	Y
0109462101	RE J1149+28	11 49 55.7	+28 45 07	4700	4	Y
0109462201	EV UMa	13 07 54.0	+53 51 30	7588	4	Y
0109462301	RE J1313-32	13 13 17.1	-32 59 12	6406	4	Y
0109462401	V834 Cen	14 09 07.5	-45 17 17	868	4	Y
0109462501	V895 Cen	14 29 27.2	-38 04 10	6881	4	Y
0109462901	V347 Pav	18 44 48.0	-74 18 33	5700	4	Y
0109463101	RE J1957-57	19 57 11.5	-57 38 22	11344	4	Y
0109463201	V2009-65	20 08 55.8	-65 27 43	6600	4	Y
0109463301	RX J2022-39	20 22 37.5	-39 54 13	7265	4	Y
0109463401	V1500 Cyg	21 11 36.5	+48 09 02	6547	4	Y
0109463501	CE Gru	21 37 56.6	-43 42 14	7591	4	Y
0109463601	CP Tuc	23 15 19.0	-59 10 28	5197	4	Y
0109463801	V834 Cen	14 09 07.5	-45 17 17	5720	4	Y
0109464201	MN Hya	09 29 07.1	-24 05 05	6900	4	Y
0109464501	EP Dra	19 07 06.0	+69 08 42	5900	4	Y
0109464801	EXO 032957-2606.9	03 32 04.6	-25 56 56	1212	4	Y
0109464901	MR Ser	15 52 47.2	+18 56 28	7209	4	Y
0109470101	WR 22	10 41 18.0	-59 40 37	3400	4	Y
0109480101	WR 47	12 44 25.0	-63 05 16	51744	4	Y
0109480401	WR 47	12 44 25.0	-63 05 16	44749	4	Y
0109500101	RX J1914+24	19 14 26.1	+24 56 44	9559	4	Y
0109500201	RX J1914+24	19 14 26.1	+24 56 44	6060	4	Y
0109510301	PQ Gem	07 51 17.4	+14 44 25	28578	6	Y
0109520101	XMDSOM_1	02 23 20.0	-04 10 00	26019	7	Y
0109520301	XMDSOM_3	02 25 60.0	-04 49 60	22012	7	Y
0109520501	XMDSOM_5	02 23 20.0	-04 49 60	24216	7	Y
0109520601	XMDSOM_6	02 22 40.0	-04 30 00	22884	7	Y
0109540101	WARP J0152.7-1357	01 52 42.5	-13 57 55	53055	3	N
0109660801	Deep Field 1334+37	13 34 37.0	+37 54 44	49356	7	Y
0109660901	Deep Field 1334+37	13 34 37.0	+37 54 44	22472	7	Y
0109661001	Deep Field 1334+37	13 34 37.0	+37 54 44	67406	7	Y
0109661101	Deep Field 0145-04	01 45 27.0	-04 34 42	48004	7	Y
0109661201	Deep Field 0145-04	01 45 27.0	-04 34 42	53079	7	Y
0109661401	Deep Field 0145-04	01 45 27.0	-04 34 42	8497	7	Y
0109860101	A 189	01 25 33.2	+01 45 38	38686	3	N
0109860201	A 189	01 25 33.2	+01 45 38	5840	3	N
0109860401	A 189	01 25 32.0	+01 45 30	7817	3	N
0109890401	A 665	08 31 01.2	+65 50 15	9261	3	N
0109900101	IRAS 16007+8137	15 56 50.6	+81 28 56	13058	1	Y
0109920301	A 2052	15 16 44.0	+07 01 18	2400	3	N
0109960101	NGC 5548	14 17 59.0	+25 08 12	23131	1	Y
0109970101	NGC 4593	12 39 39.0	-05 20 39	13039	1	Y
0109980301	Hydra A cluster	09 18 00.8	-12 05 18	27537	3	N
0109980501	Hydra A cluster	09 18 00.8	-12 05 18	3736	3	N
0110000201	IKT 18	00 59 26.0	-72 10 11	16641	5	N

0110070401	U Gem	07 55 05.2	+22 00 05	22300	4	Y
0110660101	MBM 12	02 56 04.9	+19 28 35	14468	5	N
0110660201	HVC Complex A	09 06 01.6	+62 03 00	8724	5	N
0110660301	Polaris Flare	11 01 00.0	+86 10 00	7300	5	N
0110660401	HVC Complex M	11 25 60.0	+42 52 60	12185	5	N
0110660601	HVCs/ Draco 2	16 34 60.0	+63 52 60	11066	5	N
0110661101	MBM 16	03 19 60.0	+11 13 60	11589	5	N
0110661301	MBM 16	03 19 60.0	+11 13 60	7192	5	N
0110661601	Polaris Flare	11 01 00.0	+86 10 00	10025	5	N
0110661701	HVC Complex A	09 06 01.6	+62 03 00	3184	5	N
0110662501	HVCs/ Draco 1	16 19 20.0	+60 00 00	11814	5	N
0110662701	Finger/Draco 1	17 00 00.0	+59 40 00	3600	5	N
0110860101	HU Aqr	21 07 58.3	-05 17 39	33669	6	Y
0110870101	CL0500-24	05 01 06.0	-24 25 03	24784	3	N
0110890101	IRAS 13224-3809	13 25 20.0	-38 24 55	59222	1	Y
0110890201	1H 0707-495	07 08 41.0	-49 33 06	42930	1	Y
0110890301	I Zw 1	00 53 35.0	+12 41 36	21034	1	Y
0110890401	Ton S 180	00 57 20.0	-22 22 59	29597	1	Y
0110890701	Ton S 180	00 57 20.0	-22 22 59	18146	1	Y
0110890901	PHL 1092	01 39 56.0	+06 19 21	25773	1	Y
0110910201	M 83	13 37 00.0	-29 51 51	25100	2	Y
0110920101	NGC 4258	12 18 58.0	+47 18 14	19226	1	Y
0110930101	NGC2146	06 18 40.0	+78 21 23	19100	2	Y
0110930201	NGC3079	10 01 58.0	+55 40 47	13051	2	Y
0110930401	NGC5689	14 35 30.0	+48 44 30	9756	2	Y
0110930501	NGC5005	13 10 56.0	+37 03 33	13239	2	Y
0110930701	NGC 4388	12 25 47.0	+12 39 41	11658	2	Y
0110930901	NGC5689	14 35 30.0	+48 44 30	7105	2	Y
0110940101	QSO Concentration N	13 38 31.0	+28 05 47	18865	3	N
0110950101	HE 1029-1401	10 31 54.0	-14 16 51	7297	1	Y
0110950201	TON S210	01 21 51.0	-28 20 57	7554	1	Y
0110950401	PG 1307+085	13 09 47.0	+08 19 49	12292	1	Y
0110960101	Q2237+0305	22 40 30.0	+03 21 30	24076	1	Y
0110970101	Marano01	03 13 09.0	-55 03 54	10277	7	Y
0110970201	Marano02	03 14 15.0	-55 11 22	8488	7	Y
0110970301	Marano03	03 14 15.0	-55 16 32	8475	7	Y
0110970401	Marano04	03 14 15.0	-55 21 41	8479	7	Y
0110970501	Marano05	03 14 51.0	-55 06 13	7787	7	Y
0110970601	Marano06	03 14 51.0	-55 11 22	8090	7	Y
0110970701	Marano07	03 14 51.0	-55 16 32	7892	7	Y
0110970801	Marano08	03 14 51.0	-55 21 41	4000	7	Y
0110980101	NGC 3628	11 20 16.9	+13 35 20	48832	2	Y
0110980201	NGC 4666	12 45 08.9	-00 27 38	56490	2	Y
0110980401	NGC 1511	03 59 35.7	-67 38 07	34988	2	Y
0110980601	NGC 5073	13 19 20.8	-14 50 35	43211	2	Y
0110980801	NGC 1808	05 07 42.3	-37 30 46	39303	2	Y
0110990101	AO0235+164	02 38 38.0	+16 37 00	18709	2	Y
0110990201	HI1225+01	12 27 19.0	+01 29 24	13896	2	Y
0110990301	NGC247/PHL6625	00 46 52.0	-20 43 29	6100	2	Y
0111000101	CL 0016+16	00 18 33.0	+16 26 18	31420	3	N
0111000201	CL 0016+16	00 18 33.0	+16 26 18	5530	3	N
0111010101	Cen X-3	11 21 15.2	-60 37 24	66192	6	Y
0111020201	EX Hydrae	12 52 24.4	-29 14 56	34837	6	Y
0111030101	Vela X-1	09 02 06.9	-40 33 17	54796	6	Y
0111060101	Her X-1	16 57 49.8	+35 20 33	9397	6	Y
0111061201	Her X-1	16 57 49.8	+35 20 33	10939	6	Y
0111061301	Her X-1	16 57 49.8	+35 20 33	8114	6	Y
0111061401	Her X-1	16 57 49.8	+35 20 33	7812	6	Y
0111061501	Her X-1	16 57 49.8	+35 20 33	1972	6	Y
0111061601	Her X-1	16 57 49.8	+35 20 33	8000	6	Y
0111061701	Her X-1	16 57 49.8	+35 20 33	6000	6	Y
0111062101	Her X-1	16 57 49.8	+35 20 33	2100	6	Y
0111062601	Her X-1	16 57 49.8	+35 20 33	500	6	Y
0111070201	4U1626-67	16 32 17.0	-67 27 43	15578	6	Y
0111100101	PSR J0218+42	02 18 06.0	+42 32 17	24023	5	N
0111100201	PSR J1012+53	10 12 33.0	+53 07 03	1592	5	N
0111100301	PSR J0751+18	07 51 09.0	+18 07 39	33435	5	N

0111110101	XMDS SSC_1	02 28 00.0	-05 10 00	22300	7	Y
0111110201	XMDS SSC_2	02 26 40.0	-05 10 00	8800	7	Y
0111110301	XMDS SSC_3	02 25 20.0	-05 10 00	22561	7	Y
0111110401	XMDS SSC_4	02 24 00.0	-05 10 00	28103	7	Y
0111110501	XMDS SSC_5	02 22 40.0	-05 10 00	23892	7	Y
0111110701	XMDS SSC_2	02 26 40.0	-05 10 00	12154	7	Y
0111120101	R CR A	19 01 54.4	-36 57 04	17891	4	Y
0111120201	Rho Oph Core	16 27 26.0	-24 40 48	31665	4	Y
0111160101	RXJ1334.3+5030	13 34 20.0	+50 30 54	45060	3	N
0111160201	SHARC-2	05 05 20.0	-28 49 05	45755	3	N
0111170101	geminga	06 33 54.2	+17 46 13	79335	5	N
0111180201	AE Aqr	20 40 10.0	-00 52 16	14309	6	Y
0111180401	rxj0558.0+5353	05 58 00.0	+53 53 59	27056	6	Y
0111200101	NGC 1068	02 42 41.0	-00 00 48	36566	1	Y
0111200201	NGC 1068	02 42 41.0	-00 00 48	33084	1	Y
0111220101	Markarian 3	06 15 34.7	+71 02 07	39184	1	Y
0111220201	Markarian 3	06 15 34.7	+71 02 07	48032	1	Y
0111230101	X1822-371	18 25 46.8	-37 06 18	32446	6	Y
0111240101	Circinus Galaxy	14 13 10.1	-65 20 23	96077	1	Y
0111250101	EUVE J2115.7-5840	21 15 41.0	-58 40 52	14070	6	Y
0111251401	EUVE J2115.7-5840	21 15 41.0	-58 40 52	15282	6	Y
0111251501	EUVE J2115.7-5840	21 15 41.0	-58 40 52	15585	6	Y
0111251601	EUVE J2115.7-5840	21 15 41.0	-58 40 52	5590	6	Y
0111251701	EUVE J2115.7-5840	21 15 41.0	-58 40 52	10373	6	Y
0111251801	EUVE J2115.7-5840	21 15 41.0	-58 40 52	3699	6	Y
0111251901	EUVE J2115.7-5840	21 15 41.0	-58 40 52	7234	6	Y
0111260101	GB1428+4217	14 30 24.0	+42 04 36	4300	1	Y
0111260201	GB1508+5714	15 10 03.0	+57 02 44	11958	1	Y
0111260701	GB1428+4217	14 30 24.0	+42 04 36	14373	1	Y
0111270101	A2390	21 53 37.0	+17 41 45	15389	3	N
0111270201	A2029	15 10 56.0	+05 44 42	12400	3	N
0111280101	SGP-1	00 55 19.0	-27 36 00	2012	7	Y
0111280301	SGP-3	00 58 51.0	-27 36 00	7600	7	Y
0111280601	SGP-6	00 58 51.0	-28 00 00	10537	7	Y
0111280701	SGP-7	00 55 19.0	-28 24 00	5459	7	Y
0111280801	SGP-8	00 57 00.0	-28 24 00	8071	7	Y
0111281001	F864-1	13 41 24.0	+00 24 00	9871	7	Y
0111281301	F864-4	13 41 24.0	+00 00 00	5392	7	Y
0111281401	F864-5	13 43 00.0	+00 00 00	4271	7	Y
0111281501	F864-6	13 44 36.0	+00 00 00	6569	7	Y
0111281601	F864-7	13 41 24.0	-00 24 00	7121	7	Y
0111281701	F864-8	13 43 00.0	-00 24 00	5817	7	Y
0111281801	F864-9	13 44 36.0	-00 24 00	3818	7	Y
0111282001	SGP-2	00 57 00.0	-27 36 00	7900	7	Y
0111282201	SGP-4	00 55 19.0	-28 00 00	8371	7	Y
0111282301	SGP-9	00 58 51.0	-28 24 00	1098	7	Y
0111282401	F864-2	13 43 00.0	+00 24 00	6617	7	Y
0111282501	F864-9	13 44 36.0	-00 24 00	8371	7	Y
0111282601	F864-3	13 44 36.0	+00 24 00	7765	7	Y
0111290101	PG0947+396	09 50 48.4	+39 26 51	21359	1	Y
0111290201	PG0953+414	09 56 52.4	+41 15 22	14209	1	Y
0111290301	PG1115+407	11 18 30.3	+40 25 54	19928	1	Y
0111290401	PG1116+215	11 19 08.7	+21 19 18	8512	1	Y
0111290601	PG1425+267	14 27 35.5	+26 32 14	33058	1	Y
0111291001	PG1512+370	15 14 43.0	+36 50 50	18838	1	Y
0111291101	PG1216+069	12 19 20.9	+06 38 38	16300	1	Y
0111300101	M 55	19 39 59.0	-30 57 44	24196	6	Y
0111310101	HT Cas	01 10 13.0	+60 04 35	41345	6	Y
0111310201	SS Cyg	21 42 42.8	+43 35 10	11234	6	Y
0111320101	UZ For	03 35 29.0	-25 44 23	20765	6	Y
0111320401	EF Eri	03 14 13.0	-22 35 42	2345	6	Y
0111320501	EF Eri	03 14 13.0	-22 35 42	6660	6	Y
0111370101	AR Lacertae	22 08 40.8	+45 44 32	19172	4	Y
0111390101	UX Arietis	03 26 35.3	+28 42 54	6742	4	Y
0111390301	UX Arietis	03 26 35.3	+28 42 54	28534	4	Y
0111400101	pi1 Ursae Majoris	08 39 11.7	+65 01 15	47125	4	Y
0111410101	kappa1 Ceti	03 19 21.7	+03 22 13	32195	4	Y

0111420101	AU Microscopii	20 45 09.5	-31 20 27	53591	4	Y
0111430101	UV Ceti	01 39 01.4	-17 57 02	33706	4	Y
0111440101	AD Leonis	10 19 36.3	+19 52 12	33263	4	Y
0111450101	EV Lacertae	22 46 49.7	+44 20 02	25792	4	Y
0111460101	YZ Canis Minoris	07 44 40.2	+03 33 09	23491	4	Y
0111470101	Sigma2 CrB	16 14 41.7	+33 51 35	1708	4	Y
0111470201	Sigma2 CrB	16 14 41.7	+33 51 35	10293	4	Y
0111470301	Sigma2 CrB	16 14 41.7	+33 51 35	12600	4	Y
0111490101	VY Arietis	02 48 43.7	+31 06 55	10098	4	Y
0111490401	VY Arietis	02 48 43.7	+31 06 55	30575	4	Y
0111500101	Chi1 Orionis	05 54 23.0	+20 16 34	29113	4	Y
0111510101	AT Microscopii	20 41 51.2	-32 26 07	16905	4	Y
0111520101	47 Cassiopeiae	02 05 07.4	+77 16 53	40779	4	Y
0111530101	EK Draconis	14 39 00.2	+64 17 30	51821	4	Y
0111540201	Alpha CrB	15 34 41.3	+26 42 53	32950	4	Y
0111550101	Hubble Deep Field N	12 36 50.0	+62 13 00	41519	7	Y
0111550201	Hubble Deep Field N	12 36 50.0	+62 13 12	39562	7	Y
0111550301	Hubble Deep Field N	12 36 53.0	+62 13 12	30285	7	Y
0111550401	Hubble Deep Field N	12 36 57.0	+62 13 30	87695	7	Y
0111570101	MCG-6-30-15	13 35 54.0	-34 17 45	37597	1	Y
0111570201	MCG-6-30-15	13 35 54.0	-34 17 45	44495	1	Y
0111790101	NGC7314	22 35 46.0	-26 03 02	36483	1	Y
0111800101	M81	09 55 33.0	+69 03 55	80467	1	Y
0111810101	NGC7213	22 09 16.0	-47 10 00	48512	1	Y
0111830201	PKS 0548-32	05 50 40.8	-32 16 18	42778	1	Y
0111840101	1H1219+301	12 21 22.0	+30 10 37	22358	1	Y
0111850201	H1426+428	14 28 32.7	+42 40 21	45498	1	Y
0111870301	A2142	15 57 32.3	+27 24 24	17579	3	N
0111870601	A2142	15 49 07.7	+27 03 11	14800	3	N
0111970101	TY PsA	22 49 40.0	-27 06 55	12600	6	Y
0111970301	VW Hyi	04 09 11.2	-71 17 42	18708	6	Y
0111970401	WX Hyi	02 09 50.8	-63 18 40	9700	6	Y
0111970701	T Leo	11 38 27.0	+03 22 07	12281	6	Y
0111970801	SU UMa	08 12 28.0	+62 36 22	8800	6	Y
0111970901	WW Cet	00 11 25.0	-11 28 43	12100	6	Y
0111971001	IX Vel	08 15 19.0	-49 13 21	21462	6	Y
0111971301	EI UMa	08 38 22.0	+48 38 01	4771	6	Y
0111971601	AB Dra	19 49 06.7	+77 44 24	9857	6	Y
0111971701	EI UMa	08 38 22.0	+48 38 01	9373	6	Y
0112170101	NGC7469	23 03 16.0	+08 52 26	17937	1	Y
0112170301	NGC7469	23 03 16.0	+08 52 26	23446	1	Y
0112190101	MS0302.5+1717	03 05 18.8	+17 28 24	13050	3	N
0112190201	MS1208.7+3928	12 11 15.4	+39 11 38	13911	3	N
0112190401	MS1532.5+0130	15 35 01.8	+01 20 49	14048	3	N
0112190601	MS2053.7-0449	20 56 21.8	-04 37 51	16725	3	N
0112190701	MS1621.5+2640	16 23 35.5	+26 34 13	2300	3	N
0112190801	MS1621.5+2640	16 23 35.5	+26 34 13	2494	3	N
0112200101	PSR0656+14	06 59 48.0	+14 14 22	26794	5	N
0112200201	PSR J0117+5914	01 17 39.0	+59 14 38	7979	5	N
0112200301	PSR J0358+5413	03 58 54.0	+54 13 14	28035	5	N
0112200401	PSR J0538+2817	05 38 25.0	+28 17 11	14933	5	N
0112200501	PSR J1705-1906	17 05 36.0	-19 06 38	4771	5	N
0112200601	PSR J1709-4428	17 09 42.0	-44 28 57	30578	5	N
0112201001	PSR J1825-0935	18 25 31.0	-09 35 23	5040	5	N
0112210101	NCG3783	11 39 02.0	-37 44 19	36610	1	Y
0112210201	NGC3783	11 39 01.8	-37 44 19	63361	1	Y
0112210501	NGC3783	11 39 01.8	-37 44 19	124186	1	Y
0112220101	Omega Cen	13 26 46.0	-47 28 33	38204	6	Y
0112220201	NGC 6656	18 36 24.0	-23 54 22	20948	6	Y
0112230201	A1914	14 26 02.0	+37 49 48	24708	3	N
0112230301	A2204	16 32 46.0	+05 34 48	20270	3	N
0112230501	A1413	11 55 19.0	+23 24 36	25415	3	N
0112230701	A2163 of1	16 16 48.0	-06 09 00	17284	3	N
0112230801	A2163 of2	16 15 46.0	-05 51 00	19175	3	N
0112230901	A2163 of3	16 14 34.0	-06 09 00	15092	3	N
0112231001	A2163 of4	16 15 46.0	-06 27 00	26580	3	N
0112231501	A2163	16 15 46.0	-06 09 00	4911	3	N

0112231801	A2219	16 40 24.0	+46 42 36	1026	3	N
0112231901	A2219	16 40 24.0	+46 42 36	1741	3	N
0112240401	A2142	15 59 20.4	+27 31 37	1724	3	N
0112250101	RXJ1354.3-0222	13 54 17.0	-02 21 46	24755	3	N
0112250201	QSO 1345+584	13 47 41.0	+58 12 42	31679	3	N
0112250301	H1413+117	14 15 46.0	+11 29 44	25500	3	N
0112251301	H1413+117	14 15 46.0	+11 29 44	29371	3	N
0112270301	HCG51	11 22 21.0	+24 17 35	14055	3	N
0112270601	N79-299A	12 04 10.0	+20 13 18	6865	3	N
0112270701	HCG62	12 53 06.0	-09 12 00	12526	3	N
0112271001	N79-299A	12 04 10.0	+20 13 18	7713	3	N
0112271101	N79-299A	12 04 10.0	+20 13 18	5382	3	N
0112280101	NGC891	02 22 31.0	+42 20 15	13012	2	Y
0112280201	NGC4490	12 30 36.0	+41 38 41	16900	2	Y
0112290501	NGC5408	14 03 19.0	-41 23 05	6600	2	Y
0112290601	NGC5408	14 03 19.0	-41 23 05	6199	2	Y
0112290701	NGC5408	14 03 19.0	-41 23 05	7400	2	Y
0112290801	NGC1569	04 30 46.0	+64 50 53	16876	2	Y
0112291201	NGC5408	14 03 19.0	-41 23 05	4300	2	Y
0112300101	ngc 720	01 53 01.0	-13 44 14	29302	2	Y
0112310101	NGC 4151	12 10 32.0	+39 24 20	29651	1	Y
0112310201	NGC 7582	23 18 23.0	-42 22 11	22400	1	Y
0112310301	NGC 4945	13 05 26.0	-49 28 14	22391	1	Y
0112310401	NGC 6552	18 00 07.0	+66 36 54	2810	1	Y
0112310801	NGC 6552	18 00 07.0	+66 36 54	6865	1	Y
0112320101		-1 00 00.0	+00 30 27	22058	5	N
0112370101	SDS-1	02 18 00.0	-05 00 00	42877	7	Y
0112370301	SDS-2	02 19 36.0	-05 00 00	41279	7	Y
0112370401	SDS-3	02 18 48.0	-04 39 13	21365	7	Y
0112370601	SDS-5	02 16 24.0	-05 00 00	35232	7	Y
0112370701	SDS-6	02 17 12.0	-05 20 47	48964	7	Y
0112370801	SDS-7	02 18 48.0	-05 20 47	37930	7	Y
0112371001	SDS-1	02 18 00.0	-05 00 00	44582	7	Y
0112371501	SDS-3	02 18 48.0	-04 39 13	7490	7	Y
0112371701	SDS-4	02 17 12.0	-04 39 13	22527	7	Y
0112372001	SDS-4	02 17 12.0	-04 39 13	27336	7	Y
0112380101	SCO-CEN PT1	15 56 25.0	-23 37 47	40179	4	Y
0112390101	Pleiades	03 43 44.0	+24 43 17	48734	4	Y
0112400101	Epsilon Ori	05 36 12.0	-01 12 07	12319	4	Y
0112410101	GRS 1716-249	17 19 37.0	-25 01 03	10416	6	Y
0112420101	IC 2391	08 41 59.0	-53 00 35	43932	4	Y
0112430101	LSI +61 303	02 40 32.0	+61 13 47	4600	6	Y
0112430102	LSI +61 303	02 40 32.0	+61 13 47	5800	6	Y
0112430401	LSI +61 303	02 40 32.0	+61 13 47	6154	6	Y
0112440101	Aql X-1	19 11 16.0	+00 35 06	2500	6	Y
0112440301	Aql X-1	19 11 16.0	+00 35 06	7165	6	Y
0112440401	Aql X-1	19 11 16.0	+00 35 06	13336	6	Y
0112450301	HD49798	06 48 05.0	-44 18 54	7273	6	Y
0112450501	HD49798	06 48 05.0	-44 18 54	2565	6	Y
0112450601	HD49798	06 48 05.0	-44 18 54	11739	6	Y
0112460201	GRO J1655-40	16 54 00.2	-39 50 45	27456	6	Y
0112480101	oph_pos1	16 40 48.0	-24 06 00	19529	5	N
0112480201	oph_pos2	16 40 48.0	-24 23 60	17198	5	N
0112480301	oph_pos3	16 40 48.0	-24 41 60	17463	5	N
0112490101	aqui_pos1	18 27 59.9	-03 30 00	21554	5	N
0112490201	aqui_pos3	18 29 36.0	-03 30 00	3295	5	N
0112490301	aqui_pos3	18 31 12.0	-03 30 00	23000	5	N
0112500101	A2256 offset	16 56 46.5	+79 01 16	25204	3	N
0112510301	MBM 12 Pos_2	02 56 05.0	+19 22 60	28092	5	N
0112520101	IZw18	09 34 02.0	+55 14 20	30314	2	Y
0112520201	IZw18	09 34 02.0	+55 14 20	10800	2	Y
0112520601	Holmberg II	08 19 29.0	+70 42 23	9761	2	Y
0112520701	Holmberg II	08 19 29.0	+70 42 23	6873	2	Y
0112520901	Holmberg II	08 19 29.0	+70 42 23	6509	2	Y
0112521001	Holmberg IX	09 57 53.0	+69 03 40	10100	2	Y
0112521101	Holmberg IX	09 57 53.0	+69 03 40	9583	2	Y
0112521301	NGC 7714	23 36 15.0	+02 09 18	16144	2	Y

0112521701	NGC 4449	12 28 09.0	+44 05 10	15165	2	Y
0112521901	NGC 4395	12 25 48.0	+33 32 50	14793	2	Y
0112522601	NGC 7714	23 36 15.0	+02 09 18	15890	2	Y
0112522701	NGC 4395	12 25 48.0	+33 32 50	8175	2	Y
0112530101	Zeta Orionis	05 40 45.5	-01 56 33	41469	4	Y
0112540101	Tau Scorpii	16 35 52.9	-28 12 58	22332	4	Y
0112550101	ngc3486	11 00 23.0	+28 58 29	4500	1	Y
0112550201	ngc1058	02 43 29.0	+37 20 27	10000	1	Y
0112550301	ngc4565	12 36 20.0	+25 59 16	14260	1	Y
0112550401	ngc4725	12 50 26.0	+25 30 05	17419	1	Y
0112550501	ngc4168	12 12 16.0	+13 12 23	21853	1	Y
0112550701	ngc4477	12 30 02.0	+13 38 10	800	1	Y
0112550801	ngc4501	12 31 58.0	+14 25 09	13159	1	Y
0112551001	ngc4639	12 42 52.0	+13 15 26	14364	1	Y
0112551101	ngc4698	12 48 22.0	+08 29 14	14106	1	Y
0112551201	ngc4138	12 09 30.0	+43 41 04	14341	1	Y
0112551401	ngc3941	11 52 55.0	+36 59 10	6525	1	Y
0112551501	ngc676	01 48 57.0	+05 54 26	16954	1	Y
0112551701	ngc5273	13 42 08.0	+35 39 14	16092	1	Y
0112552001	ngc3185	10 17 38.0	+21 41 17	13700	1	Y
0112552101	ngc4477	12 30 02.0	+13 38 10	13522	1	Y
0112570201	M31 South 1	00 41 25.0	+40 55 35	57152	2	Y
0112570301	M31 South 2	00 40 06.0	+40 35 24	49263	2	Y
0112600301	MRK 1044	02 30 05.0	-08 59 53	6700	1	Y
0112600401	1H 0419-577	04 25 44.0	-57 13 35	7497	1	Y
0112600501	Mrk 896	20 46 20.0	-02 48 46	10539	1	Y
0112600601	Mrk 359	01 27 32.0	+19 10 39	6893	1	Y
0112600801	Mrk 493	15 59 10.0	+35 01 45	17360	1	Y
0112610101	PG 1211+143	12 14 17.0	+14 03 12	54481	1	Y
0112620101	S5 0836+716	08 41 24.0	+70 53 41	28568	1	Y
0112620201	S5 0014+813	00 17 08.0	+81 35 08	18187	1	Y
0112630101	HE 1104-1805	11 06 33.0	-18 21 24	12600	1	Y
0112630201	QSO 0130-403	01 33 02.0	-40 06 31	26300	1	Y
0112640201	NGC 2023	05 41 47.2	-02 16 37	19559	4	Y
0112650101	NGP Rift 1	12 31 12.0	+20 48 00	23080	5	N
0112650201	NGP Rift 2	12 31 12.0	+21 18 00	24110	5	N
0112650301	NGP Rift 3	12 31 12.0	+21 48 00	18858	5	N
0112650401	G133-69 Pos_1	01 04 24.0	-06 24 00	23583	5	N
0112650501	G133-69 Pos_2	01 04 00.0	-06 42 00	22787	5	N
0112670101	Gamma2 Velorum	08 09 32.0	-47 20 12	4322	4	Y
0112670201	Gamma2 Velorum	08 09 32.0	-47 20 12	11300	4	Y
0112670401	Gamma2 Velorum	08 09 32.0	-47 20 12	14095	4	Y
0112670501	Gamma2 Velorum	08 09 32.0	-47 20 12	28338	4	Y
0112680101	MLS-1	02 27 20.0	-04 10 00	25279	7	Y
0112680201	MLS-2	02 25 60.0	-04 10 00	14669	7	Y
0112680301	MLS-3	02 24 40.0	-04 10 00	22190	7	Y
0112680401	MLS-5	02 28 00.0	-04 30 00	24064	7	Y
0112680501	MLS-8	02 24 00.0	-04 30 00	21757	7	Y
0112681001	MLS-7	02 25 20.0	-04 30 00	33700	7	Y
0112681301	MLS-6	02 26 40.0	-04 30 00	17079	7	Y
0112770101	3C 273	12 29 06.0	+02 03 07	5093	1	Y
0112770201	3C 273	12 29 06.0	+02 03 07	5549	1	Y
0112770501	3C 273	12 29 06.0	+02 03 07	8086	1	Y
0112770601	3C 273	12 29 06.0	+02 03 07	4689	1	Y
0112770701	3C 273	12 29 06.0	+02 03 07	5139	1	Y
0112770801	3C 273	12 29 06.0	+02 03 07	5048	1	Y
0112771001	3C 273	12 29 06.0	+02 03 07	5663	1	Y
0112771101	3C 273	12 29 06.0	+02 03 07	8665	1	Y
0112780201	RX J0059.2-7138	00 59 13.0	-71 38 50	4870	6	Y
0112780401	1E 1048.1-5937	10 50 09.0	-59 53 19	7246	6	Y
0112781001	4U 0115+63	01 18 32.0	+63 44 24	4135	6	Y
0112790101	RX J1940.1-1025	19 40 11.5	-10 25 25	21820	6	Y
0112800101	NGC 300	00 54 55.0	-37 40 60	43689	6	Y
0112800201	NGC 300	00 54 55.0	-37 40 60	32524	6	Y
0112810101	NGC 3690	11 28 30.0	+58 33 43	20212	2	Y
0112810201	NGC 3256	10 27 50.0	-43 54 14	11109	2	Y
0112810301	NGC 3310	10 38 45.0	+53 30 11	5600	2	Y

0112830201	NGC4151	12 10 32.6	+39 24 21	59155	1	Y
0112830301	MCG-5-23-16	09 47 40.2	-30 56 54	12159	1	Y
0112830401	MCG-5-23-16	09 47 40.2	-30 56 54	24174	1	Y
0112830501	NGC4151	12 10 32.6	+39 24 21	22089	1	Y
0112840101	NGC4579	12 37 43.5	+11 49 05	18519	1	Y
0112850101	0952+179	09 54 56.8	+17 43 31	16930	2	Y
0112850201	1127-145	11 30 07.0	-14 49 27	19091	2	Y
0112850301	0738+313	07 41 10.7	+31 12 00	3620	2	Y
0112860101	Q0226-1024	02 28 56.5	-10 10 39	7632	1	Y
0112860201	Q0932+5006	09 35 52.9	+49 53 13	3227	1	Y
0112860301	Q1524+5147	15 25 53.9	+51 36 50	2200	1	Y
0112880101	CoD-33_7795	11 31 55.0	-34 36 25	29537	4	Y
0112880201	TW Hya	11 01 51.9	-34 42 17	28644	4	Y
0112880301	EQ Peg	23 31 50.0	+19 56 17	14491	4	Y
0112880401	Gl 182	04 59 35.0	+01 47 09	18993	4	Y
0112880501	HR 1084	03 32 55.8	-09 27 30	13162	4	Y
0112880601	HR 188	00 43 35.0	-17 59 14	12495	4	Y
0112880801	YY Gem	07 34 38.2	+31 52 15	51770	4	Y
0112880901	CF Tuc	00 53 04.8	-74 39 07	38740	4	Y
0112900201	GX 339-4	17 02 49.0	-48 47 22	6231	6	Y
0112910101	ESO 198-G24	02 38 11.0	-52 10 40	9726	1	Y
0112910201	MKN 841	15 04 01.2	+10 26 16	8677	1	Y
0112910301	MR 2251-178	22 53 59.0	-17 33 50	4926	1	Y
0112940101	Marano pointing 9	03 15 27.0	-55 06 13	5991	7	Y
0112940201	Marano pointing 16	03 16 03.0	-55 21 41	9187	7	Y
0112940301	Marano pointing 10	03 15 27.0	-55 11 22	6400	7	Y
0112940401	Marano pointing 11	03 15 27.0	-55 16 32	8889	7	Y
0112940501	Marano pointing 12	03 15 27.0	-55 21 41	5900	7	Y
0112950601	A2256_f2	17 07 57.5	+78 31 41	12320	3	N
0112960301	AXJ2019+112	20 19 18.0	+11 27 15	13461	3	N
0112960501	AXJ2019+112	20 19 18.0	+11 27 15	13255	3	N
0112960601	AXJ2019+112	20 19 18.0	+11 27 15	12143	3	N
0112970101	GC1	17 48 44.0	-28 05 06	14000	7	Y
0112970201	GC2	17 47 21.0	-28 09 02	16789	7	Y
0112970401	GC4	17 46 10.0	-28 38 37	23088	7	Y
0112971501	GC3	17 47 10.0	-28 28 03	12198	7	Y
0112971601	GC6	17 45 40.0	-29 00 23	799	7	Y
0112971801	GC9	17 43 27.0	-29 47 34	10223	7	Y
0112971901	GRO J1744-28	17 44 34.0	-28 45 22	9189	7	Y
0112980101	A2218	16 35 48.0	+66 12 36	18163	3	N
0112980201	RXJ0658-55	06 58 16.8	-55 57 36	40148	3	N
0112980401	A2218	16 35 48.0	+66 12 36	14960	3	N
0112980501	A2218	16 35 48.0	+66 12 36	12300	3	N
0113040801	C2001/A2 LIN	01 20 39.9	-10 56 34	6400	4	Y
0113041401	c2002/t7	08 43 40.0	-13 50 23	20179	4	Y
0113050101	PSR 1055-52	10 57 58.8	-52 26 56	21039	5	N
0113050201	PSR 1055-52	10 57 58.8	-52 26 56	53850	5	N
0113060201	MKN501	16 53 52.2	+39 45 37	5398	1	Y
0113060401	MKN501	16 53 52.2	+39 45 37	5700	1	Y
0113070101	nps_pos1	16 53 59.9	+14 18 00	21302	5	N
0113070901	nps_pos2	16 53 59.9	+14 54 00	6697	5	N
0113071001	nps_pos3	16 53 59.9	+15 30 00	3000	5	N
0119100201	PKS0558	05 59 47.0	-50 26 51	8100	4	Y
0119710201	EXO0748-67	07 48 25.0	-67 45 00	21177	6	Y
0119940201	SAX J1808.4-3658	18 08 27.6	-36 58 42	16277	6	Y
0119940501	SAX J1808.4-3658	18 08 27.6	-36 58 42	4296	6	Y
0121920101	Capella	05 16 41.0	+46 00 14	17045	4	Y
0122321101	EXO0748-67	07 48 25.0	-67 45 00	19000	6	Y
0122520201	PKS0312-770	03 11 55.0	-76 51 52	27184	2	Y
0122901001	Canopus z-0.5	06 21 06.6	-52 26 37	698	4	Y
0122901201	Canopus z+1	06 29 44.0	-53 11 13	995	4	Y
0122901301	Canopus z+1.5	06 32 40.4	-53 25 34	996	4	Y
0122901401	Canopus z+2	06 35 38.8	-53 39 37	1000	4	Y
0122901701	Canopus z+3	06 41 41.5	-54 06 55	897	4	Y
0123100101	MS0737.9+7441	07 44 04.5	+74 33 50	45654	1	Y
0123100201	MS0737.9+7441	07 44 04.5	+74 33 50	19690	1	Y
0123500101	EXO0748-676	07 48 24.5	-67 45 00	17293	6	Y

0123510101	CAL 83	05 43 33.0	-68 22 23	9591	6	Y
0123700101	Lockman Hole	10 52 43.0	+57 28 48	35100	7	Y
0123700401	Lockman Hole	10 52 43.0	+57 28 48	14328	7	Y
0123710101	YY Gem	07 34 37.3	+31 52 10	55982	4	Y
0123710201	YY Gem	07 34 37.3	+31 52 10	19390	4	Y
0123720301	AB Dor (RC 0010)	05 28 44.0	-65 27 02	54636	4	Y
0123900101	A S 1101	23 13 59.0	-42 43 36	34400	3	N
0123920101	BPM 16274	00 50 03.2	-52 08 17	18995	4	Y
0123940201	Procyon	07 39 18.1	+05 13 30	52036	4	Y
0124100101	RXj 0720.4-3125	07 20 25.1	-31 25 45	38890	5	N
0124110101	Mkn205	12 21 44.0	+75 18 37	17196	1	Y
0124710301	Coma3	12 58 32.2	+27 24 12	17003	3	N
0124710701	Coma7	12 57 27.7	+28 08 41	6100	3	N
0124900101	MS1229.2+6430	12 31 32.0	+64 14 21	28800	1	Y
0124930101	PKS2155-304	21 58 53.0	-30 13 35	27172	1	Y
0124930201	PKS2155-304	21 58 53.0	-30 13 35	45285	1	Y
0124930501	PKS2155-304	21 58 52.1	-30 13 32	97250	1	Y
0124930601	PKS2155-304	21 58 52.1	-30 13 32	56866	1	Y
0125110101	PKS0558-504	05 59 47.0	-50 26 51	8767	1	Y
0125300101	J104433.04-012502.2	10 44 33.0	-01 25 02	35126	1	Y
0125310101	Abell 2690	00 00 30.0	-25 07 30	19096	2	Y
0125320401	BPM16274	00 50 03.2	-52 08 17	21639	4	Y
0125320501	BPM16274	00 50 03.2	-52 08 17	6314	4	Y
0125320701	BPM16274	00 50 03.2	-52 08 17	17670	4	Y
0125910301	HD 224317	23 56 52.6	-24 25 31	10646	4	Y
0125910501	GD153	12 57 02.4	+22 01 56	12733	4	Y
0125910601	HD13499	02 11 22.1	-24 34 04	1647	4	Y
0125910701	HD13499	02 11 06.2	-24 33 30	4114	4	Y
0125911001	NGC 7293	22 29 48.2	-20 49 26	14238	4	Y
0125911101	GD153	12 57 02.3	+22 01 52	13649	4	Y
0125911201	GD153	12 57 02.3	+22 01 52	4300	4	Y
0125911901	GD153	12 57 02.3	+22 01 52	9033	4	Y
0125920201	G158-100	00 33 54.3	-12 07 57	21723	4	Y
0125970101	HZ43	13 16 22.0	+29 06 00	5303	4	Y
0126500101	LMC X-3	05 38 56.0	-64 05 02	21498	6	Y
0126500201	LMC X-3	05 38 56.0	-64 05 02	21695	6	Y
0126700101	3C 273off-7min	12 29 30.8	+01 59 39	7436	1	Y
0126700201	3C 273off-1.5min	12 29 03.8	+02 01 51	12837	1	Y
0126700301	3C 273	12 29 06.7	+02 03 09	61092	1	Y
0126700401	3C 273off+7min	12 28 44.8	+02 07 27	7156	1	Y
0126700501	3C 273off+1.5min	12 29 09.6	+02 04 27	2200	1	Y
0126700601	3C 273	12 29 06.7	+02 03 09	27698	1	Y
0126700701	3C 273	12 29 06.7	+02 03 09	26396	1	Y
0126700801	3C 273	12 29 06.7	+02 03 09	47599	1	Y
0127110201	IIIZW2	00 10 31.0	+10 58 30	7534	1	Y
0127720201	Nova LMC 2000	05 25 01.6	-70 14 17	22275	6	Y
0127720301	Nova LMC 2000	05 25 01.6	-70 14 17	8989	6	Y
0127720401	Nova LMC 2000	05 25 01.6	-70 14 17	6600	6	Y
0127720501	V4743 Sgr	19 01 09.4	-22 00 05	27913	6	Y
0127920401	GROTH-WESTPHAL STRI	14 17 12.0	+52 24 00	3379	7	Y
0127920901	GROTH-WESTPHAL STRI	14 17 12.0	+52 24 00	396	7	Y
0127921001	GROTH-WESTPHAL STRI	14 17 12.0	+52 24 00	53740	7	Y
0127921101	GROTH-WESTPHAL STRI	14 17 12.0	+52 24 00	7473	7	Y
0127921201	GROTH-WESTPHAL STRI	14 17 12.0	+52 24 00	18477	7	Y
0128320301	OY Car	10 06 22.3	-70 14 05	12892	6	Y
0128530301	GRB001025	08 36 36.5	-13 04 30	33791	6	Y
0128530801	GRB020322	18 00 53.0	+81 04 48	28329	6	Y
0128531101	IGR J16320-4751	16 31 60.0	-47 51 00	4984	6	Y
0128531201	GRB030227	04 57 29.0	+20 29 23	24196	6	Y
0128531401	GRB030329	10 44 50.0	+21 31 17	33093	6	Y
0128531501	GRB030329	10 44 50.0	+21 31 17	58505	6	Y
0128531601	GRB030329	10 44 50.0	+21 31 17	75289	6	Y
0129320801	Marano pointing 15	03 16 03.0	-55 16 32	9952	7	Y
0129320901	Marano pointing 13	03 16 03.0	-55 06 13	9988	7	Y
0129321001	Marano pointing 14	03 16 03.0	-55 11 22	5000	7	Y
0129350201	HR1099	03 36 47.0	+00 35 24	6614	4	Y
0129360201	PKS0558-504 (FAST t	05 59 47.0	-50 26 51	12681	1	Y

0130720101	Mkn509	20 44 09.0	-10 43 15	22700	1	Y
0130720201	Mkn509	20 44 09.0	-10 43 15	38492	1	Y
0130920101	HD 209458 / ToO	22 03 10.8	+18 53 03	16532	4	Y
0132520301	RXj 0720.4-3125	07 20 25.1	-31 25 49	25508	5	N
0133120101	AB DOR	05 28 44.0	-65 27 02	40691	4	Y
0133120201	AB DOR	05 28 44.0	-65 27 02	6270	4	Y
0133120301	BPM 16274	00 50 03.2	-52 08 17	10792	4	Y
0133120401	BPM 16274	00 50 03.2	-52 08 17	10667	4	Y
0134520301	AB Dor	05 28 44.0	-65 27 02	46272	4	Y
0134520701	AB Dor	05 28 44.0	-65 27 02	48786	4	Y
0134521301	AB Dor	05 28 44.0	-65 27 02	34531	4	Y
0134521401	AB Dor	05 28 44.0	-65 27 02	3918	4	Y
0134521501	AB Dor	05 28 44.0	-65 27 02	16150	4	Y
0134521601	AB Dor	05 28 44.8	-65 26 55	11400	4	Y
0134521701	AB Dor	05 28 44.8	-65 26 55	16100	4	Y
0134522001	AB Dor	05 28 44.8	-65 26 55	7000	4	Y
0134522101	AB Dor	05 28 44.8	-65 26 55	48529	4	Y
0134522301	AB Dor	05 28 44.8	-65 26 55	2000	4	Y
0134531401	NGC2516	07 58 22.3	-60 45 36	4922	4	Y
0134540401	HR1099	03 36 47.0	+00 35 24	16949	4	Y
0134540601	HR1099	03 36 47.3	+00 35 16	35356	4	Y
0134540801	HR1099	03 36 47.3	+00 35 16	9090	4	Y
0134561101	EXO 0748-67 off1	07 48 25.0	-67 43 00	7139	4	Y
0134561201	EXO 0748-67 on-axis	07 48 25.0	-67 45 00	5392	4	Y
0134561301	EXO 0748-67 off2	07 48 03.8	-67 45 00	5392	4	Y
0134561401	EXO 0748-67 off3	07 48 25.0	-67 46 60	5392	4	Y
0134561501	EXO 0748-67 off4	07 48 46.2	-67 45 00	5387	4	Y
0134562101	EXO0748 onaxis	07 48 33.7	-67 45 07	7978	4	Y
0134562201	EXO0748-676 off1	07 48 33.7	-67 43 07	6229	4	Y
0134562301	EXO0748-676 off2	07 48 12.6	-67 45 07	6030	4	Y
0134562401	EXO0748-676 off3	07 48 33.7	-67 47 07	5827	4	Y
0134562501	EXO0748-676 off4	07 48 54.8	-67 45 07	5825	4	Y
0134720101	Capella	05 16 41.0	+46 00 14	29558	4	Y
0134720901	Capella	05 16 42.2	+45 59 54	13063	4	Y
0134920901	SA95-42	03 53 43.7	-00 04 33	15578	4	Y
0135720601	1ES0102-72	01 03 50.0	-72 01 55	18899	5	N
0135740701	XGPS_007	18 27 25.0	-10 47 47	7230	7	Y
0135740801	XGPS_008	18 29 55.0	-11 07 05	4435	7	Y
0135740901	XGPS_009	18 28 10.5	-10 26 32	11890	7	Y
0135741001	XGPS_010	18 30 40.3	-10 45 49	3400	7	Y
0135741201	XGPS_012	18 28 55.8	-10 05 17	3400	7	Y
0135741501	XGPS_015	18 29 41.0	-09 44 01	4848	7	Y
0135741601	XGPS_016	18 32 10.6	-10 03 16	7592	7	Y
0135741701	XGPS_017	18 31 18.3	-09 43 01	7137	7	Y
0135741801	XGPS_018	18 30 26.1	-09 22 45	2700	7	Y
0135742601	XGPS_026	18 00 20.5	-22 45 40	4864	7	Y
0135742801	XGPS_028	18 01 47.3	-22 45 34	6097	7	Y
0135742901	XGPS_029	18 01 03.5	-22 28 18	6517	7	Y
0135743001	XGPS_030	18 03 14.1	-22 45 26	504	7	Y
0135743101	XGPS_031	18 02 30.1	-22 28 11	6520	7	Y
0135744801	XGPS_018	18 30 26.1	-09 22 45	2121	7	Y
0135745201	XGPS_011	18 29 48.0	-10 25 33	7604	7	Y
0135745401	RIDGE_2	18 26 44.0	-11 51 26	13646	7	Y
0135745701	XGPS_012	18 28 55.8	-10 05 17	7364	7	Y
0135745801	XGPS_008	18 29 55.0	-11 07 05	13161	7	Y
0135745901	XGPS_010	18 30 40.3	-10 45 49	9065	7	Y
0135746301	XGPS_014	18 30 33.2	-10 04 17	6659	7	Y
0135746401	XGPS_015	18 29 41.0	-09 44 01	5467	7	Y
0135746601	XGPS_014	18 30 33.2	-10 04 17	1343	7	Y
0135746701	XGPS_015	18 29 41.0	-09 44 01	2320	7	Y
0135746801	XGPS_013	18 31 25.5	-10 24 33	4700	7	Y
0135747001	RIDGE_4	18 28 19.0	-11 07 11	6647	7	Y
0135940101	AXJ131021+3019	13 10 24.6	+30 19 28	14370	1	Y
0135940201	AXJ131816+3240	13 18 17.6	+32 40 53	9400	1	Y
0135960101	Clump2	17 51 50.2	-26 38 40	14315	5	N
0135970401	IRAS20126+4104	20 14 26.0	+41 13 32	2316	4	Y
0135980201	IC1459	22 57 10.6	-36 27 44	28840	2	Y

0136000101	A1674	13 04 12.0	+67 30 25	17400	3	N
0136020501	Gamma Cygni	20 20 36.0	+40 42 00	3030	5	N
0136030101	G32.45+0.1	18 50 06.7	-00 25 40	22700	5	N
0136030201	G38.55+0.0	19 01 42.7	+04 59 54	15736	5	N
0136040101	3C324	15 49 50.1	+21 25 56	17780	2	Y
0136340101	Abell 194	01 25 50.0	-01 22 60	20664	3	N
0136550101	3C 273	12 29 06.7	+02 03 09	86892	1	Y
0136550501	3C 273	12 29 06.7	+02 03 09	8655	1	Y
0136550801	3C 273	12 29 06.7	+02 03 09	49975	1	Y
0136950201	RXJ1242	12 42 38.5	-11 19 21	29202	2	Y
0137160201	YY Mem	04 58 17.9	-75 16 38	83393	4	Y
0137550201	PKS0558-504	05 59 47.4	-50 26 52	13981	2	Y
0137550601	PKS0558-504	05 59 47.4	-50 26 52	11305	2	Y
0137551001	3C 273	12 29 06.7	+02 03 09	9048	2	Y
0137551101	N132D	05 25 02.0	-69 38 38	15174	2	Y
0137750101	G153	12 58 20.0	-59 31 00	18273	4	Y
0137950201	KS 1731-260	17 34 13.5	-26 05 19	16253	6	Y
0137950301	KS 1731-260	17 34 13.5	-26 05 19	20910	6	Y
0138950801	IRAS15480-0344	15 50 41.5	-03 53 18	2107	1	Y
0138951401	UGC4229	08 07 41.0	+39 00 15	6947	1	Y
0138951501	IRAS15480-0344	15 50 41.5	-03 53 18	3293	1	Y
0139760101	XTE J0421+560	04 19 42.1	+55 59 58	44271	6	Y
0140190101	RX J0323-4931	03 23 15.2	-49 31 04	29276	1	Y
0140210101	RXCJ0454-1808	04 54 45.1	-18 08 27	35186	3	N
0140210201	RXCJ0953-1558	09 53 14.2	-15 58 49	38452	3	N
0140350101	V851 Cen	13 44 00.9	-61 21 59	30938	4	Y
0140370401	HD 141714	15 49 35.7	+26 04 06	12733	4	Y
0140550601	PG 1004+130	10 07 26.1	+12 48 56	21851	1	Y
0140950101	NGC5643	14 32 40.7	-44 10 28	9352	1	Y
0140950201	NGC1386	03 36 45.4	-35 59 57	16664	1	Y
0140951001	NGC2273	06 50 08.7	+60 50 45	6618	1	Y
0140960101	Mrk668	14 07 00.4	+28 27 15	13740	1	Y
0141150101	I Zw 49	12 59 01.8	+34 51 40	27165	2	Y
0141150201	Mrk 71	07 28 47.6	+69 11 39	37238	2	Y
0141150501	I Zw 49	12 59 01.8	+34 51 40	11321	2	Y
0141160301	A2301	18 14 14.4	+69 39 33	5100	3	N
0141170101	EIS0954-2023/22	09 54 53.5	-20 23 05	33041	3	N
0141400301	LH0416+14	04 19 36.8	+14 33 33	12352	4	Y
0141570101	NGC 4552	12 35 39.8	+12 33 23	27727	2	Y
0141570201	NGC 4125	12 08 05.9	+65 10 27	19858	2	Y
0141610601	3EG J1809-2328	18 09 48.6	-23 32 09	13098	5	N
0141750101	RXJ0420.0-5022	04 20 02.4	-50 22 50	21538	5	N
0141750501	RXJ0806.4-4123	08 06 22.8	-41 22 33	20158	5	N
0141751001	RXJ0420.0-5022	04 20 02.4	-50 22 50	21156	5	N
0141751101	RXJ0420.0-5022	04 20 02.4	-50 22 50	22030	5	N
0141751201	RXJ0420.0-5022	04 20 02.4	-50 22 50	21666	5	N
0141960201	HH 355F	04 22 04.5	+19 14 37	22288	4	Y
0141980101	M33_10	01 33 07.0	+30 45 02	9739	2	Y
0141980201	M33_9	01 34 04.0	+30 57 25	15767	2	Y
0141980301	M33_6	01 34 08.0	+30 46 06	12000	2	Y
0141980401	M33_3	01 33 32.0	+30 52 13	5396	2	Y
0141980501	M33_1	01 33 51.0	+30 39 37	7860	2	Y
0141980601	M33_4	01 32 51.0	+30 36 49	13380	2	Y
0141980701	M33_12	01 33 38.0	+30 21 49	5700	2	Y
0141980801	M33_1	01 33 51.0	+30 39 37	10137	2	Y
0142330201	X1850-087	18 53 04.9	-08 42 20	11576	6	Y
0142330501	X1850-087	18 53 04.9	-08 42 20	8557	6	Y
0142610101	S2F1a	03 06 41.0	+00 01 12	48910	1	Y
0142630301	3 Sco	15 54 39.5	-25 14 38	18731	4	Y
0142660401	RXJ0059.1-7505	00 59 10.7	-75 05 23	16953	6	Y
0142660801	RXJ0059.4-7118	00 59 26.4	-71 18 48	8500	6	Y
0142660901	RXJ0535.5-7026	05 35 34.8	-70 26 08	7306	6	Y
0142661001	RXJ0050.5-7455	00 50 35.1	-74 55 44	14113	6	Y
0142770101	NGC 5204 X-1	13 29 38.6	+58 25 06	18664	2	Y
0142770301	NGC 5204 X-1	13 29 38.6	+58 25 06	7881	2	Y
0142970101	DW UMa	10 33 52.9	+58 46 55	18009	6	Y
0143150101	PG 1634+716	16 34 28.9	+70 31 33	15356	1	Y

0143150201	PG 1247+267	12 50 05.6	+26 31 10	24699	1	Y
0143150301	SBS 0909+532	09 13 01.6	+52 59 29	7061	1	Y
0143150601	SBS 0909+532	09 13 01.6	+52 59 29	17207	1	Y
0143200101	HD17638	02 52 11.7	+56 56 07	2500	4	Y
0143200301	HD119078	13 43 16.4	-67 24 05	12570	4	Y
0143210801	cl1216-12	12 16 45.0	-12 01 17	25925	3	N
0143230801	NEP 2300	17 41 14.4	+65 07 43	3500	3	N
0143370101	Mu Lep	05 12 55.9	-16 12 20	44300	4	Y
0143380101	G328.4+0.2	15 55 27.0	-53 19 10	47911	5	N
0143400101	PSR B1338-62	13 41 42.6	-62 20 21	5504	5	N
0143400201	PSR B1338-62	13 41 42.6	-62 20 21	6670	5	N
0143430101	HS Cam	07 19 14.5	+65 57 45	15084	6	Y
0143500101	NGC 4151	12 10 32.6	+39 24 20	18111	1	Y
0143500201	NGC 4151	12 10 32.6	+39 24 20	17456	1	Y
0143500301	NGC 4151	12 10 32.6	+39 24 20	17810	1	Y
0143630701	HD 81809	09 27 47.0	-06 04 16	6974	4	Y
0143650101	AXJ1531.9+2420	15 31 56.5	+24 20 22	6957	7	Y
0143650701	AXJ1532.3+2401	15 32 19.1	+24 01 13	5100	7	Y
0143650801	AXJ1534.0+3346	13 54 01.0	+33 46 27	9555	7	Y
0143650901	AXJ1115.4+5308	11 15 24.1	+53 08 07	7169	7	Y
0143651101	AXJ1617.0+3506	16 17 05.9	+35 06 38	1593	7	Y
0143651701	AXJ1512.0+5708	15 12 04.4	+57 08 05	3379	7	Y
0143652301	AXJ1425.2+2303	14 25 14.0	+23 03 19	1800	7	Y
0143653901	AXJ0836.3+5538	08 36 13.9	+55 38 48	9466	7	Y
0144080101	G345.7-0.2	17 07 22.0	-40 52 60	16965	5	N
0144220101	G0.9+0.1	17 47 22.8	-28 09 15	44929	5	N
0144230101	Markarian 6	06 52 12.3	+74 25 37	23302	1	Y
0144271401	HD 163296	17 56 21.3	-21 57 22	6954	4	Y
0144310101	Abell 133	01 02 41.1	-21 52 47	21546	3	N
0144490101	V4641 Sgr	18 19 21.6	-25 24 26	35024	6	Y
0144570101	Tau Boo	13 47 15.7	+17 27 25	53223	4	Y
0144630101	1E1740.7-2942	17 43 54.9	-29 44 43	4770	6	Y
0144840101	HT Cam	07 57 01.4	+63 06 02	26370	6	Y
0144920101	GRB001025	08 36 36.5	-13 04 30	9244	6	Y
0144920201	GRB001025	08 36 36.5	-13 04 30	18863	6	Y
0145020101	A 1991	14 54 32.0	+18 38 32	34498	3	N
0145020201	A 2717	00 03 12.9	-35 56 12	52851	3	N
0145050101	V1223 Sgr	18 55 02.2	-31 09 48	37849	6	Y
0145190101	NGC5907	15 15 53.6	+56 19 44	22156	7	Y
0145190201	NGC5907	15 15 53.6	+56 19 44	33348	7	Y
0145240101	3C303.1	14 43 14.4	+77 07 27	31676	1	Y
0145450101	SDSS1553+5516	15 53 31.1	+55 16 15	5700	6	Y
0145450201	SDSS015543+0028	01 55 43.4	+00 28 07	5249	6	Y
0145450301	SDSS1700+4003	17 00 53.3	+40 03 58	3054	6	Y
0145450401	SDSS0752+3628	07 52 40.5	+36 28 23	7165	6	Y
0145450501	SDSS0729+3658	07 29 10.7	+36 58 38	5956	6	Y
0145450601	SDSS1553+5516	15 53 31.1	+55 16 15	7478	6	Y
0145480101	Abell 1882	14 14 48.0	-00 24 00	21743	3	N
0145540101	IRASF01063-8034	01 07 01.7	-80 18 28	27562	1	Y
0145670101	NGC 2110	05 52 11.4	-07 27 23	30968	1	Y
0145750101	Q1120+0195	11 23 20.7	+01 37 47	27518	1	Y
0145800101	LBQS 1228+1116	12 30 54.1	+11 00 11	44096	1	Y
0145840101	G10_T1	18 07 60.0	-19 53 45	27906	7	Y
0145840201	G10_T2	18 10 30.0	-21 15 33	24971	7	Y
0145841101	G10_T2	18 10 30.0	-21 15 33	1657	7	Y
0146310201	HR 6000	16 08 34.6	-39 05 34	19273	4	Y
0146340501	PKS 1814-637	18 19 35.0	-63 45 48	2122	1	Y
0146340601	PKS 1814-637	18 19 35.0	-63 45 48	8100	1	Y
0146390101	TY CrA	19 01 40.8	-36 52 34	20800	4	Y
0146390201	TY CrA	19 01 40.8	-36 52 34	22584	4	Y
0146420101	NGC6388	17 36 20.4	-44 44 40	29834	6	Y
0146500101	UW CrB	16 05 46.1	+25 51 45	6900	6	Y
0146500201	UW CrB	16 05 46.1	+25 51 45	7900	6	Y
0146510301	NGC3411 Group	10 50 26.1	-12 50 42	22727	2	Y
0146510401	IC1860 Group	02 49 33.7	-31 11 21	34860	2	Y
0146990101	IRAS 10190+1322	10 21 41.9	+13 07 00	19662	1	Y
0146990201	IRAS 10494+4424	10 52 22.2	+44 08 59	11234	1	Y

0146990901	IRAS 10494+4424	10 52 22.2	+44 08 59	8575	1	Y
0147110101	B28	02 22 00.6	-02 49 60	11666	7	Y
0147110201	B29	02 20 40.7	-02 49 60	10664	7	Y
0147111301	B30	02 21 21.6	-05 10 00	12630	7	Y
0147111401	B31	02 20 42.0	-05 30 00	11300	7	Y
0147111501	B32	02 22 01.6	-05 30 00	3700	7	Y
0147131101	AG Draconis	16 01 40.9	+66 48 09	11393	6	Y
0147190101	Ark 120	05 16 11.5	-00 09 01	78689	1	Y
0147330201	Abell 1835	14 01 02.2	+02 52 40	36921	3	N
0147390701	AM CVn	12 34 54.6	+37 37 43	12146	6	Y
0147420201	NGC 6240	16 52 58.9	+02 24 03	8726	1	Y
0147420401	NGC 6240	16 52 58.9	+02 24 03	10161	1	Y
0147420501	NGC 6240	16 52 58.9	+02 24 03	3137	1	Y
0147420601	NGC 6240	16 52 58.9	+02 24 03	2359	1	Y
0147440101	IC 4329A	13 49 19.4	-30 18 35	91252	1	Y
0147450301	J1047+743	10 47 58.0	+74 19 30	15064	3	N
0147510101	Lockman Hole	10 51 03.4	+57 27 50	80785	7	Y
0147510801	Lockman Hole	10 51 27.7	+57 28 07	64099	7	Y
0147510901	Lockman Hole	10 52 43.0	+57 28 48	68165	7	Y
0147511001	Lockman Hole	10 52 08.1	+57 28 29	78904	7	Y
0147511101	Lockman Hole	10 53 17.9	+57 29 07	61124	7	Y
0147511201	Lockman Hole	10 53 58.3	+57 29 29	43048	7	Y
0147511301	Lockman Hole	10 54 29.5	+57 29 46	50496	7	Y
0147511601	Lockman Hole	10 52 43.0	+57 28 48	106957	7	Y
0147511701	Lockman Hole	10 52 40.6	+57 28 29	96929	7	Y
0147511801	Lockman Hole	10 52 45.3	+57 29 07	85304	7	Y
0147540101	3C 292	13 50 41.9	+64 29 35	21630	3	N
0147570101	IRAS P00182-7112	00 20 34.7	-70 55 27	6554	1	Y
0147570601	IRAS F14218+3845	14 23 55.0	+38 32 14	13100	1	Y
0147580101	1AXGJ133937+2730	13 39 37.3	+27 30 27	6000	1	Y
0147580201	1AXGJ160118+0844	16 01 18.8	+08 44 31	4600	1	Y
0147580301	1AXGJ233200+1945	23 32 00.5	+19 45 13	11314	1	Y
0147580401	1AXGJ234725+0053	23 47 25.2	+00 53 58	15116	1	Y
0147580501	1AXGJ133937+2730	13 39 37.3	+27 30 27	6567	1	Y
0147610101	NGC 4254	12 18 49.6	+14 24 59	18274	2	Y
0147630101	ABELL 1068	10 40 44.6	+39 57 12	21742	3	N
0147670201	PKS B1334-127	13 37 39.8	-12 57 25	13664	1	Y
0147670301	3C 207	08 40 47.6	+13 12 23	12473	1	Y
0147671001	IRAS 09104+4109	09 13 45.5	+40 56 28	12770	1	Y
0147760101	SN2001ci	10 01 60.0	+55 42 00	31700	5	N
0147860101	1E1048.1-5937	10 50 06.0	-59 53 17	48710	6	Y
0147890101	RXCJ2228+2037	22 28 33.3	+20 37 12	24968	3	N
0147920101	MRK 1152	01 13 50.1	-14 50 45	23028	1	Y
0147920301	NGC 2992	09 45 42.0	-14 19 35	22320	1	Y
0147920601	NGC 7172	22 02 01.9	-31 52 08	13637	1	Y
0147920701	H1846-786	18 47 01.7	-78 31 59	3494	1	Y
0148000201	1H 0419-577	04 26 00.8	-57 12 00	13550	1	Y
0148000301	1H 0419-577	04 26 00.8	-57 12 00	4400	1	Y
0148000401	1H 0419-577	04 26 00.8	-57 12 00	13455	1	Y
0148000501	1H 0419-577	04 26 00.8	-57 12 00	11500	1	Y
0148000601	1H 0419-577	04 26 00.8	-57 12 00	13505	1	Y
0148010301	1H 0707-495	07 08 40.9	-49 33 06	76295	1	Y
0148060201	BPS CS 22892-052	22 17 01.5	-16 39 26	3797	4	Y
0148060401	BPS CS 31082-001	01 29 31.2	-16 00 48	7861	4	Y
0148090101	V4643 Sgr	17 54 40.4	-26 14 15	6946	6	Y
0148090501	V4643 Sgr	17 54 40.4	-26 14 15	7764	6	Y
0148200101	HD209458	22 03 10.8	+18 53 03	5395	4	Y
0148210101	SGR 1806–20	18 08 39.3	-20 24 39	7289	5	N
0148210401	SGR 1806–20	18 08 39.3	-20 24 39	12630	5	N
0148250101	RXJ1416.4+2315	14 16 26.9	+23 15 32	1201	2	Y
0148250201	RXJ1416.4+2315	14 16 26.9	+23 15 32	8105	2	Y
0148300101	sigma Orionis 55	05 37 32.0	-02 33 41	30374	4	Y
0148310101	Abell 2626	23 36 30.5	+21 08 45	40735	3	N
0148440101	BL Hyi	01 41 00.2	-67 53 28	29258	6	Y
0148450101	NGC 3201	10 17 36.8	-46 24 40	28904	6	Y
0148450701	NGC 3201	10 17 36.8	-46 24 40	10800	6	Y
0148500101	TX Cam	05 00 50.4	+56 10 53	12908	4	Y

0148500201	Mira	02 19 20.8	-02 58 40	11959	4	Y
0148500501	T Cas	00 23 14.3	+55 47 33	9264	4	Y
0148520101	Daddi field	14 49 28.0	+09 00 00	23270	1	Y
0148520301	Daddi field	14 49 28.0	+09 00 00	31051	1	Y
0148560501	SDSS 1030+0524	10 30 27.1	+05 24 55	66679	1	Y
0148580101	RR242	13 21 13.0	-43 42 16	14711	2	Y
0148580201	rr143	06 48 37.0	-64 16 24	10365	2	Y
0148590201	BY Cam	05 42 48.9	+60 51 32	1498	6	Y
0148590301	BY Cam	05 42 48.9	+60 51 32	7707	6	Y
0148590401	BY Cam	05 42 48.9	+60 51 32	3300	6	Y
0148590501	BY Cam	05 42 48.9	+60 51 32	3199	6	Y
0148590701	BY Cam	05 42 48.9	+60 51 32	3084	6	Y
0148590801	BY Cam	05 42 48.9	+60 51 32	9300	6	Y
0148590901	BY Cam	05 42 48.9	+60 51 32	8205	6	Y
0148620101	ClJ1415.1+3612	14 15 11.2	+36 12 00	20248	3	N
0148650101	NGC 1705	04 54 13.7	-53 21 41	43825	2	Y
0148680101	beta Comae	13 11 52.2	+27 52 44	47553	4	Y
0148690101	1RXS J170849.0-4009	17 08 49.0	-40 09 10	36799	5	N
0148740101	0854+0915	08 57 24.0	+09 03 49	5933	1	Y
0148740301	1202+3538	12 05 04.4	+35 22 08	4908	1	Y
0148740401	1824+6507	18 24 46.7	+65 09 25	1800	1	Y
0148740801	1422+4224	14 24 36.0	+42 10 31	5759	1	Y
0148742101	0810+5157	08 14 22.1	+51 48 39	7059	1	Y
0148742401	1202+3538	12 05 04.4	+35 22 08	7800	1	Y
0148742501	0848+1119	08 50 45.7	+11 08 40	7800	1	Y
0148742601	1422+4224	14 24 36.0	+42 10 31	7614	1	Y
0148790101	CC Eri	02 34 22.6	-43 47 47	31286	4	Y
0148880101	Gl355	09 32 25.6	-11 11 05	28922	4	Y
0148880301	Gl355	09 32 25.6	-11 11 05	15565	4	Y
0148960101	ELAIS-S1-A	00 35 50.0	-43 19 00	46560	7	Y
0148961201	ELAIS-S1-C	00 33 50.0	-43 19 00	18493	7	Y
0148961301	ELAIS-S1-C	00 33 50.0	-43 19 00	38270	7	Y
0148961401	ELAIS-S1-C	00 33 50.0	-43 19 00	5564	7	Y
0148990101	Abell 2667	23 51 39.1	-26 05 04	26914	3	N
0149010201	CNOC2 0920+37 (SPRI	09 20 38.0	+37 11 17	54719	2	Y
0149040201	RZ Cassiopeiae	02 48 55.5	+69 38 03	84930	4	Y
0149160101	NGC 2613	08 33 22.6	-22 58 19	4100	2	Y
0149160201	NGC 2613	08 33 22.6	-22 58 19	24919	2	Y
0149170101	2MASSI234449+1221	23 44 49.6	+12 21 43	6146	1	Y
0149170501	2MASSI091848+2117	09 18 48.6	+21 17 17	10114	1	Y
0149170601	2MASSI105144+3539	10 51 44.2	+35 39 31	5100	1	Y
0149170701	2MASSI130005+1632	13 00 05.4	+16 32 15	3100	1	Y
0149170801	2MASSI140251+2631	14 02 51.2	+26 31 18	2197	1	Y
0149180901	4U 1745-203	17 48 53.4	-20 22 02	1634	6	Y
0149410401	BR 2237-0607	22 39 53.6	-05 52 20	23705	1	Y
0149420101	ESO03060170	05 40 06.2	-40 55 11	17838	3	N
0149500601	PMN-525-3343	05 25 06.2	-33 43 06	11453	1	Y
0149500701	PMN-525-3343	05 25 06.2	-33 43 06	11649	1	Y
0149500801	PMN-525-3343	05 25 06.2	-33 43 06	9914	1	Y
0149500901	PMN-525-3343	05 25 06.2	-33 43 06	9553	1	Y
0149501001	PMN-525-3343	05 25 06.2	-33 43 06	7670	1	Y
0149501201	PMN-525-3343	05 25 06.2	-33 43 06	7670	1	Y
0149550401	SAX J2103.5+4545	21 03 33.0	+45 45 00	9398	6	Y
0149610101	Herbig Haro 80/81	18 19 11.0	-20 49 43	3664	4	Y
0149610301	Herbig Haro 168	22 56 03.6	+62 01 59	37662	4	Y
0149610401	Herbig Haro 80/81	18 19 11.0	-20 49 43	32354	4	Y
0149620201	SN 1995N	14 49 28.3	-10 10 15	24786	5	N
0149630301	LMC1 Field3	05 01 26.8	-65 31 33	18600	5	N
0149670101	Abell 3827	22 01 56.0	-59 56 57	22316	3	N
0149670301	Abell 3911	22 46 17.0	-52 43 35	26567	3	N
0149750301	23545+6508	23 57 05.2	+65 25 11	12882	4	Y
0149780101	NGC 752	01 57 38.0	+37 48 00	41317	4	Y
0149880101	A2034	15 10 11.7	+33 30 30	11275	3	N
0149890301	HH 212	05 43 51.8	-01 02 55	18985	4	Y
0149900201	Abell 1314	11 34 45.7	+49 05 06	18159	3	N
0150010601	NGC 4143	12 09 36.1	+42 32 03	11958	1	Y
0150020101	Beta Cen	14 03 49.4	-60 22 23	46923	4	Y

0150050101	Galactic Halo	22 44 30.0	-72 42 00	32558	5	N
0150100101	WZ Sge	20 07 36.5	+17 42 15	4675	6	Y
0150180101	RBS 315	02 25 04.7	+18 46 48	21845	1	Y
0150190201	V393 Pav	19 57 11.5	-57 38 22	21807	6	Y
0150190301	VV Pup	08 15 06.8	-19 03 18	14600	6	Y
0150320201	IRAS10565+2448	10 59 17.4	+24 32 37	27952	2	Y
0150350101	NGC5775	14 53 57.6	+03 32 40	26206	2	Y
0150470601	NGC 985	02 34 37.8	-08 47 15	38200	1	Y
0150470701	UGC 11763	21 32 27.8	+10 08 20	32948	1	Y
0150480201	NGC1614	04 33 59.8	-08 34 44	23465	1	Y
0150480401	IC4395	14 17 21.1	+26 51 27	18932	1	Y
0150480501	NGC34	00 11 06.5	-12 06 26	16453	1	Y
0150600101	J2123-058	21 23 14.5	-05 47 53	29696	6	Y
0150610101	PG 1001+054	10 04 20.1	+05 13 01	11428	1	Y
0150610201	PG 2112+059	21 14 52.6	+06 07 42	11158	1	Y
0150610301	PG 1535+547	15 36 38.3	+54 33 33	22699	1	Y
0150620101	DLS09214+3013	09 21 22.0	+30 13 12	14919	3	N
0150620201	DLS09201+3029	09 20 08.0	+30 29 53	15385	3	N
0150620301	DLS09163+3025	09 16 16.0	+30 25 05	9338	3	N
0150650301	NGC 5204	13 29 37.0	+58 25 13	7260	6	Y
0150651101	NGC 2403	07 36 51.0	+65 36 10	4993	6	Y
0150651201	NGC 2403	07 36 51.0	+65 36 10	7469	6	Y
0150680101	RDCS1517+3127	15 17 55.5	+31 27 47	32248	3	N
0150800101	RXJ0806.3+1527	08 06 23.2	+15 27 30	25962	6	Y
0150820201	PSR B0154+61	01 57 50.0	+62 12 27	24739	5	N
0150870201	BRI0103+0032	01 06 19.2	+00 48 22	3092	1	Y
0150870301	PSS0248+1802	02 48 54.6	+18 02 50	5332	1	Y
0150870401	BRI1033-0327	10 36 23.7	-03 43 20	30716	1	Y
0150900101	Abell 1722	13 20 22.0	+69 58 43	9236	3	N
0150900501	Abell 1722	13 20 22.0	+69 58 43	7200	3	N
0150910101	NGC 1482	03 54 39.3	-20 30 09	14019	2	Y
0150940101	NGC 526A	01 23 54.4	-35 03 56	41174	1	Y
0150960201	G078.2+2.1	20 20 50.0	+40 25 60	1900	5	N
0150960301	G013.3-1.3	18 19 20.0	-18 00 00	5164	5	N
0150960801	G078.2+2.1	20 20 50.0	+40 25 60	7969	5	N
0150970101	PSR B0943+10	09 46 07.3	+09 51 57	9664	5	N
0150970301	PSR B0943+10	09 46 07.3	+09 51 57	23517	5	N
0151100201	Rabbit	14 18 39.8	-60 58 03	25108	5	N
0151160201	LS 5039	18 26 14.9	-14 50 51	10252	6	Y
0151160301	LS 5039	18 26 14.9	-14 50 51	7809	6	Y
0151230101	UN J1141-0143	11 41 11.6	-01 43 08	7868	1	Y
0151240201	4U 1700+24	17 06 34.5	+23 58 19	7700	6	Y
0151240301	4U 1700+24	17 06 34.5	+23 58 19	2208	6	Y
0151240401	4U 1700+24	17 06 34.5	+23 58 19	12092	6	Y
0151270401	Abell 3390	06 25 01.0	-37 20 45	8599	3	N
0151370101	NGC 1365-X1	03 33 34.5	-36 09 38	17657	6	Y
0151370701	NGC 1365-X1	03 33 34.5	-36 09 38	8098	6	Y
0151390101	4C 06.41	10 41 17.1	+06 10 16	47404	1	Y
0151400201	NRGb184	12 08 05.6	+25 14 13	14063	2	Y
0151450101	FK Aqr	22 38 45.6	-20 37 16	40722	4	Y
0151490101	NGC 1132	02 52 51.7	-01 16 30	24458	2	Y
0151530401	AG Dra	16 01 41.0	+66 48 10	23739	6	Y
0151560101	IC 310	03 16 43.0	+41 19 29	25399	2	Y
0151580101	M31-Halo1	00 33 36.0	+39 31 12	4100	2	Y
0151580201	M31-Halo2	00 43 12.0	+39 48 00	1298	2	Y
0151580401	M31-Halo4	00 46 07.0	+41 20 58	12877	2	Y
0151581101	M31-Halo1	00 33 36.0	+39 31 12	9650	2	Y
0151581201	M31-Halo2	00 43 12.0	+39 48 00	3869	2	Y
0151581301	M31-Halo3	00 45 59.0	+40 42 36	4927	2	Y
0151590101	pks1406-076	14 08 56.5	-07 52 35	11723	1	Y
0151590201	pks1406-076	14 08 56.5	-07 52 35	8702	1	Y
0151750101	4U 0513-40	05 14 06.4	-40 02 38	22858	6	Y
0151790701	1RXSJ130547.2+64125	13 05 47.2	+64 12 52	6673	5	N
0152000101	NGC7142	21 45 11.0	+65 46 22	5398	4	Y
0152130401	CIZAJ1410.5-4246	14 10 29.0	-42 46 49	9254	3	N
0152131201	CIZAJ1324.6-5736	13 24 47.0	-57 36 34	9450	3	N
0152150101	NGC1550	04 19 37.8	+02 24 36	22900	2	Y

0152170501	NGC4559 X1	12 35 52.0	+27 56 01	38684	6	Y
0152200101	Abell 2638	23 40 29.0	-11 42 21	53261	3	N
0152260101	IC 10 X-1 & Shell	00 20 29.0	+59 16 50	35758	5	N
0152280101	G85.4+0.7	20 50 40.2	+45 22 02	997	5	N
0152280201	G85.9-0.6	20 58 36.8	+44 52 60	6460	5	N
0152280501	G85.4+0.7	20 50 40.2	+45 22 02	6400	5	N
0152330101	SCG 0018-4854	00 21 23.3	-48 38 24	32245	2	Y
0152360101	NGC 5044	13 15 24.0	-16 45 36	38834	2	Y
0152420101	OGLE-1999-BUL-32	18 05 05.3	-28 34 43	46098	6	Y
0152460301	Chamaeleon I Field	11 00 06.0	-77 28 51	30158	4	Y
0152490201	HT Cas	01 10 13.2	+60 04 36	15211	6	Y
0152530101	YZ Cnc	08 10 56.7	+28 08 33	27415	6	Y
0152580101	NGC 3216	10 21 41.2	+23 55 23	5823	1	Y
0152620101	4U 1626-67	16 32 16.6	-67 27 43	65429	6	Y
0152630101	SXRB_1	16 18 32.8	-33 27 57	9803	5	N
0152630201	SXRB_2	15 58 54.8	-29 10 21	11169	5	N
0152630301	SXRB_3	15 40 53.0	-24 42 52	7458	5	N
0152660101	PG 1448+273	14 51 08.8	+27 09 27	21019	1	Y
0152670101	PKS 2152-69	21 57 05.9	-69 41 24	27600	1	Y
0152680201	AA Tau	04 34 55.5	+24 28 54	15760	4	Y
0152680301	AA Tau	04 34 55.5	+24 28 54	15265	4	Y
0152680401	AA Tau	04 34 55.5	+24 28 54	15240	4	Y
0152680501	AA Tau	04 34 55.5	+24 28 54	12083	4	Y
0152680601	AA Tau	04 34 55.5	+24 28 54	16960	4	Y
0152680701	AA Tau	04 34 55.5	+24 28 54	17160	4	Y
0152680801	AA Tau	04 34 55.5	+24 28 54	14084	4	Y
0152680901	AA Tau	04 34 55.5	+24 28 54	14645	4	Y
0152750101	Barnard 68	17 22 43.0	-23 48 06	42053	5	N
0152780201	4U 1538-522	15 42 23.3	-52 23 10	61575	6	Y
0152832801	NXGPS_28	18 07 22.7	-19 51 30	9318	7	Y
0152832901	NXGPS_29	18 09 31.6	-20 08 19	8667	7	Y
0152833001	NXGPS_30	18 08 47.7	-19 51 10	7965	7	Y
0152833101	NXGPS_31	18 08 04.0	-19 34 01	8560	7	Y
0152833201	NXGPS_32	18 10 12.8	-19 50 48	8516	7	Y
0152833401	NXGPS_34	18 08 45.2	-19 16 32	8659	7	Y
0152833501	NXGPS_35	18 10 53.8	-19 33 17	3312	7	Y
0152833701	NXGPS_37	18 12 12.1	-18 23 35	8661	7	Y
0152834301	NXGPS_43	18 12 55.9	-18 40 41	1795	7	Y
0152834401	NXGPS_44	18 16 48.3	-15 45 59	9543	7	Y
0152834501	NXGPS_45	18 18 55.2	-16 02 24	9442	7	Y
0152834601	NXGPS_46	18 18 11.4	-15 45 24	7470	7	Y
0152834801	NXGPS_48	18 19 34.5	-15 44 47	7763	7	Y
0152834901	NXGPS_49	18 18 50.8	-15 27 47	8270	7	Y
0152835001	NXGPS_50	18 17 32.0	-16 03 00	8157	7	Y
0152835101	NXGPS_38	18 10 50.8	-18 58 39	5268	7	Y
0152835401	NXGPS_41	18 11 31.5	-18 41 08	3248	7	Y
0152835501	NXGPS_40	18 12 15.3	-18 58 13	4392	7	Y
0152835701	NXGPS_39	18 10 07.1	-18 41 32	10184	7	Y
0152840101	3C120	04 33 11.1	+05 21 16	99023	1	Y
0152900201	1RXJ044127.8+15045	04 41 27.4	+15 04 55	6276	1	Y
0152940101	NGC 5252	13 38 15.9	+04 32 33	42651	1	Y
0153090101	HU Aqr	21 07 58.3	-05 17 39	14398	6	Y
0153090201	HU Aqr	21 07 58.3	-05 17 39	11271	6	Y
0153100101	IRAS 04505-2958	04 52 30.1	-29 53 35	13957	1	Y
0153100601	IRAS 06269-0543	06 29 24.9	-05 45 23	8387	1	Y
0153150101	HH24-26	05 46 08.5	-00 10 03	33419	4	Y
0153170101	MS 0116.3-0115	01 18 53.6	-01 00 07	14760	2	Y
0153190101	X1658-298	17 02 06.3	-29 56 45	59567	6	Y
0153210101	3C 249.1	11 04 13.8	+76 58 58	14896	1	Y
0153220101	RX J2241.8-4405	22 41 55.3	-44 04 55	8169	1	Y
0153220301	RX J1225.7+2055	12 25 41.9	+20 55 04	5129	1	Y
0153220401	PG 1543+489	15 45 30.2	+48 46 09	10460	1	Y
0153220601	PG 2233+134	22 36 07.7	+13 43 55	8570	1	Y
0153250101	CAL87	05 46 45.0	-71 08 54	55416	6	Y
0153290101	RXJ1028.6-0844	10 28 38.7	-08 44 39	19155	1	Y
0153350101	RX Pup	08 14 12.3	-41 42 29	13408	6	Y
0153450101	NGC4697	12 48 35.8	-05 48 00	50708	2	Y

0153950101	BPM16274	00 50 03.2	-52 08 17	4572	2	Y
0154150401	G 191-B2B	05 05 30.6	+52 49 52	5870	4	Y
0154150501	NGC 6712	18 53 04.3	-08 42 21	23767	4	Y
0154350201	SN2002ap	01 36 23.9	+15 45 13	24647	5	N
0154550101	GK Per	03 31 11.8	+43 54 17	7552	6	Y
0154750401	IGR J16318-4848	16 31 52.0	-48 48 30	24409	6	Y
0154750601	IGR J17544-2619	17 54 26.0	-26 19 42	2183	6	Y
0155150101	AB Dor	05 28 44.8	-65 26 55	6079	4	Y
0155560401	G93-48	21 52 25.4	+02 23 20	5662	4	Y
0155560501	BD+28 4211	21 51 11.0	+28 51 50	3663	4	Y
0155560801	Feige 110	23 19 58.4	-05 09 56	262	4	Y
0155561101	T Tau	04 21 59.4	+19 32 06	1200	4	Y
0155960601	HD154791	17 06 34.5	+23 58 19	6400	5	N
0156160101	GS 1826-238	18 29 28.3	-23 47 49	6017	6	Y
0156360101	rxj1205	12 05 52.6	+44 29 10	26760	3	N
0156960201	RXj 0720.4-3125	07 20 25.1	-31 25 49	22691	4	Y
0156960401	RXj 0720.4-3125	07 20 25.1	-31 25 49	31336	4	Y
0157160501	Zeta Puppis	08 03 35.0	-40 00 11	36438	4	Y
0157160901	Zeta Puppis	08 03 35.0	-40 00 11	43042	4	Y
0157161101	Zeta Puppis	08 03 35.0	-40 00 11	12100	4	Y
0157360101	RBS1223	13 08 48.6	+21 27 09	28555	4	Y
0157360401	RXSJ160518.8+32	16 05 18.8	+32 49 07	28488	4	Y
0157360601	RXSJ160518.8+32	16 05 18.8	+32 49 07	9398	4	Y
0157560101	NGC 4051	12 03 09.6	+44 31 53	46919	1	Y
0157960101	XTE J1807-294	18 07 00.0	-29 24 30	16318	6	Y
0157960201	XTE J0055-727	00 55 22.0	-72 42 00	18568	6	Y
0158160201	GRB031203	08 02 30.0	-39 50 48	57728	6	Y
0158160401	GRB040106	11 52 18.0	-46 47 14	38200	6	Y
0158160601	GRB040223	16 39 34.0	-41 55 45	26182	6	Y
0158360201	RXj 0720.4-3125	07 20 25.1	-31 25 49	29387	5	N
0158560301	MS1229.2+6430	12 31 32.0	+64 14 21	19916	1	Y
0158761201	Jupiter	08 46 47.2	+18 48 59	3900	4	Y
0158960101	PKS2155-304	21 58 52.1	-30 13 32	25407	1	Y
0158960901	PKS2155-304	21 58 52.1	-30 13 32	26864	1	Y
0158961001	PKS2155-304	21 58 52.1	-30 13 32	26203	1	Y
0158970701	Mkn421	11 04 27.3	+38 12 32	32649	1	Y
0159360101	zeta Puppis	08 03 35.0	-40 00 11	35447	4	Y
0159360301	zeta Puppis	08 03 35.0	-40 00 11	24700	4	Y
0159360401	zeta Puppis	08 03 40.4	-40 00 36	32489	4	Y
0159960101	3C273	12 29 06.7	+02 03 09	56874	1	Y
0160362501	AB Dor	05 28 44.8	-65 26 55	995	4	Y
0160362601	AB Dor	05 28 44.8	-65 26 55	1698	4	Y
0160362701	AB Dor	05 28 44.8	-65 26 55	11753	4	Y
0160760101	EXO 0748-676	07 48 33.8	-67 45 07	81814	6	Y
0160760201	EXO 0748-676	07 48 33.8	-67 45 07	79293	6	Y
0160760301	EXO 0748-676	07 48 33.8	-67 45 07	74138	6	Y
0160760401	EXO 0748-676	07 48 33.8	-67 45 07	67815	6	Y
0160760601	EXO 0748-676	07 48 33.8	-67 45 07	47412	6	Y
0160760801	EXO 0748-676	07 48 33.8	-67 45 07	51508	6	Y
0160761301	EXO 0748-676	07 48 33.8	-67 45 07	78829	6	Y
0161160101	1H 0414+009	04 16 52.4	+01 05 24	48388	1	Y
0161360301	XTE J1809-197	18 09 51.1	-19 43 51	7642	6	Y
0161360401	XTE J1809-197	18 09 51.1	-19 43 51	800	6	Y
0161360501	XTE J1810-197	18 09 51.2	-19 43 51	9900	6	Y
0162160101	SEP-r725	06 00 00.0	-66 33 38	13048	5	N
0162160201	HDF-r725	12 36 52.0	+62 13 15	14607	5	N
0162160301	SEP-r731	06 00 00.0	-66 33 38	10669	5	N
0162160401	HDF-r731	12 36 52.0	+62 13 15	10558	5	N
0162160501	SEP-r735	06 00 00.0	-66 33 38	10163	5	N
0162160601	HDF-r735	12 36 52.0	+62 13 15	10617	5	N
0163360201	zeta Puppis	08 03 14.2	-39 56 24	42145	4	Y
0163560101	RBS1223	13 08 48.6	+21 27 09	29868	6	Y
0164160201	HZ 15	04 40 39.0	+08 40 46	9400	4	Y
0164560201	IRAS 05436-0007	05 46 13.1	-00 06 05	33210	6	Y
0164560501	RXJ 0720.4-3125	07 20 25.1	-31 25 49	24960	6	Y
0164560701	CXOUJ140332.3+54210	14 03 32.3	+54 21 03	26562	6	Y
0164560801	SN 2004dk	16 21 48.9	-02 16 17	10600	6	Y

0164570401	GRB040827	15 16 57.7	-16 09 29	43188	6	Y
0165770101	H1426+428	14 28 32.7	+42 40 21	59083	1	Y
0165770201	H1426+428	14 28 32.7	+42 40 21	57265	1	Y
0200240401	NGC 3242	10 24 46.1	-18 38 33	18995	4	Y
0200730201	PSS 1326+0743	13 26 11.9	+07 43 58	31463	1	Y
0201200201	SAO 49725	20 30 30.8	+47 51 51	8476	6	Y
0201230101	3C436	21 44 11.7	+28 10 19	29077	1	Y
0201900101	RXCJ0003.8+0203	00 03 50.6	+02 03 48	26380	3	N
0201900301	RXCJ0020.7-2542	00 20 42.8	-25 42 37	27001	3	N
0201900701	RXCJ0225.1-2928	02 25 10.5	-29 28 26	6350	3	N
0201900801	RXCJ0345.7-4112	03 45 45.7	-41 12 27	25281	3	N
0201900901	RXCJ0547.6-3152	05 47 38.2	-31 52 31	24100	3	N
0201901101	RXCJ0616.8-4748	06 16 53.6	-47 48 18	13098	3	N
0201901201	RXCJ0645.4-5413	06 45 29.3	-54 13 08	14409	3	N
0201901601	RXCJ1141.4-1216	11 41 24.3	-12 16 20	28800	3	N
0201901701	RXCJ1236.7-3354	12 36 44.7	-33 54 10	11900	3	N
0201901801	RXCJ1302.8-0230	13 02 50.7	-02 30 22	25498	3	N
0201901901	RXCJ1350.7-3343	13 50 43.9	-33 43 17	24398	3	N
0201902001	RXCJ1516.3+0005	15 16 19.2	+00 05 52	27368	3	N
0201902101	RXCJ1516.5-0056	15 16 34.0	-00 56 56	29962	3	N
0201902401	RXCJ2048.1-1750	20 48 10.6	-17 50 38	26095	3	N
0201903301	RXCJ2319.6-7313	23 19 41.8	-73 13 51	10662	3	N
0201903401	RXCJ0645.4-5413	06 45 29.3	-54 13 08	16662	3	N
0201903501	RXCJ0958.3-1103	09 58 22.2	-11 03 35	11432	3	N
0202140301	PSS J2322+1944	23 22 07.2	+19 44 23	34506	1	Y
0202190201	NGC 57	00 15 30.9	+17 19 43	23271	3	N
0202520501	B2352+495	23 55 09.5	+49 50 08	17149	1	Y
0203060101	HD 220140	23 19 26.9	+79 00 13	27459	4	Y
0203130201	LHB-3	23 09 27.8	+61 38 47	22469	5	N
0203160401	WGAJ0110.5-1647	01 10 35.5	-16 48 29	5485	1	Y
0203360701	COSMOS FIELD 7	10 01 26.4	+02 27 36	34194	1	Y
0203361201	COSMOS FIELD 12	10 00 26.4	+02 27 36	26958	1	Y
0203361301	COSMOS FIELD 13	10 00 26.4	+02 12 36	26570	1	Y
0203361401	COSMOS FIELD 14	10 00 26.4	+01 57 36	31588	1	Y
0203361801	COSMOS FIELD 18	09 59 26.4	+02 12 36	27766	1	Y
0204710101	S689	12 10 42.5	-46 44 30	3897	3	N
0204790401	NGC 205	00 40 22.3	+41 41 09	15871	2	Y
0205680101	Q0056-363	00 58 37.2	-36 06 08	96914	3	N
0205770101	Z CHA	08 07 28.6	-76 32 02	100154	6	Y
0207060201	MZ 5383	12 34 53.0	-03 35 54	17803	3	N

Table A.1: Observation log for XCS. The value t_{exp} is the duration of the exposure (not to be mistaken with the 'livetime' obtained after background flares and are removed and other instrumental factors are accounted for). The description of the seven pointing types is given in Table 4.1. Also included is a binary flag (Y/N) representing whether an observation was deemed suitable for the XCS Statistical Sample.

Appendix B

XCS Statistical Sample Known Clusters

Id	Literature Name	Obsid	RA(J2000)	Dec(J2000)	θ	Scts	t_{max}	Flux	σ_F	Sig	FN_P	Flags	z
XMMXCS J004252.7+004302.6	SDSS CE J010.717058+00.725393	0090070201	00 42 52.8	+00 43 03	10.6	406.6	11375	4.75	0.25	120.31	0.26	0100	0.265
XMMXCS J004333.8+010107.8	SDSS CE J010.888028+01.015296	0090070201	00 43 33.8	+01 01 08	10.5	689.3	8796	10.59	0.42	227.84	0.28	0100	0.186
XMMXCS J004350.0+004720.3	SDSS CE J010.964841+00.774039	0090070201	00 43 50.0	+00 47 20	8.5	257.1	11176	3.11	0.21	118.87	0.16	0100	0.311
XMMXCS J004616.1+853116.7	ClG J0046+8530	0100640201	00 46 16.1	+85 31 17	11.1	1688.8	29361	8.25	0.21	NaN	0.28	0010	0.624
XMMXCS J005558.3-373301.2	RXCJ0056.0-3732	0112800101	00 55 58.3	-37 33 01	14.9	3654.4	13739	125.74	2.11	NaN	0.60	1110	0.162
XMMXCS J005655.6-221358.7	[VMF98]005	0110890701	00 56 55.7	-22 13 59	10.6	340.5	9456	10.37	0.59	130.59	0.29	1110	0.116
XMMXCS J005656.6-274032.0	J1888.16CL	0111282001	00 56 56.7	-27 40 32	4.6	399.7	5792	9.59	0.50	227.28	0.21	1110	0.560
XMMXCS J010607.9+005013.2	SDSS CE J016.528793+00.817471	0150870201	01 06 08.0	+00 50 13	3.4	549.2	2583	26.71	1.19	295.81	0.30	0100	0.277
XMMXCS J011942.5-441022.5	LCLG -45 044	0103860901	01 19 42.6	-44 10 23	7.2	666.8	13936	6.04	0.24	180.78	0.29	0110	0.123
XMMXCS J011952.1-441519.9	LCLG -45 045	0103860901	01 19 52.2	-44 15 20	9.1	419.8	13418	3.59	0.18	109.90	0.24	0110	0.118
XMMXCS J012358.7-350733.2	SCG 0121-3521	0150940101	01 23 58.8	-35 07 33	3.7	34.1	26688	0.15	0.03	9.91	0.02	0110	...
XMMXCS J012434.8+040054.8	[VMF98]011	0025541601	01 24 34.8	+04 00 55	13.4	135.2	4553	4.24	0.40	46.13	0.34	1110	0.316
XMMXCS J015415.3-593756.7	[VMF98]020	0109460201	01 54 15.3	-59 37 57	10.0	248.6	4067	9.00	0.61	81.15	0.23	1110	0.360
XMMXCS J020019.2+001929.5	SEXCLAS_3	0101640201	02 00 19.2	+00 19 30	8.4	141.5	4735	3.96	0.36	58.53	0.13	0001	0.510
XMMXCS J021734.5-051315.8	SEXCLAS_4	0112370701	02 17 34.5	-05 13 16	9.4	573.5	29623	2.45	0.11	178.49	0.23	0001	...
XMMXCS J021944.6-045317.7	SEXCLAS_7	0112370301	02 19 44.7	-04 53 18	7.0	454.4	31754	1.77	0.09	139.87	0.19	0001	...
XMMXCS J021945.3-044833.7	SEXCLAS_8	0112370301	02 19 45.4	-04 48 34	11.7	103.9	21674	0.59	0.06	22.37	0.16	0001	...
XMMXCS J022145.3-034617.7	XLSSC 006	0037982501	02 21 45.4	-03 46 18	7.3	1855.9	6958	35.82	0.85	NaN	0.29	0011	0.429
XMMXCS J022253.2-032832.6	XLSS J022253.5-032824	0037980701	02 22 53.3	-03 28 33	6.8	128.2	8412	2.17	0.21	30.66	0.12	0001	1.000
XMMXCS J022303.0-043620.6	XLSS J022303.0-043622	0109520601	02 23 03.0	-04 36 21	8.6	79.6	14249	0.66	0.08	25.03	0.08	0001	1.300
XMMXCS J022400.1-032515.0	XLSS J022400.5-032526	0037980801	02 24 00.2	-03 25 15	11.0	79.2	5362	2.09	0.26	22.44	0.11	0001	0.810
XMMXCS J022401.8-050527.9	XLSSC 018	0111110401	02 24 01.9	-05 05 28	4.6	490.5	24460	2.54	0.12	114.04	0.14	0011	0.322
XMMXCS J022404.2-041327.9	XLSS J022403.9-041328	0112680301	02 24 04.2	-04 13 28	9.6	405.7	12974	4.18	0.22	212.89	0.24	0001	1.050
XMMXCS J022406.1-035502.7	XLSSC 007	0037980201	02 24 06.1	-03 55 03	5.3	184.7	10871	2.32	0.18	33.16	0.11	0011	0.557
XMMXCS J022457.7-034852.6	XLSS J022457.1-034853	0037980301	02 24 57.8	-03 48 53	5.7	699.2	10008	9.43	0.37	476.18	0.25	0011	...
XMMXCS J022632.9-050016.9	XLSSC 020	0109520301	02 26 32.8	-05 00 17	13.2	236.9	8801	5.47	0.38	54.91	0.40	0011	0.494
XMMXCS J022634.7-040407.4	XLSSC 014	0112680101	02 26 34.8	-04 04 07	12.7	245.7	11558	2.59	0.18	78.40	0.40	0011	0.344
XMMXCS J022709.4-041806.4	XLSS J022709.7-041805	0112680101	02 27 09.4	-04 18 06	8.5	165.1	16390	1.19	0.10	69.28	0.13	0011	...
XMMXCS J022722.1-032145.3	XLSSC 010	0037981001	02 27 22.2	-03 21 45	8.3	378.1	9260	5.30	0.29	223.23	0.16	0011	0.329
XMMXCS J022726.8-043207.3	XLSSC 013	0112680401	02 27 26.9	-04 32 07	8.5	330.6	14809	2.78	0.16	124.38	0.16	0011	0.307
XMMXCS J022738.5-031800.7	XLSS J022738.2-031757	0037981501	02 27 38.6	-03 18 01	9.6	294.4	6374	6.73	0.42	119.15	0.16	0011	...
XMMXCS J022812.3-100537.5	WARPJ0228.1-1005	0112860101	02 28 12.4	-10 05 38	12.0	378.9	3222	19.60	1.06	167.59	0.46	1110	0.149
XMMXCS J022827.3-042536.3	XLSSC 012	0112680401	02 28 27.4	-04 25 36	8.1	541.6	12631	5.11	0.23	162.25	0.23	0011	0.433
XMMXCS J023605.1-522508.8	WARPJ0236.0-5224	0098810101	02 36 05.2	-52 25 09	6.0	898.7	18042	5.03	0.17	493.56	0.29	1110	...
XMMXCS J023759.8-522407.6	WARPJ0238.0-5224	0067190101	02 37 59.9	-52 24 08	12.9	2344.8	13111	45.43	0.96	NaN	0.57	1110	0.135
XMMXCS J030205.5-00000-2.4	SDSS CE J045.491806+00.008648	0041170101	03 02 05.6	-00 00 02	11.3	452.1	24911	2.55	0.13	237.24	0.26	0100	0.333
XMMXCS J030617.3-000837.7	ABELL 0412	0142610101	03 06 17.4	-00 08 38	11.5	2686.6	25797	14.21	0.28	689.98	0.28	0110	0.107
XMMXCS J030625.3+001306.1	SDSS CE J046.580116+00.232915	0142610101	03 06 25.4	+00 13 06	12.5	236.8	19429	1.42	0.10	29.46	0.40	0100	0.163
XMMXCS J031816.8-030205.2	RX J0318.2-0301	0056022201	03 18 16.8	-03 02 05	2.2	821.9	16797	7.44	0.27	488.73	0.30	0110	0.370
XMMXCS J031833.0-030258.1	RXJ0318.5-0302	0056022201	03 18 33.1	-03 02 58	2.4	4352.8	16865	34.89	0.54	NaN	0.30	1110	0.370
XMMXCS J033556.1+003215.3	SDSS CE J053.980568+00.534098	0134540601	03 35 56.2	+00 32 15	13.1	727.0	12263	7.23	0.28	199.80	0.57	0100	0.402

XMMXCS J033833.4-352654.0	NGC1399GROUP	0055140101	03 38 33.3	-35 26 54	12.5	40898.4	21827	307.65	1.53	NaN	0.57	1110	0.005
XMMXCS J034747.1+241901.6	ZwCl 0344.7+2409	0094780101	03 47 47.1	+24 19 02	7.5	807.7	21221	6.01	0.22	171.18	0.29	0100	...
XMMXCS J040646.7-711630.7	MS0407.2-7123	0111970301	04 06 46.7	-71 16 31	11.7	2306.0	7821	37.96	0.81	NaN	0.28	1110	0.229
XMMXCS J041704.8+011327.2	ZwCl 0414.3+0103	0161160101	04 17 04.8	+01 13 27	8.6	718.4	30318	127.26	4.93	328.15	0.23	0110	0.320
XMMXCS J043418.4-083003.7	[VMF98]037	0150480201	04 34 18.4	-08 30 04	6.6	346.9	15308	6.29	0.36	136.31	0.18	1110	0.240
XMMXCS J052110.9-253106.5	[VMF98]040	0085640101	05 21 10.9	-25 31 07	9.6	126.3	5416	2.99	0.29	59.98	0.13	1110	0.581
XMMXCS J052215.3-362514.2	[VMF98]041	0065760201	05 22 15.3	-36 25 14	8.9	1926.9	15731	14.17	0.33	NaN	0.23	1110	0.472
XMMXCS J062144.3-524130.9	MS0620.6-5239	0122901001	06 21 44.3	-52 41 31	16.0	102.3	205	79.23	8.64	55.57	0.53	1100	0.051
XMMXCS J081919.5+705508.4	[VMF98]049	0112520601	08 19 19.6	+70 55 08	12.8	205.9	3944	8.51	0.64	64.28	0.40	1110	0.226
XMMXCS J084834.5+445340.9	RDCSJ0848+4453	0085150101	08 48 34.6	+44 53 41	7.4	125.2	24769	0.62	0.06	27.19	0.12	1110	1.270
XMMXCS J084848.1+445606.6	RXJ0848.7+4457	0085150101	08 48 48.1	+44 56 07	7.1	902.8	26286	4.17	0.14	314.53	0.29	1110	0.574
XMMXCS J084859.0+445149.6	RXJ0848.9+4452	0085150101	08 48 59.0	+44 51 50	2.7	413.3	38374	1.32	0.07	158.93	0.18	1110	1.261
XMMXCS J091939.3+370753.4	NSC J091944+370751	0149010201	09 19 39.3	+37 07 53	12.2	1999.6	27500	9.62	0.22	NaN	0.57	0110	0.141
XMMXCS J092039.3+370610.3	NSC J092040+370507	0149010201	09 20 39.3	+37 06 10	5.1	65.5	45737	0.21	0.03	30.35	0.06	0110	0.208
XMMXCS J094632.7-140949.9	RX J0946.5-1410	0147920301	09 46 32.8	-14 09 50	15.7	84.4	5766	2.80	0.34	22.51	0.28	0110	0.230
XMMXCS J095341.4+014201.6	XBS J095341.1+014204	0070940401	09 53 41.4	+01 42 02	7.3	2905.3	8313	82.04	1.55	NaN	0.29	0010	0.100
XMMXCS J095418.1+685446.4	[B2002a] 16	0111800101	09 54 18.1	+68 54 46	11.3	785.8	40496	5.03	0.19	163.90	0.28	0100	...
XMMXCS J095603.5+410708.3	[VMF98]079	0111290201	09 56 03.6	+41 07 08	12.3	327.3	5451	19.28	1.13	185.71	0.46	1110	0.587
XMMXCS J100655.6+123911.0	[RPG97] 075	0140550601	10 06 55.6	+12 39 11	12.3	67.6	10563	0.72	0.10	31.44	0.15	0100	0.009
XMMXCS J101931.6+080345.2	ABELL 0973	0093640301	10 19 31.6	+08 03 45	12.1	515.5	7233	20.19	0.93	198.53	0.57	0110	0.172
XMMXCS J102246.0+194734.3	[M98j] 086	0101040301	10 22 46.1	+19 47 34	11.3	511.8	13825	3.86	0.18	76.62	0.28	0110	0.005
XMMXCS J102744.6+681118.6	ABELL1005	0026340301	10 27 44.6	+68 11 19	13.8	242.8	8381	5.59	0.38	121.79	0.40	1000	0.200
XMMXCS J103100.2+305138.7	NSC J103056+305225	0102040301	10 31 00.3	+30 51 39	11.3	1106.5	12195	12.65	0.39	363.98	0.28	0110	0.222
XMMXCS J105030.6-124141.8	LCDCS 0158	0146510301	10 50 30.6	-12 41 42	9.1	162.7	13073	1.30	0.11	42.38	0.13	0110	0.350
XMMXCS J105236.8+573053.8	SEXCLAS_12	0022740201	10 52 36.8	+57 30 54	2.3	259.6	78959	1.09	0.07	57.82	0.11	0001	0.610
XMMXCS J105250.8+574115.4	RX J105244.4+574045	0147511601	10 52 50.9	+57 41 15	12.5	2477.2	48755	10.96	0.22	628.20	0.57	0110	0.074
XMMXCS J105254.7+573217.7	SEXCLAS_13	0147511001	10 52 54.7	+57 32 18	7.3	276.9	98064	0.67	0.04	55.07	0.18	0001	0.580
XMMXCS J105258.6+572402.1	[dZP97] X034	0123700101	10 52 58.7	+57 24 02	5.2	171.1	26859	0.72	0.06	42.07	0.11	0110	0.340
XMMXCS J105318.5+572046.3	[VMF98]093	0147511801	10 53 18.5	+57 20 46	9.5	708.9	60449	2.05	0.08	243.90	0.23	1110	0.340
XMMXCS J105322.0+573522.6	RXJ1053.7+5735	0147511701	10 53 22.0	+57 35 23	8.9	148.7	64242	0.26	0.02	56.80	0.13	1110	1.140
XMMXCS J105343.6+573518.6	RXJ1053.7+5735	0147511601	10 53 43.6	+57 35 19	10.4	1883.3	62884	4.03	0.10	644.45	0.28	1110	1.140
XMMXCS J111726.1+074327.4	[VMF98]097	0082340101	11 17 26.1	+07 43 27	12.8	1176.2	19059	8.30	0.25	504.59	0.57	1110	0.477
XMMXCS J111729.0+074631.6	RIXOS F258_101	0082340101	11 17 29.0	+07 46 32	11.9	800.6	21356	4.49	0.16	193.95	0.28	0110	0.160
XMMXCS J111729.8+174452.9	[VMF98]098	0099030101	11 17 29.9	+17 44 53	13.2	467.7	7871	9.20	0.45	174.58	0.53	1110	0.548
XMMXCS J111834.6+074433.9	PG1150+080GROUP	0082340101	11 18 34.6	+07 44 34	4.6	175.3	50512	0.44	0.04	71.85	0.11	1000	0.310
XMMXCS J111926.5+210650.8	NSC J111920+210546	0111290401	11 19 26.6	+21 06 51	13.1	175.1	3781	11.79	0.96	80.62	0.34	0110	...
XMMXCS J111941.9+212641.7	[VMF98]099	0111290401	11 19 42.0	+21 26 42	10.7	72.2	4732	4.52	0.60	25.32	0.11	1110	0.061
XMMXCS J113844.5+031539.1	[VMF98]105	0111970701	11 38 44.5	+03 15 39	7.8	690.4	6376	11.95	0.47	408.00	0.29	1110	0.127
XMMXCS J115123.6+545011.2	ABELL 1396	0049340301	11 51 23.7	+54 50 11	14.8	550.7	7738	12.29	0.55	163.95	0.60	0110	0.144
XMMXCS J121334.9+025350.7	[VMF98]116	0081340801	12 13 34.8	+02 53 51	5.9	2161.8	16076	15.18	0.33	NaN	0.25	1110	0.409
XMMXCS J121743.8+472915.4	ZWCL1215.3+4745	0032140101	12 17 43.8	+47 29 15	9.9	451.7	5258	57.28	2.82	144.46	0.24	1110	...
XMMXCS J121806.4+295826.3	NSC J121805+295932	0096020101	12 18 06.4	+29 58 26	10.6	52.3	15699	1.00	0.16	8.04	0.06	0110	0.032
XMMXCS J122008.5+751428.4	[M98j] 168	0124110101	12 20 08.5	+75 14 28	7.3	289.6	11897	1.39	0.09	19.60	0.18	0110	0.007

XMMXCS J122018.7+752213.8	NGC 4291	0124110101	12 20 18.8	+75 22 14	6.5	16246.4	11910	57.63	0.46	NaN	0.29	0110	0.006
XMMXCS J123144.3+413729.5	NSC J123154+413714	0112280201	12 31 44.4	+41 37 30	12.8	589.7	5834	18.55	0.80	241.18	0.57	0010	0.191
XMMXCS J123615.5+255438.7	RX J1236.2+2554	0112550301	12 36 15.6	+25 54 39	4.7	157.2	11805	1.55	0.13	108.39	0.11	0100	...
XMMXCS J124312.2+131304.4	RSCG 66	0112551001	12 43 12.3	+13 13 04	5.5	384.6	11380	4.34	0.23	136.49	0.21	0110	0.003
XMMXCS J124323.1+131151.6	RSCG 66	0112551001	12 43 23.1	+13 11 52	8.4	59.3	8533	0.83	0.12	29.77	0.05	0110	0.003
XMMXCS J124454.3-003331.8	SDSS CE J191.220871-00.560489	0110980201	12 44 54.4	-00 33 32	6.9	1428.3	39669	3.97	0.11	385.43	0.29	0100	0.231
XMMXCS J125204.0-292035.1	[VMF98]124	0111020201	12 52 04.0	-29 20 35	7.2	1048.7	21536	14.35	0.46	511.23	0.29	1110	0.188
XMMXCS J125233.6-292506.7	CXOU J1252.6-2925	0111020201	12 52 33.7	-29 25 07	10.4	149.8	51927	2.59	0.23	32.18	0.16	0110	...
XMMXCS J125313.9+155544.7	RX J1253.2+1556	0082990101	12 53 13.9	+15 55 45	14.0	1018.0	14619	14.45	0.47	364.35	0.60	0110	0.275
XMMXCS J125527.5+564634.7	RX J1255528.1+564640	0081340201	12 55 27.6	+56 46 35	8.6	146.0	13670	1.27	0.11	38.89	0.13	0010	...
XMMXCS J131022.3+081934.0	ZwCl 1307.8+0835	0110950401	13 10 22.4	+08 19 34	8.8	116.4	6100	2.32	0.24	41.17	0.13	0100	...
XMMXCS J131302.4+351944.4	ZwCl 1310.6+3536	0109080201	13 13 02.4	+35 19 44	10.1	181.2	11769	6.06	0.48	153.08	0.16	0100	...
XMMXCS J131339.6-325038.3	RX J1313.6-3251	0109462301	13 13 39.6	-32 50 38	9.8	207.2	3135	17.37	1.29	40.88	0.16	0110	0.052
XMMXCS J131605.9+285451.5	GHO 1313+2911	0125970101	13 16 06.0	+28 54 52	11.7	55.6	2396	3.26	0.50	13.87	0.06	0110	...
XMMXCS J132053.9+335522.9	ABELL1716	0093640401	13 20 53.9	+33 55 23	13.6	719.3	8503	22.75	0.88	401.49	0.57	1110	0.182
XMMXCS J132501.4-381324.5	RX J1325.0-3814	0110890101	13 25 01.5	-38 13 25	12.1	2563.5	22785	12.53	0.25	642.37	0.57	0110	0.296
XMMXCS J132546.2-382520.0	RXJ1325.5-3826	0110890101	13 25 46.3	-38 25 20	5.2	146.5	38947	0.54	0.05	26.64	0.11	1110	0.445
XMMXCS J133129.7+110756.1	RX J1331.5+1108	0061940101	13 31 29.7	+11 07 56	10.4	161.9	3319	6.70	0.57	106.04	0.16	0010	0.081
XMMXCS J133434.9+375656.2	[VMF98]138	0109660801	13 34 35.0	+37 56 56	2.2	644.1	63644	1.65	0.07	228.37	0.30	1110	0.308
XMMXCS J133459.5+375024.5	[VMF98]139	0109660801	13 34 59.5	+37 50 25	6.2	651.2	50151	2.54	0.10	177.53	0.29	1110	0.382
XMMXCS J133514.4+374908.0	[MJM98] 034	0109661001	13 35 14.4	+37 49 08	9.3	409.2	30868	1.46	0.08	136.78	0.24	0110	0.595
XMMXCS J134139.0+001733.4	SDSS CE J205.412231+00.303271	0111281001	13 41 39.1	+00 17 33	7.5	251.8	6128	6.26	0.42	133.62	0.18	0100	0.390
XMMXCS J134326.7+554655.2	[VMF98]150	0101640401	13 43 26.7	+55 46 55	12.3	240.9	9199	4.05	0.28	38.63	0.40	1110	0.069
XMMXCS J134500.1-002040.9	SDSS CE J206.237427-00.357679	0111282501	13 45 00.2	-00 20 41	6.9	51.4	6258	1.16	0.19	8.58	0.06	0100	0.414
XMMXCS J134513.7-000854.5	SDSS CE J206.296951-00.146028	0111281501	13 45 13.8	-00 08 55	13.0	133.0	2247	10.44	0.99	27.09	0.34	0100	0.118
XMMXCS J135047.8+600709.4	RDCSJ1350+6007	0071340501	13 50 47.9	+60 07 09	12.3	373.1	8672	13.19	0.72	137.09	0.46	1110	0.804
XMMXCS J135452.9+691722.9	RX J1354.8+6917	0083960101	13 54 52.9	+69 17 23	9.7	372.8	12209	4.51	0.25	75.87	0.16	0110	0.207
XMMXCS J140615.7+283049.2	WARPJ1406.2+2830	0140960101	14 06 15.8	+28 30 49	10.4	388.1	6089	7.75	0.41	160.62	0.29	1110	0.546
XMMXCS J140646.6+283307.6	WARPJ1406.9+2834	0140960101	14 06 46.7	+28 33 08	6.6	137.8	10019	1.71	0.16	27.94	0.12	1010	0.118
XMMXCS J141223.6-030950.4	MS1409.9-0255	0013140101	14 12 23.7	-03 09 50	13.0	46.3	5606	0.91	0.15	16.30	0.08	1000	0.221
XMMXCS J141558.4+230718.9	OC03 J1415+2307	0148250201	14 15 58.4	+23 07 19	10.5	289.1	3677	12.89	0.80	216.00	0.23	0110	0.300
XMMXCS J141628.2+444641.3	[VMF98]158	0109080501	14 16 28.3	+44 46 41	11.0	2033.2	11181	49.63	1.13	NaN	0.28	1110	0.400
XMMXCS J141652.4+522052.5	HST J141653+52210	0127921001	14 16 52.4	+52 20 53	4.3	872.4	48317	1.97	0.07	NaN	0.25	0110	...
XMMXCS J141832.1+251107.0	WARPJ1418.5+2511	0089960301	14 18 32.1	+25 11 07	7.9	6300.1	31642	49.45	0.63	NaN	0.29	1110	0.296
XMMXCS J142907.7+424105.6	CRSS J1429.1+4241	0165770201	14 29 07.8	+42 41 06	6.5	1134.9	34994	7.57	0.23	723.01	0.29	0100	...
XMMXCS J143252.1-441909.5	ABELL3602	0140950101	14 32 52.2	-44 19 10	8.9	8314.0	5478	203.28	2.25	NaN	0.23	1110	...
XMMXCS J143857.3+642333.4	ZWCL1437.3+6436	0111530101	14 38 57.3	+64 23 33	6.1	1388.5	33075	6.47	0.18	312.50	0.29	1110	0.146
XMMXCS J151424.7+363710.1	MS1512.4+3647	0111291001	15 14 24.7	+36 37 10	14.1	514.3	7792	31.57	1.45	344.86	0.60	1110	0.372
XMMXCS J154404.7+534710.8	[VMF98]173	0060370901	15 44 04.7	+53 47 11	11.9	255.4	10489	3.67	0.24	28.87	0.23	1110	0.112
XMMXCS J154932.3+213301.7	[B2002a] 30	0136040101	15 49 32.3	+21 33 02	8.2	458.4	10770	5.16	0.25	232.75	0.24	0100	0.800
XMMXCS J161132.8+541635.5	NSC J161132+541649	0059752301	16 11 32.8	+54 16 36	5.8	818.2	5002	24.02	0.87	361.41	0.25	0110	0.379
XMMXCS J161719.7+345411.0	RXCJ1617.5+3458	0143651101	16 17 19.7	+34 54 11	12.8	77.1	580	17.00	2.17	89.03	0.21	1110	0.032
XMMXCS J162659.9+552819.7	ABELL2201	0109081101	16 26 60.0	+55 28 20	9.8	51.2	674	32.34	5.18	16.34	0.05	1110	0.130

XMMXCS J163341.4+571417.1	[VMF98]181	0049540401	16 33 41.5	+57 14 17	6.9	125.7	14651	1.33	0.13	64.15	0.12	1110	0.239
XMMXCS J190816.9+690347.9	ABELL2317	0109464501	19 08 16.9	+69 03 48	8.0	1345.5	3234	87.17	2.44	701.27	0.23	1110	0.211
XMMXCS J210849.1-051640.2	WARPJ2108.8-0516	0110860101	21 08 49.2	-05 16 40	12.7	748.5	15372	13.73	0.52	279.54	0.57	1110	0.319
XMMXCS J220206.1-315909.0	HCG90	0147920601	22 02 06.1	-31 59 09	7.1	1935.1	9628	22.07	0.51	NaN	0.29	1110	0.009
XMMXCS J223520.3-255742.2	XMMU J2235.3-2557	0111790101	22 35 20.4	-25 57 42	7.8	142.0	22907	4.31	0.39	85.40	0.12	0001	1.393
XMMXCS J223924.4-054718.5	WARPJ2239.4-0547	0149410401	22 39 24.4	-05 47 19	8.8	2487.9	13389	21.67	0.44	NaN	0.23	1110	0.242
XMMXCS J223934.0-060019.1	WARPJ2239.5-0600	0149410401	22 39 34.0	-06 00 19	9.4	652.0	10929	7.10	0.29	181.70	0.23	1110	0.173
XMMXCS J223939.4-054327.4	WARPJ2239.6-0543	0149410401	22 39 39.4	-05 43 27	9.6	2765.8	13649	25.26	0.49	NaN	0.23	1110	0.243
XMMXCS J225145.7-180528.4	SEXCLAS_18	0081340901	22 51 45.7	-18 05 28	13.1	144.0	7987	35.80	3.24	32.82	0.34	0001	...
XMMXCS J230247.4+084812.9	[B2002a] 36	0112170301	23 02 47.4	+08 48 13	8.2	58.4	14989	1.15	0.17	29.50	0.05	0100	...
XMMXCS J230247.7+084354.0	WARPJ2302.8+0843	0112170301	23 02 47.8	+08 43 54	11.0	328.1	12333	7.00	0.41	187.27	0.29	1110	0.722
XMMXCS J230252.2+084135.4	WARPJ2302.8+0843	0032140201	23 02 52.2	+08 41 35	7.5	96.8	5867	2.41	0.27	72.40	0.08	1000	0.722
XMMXCS J231805.9-423535.8	1AXGJ231807-4236	0112310201	23 18 05.9	-42 35 36	13.8	573.1	7716	49.06	2.14	172.46	0.57	1110	0.209
XMMXCS J233227.3+195825.1	SEXCLAS_19	0112880301	23 32 27.4	+19 58 25	9.0	279.6	8843	4.57	0.29	70.01	0.16	0001	0.270
XMMXCS J233756.6+271120.7	ABELL 2634:[SM98] 02	0002960101	23 37 56.7	+27 11 21	11.9	2386.2	5067	66.10	1.38	NaN	0.28	0110	0.123

Table B.1: XCS Statistical Cluster Sample: Known Clusters. The column descriptions are given in Section 4.2.1.

Appendix C

XCS Statistical Sample New Candidates

Id	Obsid	RA(J2000)	Dec(J2000)	θ	Scts	t_{exp}	Flux	σ_F	Sig	FN_P	z_{est}	σ_z	z_{flag}
XMMXCS J000014.0-251057.3	0125310101	00 00 14.1	-25 10 57	5.0	1264.5	11852	11.72	0.34	328.34	0.25	0.085	0.001	1
XMMXCS J000018.8-245711.8	0125310101	00 00 18.9	-24 57 12	10.6	46.7	10227	0.49	0.08	13.02	0.04	...	...	...
XMMXCS J000047.1-251546.2	0125310101	00 00 47.1	-25 15 46	9.1	56.4	9055	0.69	0.10	13.67	0.05	0.087	0.001	1
XMMXCS J000103.5-250352.6	0125310101	00 01 03.6	-25 03 53	8.4	470.4	11287	4.63	0.22	121.18	0.24	...	...	...
XMMXCS J000209.9-301433.5	0041750101	00 02 09.9	-30 14 34	16.6	82.4	12628	3.66	0.45	28.48	0.28	...	...	...
XMMXCS J000218.9-295655.9	0041750101	00 02 18.9	-29 56 56	7.0	231.9	34649	0.84	0.06	67.78	0.18	...	...	...
XMMXCS J000259.0-295504.8	0041750101	00 02 59.1	-29 55 05	5.5	1009.6	43289	2.50	0.08	266.25	0.25	0.099	0.032	3
XMMXCS J000300.4-295157.4	0041750101	00 03 00.4	-29 51 57	8.5	694.5	33059	2.36	0.09	90.25	0.23	...	...	...
XMMXCS J000309.5-295742.2	0041750101	00 03 09.5	-29 57 42	5.2	112.2	39610	0.28	0.03	24.96	0.11	...	...	...
XMMXCS J000313.9-255056.9	0103060301	00 03 13.9	-25 50 57	12.5	100.5	18807	1.04	0.11	17.28	0.34	...	...	...
XMMXCS J000314.0-260928.6	0103060301	00 03 14.0	-26 09 29	6.5	138.3	25756	0.59	0.05	23.05	0.12	...	...	...
XMMXCS J000317.1-295847.4	0041750101	00 03 17.1	-29 58 47	6.4	801.4	36723	2.14	0.08	NaN	0.29	...	...	...
XMMXCS J000324.2-255807.7	0103060301	00 03 24.3	-25 58 08	5.2	181.6	33136	0.69	0.06	38.00	0.11	...	...	...
XMMXCS J000341.5-300729.9	0041750101	00 03 41.5	-30 07 30	13.8	290.6	21295	3.51	0.22	69.68	0.40	0.060	0.001	1
XMMXCS J000429.1+633127.1	0109120101	00 04 29.2	+63 31 27	14.0	901.2	12628	12.99	0.45	312.67	0.60	0.374	...	3
XMMXCS J000626.3+195937.3	0101040101	00 06 26.4	+19 59 37	12.8	164.6	15668	2.95	0.25	31.09	0.34	...	...	...
XMMXCS J000634.9+201722.3	0101040101	00 06 34.8	+20 17 22	6.2	251.6	19046	2.30	0.15	56.87	0.18	...	...	...
XMMXCS J001026.8+110549.4	0127110201	00 10 26.9	+11 05 49	7.4	108.9	5287	5.07	0.53	42.35	0.12	...	...	...
XMMXCS J001042.5-112743.3	0111970901	00 10 42.5	-11 27 43	10.5	296.0	6643	6.50	0.40	265.56	0.23	...	...	...
XMMXCS J001210.7-112439.2	0111970901	00 12 10.8	-11 24 39	11.9	46.8	4525	1.19	0.20	21.91	0.04	...	...	...
XMMXCS J001339.2-390145.1	0028740101	00 13 39.3	-39 01 45	13.8	35.2	10464	0.18	0.04	15.90	0.05	...	...	...
XMMXCS J001436.0-385555.1	0028740101	00 14 36.0	-38 55 55	14.9	32.1	6378	1.07	0.22	25.40	0.08	...	...	...
XMMXCS J001436.6-390008.2	0028740101	00 14 36.7	-39 00 08	10.7	161.8	12542	1.53	0.13	19.32	0.16	...	...	...
XMMXCS J001530.6-392645.8	0028740201	00 15 30.7	-39 26 46	11.7	155.6	16025	1.05	0.09	21.52	0.16	0.086	0.020	2
XMMXCS J001610.6-391701.7	0028740201	00 16 10.6	-39 17 02	5.0	477.1	25982	2.10	0.10	137.86	0.14	...	...	...
XMMXCS J001636.2-392512.3	0028740201	00 16 36.2	-39 25 12	13.8	75.9	10756	23.92	3.07	9.49	0.21	...	...	...
XMMXCS J001816.8+812219.0	0112620201	00 18 16.8	+81 22 19	13.1	148.0	6167	5.14	0.46	55.53	0.34	...	...	...
XMMXCS J001850.4+814017.4	0112620201	00 18 50.5	+81 40 17	6.4	403.0	12949	4.60	0.24	112.15	0.19	...	...	...
XMMXCS J001857.4-705016.7	0147570101	00 18 57.5	-70 50 17	9.5	78.6	3463	1.82	0.23	17.76	0.08	...	...	...
XMMXCS J001955.1+214415.8	0047940101	00 19 55.1	+21 44 16	12.7	140.0	22577	1.64	0.15	17.28	0.34	...	...	...
XMMXCS J002202.0-772041.9	0006010401	00 22 02.0	-77 20 42	13.4	187.2	14108	5.00	0.39	76.90	0.34	...	...	...
XMMXCS J002229.0-484327.3	0152330101	00 22 29.1	-48 43 27	12.0	142.0	13016	1.44	0.13	52.30	0.34	...	...	...
XMMXCS J002402.4-771052.0	0006010401	00 24 02.5	-77 10 52	7.2	30.9	23950	0.19	0.04	10.57	0.03	...	...	...
XMMXCS J002530.5-772851.2	0006010401	00 25 30.6	-77 28 51	13.6	231.3	11506	5.32	0.37	47.35	0.40	0.055	0.001	1
XMMXCS J002631.0+105225.5	0001930101	00 26 31.1	+10 52 26	12.6	78.4	5520	1.95	0.25	23.64	0.21	0.067	0.021	3
XMMXCS J002635.9+103445.0	0001930101	00 26 36.0	+10 34 45	9.7	446.1	8965	7.32	0.36	107.18	0.24	...	...	...
XMMXCS J003247.5-431427.9	0148961201	00 32 47.6	-43 14 28	12.2	175.9	16162	3.16	0.26	43.49	0.34	...	...	...
XMMXCS J003252.9+392625.4	0151581101	00 32 53.0	+39 26 25	9.6	45.6	5962	1.03	0.18	7.04	0.04	...	...	...
XMMXCS J003317.9-212500.0	0044350101	00 33 17.9	-21 25 00	13.1	259.4	5887	7.37	0.49	97.15	0.40	...	...	...
XMMXCS J003354.5-433421.5	0148961301	00 33 54.6	-43 34 22	15.4	33.8	8233	41.52	8.44	12.10	0.08	...	...	...
XMMXCS J003407.3-432237.7	0148961301	00 34 07.4	-43 22 38	4.8	214.2	28885	0.86	0.06	50.91	0.10	0.343	...	3

XMMXCS J003412.4-433154.9	0148961201	00 34 12.4	-43 31 55	13.5	115.4	6214	17.69	1.81	31.02	0.34	...	...	...
XMMXCS J003413.5+392419.8	0151581101	00 34 13.6	+39 24 20	10.0	58.3	5195	1.32	0.20	31.42	0.06	...	...	...
XMMXCS J003414.9+852003.9	0100640101	00 34 15.0	+85 20 04	12.3	291.4	27565	2.97	0.18	83.39	0.40	...	...	...
XMMXCS J003427.6-431855.8	0148961301	00 34 27.7	-43 18 56	6.8	3550.9	25096	16.33	0.28	NaN	0.29	...	...	...
XMMXCS J003439.3-120716.0	0125920201	00 34 39.3	-12 07 16	11.0	487.3	11566	10.57	0.50	197.08	0.26	...	...	...
XMMXCS J003513.5-431016.2	0148960101	00 35 13.5	-43 10 16	11.0	160.4	23514	0.74	0.06	27.18	0.16	0.168	0.031	3
XMMXCS J003547.2-430530.0	0148960101	00 35 47.3	-43 05 30	13.5	66.2	18169	1.05	0.15	22.05	0.15	...	...	...
XMMXCS J003548.2-432230.6	0148960101	00 35 48.3	-43 22 31	3.5	884.3	33906	2.91	0.10	222.37	0.30	...	...	...
XMMXCS J003551.3-431217.8	0148960101	00 35 51.4	-43 12 18	6.7	479.6	32807	1.45	0.07	100.78	0.19	...	...	...
XMMXCS J003603.7+851321.4	0100640101	00 36 03.7	+85 13 21	12.4	590.7	14902	34.34	1.47	133.15	0.57	...	...	...
XMMXCS J003627.4-432835.6	0148960101	00 36 27.4	-43 28 36	11.8	1172.1	17824	7.46	0.22	207.80	0.28	...	...	...
XMMXCS J003646.4-432020.6	0148960101	00 36 46.4	-43 20 21	10.4	601.3	23636	2.71	0.12	144.86	0.28	...	...	...
XMMXCS J003832.0+853105.5	0100640101	00 38 32.0	+85 31 06	12.8	244.6	15793	4.45	0.30	131.40	0.40	...	...	...
XMMXCS J003941.8+414949.4	0204790401	00 39 41.9	+41 49 49	11.5	609.3	6933	12.67	0.53	172.90	0.28	...	...	...
XMMXCS J004038.6+410607.0	0112570201	00 40 38.6	+41 06 07	13.7	214.6	22121	1.20	0.09	20.03	0.40	...	...	...
XMMXCS J004047.2+850536.2	0100640201	00 40 47.3	+85 05 36	15.5	58.8	12370	0.92	0.14	31.09	0.17	...	...	...
XMMXCS J004049.5+415204.1	0204790401	00 40 49.6	+41 52 04	12.0	684.5	5886	17.78	0.71	174.03	0.57	...	...	...
XMMXCS J004128.7+852832.4	0100640101	00 41 28.7	+85 28 32	8.8	233.9	34937	1.60	0.11	45.60	0.16	...	...	...
XMMXCS J004231.9+005119.2	0090070201	00 42 31.9	+00 51 19	11.9	262.6	10126	4.27	0.28	63.44	0.23	0.151	0.001	1
XMMXCS J004254.7-180041.5	0112880601	00 42 54.7	-18 00 42	9.7	116.4	7236	2.41	0.24	47.21	0.13	0.241	0.029	3
XMMXCS J004328.6+413556.3	0109270701	00 43 28.6	+41 35 56	6.1	184.6	41748	0.64	0.05	57.18	0.12	...	...	...
XMMXCS J004331.3+395614.5	0151580201	00 43 31.4	+39 56 15	9.0	42.2	636	7.87	1.41	25.62	0.04	...	...	...
XMMXCS J004351.6+005702.3	0090070201	00 43 51.6	+00 57 02	9.9	67.1	9353	0.86	0.12	48.73	0.07	...	...	...
XMMXCS J004356.2-180620.0	0112880601	00 43 56.3	-18 06 20	8.7	101.6	7544	2.00	0.22	47.39	0.13	...	...	...
XMMXCS J004409.0+005647.7	0090070201	00 44 09.1	+00 56 48	13.5	145.3	6604	18.80	1.69	48.78	0.34	...	...	...
XMMXCS J004428.9-175029.2	0112880601	00 44 29.0	-17 50 29	15.5	165.2	2705	77.50	6.51	48.46	0.53	0.289	0.029	3
XMMXCS J004434.4+420630.9	0109270301	00 44 34.3	+42 06 31	13.4	29.9	13182	0.30	0.07	12.09	0.02	...	...	...
XMMXCS J004610.5+420354.1	0109270301	00 46 10.6	+42 03 54	12.2	90.7	16811	0.90	0.10	58.60	0.21	...	...	...
XMMXCS J004620.1+412421.1	0151580401	00 46 20.2	+41 24 21	4.2	153.0	9973	1.84	0.16	45.82	0.11	0.108	0.031	3
XMMXCS J004717.6+422127.1	0109270401	00 47 17.6	+42 21 27	8.9	843.0	32766	2.65	0.09	483.05	0.23	...	...	...
XMMXCS J004726.7+421347.3	0109270401	00 47 26.7	+42 13 47	9.4	97.8	32111	0.36	0.04	19.90	0.08	...	...	...
XMMXCS J004728.3+412456.6	0151580401	00 47 28.3	+41 24 57	15.8	89.0	3116	17.87	2.10	44.71	0.28	...	...	...
XMMXCS J004743.2+320332.8	0067540201	00 47 43.3	+32 03 33	14.9	27.4	5057	65.25	15.02	38.00	0.05	...	...	...
XMMXCS J004753.1+852716.9	0100640201	00 47 53.2	+85 27 17	8.1	584.7	36727	2.50	0.11	172.62	0.23	0.275	0.037	3
XMMXCS J004844.4-520246.2	0125320501	00 48 44.4	-52 02 46	13.3	48.3	2346	2.81	0.47	14.98	0.08	...	...	...
XMMXCS J005042.4-521316.7	0125320701	00 50 42.4	-52 13 17	7.8	230.5	12612	3.18	0.22	76.90	0.18	0.026	0.001	1
XMMXCS J005126.0+852456.3	0100640201	00 51 26.0	+85 24 56	9.7	120.8	29966	0.61	0.06	44.34	0.13	...	...	...
XMMXCS J005252.3-745018.4	0112880901	00 52 52.3	-74 50 18	11.2	47.3	21006	0.25	0.04	19.01	0.04	...	...	...
XMMXCS J005316.7+124923.8	0110890301	00 53 16.8	+12 49 24	9.0	110.7	12794	2.45	0.26	42.06	0.13	...	...	...
XMMXCS J005353.0-374034.5	0112800201	00 53 53.0	-37 40 35	12.3	84.2	16233	0.88	0.11	23.78	0.21	...	...	...
XMMXCS J005402.7-373343.4	0112800201	00 54 02.7	-37 33 43	12.7	101.4	14592	1.07	0.12	42.68	0.34	...	...	...
XMMXCS J005403.4-374620.8	0112800201	00 54 03.4	-37 46 21	11.5	37.2	22185	0.39	0.08	29.07	0.02	...	...	...
XMMXCS J005417.6-743439.1	0112880901	00 54 17.6	-74 34 39	6.6	33.0	25072	0.24	0.05	24.74	0.03	...	...	...

XMMXCS J005624.5-281831.4	0111280801	00 56 24.5	-28 18 31	9.5	114.8	4475	4.23	0.43	37.99	0.13	...	...	...
XMMXCS J005717.2-221402.1	0110890401	00 57 17.1	-22 14 02	9.0	89.2	15174	1.67	0.20	44.50	0.08	...	...	...
XMMXCS J005731.4-223509.6	0110890401	00 57 31.4	-22 35 10	12.5	195.8	14137	4.84	0.37	74.12	0.34	...	...	...
XMMXCS J005747.0-223446.8	0110890401	00 57 47.0	-22 34 47	13.3	46.1	12099	1.07	0.18	25.60	0.08	...	...	...
XMMXCS J005806.2-273439.8	0111280301	00 58 06.2	-27 34 40	10.0	27.5	3497	1.22	0.28	9.42	0.02	...	...	...
XMMXCS J005808.6-273644.7	0111280301	00 58 08.6	-27 36 45	9.4	39.3	3783	1.70	0.32	24.68	0.02	...	...	...
XMMXCS J005809.6-361800.0	0102040701	00 58 09.6	-36 18 00	13.2	80.1	4697	1.84	0.23	33.07	0.21	...	...	...
XMMXCS J005818.0-222023.4	0110890401	00 58 18.0	-22 20 23	13.7	91.1	10146	3.73	0.43	39.60	0.21	...	...	...
XMMXCS J005819.1-272858.9	0111280301	00 58 19.2	-27 28 59	10.0	52.4	4121	2.05	0.32	26.83	0.06	...	...	...
XMMXCS J005822.6-720032.5	0018540101	00 58 22.6	-72 00 33	10.6	380.6	11597	4.91	0.26	121.10	0.29	...	...	...
XMMXCS J005906.7-274859.0	0111280601	00 59 06.8	-27 48 59	11.6	54.1	5577	1.25	0.19	25.25	0.06	...	...	...
XMMXCS J005932.0-751120.9	0142660401	00 59 32.1	-75 11 21	6.1	29.7	13790	0.28	0.06	31.69	0.02	...	...	...
XMMXCS J010024.7-720517.7	0018540101	01 00 24.7	-72 05 18	6.4	41.4	18236	0.47	0.09	15.08	0.03	...	...	...
XMMXCS J010031.1-720105.3	0018540101	01 00 31.2	-72 01 05	10.1	648.3	11637	8.54	0.35	77.45	0.28	...	...	...
XMMXCS J010124.4-750505.9	0142660401	01 01 24.5	-75 05 06	8.6	210.9	10003	2.99	0.22	89.21	0.16	...	...	...
XMMXCS J010647.1+005618.8	0150870201	01 06 47.1	+00 56 19	10.6	30.3	1717	2.26	0.49	20.27	0.02	...	...	...
XMMXCS J010743.7-801214.7	0145540101	01 07 43.8	-80 12 15	6.5	37.6	19101	0.65	0.12	27.28	0.03	...	...	...
XMMXCS J010801.9-801836.8	0145540101	01 08 01.9	-80 18 37	2.5	416.3	22913	5.64	0.29	146.68	0.18	...	...	...
XMMXCS J011138.6-453858.9	0067170101	01 11 38.7	-45 38 59	14.1	846.1	15555	8.02	0.29	262.12	0.60	...	...	...
XMMXCS J011244.0-454237.5	0067170101	01 12 44.1	-45 42 38	9.6	69.4	20258	0.38	0.05	26.01	0.07	...	...	...
XMMXCS J011303.6-144457.8	0147920101	01 13 03.6	-14 44 58	12.6	124.4	9551	1.58	0.15	42.71	0.34	...	...	...
XMMXCS J011354.9-732705.5	0011450101	01 13 54.9	-73 27 06	13.6	396.5	16230	3.03	0.16	94.82	0.46	...	...	...
XMMXCS J011545.6-731839.1	0011450101	01 15 45.6	-73 18 39	9.8	232.1	26040	1.01	0.07	14.78	0.16	...	...	...
XMMXCS J011818.6-733801.2	0011450101	01 18 18.6	-73 38 01	12.6	217.5	16257	1.43	0.10	23.10	0.40	...	...	...
XMMXCS J011918.3-440113.1	0103860901	01 19 18.3	-44 01 13	12.8	328.7	9355	5.20	0.30	99.40	0.46	0.232	0.001	1
XMMXCS J011925.5-733459.0	0011450101	01 19 25.5	-73 34 59	13.0	170.5	16252	1.76	0.15	17.64	0.34	...	...	...
XMMXCS J011944.7-732225.9	0011450101	01 19 44.8	-73 22 26	12.1	132.4	20807	0.97	0.09	55.35	0.34	...	...	...
XMMXCS J011949.5-440434.0	0103860901	01 19 49.5	-44 04 34	6.3	503.5	13842	5.48	0.26	273.50	0.29	...	...	...
XMMXCS J012018.8-435727.1	0103860901	01 20 18.9	-43 57 27	10.3	95.5	10024	1.17	0.13	21.64	0.11	...	...	...
XMMXCS J012054.8-440402.5	0103860901	01 20 54.9	-44 04 03	7.3	55.1	13196	0.49	0.08	22.71	0.06	...	...	...
XMMXCS J012117.7-440526.2	0103860901	01 21 17.6	-44 05 26	10.6	55.1	9455	0.61	0.09	7.14	0.06	...	...	...
XMMXCS J012218.2-585830.5	0101040201	01 22 18.3	-58 58 30	15.2	116.7	7950	2.13	0.22	29.76	0.53	...	...	...
XMMXCS J012304.5-345456.3	0150940101	01 23 04.6	-34 54 56	13.6	383.1	17063	6.13	0.33	154.87	0.46	...	...	...
XMMXCS J012359.5+034442.0	0025541601	01 23 59.5	+03 44 42	9.3	51.9	7025	1.07	0.17	15.56	0.05	...	...	...
XMMXCS J012359.9+035110.2	0025541601	01 23 59.9	+03 51 10	9.5	79.9	7332	1.58	0.20	22.02	0.08	...	...	...
XMMXCS J012411.6-585558.7	0101040201	01 24 11.6	-58 55 59	8.3	208.0	17116	1.36	0.10	61.03	0.16	...	...	...
XMMXCS J012411.8-345247.6	0150940101	01 24 11.8	-34 52 48	11.7	166.1	21547	2.62	0.22	45.60	0.16	...	...	...
XMMXCS J012415.4+035653.1	0025541601	01 24 15.4	+03 56 53	10.6	104.3	6089	2.49	0.27	41.28	0.16	...	...	...
XMMXCS J012431.6-351233.8	0109130201	01 24 31.6	-35 12 34	11.5	49.1	4855	2.66	0.44	15.71	0.04	...	...	...
XMMXCS J012441.3-345747.3	0150940101	01 24 41.3	-34 57 47	11.4	127.2	20180	1.11	0.11	26.44	0.16	...	...	...
XMMXCS J013154.4+302936.0	0102641101	01 31 54.5	+30 29 36	11.2	73.2	4335	2.27	0.30	26.78	0.11	...	...	...
XMMXCS J013352.1-395703.5	0112630201	01 33 52.2	-39 57 04	13.5	37.0	9548	3.22	0.62	13.49	0.05	...	...	...
XMMXCS J013837.3-175956.9	0111430101	01 38 37.3	-17 59 57	6.4	138.7	20299	2.91	0.27	38.92	0.12	...	...	...

XMMXCS J013953.0-675421.0	0148440101	01 39 53.0	-67 54 21	6.4	84.1	20276	0.48	0.06	47.10	0.08	...	...	...
XMMXCS J014007.2+062314.8	0110890901	01 40 07.3	+06 23 15	4.8	72.0	10342	1.40	0.19	51.64	0.05	...	...	...
XMMXCS J014046.2-675033.0	0148440101	01 40 46.2	-67 50 33	3.2	83.4	24793	0.36	0.04	32.93	0.03	...	...	...
XMMXCS J014146.3-674937.1	0148440101	01 41 46.4	-67 49 37	5.8	49.0	19662	0.34	0.06	12.03	0.02	...	...	...
XMMXCS J014213.2+134333.8	0093641001	01 42 13.2	+13 43 34	12.8	29.1	4840	0.91	0.20	31.33	0.02	...	...	...
XMMXCS J014214.3-674009.0	0148440101	01 42 14.4	-67 40 09	15.0	34.7	7403	0.84	0.17	15.58	0.08	...	...	...
XMMXCS J014321.3+134859.0	0093641001	01 43 21.3	+13 48 59	11.5	71.1	4353	2.41	0.32	37.48	0.11	...	...	...
XMMXCS J014449.9-043231.5	0109661101	01 44 50.0	-04 32 32	9.5	1053.7	28190	4.96	0.16	238.81	0.23	0.133	0.022	2
XMMXCS J014506.3-043921.5	0109661201	01 45 06.4	-04 39 22	6.9	180.6	31103	0.79	0.06	27.51	0.12	...	...	...
XMMXCS J014523.2-042305.7	0109661101	01 45 23.3	-04 23 06	11.6	149.5	18969	0.95	0.08	11.98	0.16	0.042	0.001	1
XMMXCS J014525.9-044751.7	0109661101	01 45 26.0	-04 47 52	13.2	120.7	21396	1.49	0.15	45.46	0.34	...	...	...
XMMXCS J014534.1-393439.2	0090070101	01 45 34.1	-39 34 39	13.7	131.9	10150	1.43	0.14	37.64	0.34	...	...	...
XMMXCS J014547.5-042214.4	0109661101	01 45 47.5	-04 22 14	13.5	145.9	15356	1.12	0.10	13.23	0.34	0.057	0.001	1
XMMXCS J014557.3-043411.7	0109661201	01 45 57.3	-04 34 12	7.6	41.9	36434	0.23	0.04	25.18	0.03	...	...	...
XMMXCS J014603.4-044450.4	0109661201	01 46 03.4	-04 44 50	13.6	80.1	20334	47.57	5.94	31.47	0.21	...	...	...
XMMXCS J014607.1-393909.6	0090070101	01 46 07.1	-39 39 10	16.1	122.3	7977	9.39	0.93	35.35	0.53	...	...	...
XMMXCS J014607.8-391406.6	0090070101	01 46 07.9	-39 14 07	9.0	62.2	21272	0.35	0.05	26.85	0.07	...	...	...
XMMXCS J014631.4-393030.6	0090070101	01 46 31.5	-39 30 31	8.3	140.5	18213	1.01	0.09	16.85	0.13	...	...	...
XMMXCS J014652.8-392842.2	0090070101	01 46 52.9	-39 28 42	9.6	207.2	17535	1.61	0.12	51.73	0.16	...	...	...
XMMXCS J014703.5-393233.1	0090070101	01 47 03.6	-39 32 33	13.7	180.3	11995	31.28	2.51	66.76	0.34	...	...	...
XMMXCS J014801.3+055247.2	0112551501	01 48 01.4	+05 52 47	13.9	334.5	5363	7.34	0.42	137.00	0.46	...	...	...
XMMXCS J014908.5+135742.1	0094383401	01 49 08.6	+13 57 42	10.5	60.2	2368	6.88	1.01	28.94	0.07	0.071	0.001	1
XMMXCS J014920.6+055518.5	0112551501	01 49 20.7	+05 55 19	5.9	131.2	11663	1.27	0.12	44.46	0.11	...	...	...
XMMXCS J015212.6-133704.7	0112300101	01 52 12.6	-13 37 05	13.8	63.3	10255	0.85	0.12	8.10	0.15	0.105	0.031	3
XMMXCS J015241.1-133855.1	0112300101	01 52 41.2	-13 38 55	7.2	382.1	19694	2.75	0.15	147.53	0.18	...	...	...
XMMXCS J015356.3-492434.3	0092970201	01 53 56.3	-49 24 34	12.8	110.8	6755	3.40	0.35	29.44	0.34	...	...	...
XMMXCS J015423.6-493633.4	0092970201	01 54 23.6	-49 36 33	7.3	98.9	8643	1.52	0.17	27.12	0.08	...	...	...
XMMXCS J015437.6-594640.0	0109460201	01 54 37.6	-59 46 40	4.7	48.5	5788	1.33	0.22	6.57	0.02	...	...	...
XMMXCS J015656.0+375913.2	0149780101	01 56 56.1	+37 59 13	13.9	96.2	14251	0.60	0.07	35.64	0.21	...	...	...
XMMXCS J015719.5+375635.8	0149780101	01 57 19.6	+37 56 36	9.3	1343.2	20792	8.00	0.22	527.18	0.23	...	...	...
XMMXCS J015731.0+380207.1	0149780101	01 57 31.0	+38 02 07	14.2	113.9	13014	1.60	0.16	23.44	0.53	...	...	...
XMMXCS J015754.8+375239.1	0149780101	01 57 54.8	+37 52 39	5.7	250.2	26598	1.07	0.07	119.87	0.10	...	...	...
XMMXCS J015951.9+001655.4	0101640201	01 59 51.9	+00 16 55	6.8	115.4	4925	3.37	0.34	41.56	0.12	...	...	...
XMMXCS J020801.3+351410.2	0084140101	02 08 01.4	+35 14 10	11.7	100.9	18858	0.64	0.07	32.75	0.16	...	...	...
XMMXCS J020801.6+352754.5	0084140501	02 08 01.7	+35 27 55	8.8	57.1	8678	0.91	0.14	31.17	0.05	...	...	...
XMMXCS J020811.7+353155.6	0084140101	02 08 11.7	+35 31 56	10.2	136.0	18864	0.90	0.08	40.28	0.16	...	...	...
XMMXCS J020811.7+351838.5	0084140101	02 08 11.8	+35 18 39	7.0	159.4	27828	0.64	0.05	17.46	0.12	...	...	...
XMMXCS J020816.1+351257.1	0084140101	02 08 16.1	+35 12 57	11.2	104.9	20470	0.58	0.06	31.82	0.16	...	...	...
XMMXCS J020823.3+352820.6	0084140101	02 08 23.3	+35 28 21	6.0	62.7	27464	0.30	0.04	26.62	0.07	...	...	...
XMMXCS J020828.7+352003.9	0084140501	02 08 28.8	+35 20 04	3.7	33.6	13323	0.34	0.07	7.40	0.02	...	...	...
XMMXCS J020847.8-632921.8	0111970401	02 08 47.9	-63 29 22	12.8	23.8	4405	1.46	0.37	4.41	0.02	...	...	...
XMMXCS J020848.1+353001.7	0084140101	02 08 48.1	+35 30 02	7.1	138.5	22105	0.76	0.07	22.99	0.12	...	...	...
XMMXCS J020853.4+350948.1	0084140101	02 08 53.5	+35 09 48	13.8	60.9	16045	1.53	0.22	32.57	0.15	...	...	...

XMMXCS J020906.0-632153.6	0111970401	02 09 06.1	-63 21 54	6.0	111.8	6978	2.17	0.23	24.57	0.12	...	...	...	...	...
XMMXCS J020906.3+353525.4	0084140101	02 09 06.3	+35 35 25	13.5	96.2	11545	1.87	0.21	15.70	0.21	...	...	...	...	...
XMMXCS J020910.5+353704.2	0084140101	02 09 10.5	+35 37 04	15.4	55.0	8985	8.68	1.34	44.82	0.17	...	...	...	...	...
XMMXCS J020932.8+353432.1	0084140101	02 09 32.8	+35 34 32	15.9	199.0	9265	3.31	0.25	273.05	0.53	...	...	...	...	...
XMMXCS J021138.2-244225.6	0125910701	02 11 38.3	-24 42 26	11.5	146.4	1932	9.34	0.84	56.85	0.16	...	...	...	...	...
XMMXCS J021350.2-735507.7	0049150301	02 13 50.3	-73 55 08	9.0	74.0	11734	0.79	0.10	23.58	0.08	...	...	...	...	...
XMMXCS J021401.8-003950.2	0109130301	02 14 01.9	-00 39 50	10.0	46.8	5577	2.23	0.38	15.73	0.04	...	...	...	...	...
XMMXCS J021416.6-005230.7	0109130301	02 14 16.6	-00 52 31	7.8	60.5	7334	2.00	0.29	31.24	0.07	...	...	...	...	...
XMMXCS J021452.4-741726.8	0049150301	02 14 52.4	-74 17 27	16.6	46.1	3803	3.69	0.63	36.85	0.13	...	...	...	...	...
XMMXCS J021516.9-003750.9	0109130301	02 15 16.9	-00 37 51	13.6	32.1	3118	2.74	0.57	17.85	0.05	...	...	...	...	...
XMMXCS J021534.8-050503.8	0112370601	02 15 34.8	-05 05 04	13.3	116.1	11123	1.14	0.12	26.59	0.34	...	...	...	...	...
XMMXCS J021557.9-045528.8	0112370601	02 15 57.9	-04 55 29	7.9	75.7	20840	0.39	0.05	32.43	0.08	...	...	...	...	...
XMMXCS J021611.7-044627.1	0112370601	02 16 11.8	-04 46 27	13.9	87.3	13934	1.41	0.17	37.05	0.21	...	...	...	...	...
XMMXCS J021620.5-052626.2	0112370701	02 16 20.5	-05 26 26	14.0	124.8	14568	0.90	0.09	23.33	0.53	...	...	...	...	...
XMMXCS J021621.5-051702.1	0112370701	02 16 21.5	-05 17 02	13.1	21.7	17377	0.22	0.06	0.75	0.02	...	...	...	...	...
XMMXCS J021634.0-051810.8	0112370701	02 16 34.0	-05 18 11	9.8	143.0	23050	0.61	0.06	43.60	0.13	...	...	...	...	...
XMMXCS J021638.2-740601.6	0099840101	02 16 38.2	-74 06 02	8.0	102.7	11496	2.51	0.27	20.12	0.13	...	...	...	...	...
XMMXCS J021648.1-043315.4	0112372001	02 16 48.1	-04 33 15	8.4	104.8	16460	0.72	0.08	51.48	0.13	...	...	...	...	...
XMMXCS J021659.0-044921.4	0112372001	02 16 59.1	-04 49 21	10.6	233.9	15579	2.12	0.15	80.28	0.23	...	...	...	...	...
XMMXCS J021705.5-050626.9	0112370101	02 17 05.6	-05 06 27	15.0	69.9	10521	0.88	0.12	35.52	0.27	...	...	...	...	...
XMMXCS J021723.7-051308.9	0112370701	02 17 23.8	-05 13 09	8.2	145.2	35277	0.46	0.04	62.30	0.13	...	...	...	...	...
XMMXCS J021726.6-052502.3	0112370701	02 17 26.7	-05 25 02	5.6	79.8	37423	0.22	0.03	6.84	0.05	...	...	...	...	...
XMMXCS J021755.2-052704.6	0112370701	02 17 55.3	-05 27 05	12.5	236.6	23203	1.59	0.11	57.38	0.40	...	...	...	...	...
XMMXCS J021756.1-044405.1	0112371701	02 17 56.1	-04 44 05	12.0	151.3	10789	2.48	0.22	51.57	0.34	...	...	...	...	...
XMMXCS J021759.3-045215.9	0112370101	02 17 59.3	-04 52 16	7.7	100.5	31545	0.35	0.04	16.08	0.12	...	...	...	...	...
XMMXCS J021817.0-735637.6	0049150301	02 18 17.0	-73 56 38	12.3	280.9	9278	5.96	0.38	157.53	0.40	...	...	...	...	...
XMMXCS J021826.1-043142.3	0112370401	02 18 26.2	-04 31 42	9.3	46.2	11999	0.49	0.08	28.48	0.04	...	...	...	...	...
XMMXCS J021843.8-053257.5	0112370801	02 18 43.9	-05 32 58	12.2	253.4	14713	8.91	0.60	73.60	0.40	...	...	...	...	...
XMMXCS J021850.0-050947.6	0112370301	02 18 50.0	-05 09 48	15.1	73.4	9677	1.08	0.14	20.60	0.28	...	...	...	...	...
XMMXCS J021857.3-051903.3	0112370801	02 18 57.4	-05 19 03	2.9	114.3	35304	0.47	0.05	31.28	0.08	...	...	...	...	...
XMMXCS J021905.3-044829.1	0112370301	02 19 05.3	-04 48 29	13.8	107.8	15516	2.16	0.23	24.16	0.34	...	...	...	...	...
XMMXCS J021915.0-052706.5	0112370801	02 19 15.0	-05 27 07	9.2	83.3	21151	0.45	0.05	27.89	0.08	...	...	...	...	...
XMMXCS J021915.0-045100.6	0112370401	02 19 15.1	-04 51 01	13.6	152.8	8348	8.24	0.72	27.81	0.34	...	...	...	...	...
XMMXCS J021928.7-043253.7	0037982301	02 19 28.8	-04 32 54	8.3	48.4	6635	0.74	0.12	34.50	0.04	...	...	...	...	...
XMMXCS J021928.9-030618.9	0148500201	02 19 29.0	-03 06 19	7.9	73.5	7151	1.43	0.19	31.93	0.08	...	...	...	...	...
XMMXCS J021939.3-032514.8	0037982601	02 19 39.3	-03 25 15	15.9	45.8	2462	2.63	0.45	49.20	0.13	...	...	...	...	...
XMMXCS J021946.5-050751.2	0112370301	02 19 46.5	-05 07 51	8.3	137.8	23822	0.79	0.07	29.62	0.13	...	...	...	...	...
XMMXCS J021951.2-033234.3	0037982601	02 19 51.2	-03 32 34	12.4	101.8	5180	2.71	0.30	29.46	0.34	...	...	...	...	...
XMMXCS J021953.3-030353.3	0148500201	02 19 53.4	-03 03 53	9.7	27.1	6595	0.78	0.18	16.02	0.02	...	...	...	...	...
XMMXCS J021958.6-052335.2	0147111401	02 19 58.7	-05 23 35	12.5	38.3	4562	0.99	0.19	12.37	0.05	...	...	...	...	...
XMMXCS J021959.6-041721.6	0037982301	02 19 59.7	-04 17 22	12.6	95.6	3841	3.22	0.36	26.58	0.21	...	...	...	...	...
XMMXCS J022005.9-025346.5	0148500201	02 20 06.0	-02 53 47	12.3	74.6	5453	4.31	0.56	30.43	0.21	...	...	...	...	...
XMMXCS J022020.6-023847.3	0147110201	02 20 20.7	-02 38 47	12.3	53.6	4722	2.00	0.31	14.79	0.10	...	...	...	...	...

XMMXCS J022023.1-025023.7	0147110201	02 20 23.1	-02 50 24	4.4	129.5	8584	1.73	0.17	76.96	0.11	0.248	0.029	3
XMMXCS J022024.2-040305.3	0037982401	02 20 24.3	-04 03 05	7.9	71.6	11261	0.88	0.12	21.78	0.08	...	...	...
XMMXCS J022028.2-052444.9	0147111401	02 20 28.3	-05 24 45	6.3	51.3	8529	0.75	0.12	29.73	0.06	...	...	...
XMMXCS J022043.1-030114.9	0147110201	02 20 43.2	-03 01 15	11.3	174.4	4558	5.00	0.41	67.46	0.16	...	...	...
XMMXCS J022045.1-032555.8	0037982601	02 20 45.1	-03 25 56	4.3	557.2	12811	5.80	0.26	209.53	0.25	...	...	...
XMMXCS J022129.4-040537.9	0037982401	02 21 29.4	-04 05 38	13.1	92.7	6095	4.72	0.54	45.53	0.21	...	...	...
XMMXCS J022132.9-035323.7	0037982501	02 21 32.8	-03 53 24	4.7	50.5	10078	0.69	0.11	13.10	0.03	0.107	0.022	2
XMMXCS J022205.0-043240.6	0109520601	02 22 05.0	-04 32 41	9.1	315.0	13924	2.89	0.17	82.48	0.16	...	...	...
XMMXCS J022206.5-030311.2	0147110101	02 22 06.6	-03 03 11	13.3	374.0	7408	16.30	0.89	308.37	0.46	...	...	...
XMMXCS J022210.7+430619.1	0002970201	02 22 10.7	+43 06 19	13.0	212.6	8550	3.22	0.24	37.96	0.40	...	...	...
XMMXCS J022222.3-024837.8	0147110101	02 22 22.4	-02 48 38	5.6	32.5	8802	0.49	0.10	8.74	0.01	...	...	...
XMMXCS J022225.4-043735.8	0109520601	02 22 25.4	-04 37 36	8.4	43.2	15295	0.37	0.07	19.00	0.04	...	...	...
XMMXCS J022233.3-045758.7	0111110501	02 22 33.3	-04 57 59	12.1	175.0	11924	2.05	0.17	49.25	0.34	...	...	...
XMMXCS J022234.1-031612.6	0037981101	02 22 34.1	-03 16 13	6.4	33.0	8135	0.46	0.09	7.19	0.03	...	...	...
XMMXCS J022247.0-035148.6	0037980101	02 22 47.1	-03 51 49	2.5	81.1	13453	1.52	0.19	18.30	0.03	0.126	0.032	3
XMMXCS J022251.0-031147.5	0037981101	02 22 51.0	-03 11 48	3.3	116.2	10668	1.38	0.14	37.49	0.08	0.081	0.028	3
XMMXCS J022251.2-041642.5	0109520101	02 22 51.2	-04 16 43	9.8	88.0	14820	0.67	0.08	31.93	0.08	...	...	...
XMMXCS J022258.6-040639.0	0109520101	02 22 58.6	-04 06 39	6.3	91.2	17699	0.56	0.07	21.40	0.08	...	...	...
XMMXCS J022258.8-041609.5	0109520101	02 22 58.8	-04 16 10	8.1	39.4	18424	0.26	0.05	17.03	0.02	...	...	...
XMMXCS J022300.7-031834.2	0037980701	02 23 00.7	-03 18 34	12.4	71.5	4910	2.28	0.30	11.84	0.21	...	...	...
XMMXCS J022307.3-041307.3	0109520101	02 23 07.3	-04 13 07	4.4	171.2	22408	0.94	0.08	42.64	0.11	...	...	...
XMMXCS J022307.9-045930.2	0109520501	02 23 08.0	-04 59 30	10.0	102.6	10715	1.22	0.13	16.37	0.16	...	...	...
XMMXCS J022317.0-030718.5	0037981201	02 23 17.0	-03 07 19	11.1	47.5	4905	1.16	0.19	16.78	0.04	...	...	...
XMMXCS J022333.2+425349.1	0002970201	02 23 33.3	+42 53 49	7.0	2413.5	12451	22.65	0.47	NaN	0.29	...	...	...
XMMXCS J022341.7-043032.0	0109520601	02 23 41.8	-04 30 32	15.4	59.9	4914	1.88	0.28	20.75	0.17	...	...	...
XMMXCS J022341.8-025405.1	0037981601	02 23 41.8	-02 54 05	6.8	53.3	9001	0.91	0.14	23.64	0.06	...	...	...
XMMXCS J022347.5-025133.5	0037981601	02 23 47.5	-02 51 34	7.1	269.1	8680	4.38	0.28	78.31	0.18	0.202	0.027	3
XMMXCS J022348.1-051349.6	0111110401	02 23 48.2	-05 13 50	4.8	79.3	20312	0.44	0.06	25.41	0.05	...	...	...
XMMXCS J022351.0-044910.1	0109520501	02 23 51.0	-04 49 10	7.8	60.5	16525	0.46	0.07	24.83	0.07	...	...	...
XMMXCS J022351.3+424728.4	0002970201	02 23 51.4	+42 47 28	14.1	274.6	7409	153.03	9.80	119.82	0.59	0.020	0.001	1
XMMXCS J022351.4-041842.5	0109520101	02 23 51.4	-04 18 43	11.7	103.9	11776	1.50	0.16	70.75	0.16	...	...	...
XMMXCS J022356.2-030557.1	0037981201	02 23 56.2	-03 05 57	4.2	152.0	10143	1.88	0.17	35.35	0.11	...	...	...
XMMXCS J022357.4-043517.2	0112680501	02 23 57.5	-04 35 17	5.3	164.3	15361	1.40	0.12	50.35	0.11	...	...	...
XMMXCS J022401.9-044132.0	0109520501	02 24 01.9	-04 41 32	13.4	129.9	10800	2.87	0.27	21.96	0.34	0.043	0.001	1
XMMXCS J022408.7+430232.1	0002970201	02 24 08.8	+43 02 32	10.9	71.2	8001	1.43	0.19	25.78	0.11	0.162	0.031	3
XMMXCS J022417.0-050313.0	0111110401	02 24 17.0	-05 03 13	8.0	90.0	18832	0.67	0.08	28.71	0.08	0.179	0.029	3
XMMXCS J022423.0-033645.5	0037980801	02 24 23.0	-03 36 46	8.0	66.4	6156	1.76	0.24	7.71	0.07	...	...	...
XMMXCS J022428.3+183336.6	0150180101	02 24 28.3	+18 33 37	15.8	50.4	5390	2.35	0.38	31.83	0.17	...	...	...
XMMXCS J022434.4-041427.1	0112680301	02 24 34.5	-04 14 27	4.7	340.1	18615	2.23	0.13	108.54	0.21	...	...	...
XMMXCS J022436.8-043815.3	0112681001	02 24 36.8	-04 38 15	13.6	137.4	14360	2.64	0.25	52.42	0.34	...	...	...
XMMXCS J022454.0-032843.4	0037980801	02 24 54.1	-03 28 43	3.7	80.5	9981	1.17	0.15	34.81	0.03	0.164	0.031	3
XMMXCS J022458.8-044204.0	0112681001	02 24 58.8	-04 42 04	13.2	159.3	14849	4.79	0.41	16.19	0.34	...	...	...
XMMXCS J022500.0-040021.8	0112680301	02 25 00.0	-04 00 22	10.9	72.4	9324	0.83	0.11	32.35	0.11	...	...	...

XMMXCS J022508.9-040832.7	0112680201	02 25 09.0	-04 08 33	12.8	87.8	5312	2.78	0.33	30.89	0.21	...	...	...	...	...
XMMXCS J022509.6-041900.6	0112680301	02 25 09.6	-04 19 01	11.6	227.0	10195	3.89	0.28	68.92	0.23	...	...	...	...	...
XMMXCS J022510.2-040139.8	0112680301	02 25 10.3	-04 01 40	11.2	151.4	8301	2.34	0.21	35.43	0.16	0.162	0.031	3	...	...
XMMXCS J022510.9-024429.3	0037981801	02 25 10.9	-02 44 29	13.4	39.8	5988	1.10	0.20	33.13	0.05	...	...	...	...	...
XMMXCS J022529.1-040037.5	0037980301	02 25 29.1	-04 00 38	10.9	230.4	7245	5.01	0.35	56.14	0.23	0.054	0.015	2	...	...
XMMXCS J022539.3-031124.4	0037981301	02 25 39.4	-03 11 24	5.0	1125.7	5467	47.85	1.47	286.10	0.25	...	...	...	...	...
XMMXCS J022540.8-045912.2	0109520301	02 25 40.9	-04 59 12	10.4	55.6	13046	0.62	0.09	25.66	0.06	...	...	...	...	...
XMMXCS J022552.0-034518.0	0037980401	02 25 52.0	-03 45 18	12.9	70.4	5237	1.98	0.27	16.84	0.21	...	...	...	...	...
XMMXCS J022554.8-052022.7	0111110301	02 25 54.8	-05 20 23	13.5	65.9	8313	5.52	0.77	17.89	0.15	0.052	0.019	3	...	...
XMMXCS J022610.7-045812.0	0109520301	02 26 10.7	-04 58 12	8.6	659.3	13802	6.00	0.24	199.75	0.23	0.057	0.014	2	...	...
XMMXCS J022616.3-023954.2	0037981801	02 26 16.3	-02 39 54	10.9	764.3	8992	11.81	0.44	655.84	0.28	0.049	0.014	2	...	...
XMMXCS J022643.1-045913.4	0111110701	02 26 43.1	-04 59 13	10.8	20.6	6770	0.50	0.14	10.69	0.02	...	...	...	...	...
XMMXCS J022658.4-032639.2	0037981001	02 26 58.4	-03 26 39	6.3	27.1	9838	0.35	0.08	34.68	0.02	...	...	...	...	...
XMMXCS J022659.4-043521.2	0112681301	02 26 59.4	-04 35 21	7.2	243.9	11090	3.04	0.21	71.90	0.18	0.070	0.001	1	...	...
XMMXCS J022708.4-043228.1	0112680401	02 27 08.5	-04 32 28	13.1	161.6	10170	4.07	0.35	37.10	0.34	...	...	...	...	...
XMMXCS J022711.1-024904.1	0037981901	02 27 11.1	-02 49 04	2.4	38.7	12349	0.52	0.10	13.33	0.02	...	...	...	...	...
XMMXCS J022719.1-031330.4	0037981501	02 27 19.1	-03 13 30	10.8	59.5	4824	1.54	0.23	8.43	0.06	...	...	...	...	...
XMMXCS J022723.7-051232.4	0111110101	02 27 23.7	-05 12 32	9.4	54.4	11204	0.61	0.09	24.35	0.05	...	...	...	...	...
XMMXCS J022726.3-030138.5	0037981901	02 27 26.4	-03 01 39	11.8	45.6	5359	1.03	0.18	46.02	0.04	...	...	...	...	...
XMMXCS J022741.3-045740.6	0111110101	02 27 41.3	-04 57 41	13.2	79.1	9538	2.18	0.27	23.60	0.21	0.067	0.021	3	...	...
XMMXCS J022744.8-034413.0	0037980501	02 27 44.9	-03 44 13	6.9	40.9	10738	0.60	0.11	27.60	0.03	0.044	0.012	2	...	...
XMMXCS J022801.5-030256.2	0037981501	02 28 01.6	-03 02 56	7.1	64.0	8627	1.09	0.15	22.73	0.07	...	...	...	...	...
XMMXCS J022805.6-051642.2	0111110101	02 28 05.6	-05 16 42	6.8	109.8	13521	1.11	0.12	21.62	0.12	...	...	...	...	...
XMMXCS J022811.8-043843.0	0112680401	02 28 11.8	-04 38 43	9.2	62.5	14208	0.55	0.08	32.92	0.07	...	...	...	...	...
XMMXCS J022849.1-100204.0	0112860101	02 28 49.1	-10 02 04	8.8	69.2	4889	2.05	0.28	32.75	0.07	...	...	...	...	...
XMMXCS J022919.3-090821.3	0112600301	02 29 19.3	-09 08 21	14.1	16.5	1768	3.26	1.02	13.60	0.04	...	...	...	...	...
XMMXCS J022933.2-100541.5	0112860101	02 29 33.3	-10 05 42	10.3	404.2	4283	14.42	0.75	282.06	0.26	...	...	...	...	...
XMMXCS J023345.9-085043.1	0150470601	02 33 46.0	-08 50 43	13.3	188.6	11010	5.55	0.43	41.52	0.34	0.096	0.001	1	...	...
XMMXCS J023400.0-434206.1	0148790101	02 34 00.0	-43 42 06	7.0	47.2	20812	1.03	0.17	26.96	0.03	...	...	...	...	...
XMMXCS J023442.5-433636.6	0148790101	02 34 42.6	-43 36 37	11.7	63.1	16055	1.35	0.19	23.46	0.07	...	...	...	...	...
XMMXCS J023459.3-085058.9	0150470601	02 34 59.3	-08 50 59	6.5	137.4	24395	3.48	0.32	50.96	0.12	...	...	...	...	...
XMMXCS J023627.0+243112.3	0075940301	02 36 27.1	+24 31 12	10.4	93.4	26438	1.00	0.11	18.83	0.11	...	...	...	...	...
XMMXCS J023629.0-521112.7	0098810101	02 36 29.0	-52 11 13	8.5	99.4	11768	0.93	0.10	18.60	0.08	...	...	...	...	...
XMMXCS J023632.4-522333.5	0098810101	02 36 32.3	-52 23 34	5.4	230.4	19653	1.34	0.09	86.35	0.10	...	...	...	...	...
XMMXCS J023650.4-520932.1	0067190101	02 36 50.4	-52 09 32	13.8	136.0	10807	4.23	0.39	70.15	0.34	...	...	...	...	...
XMMXCS J023714.7+242555.2	0075940301	02 37 14.7	+24 25 55	13.5	67.7	18199	1.03	0.14	34.92	0.15	...	...	...	...	...
XMMXCS J023727.2-522035.1	0098810101	02 37 27.3	-52 20 35	11.7	53.0	10907	0.54	0.08	10.46	0.06	0.079	0.024	3	...	...
XMMXCS J024113.4-082619.8	0093630101	02 41 13.4	-08 26 20	11.2	55.8	7148	1.03	0.16	14.21	0.06	...	...	...	...	...
XMMXCS J024144.7-000138.0	0111200101	02 41 44.8	-00 01 38	14.1	76.9	10818	0.91	0.12	13.09	0.28	...	...	...	...	...
XMMXCS J024220.7+000852.6	0111200201	02 42 20.7	+00 08 53	10.9	42.6	15948	0.69	0.12	30.69	0.04	...	...	...	...	...
XMMXCS J024249.6+372130.6	0112550201	02 42 49.6	+37 21 31	7.9	105.1	6491	2.43	0.26	55.77	0.12	...	...	...	...	...
XMMXCS J024253.2+000732.0	0111200201	02 42 53.3	+00 07 32	8.9	0.2	20416	0.13	1.28	1.36	0.22	...	...	...	...	...
XMMXCS J024311.6+372331.3	0112550201	02 43 11.7	+37 23 31	4.6	44.6	7874	1.32	0.23	55.12	0.02	...	...	...	...	...

XMMXCS J024318.2-000751.9	0111200101	02 43 18.1	-00 07 52	11.7	296.3	17376	4.83	0.30	56.77	0.23	...	...	...
XMMXCS J024403.9+372628.4	0112550201	02 44 03.9	+37 26 28	9.2	56.7	5173	1.50	0.23	21.10	0.05	...	...	...
XMMXCS J024409.8+373128.8	0112550201	02 44 09.9	+37 31 29	13.7	818.7	3722	47.07	1.70	270.43	0.57	0.033	0.015	3
XMMXCS J024426.3+371753.4	0112550201	02 44 26.3	+37 17 53	11.7	52.9	3961	2.01	0.32	7.98	0.06	...	...	...
XMMXCS J024749.7+692606.6	0149040201	02 47 49.8	+69 26 07	13.3	190.5	26851	5.99	0.47	18.24	0.34	...	...	...
XMMXCS J024759.6+180736.7	0150870301	02 47 59.7	+18 07 37	13.9	42.3	1999	2.04	0.36	31.17	0.08	...	...	...
XMMXCS J024809.8+311523.4	0111490401	02 48 09.8	+31 15 23	11.2	172.3	14245	3.73	0.31	44.43	0.16	...	...	...
XMMXCS J024836.0+311917.4	0111490401	02 48 36.0	+31 19 17	12.5	274.8	11433	6.47	0.41	90.40	0.40	...	...	...
XMMXCS J024902.2-312010.6	0146510401	02 49 02.3	-31 20 11	11.1	165.7	18531	1.30	0.11	20.19	0.16	0.104	0.001	1
XMMXCS J024922.8+310654.2	0111490401	02 49 22.9	+31 06 54	8.4	55.4	17098	0.96	0.15	17.16	0.05	...	...	...
XMMXCS J025006.5-310400.2	0146510401	02 50 06.5	-31 04 00	10.2	740.9	14541	5.65	0.22	250.08	0.28	...	...	...
XMMXCS J025250.0-012438.0	0151490101	02 52 50.1	-01 24 38	8.1	172.6	12532	1.43	0.12	51.57	0.13	...	...	...
XMMXCS J025602.9+001515.7	0056020301	02 56 02.9	+00 15 16	11.8	101.0	8946	1.86	0.20	19.65	0.16	...	...	...
XMMXCS J025704.4-000530.7	0056020301	02 57 04.5	-00 05 31	14.1	70.2	6694	4.06	0.54	11.83	0.28	0.154	0.001	1
XMMXCS J025721.8+001148.8	0056020301	02 57 21.8	+00 11 49	13.4	65.9	5585	1.67	0.23	19.37	0.15	...	...	...
XMMXCS J030159.0-000221.0	0041170101	03 01 59.0	-00 02 21	14.1	54.6	17356	1.42	0.22	28.24	0.17	...	...	...
XMMXCS J030211.3-000133.5	0041170101	03 02 11.3	-00 01 34	11.5	193.8	25468	1.12	0.09	129.56	0.16	...	...	...
XMMXCS J030212.0+000600.6	0041170101	03 02 12.1	+00 06 01	6.8	88.2	32835	0.45	0.05	19.65	0.08	...	...	...
XMMXCS J030212.0+001119.3	0041170101	03 02 12.1	+00 11 19	7.6	186.4	30537	0.89	0.07	19.58	0.12	...	...	...
XMMXCS J030237.0-000506.4	0041170101	03 02 37.1	-00 05 06	12.8	213.2	21494	2.28	0.17	32.46	0.40	...	...	...
XMMXCS J030248.6+002131.5	0041170101	03 02 48.7	+00 21 32	14.1	628.1	14587	7.93	0.33	NaN	0.60	...	...	...
XMMXCS J030253.9-000606.6	0041170101	03 02 53.9	-00 06 07	14.3	59.5	16237	1.05	0.15	37.68	0.17	...	...	...
XMMXCS J030317.4+001239.7	0041170101	03 03 17.4	+00 12 40	10.9	138.3	18465	1.30	0.12	51.95	0.16	...	...	...
XMMXCS J030614.6-000537.0	0142610101	03 06 14.6	-00 05 37	9.5	1297.7	30810	5.01	0.14	439.85	0.23	0.109	0.001	1
XMMXCS J030817.5-765511.0	0122520201	03 08 17.6	-76 55 11	12.8	103.1	12414	1.65	0.18	18.77	0.34	...	...	...
XMMXCS J030930.4-764115.9	0122520201	03 09 30.5	-76 41 16	13.4	150.8	11326	3.91	0.35	41.93	0.34	...	...	...
XMMXCS J031140.0-770420.0	0122520201	03 11 40.0	-77 04 20	12.5	104.5	10409	1.73	0.19	25.84	0.34	...	...	...
XMMXCS J031220.9-550711.3	0110970101	03 12 21.0	-55 07 11	7.6	130.8	5691	3.34	0.32	58.50	0.12	...	...	...
XMMXCS J031231.7+363406.8	0094360201	03 12 31.7	+36 34 07	11.3	227.7	6043	7.05	0.50	57.00	0.23	...	...	...
XMMXCS J031244.5+363401.2	0094360201	03 12 44.5	+36 34 01	8.8	36.7	7769	0.68	0.13	10.76	0.02	...	...	...
XMMXCS J031427.2-224003.4	0111320501	03 14 27.2	-22 40 03	5.5	71.1	5315	1.75	0.23	32.57	0.05	...	...	...
XMMXCS J031455.5-545741.6	0110970601	03 14 55.6	-54 57 42	13.7	57.2	3211	4.42	0.67	32.63	0.10	...	...	...
XMMXCS J031528.4-551028.2	0129320901	03 15 28.5	-55 10 28	6.5	76.9	7005	1.58	0.20	44.98	0.08	...	...	...
XMMXCS J031627.8-553429.0	0112940201	03 16 27.8	-55 34 29	13.3	51.0	3052	2.66	0.43	17.02	0.10	0.072	0.001	1
XMMXCS J031628.6-551147.1	0129320901	03 16 28.6	-55 11 47	6.7	56.1	7017	1.07	0.16	15.00	0.06	...	...	...
XMMXCS J031651.4-551243.7	0129320801	03 16 51.5	-55 12 44	7.9	35.3	6964	0.75	0.15	17.53	0.03	...	...	...
XMMXCS J032241.9-371813.0	0091770101	03 22 41.9	-37 18 13	13.6	321.4	18315	4.23	0.25	49.07	0.46	0.001	0.001	1
XMMXCS J032316.7-371240.9	0091770101	03 23 16.6	-37 12 41	7.9	495.2	28684	2.35	0.11	72.12	0.19	...	...	...
XMMXCS J032330.7-371613.7	0091770101	03 23 30.7	-37 16 14	3.9	210.7	38859	0.73	0.05	53.93	0.11	...	...	...
XMMXCS J032345.0-493646.4	0140190101	03 23 45.0	-49 36 46	7.5	80.6	18752	0.48	0.06	16.41	0.08	0.087	0.001	1
XMMXCS J032410.1-492143.0	0140190101	03 24 10.2	-49 21 43	12.9	68.7	13222	0.74	0.10	22.78	0.15	...	...	...
XMMXCS J032421.3-372624.4	0091770101	03 24 21.4	-37 26 24	11.3	309.1	21709	1.90	0.11	69.17	0.29	0.258	0.035	3
XMMXCS J032431.0-372822.2	0091770101	03 24 31.0	-37 28 22	14.0	90.4	15342	2.48	0.29	19.07	0.28	...	...	...

XMMXCS J032434.2-372415.7	0091770101	03 24 34.2	-37 24 16	11.4	215.6	19564	1.54	0.11	14.53	0.23	...	...	...
XMMXCS J032535.5+303325.7	0089940201	03 25 35.5	+30 33 26	10.6	153.8	11442	2.06	0.18	19.85	0.16	...	...	...
XMMXCS J032553.4-061723.8	0103861001	03 25 53.4	-06 17 24	11.4	114.0	4278	3.33	0.34	36.60	0.16	0.277	0.037	3
XMMXCS J032609.0-061600.9	0103861001	03 26 09.1	-06 16 01	13.3	79.7	3887	2.79	0.35	36.57	0.21	...	...	...
XMMXCS J032614.8+021655.5	0094382501	03 26 14.9	+02 16 56	8.3	54.3	3480	4.21	0.65	23.33	0.05	...	...	...
XMMXCS J032630.5+484230.9	0101440101	03 26 30.5	+48 42 31	8.3	608.8	29176	2.68	0.11	117.34	0.23	...	...	...
XMMXCS J033133.5-274822.1	0108062301	03 31 33.5	-27 48 22	12.0	113.0	39591	0.37	0.04	35.70	0.34	...	...	...
XMMXCS J033140.6-275537.3	0108062301	03 31 40.7	-27 55 37	12.8	204.3	34897	1.48	0.11	28.68	0.40	...	...	...
XMMXCS J033148.0-275720.3	0108062301	03 31 48.0	-27 57 20	12.7	405.3	36497	2.80	0.15	78.96	0.53	...	...	...
XMMXCS J033151.2-274937.9	0108062301	03 31 51.3	-27 49 38	8.2	292.6	53089	0.68	0.04	42.92	0.16	...	...	...
XMMXCS J033204.3-280416.2	0108060501	03 32 04.4	-28 04 16	16.5	44.9	8774	2.12	0.37	30.27	0.13	...	...	...
XMMXCS J033210.9-275937.5	0108062101	03 32 11.0	-27 59 38	12.0	188.9	42100	1.23	0.10	20.35	0.34	...	...	...
XMMXCS J033225.3-275836.9	0108060701	03 32 25.4	-27 58 37	10.0	451.1	47103	1.29	0.06	72.14	0.26	0.124	0.001	1
XMMXCS J033231.7-280319.5	0108060501	03 32 31.7	-28 03 20	14.7	217.0	18182	119.76	8.70	93.26	0.59	0.127	0.032	3
XMMXCS J033258.2-275857.2	0108062301	03 32 58.3	-27 58 57	12.7	121.0	34214	0.89	0.09	5.67	0.34	0.128	0.032	3
XMMXCS J033310.9-275807.9	0108062101	03 33 10.9	-27 58 08	13.4	229.6	17218	4.14	0.29	31.35	0.40	...	...	...
XMMXCS J033311.8-362325.0	0151370701	03 33 11.9	-36 23 25	14.5	49.0	1820	3.80	0.62	20.73	0.13	...	...	...
XMMXCS J033321.8-274842.5	0108062301	03 33 21.9	-27 48 43	11.9	2079.0	33071	8.37	0.19	401.87	0.28	0.109	0.021	2
XMMXCS J033322.1-275537.5	0108062101	03 33 22.1	-27 55 38	13.8	48.6	16204	1.35	0.22	9.27	0.08	...	...	...
XMMXCS J033322.7-274558.4	0108061801	03 33 22.8	-27 45 58	12.4	159.0	19511	0.85	0.07	18.94	0.34	...	...	...
XMMXCS J033429.1-361418.4	0151370101	03 34 29.1	-36 14 18	12.0	227.0	7214	4.00	0.28	75.01	0.40	...	...	...
XMMXCS J033509.7-253633.8	0111320101	03 35 09.7	-25 36 34	8.9	76.1	12799	1.63	0.21	12.47	0.08	0.074	0.024	3
XMMXCS J033530.4-255514.1	0099010101	03 35 30.5	-25 55 14	10.9	41.7	11276	1.00	0.18	14.66	0.04	...	...	...
XMMXCS J033553.6+002820.4	0134540601	03 35 53.7	+00 28 20	15.1	38.7	9139	0.60	0.11	30.27	0.08	...	...	...
XMMXCS J033558.8-254230.9	0099010101	03 35 58.8	-25 42 31	7.0	92.3	11996	0.86	0.10	26.31	0.08	...	...	...
XMMXCS J033716.9+002338.3	0134540401	03 37 16.9	+00 23 38	13.9	29.3	4225	10.77	2.38	15.57	0.02	...	...	...
XMMXCS J033858.4+001531.2	0036540101	03 38 58.5	+00 15 31	9.7	70.2	10818	0.86	0.12	37.35	0.08	...	...	...
XMMXCS J034212.8-443329.5	0045940301	03 42 12.8	-44 43 30	12.8	115.3	12649	1.93	0.20	15.81	0.34	...	...	...
XMMXCS J034621.0+242813.1	0094780101	03 46 21.1	+24 28 13	14.2	136.0	11680	1.94	0.18	66.20	0.53	...	...	...
XMMXCS J034808.5+241603.0	0094780101	03 48 08.6	+24 16 03	13.2	2224.7	14794	62.39	1.35	NaN	0.57	0.110	0.031	3
XMMXCS J035317.9-000535.6	0134920901	03 53 18.0	-00 05 36	6.5	74.6	11218	1.21	0.16	15.59	0.08	...	...	...
XMMXCS J035322.2-101650.4	0093160201	03 53 22.3	-10 16 50	10.4	51.6	9499	0.62	0.10	24.50	0.06	...	...	...
XMMXCS J035325.2-101152.5	0093160201	03 53 25.3	-10 11 53	14.5	41.8	6660	1.47	0.26	30.67	0.13	...	...	...
XMMXCS J035405.4-203518.5	0150910101	03 54 05.4	-20 35 19	9.5	59.7	8616	1.03	0.15	17.94	0.05	...	...	...
XMMXCS J035415.8-001006.0	0134920901	03 54 15.9	-00 10 06	9.8	437.4	7962	9.74	0.49	124.13	0.24	0.093	0.032	3
XMMXCS J035726.1+011807.8	0094790201	03 57 26.1	+01 18 08	7.3	1244.5	15285	13.40	0.39	437.25	0.29	...	...	...
XMMXCS J035744.5+010137.0	0094790201	03 57 44.5	+01 01 37	10.9	898.0	10380	35.43	1.22	203.37	0.28	...	...	...
XMMXCS J035811.9+102547.9	0064600101	03 58 12.0	+10 25 48	10.4	395.8	6198	9.85	0.52	73.59	0.29	0.204	0.027	3
XMMXCS J035939.8+102538.3	0064600101	03 59 39.9	+10 25 38	11.2	268.3	6380	5.55	0.36	107.54	0.23	...	...	...
XMMXCS J040039.1-674000.3	0110980401	04 00 39.1	-67 40 00	6.3	66.2	24312	0.43	0.06	18.05	0.07	...	...	...
XMMXCS J040903.4-711227.8	0111970301	04 09 03.4	-71 12 28	5.3	27.5	10184	0.38	0.09	25.78	0.01	...	...	...
XMMXCS J041821.0+555329.5	0139760101	04 18 21.0	+55 53 30	13.1	123.6	19824	1.68	0.17	21.07	0.34	...	...	...
XMMXCS J041834.8+282236.8	0086360301	04 18 34.8	+28 22 37	4.7	248.7	50792	0.59	0.04	23.00	0.10	...	...	...

XMMXCS J041848.9+554807.6	0139760101	04 18 49.0	+55 48 08	14.0	216.2	18908	4.48	0.33	22.68	0.59	...	...	...
XMMXCS J041856.0+153247.4	0024140101	04 18 56.1	+15 32 47	13.3	154.1	23142	1.98	0.17	37.82	0.34	...	...	...
XMMXCS J041905.3+154439.7	0024140101	04 19 05.3	+15 44 40	12.4	73.9	24123	0.43	0.06	19.12	0.21	...	...	...
XMMXCS J041925.0+153201.4	0024140101	04 19 25.1	+15 32 01	7.8	104.7	36519	0.45	0.05	31.16	0.12	...	...	...
XMMXCS J041931.2+282054.0	0086360301	04 19 31.2	+28 20 54	14.7	159.6	16212	1.77	0.15	15.68	0.53	...	...	...
XMMXCS J041938.0+142116.4	0141400301	04 19 38.1	+14 21 16	12.3	53.9	5947	1.74	0.27	17.42	0.10	...	...	...
XMMXCS J041939.3+153420.9	0024140101	04 19 39.3	+15 34 21	3.9	202.4	47024	0.70	0.05	22.85	0.11	...	...	...
XMMXCS J041944.9+143905.9	0141400301	04 19 45.0	+14 39 06	5.9	300.1	8234	5.00	0.31	61.39	0.21	...	...	...
XMMXCS J041945.6+021319.0	0152150101	04 19 45.7	+02 13 19	11.4	281.9	11173	1.63	0.10	40.39	0.23	...	...	...
XMMXCS J042021.8+154738.4	0024140101	04 20 21.8	+15 47 38	12.9	175.8	17647	6.53	0.53	30.56	0.34	...	...	...
XMMXCS J042029.2+022645.3	0152150101	04 20 29.2	+02 26 45	13.0	87.4	7485	1.27	0.15	21.60	0.21	0.117	0.032	3
XMMXCS J042216.1+282202.1	0101440701	04 22 16.1	+28 22 02	5.4	131.0	25294	0.62	0.06	57.00	0.11	0.071	0.024	3
XMMXCS J042409.0+145917.4	0101441501	04 24 09.0	+14 59 17	13.8	66.6	13193	0.45	0.06	21.87	0.15	...	...	...
XMMXCS J042421.3+145923.6	0101441501	04 24 21.3	+14 59 24	14.0	97.8	12820	0.87	0.10	36.38	0.28	...	...	...
XMMXCS J042437.1+144331.0	0101441501	04 24 37.2	+14 43 31	6.2	162.5	27599	0.81	0.07	17.35	0.12	...	...	...
XMMXCS J042450.7-570744.3	0112600401	04 24 50.7	-57 07 44	9.3	39.4	5989	2.97	0.55	37.28	0.02	...	...	...
XMMXCS J042451.9+145525.3	0101441501	04 24 51.9	+14 55 25	13.7	85.1	12022	0.96	0.12	23.21	0.21	...	...	...
XMMXCS J042508.8+144305.1	0101440601	04 25 08.9	+14 43 05	13.7	75.5	16704	5.37	0.69	29.68	0.21	...	...	...
XMMXCS J042651.1+170147.4	0056020401	04 26 51.1	+17 01 47	12.4	266.6	8982	5.76	0.37	56.46	0.40	...	...	...
XMMXCS J042743.3-571016.1	0148000601	04 27 43.3	-57 10 16	14.0	66.2	5558	104.95	14.56	27.76	0.27	...	...	...
XMMXCS J042837.9+154825.3	0101440501	04 28 37.8	+15 48 25	9.4	66.5	21553	0.40	0.06	19.76	0.07	...	...	...
XMMXCS J042838.2+160607.6	0101440501	04 28 38.3	+16 06 08	8.4	43.7	26771	0.34	0.06	11.60	0.04	...	...	...
XMMXCS J042920.7+155603.9	0101440501	04 29 20.8	+15 56 04	11.1	49.0	21586	0.55	0.09	27.09	0.04	...	...	...
XMMXCS J042954.7+643722.9	0112290801	04 29 54.8	+64 37 23	14.6	21.6	3277	13.99	3.71	15.00	0.05	...	...	...
XMMXCS J043207.7+644129.6	0112290801	04 32 07.7	+64 41 30	12.8	67.6	6543	1.77	0.24	14.08	0.15	...	...	...
XMMXCS J043224.1+051656.4	0152840101	04 32 24.1	+05 16 56	12.5	188.4	33633	1.66	0.13	20.96	0.34	...	...	...
XMMXCS J043324.4-780747.8	0103862001	04 33 24.5	-78 07 48	8.2	105.3	3709	3.81	0.41	28.62	0.13	...	...	...
XMMXCS J043334.3+051333.2	0152840101	04 33 34.3	+05 13 33	9.6	117.6	52580	0.68	0.07	17.67	0.13	...	...	...
XMMXCS J043338.7+052307.5	0152840101	04 33 38.7	+05 23 08	7.1	275.6	67324	1.11	0.07	30.30	0.18	0.161	0.031	3
XMMXCS J043426.0+243135.3	0152680201	04 34 26.0	+24 31 35	7.2	58.1	10510	0.70	0.10	22.46	0.06	...	...	...
XMMXCS J043428.7+244124.8	0152680701	04 34 28.7	+24 41 25	13.9	42.5	5707	0.90	0.16	14.66	0.08	...	...	...
XMMXCS J043600.6+242853.6	0152680501	04 36 00.7	+24 28 54	14.8	43.1	3271	2.37	0.42	17.26	0.13	...	...	...
XMMXCS J044008.8-432635.8	0104860201	04 40 08.8	-43 26 36	6.7	87.9	8345	1.22	0.14	22.01	0.08	...	...	...
XMMXCS J044135.1-432601.5	0104860201	04 41 35.1	-43 26 02	15.8	34.5	2526	4.40	0.88	16.49	0.08	...	...	...
XMMXCS J045124.8-033759.9	0103863001	04 51 24.8	-03 37 60	11.3	78.6	3209	7.01	0.88	28.94	0.11	...	...	...
XMMXCS J045143.4-300121.5	0153100101	04 51 43.4	-30 01 22	12.8	77.3	4727	2.15	0.27	13.22	0.21	...	...	...
XMMXCS J045438.5-531907.9	0148650101	04 54 38.6	-53 19 08	4.5	65.1	35924	0.22	0.03	36.59	0.06	...	...	...
XMMXCS J045459.9-532945.4	0148650101	04 54 60.0	-53 29 45	10.6	50.7	22591	0.26	0.04	14.39	0.06	...	...	...
XMMXCS J045506.0-532342.5	0148650101	04 55 06.0	-53 23 43	8.1	803.7	25055	3.83	0.14	250.02	0.23	...	...	...
XMMXCS J045511.8-751117.7	0137160201	04 55 11.9	-75 11 18	13.0	210.8	29138	2.30	0.17	35.63	0.40	0.108	0.031	3
XMMXCS J045614.8+302138.5	0101440801	04 56 14.9	+30 21 39	12.9	141.9	47166	0.93	0.08	18.10	0.34	...	...	...
XMMXCS J045629.0-751049.6	0137160201	04 56 29.1	-75 10 50	9.0	128.2	43799	0.91	0.09	31.32	0.13	...	...	...
XMMXCS J045632.3+304101.0	0101440801	04 56 32.3	+30 41 01	10.0	178.6	70749	0.84	0.07	33.06	0.16	...	...	...

XMMXCS J045714.9-752936.5	0137160201	04 57 14.9	-75 29 37	13.6	1050.1	32174	14.92	0.47	707.39	0.57	...	...	...
XMMXCS J045841.5-750447.9	0137160201	04 58 41.5	-75 04 48	11.9	104.6	37476	0.84	0.09	31.66	0.16	0.043	0.018	3
XMMXCS J050548.0+524513.6	0154150401	05 05 48.0	+52 45 14	5.3	47.9	4524	2.67	0.44	21.37	0.02	...	...	...
XMMXCS J050815.0-373559.6	0110980801	05 08 15.1	-37 35 60	8.3	82.8	22286	0.40	0.05	22.43	0.08	...	...	...
XMMXCS J050827.3-373637.2	0110980801	05 08 27.4	-37 36 37	10.7	78.1	16487	0.73	0.09	19.16	0.11	0.053	0.001	1
XMMXCS J051200.6-161433.7	0143370101	05 12 00.6	-16 14 34	13.5	168.5	18764	2.60	0.22	25.35	0.34	0.294	0.027	3
XMMXCS J051257.8-155844.7	0143370101	05 12 57.9	-15 58 45	13.6	94.3	15803	0.72	0.08	13.01	0.21	...	...	...
XMMXCS J051326.3+792919.5	0094400101	05 13 26.3	+79 29 20	13.9	43.3	10490	0.72	0.13	10.24	0.08	...	...	...
XMMXCS J051354.1-160300.2	0143370101	05 13 54.2	-16 03 00	16.8	39.4	9680	1.24	0.23	38.21	0.08	...	...	...
XMMXCS J051509.2-395711.2	0151750101	05 15 09.3	-39 57 11	13.2	325.9	8009	12.25	0.72	125.07	0.46	...	...	...
XMMXCS J051510.9+010609.6	0010620101	05 15 11.0	+01 06 10	7.8	53.1	16231	0.59	0.09	39.03	0.06	...	...	...
XMMXCS J051528.4+793425.4	0094400101	05 15 28.5	+79 34 25	6.6	312.7	20443	1.93	0.12	84.60	0.18	...	...	...
XMMXCS J051536.7-000357.5	0147190101	05 15 36.8	-00 03 58	10.0	229.8	38425	1.70	0.12	23.05	0.23	0.134	0.030	3
XMMXCS J051549.8+794000.9	0094400101	05 15 49.9	+79 40 01	2.2	302.9	27960	1.35	0.08	152.53	0.15	...	...	...
XMMXCS J051554.0+010413.9	0010620101	05 15 54.1	+01 04 14	3.2	53.6	15252	0.59	0.09	34.21	0.02	...	...	...
XMMXCS J051609.9+010946.3	0010620101	05 16 09.9	+01 09 46	8.8	156.7	12019	1.63	0.14	29.02	0.13	...	...	...
XMMXCS J051646.7-000155.5	0147190101	05 16 46.8	-00 01 56	11.3	80.6	41615	0.53	0.07	21.30	0.11	...	...	...
XMMXCS J052104.1-251319.2	0085640101	05 21 04.2	-25 13 19	8.5	45.8	5769	1.02	0.17	34.53	0.04	...	...	...
XMMXCS J052137.6-253326.5	0085640101	05 21 37.6	-25 33 27	14.3	39.8	3250	2.13	0.39	14.63	0.08	...	...	...
XMMXCS J052149.6-363508.7	0065760201	05 21 49.6	-36 35 09	15.7	42.6	7955	0.71	0.13	21.28	0.13	...	...	...
XMMXCS J052306.5-361506.1	0065760201	05 23 06.5	-36 15 06	12.5	127.5	13586	1.82	0.18	21.87	0.34	...	...	...
XMMXCS J052331.2-362323.9	0065760201	05 23 31.3	-36 23 24	7.9	135.4	21531	0.68	0.06	26.82	0.12	...	...	...
XMMXCS J052331.6-363831.5	0065760201	05 23 31.6	-36 38 32	12.9	393.8	15080	4.20	0.22	212.59	0.46	...	...	...
XMMXCS J052402.4-334612.1	0050150301	05 24 02.5	-33 46 12	13.6	79.9	7014	1.28	0.16	14.35	0.21	...	...	...
XMMXCS J052437.3-701349.7	0127720201	05 24 37.3	-70 13 50	2.1	541.3	20942	3.25	0.15	39.92	0.30	...	...	...
XMMXCS J052520.9-335015.5	0149500701	05 25 20.9	-33 50 16	7.8	18.1	7877	0.30	0.09	4.72	0.03	...	...	...
XMMXCS J052526.8-700446.9	0127720201	05 25 26.8	-70 04 47	9.7	108.8	13323	1.08	0.11	7.10	0.13	...	...	...
XMMXCS J052532.1-334846.5	0149500601	05 25 32.2	-33 48 47	7.8	57.8	7263	0.91	0.14	15.30	0.06	...	...	...
XMMXCS J052559.1-334912.0	0149500801	05 25 59.2	-33 49 12	12.6	103.9	10637	4.18	0.45	34.23	0.34	...	...	...
XMMXCS J052607.3-334642.4	0149500801	05 26 07.4	-33 46 42	13.2	48.8	3343	1.76	0.29	13.53	0.08	...	...	...
XMMXCS J052723.2-652153.8	0123720301	05 27 23.3	-65 21 54	9.8	66.1	25657	0.70	0.10	29.94	0.07	...	...	...
XMMXCS J052751.8-653807.1	0133120101	05 27 51.9	-65 38 07	12.3	134.5	20391	1.05	0.10	19.80	0.34	...	...	...
XMMXCS J052802.8-653243.6	0134520301	05 28 02.9	-65 32 44	7.1	84.2	30147	0.77	0.09	15.22	0.08	...	...	...
XMMXCS J052816.3-654058.4	0134520701	05 28 16.4	-65 40 58	14.2	72.2	13919	3.07	0.41	16.10	0.28	...	...	...
XMMXCS J052843.8-655751.8	0104060101	05 28 43.8	-65 57 52	15.9	184.2	9291	2.90	0.23	60.06	0.53	...	...	...
XMMXCS J052852.5-660122.2	0104060101	05 28 52.6	-66 01 22	15.5	211.8	9410	3.66	0.27	26.60	0.59	0.114	0.022	2
XMMXCS J052910.4-653350.1	0155150101	05 29 10.4	-65 33 50	7.4	48.4	3349	1.32	0.22	9.80	0.03	...	...	...
XMMXCS J052922.2-652150.2	0160362701	05 29 22.3	-65 21 50	6.4	144.0	8643	4.81	0.44	40.32	0.12	...	...	...
XMMXCS J053005.9-653743.9	0123720301	05 30 05.9	-65 37 44	13.7	344.2	22140	22.57	1.28	49.77	0.46	...	...	...
XMMXCS J053031.9-660801.5	0104060101	05 30 31.9	-66 08 02	11.5	111.8	16161	0.81	0.08	21.53	0.16	...	...	...
XMMXCS J053033.8-655644.2	0104060101	05 30 33.8	-65 56 44	4.8	459.7	27895	2.19	0.11	126.04	0.14	...	...	...
XMMXCS J053056.5-463036.8	0109460701	05 30 56.6	-46 30 37	9.3	52.1	3691	3.67	0.58	8.90	0.05	...	...	...
XMMXCS J053227.5-655355.7	0104060101	05 32 27.5	-65 53 56	7.8	1880.1	26955	8.58	0.20	569.00	0.29	0.039	0.015	3

XMMXCS J053600.2-012348.8	0112400101	05 36 00.2	-01 23 49	12.1	73.0	5918	4.01	0.53	50.60	0.21	...	...	...
XMMXCS J053611.2-012117.3	0112400101	05 36 11.3	-01 21 17	9.2	83.4	7691	3.53	0.43	26.53	0.08	...	...	...
XMMXCS J053627.4-005925.2	0112400101	05 36 27.4	-00 59 25	13.3	60.6	4435	4.10	0.60	32.50	0.15	...	...	...
XMMXCS J053715.3-641416.7	0126500101	05 37 15.4	-64 14 17	14.3	131.3	6815	2.28	0.22	34.43	0.53	...	...	...
XMMXCS J053718.7-022542.7	0148300101	05 37 18.6	-02 25 43	8.6	57.2	19137	0.68	0.10	12.74	0.05	...	...	...
XMMXCS J053815.4-024203.9	0148300101	05 38 15.5	-02 42 04	13.7	127.0	11880	2.89	0.28	40.14	0.34	...	...	...
XMMXCS J053815.7-022626.4	0148300101	05 38 15.7	-02 26 26	13.1	103.8	13521	2.26	0.24	17.49	0.34	...	...	...
XMMXCS J053924.1-023442.3	0101440301	05 39 24.1	-02 34 42	9.9	270.6	19173	1.76	0.11	81.56	0.16	...	...	...
XMMXCS J053937.3-022826.4	0101440301	05 39 37.3	-02 28 26	15.1	197.0	11015	3.47	0.27	40.73	0.53	...	...	...
XMMXCS J054137.9-015845.7	0112530101	05 41 37.8	-01 58 46	13.3	627.9	17902	55.25	2.29	323.15	0.57	...	...	...
XMMXCS J054148.3-020330.2	0112640201	05 41 48.4	-02 03 30	13.1	121.8	6577	2.45	0.24	26.28	0.34	...	...	...
XMMXCS J054247.1-681740.0	0123510101	05 42 47.1	-68 17 40	6.3	1.1	6868	0.21	0.45	45.70	0.29	...	...	...
XMMXCS J054404.6-011630.2	0149890301	05 44 04.7	-01 16 30	14.0	44.3	5611	1.57	0.27	15.27	0.13	...	...	...
XMMXCS J054543.0-001116.8	0153150101	05 45 43.1	-00 11 17	6.5	69.7	22401	0.52	0.07	12.17	0.07	...	...	...
XMMXCS J054552.4-510051.8	0044740601	05 45 52.4	-51 00 52	13.7	305.3	25459	1.85	0.11	43.89	0.46	...	...	...
XMMXCS J054601.4+000310.6	0153150101	05 46 01.5	+00 03 11	13.3	178.6	14248	3.25	0.26	36.03	0.34	...	...	...
XMMXCS J054611.2-505526.2	0044740601	05 46 11.3	-50 55 26	13.4	179.8	23512	1.10	0.09	27.50	0.34	...	...	...
XMMXCS J054617.0-510744.0	0044740601	05 46 17.0	-51 07 44	10.1	202.6	37695	0.94	0.07	13.96	0.23	...	...	...
XMMXCS J054635.0+000201.3	0153150101	05 46 35.1	+00 02 01	13.8	83.3	14248	1.81	0.22	25.90	0.21	...	...	...
XMMXCS J054639.9-001537.6	0153150101	05 46 40.0	-00 15 38	9.7	177.2	17972	1.39	0.11	16.12	0.13	...	...	...
XMMXCS J054641.3-511054.2	0044740601	05 46 41.4	-51 10 54	8.9	252.1	43213	0.90	0.06	18.49	0.16	...	...	...
XMMXCS J054705.3-711152.9	0153250101	05 47 05.4	-71 11 53	3.4	150.4	48444	0.36	0.03	25.01	0.08	...	...	...
XMMXCS J054710.3-511155.0	0044740601	05 47 10.3	-51 11 55	8.0	2612.2	44749	8.58	0.17	NaN	0.23	0.143	0.031	3
XMMXCS J054716.2-505800.0	0044740601	05 47 16.3	-50 58 00	6.0	312.8	47795	1.13	0.07	78.37	0.18	...	...	...
XMMXCS J054732.7-511014.4	0044740601	05 47 32.8	-51 10 14	6.7	351.6	51920	1.01	0.06	82.15	0.18	0.076	0.024	3
XMMXCS J054754.9-711701.3	0153250101	05 47 54.9	-71 17 01	9.9	265.1	26551	1.20	0.08	67.37	0.16	...	...	...
XMMXCS J054806.1-705737.5	0153250101	05 48 06.1	-70 57 38	13.1	74.1	20722	0.42	0.05	8.63	0.21	...	...	...
XMMXCS J054817.4-505631.9	0044740601	05 48 17.4	-50 56 32	12.1	48.4	28210	0.24	0.04	7.03	0.08	...	...	...
XMMXCS J055331.4+201055.8	0111500101	05 53 31.4	+20 10 56	13.3	117.8	12848	10.29	1.04	20.50	0.34	0.123	0.032	3
XMMXCS J055355.0+201028.1	0111500101	05 53 55.0	+20 10 28	9.0	57.2	17310	2.03	0.31	28.52	0.05	...	...	...
XMMXCS J055512.9+200946.3	0111500101	05 55 13.0	+20 09 46	13.6	102.3	9396	26.75	2.92	24.21	0.34	...	...	...
XMMXCS J055548.6+221756.2	0089370501	05 55 48.7	+22 17 56	11.0	87.1	12229	1.03	0.12	19.05	0.11	...	...	...
XMMXCS J055710.3+535558.5	0111180401	05 57 10.3	+53 55 59	7.6	127.2	15941	154.56	14.96	40.96	0.12	0.049	0.018	3
XMMXCS J055835.1-502341.0	0119100201	05 58 35.1	-50 23 41	11.9	56.1	3925	2.59	0.39	10.34	0.06	...	...	...
XMMXCS J055836.4-503200.6	0129360201	05 58 36.5	-50 32 01	12.3	40.0	4123	1.00	0.18	27.28	0.08	...	...	...
XMMXCS J055902.6-501723.3	0129360201	05 59 02.6	-50 17 23	11.8	131.0	7287	2.58	0.25	45.35	0.16	...	...	...
XMMXCS J055913.8+534557.9	0111180401	05 59 13.8	+53 45 58	13.5	135.0	11058	9.60	0.90	29.08	0.34	0.261	0.027	3
XMMXCS J055919.8-503631.5	0137550601	05 59 19.8	-50 36 32	10.6	45.0	4900	1.00	0.17	14.57	0.04	...	...	...
XMMXCS J055940.4-503201.4	0137550201	05 59 40.5	-50 32 01	5.3	190.4	9509	2.58	0.20	58.95	0.11	0.197	0.030	3
XMMXCS J055953.2-503443.1	0129360201	05 59 53.3	-50 34 43	7.9	108.3	7823	1.41	0.15	15.27	0.12	...	...	...
XMMXCS J060030.2-502057.0	0129360201	06 00 30.3	-50 20 57	9.1	37.0	8614	0.41	0.08	42.14	0.02	...	...	...
XMMXCS J060112.1-503057.0	0137550201	06 01 12.1	-50 30 57	14.1	45.5	4759	1.57	0.27	20.01	0.13	...	...	...
XMMXCS J061350.0+710335.9	0009220301	06 13 50.0	+71 03 36	8.7	25.1	1286	5.31	1.29	20.77	0.02	...	...	...

XMMXCS J061555.0+782012.5	0110930101	06 15 55.1	+78 20 12	8.4	127.7	9653	1.93	0.19	11.80	0.13	...	...	...	...	...
XMMXCS J061609.4+711540.1	0009220601	06 16 09.5	+71 15 40	13.7	51.7	4050	1.97	0.31	28.53	0.10	...	...	...	...	...
XMMXCS J062210.7+781831.0	0110930101	06 22 10.8	+78 18 31	11.0	1550.7	10154	115.90	3.02	382.31	0.28	0.093	0.032	3	...	...
XMMXCS J063712.2+060130.0	0001730601	06 37 12.2	+06 01 30	7.2	94.7	13046	3.60	0.41	33.68	0.08	...	...	...	...	...
XMMXCS J063712.9+060418.5	0001730601	06 37 12.9	+06 04 19	4.7	384.5	16229	13.78	0.74	93.29	0.21	...	...	...	...	...
XMMXCS J063945.9+821849.6	0029340101	06 39 46.0	+82 18 50	4.2	1150.0	16937	58.06	1.76	607.88	0.25	...	...	...	...	...
XMMXCS J063951.5+095502.9	0011420101	06 39 51.5	+09 55 03	13.4	75.6	15506	1.28	0.16	12.29	0.21	...	...	...	...	...
XMMXCS J063952.7+094955.5	0011420101	06 39 52.8	+09 49 56	12.5	40.7	17520	1.12	0.20	13.19	0.08	...	...	...	...	...
XMMXCS J064010.3+093933.7	0011420101	06 40 10.3	+09 39 34	14.0	109.2	16095	3.54	0.37	53.96	0.53	...	...	...	...	...
XMMXCS J064021.4+094415.0	0011420101	06 40 21.4	+09 44 15	8.6	861.5	25013	4.80	0.17	308.67	0.23	...	...	...	...	...
XMMXCS J064023.4+822858.3	0029340101	06 40 23.4	+82 28 58	13.1	153.6	9796	2.16	0.19	38.78	0.34	...	...	...	...	...
XMMXCS J064035.2+093904.3	0011420101	06 40 35.2	+09 39 04	12.1	68.7	18018	0.55	0.07	18.48	0.15	...	...	...	...	...
XMMXCS J064105.4+100023.8	0011420101	06 41 05.4	+10 00 24	10.9	99.2	15420	0.82	0.09	36.60	0.11	...	...	...	...	...
XMMXCS J064246.4+822837.5	0029340101	06 42 46.4	+82 28 38	12.9	122.9	8710	1.94	0.19	22.78	0.34	0.127	0.032	3	...	...
XMMXCS J064424.1+822634.0	0029340101	06 44 24.1	+82 26 34	12.2	289.8	9878	4.92	0.31	79.73	0.40	0.247	0.029	3	...	...
XMMXCS J064637.6-441535.8	0112450601	06 46 37.6	-44 15 36	16.0	330.1	1090	56.71	3.30	720.96	0.50	...	...	...	...	...
XMMXCS J064915.1-641224.2	0148580201	06 49 15.1	-64 12 24	5.8	55.0	8428	0.89	0.14	18.41	0.03	...	...	...	...	...
XMMXCS J065046.2+742838.1	0144230101	06 50 46.2	+74 28 38	6.5	190.9	16786	2.59	0.20	44.42	0.12	...	...	...	...	...
XMMXCS J065332.0-240331.7	0092790101	06 53 32.1	-24 03 32	12.2	53.3	4515	3.10	0.49	16.55	0.10	...	...	...	...	...
XMMXCS J065444.8-235735.4	0092790101	06 54 44.8	-23 57 35	7.5	34.8	8375	1.02	0.20	5.90	0.03	...	...	...	...	...
XMMXCS J065817.0-285145.4	0069750101	06 58 17.1	-28 51 45	7.9	53.3	29116	0.57	0.09	26.03	0.06	...	...	...	...	...
XMMXCS J065928.0-285705.6	0069750101	06 59 28.1	-28 57 06	11.1	73.0	18344	1.44	0.19	12.96	0.11	...	...	...	...	...
XMMXCS J070736.8-493614.6	0110890201	07 07 36.8	-49 36 15	10.9	147.0	17392	1.27	0.11	61.75	0.16	0.044	0.001	1	...	...
XMMXCS J070741.7-492523.6	0110890201	07 07 41.8	-49 25 24	12.3	122.0	15861	0.89	0.09	13.17	0.34	...	...	...	...	...
XMMXCS J070830.9-491951.6	0148010301	07 08 31.0	-49 19 52	13.3	545.8	31426	3.47	0.15	51.35	0.57	0.045	0.001	1	...	...
XMMXCS J070830.9-494643.3	0148010301	07 08 31.0	-49 46 43	13.7	210.2	27373	2.24	0.17	41.48	0.40	...	...	...	...	...
XMMXCS J070837.5+203303.6	0093190501	07 08 37.5	+20 33 04	8.6	403.8	18321	2.88	0.15	140.43	0.24	...	...	...	...	...
XMMXCS J070846.3+204052.6	0093190501	07 08 46.4	+20 40 53	7.7	125.0	18973	0.90	0.09	27.71	0.12	0.071	0.024	3	...	...
XMMXCS J070848.2-494337.2	0110890201	07 08 48.2	-49 43 37	10.6	119.7	21184	0.59	0.06	29.85	0.16	...	...	...	...	...
XMMXCS J070857.0+202620.7	0093190501	07 08 57.1	+20 26 21	10.4	62.0	16235	0.63	0.09	24.58	0.07	0.137	0.020	2	...	...
XMMXCS J070857.5-493004.8	0148010301	07 08 57.6	-49 30 05	4.1	148.2	67374	0.24	0.02	42.60	0.11	...	...	...	...	...
XMMXCS J070902.3-492305.5	0148010301	07 09 02.4	-49 23 06	10.6	980.9	42534	3.14	0.10	129.25	0.28	...	...	...	...	...
XMMXCS J070913.7-492010.0	0148010301	07 09 13.7	-49 20 10	14.0	288.3	31125	2.55	0.16	41.35	0.59	...	...	...	...	...
XMMXCS J070928.4-492907.4	0110890201	07 09 28.4	-49 29 07	8.7	215.7	28055	0.91	0.07	51.67	0.16	...	...	...	...	...
XMMXCS J070932.0+202431.0	0093190501	07 09 32.0	+20 24 31	12.5	562.3	11970	8.87	0.39	193.78	0.57	...	...	...	...	...
XMMXCS J070933.8-492611.0	0148010301	07 09 33.8	-49 26 11	11.0	976.3	41665	3.13	0.10	164.24	0.28	...	...	...	...	...
XMMXCS J071006.4+203739.3	0093190501	07 10 06.5	+20 37 39	12.8	57.7	9115	0.65	0.10	21.46	0.10	...	...	...	...	...
XMMXCS J071735.0+660458.0	0143430101	07 17 35.1	+66 04 58	12.4	125.2	5635	3.53	0.34	18.08	0.34	...	...	...	...	...
XMMXCS J071954.6-312557.3	0156960401	07 19 54.6	-31 25 57	6.5	763.9	27715	4.63	0.17	61.39	0.29	...	...	...	...	...
XMMXCS J071955.9-311428.1	0156960401	07 19 56.0	-31 14 28	12.9	361.7	12283	4.76	0.26	59.12	0.46	...	...	...	...	...
XMMXCS J072006.7-312144.4	0164560501	07 20 06.7	-31 21 44	5.7	96.0	18317	0.58	0.07	27.40	0.05	...	...	...	...	...
XMMXCS J072020.1-313507.3	0156960401	07 20 20.1	-31 35 07	9.4	92.7	17663	0.58	0.07	23.23	0.08	...	...	...	...	...
XMMXCS J072109.1+655205.6	0143430101	07 21 09.2	+65 52 06	13.0	118.8	6741	6.35	0.64	25.74	0.34	...	...	...	...	...

XMMXCS J072118.9-313043.6	0156960401	07 21 19.0	-31 30 44	12.5	61.8	13380	1.10	0.16	13.87	0.15	...	...	...
XMMXCS J072825.8+685748.5	0141150201	07 28 25.9	+68 57 49	14.0	58.5	11655	36.14	5.37	18.41	0.17	...	...	...
XMMXCS J073417.1+320439.6	0123710101	07 34 17.1	+32 04 40	13.2	161.5	24704	2.46	0.21	46.68	0.34	...	...	...
XMMXCS J073426.5+433511.9	0083000101	07 34 26.5	+43 35 12	13.6	337.7	9943	6.70	0.38	98.53	0.46	...	...	...
XMMXCS J073439.7+315741.6	0123710101	07 34 39.8	+31 57 42	5.6	104.7	38044	3.74	0.40	17.16	0.11	...	...	...
XMMXCS J073446.5+434447.0	0083000101	07 34 46.5	+43 44 47	6.4	199.4	18476	2.03	0.15	19.49	0.12	...	...	...
XMMXCS J073455.3+313842.2	0123710101	07 34 55.4	+31 38 42	14.0	94.0	19758	6.01	0.69	44.53	0.28	...	...	...
XMMXCS J073504.1+314442.1	0123710101	07 35 04.2	+31 44 42	9.4	43.2	27912	0.48	0.08	15.03	0.04	...	...	...
XMMXCS J073509.7+315114.4	0112880801	07 35 09.8	+31 51 14	6.8	38.3	35702	0.16	0.03	40.88	0.03	...	...	...
XMMXCS J073521.7+435310.5	0083000101	07 35 21.7	+43 53 11	8.8	79.1	17165	0.76	0.10	13.54	0.08	...	...	...
XMMXCS J073552.8+434627.0	0083000101	07 35 52.9	+43 46 27	6.0	144.0	21515	0.90	0.08	43.28	0.12	...	...	...
XMMXCS J073601.7+433245.8	0083000101	07 36 01.7	+43 32 46	13.6	89.8	10941	5.41	0.63	16.74	0.21	0.115	0.001	1
XMMXCS J073603.7+433911.9	0083000101	07 36 03.8	+43 39 12	9.1	1945.9	16549	17.52	0.41	NaN	0.23	...	...	...
XMMXCS J073623.8+435133.1	0083000101	07 36 23.9	+43 51 33	13.3	85.9	10549	3.79	0.45	12.26	0.21	...	...	...
XMMXCS J073636.6+434315.5	0083000101	07 36 36.6	+43 43 16	13.5	152.5	9486	8.74	0.77	38.68	0.34	...	...	...
XMMXCS J073947.4+052519.6	0123940201	07 39 47.4	+05 25 20	13.9	81.9	22037	1.13	0.14	24.02	0.21	...	...	...
XMMXCS J074048.0+743711.4	0123100101	07 40 48.1	+74 37 11	13.5	147.2	17145	2.10	0.19	12.10	0.34	...	...	...
XMMXCS J074052.3+743137.2	0123100101	07 40 52.4	+74 31 37	13.0	142.7	19720	1.99	0.18	8.31	0.34	...	...	...
XMMXCS J074412.0+033006.9	0111460101	07 44 12.1	+03 30 07	7.6	145.5	12450	3.20	0.29	49.35	0.12	...	...	...
XMMXCS J074519.2+033541.5	0111460101	07 45 19.2	+03 35 42	10.1	45.3	13432	0.93	0.16	26.39	0.04	...	...	...
XMMXCS J074528.1+742517.4	0123100101	07 45 28.1	+74 25 17	10.2	120.6	21858	1.04	0.10	19.62	0.16	...	...	...
XMMXCS J074528.3+280010.3	0006010301	07 45 28.4	+28 00 10	2.5	1853.6	29087	8.60	0.20	660.69	0.30	...	...	...
XMMXCS J074534.4+742202.1	0123100101	07 45 34.3	+74 22 02	13.2	113.9	15809	1.15	0.12	40.71	0.34	...	...	...
XMMXCS J074534.9+275254.4	0006010301	07 45 35.0	+27 52 54	9.4	67.1	18572	0.71	0.10	35.43	0.07	...	...	...
XMMXCS J074554.5-674647.8	0134561301	07 45 54.6	-67 46 48	12.4	132.9	9122	9.55	0.90	60.96	0.34	...	...	...
XMMXCS J074723.6+743604.4	0123100101	07 47 23.7	+74 36 04	13.4	226.3	13458	2.89	0.21	10.69	0.40	...	...	...
XMMXCS J074805.8-673115.8	0160760601	07 48 05.9	-67 31 16	14.1	74.4	15830	1.17	0.15	25.44	0.28	...	...	...
XMMXCS J074812.6-674812.5	0160760101	07 48 12.7	-67 48 13	3.7	115.5	38398	1.51	0.15	17.68	0.08	...	...	...
XMMXCS J074825.4-673942.4	0134561301	07 48 25.4	-67 39 42	5.7	21.2	3540	0.95	0.25	26.25	0.01	...	...	...
XMMXCS J074921.2-674951.4	0160761301	07 49 21.2	-67 49 51	6.5	898.9	50846	5.50	0.19	334.91	0.29	0.274	0.037	3
XMMXCS J074943.7-675125.5	0134562401	07 49 43.7	-67 51 26	7.9	26.1	3395	2.60	0.62	22.39	0.02	...	...	...
XMMXCS J075014.1-675522.4	0160760601	07 50 14.1	-67 55 22	13.9	61.3	16500	8.27	1.20	32.75	0.15	...	...	...
XMMXCS J075031.9+145044.6	0109510301	07 50 31.9	+14 50 45	12.7	722.0	8880	21.46	0.83	NaN	0.57	...	...	...
XMMXCS J075043.2-673958.7	0160761301	07 50 43.2	-67 39 59	13.3	224.5	34089	2.28	0.16	25.71	0.40	...	...	...
XMMXCS J075046.2+144520.2	0109510301	07 50 46.2	+14 45 20	7.6	306.1	14038	6.55	0.40	43.68	0.18	0.077	0.024	3
XMMXCS J075056.9-675109.9	0123500101	07 50 57.0	-67 51 10	15.7	87.6	3918	46.91	5.57	68.76	0.28	...	...	...
XMMXCS J075145.5+144711.0	0109510301	07 51 45.5	+14 47 11	7.3	206.7	17124	2.64	0.20	50.10	0.18	...	...	...
XMMXCS J075148.5+144956.5	0109510301	07 51 48.5	+14 49 57	9.3	36.3	15566	0.68	0.13	11.60	0.02	...	...	...
XMMXCS J075427.9+220952.1	0110070401	07 54 27.9	+22 09 52	13.1	275.1	10316	7.60	0.49	202.37	0.40	...	...	...
XMMXCS J075433.7+214839.3	0110070401	07 54 33.7	+21 48 39	13.6	42.7	9664	1.35	0.24	11.95	0.08	...	...	...
XMMXCS J075457.7+221313.2	0110070401	07 54 57.7	+22 13 13	13.3	44.9	8546	1.29	0.22	26.06	0.08	...	...	...
XMMXCS J075534.3+220240.2	0110070401	07 55 34.3	+22 02 40	7.2	53.2	12239	0.96	0.15	37.64	0.06	...	...	...
XMMXCS J075602.0+215849.5	0110070401	07 56 02.1	+21 58 50	13.2	75.2	7109	3.43	0.44	39.18	0.21	...	...	...

XMMXCS J080207.6-395937.1	0157160501	08 02 07.7	-39 59 37	16.6	452.1	3856	11.10	0.55	NaN	0.64	...	...	...	...	...	...
XMMXCS J080226.5-394035.6	0158160201	08 02 26.5	-39 40 36	10.2	114.2	28197	0.44	0.05	16.17	0.16	...	...	...	...	...	...
XMMXCS J080247.4-401009.1	0159360301	08 02 47.4	-40 10 09	13.5	127.8	10752	3.04	0.29	20.32	0.34	...	...	...	...	...	...
XMMXCS J080322.0-400004.6	0158160201	08 03 22.0	-40 00 05	13.6	399.3	24227	79.68	4.19	101.26	0.46	...	...	...	...	...	...
XMMXCS J080331.7-395750.3	0158160201	08 03 31.8	-39 57 50	13.8	151.9	25737	1.97	0.17	53.03	0.34	...	...	...	...	...	...
XMMXCS J080344.8-400719.1	0157160901	08 03 44.9	-40 07 19	7.4	108.6	28112	0.53	0.06	34.63	0.12	...	...	...	...	...	...
XMMXCS J080344.9-401345.1	0159360401	08 03 45.0	-40 13 45	13.2	215.1	11808	5.64	0.41	27.71	0.40	...	...	...	...	...	...
XMMXCS J080411.2-395644.1	0095810401	08 04 11.3	-39 56 44	7.8	62.1	30539	0.89	0.13	12.60	0.07	...	...	...	...	...	...
XMMXCS J080509.4-763240.7	0205770101	08 05 09.5	-76 32 41	8.1	207.1	54189	0.45	0.03	36.92	0.16	...	...	...	...	...	...
XMMXCS J080513.7-281744.6	0057570101	08 05 13.8	-28 17 45	11.5	161.4	10766	1.86	0.16	55.55	0.16	0.065	0.021	3			
XMMXCS J080524.8-763839.2	0205770101	08 05 24.8	-76 38 39	9.8	369.2	50875	1.00	0.05	67.65	0.16	...	...	...	...	...	...
XMMXCS J080532.0+152136.9	0150800101	08 05 32.1	+15 21 37	13.7	86.7	8061	1.59	0.19	23.21	0.21	...	...	...	...	...	...
XMMXCS J080613.2+152243.8	0150800101	08 06 13.3	+15 22 44	5.3	153.6	17491	1.27	0.11	21.53	0.11	0.319	...	3			
XMMXCS J080633.4+153224.5	0150800101	08 06 33.5	+15 32 25	5.5	83.0	20288	0.78	0.10	20.42	0.05	0.252	0.035	3			
XMMXCS J080635.4+650336.2	0094400301	08 06 35.5	+65 03 36	13.5	104.4	8100	5.01	0.54	19.10	0.34	...	...	...	...	...	...
XMMXCS J080713.6+152658.8	0150800101	08 07 13.7	+15 26 59	12.2	722.1	12266	57.35	2.21	121.53	0.57	0.065	0.021	3			
XMMXCS J080752.5-762335.9	0205770101	08 07 52.5	-76 23 36	8.5	53.1	54526	0.19	0.03	12.83	0.05	0.280	0.037	3			
XMMXCS J080803.3+390717.7	0138951401	08 08 03.3	+39 07 18	8.3	246.9	3758	9.35	0.63	150.55	0.16	0.072	0.024	3			
XMMXCS J080829.9-762847.5	0205770101	08 08 30.0	-76 28 48	4.8	882.6	71390	1.92	0.07	258.31	0.25	...	...	...	...	...	...
XMMXCS J080854.4-491345.1	0066940101	08 08 54.4	-49 13 45	12.7	208.8	15332	3.18	0.24	53.64	0.40	...	...	...	...	...	...
XMMXCS J080858.6-761950.2	0205770101	08 08 58.7	-76 19 50	13.3	192.6	38714	0.57	0.04	25.23	0.34	...	...	...	...	...	...
XMMXCS J080944.7-473137.1	0112670501	08 09 44.8	-47 31 37	11.6	224.4	12837	3.08	0.22	58.57	0.23	...	...	...	...	...	...
XMMXCS J080949.0-491224.9	0066940101	08 09 49.0	-49 12 25	3.8	341.9	30939	1.81	0.10	111.00	0.15	...	...	...	...	...	...
XMMXCS J080949.0-471655.5	0112670201	08 09 49.1	-47 16 56	4.4	130.8	14064	3.51	0.33	82.39	0.11	...	...	...	...	...	...
XMMXCS J081044.7-492359.2	0066940101	08 10 44.7	-49 23 59	12.2	3084.7	16425	67.90	1.24	NaN	0.57	0.065	0.001	1			
XMMXCS J081101.8-472405.0	0112670501	08 11 01.8	-47 24 05	15.7	38.2	5712	2.39	0.45	32.53	0.08	...	...	...	...	...	...
XMMXCS J081128.6+275641.6	0152530101	08 11 28.7	+27 56 42	13.8	127.9	11254	2.55	0.25	17.24	0.34	...	...	...	...	...	...
XMMXCS J081507.8-191656.3	0150190301	08 15 07.8	-19 16 56	13.6	124.1	5529	13.66	1.34	60.68	0.34	...	...	...	...	...	...
XMMXCS J081515.6-190331.4	0150190301	08 15 15.7	-19 03 31	2.1	119.7	7714	2.83	0.28	10.18	0.08	...	...	...	...	...	...
XMMXCS J081518.6-490437.3	0111971001	08 15 18.6	-49 04 37	8.7	157.6	11784	1.72	0.15	24.28	0.13	...	...	...	...	...	...
XMMXCS J081548.5-490510.1	0111971001	08 15 48.6	-49 05 10	9.5	78.7	12207	0.77	0.10	14.24	0.08	...	...	...	...	...	...
XMMXCS J081554.3-190346.9	0150190301	08 15 54.3	-19 03 47	11.2	106.0	7642	4.35	0.47	55.14	0.16	...	...	...	...	...	...
XMMXCS J081556.3-491847.5	0111971001	08 15 56.4	-49 18 48	8.2	138.7	13518	1.17	0.11	38.82	0.13	...	...	...	...	...	...
XMMXCS J081626.0-491503.5	0111971001	08 16 26.1	-49 15 04	11.1	203.6	11405	2.33	0.18	58.63	0.23	...	...	...	...	...	...
XMMXCS J081831.2+704715.4	0112520601	08 18 31.3	+70 47 15	6.8	117.2	6537	2.94	0.30	31.76	0.12	0.189	0.028	3			
XMMXCS J082015.4+705240.6	0112520601	08 20 15.5	+70 52 41	11.0	76.2	4337	2.42	0.31	17.82	0.11	...	...	...	...	...	...
XMMXCS J083025.8+524129.1	0092800201	08 30 25.8	+52 41 29	12.1	3886.6	37575	16.59	0.27	NaN	0.57	...	...	...	...	...	...
XMMXCS J083054.3+524538.9	0092800201	08 30 54.4	+52 45 39	7.1	63.1	52618	0.27	0.04	35.32	0.07	...	...	...	...	...	...
XMMXCS J083115.4+523453.8	0092800201	08 31 15.4	+52 34 54	11.1	263.1	38806	1.26	0.08	50.42	0.23	...	...	...	...	...	...
XMMXCS J083147.8+525036.1	0092800201	08 31 47.8	+52 50 36	5.4	668.9	53061	1.86	0.07	251.15	0.25	...	...	...	...	...	...
XMMXCS J083154.4+523217.7	0092800201	08 31 54.4	+52 32 18	13.1	180.0	29828	1.40	0.11	30.92	0.34	0.141	0.001	1			
XMMXCS J083213.6+524830.2	0092800201	08 32 13.6	+52 48 30	5.8	360.8	51116	0.85	0.05	253.78	0.21	...	...	...	...	...	...
XMMXCS J083215.3+525808.9	0092800201	08 32 15.3	+52 58 09	13.8	104.7	24555	0.69	0.07	8.90	0.34	...	...	...	...	...	...

XMMXCS J083216.6+523201.8	0092800201	08 32 16.6	+52 32 02	14.3	110.1	24705	1.23	0.13	29.85	0.53	...	...	...
XMMXCS J083237.0-225733.2	0149160201	08 32 37.1	-22 57 33	10.5	101.8	13802	0.98	0.11	50.18	0.16	0.033	0.015	3
XMMXCS J083352.5-230510.1	0149160201	08 33 52.6	-23 05 10	9.7	50.1	11995	0.56	0.09	33.74	0.05	...	...	...
XMMXCS J083414.8-225235.6	0149160201	08 34 14.8	-22 52 36	13.3	218.5	8770	4.58	0.33	55.38	0.40	0.069	0.014	2
XMMXCS J083454.8+553420.3	0143653901	08 34 54.9	+55 34 20	12.0	5497.7	3840	219.25	3.00	NaN	0.57	0.182	0.028	3
XMMXCS J083604.2-131043.1	0128530301	08 36 04.2	-13 10 43	10.0	83.4	15508	0.96	0.12	21.87	0.11	...	...	...
XMMXCS J083606.0-125305.8	0144920201	08 36 06.0	-12 53 06	13.6	62.1	7680	0.92	0.13	41.57	0.15	...	...	...
XMMXCS J083615.3-125203.0	0128530301	08 36 15.4	-12 52 03	13.5	350.6	13328	4.22	0.24	51.85	0.46	...	...	...
XMMXCS J083637.8-131033.7	0128530301	08 36 37.8	-13 10 34	6.1	80.1	23424	0.44	0.05	25.87	0.08	...	...	...
XMMXCS J083724.3+553250.4	0143653901	08 37 24.3	+55 32 50	11.6	290.3	4587	11.77	0.73	154.49	0.23	...	...	...
XMMXCS J083731.4-130659.1	0128530301	08 37 31.4	-13 06 59	13.6	80.7	13739	1.68	0.21	17.58	0.21	...	...	...
XMMXCS J083856.2+253806.7	0025540301	08 38 56.3	+25 38 07	10.4	57.2	4943	1.70	0.26	31.27	0.06	...	...	...
XMMXCS J083901.2+705003.7	0112620101	08 39 01.3	+70 50 04	12.2	110.2	14098	0.92	0.10	38.55	0.34	...	...	...
XMMXCS J083904.2+192304.8	0101440401	08 39 04.2	+19 23 05	15.8	91.7	10861	5.56	0.64	33.06	0.28	...	...	...
XMMXCS J083913.9+704803.1	0112620101	08 39 14.0	+70 48 03	12.1	129.7	14417	1.51	0.14	13.14	0.34	...	...	...
XMMXCS J083926.0+193657.8	0101440401	08 39 26.0	+19 36 58	8.8	138.0	25633	0.68	0.06	39.68	0.13	...	...	...
XMMXCS J083945.7+483904.3	0111971301	08 39 45.8	+48 39 04	13.9	80.3	1370	10.02	1.25	41.95	0.21	...	...	...
XMMXCS J084309.2-134345.0	0113041401	08 43 09.3	-13 43 45	10.0	934.4	7060	21.30	0.72	486.23	0.28	...	...	...
XMMXCS J084729.5+741320.2	0025540401	08 47 29.5	+74 13 20	7.8	25.9	7855	0.87	0.21	28.87	0.02	...	...	...
XMMXCS J084925.4+735439.2	0025541701	08 49 25.5	+73 54 39	12.5	57.0	3133	2.90	0.44	20.78	0.10	...	...	...
XMMXCS J084958.1+445947.4	0085150101	08 49 58.1	+44 59 47	12.4	406.1	20078	3.38	0.18	106.71	0.53	...	...	...
XMMXCS J085104.6+114209.7	0109461001	08 51 04.6	+11 42 10	7.3	23.2	5609	0.50	0.13	13.74	0.02	...	...	...
XMMXCS J085124.4+115748.9	0109461001	08 51 24.5	+11 57 49	10.9	45.4	4710	1.21	0.21	32.38	0.04	...	...	...
XMMXCS J085213.2+114631.2	0109461001	08 52 13.2	+11 46 31	11.3	59.9	4777	3.21	0.47	25.73	0.06	...	...	...
XMMXCS J085729.5+090635.0	0148740101	08 57 29.5	+09 06 35	3.1	107.9	4974	3.29	0.35	68.98	0.08	...	...	...
XMMXCS J085740.3+090112.8	0148740101	08 57 40.3	+09 01 13	4.8	99.8	4326	3.58	0.40	51.17	0.05	...	...	...
XMMXCS J091145.7+525154.1	0143150301	09 11 45.7	+52 51 54	13.7	21.4	2951	2.58	0.69	35.57	0.02	...	...	...
XMMXCS J091821.8+211447.5	0149170501	09 18 21.8	+21 14 48	6.7	345.7	7156	6.29	0.36	204.30	0.18	...	...	...
XMMXCS J091913.7-072622.6	0072340601	09 19 13.8	-07 26 23	13.1	126.1	2617	13.93	1.35	101.82	0.34	...	...	...
XMMXCS J091938.8+371614.1	0149010201	09 19 38.9	+37 16 14	12.8	84.8	23579	0.97	0.12	12.80	0.21	...	...	...
XMMXCS J092018.9+370618.0	0149010201	09 20 18.9	+37 06 18	6.3	30355.2	40616	82.93	0.48	NaN	0.29	0.235	0.001	1
XMMXCS J092026.3+744835.7	0058940101	09 20 26.4	+74 48 36	12.9	88.3	11041	1.33	0.16	37.78	0.21	0.141	0.031	3
XMMXCS J092036.7-630959.5	0051590101	09 20 36.8	-63 09 60	15.4	488.0	14780	4.70	0.22	NaN	0.64	...	...	...
XMMXCS J092042.4+372523.4	0149010201	09 20 42.4	+37 25 23	14.1	101.1	19000	0.87	0.10	28.46	0.53	...	...	...
XMMXCS J092114.4+370129.8	0149010201	09 21 14.5	+37 01 30	12.2	316.8	21183	2.13	0.13	47.50	0.46	0.253	0.035	3
XMMXCS J092119.1+371721.9	0149010201	09 21 19.1	+37 17 22	10.2	19.5	23686	0.28	0.08	42.39	0.02	...	...	...
XMMXCS J092136.7+372000.7	0149010201	09 21 36.8	+37 20 01	14.6	67.9	13773	1.84	0.25	13.95	0.27	...	...	...
XMMXCS J092229.1+745232.6	0058940101	09 22 29.2	+74 52 33	7.1	80.4	17176	0.73	0.09	16.51	0.08	...	...	...
XMMXCS J092307.3+745316.4	0058940101	09 23 07.3	+74 53 17	7.2	105.7	17139	0.87	0.09	19.12	0.12	...	...	...
XMMXCS J092322.2-630455.5	0051590101	09 23 22.2	-63 04 56	13.9	425.4	22351	5.21	0.27	232.40	0.53	0.049	0.018	3
XMMXCS J092328.5-632946.8	0051590101	09 23 28.6	-63 29 47	13.5	300.8	25765	4.10	0.25	61.10	0.46	...	...	...
XMMXCS J092411.6+745843.7	0058940101	09 24 11.6	+74 58 44	7.8	47.4	14136	0.39	0.07	12.67	0.03	...	...	...
XMMXCS J092700.6-061050.8	0032342301	09 27 00.7	-06 10 51	13.2	58.8	3494	4.87	0.72	42.75	0.10	...	...	...

XMMXCS J092916.8-235917.4	0109464201	09 29 16.9	-23 59 17	6.2	184.3	4254	103.35	8.19	119.85	0.12	...	...	...	...	...
XMMXCS J093152.3-111635.0	0148880101	09 31 52.4	-11 16 35	9.8	221.8	16889	4.10	0.29	70.70	0.16	...	...	...	...	...
XMMXCS J093259.4+551545.0	0112520101	09 32 59.5	+55 15 45	9.0	380.3	19154	2.43	0.13	75.15	0.16	0.102	0.001	1		
XMMXCS J093310.7-111227.1	0148880301	09 33 10.8	-11 12 27	11.2	60.8	8116	2.49	0.36	14.60	0.07	...	...	...	...	...
XMMXCS J093350.2+552620.1	0112520201	09 33 50.2	+55 26 20	12.1	187.3	4884	4.11	0.32	56.32	0.34	...	...	...	...	...
XMMXCS J093358.2+550946.1	0112520101	09 33 58.2	+55 09 46	4.6	52.5	26027	0.29	0.05	25.41	0.03	...	...	...	...	...
XMMXCS J093423.1+551743.5	0112520101	09 34 23.1	+55 17 44	4.5	130.0	23469	0.72	0.07	24.74	0.11	...	...	...	...	...
XMMXCS J093438.5+551335.7	0112520101	09 34 38.6	+55 13 36	5.3	172.7	22144	1.11	0.09	44.82	0.11	...	...	...	...	...
XMMXCS J093532.8+552142.6	0112520101	09 35 32.8	+55 21 43	14.9	80.0	6294	15.82	1.97	20.98	0.28	...	...	...	...	...
XMMXCS J093709.1+611612.5	0085640201	09 37 09.2	+61 16 13	10.6	512.5	18435	3.47	0.16	84.68	0.28	0.208	0.001	1		
XMMXCS J093947.0+360059.6	0021740101	09 39 47.0	+36 00 60	7.1	112.3	19596	0.89	0.09	11.60	0.12	...	...	...	...	...
XMMXCS J093959.0+711403.3	0026340101	09 39 59.1	+71 14 03	3.7	63.2	22394	0.31	0.04	18.07	0.03	...	...	...	...	...
XMMXCS J094034.7+355952.5	0021740101	09 40 34.7	+35 59 53	10.3	405.3	16963	3.91	0.20	49.28	0.26	0.355	...	3		
XMMXCS J094517.1+095432.8	0150970101	09 45 17.1	+09 54 33	12.6	74.0	4168	5.17	0.67	19.67	0.21	...	...	...	...	...
XMMXCS J094633.9-141409.0	0147920301	09 46 34.0	-14 14 09	13.7	130.2	7201	9.29	0.89	47.56	0.34	...	...	...	...	...
XMMXCS J094719.5-304933.2	0112830401	09 47 19.6	-30 49 33	8.6	66.4	13591	0.56	0.08	12.70	0.07	...	...	...	...	...
XMMXCS J094735.2-304557.7	0112830401	09 47 35.2	-30 45 58	11.0	252.6	11646	2.71	0.18	37.81	0.23	...	...	...	...	...
XMMXCS J094827.8-305217.9	0112830401	09 48 27.9	-30 52 18	11.2	75.9	13156	0.87	0.11	15.41	0.11	...	...	...	...	...
XMMXCS J095105.8+391741.3	0111290101	09 51 05.9	+39 17 41	9.8	113.3	12133	1.64	0.17	30.09	0.13	...	...	...	...	...
XMMXCS J095127.7+392009.1	0111290101	09 51 27.7	+39 20 09	10.1	48.6	12290	0.44	0.07	34.09	0.04	...	...	...	...	...
XMMXCS J095535.8+173653.6	0112850101	09 55 35.8	+17 36 54	11.4	88.0	6618	1.68	0.20	46.14	0.11	...	...	...	...	...
XMMXCS J095839.9+020442.5	0203361801	09 58 39.9	+02 04 43	14.0	108.0	8802	5477.22	579.59	33.02	0.53	...	...	...	...	...
XMMXCS J095928.6+022014.2	0203361201	09 59 28.6	+02 20 14	16.1	86.0	6461	4.49	0.54	48.96	0.28	...	...	...	...	...
XMMXCS J095931.7+022658.8	0203361201	09 59 31.7	+02 26 59	13.7	80.3	7906	1.29	0.16	29.94	0.21	...	...	...	...	...
XMMXCS J095941.1+023105.7	0203361201	09 59 41.2	+02 31 06	11.8	483.8	10043	6.11	0.29	186.68	0.26	...	...	...	...	...
XMMXCS J095948.3+690841.6	0112521001	09 59 48.3	+69 08 42	11.4	45.5	4096	1.40	0.24	35.75	0.04	...	...	...	...	...
XMMXCS J095957.8+251630.4	0041170201	09 59 57.8	+25 16 30	9.9	1740.8	20585	11.38	0.28	NaN	0.23	0.054	0.019	3		
XMMXCS J100002.0+021535.8	0203361301	10 00 02.1	+02 15 36	6.8	146.2	16974	1.06	0.10	53.38	0.12	...	...	...	...	...
XMMXCS J100002.9+020153.8	0203361301	10 00 03.0	+02 01 54	12.2	64.9	10430	0.78	0.11	28.94	0.15	0.079	0.001	1		
XMMXCS J100021.7+023158.4	0203361201	10 00 21.7	+02 31 58	4.5	132.0	22866	0.62	0.06	35.68	0.11	...	...	...	...	...
XMMXCS J100022.7+022326.3	0203361201	10 00 22.7	+02 23 26	4.3	168.6	21396	0.84	0.07	52.50	0.11	...	...	...	...	...
XMMXCS J100027.2+024055.4	0203361201	10 00 27.2	+02 40 55	13.3	162.2	10620	3.51	0.30	35.53	0.34	...	...	...	...	...
XMMXCS J100031.5+251714.3	0041170201	10 00 31.6	+25 17 14	3.5	119.8	39293	0.41	0.04	23.80	0.08	...	...	...	...	...
XMMXCS J100043.7+014606.4	0203361401	10 00 43.7	+01 46 06	12.3	140.9	14579	1.47	0.13	66.71	0.34	...	...	...	...	...
XMMXCS J100052.4+021656.6	0203360701	10 00 52.5	+02 16 57	13.6	121.4	12596	29.83	2.96	37.74	0.34	...	...	...	...	...
XMMXCS J100057.2+023344.9	0203361201	10 00 57.2	+02 33 45	9.9	209.2	17102	1.51	0.11	61.32	0.16	...	...	...	...	...
XMMXCS J100104.2+252625.0	0041170201	10 01 04.2	+25 26 25	13.2	156.4	18536	2.28	0.20	13.81	0.34	...	...	...	...	...
XMMXCS J100113.0+023558.9	0203361201	10 01 13.0	+02 35 59	14.3	24.6	10624	1.39	0.34	32.93	0.05	...	...	...	...	...
XMMXCS J100113.6+022359.4	0203361201	10 01 13.7	+02 23 59	12.3	223.3	12175	7.40	0.53	55.16	0.40	...	...	...	...	...
XMMXCS J100113.7+554849.9	0110930201	10 01 13.8	+55 48 50	10.2	57.9	7577	1.22	0.18	21.12	0.06	...	...	...	...	...
XMMXCS J100115.3+250612.4	0041170201	10 01 15.4	+25 06 12	11.3	353.6	23631	2.92	0.16	104.48	0.29	...	...	...	...	...
XMMXCS J100120.8+553212.0	0110930201	10 01 20.8	+55 32 12	10.1	41.4	7264	1.29	0.23	31.12	0.04	...	...	...	...	...
XMMXCS J100121.3+022318.4	0203360701	10 01 21.4	+02 23 18	4.5	117.7	27454	0.47	0.05	8.25	0.11	...	...	...	...	...

XMMXCS J100124.2+250653.9	0041170201	10 01 24.3	+25 06 54	12.4	50.5	22120	0.70	0.11	27.32	0.10	...	...	...
XMMXCS J100141.8+022538.2	0203360701	10 01 41.9	+02 25 38	4.3	2432.2	27692	9.59	0.20	NaN	0.25	0.124	0.001	1
XMMXCS J100144.3+021429.7	0203360701	10 01 44.3	+02 14 30	13.8	68.2	13912	1.33	0.18	29.43	0.15	...	...	...
XMMXCS J100152.7-192043.6	0109461201	10 01 52.7	-19 20 44	6.6	33.7	3750	1.16	0.24	12.66	0.03	...	...	...
XMMXCS J100157.5-193143.9	0109461201	10 01 57.5	-19 31 44	7.0	165.0	3751	6.28	0.53	51.89	0.12	...	...	...
XMMXCS J100223.7-191304.1	0109461201	10 02 23.7	-19 13 04	12.9	52.1	2386	3.95	0.63	12.46	0.10	...	...	...
XMMXCS J100245.9-192709.6	0109461201	10 02 45.9	-19 27 10	8.2	48.1	3873	1.66	0.28	51.16	0.04	...	...	...
XMMXCS J100452.5-700246.0	0099020301	10 04 52.5	-70 02 46	13.6	199.2	20735	1.66	0.13	64.90	0.34	0.063	0.021	3
XMMXCS J100456.8-702219.5	0128320301	10 04 56.8	-70 22 20	10.9	61.6	6138	1.75	0.25	32.85	0.07	...	...	...
XMMXCS J100617.6-695952.2	0128320301	10 06 17.6	-69 59 52	14.2	40.7	5165	2.08	0.38	25.93	0.13	...	...	...
XMMXCS J100635.3+124950.8	0140550601	10 06 35.3	+12 49 51	12.4	291.8	10001	7.74	0.48	111.40	0.40	...	...	...
XMMXCS J100653.6+125846.8	0140550601	10 06 53.7	+12 58 47	12.6	62.8	9647	0.82	0.12	20.58	0.15	0.038	0.001	1
XMMXCS J100744.2+123948.3	0140550601	10 07 44.3	+12 39 48	10.1	37.7	11061	0.88	0.17	35.17	0.02	...	...	...
XMMXCS J100747.7+125033.3	0140550601	10 07 47.7	+12 50 33	5.5	88.8	14526	1.07	0.13	17.68	0.05	...	...	...
XMMXCS J100750.5+125822.7	0140550601	10 07 50.5	+12 58 23	11.2	113.7	9041	1.52	0.16	36.39	0.16	...	...	...
XMMXCS J101041.0+554214.0	0085170101	10 10 41.1	+55 42 14	5.1	181.0	21825	0.91	0.07	27.24	0.11	...	...	...
XMMXCS J101055.8+555711.2	0085170101	10 10 55.8	+55 57 11	12.6	290.5	12504	3.09	0.19	68.09	0.40	0.174	0.001	1
XMMXCS J101207.0+553749.6	0085170101	10 12 07.1	+55 37 50	10.4	111.0	17393	0.76	0.08	31.34	0.16	...	...	...
XMMXCS J101339.2-450640.0	0073340201	10 13 39.3	-45 06 40	2.2	1684.2	16115	12.05	0.30	NaN	0.30	0.050	0.019	3
XMMXCS J101340.2-445113.6	0073340201	10 13 40.3	-44 51 14	13.3	185.2	7169	3.68	0.29	47.89	0.34	...	...	...
XMMXCS J101407.5-451645.7	0073340201	10 14 07.5	-45 16 46	13.4	40.1	6545	1.49	0.27	16.33	0.08	...	...	...
XMMXCS J101432.0-445535.4	0073340201	10 14 32.1	-44 55 35	13.3	43.5	5789	3.06	0.54	11.60	0.08	...	...	...
XMMXCS J101638.6-461959.2	0148450101	10 16 38.7	-46 19 59	11.1	194.7	15693	2.07	0.16	46.25	0.16	...	...	...
XMMXCS J101739.0+413234.5	0028740301	10 17 39.0	+41 32 35	13.6	111.2	7479	1.83	0.19	19.80	0.34	...	...	...
XMMXCS J101759.3+215357.7	0112552001	10 17 59.3	+21 53 58	13.6	178.1	5141	6.73	0.54	39.25	0.34	0.252	0.035	3
XMMXCS J102035.4+195133.8	0111440101	10 20 35.3	+19 51 34	13.9	43.8	9802	4.84	0.85	16.59	0.08	...	...	...
XMMXCS J102049.8+130503.2	0146990101	10 20 49.9	+13 05 03	12.8	65.0	8881	1.82	0.26	25.96	0.15	...	...	...
XMMXCS J102050.7+081557.2	0093640301	10 20 50.7	+08 15 57	12.8	32.5	4970	2.56	0.53	12.67	0.05	...	...	...
XMMXCS J102115.5+131803.8	0146990101	10 21 15.6	+13 18 04	12.8	57.1	8489	0.97	0.15	2.07	0.10	...	...	...
XMMXCS J102120.5+234303.1	0152580101	10 21 20.6	+23 43 03	13.2	73.1	2360	8.97	1.18	18.91	0.21	...	...	...
XMMXCS J102137.1+125643.6	0146990101	10 21 37.1	+12 56 44	10.3	120.1	10709	1.52	0.15	54.00	0.16	...	...	...
XMMXCS J102202.5+130010.6	0146990101	10 22 02.6	+13 00 11	8.5	209.9	10819	2.63	0.19	46.53	0.16	0.126	0.001	1
XMMXCS J102257.7+195314.4	0101040301	10 22 57.7	+19 53 14	7.9	96.5	19781	0.52	0.06	51.00	0.08	...	...	...
XMMXCS J102344.7+200020.0	0101040301	10 23 44.8	+20 00 20	9.1	68.0	21064	0.37	0.05	15.69	0.07	...	...	...
XMMXCS J102358.3-184027.0	0200240401	10 23 58.4	-18 40 27	11.5	191.5	7255	3.23	0.25	52.06	0.16	...	...	...
XMMXCS J102404.5+194917.6	0101040301	10 24 04.5	+19 49 18	8.4	115.6	21675	0.56	0.06	27.66	0.13	...	...	...
XMMXCS J102424.4+195111.5	0101040301	10 24 24.4	+19 51 12	12.7	264.8	17251	3.63	0.24	42.34	0.40	...	...	...
XMMXCS J102429.7-183048.1	0200240401	10 24 29.8	-18 30 48	8.7	182.0	10703	2.55	0.20	69.43	0.13	...	...	...
XMMXCS J102523.5-183724.2	0200240401	10 25 23.6	-18 37 24	8.9	473.2	12277	4.70	0.23	159.87	0.24	...	...	...
XMMXCS J102526.5-183501.9	0200240401	10 25 26.6	-18 35 02	10.2	78.7	11004	0.93	0.12	46.43	0.11	...	...	...
XMMXCS J102817.2-085514.9	0153290101	10 28 17.1	-08 55 15	11.9	92.3	9025	1.49	0.17	18.92	0.11	...	...	...
XMMXCS J102920.5-085306.1	0153290101	10 29 20.5	-08 53 06	13.4	149.0	6226	2.46	0.22	35.46	0.34	...	...	...
XMMXCS J102934.8+052103.6	0148560501	10 29 34.8	+05 21 04	13.6	56.0	29733	0.80	0.12	8.62	0.10	...	...	...

XMMXCS J103013.9+053209.2	0148560501	10 30 13.9	+05 32 09	7.9	99.5	40649	0.27	0.03	38.39	0.08	...	...	...	...	...
XMMXCS J103014.8+311452.1	0102040301	10 30 14.9	+31 14 52	15.2	70.6	6302	1.34	0.18	10.62	0.28	...	...	...	...	...
XMMXCS J103027.6+310805.5	0102040301	10 30 27.7	+31 08 06	8.5	148.0	14355	1.14	0.10	32.32	0.13	...	...	...	...	...
XMMXCS J103028.6+305806.9	0102040301	10 30 28.6	+30 58 07	8.1	110.4	14772	0.85	0.09	27.51	0.13	...	...	...	...	...
XMMXCS J103041.2+051621.8	0148560501	10 30 41.3	+05 16 22	9.3	170.8	34326	0.62	0.05	24.94	0.13	...	...	...	...	...
XMMXCS J103103.4+052520.9	0148560501	10 31 03.4	+05 25 21	9.1	1293.9	32681	4.81	0.14	359.12	0.23	...	...	...	...	...
XMMXCS J103131.2+311315.9	0102040301	10 31 31.3	+31 13 16	12.4	412.6	12298	5.81	0.30	135.86	0.53	...	...	...	...	...
XMMXCS J103131.7+310532.6	0102040301	10 31 31.8	+31 05 33	7.5	172.9	17656	1.28	0.10	46.75	0.12	...	...	...	...	...
XMMXCS J103154.4+504427.8	0094382701	10 31 54.4	+50 44 28	10.8	42.6	3087	3.61	0.64	29.58	0.04	...	...	...	...	...
XMMXCS J103215.5+504732.4	0094382701	10 32 15.6	+50 47 32	10.9	54.8	3176	4.60	0.71	27.73	0.06	...	...	...	...	...
XMMXCS J103346.5+590015.2	0142970101	10 33 46.5	+59 00 15	13.4	111.9	6305	15.97	1.66	21.52	0.34	...	...	...	...	...
XMMXCS J103554.5-033155.0	0150870401	10 35 54.6	-03 31 55	13.5	314.7	11231	4.00	0.24	76.70	0.46	...	...	...	...	...
XMMXCS J103619.7-033751.5	0150870401	10 36 19.7	-03 37 52	5.6	48.9	23667	0.23	0.04	21.30	0.02	...	...	...	...	...
XMMXCS J103636.3-033303.3	0150870401	10 36 36.3	-03 33 03	10.8	157.2	15847	1.33	0.11	46.07	0.16	...	...	...	...	...
XMMXCS J103946.1+532948.7	0112810301	10 39 46.2	+53 29 49	9.1	22.6	2685	1.23	0.32	33.48	0.02	...	...	...	...	...
XMMXCS J104003.6+204635.0	0059800101	10 40 03.6	+20 46 35	4.9	87.0	11300	1.51	0.18	16.14	0.05	...	...	...	...	...
XMMXCS J104053.3+062121.5	0151390101	10 40 53.4	+06 21 22	12.6	204.4	20866	0.89	0.07	45.52	0.40	...	...	...	...	...
XMMXCS J104109.1+061755.4	0151390101	10 41 09.1	+06 17 55	7.9	30.4	30462	0.10	0.02	4.62	0.03	0.034	0.001	1		
XMMXCS J104129.7+055627.9	0151390101	10 41 29.7	+05 56 28	14.2	95.8	16369	1.34	0.15	12.02	0.28	...	...	...	...	...
XMMXCS J104204.3-643442.5	0101440201	10 42 04.3	-64 34 43	14.3	214.8	10596	2.92	0.21	45.53	0.59	...	...	...	...	...
XMMXCS J104211.1+061033.0	0151390101	10 42 11.2	+06 10 33	13.4	198.4	14209	1.81	0.14	70.65	0.34	...	...	...	...	...
XMMXCS J104215.2+061516.9	0151390101	10 42 15.3	+06 15 17	15.3	180.4	11504	13.35	1.07	37.59	0.53	...	...	...	...	...
XMMXCS J104227.4-643611.0	0101440201	10 42 27.4	-64 36 11	15.2	106.7	6739	9.60	1.02	215.37	0.53	...	...	...	...	...
XMMXCS J104259.1-641838.5	0101440201	10 42 59.2	-64 18 39	3.1	182.6	29060	1.00	0.08	27.56	0.08	...	...	...	...	...
XMMXCS J104348.0-012408.2	0125300101	10 43 48.0	-01 24 08	11.3	82.8	17416	0.47	0.06	22.96	0.11	...	...	...	...	...
XMMXCS J104407.2-012722.2	0125300101	10 44 07.2	-01 27 22	6.9	86.8	24325	0.35	0.04	29.15	0.08	...	...	...	...	...
XMMXCS J104407.5+212203.0	0128531501	10 44 07.5	+21 22 03	13.5	221.1	24235	2.86	0.21	22.33	0.40	...	...	...	...	...
XMMXCS J104418.1-643011.8	0101440201	10 44 18.1	-64 30 12	13.9	105.4	10623	1.70	0.18	4.85	0.34	...	...	...	...	...
XMMXCS J104422.4+213024.7	0128531601	10 44 22.4	+21 30 25	6.5	2404.2	47761	6.29	0.13	NaN	0.29	...	...	...	...	...
XMMXCS J104426.7+212525.7	0128531601	10 44 26.8	+21 25 26	8.0	92.1	42134	0.23	0.03	38.89	0.08	0.187	0.028	3		
XMMXCS J104427.5+211844.7	0128531601	10 44 27.6	+21 18 45	13.6	229.8	26541	2.92	0.21	29.07	0.40	...	...	...	...	...
XMMXCS J104448.6-011155.7	0125300101	10 44 48.7	-01 11 56	13.7	113.6	11990	1.16	0.12	26.76	0.34	...	...	...	...	...
XMMXCS J104506.9+212125.5	0128531501	10 45 06.9	+21 21 26	10.6	387.7	25602	1.76	0.09	61.85	0.29	...	...	...	...	...
XMMXCS J104507.9-013617.7	0125300101	10 45 08.0	-01 36 18	14.3	93.6	10268	1.45	0.17	28.75	0.28	...	...	...	...	...
XMMXCS J104511.9+213917.3	0128531601	10 45 11.9	+21 39 17	9.5	130.8	46166	0.39	0.04	26.75	0.13	...	...	...	...	...
XMMXCS J104512.8+213200.0	0128531601	10 45 12.8	+21 32 00	5.4	98.6	58972	0.17	0.02	28.30	0.05	0.062	0.021	3		
XMMXCS J104514.5+214333.2	0128531401	10 45 14.5	+21 43 33	13.5	99.9	12257	1.11	0.12	24.05	0.21	...	...	...	...	...
XMMXCS J104551.0+213348.8	0128531501	10 45 51.0	+21 33 49	14.4	307.3	18120	5.06	0.31	57.37	0.50	...	...	...	...	...
XMMXCS J104822.9-595915.5	0147860101	10 48 22.9	-59 59 16	14.2	157.2	18200	1.87	0.16	37.60	0.53	...	...	...	...	...
XMMXCS J104835.7-595418.9	0147860101	10 48 35.7	-59 54 19	11.4	7941.1	24796	53.71	0.61	NaN	0.28	...	...	...	...	...
XMMXCS J104858.8-595102.3	0112780401	10 48 58.8	-59 51 02	9.1	129.7	3595	4.68	0.45	20.46	0.13	...	...	...	...	...
XMMXCS J104930.5+325040.7	0055990201	10 49 30.6	+32 50 41	9.5	112.8	9581	1.52	0.16	22.46	0.13	...	...	...	...	...
XMMXCS J104932.6-125452.7	0146510301	10 49 32.6	-12 54 53	13.7	70.5	7343	0.98	0.13	42.34	0.21	...	...	...	...	...

XMMXCS J104948.4+572401.8	0147510801	10 49 48.4	+57 24 02	14.0	169.6	19729	4.50	0.37	35.10	0.53	...	...	...
XMMXCS J104955.1-594533.1	0147860101	10 49 55.1	-59 45 33	7.9	100.2	30702	0.33	0.04	48.48	0.12	...	...	...
XMMXCS J105013.7+574030.9	0147510101	10 50 13.7	+57 40 31	14.3	169.1	25980	0.93	0.08	26.33	0.53	...	...	...
XMMXCS J105017.9-595621.6	0147860101	10 50 17.9	-59 56 22	3.4	146.0	35552	0.62	0.06	22.89	0.08	...	...	...
XMMXCS J105040.6+573741.4	0147510101	10 50 40.7	+57 37 41	10.3	446.4	36954	1.36	0.07	92.96	0.26	...	...	...
XMMXCS J105055.3+335341.6	0109080701	10 50 55.3	+33 53 42	11.5	75.2	15441	1.34	0.17	24.96	0.11	...	...	...
XMMXCS J105108.2+335035.5	0109080701	10 51 08.3	+33 50 36	11.5	74.7	15218	1.29	0.17	32.88	0.11	...	...	...
XMMXCS J105111.2+354705.8	0149170601	10 51 11.3	+35 47 06	10.1	68.6	2905	3.11	0.42	48.12	0.07	...	...	...
XMMXCS J105111.8+574106.3	0147511001	10 51 11.8	+57 41 06	14.7	73.5	24909	0.57	0.07	14.88	0.28	...	...	...
XMMXCS J105112.5+571744.0	0147511001	10 51 12.6	+57 17 44	13.1	229.9	28542	1.80	0.13	14.27	0.40	...	...	...
XMMXCS J105116.6-595313.1	0112780401	10 51 16.6	-59 53 13	8.5	27.8	4740	0.67	0.15	25.96	0.02	...	...	...
XMMXCS J105116.6-600252.7	0147860101	10 51 16.6	-60 02 53	13.0	123.8	16054	0.84	0.08	22.21	0.34	...	...	...
XMMXCS J105124.4+574248.4	0147511001	10 51 24.4	+57 42 48	15.5	204.3	19012	1.45	0.11	57.56	0.59	0.073	0.001	1
XMMXCS J105128.6+355116.0	0149170601	10 51 28.6	+35 51 16	12.2	123.2	2349	7.27	0.72	51.64	0.34	...	...	...
XMMXCS J105151.2+335100.9	0109080701	10 51 51.3	+33 51 01	8.6	84.1	16544	1.53	0.19	33.39	0.08	...	...	...
XMMXCS J105152.9+573217.5	0147511701	10 51 53.0	+57 32 18	7.4	114.8	61826	0.23	0.02	21.78	0.12	...	...	...
XMMXCS J105156.6+571626.9	0147511601	10 51 56.7	+57 16 27	13.8	121.0	36016	1.46	0.15	20.62	0.34	...	...	...
XMMXCS J105204.7+340539.9	0109080701	10 52 04.7	+34 05 40	7.6	99.7	17043	4.86	0.54	40.53	0.08	0.087	0.028	3
XMMXCS J105205.3+574115.1	0147511601	10 52 05.4	+57 41 15	13.4	854.8	39147	2.35	0.08	NaN	0.57	...	...	...
XMMXCS J105207.0+573906.5	0022740201	10 52 07.0	+57 39 07	11.4	85.2	16392	0.78	0.09	9.68	0.11	...	...	...
XMMXCS J105221.7+572224.2	0147511101	10 52 21.8	+57 22 24	10.1	101.9	39721	0.48	0.05	8.10	0.16	...	...	...
XMMXCS J105223.3+441849.2	0146990201	10 52 23.4	+44 18 49	9.8	346.9	5926	7.61	0.43	128.71	0.16	...	...	...
XMMXCS J105308.6+574212.3	0147510901	10 53 08.7	+57 42 12	13.8	62.9	23255	1.05	0.15	19.87	0.15	...	...	...
XMMXCS J105320.1+440813.8	0146990201	10 53 20.1	+44 08 14	10.4	177.8	4710	5.08	0.41	63.46	0.16	...	...	...
XMMXCS J105330.5+440434.0	0146990201	10 53 30.6	+44 04 34	13.0	42.8	3683	1.18	0.21	36.20	0.08	...	...	...
XMMXCS J105348.9+574241.1	0147511201	10 53 48.9	+57 42 41	13.3	161.7	14988	1.67	0.14	23.62	0.34	...	...	...
XMMXCS J105356.4+571739.7	0123700101	10 53 56.4	+57 17 40	14.9	59.0	9237	12.09	1.79	27.44	0.17	...	...	...
XMMXCS J105410.6+573045.0	0147511601	10 54 10.7	+57 30 45	11.9	914.4	52639	1.86	0.06	NaN	0.28	...	...	...
XMMXCS J105729.9-771008.3	0067140201	10 57 30.0	-77 10 08	9.9	71.1	21656	0.37	0.05	14.35	0.08	...	...	...
XMMXCS J105909.8+244454.9	0150320201	10 59 09.8	+24 44 55	12.4	68.9	12059	0.70	0.09	10.64	0.15	...	...	...
XMMXCS J105926.5+242326.0	0150320201	10 59 26.6	+24 23 26	9.4	100.0	15213	0.74	0.08	19.62	0.13	0.058	0.019	3
XMMXCS J105927.6+242546.1	0150320201	10 59 27.7	+24 25 46	7.2	92.0	19087	0.59	0.07	37.48	0.08	...	...	...
XMMXCS J105943.9+244405.6	0150320201	10 59 44.0	+24 44 06	13.0	209.7	10146	2.73	0.20	44.03	0.40	...	...	...
XMMXCS J110051.5-343812.2	0112880201	11 00 51.6	-34 38 12	13.1	85.6	12347	1.44	0.17	14.68	0.21	...	...	...
XMMXCS J110122.1-345253.8	0112880201	11 01 22.2	-34 52 54	12.2	509.6	12807	9.02	0.42	210.09	0.57	...	...	...
XMMXCS J110209.2-344544.9	0112880201	11 02 09.2	-34 45 45	5.0	185.6	21396	0.97	0.08	15.76	0.11	...	...	...
XMMXCS J110225.8-345431.3	0112880201	11 02 25.8	-34 54 31	14.1	230.8	9538	3.52	0.25	83.23	0.59	0.219	0.028	3
XMMXCS J110250.5-765622.7	0067140201	11 02 50.5	-76 56 23	13.7	63.2	14020	1.57	0.22	25.92	0.15	...	...	...
XMMXCS J110301.9-344251.2	0112880201	11 03 02.0	-34 42 51	14.4	173.0	8732	2.96	0.24	56.89	0.53	0.173	0.029	3
XMMXCS J110514.6+251033.0	0109461801	11 05 14.6	+25 10 33	7.0	189.8	7476	7.29	0.57	105.34	0.12	...	...	...
XMMXCS J110715.2-182244.4	0112630101	11 07 15.2	-18 22 44	10.1	71.0	5629	1.64	0.22	41.02	0.11	...	...	...
XMMXCS J110807.2+723902.8	0107460701	11 08 07.2	+72 39 03	7.7	205.3	80098	0.88	0.07	54.87	0.18	...	...	...
XMMXCS J110825.8+723023.9	0107460701	11 08 25.9	+72 30 24	8.3	232.8	71635	0.85	0.06	67.28	0.16	...	...	...

XMMXCS J110932.4+723822.4	0107460601	11 09 32.3	+72 38 22	13.0	211.6	15441	4.85	0.36	28.48	0.40	...	...	...	...	...	...	...	...	...
XMMXCS J110950.3+481938.3	0104861001	11 09 50.3	+48 19 38	14.1	118.4	13498	2.44	0.25	43.25	0.53	...	...	...	...	...	...	...	...	...
XMMXCS J110954.1+482705.2	0104861001	11 09 54.1	+48 27 05	8.5	1470.2	21378	8.44	0.23	NaN	0.23	...	...	...	...	...	...	...	...	...
XMMXCS J111054.7+482657.2	0104861001	11 10 54.8	+48 26 57	5.1	132.9	24993	0.62	0.06	23.12	0.11	...	...	...	...	...	...	...	...	...
XMMXCS J111515.3+531949.1	0143650901	11 15 15.3	+53 19 49	11.8	1743.8	3338	77.37	1.90	NaN	0.28	...	...	...	...	...	...	...	...	...
XMMXCS J111629.1+180057.2	0099030101	11 16 29.1	+18 00 57	11.6	155.5	6416	2.99	0.26	44.13	0.16	...	...	...	...	...	...	...	...	...
XMMXCS J111658.8+174947.7	0099030101	11 16 58.8	+17 49 48	8.9	252.1	9225	3.57	0.24	69.71	0.16	...	...	...	...	...	...	...	...	...
XMMXCS J111710.1+180722.4	0099030101	11 17 10.1	+18 07 22	9.8	101.3	10227	1.37	0.15	45.30	0.13	...	...	...	...	...	...	...	...	...
XMMXCS J111724.6+180928.0	0099030101	11 17 24.7	+18 09 28	12.0	155.6	8235	2.33	0.20	26.96	0.34	...	...	...	...	...	...	...	...	...
XMMXCS J111754.0+440621.8	0109080801	11 17 54.0	+44 06 22	11.2	75.0	16529	0.56	0.07	18.12	0.11	...	...	...	...	...	...	...	...	...
XMMXCS J111804.4+403454.2	0111290301	11 18 04.4	+40 34 54	10.3	125.6	11484	1.40	0.14	34.99	0.16	...	...	...	...	...	...	...	...	...
XMMXCS J111805.5+440926.8	0109080801	11 18 05.5	+44 09 27	11.4	191.0	15563	1.72	0.13	31.41	0.16	...	...	...	...	...	...	...	...	...
XMMXCS J111822.9+403459.4	0111290301	11 18 23.0	+40 34 59	9.2	36.2	11641	0.57	0.11	16.55	0.02	...	...	...	...	...	...	...	...	...
XMMXCS J111841.5+125754.0	0082140301	11 18 41.5	+12 57 54	8.4	142.3	21845	0.86	0.08	42.46	0.13	...	...	...	...	...	...	...	...	...
XMMXCS J111855.5+130028.9	0082140301	11 18 55.5	+13 00 29	5.1	143.5	27010	0.66	0.06	17.46	0.11	...	...	...	...	...	...	...	...	...
XMMXCS J111907.0+130032.9	0082140301	11 19 07.1	+13 00 33	5.8	130.3	25169	0.58	0.06	37.93	0.11	...	...	...	...	...	...	...	...	...
XMMXCS J111912.6+074937.9	0082340101	11 19 12.7	+07 49 38	14.3	139.2	22642	3.04	0.28	30.68	0.53	...	...	...	...	...	...	...	...	...
XMMXCS J111926.0+130209.9	0082140301	11 19 26.0	+13 02 10	8.2	173.2	18177	1.24	0.10	61.00	0.13	...	...	...	...	...	...	...	...	...
XMMXCS J111929.2+131126.6	0082140301	11 19 29.2	+13 11 27	10.2	227.8	14558	1.98	0.14	37.89	0.23	...	...	...	...	...	...	...	...	...
XMMXCS J112012.0+132625.1	0110980101	11 20 12.0	+13 26 25	9.0	178.5	27744	0.79	0.06	26.07	0.13	...	...	...	...	...	...	...	...	...
XMMXCS J112017.0+133033.8	0110980101	11 20 17.1	+13 30 34	4.8	38.7	38599	0.14	0.03	37.39	0.01	...	...	...	...	...	...	...	...	...
XMMXCS J112023.3+134803.9	0110980101	11 20 23.3	+13 48 04	12.8	155.3	20010	1.40	0.12	12.06	0.34	0.103	0.031	3						
XMMXCS J112216.8+052139.3	0083000301	11 22 16.8	+05 21 39	15.6	37.8	6264	1.87	0.36	16.87	0.08	...	...	...						
XMMXCS J112227.6+014223.1	0145750101	11 22 27.7	+01 42 23	14.0	55.9	11053	1.18	0.18	19.44	0.17	...	...	...						
XMMXCS J112235.3-604339.5	0111010101	11 22 35.3	-60 43 40	11.6	110.3	34297	1.36	0.14	19.53	0.16	...	...	...						
XMMXCS J112245.6+013332.7	0145750101	11 22 45.7	+01 33 33	9.7	380.1	16310	3.21	0.17	86.18	0.16	0.130	0.001	1						
XMMXCS J112252.9+013959.0	0145750101	11 22 53.0	+01 39 59	7.3	41.3	19263	0.32	0.06	2.72	0.03	...	...	...						
XMMXCS J112254.0+012650.5	0145750101	11 22 54.0	+01 26 51	12.8	269.5	12147	7.07	0.46	83.85	0.40	...	...	...						
XMMXCS J112257.8-604228.0	0111010101	11 22 57.8	-60 42 28	13.6	212.3	28417	81.51	5.99	88.70	0.40	...	...	...						
XMMXCS J112303.9+053841.9	0083000301	11 23 03.9	+05 38 42	8.5	33.0	18210	0.43	0.09	23.55	0.02	0.049	0.001	1						
XMMXCS J112309.2+013433.0	0145750101	11 23 09.2	+01 34 33	4.3	139.0	23517	0.81	0.07	30.21	0.11	0.204	0.001	1						
XMMXCS J112310.3+012721.2	0145750101	11 23 10.4	+01 27 21	10.7	84.0	14171	1.02	0.12	15.56	0.11	...	...	...						
XMMXCS J112317.2+012716.1	0145750101	11 23 17.3	+01 27 16	10.5	137.9	14015	1.25	0.12	50.37	0.16	...	...	...						
XMMXCS J112342.6+012953.5	0145750101	11 23 42.6	+01 29 54	9.6	156.1	13173	1.47	0.13	17.49	0.13	...	...	...						
XMMXCS J112349.4+052955.1	0083000301	11 23 49.5	+05 29 55	10.0	448.4	17960	4.53	0.22	217.92	0.26	...	...	...						
XMMXCS J112410.7+062229.9	0103863201	11 24 10.7	+06 22 30	9.6	61.3	4940	1.81	0.26	34.50	0.07	...	...	...						
XMMXCS J112411.6-684450.3	0085960101	11 24 11.7	-68 44 50	13.0	90.6	12169	0.51	0.06	13.65	0.21	...	...	...						
XMMXCS J112627.1-682553.6	0085960101	11 26 27.1	-68 25 54	14.6	86.8	8856	1.17	0.14	11.77	0.28	...	...	...						
XMMXCS J112702.6+582948.4	0112810101	11 27 02.6	+58 29 48	12.1	68.7	9748	1.55	0.21	6.58	0.15	...	...	...						
XMMXCS J112710.5-683429.7	0085960101	11 27 10.6	-68 34 30	7.2	46.9	20796	0.23	0.04	8.44	0.03	...	...	...						
XMMXCS J112736.9+583738.9	0112810101	11 27 37.0	+58 37 39	8.0	93.4	13046	1.13	0.13	64.71	0.08	0.197	0.001	1						
XMMXCS J112822.1-683054.0	0085960101	11 28 22.1	-68 30 54	14.3	65.0	12288	1.32	0.18	8.02	0.27	...	...	...						
XMMXCS J112836.9+581845.7	0112810101	11 28 36.8	+58 18 46	15.0	48.7	4181	1.86	0.31	23.35	0.13	...	...	...						

XMMXCS J112842.9+582802.5	0112810101	11 28 42.9	+58 28 03	5.9	86.7	13839	0.78	0.09	25.98	0.05	...	...	...
XMMXCS J112911.7+582307.3	0112810101	11 29 11.8	+58 23 07	11.9	143.9	7651	2.35	0.21	47.39	0.16	0.075	0.024	3
XMMXCS J112935.8-144304.8	0112850201	11 29 35.8	-14 43 05	9.9	137.7	11563	1.43	0.13	13.65	0.13	...	...	...
XMMXCS J112959.2-150214.3	0112850201	11 29 59.3	-15 02 14	12.9	53.6	7200	1.14	0.18	29.31	0.10	...	...	...
XMMXCS J113020.6-143632.5	0112850201	11 30 20.7	-14 36 33	13.3	4231.9	7580	79.10	1.23	NaN	0.57	...	...	...
XMMXCS J113055.0+311332.7	0102040201	11 30 55.1	+31 13 33	3.1	195.9	18433	1.53	0.12	133.71	0.08	...	...	...
XMMXCS J113228.4-343406.2	0112880101	11 32 28.5	-34 34 06	7.3	208.2	21349	1.33	0.10	51.85	0.18	...	...	...
XMMXCS J113232.3-344350.2	0112880101	11 32 32.3	-34 43 50	10.7	990.0	15469	10.64	0.35	515.75	0.28	...	...	...
XMMXCS J113803.9+031532.4	0111970701	11 38 04.0	+03 15 32	8.7	288.9	7945	5.14	0.32	131.89	0.16	...	...	...
XMMXCS J113830.9-374236.5	0112210501	11 38 31.0	-37 42 37	6.3	147.5	79033	0.48	0.04	18.34	0.12	...	...	...
XMMXCS J113837.8+170512.0	0066950201	11 38 37.8	+17 05 12	8.4	79.1	7935	0.89	0.11	12.91	0.08	0.105	0.031	3
XMMXCS J113912.6+165437.0	0066950201	11 39 12.7	+16 54 37	12.8	112.8	4880	43.77	4.52	43.75	0.34	0.113	0.032	3
XMMXCS J113930.6+170620.2	0066950201	11 39 30.6	+17 06 20	4.6	333.5	8883	5.46	0.32	46.46	0.21	...	...	...
XMMXCS J115007.2+015102.6	0044740201	11 50 07.3	+01 51 03	10.0	118.8	27447	0.63	0.06	42.75	0.16	...	...	...
XMMXCS J115009.8-284303.2	0027340101	11 50 09.9	-28 43 03	12.6	152.5	12627	1.48	0.13	15.18	0.34	...	...	...
XMMXCS J115011.3+285432.7	0109462101	11 50 11.4	+28 54 33	10.0	24.8	2369	2.77	0.68	19.05	0.02	...	...	...
XMMXCS J115012.7+014558.0	0044740201	11 50 12.8	+01 45 58	7.2	106.9	33871	0.56	0.06	45.34	0.12	...	...	...
XMMXCS J115018.4+014101.6	0044740201	11 50 18.4	+01 41 02	7.6	203.7	34020	1.10	0.08	44.52	0.18	...	...	...
XMMXCS J115018.9-283525.7	0027340101	11 50 19.0	-28 35 26	16.0	98.0	8548	1.47	0.16	33.07	0.28	...	...	...
XMMXCS J115037.4+284505.4	0109462101	11 50 37.5	+28 45 05	9.2	27.4	2249	3.15	0.72	8.89	0.02	...	...	...
XMMXCS J115043.3+545639.0	0049340301	11 50 43.3	+54 56 39	8.8	1270.3	14235	10.20	0.29	NaN	0.23	0.228	0.001	1
XMMXCS J115045.2-284239.7	0027340101	11 50 45.3	-28 42 40	6.8	53.3	24700	0.26	0.04	12.82	0.06	...	...	...
XMMXCS J115103.8+551123.5	0049340301	11 51 03.8	+55 11 24	6.7	136.2	15097	0.85	0.08	42.43	0.12	...	...	...
XMMXCS J115107.4-290130.5	0027340101	11 51 07.5	-29 01 31	13.2	193.1	15677	2.88	0.22	36.53	0.34	...	...	...
XMMXCS J115116.6+014610.9	0044740201	11 51 16.6	+01 46 11	8.8	118.5	24114	0.64	0.06	40.43	0.13	...	...	...
XMMXCS J115124.7-464037.7	0158160401	11 51 24.7	-46 40 38	11.3	130.5	15530	0.99	0.09	13.79	0.16	...	...	...
XMMXCS J115131.6+014816.5	0044740201	11 51 31.7	+01 48 17	12.7	366.4	16958	4.22	0.23	61.05	0.46	...	...	...
XMMXCS J115203.9+545837.3	0049340301	11 52 03.9	+54 58 37	10.2	257.9	10685	3.00	0.20	43.78	0.23	0.060	0.001	1
XMMXCS J115226.0+370433.2	0112551401	11 52 26.0	+37 04 33	7.9	39.4	4118	1.22	0.23	24.75	0.03	...	...	...
XMMXCS J115227.7+551216.4	0049340301	11 52 27.7	+55 12 16	13.8	54.1	8627	1.67	0.26	13.62	0.10	...	...	...
XMMXCS J115232.5-463455.9	0158160401	11 52 32.6	-46 34 56	12.6	205.8	16018	3.11	0.23	57.84	0.40	...	...	...
XMMXCS J115245.1-464916.8	0158160401	11 52 45.1	-46 49 17	5.1	92.5	30335	0.31	0.04	25.02	0.05	...	...	...
XMMXCS J115409.5+370126.3	0112551401	11 54 09.6	+37 01 26	15.1	37.8	1346	4.34	0.83	31.97	0.08	...	...	...
XMMXCS J115949.3-033423.1	0056020701	11 59 49.4	-03 34 23	16.0	52.3	6087	1.67	0.26	19.98	0.17	...	...	...
XMMXCS J115955.4-032738.6	0056020701	11 59 55.4	-03 27 39	13.1	105.4	9230	1.61	0.17	23.25	0.34	...	...	...
XMMXCS J120022.3-034003.9	0056020701	12 00 22.4	-03 40 04	13.8	69.7	10043	1.16	0.16	28.14	0.15	...	...	...
XMMXCS J120023.3-031905.3	0056020701	12 00 23.4	-03 19 05	10.7	193.4	13122	1.61	0.12	81.37	0.16	...	...	...
XMMXCS J120111.4-184307.6	0085220201	12 01 11.5	-18 43 08	13.1	339.8	17535	2.60	0.15	61.14	0.46	0.273	0.037	3
XMMXCS J120131.1-184043.4	0085220201	12 01 31.1	-18 40 43	12.3	141.8	19841	0.81	0.07	28.10	0.34	...	...	...
XMMXCS J120210.4+442706.7	0109141401	12 02 10.5	+44 27 07	11.6	354.7	37719	3.23	0.18	61.78	0.29	...	...	...
XMMXCS J120214.0-184207.3	0085220201	12 02 14.0	-18 42 07	11.0	423.4	26156	1.98	0.10	40.68	0.26	0.243	0.029	3
XMMXCS J120215.7-185507.8	0085220101	12 02 15.8	-18 55 08	6.3	89.7	13233	0.95	0.11	35.07	0.08	...	...	...
XMMXCS J120216.8+443529.1	0157560101	12 02 16.9	+44 35 29	10.1	84.1	20866	0.45	0.05	7.45	0.11	...	...	...

XMMXCS J120313.6+442719.5	0157560101	12 03 13.7	+44 27 20	4.6	149.0	29694	0.91	0.08	60.85	0.11	...	...	...			
XMMXCS J120345.2-621057.7	0109110101	12 03 45.3	-62 10 58	13.5	373.9	26567	1.58	0.09	55.10	0.46	...	...	...			
XMMXCS J120359.9-621324.0	0109110101	12 03 59.9	-62 13 24	13.8	157.7	26619	0.75	0.06	25.21	0.34	...	...	...			
XMMXCS J120440.0+351213.6	0148740301	12 04 40.1	+35 12 14	11.1	68.6	2434	4.18	0.57	31.33	0.07	...	...	...			
XMMXCS J120440.1+352242.4	0148742401	12 04 40.2	+35 22 42	5.0	54.6	6218	2.26	0.35	27.64	0.03	0.187	0.028	3			
XMMXCS J120500.7+353016.5	0148740301	12 05 00.7	+35 30 17	8.2	84.8	2925	3.84	0.46	57.57	0.08	...	...	...			
XMMXCS J120505.2-615453.8	0109110101	12 05 05.3	-61 54 54	8.4	161.8	40635	0.46	0.04	24.01	0.13	...	...	...			
XMMXCS J120525.7-615442.4	0109110101	12 05 25.8	-61 54 42	8.5	37.5	38236	0.15	0.03	12.23	0.02	...	...	...			
XMMXCS J120545.6+350950.5	0148740301	12 05 45.7	+35 09 50	14.9	150.4	1535	74.65	6.60	202.09	0.53	...	...	...			
XMMXCS J120711.9+645800.1	0141570201	12 07 12.0	+64 58 00	13.7	198.9	8132	7.44	0.57	42.57	0.34	0.112	0.001	1			
XMMXCS J120735.6+250535.9	0151400201	12 07 35.7	+25 05 36	11.0	119.5	7482	2.09	0.21	65.75	0.16	...	...	...			
XMMXCS J120745.7+252013.6	0151400201	12 07 45.8	+25 20 14	7.5	104.0	9570	1.43	0.15	40.89	0.12	...	...	...			
XMMXCS J120801.1+433928.2	0112551201	12 08 01.2	+43 39 28	16.1	346.7	2528	24.32	1.38	369.98	0.50	...	...	...			
XMMXCS J120815.5+250001.8	0151400201	12 08 15.5	+25 00 02	14.4	126.3	4788	4.85	0.47	59.50	0.53	...	...	...			
XMMXCS J120851.5+452958.5	0033540601	12 08 51.5	+45 29 59	10.7	255.1	3367	19.37	1.29	130.03	0.23	0.161	0.031	3			
XMMXCS J120930.2+392756.2	0112830201	12 09 30.2	+39 27 56	12.6	591.3	21357	3.43	0.15	91.93	0.57	...	...	...			
XMMXCS J120934.4+392234.8	0112830201	12 09 34.5	+39 22 35	11.4	717.1	23289	3.57	0.14	169.03	0.28	...	...	...			
XMMXCS J120937.8+434337.1	0112551201	12 09 37.8	+43 43 37	2.9	69.2	13659	0.66	0.09	10.94	0.03	...	...	...			
XMMXCS J120943.5+391435.1	0112830201	12 09 43.5	+39 14 35	13.6	561.0	21809	16.80	0.74	173.06	0.57	...	...	...			
XMMXCS J120947.6+392042.7	0112830201	12 09 47.7	+39 20 43	9.4	69.2	28447	0.34	0.05	22.05	0.07	...	...	...			
XMMXCS J120953.0+393735.6	0112830201	12 09 53.0	+39 37 36	15.3	93.2	15289	0.85	0.10	27.71	0.28	...	...	...			
XMMXCS J121011.7+391237.6	0112310101	12 10 11.7	+39 12 38	12.3	124.2	11845	2.84	0.28	22.60	0.34	...	...	...			
XMMXCS J121031.6+423034.3	0150010601	12 10 31.6	+42 30 34	10.3	177.6	6822	3.40	0.27	75.53	0.16	...	...	...			
XMMXCS J121034.6+393042.5	0112310101	12 10 34.7	+39 30 43	6.4	151.9	19744	5.47	0.48	36.50	0.12	...	...	...			
XMMXCS J121039.4+391154.6	0143500301	12 10 39.4	+39 11 55	12.5	107.1	6821	5.63	0.60	57.48	0.34	...	...	...			
XMMXCS J121126.0+393054.9	0112830201	12 11 26.1	+39 30 55	12.2	164.8	29361	0.86	0.07	29.39	0.34	...	...	...			
XMMXCS J121130.9+391628.6	0112830501	12 11 30.9	+39 16 29	13.8	39.2	9015	3.72	0.69	13.78	0.05	...	...	...			
XMMXCS J121205.5+131743.3	0112550501	12 12 05.5	+13 17 43	5.9	330.1	15130	2.54	0.15	127.78	0.21	...	...	...			
XMMXCS J121238.7+131447.5	0112550501	12 12 38.8	+13 14 48	6.0	36.5	16388	0.27	0.05	11.20	0.03	...	...	...			
XMMXCS J121331.7+135532.3	0112610101	12 13 31.7	+13 55 32	13.4	76.2	23899	0.75	0.10	27.35	0.21	...	...	...			
XMMXCS J121448.0+140555.7	0112610101	12 14 48.1	+14 05 56	8.0	142.5	30138	0.66	0.06	23.46	0.13	0.085	0.015	2			
XMMXCS J121507.6+362028.3	0035940201	12 15 07.6	+36 20 28	6.3	154.9	8600	3.10	0.27	27.53	0.12	0.156	0.022	2			
XMMXCS J121509.5+135448.9	0112610101	12 15 09.5	+13 54 49	15.3	1199.0	14374	12.58	0.37	NaN	0.60	...	...	...			
XMMXCS J121548.0+362308.7	0035940201	12 15 48.0	+36 23 09	3.9	297.1	11215	4.10	0.25	48.09	0.11	...	...	...			
XMMXCS J121809.5+293700.8	0109141301	12 18 09.5	+29 37 01	12.3	178.9	40457	1.37	0.11	31.27	0.34	...	...	...			
XMMXCS J121839.2+470628.3	0059140101	12 18 39.2	+47 06 28	12.2	100.1	5037	2.75	0.30	38.82	0.34	0.094	0.001	1			
XMMXCS J121859.7+472821.1	0110920101	12 18 59.8	+47 28 21	10.1	47.8	9987	0.61	0.10	25.37	0.04	...	...	...			
XMMXCS J121906.1+293843.0	0096020101	12 19 06.2	+29 38 43	13.3	80.9	8955	4.24	0.53	25.73	0.21	...	...	...			
XMMXCS J121913.5+142332.4	0147610101	12 19 13.6	+14 23 32	6.0	74.5	11759	1.20	0.16	35.99	0.08	...	...	...			
XMMXCS J121917.8+060203.5	0056340101	12 19 17.9	+06 02 04	12.6	216.9	11854	2.87	0.21	33.93	0.40	...	...	...			
XMMXCS J121930.2+053818.0	0056340101	12 19 30.3	+05 38 18	11.4	94.9	13498	0.97	0.11	7.00	0.11	...	...	...			
XMMXCS J122003.4+063153.9	0105070101	12 20 03.5	+06 31 54	10.0	87.5	5297	2.42	0.29	12.22	0.11	...	...	...			
XMMXCS J122114.6+280234.2	0104860501	12 21 14.7	+28 02 34	5.9	243.1	29870	1.15	0.08	290.43	0.10	...	...	...			

XMMXCS J122118.7+275732.3	0104860501	12 21 18.6	+27 57 32	9.5	402.0	22449	2.10	0.11	100.56	0.24	...	...	...
XMMXCS J122124.3+275410.3	0104860501	12 21 24.4	+27 54 10	12.3	170.3	15715	2.44	0.20	29.53	0.34	...	...	...
XMMXCS J122156.7+750456.2	0124110101	12 21 56.8	+75 04 56	13.7	122.4	5226	1.76	0.17	30.52	0.34	...	...	...
XMMXCS J122439.6+332434.3	0112522701	12 24 39.7	+33 24 34	16.5	31.9	1683	4.50	0.95	37.32	0.08	...	...	...
XMMXCS J122514.9+123958.9	0110930701	12 25 14.9	+12 39 59	7.8	187.9	6305	3.52	0.28	33.21	0.12	...	...	...
XMMXCS J122516.2+124600.2	0110930701	12 25 16.3	+12 46 00	9.8	141.8	5618	3.28	0.30	16.03	0.13	...	...	...
XMMXCS J122642.2+334027.6	0112521901	12 26 42.2	+33 40 28	13.6	58.8	4934	6.19	0.92	26.26	0.10	...	...	...
XMMXCS J122732.4+435519.6	0112521701	12 27 32.5	+43 55 20	11.8	56.4	7088	1.63	0.25	19.69	0.06	...	...	...
XMMXCS J122737.7+435944.2	0112521701	12 27 37.7	+43 59 44	7.8	64.2	10684	0.81	0.11	9.10	0.07	...	...	...
XMMXCS J122746.6+013253.8	0110990201	12 27 46.7	+01 32 54	7.8	91.0	7412	1.49	0.17	11.48	0.08	...	...	...
XMMXCS J122821.8+020911.2	0126700801	12 28 21.9	+02 09 11	12.7	142.7	18909	2.04	0.19	28.05	0.34	...	...	...
XMMXCS J122845.8+020528.3	0136550801	12 28 45.9	+02 05 28	5.7	104.3	35378	8.16	0.88	12.68	0.11	...	...	...
XMMXCS J122847.9+015523.4	0126700301	12 28 48.0	+01 55 23	9.1	151.9	34260	1.51	0.13	20.94	0.13	...	...	...
XMMXCS J122859.2+021133.7	0126700801	12 28 59.3	+02 11 34	8.6	174.3	36090	1.81	0.15	30.41	0.13	0.078	0.001	1
XMMXCS J122902.0+015016.3	0136550801	12 29 02.1	+01 50 16	12.9	104.4	20310	1.47	0.16	15.33	0.34	...	...	...
XMMXCS J122929.0+015126.0	0136550101	12 29 29.1	+01 51 26	13.0	823.0	22254	8.51	0.31	416.11	0.57	...	...	...
XMMXCS J122932.3+020829.5	0137551001	12 29 32.3	+02 08 30	8.3	73.6	30081	1.71	0.22	17.82	0.08	...	...	...
XMMXCS J122940.1+642020.9	0124900101	12 29 40.1	+64 20 21	13.5	102.2	12858	2.37	0.26	36.28	0.34	...	...	...
XMMXCS J122944.5+133448.4	0112552101	12 29 44.6	+13 34 48	5.4	341.1	10325	4.43	0.25	59.82	0.21	...	...	...
XMMXCS J123008.5+132526.3	0112552101	12 30 08.5	+13 25 26	12.8	137.0	5296	3.50	0.33	29.21	0.34	...	...	...
XMMXCS J123019.4+110118.5	0145800101	12 30 19.5	+11 01 19	8.6	500.5	28397	1.84	0.09	49.50	0.23	...	...	...
XMMXCS J123028.4+413129.7	0112280201	12 30 28.5	+41 31 30	7.3	20.9	11297	0.23	0.06	5.69	0.02	...	...	...
XMMXCS J123032.1+132643.8	0112552101	12 30 32.1	+13 26 44	13.6	16.6	4103	0.58	0.18	9.85	0.03	...	...	...
XMMXCS J123032.6+412342.5	0112280201	12 30 32.7	+41 23 43	15.0	33.5	3560	1.35	0.28	29.77	0.08	...	...	...
XMMXCS J123040.9+105823.8	0145800101	12 30 40.9	+10 58 24	3.7	183.3	39382	0.53	0.04	35.41	0.08	...	...	...
XMMXCS J123050.9+413410.0	0112280201	12 30 51.0	+41 34 10	5.3	248.4	12036	2.60	0.18	93.10	0.10	...	...	...
XMMXCS J123103.1+111300.0	0145800101	12 31 03.1	+11 13 00	13.0	179.1	16788	0.77	0.06	12.27	0.34	...	...	...
XMMXCS J123129.2+105151.2	0145800101	12 31 29.2	+10 51 51	12.0	348.5	17436	2.38	0.13	46.60	0.46	...	...	...
XMMXCS J123150.3+143043.9	0112550801	12 31 50.4	+14 30 44	5.9	129.0	9612	2.46	0.24	42.59	0.11	...	...	...
XMMXCS J123339.6+374053.4	0147390701	12 33 39.7	+37 40 53	15.2	189.0	2952	9.60	0.75	90.64	0.53	0.125	0.032	3
XMMXCS J123425.3+372451.6	0147390701	12 34 25.3	+37 24 52	14.1	37.1	4322	1.40	0.27	22.87	0.08	...	...	...
XMMXCS J123442.3-395217.7	0006220201	12 34 42.3	-39 52 18	10.4	116.6	18670	0.89	0.09	17.01	0.16	...	...	...
XMMXCS J123503.7+621747.8	0111550301	12 35 03.8	+62 17 48	13.5	132.4	13043	2.77	0.26	10.25	0.34	...	...	...
XMMXCS J123505.0+275135.5	0152170501	12 35 05.1	+27 51 36	11.3	104.4	21009	0.59	0.06	18.87	0.16	...	...	...
XMMXCS J123525.7+620617.5	0111550401	12 35 25.8	+62 06 18	12.9	89.3	41010	0.38	0.04	14.29	0.21	...	...	...
XMMXCS J123545.4+122013.2	0141570101	12 35 45.5	+12 20 13	13.2	142.7	10644	5.60	0.51	37.49	0.34	...	...	...
XMMXCS J123601.2+622417.6	0111550401	12 36 01.3	+62 24 18	12.6	66.7	39821	0.38	0.05	6.31	0.15	...	...	...
XMMXCS J123635.6+615815.5	0111550101	12 36 35.6	+61 58 16	14.8	74.7	11497	1.05	0.14	29.30	0.28	...	...	...
XMMXCS J123641.3+280442.0	0152170501	12 36 41.3	+28 04 42	13.9	85.0	12315	6.52	0.79	18.64	0.21	...	...	...
XMMXCS J123650.6+620335.2	0111550401	12 36 50.6	+62 03 35	9.9	195.8	43564	0.65	0.05	25.92	0.13	...	...	...
XMMXCS J123650.7+255217.3	0112550301	12 36 50.8	+25 52 17	9.8	256.9	6792	5.19	0.34	53.34	0.16	...	...	...
XMMXCS J123715.5+114732.3	0112840101	12 37 15.6	+11 47 32	7.0	117.2	13761	1.28	0.13	52.07	0.12	...	...	...
XMMXCS J123844.6-052358.5	0059830101	12 38 44.7	-05 23 59	13.9	164.7	29166	1.60	0.13	36.82	0.34	...	...	...

XMMXCS J123953.7-052530.6	0059830101	12 39 53.7	-05 25 31	6.1	75.2	44338	0.46	0.06	32.81	0.08	...	...	...	...	...	...
XMMXCS J124009.4-114748.3	0084030101	12 40 09.5	-11 47 48	10.7	185.9	21884	1.52	0.12	30.96	0.16	...	...	...	...	...	...
XMMXCS J124018.4-051332.9	0059830101	12 40 18.5	-05 13 33	12.1	235.1	26083	2.59	0.18	59.85	0.40	...	...	...	...	...	...
XMMXCS J124024.8-114806.6	0084030101	12 40 24.8	-11 48 07	12.4	923.0	20176	21.93	0.75	342.62	0.57	...	...	...	...	...	...
XMMXCS J124100.9+325955.3	0056020901	12 41 01.0	+32 59 55	11.7	144.3	10124	2.40	0.22	33.25	0.16	...	...	...	...	...	...
XMMXCS J124204.9+131741.3	0112551001	12 42 04.9	+13 17 41	11.7	81.3	5304	2.49	0.31	27.21	0.11	...	...	...	...	...	...
XMMXCS J124207.4+325946.4	0056020901	12 42 07.4	+32 59 46	11.8	207.0	8111	3.06	0.23	55.43	0.23	...	...	...	...	...	...
XMMXCS J124235.3-112412.9	0136950201	12 42 35.3	-11 24 13	4.9	986.6	24302	5.05	0.17	228.37	0.25	0.068	0.021	3	...	...	...
XMMXCS J124241.7-112843.3	0136950201	12 42 41.8	-11 28 43	9.4	1195.5	15575	8.68	0.26	249.48	0.23	0.047	0.001	1	...	...	...
XMMXCS J124300.4+113656.9	0021540201	12 43 00.4	+11 36 57	10.4	267.8	22075	1.77	0.11	60.53	0.23	...	...	...	...	...	...
XMMXCS J124303.0+113350.2	0021540201	12 43 03.1	+11 33 50	9.0	83.5	24532	0.39	0.05	22.35	0.08	...	...	...	...	...	...
XMMXCS J124319.8-630518.2	0109480401	12 43 19.8	-63 05 18	7.4	28.7	34600	0.28	0.06	13.55	0.02	...	...	...	...	...	...
XMMXCS J124333.1-625948.6	0109480101	12 43 33.1	-62 59 49	8.0	92.9	34346	0.52	0.06	17.42	0.08	...	...	...	...	...	...
XMMXCS J124339.5-630537.1	0109480101	12 43 39.5	-63 05 37	5.2	4782.1	41401	17.68	0.26	NaN	0.25	...	...	...	...	...	...
XMMXCS J124357.3+113616.2	0021540201	12 43 57.3	+11 36 16	5.3	234.3	39890	0.70	0.05	65.20	0.10	...	...	...	...	...	...
XMMXCS J124424.3+113528.5	0021540201	12 44 24.4	+11 35 29	11.2	132.3	25593	0.57	0.05	30.57	0.16	...	...	...	...	...	...
XMMXCS J124431.7+113842.9	0021540201	12 44 31.7	+11 38 43	13.9	77.4	20887	2.15	0.27	30.03	0.21	...	...	...	...	...	...
XMMXCS J124434.2-003642.9	0110980201	12 44 34.3	-00 36 43	12.6	123.0	26689	0.60	0.06	30.71	0.34	...	...	...	...	...	...
XMMXCS J124448.6-001948.7	0110980201	12 44 48.6	-00 19 49	9.3	278.1	33484	1.10	0.07	72.23	0.16	...	...	...	...	...	...
XMMXCS J124524.6-625303.6	0109480101	12 45 24.7	-62 53 04	14.0	81.7	16538	1.70	0.21	18.32	0.28	...	...	...	...	...	...
XMMXCS J124556.8-630525.5	0109480101	12 45 56.8	-63 05 26	10.4	165.9	22375	1.03	0.09	17.64	0.16	...	...	...	...	...	...
XMMXCS J124658.1+020845.1	0051760101	12 46 58.2	+02 08 45	14.6	25.9	2605	11.91	2.83	21.93	0.05	...	...	...	...	...	...
XMMXCS J124744.2+082526.4	0112551101	12 47 44.3	+08 25 26	10.1	35.6	6438	0.94	0.19	12.10	0.02	...	...	...	...	...	...
XMMXCS J124924.4-061336.4	0060370201	12 49 24.5	-06 13 36	14.5	296.6	13958	5.14	0.32	25.37	0.59	...	...	...	...	...	...
XMMXCS J124928.3-055958.8	0060370201	12 49 28.4	-05 59 59	3.7	455.3	32630	2.45	0.12	131.18	0.18	...	...	...	...	...	...
XMMXCS J124941.1+253840.5	0112550401	12 49 41.2	+25 38 41	13.3	65.6	7267	2.52	0.35	27.23	0.15	...	...	...	...	...	...
XMMXCS J124954.2+253610.4	0112550401	12 49 54.2	+25 36 10	9.4	26.2	10447	0.31	0.07	20.48	0.02	...	...	...	...	...	...
XMMXCS J124955.8+264339.7	0143150201	12 49 55.8	+26 43 40	12.7	161.8	10974	2.27	0.19	35.82	0.34	...	...	...	...	...	...
XMMXCS J125002.3+254022.9	0112550401	12 50 02.3	+25 40 23	11.6	87.5	8723	1.29	0.15	23.71	0.11	...	...	...	...	...	...
XMMXCS J125008.4+410326.4	0094360701	12 50 08.5	+41 03 26	9.2	95.6	7466	2.46	0.28	34.13	0.08	...	...	...	...	...	...
XMMXCS J125047.3+263356.4	0143150201	12 50 47.4	+26 33 56	9.7	374.5	10927	4.44	0.24	74.07	0.16	...	...	...	...	...	...
XMMXCS J125048.7+262514.9	0143150201	12 50 48.8	+26 25 15	11.3	43.1	9753	1.15	0.20	26.87	0.04	...	...	...	...	...	...
XMMXCS J125055.7+254153.3	0112550401	12 50 55.8	+25 41 53	13.6	98.6	6302	2.54	0.28	33.68	0.21	0.152	0.032	3	...	...	...
XMMXCS J125122.4-291318.2	0111020201	12 51 22.4	-29 13 18	13.6	117.7	14492	2.19	0.22	52.78	0.34	...	...	...	...	...	...
XMMXCS J125141.4+273739.4	0008220201	12 51 41.4	+27 37 39	5.2	75.0	23290	0.50	0.06	28.35	0.05	...	...	...	...	...	...
XMMXCS J125215.0+273836.9	0008220201	12 52 15.1	+27 38 37	9.6	146.5	24276	0.86	0.08	33.14	0.13	...	...	...	...	...	...
XMMXCS J125218.9+273225.1	0008220201	12 52 19.0	+27 32 25	8.2	43.4	27308	0.27	0.05	22.69	0.04	...	...	...	...	...	...
XMMXCS J125220.8+274302.0	0008220201	12 52 20.9	+27 43 02	13.7	113.7	16904	2.16	0.22	24.32	0.34	...	...	...	...	...	...
XMMXCS J125243.6-290757.8	0111020201	12 52 43.7	-29 07 58	8.1	32.3	19691	0.50	0.10	32.68	0.02	...	...	...	...	...	...
XMMXCS J125301.7+153349.2	0082990101	12 53 01.7	+15 33 49	11.5	95.7	16024	1.04	0.12	36.78	0.11	...	...	...	...	...	...
XMMXCS J125321.8+154015.2	0082990101	12 53 21.8	+15 40 15	3.5	68.2	32224	0.27	0.04	38.39	0.03	...	...	...	...	...	...
XMMXCS J125339.0+154448.8	0082990101	12 53 39.1	+15 44 49	2.7	134.4	35627	0.48	0.05	26.21	0.08	...	...	...	...	...	...
XMMXCS J125344.8+101144.5	0001930301	12 53 44.8	+10 11 45	3.8	281.3	17527	2.23	0.14	184.18	0.11	...	...	...	...	...	...

XMMXCS J125400.3+155032.8	0082990101	12 54 00.4	+15 50 33	10.4	74.4	21573	0.42	0.05	40.71	0.11	...	...	...
XMMXCS J125446.6+565723.7	0081340201	12 54 46.7	+56 57 24	12.9	82.2	9674	2.18	0.27	21.80	0.21	...	...	...
XMMXCS J125547.0+565919.6	0081340201	12 55 47.0	+56 59 20	7.8	29.5	14435	0.31	0.07	8.90	0.02	...	...	...
XMMXCS J125627.5+220713.8	0125911101	12 56 27.6	+22 07 14	9.7	37.1	6863	0.61	0.12	12.75	0.02	...	...	...
XMMXCS J125641.6+215720.1	0125911101	12 56 41.6	+21 57 20	6.6	68.7	8848	0.94	0.13	31.30	0.07	...	...	...
XMMXCS J125700.0+215002.3	0125911201	12 57 00.1	+21 50 02	11.8	28.7	2007	1.90	0.43	24.51	0.02	...	...	...
XMMXCS J125723.3+220925.1	0125910501	12 57 23.4	+22 09 25	8.9	79.7	6549	1.32	0.17	20.49	0.08	...	...	...
XMMXCS J125750.3+215933.1	0125911201	12 57 50.3	+21 59 33	11.4	30.0	1703	2.05	0.45	27.15	0.02	...	...	...
XMMXCS J125905.2-592639.7	0137750101	12 59 05.2	-59 26 40	7.2	98.7	10512	1.15	0.13	30.60	0.08	...	...	...
XMMXCS J125916.0-593617.7	0137750101	12 59 16.1	-59 36 18	8.9	102.3	9019	1.28	0.14	13.94	0.13	...	...	...
XMMXCS J125920.8+344642.6	0141150101	12 59 20.8	+34 46 43	6.3	78.7	14877	1.34	0.17	24.31	0.08	...	...	...
XMMXCS J130244.7-633715.2	0092820301	13 02 44.7	-63 37 15	12.9	36.2	15188	0.65	0.13	3.58	0.05	...	...	...
XMMXCS J130329.7-635808.6	0092820301	13 03 29.8	-63 58 09	9.2	61.2	19838	0.89	0.13	38.18	0.07	...	...	...
XMMXCS J130401.2-634419.3	0092820301	13 04 01.2	-63 44 19	10.0	73.1	17038	1.09	0.14	21.12	0.11	...	...	...
XMMXCS J130405.6-493633.8	0112310301	13 04 05.6	-49 36 34	15.5	55.4	5253	7.22	1.11	12.00	0.17	...	...	...
XMMXCS J130424.4-102932.0	0032141201	13 04 24.5	-10 29 32	14.7	109.1	4175	13.44	1.41	37.49	0.53	...	...	...
XMMXCS J130434.3-492000.1	0112310301	13 04 34.3	-49 20 00	11.8	30.8	8734	0.52	0.11	6.12	0.02	...	...	...
XMMXCS J130456.5-101012.4	0032141201	13 04 56.6	-10 10 12	11.5	86.4	5903	1.59	0.19	24.46	0.11	...	...	...
XMMXCS J130505.8-101645.5	0032141201	13 05 05.9	-10 16 46	4.6	136.7	10981	1.19	0.11	82.51	0.11	...	...	...
XMMXCS J130514.3+181418.6	0017940101	13 05 14.3	+18 14 19	15.0	58.4	10767	2.18	0.32	20.12	0.17	...	...	...
XMMXCS J130514.7-102311.5	0032141201	13 05 14.7	-10 23 12	2.2	385.9	12358	3.45	0.18	127.74	0.15	...	...	...
XMMXCS J130526.8+181156.4	0017940101	13 05 26.9	+18 11 56	11.6	2225.8	20643	13.10	0.28	NaN	0.28	...	...	...
XMMXCS J130534.8+175659.5	0017940101	13 05 34.8	+17 56 60	4.5	1356.0	30210	6.68	0.19	529.35	0.25	...	...	...
XMMXCS J130544.5+180452.1	0017940101	13 05 44.5	+18 04 52	3.8	176.4	28270	1.87	0.15	40.49	0.08	...	...	...
XMMXCS J130545.0+175318.9	0017940101	13 05 45.1	+17 53 19	7.7	676.5	28153	2.67	0.11	154.21	0.29	...	...	...
XMMXCS J130549.2-102717.5	0032141201	13 05 49.2	-10 27 18	10.9	47.3	7361	0.51	0.09	21.21	0.04	...	...	...
XMMXCS J130553.5+181439.6	0017940101	13 05 53.6	+18 14 40	13.8	397.2	18694	4.82	0.25	90.17	0.46	...	...	...
XMMXCS J130601.6+180142.3	0017940101	13 06 01.7	+18 01 42	4.4	59.0	30769	0.26	0.04	39.64	0.03	...	...	...
XMMXCS J130616.0+175039.2	0017940101	13 06 16.1	+17 50 39	13.0	98.0	21548	0.89	0.10	29.41	0.21	...	...	...
XMMXCS J130636.5+175552.2	0017940101	13 06 36.5	+17 55 52	13.6	67.0	19197	1.07	0.15	16.50	0.15	...	...	...
XMMXCS J130650.1-233129.4	0002940101	13 06 50.1	-23 31 29	9.8	306.8	3566	11.39	0.69	157.43	0.16	...	...	...
XMMXCS J130726.5+540039.6	0109462201	13 07 26.6	+54 00 40	10.0	75.4	3583	2.49	0.32	23.80	0.11	...	...	...
XMMXCS J130746.4+535510.7	0056021001	13 07 46.5	+53 55 11	14.5	43.0	8103	0.78	0.14	16.49	0.13	...	...	...
XMMXCS J130817.2+212642.6	0157360101	13 08 17.1	+21 26 43	7.3	132.2	16623	0.94	0.09	14.49	0.12	...	...	...
XMMXCS J130821.8+213126.2	0157360101	13 08 21.8	+21 31 26	7.6	94.3	17304	0.59	0.07	14.55	0.08	...	...	...
XMMXCS J130829.0+533509.9	0056021001	13 08 29.0	+53 35 10	7.2	28.4	18313	0.17	0.04	19.21	0.02	...	...	...
XMMXCS J130903.5+081736.9	0110950401	13 09 03.5	+08 17 37	11.0	109.6	6755	4.70	0.49	45.50	0.16	...	...	...
XMMXCS J130924.7+082509.7	0110950401	13 09 24.8	+08 25 10	7.7	105.0	8650	1.80	0.19	15.59	0.12	...	...	...
XMMXCS J131001.3+272431.6	0021740201	13 10 01.3	+27 24 32	14.5	94.6	12810	1.07	0.12	16.14	0.28	...	...	...
XMMXCS J131018.1+365505.8	0110930501	13 10 18.1	+36 55 06	11.3	25.0	5710	0.58	0.14	31.39	0.02	...	...	...
XMMXCS J131057.9+301054.0	0135940101	13 10 58.0	+30 10 54	11.2	28.7	7563	0.45	0.10	11.83	0.02	...	...	...
XMMXCS J131111.2+274158.6	0021740201	13 11 11.2	+27 41 59	13.9	152.7	16097	3.46	0.30	26.26	0.34	...	...	...
XMMXCS J131117.2+275157.5	0148680101	13 11 17.1	+27 51 58	7.8	91.3	33292	0.50	0.06	30.21	0.08	...	...	...

XMMXCS J131141.0+370634.4	0110930501	13 11 41.1	+37 06 34	9.5	64.5	8283	1.04	0.15	26.49	0.07	...	...	...
XMMXCS J131219.1-325258.9	0109462301	13 12 19.2	-32 52 59	13.6	34.6	2600	3.85	0.77	19.37	0.05	0.168	0.031	3
XMMXCS J131244.6+351206.2	0109080201	13 12 44.7	+35 12 06	6.4	48.5	16303	0.44	0.07	14.10	0.03	...	...	...
XMMXCS J131303.6-324810.8	0109462301	13 13 03.6	-32 48 11	11.4	59.8	3105	5.00	0.73	27.17	0.06	...	...	...
XMMXCS J131455.1-163838.3	0152360101	13 14 55.2	-16 38 38	9.8	490.0	19729	3.10	0.15	124.96	0.24	...	...	...
XMMXCS J131507.4-163206.9	0152360101	13 15 07.4	-16 32 07	14.1	707.9	13665	6.55	0.26	45.75	0.60	...	...	...
XMMXCS J131524.8-163227.9	0152360101	13 15 24.9	-16 32 28	13.1	533.0	15859	6.30	0.28	41.05	0.57	...	...	...
XMMXCS J131802.8+324819.3	0135940201	13 18 02.9	+32 48 19	8.1	101.1	5920	2.19	0.24	62.64	0.13	...	...	...
XMMXCS J131825.4-145030.3	0110980601	13 18 25.4	-14 50 30	13.4	165.5	18692	2.63	0.22	20.68	0.34	...	...	...
XMMXCS J131844.6-150133.9	0110980601	13 18 44.7	-15 01 34	14.0	208.4	18301	3.13	0.23	34.50	0.59	...	...	...
XMMXCS J131907.2+324113.9	0135940201	13 19 07.3	+32 41 14	10.5	33.0	3903	1.17	0.24	35.50	0.02	...	...	...
XMMXCS J131937.2-145444.5	0110980601	13 19 37.3	-14 54 45	5.8	250.9	30925	1.33	0.09	39.21	0.10	0.142	0.031	3
XMMXCS J131950.1-144957.5	0110980601	13 19 50.1	-14 49 58	7.1	234.5	24450	1.60	0.11	21.33	0.18	...	...	...
XMMXCS J132011.1-434003.7	0148580101	13 20 11.2	-43 40 04	11.4	85.4	7647	1.71	0.21	22.10	0.11	...	...	...
XMMXCS J132200.8-434400.9	0148580101	13 22 00.8	-43 44 01	8.8	65.7	7582	1.16	0.16	29.02	0.07	...	...	...
XMMXCS J132413.1-381935.3	0110890101	13 24 13.2	-38 19 35	14.1	135.9	15231	1.19	0.11	36.96	0.53	...	...	...
XMMXCS J132442.2-620837.2	0036140201	13 24 42.2	-62 08 37	13.3	181.8	16097	28.78	2.30	92.73	0.34	...	...	...
XMMXCS J132503.7-620005.9	0036140201	13 25 03.7	-62 00 06	13.5	39.8	15111	1.79	0.33	32.28	0.05	...	...	...
XMMXCS J132532.0-615640.5	0036140201	13 25 32.1	-61 56 41	13.7	144.5	17022	23.94	2.16	72.37	0.34	...	...	...
XMMXCS J132606.2-472906.6	0112220101	13 26 06.2	-47 29 07	6.7	1692.3	28232	9.13	0.23	446.81	0.29	...	...	...
XMMXCS J132607.6-383300.0	0110890101	13 26 07.7	-38 33 00	12.3	80.2	27664	0.95	0.12	27.34	0.21	...	...	...
XMMXCS J132611.3-474031.9	0112220101	13 26 11.3	-47 40 32	13.3	81.8	14481	1.44	0.18	17.40	0.21	...	...	...
XMMXCS J132631.0-474141.5	0112220101	13 26 31.0	-47 41 42	13.4	113.0	14322	2.07	0.21	16.43	0.34	...	...	...
XMMXCS J132631.1+074504.2	0200730201	13 26 31.2	+07 45 04	4.9	183.1	26374	0.73	0.06	43.45	0.11	...	...	...
XMMXCS J132648.4+074624.1	0200730201	13 26 48.4	+07 46 24	9.4	351.1	19652	2.31	0.13	113.96	0.16	...	...	...
XMMXCS J132659.7+074721.9	0200730201	13 26 59.8	+07 47 22	12.3	168.2	14877	1.50	0.12	49.52	0.34	...	...	...
XMMXCS J132731.7-471937.2	0112220101	13 27 31.7	-47 19 37	11.8	75.4	16118	0.75	0.10	32.18	0.11	...	...	...
XMMXCS J132746.2-621857.6	0036140201	13 27 46.2	-62 18 58	13.5	750.0	21125	214.24	8.10	289.69	0.57	...	...	...
XMMXCS J132801.8+583215.9	0142770101	13 28 01.9	+58 32 16	14.5	148.0	5537	3.40	0.30	57.18	0.53	...	...	...
XMMXCS J132822.9+581601.0	0142770101	13 28 23.0	+58 16 01	13.5	29.8	6003	1.09	0.24	4.61	0.02	...	...	...
XMMXCS J132831.5+581958.0	0150650301	13 28 31.6	+58 19 58	10.1	58.3	3723	1.93	0.29	1.50	0.06	...	...	...
XMMXCS J132832.9+583719.8	0142770101	13 28 32.8	+58 37 20	14.9	45.5	4624	11.26	1.93	20.96	0.13	...	...	...
XMMXCS J132904.5+582618.1	0142770101	13 29 04.6	+58 26 18	4.6	126.0	14250	1.32	0.13	61.85	0.11	0.157	0.001	1
XMMXCS J132949.0+583446.6	0142770101	13 29 49.1	+58 34 47	9.8	105.1	10556	1.19	0.13	12.09	0.13	...	...	...
XMMXCS J132958.8+241123.9	0100240201	13 29 58.9	+24 11 24	11.3	111.5	13629	1.14	0.12	43.60	0.16	0.143	0.031	3
XMMXCS J133003.3+241629.7	0100240201	13 30 03.4	+24 16 30	10.3	79.4	15123	0.80	0.10	15.72	0.11	...	...	...
XMMXCS J133011.3+581613.9	0142770101	13 30 11.4	+58 16 14	9.9	49.4	10534	0.59	0.10	25.37	0.04	...	...	...
XMMXCS J133016.8+240756.0	0100240101	13 30 16.9	+24 07 56	9.2	110.2	14363	0.91	0.10	10.49	0.13	...	...	...
XMMXCS J133024.4+241803.2	0100240201	13 30 24.5	+24 18 03	6.6	284.6	22423	1.37	0.09	203.96	0.18	...	...	...
XMMXCS J133027.4+582701.2	0142770101	13 30 27.4	+58 27 01	6.7	108.0	13953	0.86	0.09	30.46	0.12	...	...	...
XMMXCS J133043.6+240903.0	0100240101	13 30 43.7	+24 09 03	5.0	339.0	26095	1.93	0.11	75.60	0.21	...	...	...
XMMXCS J133055.9+242719.9	0100240201	13 30 55.9	+24 27 20	13.5	58.9	13829	1.05	0.16	26.41	0.10	...	...	...
XMMXCS J133057.4+581453.3	0150650301	13 30 57.5	+58 14 53	14.8	119.8	2213	155.22	15.52	38.66	0.53	0.311	0.001	1

XMMXCS J133109.5+112415.2	0061940101	13 31 09.5	+11 24 15	12.9	42.4	2350	2.42	0.43	5.29	0.08	...	...	...
XMMXCS J133155.4+110332.7	0061940101	13 31 55.4	+11 03 33	13.2	29.5	3056	2.37	0.52	29.17	0.02	...	...	...
XMMXCS J133422.6+380419.0	0109660801	13 34 22.6	+38 04 19	10.0	50.0	34795	0.26	0.04	27.10	0.06	...	...	...
XMMXCS J133437.1+380626.8	0109660901	13 34 37.1	+38 06 27	11.7	129.9	10669	2.03	0.19	41.64	0.16	0.235	0.001	1
XMMXCS J133502.5-341124.9	0029740801	13 35 02.6	-34 11 25	12.3	346.6	51564	1.43	0.08	79.78	0.46	...	...	...
XMMXCS J133514.7-341625.4	0029740801	13 35 14.7	-34 16 25	8.2	709.6	75579	2.39	0.09	150.75	0.23	...	...	...
XMMXCS J133522.8+515154.8	0084190201	13 35 22.9	+51 51 55	12.4	268.1	21139	2.05	0.13	44.14	0.40	...	...	...
XMMXCS J133527.1-342619.9	0111570101	13 35 27.1	-34 26 20	10.2	66.7	21933	0.88	0.12	17.46	0.07	...	...	...
XMMXCS J133530.3+380346.0	0109661001	13 35 30.3	+38 03 46	13.9	277.8	22464	11.94	0.76	37.67	0.40	...	...	...
XMMXCS J133559.7+375419.0	0109660801	13 35 59.7	+37 54 19	16.3	111.0	15797	5.27	0.55	37.75	0.53	0.267	0.027	3
XMMXCS J133604.6+514531.5	0084190201	13 36 04.6	+51 45 32	10.9	1198.6	22304	7.40	0.22	326.18	0.28	...	...	...
XMMXCS J133608.5-340505.1	0029740801	13 36 08.5	-34 05 05	13.0	276.8	43944	1.50	0.10	6.70	0.40	...	...	...
XMMXCS J133628.2+520615.5	0084190201	13 36 28.3	+52 06 16	11.6	121.0	21650	0.63	0.06	31.34	0.16	...	...	...
XMMXCS J133630.4+514706.3	0084190201	13 36 30.4	+51 47 06	7.9	130.9	28506	0.52	0.05	18.37	0.12	...	...	...
XMMXCS J133641.5-341605.2	0111570101	13 36 41.5	-34 16 05	10.0	82.2	17361	1.36	0.17	8.92	0.11	...	...	...
XMMXCS J133650.9+241244.4	0096010101	13 36 50.9	+24 12 44	12.1	58.8	17149	0.87	0.13	38.35	0.10	...	...	...
XMMXCS J133654.9+514444.8	0084190201	13 36 54.9	+51 44 45	10.3	119.9	19851	0.61	0.06	33.78	0.16	...	...	...
XMMXCS J133700.8-125357.6	0147670201	13 37 00.8	-12 53 58	10.1	50.4	6077	0.89	0.14	34.85	0.06	...	...	...
XMMXCS J133714.7+243642.9	0096010101	13 37 14.8	+24 36 43	13.7	85.1	17625	1.24	0.15	37.57	0.21	...	...	...
XMMXCS J133716.7-125203.5	0147670201	13 37 16.8	-12 52 04	7.8	31.4	7951	0.40	0.08	32.67	0.03	0.143	0.031	3
XMMXCS J133723.9+520640.8	0084190201	13 37 24.0	+52 06 41	13.6	327.8	16856	4.39	0.26	62.85	0.46	...	...	...
XMMXCS J133728.1-300201.2	0110910201	13 37 28.2	-30 02 01	11.9	66.6	11929	0.66	0.09	8.30	0.07	0.050	0.001	1
XMMXCS J133736.6-130450.0	0147670201	13 37 36.7	-13 04 50	7.5	77.7	8826	1.11	0.14	14.34	0.08	...	...	...
XMMXCS J133754.0-130349.4	0147670201	13 37 54.1	-13 03 49	7.3	90.4	8285	1.14	0.13	55.20	0.08	0.141	0.031	3
XMMXCS J133754.4+515246.4	0084190201	13 37 54.5	+51 52 46	11.5	269.0	16401	2.17	0.14	24.57	0.23	0.065	0.021	3
XMMXCS J133758.4+041904.5	0152940101	13 37 58.4	+04 19 05	14.2	56.6	16359	5.68	0.86	36.68	0.17	...	...	...
XMMXCS J133804.0+482105.9	0055990501	13 38 04.1	+48 21 06	5.1	385.3	14598	3.28	0.18	156.67	0.21	0.088	0.001	1
XMMXCS J133810.3-130054.7	0147670201	13 38 10.3	-13 00 55	8.2	72.4	8794	1.12	0.15	33.92	0.08	...	...	...
XMMXCS J133812.3-124853.1	0147670201	13 38 12.3	-12 48 53	11.6	74.7	7026	1.63	0.21	6.39	0.11	...	...	...
XMMXCS J133827.5+041841.9	0152940101	13 38 27.5	+04 18 42	14.2	151.0	14853	2.15	0.19	14.80	0.53	...	...	...
XMMXCS J133852.3+044255.1	0152940101	13 38 52.3	+04 42 55	13.8	287.0	15400	7.51	0.47	103.12	0.40	...	...	...
XMMXCS J133853.2+482032.5	0055990501	13 38 53.3	+48 20 33	7.1	83.8	11694	0.79	0.10	30.90	0.08	...	...	...
XMMXCS J133909.0+481152.8	0055990501	13 39 09.0	+48 11 53	9.7	139.8	8034	2.09	0.19	56.92	0.13	...	...	...
XMMXCS J133928.1-314837.8	0035940301	13 39 28.1	-31 48 38	11.9	105.5	17390	1.08	0.12	22.30	0.16	...	...	...
XMMXCS J133936.1+480619.6	0055990501	13 39 36.1	+48 06 20	16.6	41.5	3591	5.29	0.96	30.76	0.13	...	...	...
XMMXCS J134001.3+273347.7	0147580101	13 40 01.3	+27 33 48	6.3	58.9	3939	1.89	0.28	37.75	0.06	...	...	...
XMMXCS J134004.6-313014.8	0035940301	13 40 04.6	-31 30 15	8.4	71.5	21877	0.58	0.08	24.96	0.08	...	...	...
XMMXCS J134114.7+353335.7	0112551701	13 41 14.8	+35 33 36	12.2	75.2	8048	1.34	0.17	10.41	0.21	...	...	...
XMMXCS J134158.7-000310.4	0111281301	13 41 58.7	-00 03 10	9.2	43.6	2654	2.98	0.52	24.87	0.04	0.102	0.001	1
XMMXCS J134206.4-671313.3	0143200301	13 42 06.4	-67 13 13	12.8	87.4	5432	4.18	0.50	10.72	0.21	...	...	...
XMMXCS J134240.1-673614.0	0143200301	13 42 40.2	-67 36 14	12.6	76.1	4864	5.03	0.65	11.79	0.21	...	...	...
XMMXCS J134245.1-612949.5	0140350101	13 42 45.1	-61 29 50	12.0	88.8	10468	15.59	1.84	8.10	0.21	...	...	...
XMMXCS J134305.1+555325.7	0101640401	13 43 05.2	+55 53 26	13.6	53.1	8982	2.21	0.35	14.14	0.10	...	...	...

XMMXCS J134317.0+555812.6	0101640401	13 43 17.0	+55 58 13	12.9	122.3	10368	2.49	0.25	49.88	0.34	...	...	...	...	...
XMMXCS J134411.6+002542.4	0111282601	13 44 11.6	+00 25 42	6.3	42.8	4768	1.80	0.32	18.46	0.03	...	...	...	...	...
XMMXCS J134434.4+560443.5	0101640401	13 44 34.5	+56 04 44	11.6	83.9	11231	1.39	0.17	31.53	0.11	...	...	...	...	...
XMMXCS J134446.4-003019.6	0111282501	13 44 46.5	-00 30 20	6.9	52.0	5705	1.27	0.20	27.24	0.06	...	...	...	...	...
XMMXCS J134609.6-602128.9	0092140101	13 46 09.6	-60 21 29	5.7	204.6	23134	4.84	0.36	36.56	0.10	...	...	...	...	...
XMMXCS J134636.7+173645.9	0144570101	13 46 36.7	+17 36 46	13.2	182.1	22302	1.95	0.16	29.87	0.34	0.055	0.019	3	...	...
XMMXCS J134650.7+173443.0	0144570101	13 46 50.8	+17 34 43	9.4	43.3	32872	0.21	0.04	34.96	0.04	...	...	...	...	...
XMMXCS J134651.4+171745.7	0144570101	13 46 51.4	+17 17 46	11.3	172.8	25740	0.89	0.07	22.08	0.16	...	...	...	...	...
XMMXCS J134655.3+173211.6	0144570101	13 46 55.3	+17 32 12	6.8	144.5	36507	0.60	0.05	24.53	0.12	...	...	...	...	...
XMMXCS J134753.6+600353.6	0071340501	13 47 53.6	+60 03 54	12.6	143.3	6478	5.46	0.50	36.35	0.34	...	...	...	...	...
XMMXCS J134805.0+600622.9	0071340501	13 48 05.1	+60 06 23	10.1	62.5	8187	0.86	0.12	15.63	0.07	...	...	...	...	...
XMMXCS J134807.0+261645.0	0109070201	13 48 07.0	+26 16 45	8.2	1016.0	30312	3.60	0.12	454.43	0.23	...	...	...	...	...
XMMXCS J134813.0+260938.3	0109070201	13 48 13.0	+26 09 38	13.4	328.1	20842	11.77	0.69	58.20	0.46	...	...	...	...	...
XMMXCS J134903.1-300728.9	0147440101	13 49 03.1	-30 07 29	11.6	192.8	44258	1.19	0.09	17.05	0.16	...	...	...	...	...
XMMXCS J135358.8+335003.4	0143650801	13 53 58.9	+33 50 04	3.6	422.8	8163	6.16	0.31	283.29	0.18	...	...	...	...	...
XMMXCS J135403.7+333514.6	0143650801	13 54 03.8	+33 35 15	11.2	47.1	4428	1.73	0.29	34.99	0.04	0.092	0.021	2	...	...
XMMXCS J135432.9+690702.7	0083960101	13 54 32.8	+69 07 03	13.9	108.8	7575	4.10	0.43	19.74	0.34	...	...	...	...	...
XMMXCS J135449.9+382758.5	0072340701	13 54 49.9	+38 27 59	14.0	15.8	2508	1.27	0.41	15.54	0.04	...	...	...	...	...
XMMXCS J135512.8+182341.0	0094401201	13 55 12.8	+18 23 41	11.9	187.3	9190	2.35	0.18	22.41	0.16	...	...	...	...	...
XMMXCS J135517.1-585352.6	0007421501	13 55 17.1	-58 53 53	4.7	213.0	12022	2.06	0.15	68.18	0.10	...	...	...	...	...
XMMXCS J135527.4+182352.3	0094401201	13 55 27.4	+18 23 52	8.5	109.8	13079	0.88	0.09	17.53	0.13	...	...	...	...	...
XMMXCS J135536.1+692117.0	0083960101	13 55 36.2	+69 21 17	13.8	47.7	9047	4.75	0.79	6.37	0.08	...	...	...	...	...
XMMXCS J135537.8+383206.2	0072340701	13 55 37.8	+38 32 06	3.9	46.4	5904	1.08	0.18	31.15	0.02	...	...	...	...	...
XMMXCS J135617.9+180953.1	0094401201	13 56 18.0	+18 09 53	13.0	154.3	11274	3.10	0.27	36.50	0.34	...	...	...	...	...
XMMXCS J135708.6-604332.7	0007421101	13 57 08.6	-60 43 33	12.1	115.3	4395	3.40	0.35	30.92	0.34	...	...	...	...	...
XMMXCS J135919.3-600806.9	0007422101	13 59 19.4	-60 08 07	3.4	76.0	10917	0.87	0.11	19.94	0.03	...	...	...	...	...
XMMXCS J140108.5-620621.1	0007420701	14 01 08.6	-62 06 21	6.2	96.0	8084	1.37	0.15	32.96	0.08	...	...	...	...	...
XMMXCS J140124.5-622237.3	0007420701	14 01 24.6	-62 22 37	12.4	120.6	4971	6.42	0.64	39.31	0.34	...	...	...	...	...
XMMXCS J140235.6-614753.5	0007421701	14 02 35.6	-61 47 54	4.8	116.8	9610	1.49	0.15	58.89	0.11	...	...	...	...	...
XMMXCS J140343.5-411823.0	0112291201	14 03 43.6	-41 18 23	6.6	92.8	4986	5.02	0.58	28.21	0.08	...	...	...	...	...
XMMXCS J140408.4-341135.3	0058940301	14 04 08.5	-34 11 35	9.4	77.9	11016	1.14	0.14	5.50	0.08	...	...	...	...	...
XMMXCS J140432.6-602313.4	0150020101	14 04 32.6	-60 23 13	5.4	111.1	32744	0.56	0.06	20.51	0.11	...	...	...	...	...
XMMXCS J140436.9-334921.2	0058940301	14 04 36.8	-33 49 21	13.7	174.2	7729	5.73	0.47	34.53	0.34	...	...	...	...	...
XMMXCS J140439.3-341235.3	0058940301	14 04 39.4	-34 12 35	11.3	471.1	9942	6.98	0.34	137.67	0.26	...	...	...	...	...
XMMXCS J140509.2-601053.3	0150020101	14 05 09.2	-60 10 53	15.2	71.6	10817	3.38	0.45	27.16	0.28	...	...	...	...	...
XMMXCS J140626.6+223243.3	0051760201	14 06 26.6	+22 32 43	9.0	54.5	8132	1.54	0.24	18.84	0.05	0.068	0.021	3	...	...
XMMXCS J140837.2-074522.6	0151590101	14 08 37.3	-07 45 23	8.6	61.1	7372	2.31	0.34	22.37	0.07	...	...	...	...	...
XMMXCS J140850.1-080546.0	0151590101	14 08 50.1	-08 05 46	13.3	59.6	4659	3.97	0.58	28.57	0.10	...	...	...	...	...
XMMXCS J140919.8+262549.9	0092850501	14 09 19.8	+26 25 50	7.5	723.1	25901	3.44	0.13	215.50	0.29	...	...	...	...	...
XMMXCS J140933.1+261456.8	0092850501	14 09 33.1	+26 14 57	4.0	360.0	34565	1.23	0.07	64.01	0.21	...	...	...	...	...
XMMXCS J140935.1+262941.9	0092850501	14 09 35.2	+26 29 42	11.6	269.3	18521	2.25	0.15	43.32	0.23	0.101	0.018	2	...	...
XMMXCS J140939.0+260643.7	0092850501	14 09 39.0	+26 06 44	12.1	537.7	19217	4.29	0.19	211.46	0.57	...	...	...	...	...
XMMXCS J141246.0-653055.2	0111240101	14 12 46.1	-65 30 55	10.8	486.6	51736	2.81	0.13	29.82	0.26	...	...	...	...	...

XMMXCS J141254.6-031528.0	0013140101	14 12 54.6	-03 15 28	5.9	50.6	8468	0.97	0.16	26.98	0.03	...	...	...
XMMXCS J141255.9-032404.3	0013140101	14 12 55.9	-03 24 04	12.5	98.3	6718	4.02	0.45	32.16	0.21	...	...	...
XMMXCS J141319.0+440445.1	0103660101	14 13 19.1	+44 04 45	6.9	356.2	22765	2.08	0.12	95.34	0.18	...	...	...
XMMXCS J141330.0-652207.0	0111240101	14 13 30.1	-65 22 07	2.7	354.2	82012	0.62	0.03	54.39	0.15	...	...	...
XMMXCS J141335.4+435606.0	0103660101	14 13 35.3	+43 56 06	4.7	52.6	26914	0.24	0.04	10.54	0.03	...	...	...
XMMXCS J141414.5-653351.1	0111240101	14 14 14.5	-65 33 51	15.0	201.8	18824	4.01	0.30	46.73	0.59	...	...	...
XMMXCS J141443.2-652556.8	0111240101	14 14 43.3	-65 25 57	11.2	62.1	40648	0.27	0.04	13.28	0.07	...	...	...
XMMXCS J141458.1+440317.9	0103660101	14 14 58.1	+44 03 18	12.9	168.6	9925	2.38	0.20	35.16	0.34	...	...	...
XMMXCS J141525.6-652552.5	0111240101	14 15 25.7	-65 25 53	15.1	248.8	18238	27.28	1.84	58.60	0.59	...	...	...
XMMXCS J141544.3+522518.5	0127921001	14 15 44.4	+52 25 19	13.4	123.7	22826	1.14	0.11	25.37	0.34	...	...	...
XMMXCS J141617.1+522945.8	0127921001	14 16 17.1	+52 29 46	10.1	55.0	31091	0.20	0.03	6.89	0.06	...	...	...
XMMXCS J141629.0+522707.9	0127921001	14 16 29.1	+52 27 08	7.3	249.1	36487	1.00	0.07	70.23	0.18	...	...	...
XMMXCS J141648.4+521024.2	0127921001	14 16 48.5	+52 10 24	14.1	184.0	19773	2.55	0.20	71.70	0.53	...	...	...
XMMXCS J141648.5+522605.8	0127921101	14 16 48.5	+52 26 06	4.1	70.0	6546	1.99	0.27	45.13	0.05	...	...	...
XMMXCS J141657.6+231238.7	0148250201	14 16 57.6	+23 12 39	7.6	113.9	5441	3.31	0.34	63.53	0.12	0.116	0.001	1
XMMXCS J141701.2+450502.6	0109080501	14 17 01.3	+45 05 03	8.9	80.8	12148	1.02	0.13	24.28	0.08	0.114	0.001	1
XMMXCS J141714.1+450724.2	0109080501	14 17 14.2	+45 07 24	11.6	76.8	10320	1.92	0.25	32.53	0.11	...	...	...
XMMXCS J141730.9+251137.8	0089960301	14 17 31.0	+25 11 38	7.3	151.0	42907	1.03	0.09	37.20	0.12	0.154	0.032	3
XMMXCS J141732.0+523157.8	0127921201	14 17 32.1	+52 31 58	8.5	78.0	10333	0.93	0.12	22.62	0.08	...	...	...
XMMXCS J141755.0+245651.5	0089960301	14 17 55.1	+24 56 52	11.4	95.7	31209	0.95	0.11	16.93	0.11	...	...	...
XMMXCS J141801.2+522152.1	0127921201	14 18 01.3	+52 21 52	7.8	32.8	10098	0.40	0.08	4.42	0.03	...	...	...
XMMXCS J141803.0+264718.5	0150480401	14 18 03.1	+26 47 19	10.2	182.6	10991	2.61	0.21	51.03	0.16	...	...	...
XMMXCS J141840.9+521821.3	0127920401	14 18 41.0	+52 18 21	14.7	20.9	897	271.06	73.32	47.43	0.05	...	...	...
XMMXCS J142256.4+383318.8	0147570601	14 22 56.4	+38 33 19	11.5	90.2	6564	2.59	0.30	35.20	0.11	...	...	...
XMMXCS J142305.9+382803.8	0147570601	14 23 05.9	+38 28 04	10.5	248.8	7419	3.86	0.26	67.54	0.23	...	...	...
XMMXCS J142700.1+263438.9	0111290601	14 27 00.1	+26 34 39	8.3	175.4	20555	0.97	0.08	16.24	0.13	...	...	...
XMMXCS J142728.4+423414.9	0165770201	14 27 28.4	+42 34 15	13.3	263.0	25951	3.83	0.25	35.56	0.40	0.129	0.001	1
XMMXCS J142730.5+262859.1	0111290601	14 27 30.6	+26 28 59	3.4	1074.4	28271	4.38	0.14	262.16	0.30	...	...	...
XMMXCS J142736.5+424808.6	0165770101	14 27 36.5	+42 48 09	12.9	28.9	28917	0.68	0.15	10.97	0.02	...	...	...
XMMXCS J142747.6+423415.4	0165770101	14 27 47.7	+42 34 15	10.3	64.7	33967	0.50	0.07	29.44	0.07	...	...	...
XMMXCS J142824.1+422640.1	0165770101	14 28 24.2	+42 26 40	13.8	163.8	24218	2.54	0.21	43.00	0.34	...	...	...
XMMXCS J142902.7+474520.5	0109080901	14 29 02.8	+47 45 21	7.1	147.4	26238	8.01	0.72	60.27	0.12	...	...	...
XMMXCS J142906.3+475233.7	0109080901	14 29 06.3	+47 52 34	8.0	203.9	25552	1.14	0.09	30.87	0.16	...	...	...
XMMXCS J142927.5+424158.5	0165770201	14 29 27.6	+42 41 59	10.2	72.7	25083	0.75	0.10	33.17	0.11	...	...	...
XMMXCS J142949.1+415806.4	0111260101	14 29 49.2	+41 58 06	9.2	39.1	2214	2.96	0.55	29.28	0.02	...	...	...
XMMXCS J143001.4-380422.2	0109462501	14 30 01.5	-38 04 22	6.8	46.4	5060	1.46	0.25	12.85	0.03	...	...	...
XMMXCS J143028.6+475752.9	0109080901	14 30 28.7	+47 57 53	12.9	77.0	15381	1.84	0.23	13.01	0.21	...	...	...
XMMXCS J143043.9+475531.5	0109080901	14 30 43.9	+47 55 32	13.0	85.9	13790	1.63	0.20	23.35	0.21	...	...	...
XMMXCS J143103.4+421426.4	0111260701	14 31 03.4	+42 14 26	12.3	422.6	6983	10.35	0.53	216.95	0.53	...	...	...
XMMXCS J143117.7+415842.4	0111260701	14 31 17.6	+41 58 42	11.6	78.5	7460	1.81	0.23	20.64	0.11	...	...	...
XMMXCS J143321.1-440211.8	0140950101	14 33 21.2	-44 02 12	11.0	24.2	5176	0.60	0.15	17.44	0.02	...	...	...
XMMXCS J143516.0+483302.1	0110930401	14 35 16.0	+48 33 02	11.7	24.4	4692	1.06	0.26	11.34	0.02	...	...	...
XMMXCS J143624.6+484925.4	0110930901	14 36 24.6	+48 49 25	10.3	120.2	4165	4.40	0.44	34.85	0.16	0.075	0.001	1

XMMXCS J143711.5-150824.8	0081341401	14 37 11.5	-15 08 25	10.3	29.4	10113	0.42	0.09	13.23	0.02	...	...	...	...	...
XMMXCS J143714.8+642017.0	0111530101	14 37 14.8	+64 20 17	11.8	206.7	19254	1.44	0.11	58.50	0.23	...	...	...	...	...
XMMXCS J144100.9+642300.6	0111530101	14 41 00.9	+64 23 01	14.2	69.6	20627	1.72	0.23	24.62	0.27	0.091	0.032	3		
XMMXCS J144238.1+353719.2	0005010101	14 42 38.2	+35 37 19	12.6	79.5	11196	1.97	0.25	17.09	0.21	...	...	...		
XMMXCS J144410.1+771005.4	0145240101	14 44 10.2	+77 10 05	4.1	261.5	25268	1.47	0.10	145.14	0.10	...	...	...		
XMMXCS J144453.7+770800.4	0145240101	14 44 53.8	+77 08 00	5.6	77.2	21161	0.46	0.06	14.45	0.05	...	...	...		
XMMXCS J144512.5+292532.4	0103060201	14 45 12.5	+29 25 32	7.6	324.1	16765	2.70	0.16	100.35	0.18	0.123	0.001	1		
XMMXCS J144537.7+291047.8	0103060201	14 45 37.7	+29 10 48	12.7	106.7	10324	1.33	0.14	38.14	0.34	...	...	...		
XMMXCS J144705.0+402218.7	0109080601	14 47 05.1	+40 22 19	13.3	117.7	7459	239.96	24.23	45.06	0.34	...	...	...		
XMMXCS J144853.3+085353.5	0148520101	14 48 53.4	+08 53 54	10.5	363.4	21819	3.34	0.18	73.37	0.29	...	...	...		
XMMXCS J144857.7+090244.6	0057560301	14 48 57.7	+09 02 45	8.1	262.6	23579	1.28	0.08	38.14	0.16	...	...	...		
XMMXCS J144935.3+091341.5	0148520101	14 49 35.3	+09 13 42	13.8	144.3	11193	2.24	0.20	24.94	0.34	...	...	...		
XMMXCS J144940.6+084738.3	0057560301	14 49 40.7	+08 47 38	12.7	310.8	15474	3.32	0.20	60.45	0.46	...	...	...		
XMMXCS J145009.4+090429.9	0148520301	14 50 09.4	+09 04 30	11.2	590.7	15226	5.78	0.25	129.52	0.28	0.062	0.021	3		
XMMXCS J145015.1+270832.2	0152660101	14 50 15.2	+27 08 32	12.0	470.5	7610	7.22	0.35	161.05	0.53	...	...	...		
XMMXCS J145054.9+191800.9	0056030101	14 50 55.0	+19 18 01	13.6	50.6	19766	0.79	0.13	7.55	0.10	...	...	...		
XMMXCS J145101.3+190907.6	0056030101	14 51 01.4	+19 09 08	5.9	89.2	38739	0.92	0.11	34.07	0.05	...	...	...		
XMMXCS J145121.2+270256.4	0152660101	14 51 21.3	+27 02 56	7.1	67.5	13706	0.51	0.07	24.76	0.07	...	...	...		
XMMXCS J145324.4+034154.5	0150350101	14 53 24.5	+03 41 55	12.4	139.2	12489	1.14	0.11	20.05	0.34	...	...	...		
XMMXCS J145359.0+034435.1	0150350101	14 53 59.0	+03 44 35	11.9	202.1	11619	2.07	0.16	25.49	0.23	...	...	...		
XMMXCS J150416.0+102000.0	0070740101	15 04 16.0	+10 20 00	7.3	32.2	7378	0.97	0.20	11.27	0.03	0.085	0.028	3		
XMMXCS J150429.3+474237.8	0100650101	15 04 29.4	+47 42 38	7.8	130.5	10948	1.61	0.15	41.52	0.12	...	...	...		
XMMXCS J150429.8+474056.0	0100650101	15 04 29.8	+47 40 56	7.4	96.2	9859	1.33	0.15	78.10	0.08	...	...	...		
XMMXCS J150502.2+473109.9	0100650101	15 05 02.2	+47 31 10	15.0	56.9	4319	2.40	0.36	25.62	0.17	...	...	...		
XMMXCS J150543.3+013639.9	0021540501	15 05 43.4	+01 36 40	11.5	77.0	9303	1.94	0.25	7.79	0.11	...	...	...		
XMMXCS J150654.7+014405.4	0021540101	15 06 54.8	+01 44 05	10.0	190.3	13561	2.58	0.20	27.10	0.16	...	...	...		
XMMXCS J151443.1+370254.4	0111291001	15 14 43.2	+37 02 54	12.1	20.8	7772	0.78	0.21	16.09	0.02	...	...	...		
XMMXCS J151512.1+364106.0	0111291001	15 15 12.2	+36 41 06	11.4	112.4	8301	3.54	0.37	26.06	0.16	...	...	...		
XMMXCS J151529.2+370102.6	0111291001	15 15 29.3	+37 01 03	13.8	43.7	5650	2.07	0.36	38.52	0.08	...	...	...		
XMMXCS J151541.1+561124.6	0145190201	15 15 41.1	+56 11 25	8.5	76.0	17575	0.63	0.08	6.04	0.08	...	...	...		
XMMXCS J151620.7-161444.9	0164570401	15 16 20.8	-16 14 45	10.3	173.7	22279	1.14	0.09	39.00	0.16	...	...	...		
XMMXCS J151719.8-161811.8	0164570401	15 17 19.8	-16 18 12	10.2	113.5	20059	0.86	0.09	33.78	0.16	...	...	...		
XMMXCS J152639.0+354527.2	0081341101	15 26 39.1	+35 45 27	13.8	84.7	4921	173.33	20.96	32.93	0.21	...	...	...		
XMMXCS J152640.8+514847.2	0011830201	15 26 40.8	+51 48 47	14.0	50.9	10814	0.71	0.11	7.15	0.17	...	...	...		
XMMXCS J152708.2+513645.3	0011830201	15 27 08.3	+51 36 45	11.5	120.1	15611	1.05	0.10	18.76	0.16	0.158	0.001	1		
XMMXCS J153112.2+241657.4	0143650101	15 31 12.2	+24 16 57	10.7	40.8	3934	1.41	0.26	37.99	0.04	...	...	...		
XMMXCS J153133.9-083308.4	0100240801	15 31 34.0	-08 33 08	12.2	74.5	9112	1.42	0.18	5.87	0.21	...	...	...		
XMMXCS J153154.7+240600.7	0143650101	15 31 54.8	+24 06 01	14.4	13.8	2361	2.76	0.96	11.39	0.04	0.154	0.032	3		
XMMXCS J153226.0-084020.6	0100240801	15 32 26.0	-08 40 21	8.3	59.6	16281	0.53	0.08	36.68	0.05	...	...	...		
XMMXCS J153401.9+264648.6	0111540201	15 34 01.9	+26 46 49	9.6	80.3	20094	1.24	0.15	21.30	0.08	...	...	...		
XMMXCS J153510.1+543546.1	0150610301	15 35 10.1	+54 35 46	13.0	141.0	8606	1.72	0.16	19.52	0.34	0.110	0.001	1		
XMMXCS J153627.2+543926.2	0150610301	15 36 27.2	+54 39 26	6.1	173.7	14450	1.74	0.14	16.00	0.12	...	...	...		
XMMXCS J153648.1+543720.6	0150610301	15 36 48.1	+54 37 21	4.1	308.9	18896	2.26	0.14	25.65	0.21	...	...	...		

XMMXCS J154233.5+535932.9	0060370901	15 42 33.5	+53 59 33	12.6	280.1	8374	4.74	0.30	77.95	0.40	...	...	...
XMMXCS J154345.7+535216.2	0060370901	15 43 45.8	+53 52 16	7.1	51.1	15343	0.48	0.08	36.00	0.06	...	...	...
XMMXCS J154401.8-521608.6	0152780201	15 44 01.8	-52 16 09	16.6	124.7	13849	2.05	0.20	49.93	0.53	...	...	...
XMMXCS J154610.4+484851.6	0153220401	15 46 10.4	+48 48 52	7.2	100.3	7654	2.41	0.27	17.30	0.12	0.113	0.001	1
XMMXCS J154820.5-451633.9	0105460301	15 48 20.5	-45 16 34	12.2	91.5	7782	1.62	0.19	31.41	0.21	...	...	...
XMMXCS J154921.5+212844.6	0136040101	15 49 21.5	+21 28 45	7.2	89.0	10920	0.96	0.11	12.71	0.08	...	...	...
XMMXCS J155257.0+184711.8	0109464901	15 52 57.1	+18 47 12	9.6	53.3	3944	1.90	0.30	39.07	0.05	...	...	...
XMMXCS J155339.0+185538.9	0109464901	15 53 39.1	+18 55 39	12.3	61.5	3420	4.44	0.64	13.24	0.15	...	...	...
XMMXCS J155548.9-251222.7	0142630301	15 55 48.9	-25 12 23	15.9	712.5	3168	100.60	3.91	NaN	0.60	...	...	...
XMMXCS J155624.5-234255.2	0112380101	15 56 24.6	-23 42 55	5.1	235.1	31648	0.89	0.06	38.43	0.10	...	...	...
XMMXCS J155628.5-235138.7	0112380101	15 56 28.6	-23 51 39	13.9	284.6	14466	9.46	0.59	44.02	0.40	...	...	...
XMMXCS J155828.8+351324.2	0112600801	15 58 28.9	+35 13 24	14.4	143.5	4419	4.79	0.43	21.30	0.53	0.119	0.001	1
XMMXCS J155930.5+350439.2	0112600801	15 59 30.6	+35 04 39	5.1	28.6	8262	574.63	128.93	32.57	0.01	...	...	...
XMMXCS J160129.7+083856.6	0147580201	16 01 29.8	+08 38 57	6.2	663.7	3125	24.69	1.00	316.25	0.29	0.239	0.032	3
XMMXCS J160307.1+664755.3	0151530401	16 03 07.2	+66 47 55	8.5	72.0	12905	1.50	0.20	29.85	0.08	...	...	...
XMMXCS J160419.1+325622.3	0157360401	16 04 19.1	+32 56 22	14.5	77.2	8954	0.78	0.10	19.05	0.28	...	...	...
XMMXCS J160423.8+325216.0	0157360401	16 04 23.8	+32 52 16	12.0	167.2	10410	2.19	0.18	8.46	0.34	...	...	...
XMMXCS J160831.4-390023.6	0146310201	16 08 31.4	-39 00 24	5.2	204.3	14043	3.34	0.25	143.12	0.10	...	...	...
XMMXCS J161025.1+542332.0	0059752601	16 10 25.1	+54 23 32	11.3	100.3	3864	4.29	0.47	38.21	0.16	0.069	0.021	3
XMMXCS J161039.8+540606.4	0059752301	16 10 39.9	+54 06 06	7.9	258.1	6351	6.96	0.46	88.43	0.18	...	...	...
XMMXCS J161051.3+535955.4	0059752601	16 10 51.3	+53 59 55	13.6	44.3	3870	12.04	2.10	22.35	0.08	...	...	...
XMMXCS J161411.7-230212.7	0109060201	16 14 11.8	-23 02 13	3.5	6236.7	39956	16.64	0.21	NaN	0.30	...	...	...
XMMXCS J161414.7+334459.3	0111470301	16 14 14.8	+33 44 59	8.6	52.6	6646	2.45	0.39	22.16	0.05	...	...	...
XMMXCS J161416.6-225516.9	0109060201	16 14 16.6	-22 55 17	6.1	174.6	33495	0.60	0.05	25.46	0.12	...	...	...
XMMXCS J161554.2+121928.5	0103460801	16 15 54.3	+12 19 29	11.0	526.6	5567	12.20	0.56	180.78	0.28	...	...	...
XMMXCS J161703.7+123308.6	0103460901	16 17 03.7	+12 33 09	8.8	150.5	8331	1.97	0.17	26.37	0.13	...	...	...
XMMXCS J161706.8+122518.2	0103461001	16 17 06.8	+12 25 18	13.8	63.5	4319	1.84	0.26	19.15	0.15	...	...	...
XMMXCS J161715.7+121506.1	0103460901	16 17 15.8	+12 15 06	9.8	81.7	8353	1.17	0.14	12.19	0.08	...	...	...
XMMXCS J161736.0+122901.7	0103461001	16 17 36.0	+12 29 02	7.9	54.7	7574	0.86	0.13	33.52	0.06	0.068	0.021	3
XMMXCS J161739.7+121641.3	0103460901	16 17 39.8	+12 16 41	11.9	89.3	6790	3.74	0.44	17.69	0.11	...	...	...
XMMXCS J161746.9+124422.8	0103461001	16 17 46.9	+12 44 23	7.8	105.5	7751	1.99	0.21	43.06	0.12	...	...	...
XMMXCS J162703.7-491330.6	0098610201	16 27 03.8	-49 13 31	9.9	88.1	24984	0.97	0.11	38.10	0.08	...	...	...
XMMXCS J162709.1+550934.5	0109081101	16 27 09.1	+55 09 35	14.6	68.1	300	800.47	109.29	22.24	0.27	...	...	...
XMMXCS J162751.3-490130.4	0098610201	16 27 51.3	-49 01 30	10.7	125.8	28744	1.19	0.12	19.64	0.16	...	...	...
XMMXCS J162806.2-245025.3	0111120201	16 28 06.3	-24 50 25	13.3	133.5	13721	2.16	0.20	32.75	0.34	...	...	...
XMMXCS J163057.2-672649.9	0152620101	16 30 57.2	-67 26 50	7.7	465.5	33640	4.45	0.22	160.43	0.19	...	...	...
XMMXCS J163122.6-671643.4	0152620101	16 31 22.7	-67 16 43	12.2	154.6	22528	2.38	0.21	15.51	0.34	...	...	...
XMMXCS J163133.3+374911.1	0033540901	16 31 33.3	+37 49 11	12.6	94.8	5191	1.93	0.22	23.69	0.21	...	...	...
XMMXCS J163156.9+374651.4	0033540901	16 31 56.9	+37 46 51	9.1	86.5	7753	1.19	0.14	28.18	0.08	...	...	...
XMMXCS J163205.9+781000.8	0061940301	16 32 06.0	+78 10 01	3.8	50.9	4334	3.19	0.51	31.80	0.02	...	...	...
XMMXCS J163231.7+703141.2	0143150101	16 32 31.8	+70 31 41	9.8	156.4	8104	2.39	0.21	62.87	0.13	...	...	...
XMMXCS J163248.6+373840.6	0033540901	16 32 48.7	+37 38 41	9.5	138.2	9207	1.78	0.16	38.50	0.13	...	...	...
XMMXCS J163249.2-671650.3	0111070201	16 32 49.2	-67 16 50	11.3	95.5	5798	4.68	0.53	28.75	0.11	...	...	...

XMMXCS J163255.8+374102.5	0033540901	16 32 55.8	+37 41 03	11.3	87.7	7767	1.26	0.15	8.83	0.11	...	...	...	...	...
XMMXCS J163328.1+702957.5	0143150101	16 33 28.2	+70 29 57	5.3	126.5	11718	1.30	0.13	29.27	0.11	...	...	...	...	...
XMMXCS J163431.6+704302.9	0143150101	16 34 31.7	+70 43 03	11.5	82.6	5745	1.53	0.19	22.99	0.11	...	...	...	...	...
XMMXCS J163451.4+704232.8	0143150101	16 34 51.5	+70 42 33	11.2	35.8	6475	0.69	0.14	29.25	0.02	...	...	...	...	...
XMMXCS J163539.3+570048.0	0049540301	16 35 39.3	+57 00 48	14.0	119.3	6944	4.76	0.48	36.06	0.53	...	...	...	...	...
XMMXCS J163938.0-414134.4	0158160601	16 39 38.1	-41 41 34	14.2	57.7	9943	1.64	0.25	21.02	0.17	...	...	...	...	...
XMMXCS J164053.6+363322.9	0085280301	16 40 53.7	+36 33 23	11.2	100.2	5902	2.45	0.27	11.29	0.16	...	...	...	...	...
XMMXCS J164111.9+363223.4	0085280301	16 41 12.0	+36 32 23	7.6	139.9	8862	2.04	0.19	44.75	0.12	...	...	...	...	...
XMMXCS J164145.1+364139.3	0085280301	16 41 45.1	+36 41 39	14.1	38.1	5286	1.41	0.27	26.02	0.08	...	...	...	...	...
XMMXCS J165058.5-690548.3	0021750101	16 50 58.6	-69 05 48	13.1	61.9	5281	3.56	0.51	10.68	0.15	...	...	...	...	...
XMMXCS J165810.5+351309.1	0111061401	16 58 10.6	+35 13 09	8.5	75.0	4378	4.76	0.62	30.15	0.08	...	...	...	...	...
XMMXCS J170407.1-484426.2	0085680601	17 04 07.2	-48 44 26	13.1	78.4	5081	3.88	0.49	23.93	0.21	...	...	...	...	...
XMMXCS J170415.7-380322.0	0083280101	17 04 15.8	-38 03 22	13.3	97.7	9710	8.94	1.00	26.06	0.21	...	...	...	...	...
XMMXCS J172335.3+341202.6	0102040101	17 23 35.3	+34 12 03	6.7	108.8	3777	16.87	1.78	51.13	0.12	...	...	...	...	...
XMMXCS J172738.7-140412.5	0041160101	17 27 38.8	-14 04 13	15.4	169.8	10377	2.16	0.18	33.85	0.53	...	...	...	...	...
XMMXCS J172811.1-045409.7	0085280201	17 28 11.2	-04 54 10	12.4	73.2	4243	3.14	0.41	14.64	0.21	...	...	...	...	...
XMMXCS J172814.0-142813.9	0041160101	17 28 14.0	-14 28 14	12.4	2476.8	18790	28.17	0.58	NaN	0.57	0.191	0.030	3		
XMMXCS J172816.2-140509.6	0041160101	17 28 16.3	-14 05 10	10.8	344.4	22544	3.31	0.19	73.31	0.29	...	...	...	...	...
XMMXCS J173017.1+520519.7	0021750201	17 30 17.1	+52 05 20	12.8	54.0	3349	4.30	0.67	20.78	0.10	...	...	...	...	...
XMMXCS J173522.2-260046.3	0137950201	17 35 22.3	-26 00 46	16.1	35.8	3724	2.47	0.49	35.99	0.08	...	...	...	...	...
XMMXCS J174458.0-285127.7	0112971901	17 44 58.1	-28 51 28	8.1	568.1	5841	17.94	0.78	135.96	0.23	...	...	...	...	...
XMMXCS J174634.0-280701.3	0112970201	17 46 34.1	-28 07 01	10.5	84.3	9599	6.54	0.79	23.52	0.11	...	...	...	...	...
XMMXCS J175535.1-220325.5	0144271401	17 55 35.2	-22 03 26	12.3	58.1	3388	11.77	1.76	5.90	0.10	...	...	...	...	...
XMMXCS J175849.5-335022.0	0032940101	17 58 49.5	-33 50 22	2.8	210.9	16045	1.55	0.11	32.96	0.11	...	...	...	...	...
XMMXCS J180225.3-225054.6	0135742801	18 02 25.4	-22 50 55	10.3	40.1	3431	1.57	0.29	10.94	0.04	...	...	...	...	...
XMMXCS J180509.6-282322.8	0152420101	18 05 09.6	-28 23 23	11.4	102.1	19547	0.70	0.08	13.46	0.16	...	...	...	...	...
XMMXCS J180512.5+023637.1	0044741401	18 05 12.5	+02 36 37	7.6	198.4	6021	4.51	0.34	127.95	0.12	...	...	...	...	...
XMMXCS J180539.1+021558.0	0044741301	18 05 39.2	+02 15 58	14.3	30.3	3209	4.21	0.91	21.84	0.08	...	...	...	...	...
XMMXCS J180620.9+811048.2	0128530801	18 06 21.0	+81 10 48	14.0	167.6	12586	2.64	0.22	40.92	0.53	...	...	...	...	...
XMMXCS J180657.6-192708.1	0024940201	18 06 57.6	-19 27 08	14.4	68.4	6363	1.63	0.22	13.35	0.27	...	...	...	...	...
XMMXCS J180721.9-191437.9	0024940201	18 07 21.9	-19 14 38	12.5	91.4	10112	1.30	0.15	9.50	0.21	...	...	...	...	...
XMMXCS J180816.3-194346.7	0145840101	18 08 16.4	-19 43 47	10.7	137.2	14940	7.69	0.71	21.46	0.16	...	...	...	...	...
XMMXCS J180853.2-370534.4	0064940101	18 08 53.3	-37 05 34	8.6	144.8	22074	2.03	0.18	11.18	0.13	0.011	0.001	1		
XMMXCS J180921.2-370056.8	0064940101	18 09 21.3	-37 00 57	11.0	297.5	18942	4.12	0.25	111.62	0.23	...	...	...	...	...
XMMXCS J180941.6-191820.0	0152833401	18 09 41.7	-19 18 20	13.4	61.9	2761	2.30	0.33	16.75	0.15	...	...	...	...	...
XMMXCS J181047.7-183507.9	0152835701	18 10 47.8	-18 35 08	11.6	76.1	3723	2.42	0.31	16.60	0.11	...	...	...	...	...
XMMXCS J181659.1-153458.7	0152834401	18 16 59.1	-15 34 59	11.3	71.4	5117	2.60	0.35	12.85	0.11	...	...	...	...	...
XMMXCS J181750.2-120458.9	0008820301	18 17 50.3	-12 04 59	10.9	140.5	4873	25.25	2.32	36.82	0.16	...	...	...	...	...
XMMXCS J181817.3-204537.3	0149610401	18 18 17.4	-20 45 37	13.2	65.5	14066	1.36	0.19	41.14	0.15	...	...	...	...	...
XMMXCS J181824.9-635424.9	0146340601	18 18 25.0	-63 54 25	11.6	177.7	3189	8.84	0.71	27.26	0.16	...	...	...	...	...
XMMXCS J181836.4-634645.9	0146340601	18 18 36.3	-63 46 46	6.5	200.3	4998	7.00	0.53	67.18	0.18	...	...	...	...	...
XMMXCS J181847.7-205546.2	0149610401	18 18 47.7	-20 55 46	8.1	80.2	22116	0.46	0.06	21.12	0.08	...	...	...	...	...
XMMXCS J181851.3-204138.3	0149610401	18 18 51.4	-20 41 38	9.3	388.4	18057	2.65	0.14	48.28	0.16	...	...	...	...	...

XMMXCS J181857.8-120701.6	0008820301	18 18 57.9	-12 07 02	7.4	83.5	8046	10.21	1.24	23.71	0.08	...	...	...
XMMXCS J181902.6-634959.9	0146340601	18 19 02.7	-63 49 60	5.5	147.3	5557	4.35	0.39	54.64	0.11	...	...	...
XMMXCS J181905.8-205346.0	0149610401	18 19 05.9	-20 53 46	4.2	192.1	28585	0.84	0.07	37.34	0.11	...	...	...
XMMXCS J181917.2-253307.1	0144490101	18 19 17.1	-25 33 07	8.7	52.7	18192	1.26	0.20	28.10	0.05	...	...	...
XMMXCS J181919.2-121732.7	0008820601	18 19 19.3	-12 17 33	14.2	46.6	3854	10.52	1.78	13.96	0.13	...	...	...
XMMXCS J181923.1-204616.1	0149610401	18 19 23.1	-20 46 16	4.5	144.8	25053	0.64	0.06	31.19	0.11	0.017	0.006	2
XMMXCS J181926.4-251049.8	0144490101	18 19 26.4	-25 10 50	13.6	75.2	14562	2.13	0.28	33.23	0.21	...	...	...
XMMXCS J182007.3-204621.1	0149610401	18 20 07.3	-20 46 21	13.6	137.2	9551	1.49	0.14	54.00	0.34	...	...	...
XMMXCS J182102.4-272605.7	0085580301	18 21 02.4	-27 26 06	10.1	81.8	5188	1.94	0.24	26.35	0.11	...	...	...
XMMXCS J182155.1-273810.6	0085581201	18 21 55.2	-27 38 11	7.3	83.1	4411	2.11	0.26	27.90	0.08	...	...	...
XMMXCS J182317.3+650503.4	0148740401	18 23 17.3	+65 05 03	10.4	49.8	815	6.48	1.06	27.37	0.04	0.207	0.027	3
XMMXCS J182440.2-115925.3	0051940101	18 24 40.2	-11 59 25	10.5	57.2	3265	2.74	0.41	20.76	0.06	...	...	...
XMMXCS J182931.3+010053.9	0065820601	18 29 31.3	+01 00 54	14.1	12.9	8172	1.64	0.60	37.31	0.04	...	...	...
XMMXCS J183007.1+010050.4	0065820601	18 30 07.1	+01 00 50	12.3	104.1	8635	2.42	0.26	13.83	0.34	...	...	...
XMMXCS J183022.8+012022.0	0065820501	18 30 22.9	+01 20 22	9.3	233.6	9677	3.87	0.27	92.14	0.16	...	...	...
XMMXCS J183054.8+012215.1	0065820601	18 30 54.8	+01 22 15	16.5	105.1	3013	7.49	0.80	34.13	0.53	...	...	...
XMMXCS J183633.5-653018.8	0109130601	18 36 33.6	-65 30 19	12.0	73.1	4030	2.37	0.31	8.51	0.21	...	...	...
XMMXCS J183633.6-240617.0	0112220201	18 36 33.7	-24 06 17	12.1	433.6	9205	11.35	0.57	88.25	0.53	...	...	...
XMMXCS J183657.5-591022.8	0022940101	18 36 57.6	-59 10 23	13.8	66.4	25658	0.37	0.05	5.62	0.15	...	...	...
XMMXCS J183904.0-652301.9	0109130601	18 39 04.1	-65 23 02	5.3	75.4	6456	1.63	0.21	17.46	0.05	0.138	0.030	3
XMMXCS J184432.6-743100.9	0109462901	18 44 32.6	-74 31 01	12.5	187.9	2184	23.62	1.85	125.13	0.34	0.182	0.028	3
XMMXCS J185032.5-782920.0	0147920701	18 50 32.5	-78 29 20	10.8	76.6	1469	8.69	1.11	35.71	0.11	0.165	0.031	3
XMMXCS J185342.4-084109.7	0154150501	18 53 42.4	-08 41 10	9.5	115.9	11521	2.98	0.30	16.99	0.13	...	...	...
XMMXCS J185603.2-311225.4	0145050101	18 56 03.3	-31 12 25	13.3	63.5	15162	2.40	0.34	9.71	0.15	0.142	0.031	3
XMMXCS J191045.3+002818.7	0112440401	19 10 45.3	+00 28 19	10.2	113.4	7564	4.13	0.43	32.85	0.16	...	...	...
XMMXCS J191952.3-583224.7	0101040501	19 19 52.3	-58 32 25	13.2	33.3	16358	0.55	0.11	31.10	0.05	...	...	...
XMMXCS J193239.9-724230.6	0081341001	19 32 39.9	-72 42 31	6.6	91.6	12622	1.32	0.15	13.41	0.08	...	...	...
XMMXCS J193637.5+072526.5	0089940901	19 36 37.6	+07 25 27	10.5	74.5	8290	1.06	0.14	16.96	0.11	...	...	...
XMMXCS J193646.0+074321.2	0089940801	19 36 46.0	+07 43 21	9.9	39.0	4466	1.13	0.21	34.50	0.02	...	...	...
XMMXCS J193652.5+073425.2	0089940101	19 36 52.6	+07 34 25	2.1	47.7	11557	0.58	0.10	16.05	0.02	...	...	...
XMMXCS J193716.0+074251.0	0089940901	19 37 16.1	+07 42 51	9.4	67.2	6733	1.29	0.18	16.85	0.07	...	...	...
XMMXCS J194921.1+773051.1	0111971601	19 49 21.1	+77 30 51	13.6	142.8	3740	26.21	2.38	28.01	0.34	...	...	...
XMMXCS J195614.8-573943.7	0150190201	19 56 14.8	-57 39 44	7.7	102.8	14125	2.10	0.23	14.54	0.12	...	...	...
XMMXCS J195710.5-575244.1	0150190201	19 57 10.6	-57 52 44	14.4	36.6	8424	1.57	0.31	27.89	0.08	...	...	...
XMMXCS J195815.0-573613.4	0150190201	19 58 15.0	-57 36 13	8.8	32.7	10840	0.71	0.15	9.96	0.02	...	...	...
XMMXCS J200213.1-325013.6	0104860601	20 02 13.2	-32 50 14	15.0	123.7	4938	3.41	0.34	19.39	0.53	...	...	...
XMMXCS J200312.6-324754.9	0104860601	20 03 12.7	-32 47 55	4.5	1327.6	16117	10.02	0.28	649.36	0.25	0.172	0.029	3
XMMXCS J200406.3-330043.4	0104860601	20 04 06.3	-33 00 43	12.6	101.6	8130	1.92	0.21	9.00	0.34	...	...	...
XMMXCS J200737.1-653156.4	0109463201	20 07 37.1	-65 31 56	9.2	88.2	3099	3.53	0.42	27.42	0.08	0.188	0.028	3
XMMXCS J200758.9-110251.6	0044350501	20 07 58.9	-11 02 52	6.0	285.3	9458	3.51	0.22	97.46	0.18	0.079	0.024	3
XMMXCS J200812.5+173424.2	0150100101	20 08 12.6	+17 34 24	11.6	43.0	1933	3.59	0.64	24.18	0.04	...	...	...
XMMXCS J201338.0-415347.8	0081340501	20 13 38.1	-41 53 48	6.4	104.7	14081	1.32	0.14	26.53	0.12	...	...	...
XMMXCS J202152.0+403220.6	0150960801	20 21 52.0	+40 32 21	13.4	43.1	2535	2.18	0.39	16.85	0.08	...	...	...

XMMXCS J203801.3+754059.6	0100650201	20 38 01.4	+75 40 60	5.6	61.2	7839	1.71	0.25	11.39	0.06	...	...	...
XMMXCS J204210.6-323631.4	0111510101	20 42 10.6	-32 36 31	11.2	499.7	8047	18.35	0.86	257.10	0.26	0.079	0.024	3
XMMXCS J204428.9-311436.2	0111420101	20 44 28.9	-31 14 36	10.5	103.8	29019	1.19	0.13	18.94	0.16	...	...	...
XMMXCS J204439.5-313312.8	0111420101	20 44 39.6	-31 33 13	14.3	98.9	21372	303.93	33.75	26.94	0.28	...	...	...
XMMXCS J204931.2+451902.0	0152280501	20 49 31.2	+45 19 02	12.5	34.0	2905	19.78	4.01	21.28	0.05	...	...	...
XMMXCS J205405.6-154728.5	0083210101	20 54 05.7	-15 47 29	8.8	222.0	5922	5.31	0.38	35.00	0.16	0.184	0.021	2
XMMXCS J205434.3+441957.0	0100241101	20 54 34.3	+44 19 57	8.1	48.1	4058	11.26	1.87	23.05	0.04	...	...	...
XMMXCS J205445.3+443135.4	0100241201	20 54 45.3	+44 31 35	12.6	98.9	1918	35.25	3.91	49.93	0.21	...	...	...
XMMXCS J205505.0-155309.5	0083210101	20 55 05.0	-15 53 10	11.4	91.9	4637	3.27	0.38	15.61	0.11	...	...	...
XMMXCS J210407.0-121701.7	0038540301	21 04 07.1	-12 17 02	8.7	227.6	8021	3.28	0.23	306.49	0.16	...	...	...
XMMXCS J211354.4-584737.1	0111251501	21 13 54.4	-58 47 37	15.4	26.4	3520	1.85	0.44	35.00	0.05	...	...	...
XMMXCS J211457.0-584618.0	0111251801	21 14 57.1	-58 46 18	7.9	102.1	1840	4.70	0.51	55.00	0.12	...	...	...
XMMXCS J211503.9-585001.3	0111251501	21 15 03.9	-58 50 01	10.3	63.2	6564	1.17	0.17	45.93	0.07	...	...	...
XMMXCS J211536.4+061109.4	0150610201	21 15 36.3	+06 11 09	11.4	121.5	5564	3.64	0.36	34.78	0.16	...	...	...
XMMXCS J211544.4-585330.5	0111251501	21 15 44.5	-58 53 31	12.7	122.9	5625	9.81	0.97	43.89	0.34	0.084	0.001	1
XMMXCS J211554.2-582834.9	0111251501	21 15 54.2	-58 28 35	12.4	297.0	7644	10.49	0.64	134.12	0.40	0.127	0.001	1
XMMXCS J211610.8-584909.6	0111251701	21 16 10.8	-58 49 10	9.2	95.8	5079	5.58	0.63	19.25	0.08	...	...	...
XMMXCS J211631.4-584612.0	0111251601	21 16 31.5	-58 46 12	8.4	58.2	8931	4.91	0.73	14.58	0.05	0.102	0.031	3
XMMXCS J212320.6-053950.6	0150600101	21 23 20.6	-05 39 51	8.2	190.7	16387	1.26	0.10	26.27	0.13	0.078	0.024	3
XMMXCS J212802.0-444959.0	0088020201	21 28 02.1	-44 49 59	4.4	144.9	14313	1.71	0.15	32.53	0.11	0.223	0.030	3
XMMXCS J212807.2-445409.7	0088020201	21 28 07.3	-44 54 10	7.4	264.3	10855	3.95	0.26	34.82	0.18	...	...	...
XMMXCS J212858.6-153422.6	0103060101	21 28 58.7	-15 34 23	5.4	295.9	15238	2.81	0.17	44.66	0.10	0.199	0.030	3
XMMXCS J213739.8-424919.5	0061940201	21 37 39.9	-42 49 20	14.0	75.7	1429	18.28	2.35	43.53	0.28	...	...	...
XMMXCS J213828.9-424800.9	0061940201	21 38 28.9	-42 48 01	12.4	41.2	1701	4.06	0.74	33.43	0.08	...	...	...
XMMXCS J214427.0+282334.6	0201230101	21 44 27.0	+28 23 35	13.7	114.8	9431	1.87	0.19	15.95	0.34	...	...	...
XMMXCS J215121.8-272336.3	0062940401	21 51 21.8	-27 23 36	11.9	136.0	10436	1.25	0.12	25.01	0.16	...	...	...
XMMXCS J215123.2-302441.2	0103060401	21 51 23.2	-30 24 41	7.7	46.4	14902	0.49	0.08	41.66	0.03	...	...	...
XMMXCS J215144.8+285356.5	0155560501	21 51 44.9	+28 53 57	7.7	50.2	2160	3.05	0.49	20.74	0.06	...	...	...
XMMXCS J215211.2-274347.9	0062940401	21 52 11.3	-27 43 48	12.2	119.2	10902	1.98	0.20	23.57	0.34	...	...	...
XMMXCS J215220.9-272525.3	0062940401	21 52 21.0	-27 25 25	7.8	45.3	12550	0.35	0.06	6.94	0.03	...	...	...
XMMXCS J215221.0-273025.5	0062940401	21 52 21.0	-27 30 26	4.7	216.0	17749	1.07	0.08	69.06	0.10	...	...	...
XMMXCS J215233.1+022038.0	0155560401	21 52 33.2	+02 20 38	3.3	67.6	5195	1.64	0.22	18.87	0.03	0.061	0.021	3
XMMXCS J215734.2-695256.8	0152670101	21 57 34.3	-69 52 57	11.8	131.5	13975	1.45	0.14	32.82	0.16	...	...	...
XMMXCS J215739.6-112651.6	0103860501	21 57 39.7	-11 26 52	16.6	64.7	1309	7.13	1.00	27.02	0.27	0.091	0.001	1
XMMXCS J215811.6-301737.3	0124930501	21 58 11.7	-30 17 37	9.6	418.4	42286	2.81	0.14	50.68	0.24	...	...	...
XMMXCS J215819.9-300933.6	0124930601	21 58 20.0	-30 09 34	8.0	575.3	48319	9.08	0.39	158.87	0.23	...	...	...
XMMXCS J215829.7-301739.3	0124930601	21 58 29.8	-30 17 39	6.3	193.0	41396	1.08	0.08	24.55	0.12	...	...	...
XMMXCS J215850.5-302450.8	0124930501	21 58 50.6	-30 24 51	11.3	461.6	40743	3.16	0.15	58.27	0.26	...	...	...
XMMXCS J215855.3-300102.5	0124930501	21 58 55.4	-30 01 03	12.5	121.2	41223	0.60	0.06	24.59	0.34	...	...	...
XMMXCS J215906.9-694342.1	0152670101	21 59 06.9	-69 43 42	10.7	102.7	13335	1.14	0.12	3.98	0.16	...	...	...
XMMXCS J215933.4-693743.3	0152670101	21 59 33.3	-69 37 43	13.3	133.3	9196	1.79	0.17	13.88	0.34	...	...	...
XMMXCS J220222.4+184236.5	0148200101	22 02 22.4	+18 42 37	15.5	16.0	597	4.74	1.51	23.34	0.04	...	...	...
XMMXCS J220320.1+184837.1	0130920101	22 03 20.1	+18 48 37	5.0	74.7	14057	0.61	0.08	19.07	0.05	...	...	...

XMMXCS J220401.6+190030.1	0130920101	22 04 01.6	+19 00 30	14.1	71.9	4336	2.04	0.27	4.37	0.28	...	...	...
XMMXCS J220550.0-015930.4	0012440301	22 05 50.1	-01 59 30	10.9	79.9	15619	0.63	0.08	45.28	0.11	...	...	...
XMMXCS J220559.3-015815.7	0012440301	22 05 59.3	-01 58 16	12.7	68.2	12948	0.69	0.09	26.27	0.15	...	...	...
XMMXCS J220814.2-471550.0	0111810101	22 08 14.2	-47 15 50	12.0	106.1	16146	1.92	0.21	30.28	0.34	...	...	...
XMMXCS J220819.7-471845.7	0111810101	22 08 19.7	-47 18 46	13.0	68.4	15292	1.29	0.18	33.17	0.15	...	...	...
XMMXCS J220824.1-470336.5	0111810101	22 08 24.1	-47 03 37	10.9	605.5	21542	7.80	0.33	157.55	0.28	...	...	...
XMMXCS J220952.4-471424.8	0111810101	22 09 52.4	-47 14 25	7.6	27.2	27367	0.37	0.09	13.06	0.02	...	...	...
XMMXCS J221447.3-175248.3	0106660601	22 14 47.3	-17 52 48	13.7	501.0	39571	3.97	0.19	80.54	0.57	...	...	...
XMMXCS J221459.6-175036.8	0106660601	22 14 59.6	-17 50 37	10.0	231.6	56004	0.45	0.03	31.16	0.23	...	...	...
XMMXCS J221537.3-172903.3	0106660601	22 15 37.3	-17 29 03	15.1	67.5	19318	0.80	0.11	13.60	0.27	...	...	...
XMMXCS J221548.4-173827.4	0106660401	22 15 48.4	-17 38 27	6.9	33.8	17684	0.95	0.19	16.37	0.03	...	...	...
XMMXCS J221555.9-175149.8	0106660601	22 15 56.0	-17 51 50	9.7	106.7	51699	0.24	0.03	15.48	0.13	...	...	...
XMMXCS J221559.4-173815.5	0106660101	22 15 59.4	-17 38 16	8.8	443.7	28188	1.75	0.09	116.32	0.24	...	...	...
XMMXCS J221605.1-175418.3	0106660601	22 16 05.1	-17 54 18	12.9	160.8	37256	2.72	0.23	18.19	0.34	...	...	...
XMMXCS J221613.6-173519.9	0106660601	22 16 13.6	-17 35 20	13.3	247.0	28314	0.91	0.06	31.83	0.40	...	...	...
XMMXCS J221622.4-173308.2	0106660101	22 16 22.5	-17 33 08	16.3	89.6	20502	1.88	0.22	28.94	0.28	...	...	...
XMMXCS J221656.7+002405.9	0094310101	22 16 56.8	+00 24 06	13.0	508.7	21180	2.96	0.14	NaN	0.57	...	...	...
XMMXCS J221659.5+002505.7	0094310101	22 16 59.6	+00 25 06	13.3	153.9	24010	0.78	0.07	35.67	0.34	...	...	...
XMMXCS J221705.0+002633.7	0094310201	22 17 05.1	+00 26 34	13.6	355.6	26243	1.81	0.10	69.53	0.46	...	...	...
XMMXCS J221712.9-082740.8	0009650201	22 17 12.9	-08 27 41	12.4	39.0	6676	1.50	0.28	14.97	0.05	...	...	...
XMMXCS J221713.4+000158.2	0094310201	22 17 13.5	+00 01 58	14.0	106.6	29663	1.55	0.17	31.82	0.53	...	...	...
XMMXCS J221714.3+000542.4	0094310201	22 17 14.3	+00 05 42	10.6	206.7	39995	0.70	0.05	46.63	0.23	...	...	...
XMMXCS J221714.6+142805.5	0103660301	22 17 14.7	+14 28 06	13.8	95.2	7237	5.38	0.61	13.10	0.21	...	...	...
XMMXCS J221720.4+141808.7	0103660301	22 17 20.5	+14 18 09	4.3	160.4	15195	1.90	0.16	24.24	0.11	...	...	...
XMMXCS J221725.9-082537.6	0009650201	22 17 25.9	-08 25 38	8.6	86.7	10060	2.40	0.29	53.32	0.08	0.085	0.001	1
XMMXCS J221744.7-163810.6	0148060201	22 17 44.8	-16 38 11	10.4	71.9	2036	3.54	0.47	33.06	0.11	...	...	...
XMMXCS J221752.5+001635.6	0094310201	22 17 52.6	+00 16 36	4.9	91.0	54126	0.17	0.02	29.84	0.05	...	...	...
XMMXCS J221809.2+002715.1	0094310201	22 18 09.3	+00 27 15	15.0	83.9	17235	0.71	0.09	21.39	0.28	...	...	...
XMMXCS J221810.7-082606.1	0009650201	22 18 10.8	-08 26 06	6.3	79.8	12576	1.38	0.17	48.81	0.08	...	...	...
XMMXCS J221825.0+002425.0	0094310101	22 18 25.0	+00 24 25	15.8	613.6	16122	11.50	0.48	NaN	0.60	...	...	...
XMMXCS J221829.6+001209.2	0094310101	22 18 29.7	+00 12 09	14.2	152.7	20617	1.50	0.13	16.66	0.53	...	...	...
XMMXCS J221853.9+121334.5	0103861201	22 18 54.0	+12 13 35	8.3	59.5	7535	1.16	0.17	11.06	0.05	...	...	...
XMMXCS J221911.5+121753.5	0103861201	22 19 11.6	+12 17 54	10.1	33.3	7120	0.65	0.13	13.66	0.02	...	...	...
XMMXCS J222044.1-242816.5	0049340201	22 20 44.1	-24 28 17	12.4	76.1	10104	0.95	0.12	18.49	0.21	...	...	...
XMMXCS J222300.6-020532.7	0090050601	22 23 00.6	-02 05 33	12.3	225.9	11720	7.72	0.55	95.26	0.40	...	...	...
XMMXCS J222332.9-021805.9	0090050601	22 23 32.8	-02 18 06	12.6	252.7	10857	6.84	0.46	407.37	0.40	...	...	...
XMMXCS J222736.8-052113.6	0100440101	22 27 36.8	-05 21 14	13.5	151.8	14638	1.55	0.14	41.77	0.34	...	...	...
XMMXCS J222759.3-052858.7	0100440101	22 27 59.4	-05 28 59	12.7	196.1	15071	2.38	0.18	46.50	0.34	...	...	...
XMMXCS J222818.4-053405.3	0100440101	22 28 18.4	-05 34 05	15.5	279.1	11003	132.02	8.39	141.09	0.59	...	...	...
XMMXCS J222818.8-050746.8	0100440101	22 28 18.8	-05 07 47	11.5	351.4	22511	2.91	0.16	39.50	0.29	0.132	0.030	3
XMMXCS J222820.6-051329.1	0100440101	22 28 20.7	-05 13 29	5.9	139.0	35144	0.67	0.06	28.85	0.11	...	...	...
XMMXCS J222833.2-052826.2	0100440101	22 28 33.3	-05 28 26	9.5	333.7	21669	2.40	0.14	61.56	0.16	0.146	0.031	3
XMMXCS J222856.9-053053.5	0100440101	22 28 57.0	-05 30 54	13.7	237.4	17523	8.14	0.56	29.28	0.40	...	...	...

XMMXCS J223003.6-204919.3	0125911001	22 30 03.7	-20 49 19	3.6	133.0	12283	1.21	0.11	14.51	0.08	...	...	...	
XMMXCS J223018.9+392403.9	0002970101	22 30 19.0	+39 24 04	12.2	96.0	10123	1.11	0.13	16.93	0.21	...	...	...	
XMMXCS J223022.9-203952.2	0125911001	22 30 23.0	-20 39 52	12.6	74.7	4877	2.45	0.32	17.67	0.21	...	...	...	
XMMXCS J223031.7+392601.1	0002970101	22 30 31.7	+39 26 01	10.5	69.7	11359	0.81	0.11	18.21	0.07	0.183	0.028	3	
XMMXCS J223219.8+393015.3	0002970101	22 32 19.9	+39 30 15	14.4	59.6	5880	1.20	0.18	33.85	0.17	...	...	...	
XMMXCS J223228.7+391518.3	0002970101	22 32 28.7	+39 15 18	14.6	613.0	7390	82.21	3.46	302.81	0.60	0.271	0.037	3	
XMMXCS J223447.3-260459.4	0111790101	22 34 47.3	-26 04 59	13.3	68.4	11744	1.82	0.25	27.35	0.15	...	...	...	
XMMXCS J223528.6+341001.2	0021140201	22 35 28.7	+34 10 01	13.0	155.5	16416	0.90	0.08	36.52	0.34	...	...	...	
XMMXCS J223547.9+335250.1	0021140201	22 35 47.9	+33 52 50	7.1	236.6	30954	0.94	0.07	55.23	0.18	...	...	...	
XMMXCS J223555.0-255554.3	0111790101	22 35 55.1	-25 55 54	7.4	66.6	26418	0.68	0.09	15.55	0.07	...	...	...	
XMMXCS J223557.3-254928.4	0111790101	22 35 57.4	-25 49 28	13.8	57.0	15773	1.19	0.18	11.71	0.10	...	...	...	
XMMXCS J223606.5+341132.2	0021140201	22 36 06.5	+34 11 32	12.4	111.4	15873	1.15	0.12	44.43	0.34	...	...	...	
XMMXCS J223626.0-152337.5	0056021601	22 36 26.0	-15 23 38	11.1	79.5	12939	0.77	0.10	28.74	0.11	...	...	...	
XMMXCS J223633.7+342959.3	0103863101	22 36 33.7	+34 29 59	8.1	742.3	5874	15.35	0.58	437.25	0.23	0.059	0.019	3	
XMMXCS J223646.4-150806.2	0056021601	22 36 46.5	-15 08 06	8.7	109.1	13596	0.95	0.10	42.55	0.13	...	...	...	
XMMXCS J223651.0+133917.5	0153220601	22 36 51.1	+13 39 18	11.5	55.1	3819	1.65	0.25	43.31	0.06	...	...	...	
XMMXCS J223654.9-152439.1	0056021601	22 36 54.9	-15 24 39	8.6	67.2	16425	0.53	0.07	28.71	0.07	...	...	...	
XMMXCS J223656.7-152924.3	0056021601	22 36 56.7	-15 29 24	13.3	323.8	11912	10.81	0.63	110.15	0.46	0.093	0.032	3	
XMMXCS J223757.7+341631.3	0103863101	22 37 57.7	+34 16 31	13.8	32.1	3399	2.21	0.46	25.60	0.05	...	...	...	
XMMXCS J223814.7-204710.6	0151450101	22 38 14.8	-20 47 11	12.3	82.0	14211	1.92	0.24	24.46	0.21	...	...	...	
XMMXCS J223852.1-202610.3	0151450101	22 38 52.1	-20 26 10	11.2	324.6	21669	4.62	0.27	118.65	0.29	...	...	...	
XMMXCS J223925.9+032144.0	0110960101	22 39 25.9	+03 21 44	16.0	49.0	4238	1.66	0.27	20.98	0.13	...	...	...	
XMMXCS J223939.0+080554.1	0103860301	22 39 39.0	+08 05 54	10.0	83.8	3173	6.90	0.84	21.28	0.11	...	...	...	
XMMXCS J224025.2-055816.5	0149410401	22 40 25.2	-05 58 17	9.9	126.0	12608	1.25	0.12	47.96	0.13	...	...	...	
XMMXCS J224040.0+081017.3	0103860301	22 40 40.0	+08 10 17	8.9	99.9	4285	4.37	0.48	19.05	0.08	0.141	0.001	1	
XMMXCS J224041.7-435849.1	0153220101	22 40 41.7	-43 58 49	14.6	23.2	2744	135.72	34.48	18.99	0.05	...	...	...	
XMMXCS J224100.0+075818.7	0103860301	22 41 00.0	+07 58 19	11.5	50.1	3248	2.95	0.48	27.60	0.06	...	...	...	
XMMXCS J224113.3+032833.0	0110960101	22 41 13.4	+03 28 33	12.9	409.2	10940	10.18	0.53	115.99	0.53	0.128	0.032	3	
XMMXCS J224729.1-510211.0	0109070401	22 47 29.2	-51 02 11	13.7	67.7	5006	3.49	0.48	22.55	0.15	...	...	...	
XMMXCS J224826.9-511858.3	0109070401	22 48 27.0	-51 18 58	9.3	69.7	8484	2.18	0.29	24.57	0.07	...	...	...	
XMMXCS J224855.3-270732.4	0111970101	22 48 55.4	-27 07 32	10.0	233.2	7496	4.12	0.29	79.57	0.23	...	...	...	
XMMXCS J224923.2-265347.0	0111970101	22 49 23.3	-26 53 47	13.7	144.4	4500	4.48	0.40	55.93	0.34	...	...	...	
XMMXCS J225108.1-175418.9	0081340901	22 51 08.2	-17 54 19	10.0	65.1	10403	0.64	0.09	35.89	0.07	...	...	...	
XMMXCS J225116.2-175902.5	0081340901	22 51 16.3	-17 59 03	10.3	154.4	9715	1.84	0.16	53.60	0.16	...	...	...	
XMMXCS J225125.3-174541.1	0081340901	22 51 25.4	-17 45 41	8.8	77.9	13692	0.69	0.09	32.18	0.08	...	...	...	
XMMXCS J225143.7-175859.6	0081340901	22 51 43.7	-17 58 60	6.7	91.9	14169	0.74	0.09	32.57	0.08	...	...	...	
XMMXCS J225240.3-175021.9	0081340901	22 52 40.4	-17 50 22	12.3	155.7	10283	3.88	0.34	41.07	0.34	0.070	0.001	1	
XMMXCS J225417.6-174043.8	0012940101	22 54 17.6	-17 40 44	6.4	91.1	12996	1.53	0.18	22.85	0.08	0.065	0.001	1	
XMMXCS J225635.3-363200.2	0135980201	22 56 35.3	-36 32 00	8.3	101.3	15836	0.79	0.09	52.46	0.13	...	...	...	
XMMXCS J230217.6+082406.8	0032140201	23 02 17.6	+08 24 07	12.8	46.9	2914	2.06	0.35	17.44	0.08	...	...	...	
XMMXCS J230227.2+083911.7	0032140201	23 02 27.3	+08 39 12	2.7	83.9	7740	1.25	0.15	13.55	0.03	...	...	...	
XMMXCS J230244.9+085951.2	0112170101	23 02 44.9	+08 59 51	10.7	34.0	8976	0.98	0.20	22.50	0.02	...	...	...	
XMMXCS J230256.6+083132.0	0032140201	23 02 56.6	+08 31 32	8.4	53.3	4963	1.37	0.21	12.37	0.05	...	...	...	

XMMXCS J230337.6+085459.6	0112170101	23 03 37.7	+08 54 60	5.9	72.0	12258	2.06	0.27	18.60	0.05	...	...	...
XMMXCS J230548.1+031033.1	0033541001	23 05 48.2	+03 10 33	15.8	71.2	2574	9.98	1.33	85.04	0.28	...	...	...
XMMXCS J230854.2+613417.7	0203130201	23 08 54.3	+61 34 18	6.0	128.4	17866	0.81	0.08	14.70	0.12	0.006	0.005	2
XMMXCS J230910.5+614442.0	0203130201	23 09 10.5	+61 44 42	6.3	104.4	15842	0.77	0.08	32.28	0.12	...	...	...
XMMXCS J231443.2-590344.4	0081340301	23 14 43.3	-59 03 44	8.2	231.7	9831	3.76	0.26	44.38	0.16	...	...	...
XMMXCS J231502.8-585609.9	0081340301	23 15 02.8	-58 56 10	9.1	107.4	8587	1.93	0.20	41.85	0.13	...	...	...
XMMXCS J231625.5+791123.4	0203060101	23 16 25.5	+79 11 23	14.1	6.3	9832	0.03	0.02	21.41	0.03	...	...	...
XMMXCS J231648.3-424228.4	0093640701	23 16 48.4	-42 42 28	10.2	374.8	8331	11.39	0.62	55.00	0.29	0.098	0.001	1
XMMXCS J231727.9-421601.2	0112310201	23 17 28.0	-42 16 01	11.9	73.7	9787	1.12	0.15	5.77	0.11	...	...	...
XMMXCS J231851.8-423130.3	0112310201	23 18 51.8	-42 31 30	10.7	784.5	10194	10.01	0.37	160.49	0.28	0.115	0.001	1
XMMXCS J232023.4+784842.1	0203060101	23 20 23.4	+78 48 42	11.8	77.5	13483	1.81	0.23	31.91	0.11	...	...	...
XMMXCS J232124.6+194515.9	0202140301	23 21 24.7	+19 45 16	10.0	4335.9	19256	25.64	0.40	NaN	0.28	0.245	0.029	3
XMMXCS J232152.7+195333.2	0202140301	23 21 52.7	+19 53 33	9.8	456.4	17216	3.11	0.15	120.12	0.24	...	...	...
XMMXCS J232155.9+193802.4	0202140301	23 21 55.9	+19 38 02	6.9	145.0	25481	0.63	0.06	42.91	0.12	...	...	...
XMMXCS J232221.3+193855.8	0202140301	23 22 21.4	+19 38 56	6.4	660.4	23841	3.08	0.12	171.71	0.29	0.158	0.032	3
XMMXCS J232227.7+195948.2	0202140301	23 22 27.7	+19 59 48	16.1	35.8	8448	4.13	0.81	14.47	0.08	...	...	...
XMMXCS J233219.2+195500.3	0112880301	23 32 19.3	+19 55 00	7.0	217.9	9733	3.27	0.24	76.65	0.18	0.227	0.030	3
XMMXCS J233230.5+195106.4	0112880301	23 32 30.5	+19 51 06	10.8	48.5	7022	1.14	0.19	17.30	0.04	...	...	...
XMMXCS J233231.0+485406.9	0093552701	23 32 31.0	+48 54 07	12.4	397.4	8697	8.54	0.45	102.75	0.46	0.111	0.032	3
XMMXCS J233402.4+485108.5	0093552701	23 34 02.5	+48 51 09	4.2	6010.2	15078	63.46	0.83	NaN	0.25	0.253	0.035	3
XMMXCS J233537.1+021737.0	0112522601	23 35 37.1	+02 17 37	12.6	266.6	6921	8.30	0.54	72.76	0.40	...	...	...
XMMXCS J233745.6-562757.6	0083210201	23 37 45.7	-56 27 58	3.4	229.7	8687	3.36	0.24	110.70	0.11	...	...	...
XMMXCS J233802.3+462210.1	0099320101	23 38 02.3	+46 22 10	7.2	140.9	20012	3.04	0.28	10.35	0.12	...	...	...
XMMXCS J233831.2+462106.2	0099320101	23 38 31.2	+46 21 06	11.8	92.5	12822	3.08	0.35	36.96	0.11	...	...	...
XMMXCS J233911.2-561346.5	0083210201	23 39 11.3	-56 13 47	15.7	21.2	1868	2.91	0.78	31.49	0.05	...	...	...
XMMXCS J233949.7-121307.1	0055990301	23 39 49.8	-12 13 07	4.5	330.3	10679	4.20	0.24	237.03	0.21	...	...	...
XMMXCS J233950.6-120641.8	0055990301	23 39 50.7	-12 06 42	10.9	55.4	6228	1.13	0.17	17.02	0.06	...	...	...
XMMXCS J234652.9+005404.2	0147580401	23 46 53.0	+00 54 04	8.1	70.0	10060	0.93	0.13	30.82	0.08	...	...	...
XMMXCS J235001.5+362521.9	0100241001	23 50 01.6	+36 25 22	4.1	751.7	7121	19.05	0.72	303.42	0.25	...	...	...
XMMXCS J235109.5+201538.2	0093190301	23 51 09.5	+20 15 38	10.3	373.7	17609	2.49	0.14	69.65	0.29	0.200	0.027	3
XMMXCS J235149.9+195359.6	0093190301	23 51 49.9	+19 53 60	13.4	147.4	12246	5.08	0.45	47.43	0.34	...	...	...
XMMXCS J235204.9+195726.9	0093190301	23 52 04.9	+19 57 27	13.0	517.1	13580	1401.88	64.40	124.20	0.57	...	...	...
XMMXCS J235708.5-241453.7	0125910301	23 57 08.6	-24 14 54	11.2	370.9	5765	9.05	0.49	126.75	0.29	...	...	...

Table C.1: XCS Statistical Cluster Sample: New Candidates. The column descriptions are given in Section 4.2.1.

Appendix D

XCS Manual Cluster Candidates

Id	Obsid	RA(J2000)	Dec(J2000)	Flags	Comment	Literature Name	z
XMMXCS J000029.7-251216.0	0125310101	00 00 29.7	-25 12 16	0000	PSF-sized	...	...
XMMXCS J000322.2-260017.3	0103060301	00 03 22.2	-26 00 17	0000	PSF-sized	...	...
XMMXCS J000400.2-355653.5	0145020201	00 04 00.2	-35 56 54	0000	Cuspy central emission	...	...
XMMXCS J001526.8+171725.1	0202190201	00 15 26.8	+17 17 25	0000	Removed as lobe	...	...
XMMXCS J002808.8-771103.3	0006010401	00 28 08.9	-77 11 03	0000	Cuspy source on chip gap	...	...
XMMXCS J003534.7-430856.8	0148960101	00 35 34.8	-43 08 57	0000	PSF-sized	...	...
XMMXCS J011136.1-381115.6	0002942301	01 11 36.1	-38 11 16	1110	PSF-sized, orientation not that of PSF	WARPJ0111.6-3811	0.122
XMMXCS J012105.4-440714.4	0103860901	01 21 05.4	-44 07 14	0000	PSF-sized	...	...
XMMXCS J012654.3+191253.3	0112600601	01 26 54.4	+19 12 53	1000	PSF-sized	ABELL0195	0.043
XMMXCS J015916.9+003011.3	0101640201	01 59 16.9	+00 30 11	1110	Cuspy extended source	[VMF98]021	0.386
XMMXCS J021741.6-052541.9	0112370701	02 17 41.7	-05 25 42	0000	PSF-sized	...	...
XMMXCS J021831.8-050108.9	0112371001	02 18 31.9	-05 01 09	0000	Cuspy emission near centre	...	...
XMMXCS J022342.0-050200.5	0111110401	02 23 42.0	-05 02 01	0000	PSF-sized	...	...
XMMXCS J022456.0-050801.5	0111110301	02 24 56.1	-05 08 02	0000	PSF-sized	...	...
XMMXCS J022524.7-044044.0	0112681001	02 25 24.7	-04 40 44	0000	PSF-sized	...	...
XMMXCS J022530.7-041418.2	0112680301	02 25 30.7	-04 14 18	0000	PSF-sized	...	...
XMMXCS J022532.1-035511.5	0037980301	02 25 32.1	-03 55 12	0011	Strong central point-like emission	XLSS J022532.5-035510	...
XMMXCS J022644.8-034106.1	0037980401	02 26 44.9	-03 41 06	0011	PSF-sized	XLSSC 009	0.327
XMMXCS J022724.0-033401.7	0037981001	02 27 24.0	-03 34 02	0000	PSF-sized	...	...
XMMXCS J024259.4+000221.0	0111200201	02 42 59.4	+00 02 21	0000	PSF-sized	...	...
XMMXCS J030518.0+172826.9	0112190101	03 05 18.0	+17 28 27	1110	Cuspy central emission	MS0302.5+1717	0.425
XMMXCS J031527.3+420533.3	0002942401	03 15 27.3	+42 05 33	0000	Low count, large scale extent	...	...
XMMXCS J034411.5+243958.2	0112390101	03 44 11.5	+24 39 58	0000	PSF-sized	...	...
XMMXCS J040013.6-673558.6	0110980401	04 00 13.6	-67 35 59	0000	Removed as lobe	...	...
XMMXCS J042017.6-503157.1	0141751101	04 20 17.6	-50 31 57	0000	Cuspy central emission	...	...
XMMXCS J042606.0-570603.6	0112600401	04 26 06.1	-57 06 04	0000	Low counts, large angular extent	...	...
XMMXCS J045421.5-531539.9	0148650101	04 54 21.6	-53 15 40	0000	Cuspy central emission	...	...
XMMXCS J045716.9-752517.0	0137160201	04 57 16.9	-75 25 17	0110	PSF-sized	AM 0459-753	...
XMMXCS J051544.7-001035.1	0147190101	05 15 44.8	-00 10 35	0000	PSF-sized	...	...
XMMXCS J051743.6-542825.0	0042340701	05 17 43.7	-54 28 25	0000	PSF-sized, probably nearby galaxy	...	...
XMMXCS J053438.1-670141.2	0071740501	05 34 38.2	-67 01 41	0000	PSF-sized	...	...
XMMXCS J063819.8+821249.0	0029340101	06 38 19.9	+82 12 49	0000	PSF-sized	...	...
XMMXCS J083839.1+255020.1	0025540301	08 38 39.1	+25 50 20	0000	Strong central point-like emission	...	...
XMMXCS J084013.1+192806.5	0101440401	08 40 13.2	+19 28 07	0000	Misclassified source	...	...
XMMXCS J084143.1+704625.0	0112620101	08 41 43.2	+70 46 25	1110	Over zealous point source removal	[VMF98]057	0.235
XMMXCS J095419.6+173559.3	0112850101	09 54 19.7	+17 35 59	0000	PSF-sized	...	...
XMMXCS J101307.9-445911.6	0073340201	10 13 07.9	-44 59 12	0000	Cuspy central source	...	...
XMMXCS J101641.0+385450.3	0084230701	10 16 41.0	+38 54 50	0000	Cuspy extended source	...	...
XMMXCS J102451.1-183342.9	0200240401	10 24 51.1	-18 33 43	0000	PSF-sized	...	...
XMMXCS J103008.6+051929.4	0148560501	10 30 08.6	+05 19 29	0000	Very large angular extent, low counts	...	...
XMMXCS J103111.7-461506.5	0092970301	10 31 11.8	-46 15 07	0010	Cuspy extended source	*NGC 3283	0.010

XMMXCS J104133.5+061525.2	0151390101	10 41 33.6	+06 15 25	0110	Central point source emission	WBL 280	0.031
XMMXCS J104443.9-011952.5	0125300101	10 44 43.9	-01 19 53	0000	Removed as lobe	...	...
XMMXCS J105624.2-033524.0	0094800101	10 56 24.2	-03 35 24	0000	Extent around very cuspy emission	...	...
XMMXCS J105652.8-764835.8	0067140201	10 56 52.8	-76 48 36	0000	Cuspy extended source	...	...
XMMXCS J111654.7+180305.6	0099030101	11 16 54.7	+18 03 06	1110	Cuspy central source in large extent	NGC3607GROUP	0.003
XMMXCS J111817.5+075821.6	0082340101	11 18 17.5	+07 58 22	0000	PSF-sized, but not PSF orientation	...	...
XMMXCS J111951.3+132854.6	0110980101	11 19 51.4	+13 28 55	0000	PSF-sized	...	...
XMMXCS J112524.2+385400.5	0052140201	11 25 24.2	+38 54 01	0000	Cuspy extended source	...	...
XMMXCS J113103.1+311013.4	0102040201	11 31 03.1	+31 10 13	0000	PSF-sized	...	...
XMMXCS J115027.6+014531.6	0044740201	11 50 27.6	+01 45 32	0000	Removed as lobe of nearby P	...	...
XMMXCS J120409.8+202033.5	0112270601	12 04 09.8	+20 20 34	0010	Cuspy emission near centre	NGC 4066	0.025
XMMXCS J120440.7-615730.7	0109110101	12 04 40.8	-61 57 31	0000	PSF-sized	...	...
XMMXCS J121408.4+140934.1	0112610101	12 14 08.4	+14 09 34	0000	Potential point source blend	...	...
XMMXCS J123046.8+111114.5	0145800101	12 30 46.8	+11 11 15	0000	Cuspy source near centre	...	...
XMMXCS J123707.6+622144.9	0111550201	12 37 07.7	+62 21 45	0000	PSF-sized, possibly blend	...	...
XMMXCS J123812.2-830752.4	0092360801	12 38 12.2	-83 07 52	0000	PSF-sized	...	...
XMMXCS J124454.7-002702.8	0110980201	12 44 54.7	-00 27 03	0100	Large angular extent	SDSS CE J191.220749-00.444507	0.220
XMMXCS J130514.3+180208.5	0017940101	13 05 14.4	+18 02 09	0000	PSF-sized	...	...
XMMXCS J131152.8+352139.8	0109080201	13 11 52.8	+35 21 40	0000	Low counts, large extent	...	...
XMMXCS J132457.3+300729.0	0025740201	13 24 57.4	+30 07 29	0110	PSF-sized	PDCS 013S	0.600
XMMXCS J134851.5+600925.0	0071340501	13 48 51.6	+60 09 25	0000	PSF-sized	...	...
XMMXCS J135545.8+182253.1	0094401201	13 55 45.8	+18 22 53	0000	Significance underestimated due to background	...	...
XMMXCS J140654.0+283417.9	0140960101	14 06 54.0	+28 34 18	1110	Removed as lobe	WARPJ1406.9+2834	0.118
XMMXCS J142855.4+474224.6	0109080901	14 28 55.4	+47 42 25	0000	PSF-sized	...	...
XMMXCS J145317.5+033447.0	0150350101	14 53 17.5	+03 34 47	0000	PSF-sized	...	...
XMMXCS J155912.4+635348.0	0070341201	15 59 12.5	+63 53 48	0000	PSF-sized	...	...
XMMXCS J162726.8-243221.3	0111120201	16 27 26.9	-24 32 21	0000	Misclassified as point source	...	...
XMMXCS J162816.0-492016.4	0098610101	16 28 16.1	-49 20 16	0000	PSF-sized, possibly blend	...	...
XMMXCS J165843.1+790716.8	0112500101	16 58 43.2	+79 07 17	0000	Extended sources removed each other	...	...
XMMXCS J170042.0+641300.1	0107860301	17 00 42.0	+64 13 00	1110	PSF-sized	ABELL2246	0.225
XMMXCS J170428.7-374807.3	0083280101	17 04 28.8	-37 48 07	0000	PSF-sized, possibly blend	...	...
XMMXCS J173053.0+520900.6	0021750201	17 30 53.0	+52 09 01	0000	Low count PSF-sized	...	...
XMMXCS J175708.4-300338.8	0050940201	17 57 08.4	-30 03 39	0000	PSF-sized	...	...
XMMXCS J181927.3+682413.9	0004610301	18 19 27.4	+68 24 14	0000	Low count, large scale extent	...	...
XMMXCS J183551.5-234656.0	0112220201	18 35 51.6	-23 46 56	0000	Cuspy central emission	...	...
XMMXCS J184500.9+005325.8	0017740701	18 45 01.0	+00 53 26	0000	PSF-sized	...	...
XMMXCS J190104.3-370339.6	0111120101	19 01 04.3	-37 03 40	0000	PSF-sized	...	...
XMMXCS J212749.4-450149.2	0088020201	21 27 49.4	-45 01 49	0000	Cuspy, PSF-sized source	...	...
XMMXCS J214411.7+281014.3	0201230101	21 44 11.8	+28 10 14	0000	Extent remove each other	...	...
XMMXCS J215134.3-302624.7	0103060401	21 51 34.3	-30 26 25	0000	Cuspy central emission	...	...
XMMXCS J221557.3-174941.0	0106660601	22 15 57.4	-17 49 41	0000	PSF-sized	...	...
XMMXCS J221744.8+001726.7	0094310101	22 17 44.9	+00 17 27	0000	Mistakenly removed as lobe	...	...
XMMXCS J222341.7-020000.6	0090050601	22 23 41.8	-02 00 01	0000	Low counts extended source, misclassified	...	...

XMMXCS J224448.7-724407.2	0150050101	22 44 48.7	-72 44 07	0000	Misclassified point	...	...
XMMXCS J225209.6-175517.5	0081340901	22 52 09.6	-17 55 18	0000	Removed as lobe	...	...
XMMXCS J225653.0-363310.5	0135980201	22 56 53.0	-36 33 11	0110	PSF-sized	HST J225657-36342	...
XMMXCS J231622.8-590434.1	0081340301	23 16 22.8	-59 04 34	0000	PSF-sized	...	...
XMMXCS J233935.5-121417.5	0055990301	23 39 35.5	-12 14 18	0000	Cuspy extended source	...	...
XMMXCS J235147.7+200624.6	0093190301	23 51 47.8	+20 06 25	0000	Cuspy extended source	...	...

Table D.1: XCS Manual Cluster Candidates. The column descriptions are given in Section 4.2.1. The additional column 'Comment' explains why the sources were missed by the detection algorithms.

Appendix E

XCS Database Attributes

Table	Attribute	Description
Observation	obsID	XMM pointing identifier
	dateObs	Date and time of beginning of exposure
	dateEnd	Date and time of end of exposure
	revolution	XMM Revolution number
	target	Name of observed object
	observer	Name of observer
	raTarget	[deg] Right Ascension of target
	decTarget	[deg] Declination of target
	raNom	[deg] Right Ascension of nominal boresight
	decNom	[deg] Declination of nominal boresight
	raPnt	[deg] Actual (mean) pointing Right Ascension
	decPnt	[deg] Actual (mean) pointing Declination
	paPnt	[deg] Actual (mean) position angle
	equinox	Equinox for sky coordinates
	cdelt2	[deg] Pixel size
	nHVal	Hydrogen column density
	pointingType	XMM target pointing type
	mask	Binary flag representing whether a XCS mask exists
	xcsStatus	Binary flag for suitability of obsID for XCS
	observationID	Index for table
	htmid	Hierarchical Triangular Mesh id
	cx	Hierarchical Triangular Mesh cartesian x
	cy	Hierarchical Triangular Mesh cartesian y
	cz	Hierarchical Triangular Mesh cartesian z
Exposure	expID	Index for table
	obsID	XMM pointing identifier
	camera	EPIC camera
	exposure	Exposure identifier
	filter	Filter used for exposure
	submode	Submode used for exposure
	livetime	Actual exposure time after removal of bad periods
	band	Exposure band [soft/hard]
PointingTypesCode	pointingType	Index for table
	pointingTypeString	Description of type
Detection	DetectionID	Index for table
	xcsName	IAU XCS name
	obsID	XMM pointing identifier
	ra	[deg] Right Ascension
	dec	[deg] Declination
	x	Image x position
	y	Image y position
	xErr	1σ error on x
	yErr	1σ error on y
	majAx	Object ellipse major axis
	minAx	Object ellipse minor axis
	orient	Object ellipse orientation
	offaxis	[arcmin] Off-axis angle
	azi	[deg] Azimuthal angle
	scts	Soft band source counts
	tmax	Maximum source exposure
	flux	Soft band source flux
	fluxerr	1σ error on soft band source flux
	sig	Source significance
	pPoint	Probability of source being point-like
	class	Source classification
	psfSizeFlag	Potential misclassification flag
	pntConFlag	Potential point source contamination
	run1ConFlag	Potential Run1 source contamination
	rInnerMaj	Background annulus inner edge major axis
	rInnerMin	Background annulus inner edge minor axis
	rOuterMaj	Background annulus outer edge major axis
	rOuterMin	Background annulus outer edge minor axis
	srcPix	Number of pixels used for source aperture
	bkgPix	Number of pixels used for background aperture
	avSrcExp	Average exposure across source

	avBkgExp	Average exposure across background
	bkgCts	Counts in background annulus
	bkgCtsSrc	Background counts in source aperture
	totCts	Total counts in source aperture
	srcCts	Source counts
	masterDetectionID	ID for parent detection
	htmid	Hierarchical Triangular Mesh id
	cx	Hierarchical Triangular Mesh cartesian x
	cy	Hierarchical Triangular Mesh cartesian y
	cz	Hierarchical Triangular Mesh cartesian z
HardbandProperties	DetectionID	Index for table
	hScts	Hard band source counts
	hSig	Hard band source significance
IndivExpProp	IndivID	Index for table
	xcsName	IAU XCS name
	DetectionID	ID from Detection table
	MasterID	Master ID from Detection table
	obsID	XMM pointing identifier
	camera	EPIC camera
	ident	Exposure identifier
	scts	Individual exposure soft band source counts
	ctRate	Individual exposure count-rate
	flux	Individual exposure source flux
	sig	Source significance
	rInnerMaj	Background annulus inner edge major axis
	rInnerMin	Background annulus inner edge minor axis
	rOuterMaj	Background annulus outer edge major axis
	rOuterMin	Background annulus outer edge minor axis
	srcPix	Number of pixels used for source aperture
	bkgPix	Number of pixels used for background aperture
	avSrcExp	Average exposure across source
	avBkgExp	Average exposure across background
	bkgCts	Counts in background annulus
	bkgCtsSrc	Background counts in source aperture
	totCts	Total counts in source aperture
Source	xcsName	IAU XCS name
	obsID	XMM pointing identifier
	ra	Right Ascension
	dec	Declination
	softCts	Soft band source counts
	tmax	Maximum source exposure in soft band
	softFlux	Soft band source flux
	hardCts	Hard band source counts
	tmaxhard	Maximum source exposure in hard band
	hardnessRatio	Hardness ratio for source
	softSig	Soft band source significance
	hardSig	Hard band source significance
	softPpoint	Probability of source being point-like (soft band)
	class	Source classification
	masterDetectionID	Master ID in Detection table
	masterPSFSizeFlag	Master Detection PSF size warning
	masterPntConFlag	Master Detection point contamination
	masterRun1ConFlag	Master Detection Run1 contamination
	targetFlag	Warning that source may be pointing target
	clObsFlag	Warning that source is in a Cluster Pointing
	snrObsFlag	Warning that source is in a SNR Pointing
	htmid	Hierarchical Triangular Mesh id
	cx	Hierarchical Triangular Mesh cartesian x
	cy	Hierarchical Triangular Mesh cartesian y
	cz	Hierarchical Triangular Mesh cartesian z
	sourceID	Index for table
FollowUp	FUID	Index for table
	xcsName	IAU XCS name
	ra	Right Ascension
	dec	Declination
	telescope	Telescope
	PI	Principal Investigator

	propID	Proposal Identifier
	propStatus	Status of Proposal
	propType	Type of Proposal
	obsStatus	Status of observation
	obsDate	Date of Observation
	confirmCls	Confirmation of cluster
	redshift	Measured cluster redshift
	comments	Comments on proposal or observation
ManualCandidate	manualCandidateID	Index for table
	xcsName	IAU XCS name
	ra	Right Ascension
	dec	Declination
	omissionReason	Reason for object not being in Source
	obsID	XMM pointing identifier
	known	Association with known cluster
OmissionReasonCode	omissionReason	Index for table
	omissionReasonString	Description of reason
KnownBAXCluster	knownBAXClusterID	Index for table
	baxName	Source name
	baxRA	BAX Right Ascension
	baxDec	BAX Declination
	baxRedshift	BAX redshift
	htmid	Hierarchical Triangular Mesh id
	cx	Hierarchical Triangular Mesh cartesian x
	cy	Hierarchical Triangular Mesh cartesian y
	cz	Hierarchical Triangular Mesh cartesian z
KnownNEDObject	knownNEDObjectID	Index for table
	nedName	Source name
	nedRA	NED Right Ascension
	nedDec	NED Declination
	nedRedshift	NED redshift
	nedType	NED source type
	htmid	Hierarchical Triangular Mesh id
	cx	Hierarchical Triangular Mesh cartesian x
	cy	Hierarchical Triangular Mesh cartesian y
	cz	Hierarchical Triangular Mesh cartesian z
KnownSIMBADObject	knownSIMBADObjectID	Index for table
	simbadName	Source name
	simbadRA	SIMBAD Right Ascension
	simbadDec	SIMBAD Declination
	simbadRedshift	SIMBAD redshift
	simbadType	SIMBAD source type
	htmid	Hierarchical Triangular Mesh id
	cx	Hierarchical Triangular Mesh cartesian x
	cy	Hierarchical Triangular Mesh cartesian y
	cz	Hierarchical Triangular Mesh cartesian z
KnownOtherCluster	knownOtherClusterID	Index for table
	ra	Right Ascension
	dec	Declination
	name	Source literature name
	redshift	Source literature redshift
	bibcode	Literature reference
	htmid	Hierarchical Triangular Mesh id
	cx	Hierarchical Triangular Mesh cartesian x
	cy	Hierarchical Triangular Mesh cartesian y
	cz	Hierarchical Triangular Mesh cartesian z

Table E.1: Description of the XCS Database Table Attributes.